PO Box 2345, Beijing 100023, China
Fax: +86-10-85381893
E-mail: wjg@wjgnet.com www.wjgnet.com

World J Gastroenterol 2004;10(13):1849-1853
World Journal of Gastroenterology
 ISSN 1007-9327

• REVIEW •

Biological functions of melanoma-associated antigens

Jiang Xiao, Hong-Song Chen

Jiang Xiao, Hong-Song Chen, Hepatology Institute, People's Hospital, Peking University, Beijing 100044, China
Supported by National Natural Science Foundation, No. 30170047, the State "863" Program, No. 2001AA217151 and No. 2002AA217071 and "211" project of Peking University
Correspondence to: Dr. Hong-Song Chen, Hepatology Institute, People's Hospital, Peking University, Beijing 100044, China. chen2999@sohu.com
Telephone: +86-10-68314422 Ext. 5726 **Fax**: +86-10-68321900
Received: 2003-12-17 **Accepted:** 2004-01-08

Abstract

To date, dozens of melanoma-associated antigens (MAGEs) have been identified and classified into 2 subgroups, I and II. Subgroup I consists of antigens which expression is generally restricted to tumor or germ cells, also named as cancer/testis (CT) antigen. Proteins and peptides derived from some of these antigens have been utilized in promising clinical trials of immunotherapies for gastrointestinal carcinoma, esophageal carcinoma, pulmonary carcinoma and so on. Various MAGE family members play important physiological and pathological roles during embryogenesis, germ cell genesis, apoptosis, etc. However, little is known regarding the role of MAGE family members in cell activities. It is reasonable to speculate that the genes for subgroup I MAGEs, which play important roles during embryogenesis, could be later deactivated by a genetic mechanism such as methylation. In the case of tumor formation, these genes are reactivated and the resultant proteins may be recognized and attacked by the immune system. Thus, the subgroup I MAGEs may play important roles in the immune surveillance of certain tumor types. Here, we review the classifications of MAGE family genes and what is known of their biological functions.

Xiao J, Chen HS. Biological functions of melanoma-associated antigens. *World J Gastroenterol* 2004; 10(13): 1849-1853
http://www.wjgnet.com/1007-9327/10/1849.asp

INTRODUCTION

In 1991, researchers first isolated a melanoma-associated antigen (MAGE) gene, MAGE-A1[1]. This antigen, isolated from an MZ-2 human melanoma cell line, could be recognized by cytotoxic T lymphocytes (CTLs). In the following years, dozens of new MAGE gene were identified. MAGE proteins act as anti-tumoral immune targets, making these antigens a popular focus of immunotherapy researches on gastrointestinal carcinoma and other cancers[2]. Although much work has investigated the expression of MAGE genes and HLA-restricted epitopes, relatively little is known about the functions of the MAGE proteins. In this paper, we review the classifications of MAGE family genes and what is known of their biological functions.

CLASSIFICATIONS OF THE HUMAN MAGE PROTEIN FAMILY

In 1991, Terry Boon's laboratory established a method for identifying tumor antigens based on tumor-specific CTLs recognition[1]. Using this method, the group identified a new tumor antigen which they called MAGE-1. Subsequently, this and other screening methods were used to identify a large number of tumor-specific and tumor-related antigens, including dozens of MAGEs (Table 1)[3-7]. The MAGE family proteins share certain homologous regions, including the MAGE homology domain (MHD). Sequence comparison and analysis revealed 3 subgroups of acidic MAGEs, termed A, B, and C, and one basic subgroup, MAGE-D, which includes Necdin, Restin and others[8]. Based on expression patterns, the MAGEs were further classified as belonging to either subgroup I or II. Members of subgroup I, including MAGE-A, -B, and -C, are expressed in malignant tumors and testis, but not in other normal tissues. These members are also named as cancer/testis (CT) antigen and tumor-specific antigen. In contrast, subgroup II MAGEs are expressed in various normal adult human tissues[4,9]. Interestingly, testis germ cells do not express MHC I/II molecules and cannot present the MAGE proteins, so testis tissue is generally immune-exempt. Based on this, tumor-expressed MAGE-A, -B, and -C proteins have become important targets for cancer immunotherapy, and some clinical trials are ongoing for treating gastrointestinal carcinoma, esophageal carcinoma, pulmonary carcinoma and so on. Now researchers are continuing to identify additional MAGE genes in the hope of identifying better therapeutic targets.

CELLULAR FUNCTIONS OF MAGE PROTEINS

Regulation of subgroup I MAGE gene expression in normal somatic cells

In normal mature somatic cells, subgroup I MAGE genes are static. When cells become neoplastic, MAGE genes are activated and the corresponding proteins are expressed. Interestingly, some non-MAGE-A1-expressing tumor cells have been found to contain transcription factors capable of activating the MAGE-A1 promoter[10]. This suggests that the presence of the relevant transcription factor is not sufficient to trigger expression, indicating that alternative regulatory mechanisms may exist in terms of MAGE-1 gene activation.

Recent studies have shown that MAGE gene activation may be related to promoter demethylation[11]. The promoter of the MAGE-A1 gene contains several cis-regulatory sequences located from nt -792 to +47. Among them, the B and B' domains are critical for MAGE-1 gene expression. Both domains contain Ets transcription factor binding sites, including a critical CpG bi-nucleotide site. When this CpG is methylated, the Ets transcription factor cannot bind to the B and B' domains, and expression of MAGE-1 is inhibited. Therefore, promoter methylation inhibits the expression of MAGE-1[10]. Indeed, when non-MAGE-A1-expressing tumor cells were treated with the demethylating reagent, 5-aza-2-deoxycytidine (5DC), MAGE-A1 expression was induced[11]. When normally non-MAGE-expressing cells (i.e. fibroblasts) were treated with 5DC, some cells expressed MAGE genes[11], while others did not[12]. In explanation of this, the authors proposed that most normal cells possess strong methylating actions, and that demethylating reagents such as 5DC are insufficient to demethylate MAGE promoters to a degree that would allow for MAGE gene expression. Taken together, these studies suggest that both normal and tumor cells contain the transcription factors that activate subgroup I MAGEs, and that expression of these genes is regulated by promoter demethylation.

Table 1 The MAGE family genes

Subtype	Gene name	Access number	Expression status	Length of amino acids
MAGE-A	MAGE-A1	JC2358[27-29]	T	280
	MAGE-A2	AAH13098[30]	T	314
	MAGE-A3	AAH00340[30]	T	314
	MAGE-A4	BAA06841[31]	T	317
	MAGE-A5	NP_064402[32]	T	320
	MAGE-A6	AAA68875[5]	T	314
	MAGE-A7	NP_064677[33]	P	80
	MAGE-A8	AAH02455[30]	T	318
	MAGE-A9	P43362[5]	T	315
	MAGE-A10	AAA68869[5]	T	369
	MAGE-A11	P43364[5]	T	319
	MAGE-A12	AAF44789[34]	T	314
	MAGE-A13	U71148	P	–
	MAGE-A14	NT_011534.1	P	–
	MAGE-A15	NT_025309.1	P	–
MAGE-B	MAGE-B1	AAC23616[35]	T	347
	MAGE-B2	AAC23617[35]	T	319
	MAGE-B3	AAC23618[35]	T	346
	MAGE-B4	AAC23619[35]	T	346
	MAGE-B5	Q9BZ81[36]	T	111
	MAGE-B6	Q8N7X4[37]	T	407
	MAGE-B7	AC005297.1	P	–
	MAGE-B8	AC005297.1	P	–
	MAGE-B9	AC005297.1	P	–
	MAGE-B10	AC011693.5	T	348
	MAGE-B11	AC011693.5	P	–
	MAGE-B12	AC011693.5	P	–
	MAGE-B13	AC011693.5	P	–
	MAGE-B14	NT_025279.3	P	–
	MAGE-B15	NT_011752.1	P	–
	MAGE-B16	NT_025279.3	T	320
	MAGE-B17	NT_011766.3	T	203
MAGE-C	MAGE-C1	NP_005453[38-40]	T	1 142
	MAGE-C2	NP_057333[41-42]	T	373
	MAGE-C3	AAK00358[36]	T	346
	MAGE-C4	AL023279.1	T	115
	MAGE-C5	NT_025337.2	P	–
	MAGE-C6	NT_025337.2	P	–
	MAGE-C7	NT_025337.2	P	–
MAGE-D	MAGE-D1	AAG09704[25,43]	N	778
	MAGE-D2	CAB10841[44-46]	N	606
	MAGE-D3	Q12816[47,48]	N	1 387
	MAGE-D4	Q96JG8[49-52]	N	741
MAGE-E	MAGE-E1	Q96JG8[49-52]	N	741
	MAGE-E2	–	N	–
	MAGE-E3	NP_032879[53-55]	N	424
MAGE-F	MAGE-F1	NP_071432[56]	N	307
MAGE-G	MAGE-G1	AAG38607[57]	N	100
MAGE-H	MAGE-H1	AAG38608[58]	N	219
MAGE-I	MAGE-I1	NT_011638.3	P	–
	MAGE-I2	NT_011638.3	P	–
MAGE-J	MAGE-J1	NT_011577	P	–
MAGE-K	MAGE-K1	Z81311	P	–
MAGE-L2	MAGE-L2	NP_061939[59,60]	N	529
Necdin	Necdin	XM_007686[61-65]	N	321
Restin	Restin (Apr-1)	NP_054780[66-70]	N	219

T: Only expressed in tumor cells or germ cells. P: Pseudogene; N: Expressed in normal cells. -: Unknown.

The functions of MAGE genes in germ cells

Most MAGE genes are expressed in germ cells under physiological conditions, but their functions remain unclear. Early work has focused on the functions of the mouse MAGE-b4 gene during embryonic development[13]. The mouse MAGE-b4 gene is expressed in adult and fetal reproductive gland cells and shares high homology with members of the human MAGE-B subtype. The MAGE-b4 protein is located in the cytoplasm but not in the nucleus. In male testes, germ cells (gonocytes) continuously proliferate until they arrest at the G0/G1 stage, differentiate into foot cells and form the spermatic cords. After birth, the gonocytes differentiate into spermatogonia, which in turn undergo meiosis during adolescence and differentiate into sperm cells. The MAGE-b4 gene is highly expressed in germ cells suspended in G0/G1; in contrast, the gene is barely expressed in meiotic spermatogonia. Thus, MAGE-b4 likely plays an important role in male germ cells, perhaps by maintaining gonocytes in a non-proliferative state.

In female germ cells, MAGE-b4 is expressed prior to meiosis, and also during the pachytene and telophase portions of meiosis. Other cell cycle proteins have shown similar differences in expression in the two sexes. For instance, cyclin A1 deficiency in male germ cells inhibits meiosis but does not affect that in female germ cells[14]. Similarly, deficiencies of Hsp70-2 or A-myb suppress the development of male germ cells and male fertility but do not affect female development[15]. Therefore, we speculate that MAGE-b4 may similarly play an important role in the control of the cycle of male germ cells, while playing a less dramatic role in female germ cells.

Another member of the MAGE family Magphinin plays an important role in germ cell development. Mouse Trophinin is a membrane protein that plays an adhesive role in the process of zygotic implantation into the uterine endometrium; an alternative transcript of the Trophinin gene encodes Magphinin[16]. Although the Trophinin protein is not homologous with the MAGE family members, the mouse Magphinin protein shares high homology with Necdin, Dlxin and NRAGE. Of these, Necdin can bind transcription factor E_2F-1, which is responsible for inducing the expression of cyclin and promoting cell cycle progression from G1 to S. Thus, it is possible that the Necdin homolog, Magphinin, acts similarly to bind E_2F-1 and inhibit cell proliferation. Magphinin has three alternatively spliced forms: magphinin-a, β and γ. Northern blot analysis reveals that Magphinin protein is expressed in mouse brain, ovary, testis, and epididymis. Western blot analysis indicates that in mouse ovary and epididymis, Magphinin is derived from alternative translation of the Trophinin transcript beginning at the second start codon (AUG). The Magphinin protein sequence contains a nuclear localization signal that allows it to enter the nucleus and inhibit cell proliferation. Immunohistochemical studies suggest that the localization of Magphinin protein varies between male and female germ cells at various stages of the cell cycle. Before meiosis, Magphinin-β is mainly distributed in the cytoplasm of male germ cells. After the first meiosis, when primary spermatocytes differentiate into secondary spermatocytes, Magphinin is localized in both the cytoplasm and the nucleus, and after this nuclear translocation, cell division terminates. Based on this, we speculate that Magphinin regulates the cell cycle during the formation of male spermatocytes. In the female germ cell, the distribution of Magphinin is somewhat different. When the oocyte has only single- or double-layer vesicles, intracellular Magphinin (especially Magphinin-γ) is strictly cytoplasmic. When the oocyte has divided into multi-layer vesicles, the protein is only located in nucleus. In this case, meiosis terminates at stage G2, suggesting that Magphinin also controls the formation of the female ovum.

May these expression patterns and functional roles be generalized to other members of the MAGE family? This remains to be shown. Indeed, at present, little is known about the functions of MAGE family proteins inside germ cells. Further studies will show whether human MAGE proteins control the cell cycle in manners similar to the actions of MAGE-b4 and Magphinin.

Below, we will discuss several specific examples of MAGEs and what is known of their cellular functions.

MAGE-A4

In terms of cancer biology, yeast two-hybrid studies identified binding between the MAGE-A4 protein and a cancer protein: the gann ankyrin repeat protein (also called Gankyrin, PSMD10 or p28). This MAGE- A4-specific binding is mediated by its C-terminus[17]. Gankyrin, which consists of six gann ankyrin repeats and a 38 amino acid N-terminus, can bind the cancer-suppressing protein Rb, the S6 ATP enzyme subunit of the 26S protein, and cell cycle-dependent kinase 4 (Cdk4). Gankyrin expression is increased in the livers of hepatocellular carcinoma patients; this increase is seen at the earliest stages of tumor genesis[18,19]. Overexpression of Gankyrin can increase the phosphorylation and degradation of Rb, as well as immortalization of NIH/3T3 cells. In addition, the binding of Gankyrin to Cdk4 counteracts the cancer-inhibiting functions of $p16^{INK4A}$ and $p18^{INK4C}$[20]. Therefore, Gankyrin plays an important role in controlling cell cycle during liver cancer tumorigenesis. Studies have shown that exogenous MAGE-A4 can partly inhibit the adhesion-independent growth of Gankyrin-overexpressing cells *in vitro* and suppress the formation of migrated tumors from these cells in nude mice. This inhibition is dependent upon binding between MAGE-A4 and Gankyrin, suggesting that interactions between Gankyrin and MAGE-A4 inhibit Gankyrin-mediated carcinogenesis[17].

Necdin

Necdin, first identified in 1991, is the best-characterized member of the MAGE protein family. The gene was isolated from P19 neural cells; the encoded protein consists of 325 amino acids and shares about 30% homology with other MAGE proteins[21]. Studies have shown that overexpression of Necdin may induce cell cycle arrest in NIH3T3 and SAOS2 cell lines, suggesting that Necdin functions in cell cycle arrest and maintenance of cell stability. *In vivo*, Necdin can interact with cell cycle promoting proteins such as the SV40 big-T protein, adenovirus EIA and transcription factor E_2F-1, which acts as a cell cycle regulator by trans-activating the relevant genes in an Rb-regulated pathway. The latter binds to E_2F-1 protein during G1 stage and inhibits the binding ability of E_2F-1, leading to inhibition of gene activation. Similarly, Necdin can bind to E_2F-1 and initiate conformational changes to decrease E_2F-1 binding and inhibit cell growth[22]. In addition, Necdin can bind to and inhibit p53, which normally induces cell cycle arrest and cell death[23]. Thus, Necdin plays important roles in inhibiting cell growth and apoptosis through its interactions with E_2F-1 and p53.

The human Necdin gene is localized at $15q^{11-13}$, an area genetically associated with the neurological behavior disorder, Prader-willi Syndrome (PWS). Newborn PWS patients generally suffer respiratory failure and myasthenia, and adolescent PWS patients show psychonosema, sexual dysfunction and obesity. The PWS chromosomal region contains several genes, including Necdin and MAGE-L2. Indeed, knockouts of the mouse Necdin homolog show symptoms similar to human PWS[24], suggesting that Necdin plays a role in proper development, and that lack of Necdin may be involved in the pathogenesis of PWS.

MAGE-D1

The MAGE-D1, also named as NRAGE or Dlxin, plays important roles in mediating apoptosis and transcription. NRAGE interacts with $p75^{NTR}$, a TNF receptor responsible for binding the Trk receptor and forming a complex that facilitates binding of neurotrophin, which in turn activates the Trk receptor. $p75^{NTR}$ is also capable of mediating cell death. NRAGE- $p75^{NTR}$ binding, identified by yeast two-hybrid screening, occurs through an 80 amino acid intracellular segment of $p75^{NTR}$ located near the plasma membrane. Overexpression of NRAGE inhibited the interaction between $p75^{NTR}$ and the Trk receptor and induced cell apoptosis. In contrast, overexpression of the Trk receptor increased binding between Trk and $p75^{NTR}$, leading to inhibition of NRAGE-$p75^{NTR}$ complex-induced cell death. This indicates that NRAGE-$p75^{NTR}$ and Trk receptor-$p75^{NTR}$ binding are mutually exclusive.

Another NRAGE-binding protein, XIAP, can inhibit apoptosis by binding to activated Caspases. The NRAGE-XIAP complex accelerates the decomposition of XIAP, suggesting that NRAGE accelerates cell death by degrading XIAP and activating Caspases[4].

Indeed, members of the MAGE-D1 subgroup can bind to several proteins that control apoptosis and cell cycle[4]. The MAGE-D1 repeat regions can directly interact with Msx2, Dlx7 and Dlx5. Msx generally acts as a transcription inhibitor, whereas Dlx acts as a transcriptional activator. In addition, Msx1 and Msx2 play roles in the control of cell cycle, and Msx2 can promote cell death. The effect of MAGE-D1 on Msx remains unknown, but MAGE-D1 is necessary for Dlx5 to promote transcription.

CONCLUSION

Although subgroup I and II MAGE genes are expressed in different tissue-specific patterns, all family members contain the MAGE homology domain (MHD), suggesting some functional conservation. Biochemical analyses of these two subgroups have provided some insights into the physiological effects of the MAGE genes. Embryonic cells have much less CpG methylation at the MAGE genes than do somatic cells[25,26]. Similarly, MAGE genes in tumor cells are hypomethylated; indeed, the entire tumor genome is generally hypomethylated[10]. Thus, it is likely that MAGE gene expression in tumor tissues is the result of tumor genesis, not a cause. It is reasonable to speculate that this family of proteins functions during embryonic development, and that the genes are subsequently deactivated, perhaps by methylation. During neoplastic transformation, these genes are re-activated, expressed, and may become antigenic targets that are recognized and attacked by the immune system[8]. Therefore, MAGE genes take part in the immune process by targeting some early tumor cells for immune destruction. Consequently, these genes should be studied further in terms of their various functions as they relate to the pathogenic mechanism of tumors, immunotherapy, and other important fields.

REFERENCES

1 **van der Bruggen P**, Traversari C, Chomez P, Lurquin C, De Plaen E, Van den Eynde B, Knuth A, Boon T. A gene encoding an antigen recognized by cytolytic T lymphocytes on a human melanoma. *Science* 1991; **254**: 1643-1647

2 **Sadanaga N**, Nagashima H, Mashino K, Tahara K, Yamaguchi H, Ohta M, Fujie T, Tanaka F, Inoue H, Takesako K, Akiyoshi T, Mori M. Dendritic cell vaccination with MAGE peptide is a novel therapeutic approach for gastrointestinal carcinomas. *Clin Cancer Res* 2001; **7**: 2277-2284

3 **Chen YT**, Scanlan MJ, Sahin U, Tureci O, Gure AO, Tsang S, Williamson B, Stockert E, Pfreundschuh M, Old LJ. A testicular antigen aberrantly expressed in human cancers detected by autologous antibody screening. *Proc Natl Acad Sci U S A* 1997; **94**: 1914-1918

4 **Barker PA**, Salehi A. The MAGE proteins: emerging roles in cell cycle progression, apoptosis, and neurogenetic disease. *J Neurosci Res* 2002; **67**: 705-712

5 **Chomez P**, De Backer O, Bertrand M, De Plaen E, Boon T, Lucas S. An overview of the MAGE gene family with the identification of all human members of the family. *Cancer Res* 2001; **61**: 5544-5551

6 **De Plaen E**, Arden K, Traversari C, Gaforio JJ, Szikora JP, De Smet C, Brasseur F, van der Bruggen P, Lethe B. Structure, chromosomal localization and expression of 12 genes of the MAGE family. *Immunogenetics* 1994; **40**: 360-369

7 http://www.ncbi.nlm.nih.gov/Genebank

8 **Zhao ZL**, Lu F, Zhu F, Yang H, Chai YB, Chen SM. Cloning and biological comparison of Restin, a novel member of Mage superfamily. *Sci China* 2002; **45**: 412-420

9 **Chiba T**, Yokosuka O, Kanda T, Fukai K, Imazeki F, Saisho H, Nishimura M, Saito Y. Hepatic graft-versus-host disease resembling acute hepatitis: additional treatment with ursodeoxycholic acid. *Liver* 2002; **22**: 514-527

10 **De Smet C**, Lurquin C, Lethe B, Martelange V, Boon T. DNA methylation is the primary silencing mechanism for a set of germ line- and tumor-specific genes with a CpG-rich promoter. *Mol Cell Biol* 1999; **19**: 7327-7335

11 **De Smet C**, De Backer O, Faraoni I, Lurquin C, Brasseur F, Boon T. The activation of human gene MAGE-1 in tumor cells is correlated with genome-wide demethylation. *Proc Natl Acad Sci U S A* 1996; **93**: 7149-7153

12 **Weber J**, Salgaller M, Samid D, Johnson B, Herlyn M, Lassam N, Treisman J, Rosenberg SA. Expression of the MAGE-1 tumor antigen is up-regulated by the demethylating agent 5-aza-2'-deoxycytidine. *Cancer Res* 1994; **54**: 1766-1771

13 **Osterlund C**, Tohonen V, Forslund KO, Nordqvist K. Mage-b4, a novel melanoma antigen (MAGE) gene specifically expressed during germ cell differentiation. *Cancer Res* 2000; **60**: 1054-1061

14 **Liu D**, Matzuk MM, Sung WK, Guo Q, Wang P, Wolgemuth DJ. Cyclin A1 is required for meiosis in the male mouse. *Nat Genet* 1998; **20**: 377-380

15 **Toscani A**, Mettus RV, Coupland R, Simpkins H, Litvin J, Orth J, Hatton KS, Reddy EP. Arrest of spermatogenesis and defective breast development in mice lacking A-myb. *Nature* 1997; **386**: 713-717

16 **Saburi S**, Nadano D, Akama TO, Hirama K, Yamanouchi K, Naito K, Tojo H, Tachi C, Fukuda MN. The trophinin gene encodes a novel group of MAGE proteins, magphinins, and regulates cell proliferation during gametogenesis in the mouse. *J Biol Chem* 2001; **276**: 49378-49389

17 **Meier S**, Haussinger D, Jensen P, Rogowski M, Grzesiek S. High-accuracy residual 1HN-13C and 1HN-1HN dipolar couplings in perdeuterated proteins. *J Am Chem Soc* 2003; **125**: 44-45

18 **Higashitsuji H**, Itoh K, Nagao T, Dawson S, Nonoguchi K, Kido T, Mayer RJ, Arii S, Fujita J. Reduced stability of retinoblastoma protein by gankyrin, an oncogenic ankyrin-repeat protein overexpressed in hepatomas. *Nat Med* 2000; **6**: 96-99

19 **Park TJ**, Kim HS, Byun KH, Jang JJ, Lee YS, Lim IK. Sequential changes in hepatocarcinogenesis induced by diethylnitrosamine plus thioacetamide in Fischer 344 rats: induction of gankyrin expression in liver fibrosis, pRB degradation in cirrhosis, and methylation of p16(INK4A) exon 1 in hepatocellular carcinoma. *Mol Carcinog* 2001; **30**: 138-150

20 **Li J**, Tsai MD. Novel insights into the INK4-CDK4/6-Rb pathway: counter action of gankyrin against INK4 proteins regulates the CDK4-mediated phosphorylation of Rb. *Biochemistry* 2002; **41**: 3977-8339

21 **Maruyama K**, Usami M, Aizawa T, Yoshikawa K. A novel brain-specific mRNA encoding nuclear protein (necdin) expressed in neurally differentiated embryonal carcinoma cells. *Biochem Biophys Res Commun* 1991; **178**: 291-296

22 **Taniura H**, Taniguchi N, Hara M, Yoshikawa K. Necdin, a postmitotic neuron-specific growth suppressor, interacts with viral transforming proteins and cellular transcription factor E2F1. *J Biol Chem* 1998; **273**: 720-728

23 **Taniura H**, Matsumoto K, Yoshikawa K. Physical and functional interactions of neuronal growth suppressor necdin with p53. *J Biol Chem* 1999; **274**: 16242-16248

24 **Nakada Y**, Taniura H, Uetsuki T, Inazawa J, Yoshikawa K. The human chromosomal gene for necdin, a neuronal growth suppressor, in the Prader-Willi syndrome deletion region. *Gene* 1998; **213**: 65-72

25 **Salehi AH**, Roux PP, Kubu CJ, Zeindler C, Bhakar A, Tannis LL, Verdi JM, Barker PA. NRAGE, a novel MAGE protein, interacts with the p75 neurotrophin receptor and facilitates nerve growth factor-dependent apoptosis. *Neuron* 2000; **27**: 279-288

26 **Reik W**, Dean W, Walter J. Epigenetic reprogramming in mammalian development. *Science* 2001; **293**: 1089-1093

27 **Ding M**, Beck RJ, Keller CJ, Fenton RG. Cloning and analysis of MAGE-1-related genes. *Biochem Biophys Res Commun* 1994; **202**: 549-555

28 **Suyama T**, Ohashi H, Nagai H, Hatano S, Asano H, Murate T, Saito H, Kinoshita T. The MAGE-A1 gene expression is not determined solely by methylation status of the promoter region in hematological malignancies. *Leuk Res* 2002; **26**: 1113-1118

29 **Chen YT**, Stockert E, Chen Y, Garin-Chesa P, Rettig WJ, van der Bruggen P, Boon T, Old LJ. Identification of the MAGE-1 gene product by monoclonal and polyclonal antibodies. *Proc Natl Acad Sci U S A* 1994; **91**: 1004-1008

30 **Strausberg RL**, Feingold EA, Grouse LH, Derge JG, Klausner RD, Collins FS, Wagner L, Shenmen CM, Schuler GD, Altschul SF, Zeeberg B, Buetow KH, Schaefer CF, Bhat NK, Hopkins RF, Jordan H, Moore T, Max SI, Wang J, Hsieh F, Diatchenko L, Marusina K, Farmer AA, Rubin GM, Hong L, Stapleton M, Soares MB, Bonaldo MF, Casavant TL, Scheetz TE, Brownstein MJ, Usdin TB, Toshiyuki S, Carninci P, Prange C, Raha SS, Loquellano NA, Peters GJ, Abramson RD, Mullahy SJ, Bosak SA, McEwan PJ, McKernan KJ, Malek JA, Gunaratne PH, Richards S, Worley KC, Hale S, Garcia AM, Gay LJ, Hulyk SW, Villalon DK, Muzny DM, Sodergren EJ, Lu X, Gibbs RA, Fahey J, Helton E, Ketteman M, Madan A, Rodrigues S, Sanchez A, Whiting M, Madan A, Young AC, Shevchenko Y, Bouffard GG, Blakesley RW, Touchman JW, Green ED, Dickson MC, Rodriguez AC, Grimwood J, Schmutz J, Myers RM, Butterfield YS, Krzywinski MI, Skalska U, Smailus DE, Schnerch A, Schein JE, Jones SJ, Marra MA. Mammalian Gene Collection Program Team. Generation and initial analysis of more than 15,000 full-length human and mouse cDNA sequences. *Proc Natl Acad Sci U S A* 2002; **99**: 16899-16903

31 **Imai Y**, Shichijo S, Yamada A, Katayama T, Yano H, Itoh K. Sequence analysis of the MAGE gene family encoding human tumor-rejection antigens. *Gene* 1995; **160**: 287-290

32 **Wang PJ**, McCarrey JR, Yang F, Page DC. An abundance of X-linked genes expressed in spermatogonia. *Nat Genet* 2001; **27**: 422-426

33 **De Plaen E**, De Backer O, Arnaud D, Bonjean B, Chomez P, Martelange V, Avner P, Baldacci P, Babinet C, Hwang SY, Knowles B, Boon T. A new family of mouse genes homologous to the human MAGE genes. *Genomics* 1999; **55**: 176-184

34 **Mallon AM**, Platzer M, Bate R, Gloeckner G, Botcherby MR, Nordsiek G, Strivens MA, Kioschis P, Dangel A, Cunningham D, Straw RN, Weston P, Gilbert M, Fernando S, Goodall K, Hunter G, Greystrong JS, Clarke D, Kimberley C, Goerdes M, Blechschmidt K, Rump A, Hinzmann B, Mundy CR, Miller W, Poustka A, Herman GE, Rhodes M, Denny P, Rosenthal A, Brown SD. Comparative genome sequence analysis of the Bpa/Str region in mouse and Man. *Genome Res* 2000; **10**: 758-775

35 **Lurquin C**, De Smet C, Brasseur F, Muscatelli F, Martelange V, De Plaen E, Brasseur R, Monaco AP, Boon T. Two members of the human MAGEB gene family located in Xp21.3 are expressed in tumors of various histological origins. *Genomics* 1997; **46**: 397-408

36 **Lucas S**, De Plaen E, Boon T. MAGE-B5, MAGE-B6, MAGE-C2, and MAGE-C3: four new members of the MAGE family with tumor-specific expression. *Int J Cancer* 2000; **87**: 55-60

37 **Ota T**, Suzuki Y, Nishikawa T, Otsuki T, Sugiyama T, Irie R, Wakamatsu A, Hayashi K, Sato H, Nagai K, Kimura K, Makita H, Sekine M, Obayashi M, Nishi T, Shibahara T, Tanaka T, Ishii S, Yamamoto J, Saito K, Kawai Y, Isono Y, Nakamura Y, Nagahari K, Murakami K, Yasuda T, Iwayanagi T, Wagatsuma M, Shiratori A, Sudo H, Hosoiri T, Kaku Y, Kodaira H, Kondo H, Sugawara M, Takahashi M, Kanda K, Yokoi T, Furuya T, Kikkawa E, Omura Y, Abe K, Kamihara K, Katsuta N, Sato K, Tanikawa M, Yamazaki M, Ninomiya K, Ishibashi T, Yamashita H, Murakawa K, Fujimori K, Tanai H, Kimata M, Watanabe M, Hiraoka S, Chiba Y, Ishida S, Ono Y, Takiguchi S, Watanabe S, Yosida M, Hotuta T, Kusano J, Kanehori K, Takahashi-Fujii A, Hara H, Tanase TO, Nomura Y, Togiya S, Komai F, Hara R, Takeuchi K, Arita M, Imose N, Musashino K, Yuuki H, Oshima A, Sasaki N, Aotsuka S, Yoshikawa Y, Matsunawa H, Ichihara T, Shiohata N, Sano S, Moriya S, Momiyama H, Satoh N, Takami S, Terashima Y, Suzuki O, Nakagawa S, Senoh A, Mizoguchi H, Goto Y, Shimizu F, Wakebe H, Hishigaki H, Watanabe T, Sugiyama A, Takemoto M, Kawakami B, Yamazaki M, Watanabe K, Kumagai A, Itakura S, Fukuzumi Y, Fujimori Y, Komiyama M, Tashiro H, Tanigami A, Fujiwara T, Ono T, Yamada K, Fujii Y, Ozaki K, Hirao M, Ohmori Y, Kawabata A, Hikiji T, Kobatake N, Inagaki H, Ikema Y, Okamoto S, Okitani R, Kawakami T, Noguchi S, Itoh T, Shigeta

K, Senba T, Matsumura K, Nakajima Y, Mizuno T, Morinaga M, Sasaki M, Togashi T, Oyama M, Hata H, Watanabe M, Komatsu T, Mizushima-Sugano J, Satoh T, Shirai Y, Takahashi Y, Nakagawa K, Okumura K, Nagase T, Nomura N, Kikuchi H, Masuho Y, Yamashita R, Nakai K, Yada T, Nakamura Y, Ohara O, Isogai T, Sugano S. Complete sequencing and characterization of 21,243 full-length human cDNAs. *Nat Genet* 2004; **36**: 40-45

38 **Jungbluth AA**, Chen YT, Busam KJ, Coplan K, Kolb D, Iversen K, Williamson B, Van Landeghem FK, Stockert E, Old LJ. CT7 (MAGE-C1) antigen expression in normal and neoplastic tissues. *Int J Cancer* 2002; **99**: 839-845

39 **Lim SH**, Bumm K, Chiriva-Intemati M, Xue Y, Wang Z. MAGE-C1 (CT7) gene expression in multiple myeloma: relationship to sperm protein 17. *Eur J Haematol* 2001; **67**: 332-334

40 **Chen YT**, Gure AO, Tsang S, Stockert E, Jager E, Knuth A, Old LJ. Identification of multiple cancer / testis antigens by allogeneic antibody screening of a melanoma cell line library. *Proc Natl Acad Sci U S A* 1998; **95**: 6919-6923

41 **Lucas S**, De Smet C, Arden KC, Viars CS, Lethe B, Lurquin C, Boon T. Identification of a new MAGE gene with tumor-specific expression by representational difference analysis. *Cancer Res* 1998; **58**: 743-752

42 **Gure AO**, Stockert E, Arden KC, Boyer AD, Viars CS, Scanlan MJ, Old LJ, Chen YT. CT10: a new cancer-testis (CT) antigen homologous to CT7 and the MAGE family, identified by representational-difference analysis. *Int J Cancer* 2000; **85**: 726-732

43 **Hennuy B**, Reiter E, Cornet A, Bruyninx M, Daukandt M, Houssa P, N'Guyen VH, Closset J, Hennen G. A novel messenger ribonucleic acid homologous to human MAGE-D is strongly expressed in rat Sertoli cells and weakly in Leydig cells and is regulated by follitropin, lutropin, and prolactin. *Endocrinology* 2000; **141**: 3821-3831

44 **Kurt RA**, Urba WJ, Schoof DD. Isolation of genes overexpressed in freshly isolated breast cancer specimens. *Breast Cancer Res Treat* 2000; **59**: 41-48

45 **Langnaese K**, Kloos DU, Wehnert M, Seidel B, Wieacker P. Expression pattern and further characterization of human MAGED2 and identification of rodent orthologues. *Cytogenet Cell Genet* 2001; **94**: 233-240

46 **Lucas S**, Brasseur F, Boon T. A new MAGE gene with ubiquitous expression does not code for known MAGE antigens recognized by T cells. *Cancer Res* 1999; **59**: 4100-4103

47 **Kikuno R**, Nagase T, Ishikawa K, Hirosawa M, Miyajima N, Tanaka A, Kotani H, Nomura N, Ohara O. Prediction of the coding sequences of unidentified human genes. XIV. The complete sequences of 100 new cDNA clones from brain which code for large proteins *in vitro*. *DNA Res* 1999; **6**: 197-205

48 **Fukuda MN**, Sato T, Nakayama J, Klier G, Mikami M, Aoki D, Nozawa S. Trophinin and tastin, a novel cell adhesion molecule complex with potential involvement in embryo implantation. *Genes Dev* 1995; **9**: 1199-1210

49 **Sasaki M**, Nakahira K, Kawano Y, Katakura H, Yoshimine T, Shimizu K, Kim SU, Ikenaka K. MAGE-E1, a new member of the melanoma-associated antigen gene family and its expression in human glioma. *Cancer Res* 2001; **61**: 4809-4814

50 **Kawano Y**, Sasaki M, Nakahira K, Yoshimine T, Shimizu K, Wada H, Ikenaka K. Structural characterization and chromosomal localization of the MAGE-E1 gene. *Gene* 2001; **277**: 129-137

51 **Wiemann S**, Weil B, Wellenreuther R, Gassenhuber J, Glassl S, Ansorge W, Bocher M, Blocker H, Bauersachs S, Blum H, Lauber J, Dusterhoft A, Beyer A, Kohrer K, Strack N, Mewes HW, Ottenwalder B, Obermaier B, Tampe J, Heubner D, Wambutt R, Korn B, Klein M, Poustka A. Toward a catalog of human genes and proteins: sequencing and analysis of 500 novel complete protein coding human cDNAs. *Genome Res* 2001; **11**: 422-435

52 **Nagase T**, Nakayama M, Nakajima D, Kikuno R, Ohara O. Prediction of the coding sequences of unidentified human genes. XX. The complete sequences of 100 new cDNA clones from brain which code for large proteins *in vitro*. *DNA Res* 2001; **8**: 85-95

53 **Sasaki A**, Masuda Y, Iwai K, Ikeda K, Watanabe K. A RING finger protein Praja1 regulates Dlx5-dependent transcription through its ubiquitin ligase activity for the Dlx / Msx-interacting MAGE / Necdin family protein, Dlxin-1. *J Biol Chem* 2002; **277**: 22541-22546

54 **Stork O**, Stork S, Pape HC, Obata K. Identification of genes expressed in the amygdala during the formation of fear memory. *Learn Mem* 2001; **8**: 209-219

55 **Mishra L**, Tully RE, Monga SP, Yu P, Cai T, Makalowski W, Mezey E, Pavan WJ, Mishra B. Praja1, a novel gene encoding a RING-H2 motif in mouse development. *Oncogene* 1997; **15**: 2361-2368

56 **Stone B**, Schummer M, Paley PJ, Crawford M, Ford M, Urban N, Nelson BH. MAGE-F1, a novel ubiquitously expressed member of the MAGE superfamily. *Gene* 2001; **267**: 173-182

57 **Kuwako K**, Taniura H, Yoshikawa K. Necdin-related MAGE proteins differentially interact with the E2F1 transcription factor and the p75 neurotrophin receptor. *J Biol Chem* 2004; **279**: 1703-1712

58 **Tcherpakov M**, Bronfman FC, Conticello SG, Vaskovsky A, Levy Z, Niinobe M, Yoshikawa K, Arenas E, Fainzilber M. The p75 neurotrophin receptor interacts with multiple MAGE proteins. *J Biol Chem* 2002; **277**: 49101-49104

59 **Lee S**, Kozlov S, Hernandez L, Chamberlain SJ, Brannan CI, Stewart CL, Wevrick R. Expression and imprinting of MAGEL2 suggest a role in Prader-willi syndrome and the homologous murine imprinting phenotype. *Hum Mol Genet* 2000; **9**: 1813-1819

60 **Boccaccio I**, Glatt-Deeley H, Watrin F, Roeckel N, Lalande M, Muscatelli F. The human MAGEL2 gene and its mouse homologue are paternally expressed and mapped to the Prader-Willi region. *Hum Mol Genet* 1999; **8**: 2497-2505

61 **Andrieu D**, Watrin F, Niinobe M, Yoshikawa K, Muscatelli F, Fernandez PA. Expression of the Prader-Willi gene Necdin during mouse nervous system development correlates with neuronal differentiation and p75NTR expression. *Gene Expr Patterns* 2003; **3**: 761-765

62 **Hu B**, Wang S, Zhang Y, Feghali CA, Dingman JR, Wright TM. A nuclear target for interleukin-1alpha: interaction with the growth suppressor necdin modulates proliferation and collagen expression. *Proc Natl Acad Sci U S A* 2003; **100**: 10008-10013

63 **Matsuda T**, Suzuki H, Oishi I, Kani S, Kuroda Y, Komori T, Sasaki A, Watanabe K, Minami Y. The receptor tyrosine kinase Ror2 associates with the melanoma-associated antigen (MAGE) family protein Dlxin-1 and regulates its intracellular distribution. *J Biol Chem* 2003; **278**: 29057-29064

64 **Ren J**, Lee S, Pagliardini S, Gerard M, Stewart CL, Greer JJ, Wevrick R. Absence of Ndn, encoding the Prader-Willi syndrome-deleted gene necdin, results in congenital deficiency of central respiratory drive in neonatal mice. *J Neurosci* 2003; **23**: 1569-1573

65 **Takazaki R**, Nishimura I, Yoshikawa K. Necdin is required for terminal differentiation and survival of primary dorsal root ganglion neurons. *Exp Cell Res* 2002; **277**: 220-232

66 **Zhu F**, Yan W, Zhao ZL, Chai YB, Lu F, Wang Q, Peng WD, Yang AG, Wang CJ. Improved PCR-based subtractive hybridization strategy for cloning differentially expressed genes. *Biotechniques* 2000; **29**: 310-313

67 **Sahin U**, Neumann F, Tureci O, Schmits R, Perez F, Pfreundschuh M. Hodgkin and Reed-Sternberg cell-associated autoantigen CLIP-170 / restin is a marker for dendritic cells and is involved in the trafficking of macropinosomes to the cytoskeleton, supporting a function-based concept of Hodgkin and Reed-Sternberg cells. *Blood* 2002; **100**: 4139-4145

68 **Ramchandran R**, Dhanabal M, Volk R, Waterman MJ, Segal M, Lu H, Knebelmann B, Sukhatme VP. Antiangiogenic activity of restin, NC10 domain of human collagen XV: comparison to endostatin. *Biochem Biophys Res Commun* 1999; **255**: 735-739

69 **Griparic L**, Keller TC. Identification and expression of two novel CLIP-170 / Restin isoforms expressed predominantly in muscle. *Biochim Biophys Acta* 1998; **1405**: 35-46

70 **Delabie J**, Bilbe G, Bruggen J, Van Leuven F, De Wolf-Peeters C. Restin in Hodgkin's disease and anaplastic large cell lymphoma. *Leuk Lymphoma* 1993; **12**: 21-26

Edited by Zhu LH **Proofread by** Xu FM

PO Box 2345, Beijing 100023, China
Fax: +86-10-85381893
E-mail: wjg@wjgnet.com www.wjgnet.com

World J Gastroenterol 2004;10(13):1854-1856
World Journal of Gastroenterology
 ISSN 1007-9327

• REVIEW •

Theory of traditional Chinese medicine and therapeutic method of diseases

Ai-Ping Lu, Hong-Wei Jia, Cheng Xiao, Qing-Ping Lu

Ai-Ping Lu, Hong-Wei Jia, Cheng Xiao, Institute of Basic Theory, China Academy of Traditional Chinese Medicine, Beijing 100700, China
Qing-Ping Lu, National Pharmaceutical Engineering Research Center, Nanchang 330077, Jiangxi Province, China
Supported by the Key Grant Program in National Administration of Traditional Chinese Medicine, No.2000-J-Z-02 and the Key Program in National Natural Science Foundation of China, No. 90209002
Correspondence to: Dr. Ai-Ping Lu, Institute of Basic Theory, China Academy of Traditional Chinese Medicine, Beijing 100700, China. catcm@public.bta.net.cn
Telephone: +86-10-64067611 **Fax:** +86-10-64013896
Received: 2003-11-18 **Accepted:** 2004-02-01

Abstract

Traditional Chinese medicine, including herbal medicine and acupuncture, as one of the most important parts in complementary and alternative medicine (CAM), plays the key role in the formation of integrative medicine. Why do not the modern drugs targeting the specificity of diseases produce theoretical effects in clinical observation? Why does not the traditional Chinese medicine targeting the Zheng (syndrome) produce theoretical effects in clinic? There should have some reasons to combine Western medicine with Chinese herbal medicine so as to form the integrative medicine. During the integration, how to clarify the impact of CAM theory on Western medicine has become an emergent topic. This paper focuses on the exploration of the impact of theory of traditional Chinese medicine on the therapy of diseases in Western medicine.

Lu AP, Jia HW, Xiao C, Lu QP. Theory of traditional Chinese medicine and therapeutic method of diseases. *World J Gastroenterol* 2004; 10(13): 1854-1856
http://www.wjgnet.com/1007-9327/10/1854.asp

INTRODUCTION

More than one third of patients in the United States use complementary and alternative medicine (CAM)[1], and more and more scientists are interested in integrative medicine research in USA. Recent research showed that integrative medicine (also complementary and alternative medicine) could contribute to primary health care[2,3]. Traditional Chinese medicine (TAM), including herbal medicine and acupuncture, as one of the most important parts in CAM, should play the key role in the formation of integrative medicine. During the integration, how to clarify the impact of CAM theory on Western medicine has become the emergent topic.

TCM was formed two thousand years ago, and developed in the following centuries. TCM recognizes human body by system discrimination and cybernetic way. TCM can be characterized as holistic with emphasis on the integrity of the human body and the close relationship between human and its social and natural environment. TCM focuses on health maintenance and in the treatment of disease emphasizes on enhancing the body's resistance to diseases. For improving health, TCM applies multiple natural therapeutic methods.

Zheng (syndrome) is the basic unit and key term in TCM theory. Zheng is an outcome after analyzing all symptoms and signs. All therapeutic methods in TCM come from the differentiation of Zheng. The methods have been used for thousands of years, which proves that TCM therapeutic approach is effective. From this point of view, Zheng should play an important role in determining the effect. Combined with modern medicine, Zheng should have an impact on disease pathogenesis that directly influences the therapeutic effect.

HISTORICAL BACKGROUND

At the time when TCM formed, there was nothing modernized in medical and biological fields, but there was something developed in Chinese philosophy, astronomy and literature. Also at that time, people got a great amount of experiences on how to deal with the disorders by natural methods, such as puncture, Qigong (mind controlling), taking plants. Some talents in China began to summarize those phenomena and sublimated to theory based on their philosophical and social knowledge at that time. The theory is the original TCM. Thus TCM handles human physiology and pathology following old Chinese philosophical thinking. In the following centuries, accumulation of experiences and addition of relative knowledge (such as clinical observation data and less anatomical experience) made TCM developed. The terminology TCM is partially originated from Chinese philosophy. Other terms in TCM, even same as those in modern medicine, have completely different meanings. It is believed that to understand the physiology of TCM, to some extent, should have some knowledge about Chinese philosophy.

PHYSIOLOGY AND PATHOLOGY IN TCM

During the formation and development of TCM, there are two ideological ideas that fully penetrate into the whole process. The first is the homeostasis idea that focuses on the integrity of human body, and emphasizes the close relationship between human body and its social and natural environment (integrity between human and cosmos). The second is the dynamic balance idea that takes emphasis on the movement in the integrity. Physiologically TCM recognizes human body by system discrimination and cybernetic way. In system discrimination approach, the intrinsic activities of human body can be clarified by analyzing the audio-visual information. The human body, a complicated system, could be identified as different closely related systems that form a network (integrity). The external information should reflect something intrinsic because of the integrity between human body and its social and natural environment. For example, the heart as a center, together with blood, vessel, mind, tongue, small intestine, consists of the heart system in TCM. Any information from any parts in the system can demonstrate the system's activity even the structure of the part is unclear. In cybernetic approach, TCM takes human body as a self-controlled system network. The network is connected by the meridian that exists in whole body. Blood

and vital energy flow also contributes to the connection. The Five elements theory in TCM, named as wood, fire, earth, metal and water, divides human body into five systems. Each system has its own specific features that can be inferred by analyzing those natural materials. The movement and interchange among the five elements are used to explain human body's physiology.

Since TCM has its unique physiology in understanding human body, it has its special understanding on human body's disorders. Pathologically, TCM focuses on the pathogeneicity of social and natural factors. The factors have a close relationship with humans to consist of the integrity. Mostly they are non-direct and non-specific factors if we say bacteria or viruses are direct and specific ones. TCM is not completely to seek the specific pathogen, and pathological changes in a specific organ, while it is to seek the disturbances among the self-controlled systems by analyzing all symptoms and signs. In the heart system, any disturbance in any part of the system is useful to clarify the pathology. At the same time, comparison of the disturbance happened in different period is also important in pathological analyses. TCM takes emphasis on the dynamic changes in any parts and any connections in the self-controlled system.

THERAPEUTIC MECHANISM IN TCM

Physiology in TCM is featured with self-controlled system discrimination and its pathology is featured with dynamic changes in the system (whether direct or indirect, specific or non-specific). The therapeutic mechanism in TCM focuses on enhancing human body's resistance to diseases and prevention by improving the inter-connections among self-controlled systems. To reach the approach, TCM uses different therapeutic methods, such as mind-spiritual methods (such as Qigong, Taiji boxing), natural methods (acupuncture, moxibustion, herbal medicine). These therapeutic methods are characterized by fewer side effects since they are natural. TCM evaluates the therapeutic results by comparing the symptoms before and after the treatment. The treatment is based on the differentiation of symptoms to clarify what is wrong in the self-controlled system. TCM seeks the therapeutic mechanism from the integrity. The integrity includes the human itself as integrity, and the integrity between human and its social and natural environment. The therapeutic mechanism can be achieved by activating systems, improving system connection and enhancing human resistance. The mechanism in TCM is not like modern medicine that seeks the mechanism from cellular or molecular level (such as killing bacteria and virus, antagonistic method). If someone lives well (no symptoms), she is healthy in TCM, whether she has some signs in cellular and molecular level such as high blood pressure.

KEY TERM IN TCM THERAPEUTIC APPROACH: DIFFERENTIATION OF ZHENG

Zheng (syndrome), a basic unit in TCM, decides the therapeutic methods. Zheng is the outcome after a careful analysis of all symptoms and signs (tongue appearance and pulse feeling included). Zheng outcome might change since the symptoms and signs might change. There are many Zhengs in TCM, either simple Zheng or combined ones.

Zheng, as the key term and basic unit in TCM therapeutic theory, develops following the progress in disease theory progress. Tens of years ago, Zheng did not include any signs from modern diagnostic instruments, and nowadays, Zheng is combined with or referred to disease diagnosis during the therapeutic process to some content.

The process of how to get the outcome is called differentiation of Zheng, which is based on the physiology and pathology of TCM.

IMPACT OF ZHENG ON DISEASE TREATMENT

Disease's key units usually contain etiology, pathology and disease location. Modern medicine is trying to get the specificity of the cause, pathology and location, and as a result, the therapeutic approach is targeting on the specificity. New drugs in modern medicine are developed from strictly designed scientific pharmacological tests that are targeting on the specificity. Pharmacological tests show better effect than the effect shown in clinic.

In differentiation of Zheng, clinical effect should be better if the theory of differentiation of Zheng and physiology of TCM are followed. Unfortunately the effect in practice, even completely following the differentiation of Zheng, is not as good as the theoretical one. There should have some reasons to explain the difference between theoretical and clinical effects in TCM practice.

As summarized, there are two questions about the therapeutic problem in medical science. One is why is there difference between the pharmacological and clinical effects in modern medicine? The other is why is there difference between the theoretical and clinical effects in traditional Chinese medicine?

The questions refer to that there are some shortages of therapeutic approach both in modern medicine and in traditional Chinese medicine.

Any disease (morbidity) could contain two parts of appearance. One is the so-called specificity to the realities of morbidity, such as the pathological change. The other is the non-specificity that refers to the reactions caused by interactions between personal physique and environments, such as heterogeneous manifestations. Modern medicine is aimed to explore the specificity of morbidity, while traditional Chinese medicine is mainly aimed to explore the reality of the morbidity by checking the external appearance (that is the differentiation of Zheng). It is believed that the non-specificity sometimes could influence or change the process of morbidity, and only targeting the specificity is not enough to stop the progress of morbidity[4].

Disease mainly refers to the specificity of cause and pathology with less emphasis on the non-specificity. Non-specificity includes all symptoms and signs not directly induced by the specific cause and pathology. Usually the specificity decides the process of diseases. Drugs in modern medicine are targeting the specific cause and pathology, and it usually gives good effect even though the effect is not as good as the pharmacological effect. Since the specific cause and pathology cannot be found in all diseases, the effect of modern drugs depends on whether the cause and pathology are clear or not. In reality, modern drugs are good at curing those diseases with clarified cause and pathology, and not good at curing those diseases due to multiple factors in the pathogenesis, which have become more common in medical science.

However, whenever the non-specificity influences on the specificity, drugs targeting the specificity have no good effect. That is the main reason why modern drugs sometimes are not effective in some cases in the treatment of a disease with a clarified cause and pathology.

Zheng mainly refers to the non-specificity and part of specificity that is only obtained from symptoms and signs by asking, watching and feeling since there are no modern diagnostic instruments. Chinese herbal medicine, based on the Zheng which is taken as an outcome of differentiation of symptoms and signs, targets to the non-specificity and part of the specificity. The effect of herbal medicine is not so good in curing a disease with specific signs, which can be only obtained

by modern diagnostic instruments since Zheng does not refer to those signs. However, the effect of herbal medicine is better in treating some cases when the non-specificity decides the process of a disease. Thus, the reason why there is a difference between the theoretical effect based on Zheng differentiation and the clinical effect is that Zheng differentiation can not exactly differentiate the specificity of a disease.

COMBINING ZHENG WITH DISEASE: NEW STRATEGY IN THERAPEUTIC APPROACH

Following TCM Zheng theory, different diseases may be treated by a same therapeutic approach if they show same Zhengs. One herbal preparation can be used to treat different diseases, a common phenomenon in TCM. Similarly, the same disease may be treated by different therapeutic approaches if the disease shows different Zhengs. It is common in TCM that one kind of disease is treated with different therapies. As mentioned above, Zheng is the outcome of differentiation of symptoms and primary signs obtained by getting from watching (tongue watching) and feeling (pulse feeling), and definitely Zheng is not so accurate. The following example can be used to explain the shortage of Zheng information. Gastritis and stomach cancer could show similar symptoms and primary signs, suggesting that they could be differentiated as the same Zheng in TCM, and could be treated by the same TCM approach. The effect, there is no doubt, should be different since stomach cancer is difficult to be cured by herbal medicine. Thus, the differentiation of Zheng would not give any good effect when the specificity is not clarified resulting from the decisive factor in the evaluation of effects.

It was reported that the effects of two herbal preparations that targeted on coronary heart disease with different Zhengs were at least partially dependent on the Zhengs. The results showed that for coronary heart disease cases with Qi deficiency, Zheng could be alleviated by herbal medicine to reinforce Qi deficiency at effective rate of 89%, while the cases could be alleviated by herbal medicine targeting coronary heart disease and nourishing Yin at effective rate of 60%. For the coronary heart disease cases with Yin deficiency, Zheng could be alleviated by herbal medicine to nourish Yin at the effective rate of 87%, while the cases could be alleviated by herbal medicine to reinforce Qi at effective rate of 65%. Thus, the differentiation of Zheng plays an important role in the therapeutic process and affects the therapeutic result of a specific disease.

Following the disease theory there should have a specific therapy targeting the specific cause, pathology and location. If the specificity is clarified, the disease would be cured. Actually, there might not be so good effect in alleviating some diseases or symptoms even the specificity is clarified. The reason is that the non-specificity influences the specificity. Thus, targeting the specificity of a disease may not result in a good effect or give no effect at all when the non-specificity is decisive in the effect evaluation. The example about drugs in lowing blood pressure would be helpful to explain the reason. In patients with hypertension, there are some good drugs in decreasing blood pressure, and the real thing is that there always have some cases showing any effect after taking drugs. The partial reason is that, in some cases of hypertension, the non-specific appearance could play a key role in influencing the effect of drugs. At this point, new anti-hypertension drugs for the cases in which the non-specificity is a decisive factor need to be developed.

Combining the differentiation of Zheng with diagnosis of disease, which is combining herbal medicine mainly targeting non-specificity with modern drugs targeting the specificity, would achieve the best therapeutic effect.

Many clinical studies have shown that combining modern drugs with herbal medicine would dominantly increase the effect. For example, the effect rate in treating coronary heart disease with modern drugs (routine therapy) was 45.5%, while combing with herbal medicine it was up to 87.3%[5]. The importance is to explore how to combine the two therapies.

More double-blinded clinical trials need to be conducted, both for modern drugs and herbal medicine. All specific and non-specific information needs to be collected for further analysis.

Any new drug, even targeting the exact specific pathology, does not act on all cases of diseases since the effect of non-specificity may affect the process of pathogenesis. Any herbal medicine originating from the exact differentiation of Zheng does not act on all cases with Zheng since lack of enough specificity may lose the decisive factor in the treatment.

After the information about new drug classification is obtained, the best effect could be achieved by either combination of drugs targeting the specificity with herbal medicine targeting the non-specificity, or by complex new drug development focusing both on specificity and non-specificity.

TCM focuses on the integrity of human body and the close relationship with its social and natural environments. It recognizes human physiology by analyzing external information by system discrimination and cybernetic approach, and regards that any disorders are caused by the disturbance in any part of the self-controlled system in the integrity. In therapeutics, TCM targets the non-specificity and part of specificity by natural ways.

Why modern drugs cannot achieve the effect as the pharmacological study and the same effect in a same disease is that Zheng in TCM contributes to the progress of a disease. It is important to clarify that in what situation drugs targeting the disease specificity would be effective and how to make the drug become more effective.

REFERENCES

1 **Eisenberg DM**, Davis RB, Ettner SL, Appel S, Wilkey S, Van Rompay M, Kessler RC. Trends in alternative medicine use in the United States, 1990-1997: results of a follow-up national survey. *JAMA* 1998; **280**: 1569-1575

2 **Bell IR**, Caspi O, Schwartz GE, Grant KL, Gaudet TW, Rychener D, Maizes V, Weil A. Integrative medicine and systemic outcomes research: issues in the emergence of a new model for primary health care. *Arch Intern Med* 2002; **162:** 133-140

3 **Corbin Winslow L,** Shapiro H. Physicians want education about complementary and alternative medicine to enhance communication with their patients. *Arch Intern Med* 2002; **162:** 1176-1181

4 **Tsokos GC,** Nepom GT. Gene therapy in the treatment of autoimmune diseases. *J Clin Invest* 2000; **106:** 181-183

5 **Wang X,** Chen K, Wang W. Clinical study of purified *Xuefu* capsule in the treatnent of angina pectoris. *Zhongguo Zhongxiyi Jiehe Zazhi* 1998; **18:** 399-401

Edited by Wang XL **Proofread by** Chen WW and Xu FM

PO Box 2345, Beijing 100023, China
Fax: +86-10-85381893
E-mail: wjg@wjgnet.com www.wjgnet.com

World J Gastroenterol 2004;10(13):1857-1861
World Journal of Gastroenterology
 ISSN 1007-9327

• REVIEW •

Cytomegalovirus and chronic allograft rejection in liver transplantation

Liang-Hui Gao, Shu-Sen Zheng

Liang-Hui Gao, Shu-Sen Zheng, Department of Hapatobiliary and Pancreatic Surgery, First Affiliated Hospital, Zhejiang University, Hangzhou 310003, Zhejiang Province, China
Supported by the National Natural Science Foundation of China, No. 30170899
Correspondence to: Liang-Hui Gao, PO Box 4193, Hubin Campus, 353 Yan' an Road, Hangzhou 310031, Zhejiang Province, China. gaolh@zju.edu.cn
Telephone: +86-571-87230531 **Fax:** +86-571-87072577
Received: 2004-02-20 **Accepted:** 2004-03-12

Abstract

Cytomegalovirus (CMV) remains one of the most frequent viral infections and the most common cause of death after liver transplantation (LT). Chronic allograft liver rejection remains the major obstacle to long-term allograft survival and CMV infection is one of the suggested risk factors for chronic allograft rejection. The precise relationship between cytomegalovirus and chronic rejection remains uncertain. This review addresses the morbidity of cytomegalovirus infection and the risk factors associated with it, the relationship between cytomegalovirus and chronic allograft liver rejection and the potential mechanisms of it.

Gao LH, Zheng SS. Cytomegalovirus and chronic allograft rejection in liver transplantation. *World J Gastroenterol* 2004; 10(13): 1857-1861

http://www.wjgnet.com/1007-9327/10/1857.asp

INTRODUCTION

Chronic allograft liver transplantation, also termed vanishing bile duct syndrome (VBDS), develops slowly over a period of months or years and is a main cause of late graft loss. In fact, the onset is usually within several months after transplantation. Diagnostic criteria for chronic rejection are (1) the presence of bile duct atrophy/pyknosis, affecting the majority of bile ducts, with or without bile duct loss; (2) convincing foam cell obliterative arteriopathy; or (3) bile duct loss affecting greater than 50% of the portal tracts[1]; (4) total fibrous obliteration of main portal vein and portal foam cell venopathy[2]. Risk factors for chronic liver rejection include transplantation for primary sclerosing cholangitis (PSC)[3], primary biliary cirrhosis (PBC)[4], certain patterns of HLA match between donor and recipient[5-7], positive lymphocyte cross-match[8], cytomegalovirus infection, transplantation between donor and recipient of different ethnic origins[9], sex mismatch[10], and absence of azathioprine from the immunosuppressive regimen[11]. Not all these risk factors have subsequently been confirmed. Cytomegalovirus infection is one of the suggested risk factors for chronic allograft liver rejection. Some results showed there was no direct correlation between them, others demonstrated CMV infection somehow implicated in mechanisms of chronic rejection and played a key role in the pathological changes of atrophy of bile duct and generation of graft arteriosclerosis, characteristic of chronic rejection.

The review addresses several questions. First, CMV infection and risk factors associated with it in liver transplantation. Second, CMV infection and cytokines. Third, relation between CMV infection and chronic liver rejection, potential etiological mechanism of CMV infection in chronic liver transplantation. Is the actual incidence of CMV infection a cause of VBDS?

CMV INFECTION AND RISK FACTORS

Human cytomegalovirus (HCMV) infection occurred in 30-65% of liver transplantation recipients, of which 18-40% were symptomatic infection and mostly developed 1 to 3 mo after transplantation. HCMV infection has two pathways: primary infection and infection activated by latent infection. Many factors are involved in HCMV infection. A prospective study of 218 LT recipients by Paya CV showed that 55% of patients developed CMV infection during the 1st year post-transplantation[12]. Symptomatic CMV infection developed in 25% of all patients, being a major cause of death (21% of all deaths). Of the 62 episodes of documented organ invasion, liver was the major site (38 episodes), followed by lung, gastrointestinal tract and retina. Multivariate statistical analysis of risk factors indicated that the R-/D+ group was the main risk factor for CMV infection and symptomatic infection. Use of antilymphocyte preparations, retransplantation, donor CMV seropositivity, use of antilymphocyte preparations, and retransplantation were risk factors for the development of CMV diseases following liver transplantation[13]. A higher incidence of cytomegalovirus infection was seen in the liver recipients of alcoholic sclerosis[14]. Intraoperative hypothermia during liver transplantation increased the risk of CMV infection in the 1st month postoperation and active warming seemed to reduce this risk[15]. Early application of OKT-3 was the risk factor for development of spreading HCMV diseases; FK506 could reverse rejection effectively, but increased the incidence of HCMV diseases[16]. Others found that immunosuppressant FK506 after liver transplantation augmented inducible NK cell activity and alleviated CMV infection[17]. Among immunosuppressive drugs, only anti- interleukin-2Rab was proved to significantly reduce the incidence of CMV[18]. The role of antirejection therapy may be particularly important, since it could suppress CMV specific cytotoxic T-cell responses and result in prolonged viraemia, which in turn could cause a prolonged alloreactive cytotoxic response. HCMV infection is associated with human herpesviruses (HHV) 6 and 7. Lautenschlager *et al*.[19] analyzed it in consecutive 34 adult liver allograft recipients, CMV disease was diagnosed in 12 patients, in which 10 patients had concurrent HHV-6 infection and 9 had HHV-7 infection. A prolonged prothrombin time, acute fulminant hepatitis diagnosed as the underlying liver disease and hepatic artery thrombosis were found to be significant risk factors for CMV infection[20]. Total number of units of blood transfusion and transfusion of seropositive CMV blood had no effect on primary CMV infection after liver transplantation, though it had an influence on the severity of CMV infection and seropositive CMV recipients. The study about the effect of cytomegalovirus infection status on the first-year mortality among orthotopic liver transplantation recipients showed[21]:

seronegative donors and recipients (11%), seronegative donors and seropositive recipients (22%), seropositive donors and recipients (30%), and seropositive donors and seronegative recipients (44%). Multivariate analysis showed that retransplantation, total number of units of blood products administered during transplantation, CMV infection and bacteremia were associated with higher mortality rates. Thus donor and recipient CMV serologic status is a significant pretransplantation determinant for death in liver transplant recipients.

HCMV INFECTION AND CYTOKINES

The significance of some cytokines highly expressed in grafts and blood serum after liver transplantation with HCMV infection remains unknown. Vascular adhesion molecules and their ligands are important both in leukocyte-endothelial cell interactions and in T-cell activation of rejection cascade. A significant induction of intercellular adhesion molecule-1 and vascular cell adhesion molecule-1 was seen in vascular and sinusoidal endothelium associated with both CMV and rejection, and induction of endothelial leukocyte adhesion molecule-1 in vascular endothelium was seen in rejection only. In both cases, the number of leukocytes expressing leukocyte function antigen-1 was significantly increased, but very late antigen-4-positive cells were more characteristic for CMV[22]. IL2-receptor (IL2R) positivity was practically seen in rejection only, but both IL2R and CD8 were increased in cytomegalovirus hepatitis. Simultaneously increased IL2R and CD8 may mean the development of cytomegalovirus hepatitis on the basis of acute rejection. Vascular adhesion protein-1 (VAP-1), an adhesion molecule involved in lymphocyte adhesion, was up-regulated in acute liver rejection of sinusoids, hepatocytes in bile duct and this up-regulation was prolonged by RCMV infection[23]. Thus the severity of acute rejection was intensified. Tumor necrosis factor-alpha (TNF-a) plays a key role in regulating reactivation of CMV infection. TNF-a could activate CMV-IE enhancer and result in high CMV-IE antigen expression in peripheral blood mononuclear cells particularly in monocytes. Increased tumor necrosis factor-a (TNF-a) could lead to occurrence of cachexy after CMV infection and mediate development of vanishing bile duct syndrome. Inhibition of TNF-a release or action might be an alternative strategy for preventing CMV-associated morbidity in allograft recipients[24].

CMV-IE protein could activate transforming growth factor-β1 (TGF-β1) promotor during CMV infection and result in early high expression of TGF-β1 mRNA[25]. In chronic human allograft rejection, increased infiltrated macrophages and up-regulated platelet-derived growth factor (PDGF), fibroblast growth factor (FGF) could lead to transformation of lipocytes to myofibroblast-like cells, which would lead to increase secretion of extracellular matrix and were engaged in hepatic fibrosis[26]. TGF-β1 increased levels of FGF and FGF receptor mRNAs in myofibroblast cells and expression levels of PDGF mRNA[27]. Thereafter CMV infection may implicate in chronic rejection by secretion of chronic fibroblast factors. Whether by regulating some of the cytokines which were thought to be involved in chronic rejection, skewing of immunity towards Th2 cytokines (TGF-β, IL-4, IL-10) and humoral response, expression of adhesive molecules and antigens can be induced in graft, to mediate occurrence of chronic rejection, needs further research.

HCMV INFECTION AND CHRONIC REJECTION IN TRANSPLANT LIVER

Many studies have demonstrated a close relationship between HCMV infection and chronic liver rejection. Analysis of ten liver transplants whose graft was lost due to histologically confirmed chronic rejection showed[28] that there was at least one episode or many times of rejection early after transplantation. All patients had a history of CMV infection usually following acute rejection. Persistent CMV-DNA was found in all of those grafts examined by DNA-hybridization *in situ*, CMV-DNA was strongly expressed in the remaining bile ducts and moderately expressed in endothelial cells of the vascular structures. Persistent CMV genome was found in those structures that were the major targets of chronic rejection process in the liver. These findings support the suggestion that CMV infection is one of the risk factors for chronic allograft rejection. Arnold *et al*.[29] found that CMV- DNA was identified in hepatocytes in 10 of 12 patients with VBDS, of whom 1 had no serological evidence of CMV infection, 9 developed cytomegalovirus infection at 1 wk until death or retransplantation. Cytomegalovirus DNA was identified in hepatocytes and never identified in either biliary or endothelial tissue. CMV-DNA was identified in all 18 patients with HCMV infection but no bile duct was injured. However in those with uncomplicated cytomegalovirus, infection occurred earlier but was eliminated more quickly, and the number of infected hepatocytes was greater when compared with those with vanishing bile duct syndrome. The data indicated that vanishing bile duct syndrome was associated with persistent cytomegalovirus replication within hepatocytes. Further study showed[30] that interferon-alpha (IFN-α) was identified more frequently and patients developed VBDS after a longer period in the bile duct cytoplasm compared with those with acute HCMV infection without evidence of VBDS. These indicate that persistent CMV infection of bile duct cells resulting in increased IFN-α is likely a co-factor linked to progression to VBDS. Martelius *et al*.[31] performed liver transplantations in a rat strain combination with PVG (RT1c) → BN (RT1n). One group of animals was infected with RCMV intraperitoneally. They found in liver allografts undergoing acute rejection, CMV significantly increased portal inflammation and caused more severe bile duct damage linked to the induction of VCAM-1 in endothelial cells. The ongoing infection was found to vary over time in different structures of liver grafts. These results support an association between CMV infection and the immunological mechanisms of rejection, as well as the role of CMV in the development of bile duct damage in liver allografts. In the same rat strain combination, Martelius *et al*.[32] examined CMV infection of the graft at various time points and found that rat cytomegalovirus (RCMV) caused an active infection in the graft from 5 d to 2 wk after transplantation. Thereafter the cultures were negative. RCMV antigens and DNA were found in hepatocytes, endothelial, inflammatory, and bile duct cells during the active infection. At 4 wk, RCMV DNA positive cells decreased. IE-1 mRNA expression was, however, only detected during the active infection, but not at 4 wk postinfection. They concluded the CMV-induced graft damage did not require the continued expression of IE-1. Halme *et al*.[33] demonstrated that CMV infection was a risk factor for development of biliary complication after liver transplantation.

A variety of risk factors for VBDS have been postulated, but they are controversial. O' Grady *et al*.[34] confirmed A 1-2 antigen matched for HLA DR antigens, a zero matched for HLA A/B antigens, and active CMV infection were independently associated with an increased risk of VBDS. Hoffmann *et al*.[35] examined 120 liver transplants retrospectively and analyzed the risk factors for VBDS. Ten patients (8.3%) developed VBDS. Seventeen patients had hepatitis C virus infections after liver transplantation. In this group, the incidence of VBDS was the highest (4 of 17, or 23.5%) and reached statistical significance. They found hepatitis C infection predisposed one to the development of VBDS after OLT.

The potential mechanisms of CMV cause VBDS. (1) Virus itself directly destroys or liquefies the infected structure. (2) Cytotoxic T lymphocyte plays a role in inducing VBDS. CMV infection may trigger an immune response by inducing MHC antigens and adhesion molecules on the bile ductal cell surface and make the ductal cells a target for immunological attack. For example, a cross-reaction between the viral protein and MHC molecules is possible because CMV has been shown to code a protein homologous to MHC class I antigen[36], and a CMV IE_2 protein has been found to share an epitope with the HLA-DRβ chain[37]. CMV is known to increase expression of class II human leukocyte antigens on bile duct epithelial cells. After immune recognition of these foreign antigens by host antigen-presenting cells, CD_4^+T would release cytokines and stimulate differentiation and proliferation of cytotoxic T cells (CD_8^+T). The activated CD_8^+T then plays a immune killing role. CMV has been shown to induce proinflammatory cytokines, such as IFN-γ and TNF-α, which could lead to other immunological events. (3) Dystrophy and ischemic sequelae caused by obliterative arteriopathy. Although CMV-DNA can not be detected on some bile duct epithelial cells in VBDS, CMV might play a pathogenetic role in the development of VBDS[38]. The sequelae of clearing infection, host immune response would selectively kill these bile duct epithelial cells with CMV infection. CMV infection of hepatocytes would in some way up-regulate the expression of HLA antigens on biliary epithelial cells. CMV viral antigens are present and bound to HLAs on the surface of bile duct cells. So even though CMV was cleared *in vivo*, they could exhibit their episode role.

Few studies about the relation of CMV infection and angiopathy are available. Grefte *et al*.[39] demonstrated that in patients with active CMV infection, distinctive large cells were present in peripheral blood. Moreover, these cells were shown to express CMV antigens and to have endothelial origin with immunologic staining, indicating an association between CMV infection and widespread occult vascular damage. CMV-induced endothelial damage may be a potent antigenic stimulus, leading to the production of anti-endothelial cells autoantibodies. Anti-endothelial cell autoantibodies may represent not only a marker of cell injury but also contribute to the progression of inflammatory response leading to the exposure of tissue-privileged self-antigens and induction of other autoantibodies such as SMA. These would further aggravate pathological damages. Analysis of autoantibody was carried out in sequential sera from 40 liver transplantation patients by Varani *et al*.[40]. Ten out of 23 antigenemia-positive and none of antigenemia-negative patients developed serum autoantibodies. Anti-endothelial cell autoantibodies were found in 9 cases and SMA in 4 patients. Antinuclear antibodies were detected in 1 autoantibody-negative patient. All but 1 case of autoantibody positivity were observed in the high antigenemia group and detected in blood during the antigenemia phase and in most cases in coincidence with or after the antigenemia peak.

In the arteries of an allografted organ, endothelial injury may arise from immune injury, ischemia/reperfusion injury, and injuries due to dyslipidemia, hypertension, or infectious agents. The injured endothelial cells can elaborate small molecules and cytokines that can activate macrophages and smooth muscle cells to express functions that may contribute to arterial lesion formation. The precise immunological mechanisms underlying chronic vascular rejection are unknown. Three potential effector mechanisms have been implicated in allograft rejection[41]: alloreactive $CD4^+$ cytokine-producing "helper" T (TH) lymphocytes, alloreactive $CD8^+$ cytolytic T lymphocytes (CTL), and alloreactive antibodies (produced by B lymphocytes). Chronic delayed-type hypersensitivity mediated by host $CD4^+$ T cells activated by graft alloantigens presented directly by graft endothelial and dendritic cells or indirectly by host dendritic cells, is likely a candidate. All of which contribute to atherosclerotic vascular disease, and chronic vascular rejection.

CMV infection might directly increase MHC antigens on the surface of graft cells through the induction of release of mediators such as interferon and may activate cytotoxic T cells, which can trigger acute rejection in association with concurrent alloantigen stimulation. Acute rejection results in a generalized inflammatory response. Kas-Deelen and colleagues have postulated that the occurrence of acute rejection at the allograft site could sensitize the endothelial surface of the host to CMV-induced damage[42]. These endothelial cells then became a target for alloreactive T cells. According to these *in vitro* studies, even a few CMV-infected endothelial cells in a transplanted organ might trigger autoreactivity[43]. CMV infection enhances several steps, with ensuing chronic rejection. Endothelial adhesion molecule expression, in particular, could provoke influx of inflammatory cells and smooth muscle cell proliferation. In addition, CMV infection could induce vascular wall changes resembling fatty streaks reported in the early stages of classic atherosclerosis[44].

There is still a controversy concerning the relationship between CMV infection and chronic allograft rejection. Paya *et al*.[45] studied 81 liver transplant recipients and found that cytomegalovirus infection developed in 46 recipients (57%), and VBDS occurred in 9 recipients (11%). CMV infection developed in only 5 of the 9 patients with VBDS. Univariate analysis of pretransplantation recipient/donor CMV serological tests and human leukocyte antigen typing showed they were not significant risk factors for the development of VBDS. The data indicated no association was found between CMV infection alone or in relation to class I or II human leukocyte antigen match and the subsequent development of VBDS. van den Berg *et al*.[46] in a retrospective study confirmed there was no association among CMV infection, HLA-DR and VBDS. Wright TL in an editorial postulated that CMV was indeed an innocent bystander rather than a culprit. In the pathogenesis of VBDS, it is the immune responsiveness of the patient that is important. It is quite possible that patients with VBDS have an inherent defect in immune response that allows persistence of CMV infection, and CMV is unrelated to destruction of bile ducts. On the other hand, if CMV infection is really an etiological factor for VBDS, antiviral therapy would be effective in decreasing incidence of the chronic rejection. Unfortunately, many studies about antiviral therapy for CMV failed to show an association between the development of CMV disease and the occurrence of rejection[47].

CONCLUSION

Many studies have demonstrated a close association between CMV infection and chronic allograft liver transplantation, but it did not prove an etiological role for the virus in this syndrome. CMV infection may be one of the risk factors for development of VBDS. A better understanding of the etiologic role of CMV in VBDS, is important for designing effective therapeutic strategies to ameliorate this process.

ACKNOWLEDGMENTS

We thank Dr. Ran Tao, Department of Starzl Transplantation Center, University of Pittsburgh, for critically reading this paper and discussion.

REFERENCES

1 **Demetris A,** Adams D, Bellamy C, Blakolmer K, Clouston A, Dhillon AP, Fung J, Gouw A, Gustafsson B, Haga H, Harrison D, Hart J, Hubscher S, Jaffe R, Khettry U, Lassman C, Lewin

K, Martinez O, Nakazawa Y, Neil D, Pappo O, Parizhskaya M, Randhawa P, Rasoul-Rockenschaub S, Reinholt F, Reynes M, Robert M, Tsamandas A, Wanless I, Wiesner R, Wernerson A, Wrba F, Wyatt J, Yamabe H. Update of the international banff schema for liver allograft rejection: working recommendations for the histopathologic staging and reporting of chronic rejection. *Hepatology* 2000; **31**: 792-799

2 **Jain D**, Robert ME, Navarro V, Friedman AL, Crawford JM. Total fibrous obliteration of main portal vein and portal foam cell venopathy in chronic hepatic allograft rejection. *Arch Pathol Lab Med* 2004; **128**: 64-67

3 **Wiesner RH**, Ludwig J, van Hoek B, Krom RA. Current concepts in cell-mediated hepatic allograft rejection leading to ductopenia and liver failure. *Hepatology* 1991; **14**(4 Pt 1): 721-729

4 **Demetris AJ**, Markus BH, Esquivel C, Van Thiel DH, Saidman S, Gordon R, Makowka L, Sysyn GD, Starzl TE. Pathologic analysis of liver transplantation for primary biliary cirrhosis. *Hepatology* 1988; **8**: 939-947

5 **Gubernatis G**, Kemnitz J, Tusch G, Pichlmayr R. HLA compatibility and different features of liver allograft rejection. *Transpl Int* 1988; **1**: 155-160

6 **Manez R**, White LT, Linden P, Kusne S, Martin M, Kramer D, Demetris AJ, Van Thiel DH, Starzl TE, Duquesnoy RJ. The influence of HLA matching on cytomegalovirus hepatitis and chronic rejection after liver transplantation. *Transplantation* 1993; **55**: 1067-1071

7 **Bismuth A**, Ducot B, Samuel D, Arulnaden JL, Gugenheim J, Debat P, Azoulay D, Farrokhi P, Pillier-Loriette C, Bourdon G. Liver transplantation and the major histocompatibility complex. *Rev Fr Transfus Hemobiol* 1991; **34**: 449-457

8 **Batts KP**, Moore SB, Perkins JD, Wiesner RH, Grambsch PM, Krom RA. Influence of positive lymphocyte crossmatch and HLA mismatching on vanishing bile duct syndrome in human liver allografts. *Transplantation* 1988; **45**: 376-379

9 **Devlin JJ**, O'Grady JG, Tan KC, Calne RY, Williams R. Ethnic variations in patient and graft survival after liver transplantation. Identification of a new risk factor for chronic allograft rejection. *Transplantation* 1993; **56**: 1381-1384

10 **Candinas D,** Gunson BK, Nightingale P, Hubscher S, McMaster P, Neuberger JM. Sex mismatch as a risk factor for chronic rejection of liver allografts. *Lancet* 1995; **346**: 1117-1121

11 **Van Hoek B**, Wiesner RH, Ludwig J, Gores GJ, Moore B, Krom RA. Combination immunosuppression with azathioprine reduces the incidence of ductopenic rejection and vanishing bile duct syndrome after liver transplantation. *Transplant Proc* 1991; **23** (1 Pt 2): 1403-1405

12 **Paya CV**, Marin E, Keating M, Dickson R, Porayko M, Wiesner R. Solid organ transplantation: results and implications of acyclovir use in liver transplants. *J Med Virol* 1993; **1**(Suppl): 123-127

13 **Wiesner RH**, Marin E, Porayko MK, Steers JL, Krom RA, Paya CV. Advances in the diagnosis, treatment, and prevention of cytomegalovirus infections after liver transplantation. *Gastroenterol Clin North Am* 1993; **22**: 351-366

14 **Stefanini GF**, Biselli M, Grazi GL, Iovine E, Moscatello MR, Marsigli L, Foschi FG, Caputo F, Mazziotti A, Bernardi M, Gasbarrini G, Cavallari A. Orthotopic liver transplantation for alcoholic liver disease: rates of survival, complications and relapse. *Hepatogastroenterology* 1997; **44**: 1356-1359

15 **Paterson DL**, Staplefeldt WH, Wagener MM, Gayowski T, Marino IR, Singh N. Intraoperative hypothermia is an independent risk factor for early cytomegalovirus infection in liver transplant recipients. *Transplantation* 1999; **67**: 1151-1155

16 **Woodle ES**, Perdrizet GA, So S, Jendrisak MD, White HM, Marsh JW. FK 506 rescue therapy: the rapidity of rejection reversal is related to the subsequent development of CMV disease. *Transplant Proc* 1993; **25**: 1992-1993

17 **Kageyama S**, Matsui S, Hasegawa T, Yoshida Y, Sato H, Yamamura J, Kurokawa M, Yamamoto H, Shiraki K. Augmentation of natural killer cell activity induced by cytomegalovirus infection in mice treated with FK506. *Acta Virol* 1997; **41**: 215-220

18 **Oldakowska-Jedynak U**, Niewczas M, Ziolkowski J, Mucha K, Foroncewicz B, Bartlomiejczyk I, Senatorski G, Wyzgal J, Krawczyk M, Zieniewicz K, Nyckowski P, Paczek L. Cytomegalovirus infection as a common complication following liver transplantation. *Transplant Proc* 2003; **35**: 2295-2297

19 **Lautenschlager I**, Lappalainen M, Linnavuori K, Suni J, Hockerstedt K. CMV infection is usually associated with concurrent HHV-6 and HHV-7 antigenemia in liver transplant patients. *J Clin Virol* 2002; **25**(Suppl 2): S57-S61

20 **Paya CV**, Wiesner RH, Hermans PE, Larson-Keller JJ, Ilstrup DM, Krom RA, Rettke S, Smith TF. Risk factors for cytomegalovirus and severe bacterial infections following liver transplantation: a prospective multivariate time-dependent analysis. *J Hepatol* 1993; **18**: 185-195

21 **Falagas ME**, Snydman DR, Griffith J, Ruthazer R, Werner BG. Effect of cytomegalovirus infection status on first-year mortality rates among orthotopic liver transplant recipients. The Boston Center for Liver Transplantation CMVIG Study Group. *Ann Intern Med* 1997; **126**: 275-279

22 **Lautenschlager I**, Hockerstedt K, Taskinen E, von Willebrand E. Expression of adhesion molecules and their ligands in liver allografts during cytomegalovirus (CMV) infection and acute rejection. *Transpl Int* 1996; **9**(Suppl 1): S213-215

23 **Martelius T**, Salmi M, Wu H, Bruggeman C, Hockerstedt K, Jalkanen S, Lautenschlager I. Induction of vascular adhesion protein-1 during liver allograft rejection and concomitant cytomegalovirus infection in rats. *Am J Pathol* 2000; **157**: 1229-1237

24 **Fietze E**, Prosch S, Reinke P, Stein J, Docke WD, Staffa G, Loning S, Devaux S, Emmrich F, von Baehr R. Cytomegalovirus infection in transplant recipients. The role of tumor necrosis factor. *Transplantation* 1994; **58**: 675-680

25 **Michelson S**, Alcami J, Kim SJ, Danielpour D, Bachelerie F, Picard L, Bessia C, Paya C, Virelizier JL. Human cytomegalovirus infection induces transcription and secretion of transforming growth factor beta 1. *J Virol* 1994; **68**: 5730-5737

26 **Hoshino K**, Demirci G, Schlitt HJ, Wonigeit K, Pichlmayr R, Nashan B. Evidence for transformation of lipocytes to myofibroblast-like cells as source of transplant fibrosis in chronic human allograft rejection. *Transplant Proc* 1995; **27**: 1144-1145

27 **Rosenbaum J**, Blazejewski S, Preaux AM, Mallat A, Dhumeaux D, Mavier P. Fibroblast growth factor 2 and transforming growth factor beta 1 interactions in human liver myofibroblasts. *Gastroenterology* 1995; **109**: 1986-1996

28 **Lautenschlager I**, Hockerstedt K, Jalanko H, Loginov R, Salmela K, Taskinen E, Ahonen J. Persistent cytomegalovirus in liver allografts with chronic rejection. *Hepatology* 1997; **25**: 190-194

29 **Arnold JC**, Portmann BC, O'Grady JG, Naoumov NV, Alexander GJ, Williams R. Cytomegalovirus infection persists in the liver graft in the vanishing bile duct syndrome. *Hepatology* 1992; **16**: 285-292

30 **Arnold JC**, Nouri-Aria KT, O'Grady JG, Portmann BC, Alexander GJ, Williams R. Hepatic alpha-interferon expression in cytomegalovirus-infected liver allograft recipients with and without vanishing bile duct syndrome. *Clin Investig* 1993; **71**: 191-196

31 **Martelius T**, Krogerus L, Hockerstedt K, Bruggeman C, Lautenschlager I. Cytomegalovirus infection is associated with increased inflammation and severe bile duct damage in rat liver allografts. *Hepatology* 1998; **27**: 996-1002

32 **Martelius TJ**, Blok MJ, Inkinen KA, Loginov RJ, Hockerstedt KA, Bruggeman CA, Lautenschlager IT. Cytomegalovirus infection, viral DNA, and immediate early-1 gene expression in rejecting rat liver allografts. *Transplantation* 2001; **71**: 1257-1261

33 **Halme L**, Hockerstedt K, Lautenschlager I. Cytomegalovirus infection and development of biliary complications after liver transplantation. *Transplantation* 2003; **75**: 1853-1858

34 **O'Grady JG**, Alexander GJ, Sutherland S, Donaldson PT, Harvey F, Portmann B, Calne RY, Williams R. Cytomegalovirus infection and donor/recipient HLA antigens: interdependent co-factors in pathogenesis of vanishing bile-duct syndrome after liver transplantation. *Lancet* 1988; **2**: 302-305

35 **Hoffmann RM**, Gunther C, Diepolder HM, Zachoval R, Eissner HJ, Forst H, Anthuber M, Paumgartner G, Pape GR. Hepatitis C virus infection as a possible risk factor for ductopenic rejection (vanishing bile duct syndrome) after liver transplantation. *Transpl Int* 1995; **8**: 353-359

36 **Beck S**, Barrell BG. Human cytomegalovirus encodes a glycoprotein homologous to MHC class I antigens. *Nature* 1988; **331**:

269-272
37 **Fujinami RS**, Nelson JA, Walker L, Oldstone MB. Sequene homology and immunologic-cross-reactivity of human cytomegalovirus with HLA-DR beta chain: a means for graft rejection and immunosuppression. *J Virol* 1988; **62**: 100-105
38 **Wright TL**. Cytomegalovirus infection and vanishing bile duct syndrome: culprit or innocent bystander? *Hepatology* 1992; **16**: 494-496
39 **Grefte A**, van der Giessen M, van Son W, The TH. Circulating cytomegalovirus (CMV)-infected endothelial cells in patients with an active CMV infection. *J Infect Dis* 1993; **167**: 270-277
40 **Varani S**, Muratori L, De Ruvo N, Vivarelli M, Lazzarotto T, Gabrielli L, Bianchi FB, Bellusci R, Landini MP. Autoantibody appearance in cytomegalovirus-infected liver transplant recipients: correlation with antigenemia. *J Med Virol* 2002; **66**: 56-62
41 **Libby P**, Pober JS. Chronic rejection. *Immunity* 2001; **14**: 387–397
42 **Kas-Deelen AM**, Harmsen MC, de Maar EF, Oost-Kort WW, Tervert JW, van der Meer J, van Son WJ, The TH. Acute rejection before cytomegalovirus infection enhances von Willebrand factor and soluble VCAM-1 in blood. *Kidney Int* 2000; **58**: 2533–2542
43 **Waldman WJ**, Adams PW, Knight DA, Sedmak DD. CMV as an exacerbating agent in transplant vascular sclerosis: potential immune-mediated mechanisms modelled *in vitro*. *Transplant Proc* 1997; **29**: 1545–1546
44 **Span AH**, Grauls G, Bosman F, Van Boven CP, Bruggeman CA. Cytomegalovirus infection induces vascular injury in the rat. *Arteriosclerosis* 1992; **93**: 41–52
45 **Paya CV**, Wiesner RH, Hermans PE, Larson-Keller JJ, Ilstrup DM, Krom RA, Moore SB, Ludwig J, Smith TF. Lack of association between cytomegalovirus infection, HLA matching and the vanishing bile duct syndrome after liver transplantation. *Hepatology* 1992; **16**: 66-70
46 **van den Berg AP**, Klompmaker IJ, Hepkema BG, Gouw AS, Haagsma EB, Lems SP, The TH, Slooff MJ. Cytomegalovirus infection does not increase the risk of vanishing bile duct syndrome after liver transplantation. *Transpl Int* 1996; **9**(Suppl 1): S171-173
47 **Shibolet O**, Ilan Y, Kalish Y, Safadi R, Ashur Y, Eid A, Shouval D, Wolf D. Late cytomegalovirus disease following liver transplantation. *Transpl Int* 2003; **16**: 861-865

Edited by Wang XL **Proofread by** Chen WW and Xu FM

PO Box 2345, Beijing 100023, China
Fax: +86-10-85381893
E-mail: wjg@wjgnet.com www.wjgnet.com

World J Gastroenterol 2004;10(13):1862-1866
World Journal of Gastroenterology
 ISSN 1007-9327

• GASTRIC CANCER •

Expression of COX-2, iNOS, p53 and Ki-67 in gastric mucosa-associated lymphoid tissue lymphoma

Hong-Ling Li, Bing-Zhong Sun, Fu-Cheng Ma

Hong-Ling Li, Bing-Zhong Sun, Department of Hematology, Xijing Hospital, Fourth Military Medical University, Xi' an 710032, Shaanxi Province, China
Fu-Cheng Ma, Department of Pathology, Xijing Hospital, Fourth Military Medical University, Xi' an 710032, Shaanxi Province, China
Correspondence to: Dr. Hong-Ling Li, Department of Hematology, Xijing Hospital, Fourth Military Medical University, 127 Changle West Road, Xi' an 710032, Shaanxi Province, China. lhl882002@hotmail.com
Telephone: +86-29-3375579
Received: 2003-11-12 **Accepted:** 2004-01-15

Abstract

AIM: To assess the expression of cyclooxygenase-2 (COX-2), nitric oxide synthase (iNOS), p53 and Ki-67 in gastric mucosa-associated lymphoid tissue (MALT) lymphoma and clarify the relationship between COX-2 expression and iNOS or p53 expression in these patients.

METHODS: The expressions of COX-2, iNOS, p53 and Ki-67 were detected in 32 gastric MALT lymphoma specimens and 10 adjacent mucosal specimens by immunohistochemical Envision method.

RESULTS: COX-2 and iNOS expressions were significantly higher in gastric MALT lymphoma tissues than those in adjacent normal tissues. The expression of COX-2 was observed in 22 of 32 cases of MALT lymphoma tissues (68.8%). A positive cytoplasmic immunoreactivity for iNOS was detected in 17 of 31 cases (53.1%). COX-2 expression in gastric MALT lymphoma tissues was positively correlated with iNOS expression (r=0.448, P=0.010) and cell proliferative activity analyzed by Ki-67 labeling index (r=0.410, P=0.020). The expression of COX-2 protein did not correlate with age, sex, stage of disease, lymph node metastasis or differentiation. The accumulation of p53 nuclear phosphoprotein was detected in 19(59.4%) of tumors. p53 protein was expressed in 11 of 23 assessed LG tumors and in 8 of 9 assessed HG tumors. The difference of p53 positivity was found statistically significant between LG and HG cases (P=0.0302). The p53 accumulation correlated with advanced clinical stage (stage III+IV *vs* stage I+II, P=0.017). There was a significant positive correlation between COX-2 expression and p53 accumulation status (r=0.403, P=0.022). The mean PI of Ki-67 in each grade group were 36.0±7.73% in HG and 27.4±9.21% in LG. High-proliferation rate correlated with HG tumors (r=0.419, P=0.017). The correlation coefficient showed a significant positive correlation between PI and COX-2 expression in MALT lymphoma patients (r=0.410, P=0.020).

CONCLUSION: COX-2 expresses in the majority of gastric MALT lymphoma tissues and correlates with cellular proliferation and iNOS expression. COX-2 overexpression is closely associated with p53 accumulation status. iNOS and COX-2 may play a synergistic role in the pathogenesis of gastric MALT lymphoma.

Li HL, Sun BZ, Ma FC. Expression of COX-2, iNOS, p53 and Ki-67 in gastric mucosa-associated lymphoid tissue lymphoma. *World J Gastroenterol* 2004; 10(13): 1862-1866
http://www.wjgnet.com/1007-9327/10/1862.asp

INTRODUCTION

Lymphomas of mucosa-associated lymphoid tissue (MALT) are a distinct subgroup of extranodal B-cell non-Hodgkin's lymphomas. Gastric MALT lymphomas are the majority of the cases and account for 1-10% of all gastric malignant neoplasms[1]. Epidemiological and clinical studies demonstrated a link between gastric MALT lymphoma and chronic infection with *Helicobacter pylori* (*H pylori*)[2,3]. Cyclooxygenase-2 (COX-2) and nitric oxide synthase (iNOS) are important enzymes that mediate inflammatory processes. In recent years, it has been demonstrated that both COX-2 and iNOS play important roles in various tumors, including gastric MALT lymphoma[4,5]. COX-2, a key isoenzyme in conversion of arachidonic acid to prostaglandins, is inducible by various agents such as growth factors and tumor promoters, and is frequently overexpressed in various tumors[6,7]. iNOS are isoenzymes that catalyze the synthesis of nitric oxide (NO). Overexpression of iNOS has been demonstrated in various human neoplasms, such as breast cancer[8], colorectal cancer[9], and gastric cancer[10]. The p53 tumor suppressor protein is a critical mediator of apoptosis and tumorigenesis. Although studies have suggested interactions between COX-2 and iNOS or p53 in different tumors, the relationship between COX-2 expression and a variety of other molecular markers of tumor progression has not been reported for gastric MALT lymphomas. In the present study, we conducted to determine the expressions of COX-2, iNOS and p53 expression as well as cell proliferative index (Ki-67) in 32 gastric MALT lymphomas by using immunohistochemistry.

MATERIALS AND METHODS

Specimens

Thirty-two gastric MALT lymphoma specimens and 10 adjacent specimens were obtained from surgical resection. The patients underwent surgery at Xijing Hospital of the Fourth Military Medical University (Xi' an, China) between January 1996 and September 2002. The tumor specimens were retrieved from the archives of the Department of Pathology, Xijing Hospital. The mean age of the gastric MALT lymphoma group was 52.8 years (range 29-70 years), and there were 22 males and 10 females. All cases were of B-cell origin as immunohistochemistry showed CD20 expression in all MALT cases. The cases were categorized in two basic groups, according to (REAL) Classification[11] and the WHO Classification[12] for MALT lymphomas: low-grade lymphoma of MALT (composed of centrocyte-like cells, lymphoid follicles and plasma cell differentiation) and high-grade lymphoma of MALT (diffuse large B cell lymphoma (DLBCL) with or without low grade MALT +lymphoma component). Of the 32 patients, 23 were low grade MALT lymphoma (LG) and 9 high grade MALT lymphoma (HG). Patients were staged according to the Ann Arbor system. All specimens

were fixed in 40 g/L buffered formaldehyde, and embedded in paraffin wax.

Immunohistochemical assay for expression of COX-2, iNOS, p53 and Ki-67

The expression of COX-2, iNOS, p53 and Ki-67 was studied by immunohistochemical Envision method according to the manufacturer's instructions. H-62 (COX-2) is a rabbit polyclonal antibody raised against a recombinant protein corresponding to amino acids 50-111 mapping near the amino terminus of COX-2 of human origin (sc-7951, Santa Cruz Biotechnology, dilution 1:50). M-19 (iNOS) was provided as a rabbit affinity-purified polyclonal antibody raised against a peptide mapping at the carboxyl terminus of iNOS of mouse origin (sc-650, Santa Cruz Biotechnology, dilution 1:50). The Ki-67 antibody recognizes the Ki-67 antigen of paraffin-embedded tissues. To detect the p53 protein, a mouse monoclonal antibody (sc-126, Santa Cruz Biotechnology, dilution 1:50) was used which recognizes an epitope in the N-terminus of the human p53 protein. Staining for Ki-67 was performed by using an anti-Ki-67 monoclonal mouse antibody (ZM-0166, Zhongshan Biotechnology, dilution 1:50). Briefly, 5-μm sections cut from formalin-fixed, paraffin-embedded specimens were deparaffinized in xylene and rehydrated in graded alcohol. For antigen retrieval, the deparaffinized slides were microwaved in 0.01 mol/L sodium citrate buffer (pH 6.0) for 10 min. Endogenous peroxidase activity was then blocked by incubating the sections with 30 mL/L H_2O_2 in 0.05 mol/L phosphate buffer (pH 7.4), containing 0.45 mol/L NaCl for 15 min. Non-specific antibody binding was blocked by pretreatment with PBS containing 5 g/L bovine serum albumin. The sections were then incubated with the primary antibodies diluted as described above. After incubation, these sections were washed with 0.02 mol/L sodium phosphate buffer. The slides were then incubated with a secondary antibody for 30 min. Diaminobenzidine was used as chromogen and the sections were counterstained with hematoxylin. Negative controls were established by replacing the primary antibody with PBS.

Assessment of immunohistochemical results

The slides were evaluated independently by two observers who were unknown to the histological status. At the cellular level, COX-2 and iNOS staining was cytoplasmic in most cases, however, p53 and Ki-67 staining was nuclear. COX-2 is cytoplasmic enzyme detectable in tumor cells, epithelial cells, endothelial cells, smooth muscle cells and inflammatory cells. For final analysis, the expression of COX-2 was scored in the tumor cells. Staining for COX-2 and iNOS was considered positive only when more than 10% of the tumor cells in the entire tumor area were judged to be positive. The level of p53 was calculated by expressing the number of p53-positive cancer cells as a percentage of the total number of cancer cells in a high-power field. For analysis, tumors were classified as p53-negative (less than 10% positive nuclei) or p53-positive (more than 10% positive nuclei). The Ki-67 labeling index (proliferation index, PI) was determined by counting the percentage of positive cells among 1 000 tumor cells in 10 random regions in 400-fold fields.

Statistical analysis

Statistical comparisons for significance were made with the Student's *t* test and Chi-square test. Spearman correlation test was used for the correlation between positive rates. A P value <0.05 was considered statistically significant.

RESULTS

Expression of COX-2 and iNOS in gastric MALT lymphoma

The expression of COX-2 was observed in 22 of 32 cases of MALT lymphoma tissues (68.8%). Immunohistochemically, COX-2 was stained diffusely in cytoplasm of the tumor cells (Figure 1A). In contrast, no or very faint signal was found in neighboring normal tissues. A positive cytoplasmic immunoreactivity for iNOS was detected in 17 of 31 cases (53.1%, Figure 1B). However, no staining could be observed in neighboring normal tissues.

There was a significant correlation between COX-2 and iNOS expression (r = 0.448, P=0.010). The positive expression

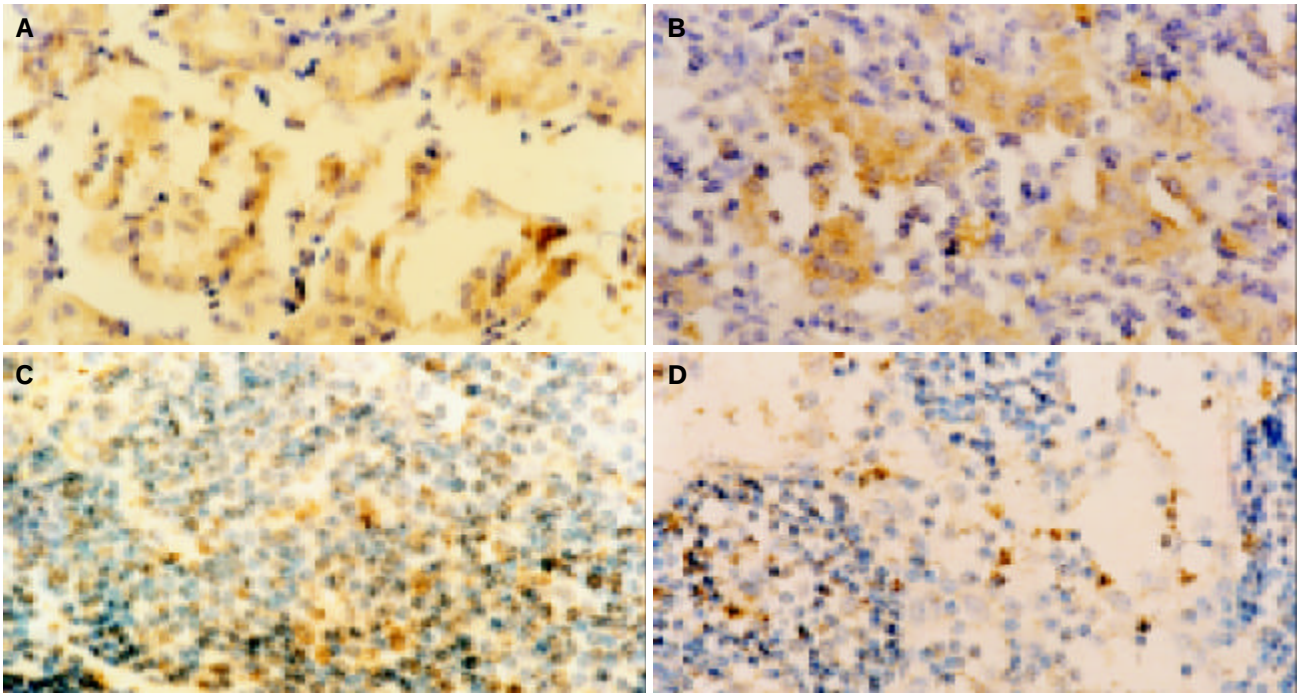

Figure 1 Results of immunohistochemical staining (Original magnification: ×400). A: Expression of COX-2 in gastric MALT lymphoma; B: Expression of iNOS in gastric MALT lymphoma; C: Expression of p53 in gastric MALT lymphoma; D: Expression of Ki-67 in gastric MALT lymphoma.

rate of iNOS (88.2%) in the COX-2 positive group was significantly higher than that in the COX-2-negative group (46.7%, P=0.011).

Correlation between COX-2 expression and clinicopathological factors

The correlation between COX-2 expression and the clinicopathologic findings was analyzed by Spearman correlation test. All the parameters analyzed in COX-2 positive cases, including age, gender, stage of disease, lymph node metastasis and differentiation degree of the tumor, did not reached statistical significance (P>0.05, Table 1).

Expression of p53 in gastric MALT lymphoma

The accumulation of p53 nuclear phosphoprotein was detected in 19(59.4%) of tumors (Table 1, Figure 1C), whereas the p53 accumulation was undetectable in normal gastric tissues. A relationship between p53 status and several clinicopathological characteristics was investigated. p53 protein was expressed in 11 of 23 assessed LG tumors and in 8 of 9 assessed HG tumors. The difference of p53 positivity was found statistically significant between LG and HG cases (P=0.033). The p53 accumulation correlated with advanced clinical stage (stage III+IV *vs* stage I+II, P=0.017). The other parameters, such as age, gender and lymph node metastasis did not show any significant relation to the expression of p53.

There was a significant positive correlation between COX-2 expression and p53 accumulation status (r=0.403, P=0.022). Tumors that overexpressed p53 had higher expression levels of COX-2 than those without p53 overexpression (P=0.022, Table 1).

Expression of Ki-67 in gastric MALT lymphoma

Ki-67 staining was nuclear (Figure 1D). Very few cells were positive for Ki-67 in non-neoplastic gastric tissues. The mean PI of Ki-67 in the tumors was 29.81±9.54% (mean±SD). Mean values in each grade group were 36.0±7.73% in HG and 27.4±9.21% in LG. A significant correlation was observed between the high-proliferation rate and HG tumors (r=0.419, P=0.017).

The PI in COX-2 positive group was significantly higher than that in COX-2 negative group (P=0.031). The correlation coefficient showed a significant positive correlation between PI and COX-2 expression in MALT lymphoma patients (r=0.410, P=0.020). However, no significant correlation between PI and iNOS expression was found (r= -0.037, P=0.839).

Table 1 Correlation between expression of COX-2 and iNOS / p53 and clinicopathological factors in gastric MALT lymphoma (n, %)

Variable		Total	COX-2 positive	COX-2 negative	P value
Gender	Male	22	15(68.2)	7(31.8)	0.918
	Female	10	7(70.0)	3(30.0)	
Age (yr)	≤50	9	6(66.7)	3(33.3)	0.874
	>50	23	16(69.6)	7(30.4)	
Lymph node	+	10	8(80.0)	2(20.0)	0.355
Metastasis	-	22	14(63.6)	8(36.4)	
Histological	Low	23	14(60.7)	9(39.1)	0.124
Grade	High	9	8(88.9)	1(11.1)	
Histological	I+II	22	16(72.7)	6(27.3)	0.472
Stage	III+IV	10	6(60.0)	4(40.0)	
INOS	+	17	15(88.2)	2(11.8)	0.011
	-	15	7(46.7)	8(53.3)	
p53	+	19	16(84.2)	3(15.8)	0.022
	-	13	6(46.2)	7(53.8)	

DISCUSSION

Gastric MALT lymphoma is a unique disease. Normal human gastric mucosa is devoid of MALT. MALT accumulates within gastric mucosa as a result of long-standing *H pylori* infection in a subset of infected patients, and from this acquired MALT, low-grade B cell MALT lymphoma may eventually develop[13]. *H pylori* can be demonstrated in the gastric mucosa of the majority of cases of gastric MALT lymphoma[14,15]. Additionally, eradication of *H pylori* was reported to result in the complete regression of the majority of these tumors[16,17]. However, the exact mechanism responsible for the development of MALT lymphoma still remains obscure.

The contribution of COX-2 to carcinogenesis and the malignant phenotype of tumor cells have been thought to be related to its abilities: (1) increase production of prostaglandins[18]; (2) convert procarcinogens to carcinogens[19]; (3) inhibit apoptosis[20]; (4) promote angiogenesis[21]; (5) modulate inflammation and immune function[22,23]; (6) increase tumor cell invasiveness[24,25]. Like COX-2, iNOS is also involved in the process of carcinogenesis. Sustained induction of iNOS in chronic inflammation may be mutagenic through NO-mediated DNA damage or hindrance to DNA repair, and thus potentially carcinogenic. In addition, NO can favour tumor growth and development by stimulating angiogenesis[10,26-28] and causing immunosuppression[29].

In the current study, we demonstrated that a high positive immunostaining rate for COX-2 and iNOS was observed in gastric MALT lymphoma. Our results agree with the findings of previous investigations[4,5,14,17]. The present results indicated that the increased expression of COX-2 and iNOS might be important molecular events that contribute to gastric MALT lymphoma carcinogenesis. We speculate that *H pylori* infection might induce gastric carcinogenesis via overexpression of COX-2. These processes may be completed by the expression of COX-2 as an inflammation enzyme to release excessive amounts of prostaglandins, leading to further proliferation, reduction in apoptosis, angiogenesis and tumor growth.

It has been reported that COX-2 overexpression in tumors significantly correlates with iNOS overexpression[4,5]. In the current study, we also discovered that COX-2 expression was positively correlated with iNOS expression, suggesting a link between the COX-2 and iNOS pathways. In addition, iNOS and COX-2 may play a synergistic role in the pathogenesis of gastric MALT lymphoma. Because the product of iNOS catalysis, NO, is an important regulator of COX-2 activity and expression[30,31], and the products of COX-2 (diverse prostaglandins) may also influence iNOS expression[32]. Furthermore, prostaglandins and NO have been proposed to be involved in angiogenesis *in vivo*[33]. The inhibition of NO production by COX-2 inhibitors suggests NO-COX cross-talk between COX-2 and iNOS pathways[34].

Our results demonstrated that COX-2 expression in MALT lymphoma tissues was positively correlated with cell proliferative activity analyzed by Ki-67 labeling index. Ki-67 is expressed in cells that undergo active proliferation and have left the G_0 phase of the cell cycle[35]. These results suggest that COX-2 expression may be actively associated with the modulation of cellular proliferation and transformation during the evolution of *H pylori*-associated gastritis to MALT lymphoma.

So far, there have been some ambiguous points with regard to relationships between COX-2 overexpression and clinicopathological characteristics of tumors. Several reports have demonstrated that COX-2 expression in various tumors influences tumor cell differentiation, invasiveness, size, and survival[36]. However, we found no significant relation between COX-2 expression and clinicopathological characteristics in our study, which was compatible with previous reports on other organs[37].

Low-grade MALT lymphoma can transform into high-grade lymphoma and is associated with other genetic events such as p53 inactivation[38,39]. In the current study, p53 positivity increased significantly as the histological grade advanced. The results of our study support the concept that the expression of p53 in gastric lymphomas may be associated with transformation from low-grade to high-grade disease. In addition, there have been many workers reporting that high-proliferation rate is associated with the presence of a large cell component of MALT lymphoma[40,41]. The results of our experiments showed that high proliferation rate expressed by Ki-67 was correlated with HG tumors. These suggested that high proliferation index in MALT lymphoma may help in identifying a population of patients with an increased risk of developing MALT lymphoma.

Consistent with the findings of others[40], we found that COX-2 overexpression was closely associated with p53 accumulation status. With regard to the negative regulation of COX-2, it has recently been shown that wild-type p53 suppresses promoter activities of COX-2 and the expression of COX-2 protein. Wild-type p53 was shown to suppress COX-2 promoter activity by competing with TATA-binding proteins[41]. Han *et al*.[42] identified that COX-2 expression was inducible by wild-type p53 and DNA damage. They also found that p53-induced COX-2 expression resulted from p53-mediated activation of the Ras/Raf/MAPK cascade, as demonstrated by suppression of COX-2 induction in response to p53 by dominant-negative Ras or Raf1 mutants. Furthermore, heparin-binding epidermal growth factor-like growth factor (HB-EGF), a p53 downstream target gene, induced COX-2 expression, implying that COX-2 is an ultimate effector in the p53→HB-EGF→Ras/Raf/MAPK→COX-2 pathway.

In conclusion, COX-2 is expressed in the majority of gastric MALT lymphoma tissues and correlates with cellular proliferation and iNOS expression. iNOS and COX-2 may play a synergistic role in the pathogenesis of gastric MALT lymphoma. COX-2 overexpression is closely associated with p53 accumulation status. The molecular basis for the expression of COX-2 and iNOS and their roles in the evolution of *H pylori*-associated gastritis to gastric MALT lymphoma requires to be carefully investigated in follow-up studies.

REFERENCES

1 **Nakamura S,** Akazawa K, Yao T, Tsuneyoshi M. A clinicopathologic study of 233 cases with special reference to evaluation with the MIB-1 index. *Cancer* 1995; **76:** 1313-1324

2 **Konturek PC**, Konturek SJ, Starzyska T, Marlicz K, Bielanski W, Pierzchalski P, Karczewska E, Hartwich A, Rembiasz K, Lawniczak M, Ziemniak W, Hahn EC. *Helicobacter pylori*-gastrin link in MALT lymphoma. *Aliment Pharmacol Ther* 2000; **14:** 1311-1318

3 **Fu S,** Ramanujam KS, Wong A, Fantry GT, Drachenberg CB, James SP, Meltzer SJ, Wilson KT. Increased expression and cellular localization of inducible nitric oxide synthase and cyclooxygenase 2 in *Helicobacter pylori* gastritis. *Gastroenterology* 1999; **116**: 1319-1329

4 **Kong G**, Kim EK, Kim WS, Lee KT, Lee YW, Lee JK, Paik SW, Rhee JC. Role of cyclooxygenase-2 and inducible nitric oxide synthase in pancreatic cancer. *J Gastroenterol Hepatol* 2002; **17:** 914-921

5 **Nose F**, Ichikawa T, Fujiwara M, Okayasu I. Up-regulation of cyclooxygenase-2 expression in lymphocytic thyroiditis and thyroid tumors: significant correlation with inducible nitric oxide synthase. *Am J Clin Pathol* 2002; **117:** 546-551

6 **Denkert C**, Winzer KJ, Muller BM, Weichert W, Pest S, Kobel M, Kristiansen G, Reles A, Siegert A, Guski H, Hauptmann S. Elevated expression of cyclooxygenase-2 is a negative prognostic factor for disease free survival and overall survival in patients with breast carcinoma. *Cancer* 2003; **97:** 2978-2987

7 **Liu JW**, Li KZ, Dou KF. Expression of cyclooxygenase-2 in pancreatic cancer and its correlation with p53. *Shijie Huaren Xiaohua Zazhi* 2003; **11:** 229-232

8 **Bing RJ**, Miyataka M, Rich KA, Hanson N, Wang X, Slosser HD, Shi SR. Nitric oxide, prostanoids, cyclooxygenase, and angiogenesis in colon and breast cancer. *Clin Cancer Res* 2001; **7:** 3385-3392

9 **Xu MH**, Deng CS, Zhu YQ, Lin J. Role of inducible nitric oxide synthase expression in aberrant crypt foci-adenoma-carcinoma sequence. *World J Gastroenterol* 2003; **9:** 1246-1250

10 **Song ZJ**, Gong P, Wu YE. Relationship between the expression of iNOS, VEGF, tumor angiogenesis and gastric cancer. *World J Gastroenterol* 2002; **8:** 591-595

11 **Harris NL**, Jaffe ES, Stein H, Banks PM, Chan JK, Cleary ML, Delsol G, De Wolf-Peeters C, Falini B, Gatter KC. A revised European-American classification of lymphoid neoplasms: a proposal from the International Lymphoma Study Group. *Blood* 1994; **84:** 1361-1392

12 **Harris NL,** Jaffe ES, Diebold J, Flandrin G, Muller-Hermelink HK, Vardiman J, Lister TA, Bloomfield CD. World Health Organization classification of neoplastic diseases of the hematopoietic and lymphoid tissues: report of the clinical advisory committee meeting-airlie house, virginia, november 1997. *J Clin Oncol* 1999; **17**: 3835-3849

13 **Du MQ**, Isaacson PG. Recent advances in our understanding of the biology and pathogenesis of gastric mucosa-associated lymphoid tissue (malt) lymphoma. *Forum* 1998; **8:** 162-173

14 **Konturek PC**, Konturek SJ, Pierzchalski P, Bielanski W, Duda A, Marlicz K, Starzynska T, Hahn EG. Cancerogenesis in *Helicobacter pylori* infected stomach-role of growth factors, apoptosis and cyclooxygenases. *Med Sci Monit* 2001; **7**: 1092-1107

15 **Konturek SJ**, Konturek PC, Hartwich A, Hahn EG. *Helicobacter pylori* infection and gastrin and cyclooxygenase expression in gastric and colorectal malignancies. *Regul Pept* 2000; **93:** 13-19

16 **Ohashi S**, Segawa K, Okamura S, Urano H, Kanamori S, Ishikawa H, Hara K, Hukutomi A, Shirai K, Maeda M. A clinicopathologic study of gastric mucosa-associated lymphoid tissue lymphoma. *Cancer* 2000; **88**: 2210-2219

17 **Konturek PC**, Konturek SJ, Pierzchalski P, Starzynska T, Marlicz K, Hartwich A, Zuchowicz M, Darasz Z, Papiez D, Hahn EG. Gastric MALT-lymphoma, gastrin and cyclooxygenases. *Acta Gastroenterol Belg* 2002; **65**: 17-23

18 **Zweifel BS**, Davis TW, Ornberg RL, Masferrer JL. Direct evidence for a role of cyclooxygenase 2-derived prostaglandin E2 in human head and neck xenograft tumors. *Cancer Res* 2002; **62:** 6706-6711

19 **Hosomi Y**, Yokose T, Hirose Y, Nakajima R, Nagai K, Nishiwaki Y, Ochiai A. Increased cyclooxygenase 2 (COX-2) expression occurs frequently in precursor lesions of human adenocarcinoma of the lung. *Lung Cancer* 2000; **30:** 73-81

20 **Miyata Y**, Koga S, Kanda S, Nishikido M, Hayashi T, Kanetake H. Expression of cyclooxygenase-2 in renal cell carcinoma: correlation with tumor cell proliferation, apoptosis, angiogenesis, expression of matrix metalloproteinase-2, and survival. *Clin Cancer Res* 2003; **9:** 1741-1749

21 **Kim MH**, Seo SS, Song YS, Kang DH, Park IA, Kang SB, Lee HP. Expression of cyclooxygenase-1 and -2 associated with expression of VEGF in primary cervical cancer and at metastatic lymph nodes. *Gynecol Oncol* 2003; **90:** 83-90

22 **Ermert L**, Dierkes C, Ermert M. Immunohistochemical expression of cyclooxygenase isoenzymes and downstream enzymes in human lung tumors. *Clin Cancer Res* 2003; **9**: 1604-1610

23 **Sharma S**, Stolina M, Yang SC, Baratelli F, Lin JF, Atianzar K, Luo J, Zhu L, Lin Y, Huang M, Dohadwala M, Batra RK, Dubinett SM. Tumor Cyclooxygenase 2-dependent suppression of dendritic cell function. *Clin Cancer Res* 2003; **9:** 961-968

24 **Zhang H**, Sun XF. Overexpression of cyclooxygenase-2 correlates with advanced stages of colorectal cancer. *Am J Gastroenterol* 2002; **97:** 1037-1041

25 **Wu QM**, Li SB, Wang Q, Wang DH, Li XB, Liu CZ. The expression of COX-2 in esophageal carcinoma and its relation to clinicopathologic characteristics. *Shijie Huaren Xiaohua Zazhi* 2001; **9**: 11-14

26 **Cianchi F**, Cortesini C, Fantappie O, Messerini L, Schiavone N, Vannacci A, Nistri S, Sardi I, Baroni G, Marzocca C, Perna F, Mazzanti R, Bechi P, Masini E. Inducible nitric oxide synthase

expression in human colorectal cancer: correlation with tumor angiogenesis. *Am J Pathol* 2003; **162**: 793-801

27 **Tao WH**, Deng CS, Zhu YQ. Expression of inducible nitric oxide synthase and angiogenesis in gastric cancer. *Shijie Huaren Xiaohua Zazhi* 2003; **11:** 33-35

28 **Franchi A**, Gallo O, Paglierani M, Sardi I, Magnelli L, Masini E, Santucci M. Inducible nitric oxide synthase expression in laryngeal neoplasia: correlation with angiogenesis. *Head Neck* 2002; **24**: 16-23

29 **Kojima M**, Morisaki T, Tsukahara Y, Uchiyama A, Matsunari Y, Mibu R, Tanaka M. Nitric oxide synthase expression and nitric oxide production in human colon carcinoma tissue. *J Surg Oncol* 1999; **70**: 222-229

30 **Liu Q**, Chan ST, Mahendran R. Nitric oxide induces cyclooxygenase expression and inhibits cell growth in colon cancer cell lines. *Carcinogenesis* 2003; **24**: 637-642

31 **Perez-Sala D**, Lamas S. Regulation of cyclooxygenase-2 expression by nitric oxide in cells. *Antioxid Redox Signal* 2001; **3:** 231-248

32 **Kobayashi O**, Miwa H, Watanabe S, Tsujii M, Dubois RN, Sato N. Cyclooxygenase-2 downregulates inducible nitric oxide synthase in rat intestinal epithelial cells. *Am J Physiol Gastrointest Liver Physiol* 2001; **281:** G688-G696

33 **Davel L**, D'Agostino A, Espanol A, Jasnis MA, Lauria de Cidre L, de Lustig ES, Sales ME. Nitric oxide synthase-cyclooxygenase interactions are involved in tumor cell angiogenesis and migration. *J Biol Regul Homeost Agents* 2002; **16**: 181-189

34 **Fantappie O**, Masini E, Sardi I, Raimondi L, Bani D, Solazzo M, Vannacci A, Mazzanti R. The MDR phenotype is associated with the expression of COX-2 and iNOS in a human hepatocellular carcinoma cell line. *Hepatology* 2002; **35**: 843-852

35 **Scholzen T**, Gerdes J. The Ki-67 protein: from the known and the unknown. *J Cell Physiol* 2000; **182**: 311-322

36 **Rajnakova A**, Moochhala S, Goh PM, Ngoi S. Expression of nitric oxide synthase, cyclooxygenase, and p53 in different stages of human gastric cancer. *Cancer Lett* 2001; **172**: 177-185

37 **Kokawa A**, Kondo H, Gotoda T, Ono H, Saito D, Nakadaira S, Kosuge T, Yoshida S. Increased expression of cyclooxygenase-2 in human pancreatic neoplasms and potential for chemoprevention by cyclooxygenase inhibitors. *Cancer* 2001; **91:** 333-338

38 **Insabato L**, Di Vizio D, Tornillo L, D'Armiento FP, Siciliano A, Milo M, Palmieri G, Pettinato G, Terracciano LM. Clinicopathologic and immunohistochemical study of surgically treated primary gastric MALT lymphoma. *J Surg Oncol* 2003; **83:** 106-111

39 **Pozzi B**, Hotz AM, Feltri M, Cornaggia M, Campiotti L, Bonato M, Pinotti G, Capella C. Primary gastric lymphomas. Clinicopathological study and evaluation of prognostic factors in 65 cases treated surgically. *Pathologica* 2000; **92**: 503-515

40 **Niki T**, Kohno T, Iba S, Moriya Y, Takahashi Y, Saito M, Maeshima A, Yamada T, Matsuno Y, Fukayama M, Yokota J, Hirohashi S. Frequent co-localization of Cox-2 and laminin-5 gamma2 chain at the invasive front of early-stage lung adenocarcinomas. *Am J Pathol* 2002; **160**: 1129-1141

41 **Subbaramaiah K**, Altorki N, Chung WJ, Mestre JR, Sampat A, Dannenberg AJ. Inhibition of cyclooxygenase-2 gene expression by p53. *J Biol Chem* 1999; **274**: 10911-10915

42 **Han JA**, Kim JI, Ongusaha PP, Hwang DH, Ballou LR, Mahale A, Aaronson SA, Lee SW. P53-mediated induction of Cox-2 counteracts p53- or genotoxic stress-induced apoptosis. *EMBO J* 2002; **21:** 5635-5644

Edited by Kumar M **Proofread by** Chen WW and Xu FM

PO Box 2345, Beijing 100023, China
Fax: +86-10-85381893
E-mail: wjg@wjgnet.com www.wjgnet.com

World J Gastroenterol 2004;10(13):1867-1871
World Journal of Gastroenterology
 ISSN 1007-9327

• LIVER CANCER •

Endostatin gene therapy for liver cancer by a recombinant adenovirus delivery

Li Li, Jia-Ling Huang, Qi-Cai Liu, Pei-Hong Wu, Ran-Yi Liu, Yi-Xin Zeng, Wen-Lin Huang

Li Li, Jia-Ling Huang, Ran-Yi Liu, Pei-Hong Wu, Yi-Xin Zeng, Wen-Lin Huang, Cancer Center, Sun Yat-sen University, 651 Dongfeng Road East, Guangzhou 510060, Guangdong Province, China
Qi-Cai Liu, Experimental Medical Research Center, Guangzhou Medical College, 195 Dongfeng Road West, Guangzhou 510182, Guangdong Province, China
Supported by the National High Technology Research and Development Program of China (863 Program), No. 2003AA216061 and CMB-SUMS Scholar Program, No. 98-677 and Guangdong Provincial Science and Technology Program, No. 2003A10902
Co-first-authors: Jia-Ling Huang and Qi-Cai Liu
Correspondence to: Dr. Wen-Lin Huang, Cancer Center, Sun Yat-sen University, 651 Dongfeng Road East, Guangzhou 510060, Guangdong Province, China. wl_huang@hotmail.com
Telephone: +86-20-87343146 **Fax:** +86-20-87343392
Received: 2004-01-15 **Accepted:** 2004-02-21

Abstract

AIM: To investigate the expression of adenovirus-mediated human endostatin (Ad/hEndo) gene transfer and its effect on the growth of hepatocellular carcinoma (HCC) BEL-7402 xenografted tumors.

METHODS: Immunohistochemistry analysis with an anti-endostatin antibody was preformed to detect endostatin protein expression in HCC BEL-7402 cells infected with Ad/hEndo. MTT assay was used to investigate the effects of Ad/hEndo on proliferation of human umbilical vein endothelial cells (HUVEC). Intra-tumoral injections of 1×10^9 pfu Ad/hEndo was given to treat BEL-7402 xenografted tumors in nude mice once weekly for 6 wk. Mice received injections of Ad/LacZ and DMEM were regarded as control groups. After intra-turmoral administration with Ad/hEndo, the endostatin mRNA expression in tumor tissue was analyzed by Northern blotting, and plasma endostatin levels were determined using enzyme-linked immunosorbent assay (ELISA).

RESULTS: High level expression of endostatin gene was detected in the infected HCC BEL-7402 cells. Ad/hEndo significantly inhibited HUVEC cell proliferation by 57.2% at a multiplicity of infection (MOI) of 20. After 6-week treatment with Ad/hEndo, the growth of treated tumors was inhibited by 46.50% compared to the Ad/*LacZ* control group (t=2.729, P<0.05) and by 48.56% compared to the DMEM control group (t=2.485, P<0.05). The ratio of mean tumor volume in treated animals to mean tumor volume in the control animals (T:C ratio) was less than 50% after 24 d of treatment. Endostatin mRNA in tumor tissue was clearly demonstrated as a band of approximately 1.2 kb, which was the expected size of intact and functional endostatin. Plasma endostatin levels peaked at 87.52±8.34 ng/mL at d 3 after Ad/hEndo injection, which was significantly higher than the basal level (12.23±2.54 ng/mL). By d 7, plasma levels dropped to nearly half the peak level (40.34±4.80 ng/mL).

CONCLUSION: Adenovirus-mediated human endostatin gene can successfully express endogenous endostatin *in vitro* and *in vivo*, and significantly inhibit the growth of BEL-7402 xenografted liver tumors in nude mice.

Li L, Huang JL, Liu QC, Wu PH, Liu RY, Zeng YX, Huang WL. Endostatin gene therapy for liver cancer by a recombinant adenovirus delivery. *World J Gastroenterol* 2004; 10(13): 1867-1871
http://www.wjgnet.com/1007-9327/10/1867.asp

INTRODUCTION

Increasing evidence suggests that solid tumors and their metastasis are angiogenesis dependent[1]. Angiogenesis, the formation of new microvessels generated by vascular endothelial cells, provides essential nutrition for rapid growth of malignant cells. Without angiogenesis, neoplasm might remain in dormancy[2]. Anti-angiogenesis therapies, which block the blood supply of a growing tumor by inhibiting proliferation of endothelial cells, provide a new strategy for treatment of solid tumors[3]. Vascular endothelial cells, the target of anti-angiogenic treatment are genetically stable. So it is unlikely that anti-angiogenic agents would induce the drug resistance[4].

Transcatheter arterial embolization (TAE) has been widely practiced in the treatment of unresectable hepatocellular carcinoma (HCC)[5]. However, the obstruction of hepatic artery induces extensive ischemic necrosis or hypoxia which are strongly correlated with increased expression of angiogenic factors, such as vascular endothelial growth factor (VEGF), basic fibroblast growth factor (bFGF)[6]. The proliferative activity of vascular endothelial cells and tumour cells was increased in residual tumor following arterial embolization[7]. Combination of antiangiogenesis and TAE therapy could inhibit increased proliferation of vascular endothelial cells and capillary vessel formation induced by arterial embolization, and improve the therapeutic effect[5].

Endostatin, a carboxyl-terminal proteolytic fragment of collagen XVIII, was regarded as one of the most potent inhibitors of tumor angiogenesis[8]. Several studies have shown that recombinant endostatin protein generated from *Escherichia coli* and *Pichia pastoris* yeast significantly inhibited growth and metastasis of xenografted tumor in different tumor models with no drug resistance and side effects[9,10]. However, its widespread application has been hampered by difficulties in the large-scale production of high bioactive protein[11,12].

In this study, we constructed a replication-defective recombinant adenoviral vector harboring a human endostatin gene (Ad/hEndo), and demonstrated efficient expression of endostatin gene *in vivo* and its antitumoral effect on BEL-7402 xenografted liver tumors in nude mice.

MATERIALS AND METHODS

Materials

Cells and adenoviruses BEL-7402 cells (Hepatocellular

carcinoma, HCC) and human umbilical vein endothelial cells (HUVEC) were maintained in RPMI 1640 supplemented with 100 mL/L fetal bovine serum (FBS). The culture medium contained 100 U/mL of penicillin and 100 μg/mL of streptomycin (GIBCO BRL, Gathersburg, MD).

Recombinant adenovirus vectors carrying the human endostatin gene (Ad/hEndo) and *LacZ* gene (Ad/*LacZ*) were generated as described previously[12,13]. All virus particles were amplified in 293 cells and purified by cesium chloride gradient centrifugation. Viruses were titered using a standard plaque-forming unit (pfu) assay.

Animals Four to 6-week-old male BALB/c nude mice (with body weight of 19 to 23 g) were purchased from Animal Experiment Center (Medial College, Sun Yat-sen University) and maintained in a specific pathogen-free (SPF) environment (certificate: 26-99S029).

Agents Human endostatin protein accucyte EIA (Oncogene Research Products, Boston, MA), rabbit anti-human endostatin polyclonal antibody (Chemicon International, Temecula, CA).

Methods

Immunohistochemistry for expression of endostatin protein *in vitro* BEL-7402 cells were infected with Ad/hEndo at a multiplicity of infection (MOI) of 10. At 2 h postinfection, the medium was replaced with Dulbecco's minimal essential medium (DMEM) containing 100 mL/L FBS. After 72-h incubation, cells were collected and plated on slides. The slides were washed, fixed and blocked for 20 min in Tris-buffered saline (TBS) containing 10 mL/L goat serum, then incubated with rabbit anti-human endostatin polyclonal antibody diluted 1:50 in PBS overnight. After washing 3 times, biotinylated goat anti-rabbit secondary antibody (Dako Corp., Carpinteria, CA) diluted 1:200 in PBS was added, and slides were incubated for an additional 30 min. Slides were then washed 3 times with PBS and stained with streptavidin-biotinylated horseradish peroxide complex.

HUVEC cells proliferation assay Human umbilical vein endothelial cells (HUVEC) were seeded in a 96-well plate at a density of 1×10^4/well and allowed to adhere overnight. Cells were then infected for 2 h with Ad/hEndo at MOIs of 0.05, 0.5, 1.0, 5.0, 10 and 20, and with Ad/LacZ at an MOI of 20. Cells were washed 3 times with PBS and incubated at 37 ℃ in fresh medium. Seventy-two hours later, 20 μL of 3-(4,5-dimethylthiazol-2-yl)-2,5-diphenyl-2H-tetrazolium bromide (MTT) (Fluka Biochemika, Buchs, Switzerland) was added to the wells and the plate was incubated for an additional 4 h at 37 ℃. Then, 100 μL DMSO was added to the wells and the plate was incubated for 10 min at 37 ℃. Absorbance was read using a Bio-Rad 550 microplate reader (Bio-Rad Laboratories, Hercules, CA) at 570 nm. The value of the treated cells was calculated as percent of the untreated control.

***In vivo* tumor growth inhibition** BEL-7402 cells were subcutaneously inoculated into the flanks of 6-week-old female BALB/c nude mice (5×10^6 cells in 200 μL). Ten days after tumor cell inoculation, intra-tumoral injections of virus (Ad/hEndo or Ad/*LacZ*; 1×10^9 pfu in 100 μL) was given once weekly for 6 wk. An additional 7 animals received injections of 100 μL of DMEM as a negative control. Tumors were measured with a caliper gauge twice a week over a 6-week period following the initial virus injections. Tumor volume was calculated according to the formula: volume = width$^2\times$length$\times0.52$[10]. One week after the 6th injection of Ad/hEndo, the mice were sacrificed and the xenografted tumors were excised and weighed. The inhibition rates of growth of BEL-7402 xenografted tumors were calculated according to the formula: Inhibition rate (%)=(1-mean Weight$_{(Ad/hEndo)}$/mean Weight$_{(control)}$)×100.

Northern blotting for expression of endostatin mRNA *in vivo* On d 1, 4 and 8 after intra-tumoral administration with 100 μL of 1×10^9 pfu Ad/hEndo, the mice were sacrificed. The xenografted tumors were excised and snap frozen in liquid nitrogen. Total RNA was isolated from tumor tissues using the Trizol reagent (Invitrogen) according to the manufacturer's instructions. RNA isolated from the tumors injected with DMEM was used as a negative control. Total RNA of 15 μg was resolved on a 10 g/L formaldehyde agarose gel, and transferred to nylon membrane. The RNA was fixed onto the membrane by UV cross-linking. The membrane was prehybridized in DIG Easy Hyb hybrization solution (Roche, Basel, Switzerland) at 68 ℃ for 30 min, then hybridized in DIG Easy Hyb hybrization solution containing digoxin (DIG)-labeled endostatin probe at 68 ℃ overnight. The membrane was incubated with anti-DIG antibody for 30 min and stained with NBT/BCIP for 10 min.

Plasma endostatin levels detected by ELISA Blood samples were harvested on d 0, 3 and 7 after intra-tumoral administration with 100 μL of 1×10^9 pfu Ad/hEndo. Samples were centrifuged, and plasma endostatin levels were determined using a human endostatin enzyme-linked immunosorbent assay (ELISA) kit (Oncogene Research Products, Boston, MA), according to the manufacturer's instructions.

Pathological observation One week after the 6th course of treatment, the animals were sacrificed. The major organs including heart, liver, spleen, kidney, lung and brain were extracted from the nude mice, fixed in 40 g/L buffered formaldehyde phosphate, cut into 4 μm thick for tissue section and stained with haematoxylin and eosin.

RESULTS

High level transgene expression in BEL-7402 cells infected with Ad/hEndo

Three days after transfection with Ad/hEndo at a MOI of 10, BEL-7402 cells were probed with rabbit anti-human endostatin antibody. Immunohistochemistry with an anti-endostatin antibody clearly demonstrated that endostatin protein was expressed in the transduced BEL-7402 cells. Extensive positive staining was observed in the cytoplasm of transduced cells (Figure 1). This indicated that human endostatin gene mediated by recombinant adenovirus was highly expressed in BEL-7402 cells and provided evidence for the feasibility of local gene therapy for HCC BEL-7402 xenografted tumors.

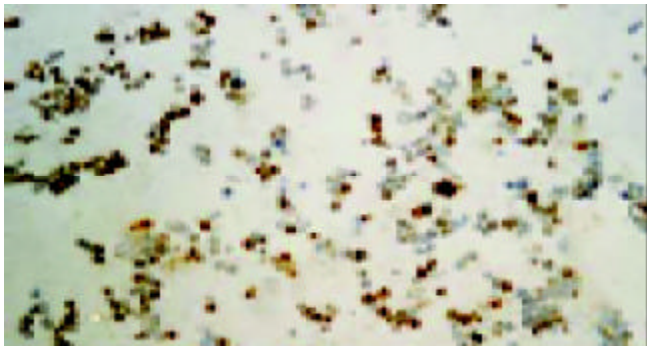

Figure 1 Immunohistochemistry analysis for endostatin protein *in vitro* (×100). Extensive positive staining was observed in the cytoplasm of transduced cells. This indicated that human endostatin gene mediated by recombinant adenovirus was highly expressed in BEL-7402 cells.

Inhibition of proliferation of HUVEC cells by Ad/hEndo

In order to investigate the effects of this secreted endostatin on proliferation of HUVEC cells, cell proliferation assays were performed by MTT assay. Ad/hEndo inhibited HUVEC cell proliferation by 7.61%, 12.61%, 24.8%, 29.86%, 38.78% and 57.2% at MOIs of 0.05, 0.5, 1.0, 5, 10 and 20, respectively. The

Ad/*LacZ* control group showed inhibition of cellular proliferation by 7.25% at a MOI of 20 (Figure 2). These results indicated that the endostatin protein secreted by the transduced cells was highly bioactive and inhibited the proliferation of vascular endothelial cells *in vitro* in a dose-dependent manner, while the viral vector alone did not.

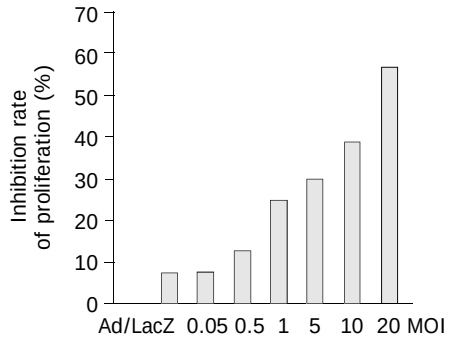

Figure 2 Effect of Ad / hEndo on the proliferation of HUVEC cells.

Inhibition of the growth of BEL-7402 xenograft tumors by Ad/hEndo

In order to observe the effect of Ad/hEndo on the growth of tumors, we established a BEL-7402 xenograft tumor model in BALB/c nude mice. After 6 wk of treatment, the growth of treated tumors was inhibited by 46.50% compared to the Ad/*LacZ* control group (t=2.729, P<0.05) and by 48.56% compared to the DMEM control group (t=2.485, P<0.05). The ratio of mean tumor volume in treated animals to that of the control animals (T:C ratio) was <50% after 24 d of treatment (Figure 3). These results showed that Ad/hEndo significantly inhibited the growth of BEL-7402 xenografted tumors.

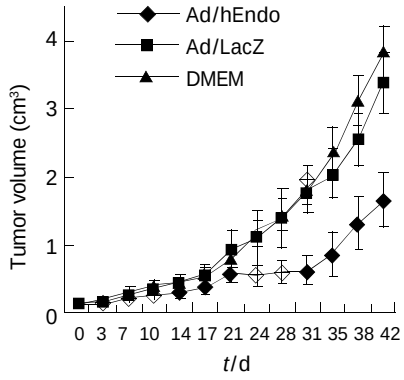

Figure 3 Effect of Ad / hEndo on growth of BEL-7402 xenografted liver tumors.

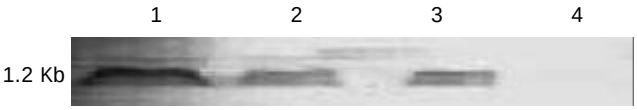

Figure 4 Northern blotting of endostatin mRNA *in vivo*. Lanes 1-3: RNA extracted from tumors on d 1, 4 and 8 after Ad / hEndo injection, respectively; Lane 4: RNA extracted from control tumors injected with DMEM.

Full-length expression of endostatin mRNA in vivo

Northern blotting was performed to test whether the *in vivo* expressed endostatin mRNA was of full-length. After hybridization, the membrane was stained with NBT/BCIP, and endostatin mRNA was clearly demonstrated as a band of approximately 1.2 kb (Figure 4), which was the expected size of intact and functional endostatin. The highest level of endostatin mRNA *in vivo* was detected 1 d after intra-tumoral administration of Ad/hEndo. On d 4 and 8, endostatin mRNA levels significantly decreased. Therefore, Northern blotting showed that adenovirus-mediated human endostatin gene transfer resulted in expression of intact endostatin mRNA *in vivo*.

Plasma levels of endostatin protein

ELISA was used to measure the plasma endostatin levels. Plasma endostatin levels peaked at 87.52±8.34 ng/mL on d 3 after Ad/hEndo injection, which was significantly higher than the basal level (12.23±2.54 ng/mL). By d 7, plasma levels dropped to half the peak level (40.34±4.80 ng/mL) (Figure 5). These results showed that intra-tumoral delivery of the endostatin gene resulted in high plasma endostatin concentrations.

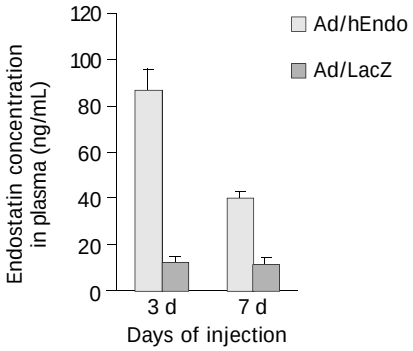

Figure 5 Detection of endostatin concentration in plasma by ELISA.

Pathological changes of main organs

All animals were survived and appeared to be physically normal. There were no histological changes in main organs of DMEM control animals. However, histological examination in several mice of the Ad/hEndo (3/8) and Ad/LacZ (3/8) groups revealed slight to modest hepatocyte fatty degeneration, cloudy swelling and occasional necrosis companied with infiltration of lymphocyte and inflammatory cells.(Figure 6) One mouse in Ad/hEndo group (1/8) and 1 in Ad/LacZ (1/8) group demonstrated slight cloudy swelling in some proximal renal tubule cells and distal renal tubule cells. No histological changes were found in spleen, lung, heart and brain of both these groups. There was no significant difference in histological changes between Ad/hEndo group and Ad/LacZ group. These results suggested that it was the recombinant adenoviruses, not endostatin protein that caused the liver and kidney toxicity.

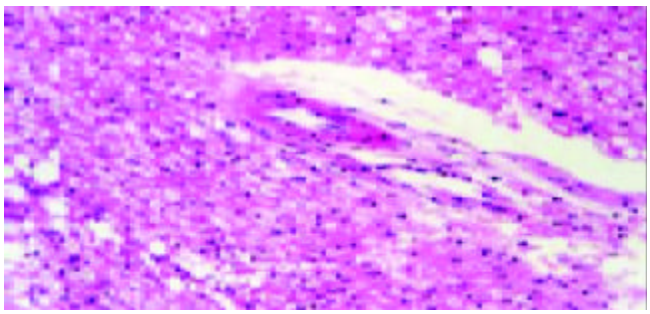

Figure 6 Pathological changes of liver 1 wk after 6 wk of treatment with Ad / hEndo (HE, original magnification: ×200).

DISCUSSION

Animal experiments on angiogenesis have frequently been conducted on tumors recently implanted in mice. However, in

the human situation, tumors are often established for months or years and may possess mature vasculature that is less sensitive to anti-angiogenic therapy[1,2]. Indeed, antiangiogenesis therapies, which inhibit the growth and metastasis of neoplasms by blocking the formation of new blood vessels from existing vessels, appear to require long-term administration of the angiogenic inhibitor to ensure tumor growth suppression[3]. Endostatin protein derived from yeast (*Pichia pastoris*) had been introduced into clinical trials as a possible antiangiogenic tumor fighting drug[15]. The clinical studies showed that the mean half-life of recombinant human endostatin was only 10.7±4.1 h in the human body, suggesting that this protein-based therapy was likely to require repeated daily or long-term administration of high-quality protein for optimal therapeutic benefits[16].

It is hoped that these difficulties of protein-based therapy may be overcome by direct expression of therapeutic gene in the body[17]. Endostatin gene therapy is a promising strategy for anti-angiogenic therapy, for a single transduction of endostatin gene could achieve a relatively long-term and high-quality protein expression *in vivo*[17,18]. Adenoviral vectors are commonly used as carriers for gene transfer due to their high efficiency and high capacity[19,20]. We cloned the human endostatin gene into an adenoviral shuttle plasmid and generated an adenoviral expressing system which resulted in highly efficient expression of endostatin gene and demonstrated high level of bioactivity by significantly inhibiting the proliferation of endothelial cells. In our studies, endostatin gene therapy using a recombinant adenovirus delivery significantly inhibited the growth of BEL-7402 xenografted liver tumors. Since d 24 of treatment with intra-tumoral injection with Ad/hEndo, the T:C ratio of mean tumor volume was less than 50%. After 6 courses of treatment, the growth of xenografted tumors treated with Ad/hEndo was markedly inhibited as compared with the control group.

Adenovirus can infect dividing and nondividing cells and obtain high efficiency of transgene expression[21,22]. These properties of adenoviral vector provide the possibility of local treatment, such as intra-tumoral injection and transcatheter arterial infusion of recombinant adenovirus[23]. In this study, we investigated the possibility of tumor-targeted endostatin gene therapy for liver cancer. First, we demonstrated high level transgene expression in BEL-7402 cells infected with Ad/hEndo. Then, intra-tumoral endostatin mRNA expression was clearly detected by Northern blotting on d 1 after injection with Ad/hEndo. Northern blotting indicated that the endostatin mRNA expressed inside tumor tissue was intact, thus the resultant endostatin protein could be biologically active *in vivo*. These positive results had provided solid evidence for local endostatin gene therapy for liver cancer.

The tumor-targeted gene therapy produced endostatin protein mostly inside the tumors[23,24], however, some of the protein entered the circulation, resulting in the peak of plasma endostatin concentration of 87.52±8.34 ng/mL by d 3 post-administration. Although this plasma level was considerably lower than those reached by intravenous delivery of recombinant adenoviral vector for endostatin gene therapy[19,20], it had been shown that circulating endostatin levels of 35-40 ng/mL was sufficient to exert an antiangiogenic effect *in vivo*[24], suggesting that our delivery system was able to induce therapeutically relevant circulating endostatin levels.

The transient expression is a key problem for any therapeutic use[23,25], while the reason for the transient *in vivo* transgene expression is unclear[26,27]. Repetition of administration with therapeutic gene *in vivo* using a transgene vector was recommended to achieve better therapeutic effect[23,28,29]. However, multiple injections of immunogenic transgene vector will get an immune response to the vector which not only make expression even worse, but also cause systemic toxicity[30,31]. Indeed, we observed slight liver and renal damage in mice after 6 courses of endostatin gene therapy using a recombinant adenovirus delivery. Histological examination in several mice administrated with adenoviral vector revealed slight to modest hepatocyte and renal tubule cell degeneration and some degree of inflammatory reaction. It was the recombinant adenovirus, not endostatin protein that caused the liver and kidney toxicity[27,32]. Our results suggested that cautions should be taken for clinical repeated administration within a short time of the recombinant adenoviral vector carrying endostatin gene.

In conclusion, a recombinant adenoviral vector carrying human endostatin gene can be successfully constructed, with highly efficient expression of endostatin gene both *in vitro* and *in vivo*, thereby significantly inhibiting the growth of BEL-7402 xenografted liver tumors in nude mice.

REFERENCES

1 **Folkman J**. What is the evidence that tumors are angiogenesis-dependent? *J Natl Cancer Inst* 1990; **82**: 4-6
2 **Folkman J.** Seminars in medicine of the beth israe1 hospital, boston. Clinical applications of research on angiogenesis. *N Engl J Med* 1995; **333**: 1757-1763
3 **Bergers G,** Javaherian K, Lo KM, Folkman J, Hanahan D. Effects of angiogenesis inhibitors on multistage carcinogenesis in mice. *Science* 1999; **284**: 808-812
4 **Boehm T,** Folkman J, Browder T, O'Reilly MS. Antiangiogenic therapy of experimental cancer does not induce acquired drug resistance. *Nature* 1997; **390**: 404-407
5 **Qian J,** Feng GS, Vogl T. Combined interventional therapies of hepatocellular carcinoma. *World J Gastroenterol* 2003; **9**: 1885-1891
6 **Li X,** Feng GS, Zheng CS, Zhuo CK, Liu X. Influence of transarterial chemoembolization on angiogenesis and expression of vascular endothelial growth factor and basic fibroblast growth factor in rat with Walker-256 transplanted hepatoma: An experimental study. *World J Gastroenterol* 2003; **9**: 2445-2449
7 **Kim YB,** Park YN, Park C. Increased proliferation activities of vascular endothelial cells and tumour cells in residual hepatocellular carcinoma following transcatheter arterial embolization. *Histopathology* 2001; **38**: 160-166
8 **O'Reilly MS,** Boehm T, Shing Y, Fukai N, Vasios G, Lane WS, Flynn E, Birkhead JR, Olsen BR, Folkman J. Endostatin: an endogenous inhibitor of angiogenesis and tumor growth. *Cell* 1997; **88**: 277-285
9 **Dhanabal M,** Ramchandran R, Volk R, Stillman IE, Lombardo M, Iruela-Arispe ML, Simons M, Sukhatme VP. Endostatin: yeast production, mutants, and antitumor effect in renal cell carcinoma. *Cancer Res* 1999; **59**: 189-197
10 **Huang X,** Wong MK, Zhao Q, Zhu Z, Wang KZ, Huang N, Ye C, Gorelik E, Li M. Soluble recombinant endostatin purified from *Escherichia coli*: antiangiogenic activity and antitumor effect. *Cancer Res* 2001; **61**: 478-481
11 **Chen QR,** Kumar D, Stass SA, Mixson AJ. Liposomes complexed to plasmids encoding angiostatin and endostatin inhibit breast cancer in nude mice. *Cancer Res* 1999; **59**: 3308-3312
12 **Ding I,** Sun JZ, Fenton B, Liu WM, Kimsely P, Okunieff P, Min W. Intratumoral administration of endostatin plasmid inhibits vascular growth and perfusion in MCa-4 murine mammary carcinomas. *Cancer Res* 2001; **61**: 526-531
13 **Huang W,** Flint SJ. The tripartite leader sequence of subgroup C adenovirus major late mRNAs can increase the efficiency of mRNA export. *J Virol* 1998; **72**: 225-235
14 **Huang W,** Flint SJ. Unusual properties of adenovirus E2E transcription by RNA polymerase III. *J Virol* 2003; **77**: 4015-4024
15 **Mundhenke C,** Thomas JP, Wilding G, Lee FT, Kelzc F, Chappell R, Neider R, Sebree LA, Friedl A. Tissue examination to monitor antiangiogenic therapy: a phase I clinical trial with endostatin. *Clin Cancer Res* 2001; **7**: 3366-3374
16 **Herbst RS,** Hess KR, Tran HT, Tseng JE, Mullani NA, Charnsangavej C, Madden T, Davis DW, McConkey DJ, O'Reilly MS, Ellis LM, Pluda J, Hong WK, Abbruzzese JL. Phase I study of recombinant human endostatin in patients

with advanced solid tumors. *J Clin Oncol* 2002; **20**: 3792-3803
17 **Folkman J.** Antiangiogenic gene therapy. *Proc Natl Acad Sci U S A* 1998; **95**: 9064-9066
18 **Szary J,** Szala S. Intra-tumoral administration of naked plasmid DNA encoding mouse endostatin inhibits renal carcinoma growth. *Int J Cancer* 2001; **91**: 835-839
19 **Sauter BV,** Martinet O, Zhang WJ, Mandeli J, Woo SL. Adenovirus-mediated gene transfer of endostatin *in vivo* results in high level of transgene expression and inhibition of tumor growth and metastases. *Proc Natl Acad Sci U S A* 2000; **97**: 4802- 4807
20 **Feldman AL,** Restifo NP, Alexander HR, Bartlett DL, Hwu P, Seth P, Libutti SK. Antiangiogenic gene therapy of cancer utilizing a recombinant adenovirus to elevate systemic endostatin levels in mice. *Cancer Res* 2000; **60**: 1503-1506
21 **St George JA.** Gene therapy progress and prospects: adenoviral vectors. *Gene Ther* 2003; **10**: 1135-1141
22 **Chen CT,** Lin J, Li Q, Phipps SS, Jakubczak JL, Stewart DA, Skripchenko Y, Forry-Schaudies S, Wood J, Schnell C, Hallenbeck PL. Antiangiogenic gene therapy for cancer via systemic administration of adenoviral vectors expressing secretable endostatin. *Hum Gene Ther* 2000; **11**: 1983-1996
23 **Kianmanesh A,** Hackett NR, Lee JM, Kikuchi T, Korst RJ, Crystal RG. Intratumoral administration of low doses of an adenovirus vector encoding tumor necrosis factor alpha together with naive dendritic cells elicits significant suppression of tumor growth without toxicity. *Hum Gene Ther* 2001; **12**: 2035-2049
24 **Shi W,** Teschendorf C, Muzyczka N, Siemann DW. Adeno-associated virus-mediated gene transfer of endostatin inhibits angiogenesis and tumor growth *in vivo*. *Cancer Gene Ther* 2002; **9**: 513-521
25 **Reid T,** Warren R, Kirn D. Intravascular adenoviral agents in cancer patients: lessons from clinical trials. *Cancer Gene Ther* 2002; **9**: 979-986
26 **Molinier-Frenkel V,** Le Boulaire C, Le Gal FA, Gahery-Segard H, Tursz T, Guillet JG, Farace F. Longitudinal follow-up of cellular and humoral immunity induced by recombinant adenovirus-mediated gene therapy in cancer patients. *Hum Gene Ther* 2000; **11**: 1911-1920
27 **Wen XY,** Bai Y, Stewart AK. Adenovirus-mediated human endostatin gene delivery demonstrates strain-specific antitumor activity and acute dose-dependent toxicity in mice. *Hum Gene Ther* 2001; **12**: 347-358
28 **Liu Q,** Muruve DA. Molecular basis of the inflammatory response to adenovirus vectors. *Gene Ther* 2003; **10**: 935-940
29 **Geutskens SB,** van der Eb MM, Plomp AC, Jonges LE, Cramer SJ, Ensink NG, Kuppen PJ, Hoeben RC. Recombinant adenoviral vectors have adjuvant activity and stimulate T cell responses against tumor cells. *Gene Ther* 2000; **7**: 1410-1416
30 **Chen P,** Kovesdi I, Bruder JT. Effective repeat administration with adenovirus vectors to the muscle. *Gene Ther* 2000; **7**: 587-595
31 **Pagliaro LC,** Keyhani A, Williams D, Woods D, Liu B, Perrotte P, Slaton JW, Merritt JA, Grossman HB, Dinney CP. Repeated intravesical instillations of an adenoviral vector in patients with locally advanced bladder cancer: a phase I study of p53 gene therapy. *J Clin Oncol* 2003; **21**: 2247-2253
32 **Reid T,** Galanis E, Abbruzzese J, Sze D, Wein LM, Andrews J, Randlev B, Heise C, Uprichard M, Hatfield M, Rome L, Rubin J, Kirn D. Hepatic arterial infusion of a replication-selective oncolytic adenovirus (dl1520): phase II viral, immunologic, and clinical endpoints. *Cancer Res* 2002; **62**: 6070-6079

Edited by Kumar M **Proofread by** Chen WW and Xu FM

PO Box 2345, Beijing 100023, China
Fax: +86-10-85381893
E-mail: wjg@wjgnet.com www.wjgnet.com

World J Gastroenterol 2004;10(13):1872-1875
World Journal of Gastroenterology
 ISSN 1007-9327

• LIVER CANCER •

Primary targeting of recombinant Fv-immunotoxin hscFv$_{25}$-mTNFa against hepatocellular carcinoma

Jing Zhang, Yan-Fang Liu, Shou-Jing Yang, Qing Qiao, Hong Cheng, Chuan-Shan Zhang, Fu-Cheng Ma, Hua-Zhang Guo

Jing Zhang, Yan-Fang Liu, Shou-Jing Yang, Hong Cheng, Chuan-Shan Zhang, Fu-Cheng Ma, Hua-Zhang Guo, Department of Pathology, Xijing Hospital, Fourth Military Medical University, Xi' an 710033, Shaanxi Province, China
Qing Qiao, Department of General Surgery, Tangdu Hospital, Fourth Military Medical University, Xi' an 710038, Shaanxi Province, China
Supported by Military 95 Major Supplementary Project, No.98M098
Correspondence to: Jing Zhang, Department of Pathology, Xijing Hospital, Fourth Military Medical University, Xi' an 710033, Shaanxi Province, China. jzhang@fmmu.edu.cn
Telephone: +86-29-83375497 **Fax:** +86-29-83375497
Received: 2003-12-28 **Accepted:** 2004-01-08

Abstract

AIM: To obtain human recombinant Fv-immunotoxin hscFv$_{25}$-mTNFα (mutant human TNFα fused to human scFv$_{25}$) against hepatocellular carcinoma (HCC).

METHODS: Two relevant sites of enzymatic digestion were added to mTNFα by PCR. mTNFα was linked to the 3' end of hscFv$_{25}$ in pGEX4T-1 vector. This anti-HCC recombinant Fv-immunotoxin hscFv$_{25}$-mTNFα was expressed in *Escherichia coli* and purified from inclusions. After purified by glutathione-S-transferase affinity chromatography and thrombin digestion, it was identified by electrophoresis and Western blot. And then, the purified recombinant Fv-immunotoxin was injected into nude mice with HCC xenografts through their tail veins. mTNFα protein and PBS were used as control at the same time. After treated for two weeks, nude mice were executed. The bulk and weight of tumors were observed. The tumor tissues were stained by immunohistochemical method with TNFα antibody.

RESULTS: The expression ratio of recombinant Fv-immunotoxin hscFv$_{25}$-mTNFα was 12% of bacterial protein. The result of tumor restraining trials of hscFv$_{25}$-mTNFα showed 2/5 complete remission and 3/5 partial remission. mTNFα restraining trials showed 5/5 partial remission. The therapeutic result of hscFv$_{25}$-mTNFα was better than that of mTNFα (F=8.70, P<0.05). The hscFv$_{25}$-mTNFα remedial tumor tissues were positive for TNFα by immunohistochemical staining. The positive granules mainly existed in the cytoplasm of tumor cell.

CONCLUSION: Recombinant Fv-immunotoxin hscFv$_{25}$-mTNFα has better therapeutic effect than mTNFα. It can inhibit the cellular growth of HCC and has some potential of clinical application.

Zhang J, Liu YF, Yang SJ, Qiao Q, Cheng H, Zhang CS, Ma FC, Guo HZ. Primary targeting of recombinant Fv-immunotoxin hscFv$_{25}$-mTNFα against hepatocellular carcinoma. *World J Gastroenterol* 2004; 10(13): 1872-1875
http://www.wjgnet.com/1007-9327/10/1872.asp

INTRODUCTION

Hepatocellular carcinoma (HCC) is a common malignant tumor in China with poor prognosis[1,2]. Its diagnosis and therapy are still major challenges[3,4]. The single chain Fv (scFv) is consisted of heavy-chain and light-chain variable region of the antibody, linked with a peptide chain. They have shown a various application value in tumor therapy[5-7]. Our laboratory, through collaboration with the Academy of Military Medical Science, constructed human scFv$_{25}$ against HCC (hscFv$_{25}$) several years ago[8]. In this study, we fused human mutant tumor necrosis factor-alpha (mTNFα) to hscFv$_{25}$ and constructed prokaryotic expressing vector pGEX4T-1/hscFv$_{25}$-mTNFα. After recombinant Fv-immunotoxin hscFv$_{25}$-mTNFα was expressed, purified and identified, we used it in tumor restraining trials of the HCC (SMMC-7721) xenografts in nude mice.

MATERIALS AND METHODS

Main materials

Isopropyl-1-thio-D-galactopyranoside (IPTG), PCR marker, T4 ligase and thrombin were purchased from Promega. Glutathione-S-transferase affinity chromatogram and low molecular weight marker were purchased from Pharmacia. The plasmid extracting reagent kit was purchased from Huashun Biologic Co. (Shanghai, China). EnVision™ System was purchased from Dako. The mTNFα protein produce was offered by Biologic Center of the Fourth Military Medical University. The mouse anti-human TNFα monoclonal antibody was purchased from Santa Cruz, USA.

Vector construction

According to cDNA of mTNFα, *Sal* I site was added to its 5' -end and *Xho*l I site to its 3' -end. The 5' primer was: ACTCTCGAG TCAGAAGGCAATGATCCCAAAGTA; and the 3' primer was: ACGCGTCGACCGCAAACGTAAGCCTGTA.

The primers were synthesized by Sangon (Shanghai, China). After digested by *Sal* I and *Xho*l I restriction enzymes, mTNFα PCR products were linked to 3' -end of pGEX4T-1/hscFv$_{25}$, which was digested by the same restriction enzymes. And then, pGEX4T-1/hscFv$_{25}$-mTNFα was transformed into *E. coli*. JM109. *E. coli.* were cultivated in the Amp$^+$/LB medium at 37 ℃ for 16-22 h. The positive clones were selected and identified by *Eco*R I and *Sal* I, *Eco*R I and *Xho*l I, *Sal* I and *Xho*l I restriction enzymes analysis and 10 g/L agarose gel electrophoresis.

Recombinant Fv-immunotoxin expression and purification

E. coli. were cultivated at 37 ℃ in LB medium containing 50 g/L ampicillin. When their density reached A_{650}=1.0, bacteria were induced by 1.0 mmol/L IPTG for 3-4 h. And then they were harvested by centrifugation and their inclusions were isolated, purified, denatured and re-natured. After purified by glutathione-S-transferase affinity chromatography, glutathione-S-transferase (GST) was removed by thrombin digestion. The immunotoxin was analyzed by 120 g/L SDS-PAGE.

Western blot

When 120 g/L SDS-PAGE electrophoresis was completed, stacking gel was removed and equilibrated in transfer buffer

(25 mmol/L Tris, 190 mmol/L glycocine, 200 mL/L methanol). The expressing proteins were transferred from gel to NC membrane by electrophoresis. The membrane in heat-sealable plastic bag was blocked with buffer (TBS with 30 g/L bovine serum albumin, BSA) overnight at 4 ℃. After the blocking buffer was removed, the solution with TNFα antibody was added, which was diluted with TBS (containing 10 g/L BSA). And then the membrane was incubated for 1h at 37 ℃. After washed 3 times with TBS, the membrane was transferred to fresh plastic bag containing goat anti-mouse IgG antibody for one hour at 37 ℃ and stained with DAB for 10-20 min.

Tumor therapy

The SMMC-7721 cells were cultivated in RPMI 1640 containing 100 mL/L fetal bovine serum, which was obtained from Gibco BRL. Fifteen immunodeficient nude mice BALB/nu, purchased from our Experiment Animal Center and Shanghai Cellular and Biologic Center, were implanted s.c. 2×10^6 SMMC-7721 cells (PBS suspended) at right rear flank respectively. When tumors grew to a palpable size about 2 mm subcutaneously, fifteen mice were divided into three groups randomly. Each group had five mice. PBS was injected to the first group of mice. Twelve μg mTNFα was injected to each mouse in the second group and 16 μg hscFv$_{25}$-mTNFα was injected to each mouse in the third group. All mice were injected through their tail veins. Fourteen days were one course of therapy. At the end of the second week, the mice were dissected. Their tumors were weighed and examined for morphological evidence of damage, along with lungs and livers. The paraffin sections were prepared for histological examination and immunohistochemical staining.

Immunohistochemical staining

The sections were stained by immunohistochemical method. Those in the control groups were stained according to the same method, with the first antibody substituted by PBS, normal mouse serum and an irrelevant antibody IB$_3$ respectively. All paraffin embedded samples were deparaffined and rehydrated, pretreated for 20 min at 95 ℃ in a microwave oven. After being treated with 3 mL/L H_2O_2 for 30 min to block the endogenous peroxidase, the sections were incubated with 20 mL/L fetal calf serum for 30 min to reduce nonspecific binding, and then the primary TNFα antibody was applied to sections at 4 ℃ overnight. The sections were subsequently incubated with horseradish peroxidase (HR)-labeled goat anti-mouse immunoglobulin at 37 ℃ for 1 h, and stained with DAB-H_2O_2 for 5-10 min and counterstained with hematoxylin.

Statistical methods

The *F* test was used for statistical analysis of tumor bulk and weight among three groups. The criterion of significance was set at $P<0.05$.

RESULTS

Vector construction and verification

One ladder was observed at 450 bp, with the same size as mTNFα. After PCR products were digested by *Sal* I, *Xho*l I and linked to 3' -end of pGEX4T-1/hscFv$_{25}$, which was digested by the same restriction enzymes, the prokaryotic expressing vector pGEX4T-1/hscFv$_{25}$-mTNFα was constructed. Then it was transformed to *E.coli* JM109. The bacteria were cultivated in the Amp$^+$/LB medium at 37 ℃ for 16-22 h. Six clones were selected at random. Three clones had one ladder about 450 bp digested by *Sal* I and *Xho*l I restriction enzymes. After subsequently digested by *Eco*R I and *Xho*l I, *Eco*R I and *Sal* I, 1 180 bp and 730 bp ladders were observed, corresponding well with the size of hscFv$_{25}$-mTNFα and hscFv$_{25}$ (Figure 1).

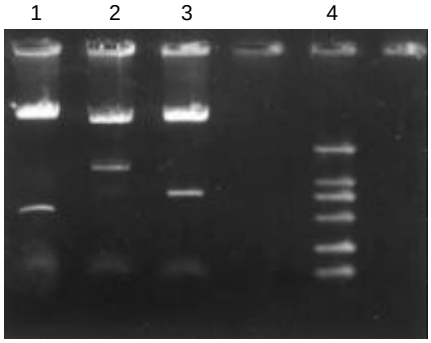

Figure 1 The result of enzyme digested pGEX4T-1 / hscFv$_{25}$-mTNFα. Lane1: mTNFα; Lane 2: hscFv$_{25}$; Line 3: hscFv$_{25}$-mTNFα; Lane 4: DNA ladder (100, 250, 500, 750, 1 000, 2 000 bp).

Fv-immunotoxin expression, purification and identification

The bacteria containing pGEX4T-1/hscFv$_{25}$-mTNFα were induced by IPTG. Compared with the same bacteria without induction by IPTG, there was a new transcript of M_r 68 000, corresponding well with the size of fusion protein GST–hscFv$_{25}$-mTNFα (GST M_r 26 000, hscFv$_{25}$ M_r 26 000, mTNFα M_r 16 000). The result of absorbance scanning showed that the expressing amount of GST-hscFv$_{25}$-mTNFα was 12% bacterial protein. The fusion protein existed in the form of infusibility inclusions. After the inclusions were denatured, renatured, purified by affinity chromatography, only 2 mg preliminarily purified GST–hscFv$_{25}$-mTNFα was obtained from 100 mL bacteria. Digested by thrombin subsequently and purified by GST affinity chromatography again, hscFv$_{25}$-mTNFα protein was obtained. The result of SDS-PAGE showed that proteins were accorded to electrophoresis purification (Figure 2). The GST-hscFv$_{25}$-mTNFα studied by Western blot was seen as a new transcript of M_r 68 000, the same as the fusion protein GST-hscFv$_{25}$-mTNFα.

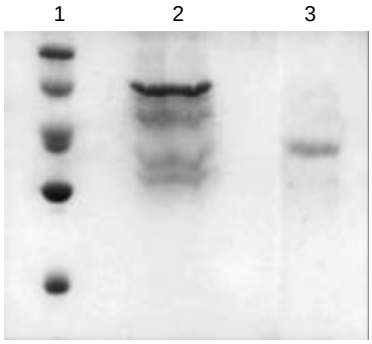

Figure 2 GST-hscFv$_{25}$-mTNFα and hscFv$_{25}$-mTNFα SDS-PAGE Lane 1: Low molecular mass marker (20.1, 31.0, 43.0, 66.2, 97.4 KD); Lane 2: Preliminarily purified GST-hscFv$_{25}$-mTNFα; Lane 3: Purified hscFv$_{25}$-mTNFα.

hscFv$_{25}$-mTNFα targeting therapy

Fifteen nude mice, weighing 16-24 g, were implanted s.c. 2×10^6 SMMC-7721 cells at their right rear flanks and received drug treatment on the tenth day. The tumor of bulk and weight of 15 nude mice were shown in Table 1. The tumor restraining trials of hscFv$_{25}$-mTNFα to HCC xenografts showed 2/5 complete remission (CR) and 3/5 partial remission (PR). The therapeutic result of mTNFα showed 5/5 PR. The therapeutic effectiveness of mTNFα was less than that of hscFv$_{25}$-mTNF-α (F=8.70, $P<0.05$). In the PBS group, tumors showed no remission

Table 1 Targeting therapy of hscFv$_{25}$-mTNFα for HCC xenografts

		Tumor bulk (mm×mm)	Tumor weight (mg)	Regression rate of tumor bulk (%)	Regression rate of tumor weight (%)	Curative effect
PBS	1	9×5	119	0	0	NR
	2	7×7	87	0	0	NR
	3	9×4	51	0	0	NR
	4	5×3	26	0	0	NR
	5	5×4	30	0	0	NR
hscFv$_{25}$	1	0.8×0.5	2	99.2	96.8	PR
-mTNFα	2	2×3	10	81.8	84.0	PR
	3	2×3	15	81.8	76.0	PR
	4	0	0	100	100	CR
	5	0	0	100	100	CR
mTNFα	1	2×2	11	87.9	82.4	PR
	2	3×3	22	72.7	64.9	PR
	3	2×4	5	75.8	76.0	PR
	4	2×3	10	81.8	84.0	PR
	5	2×3	10	81.8	84.0	PR

NR: non-remission; PR: partial remission; CR: complete remission.

(NR). After the liver and lung specimens were sliced up continuously and examined, no metastastic tumors and surviving tumor cells were seen in CR xenografts. The tissues of PR xenografts showed a large number of necrotic areas.

Immunohistochemical staining

The remnant tumor tissues treated by hscFv$_{25}$-mTNFα showed diffusely positive for TNFα. The positive granules mainly existed in the cytoplasm of tumor cells (Figure 3). Immunohistochemical staining with the irrelevant antibody IB$_3$, PBS and normal mouse serum was negative. The tumor tissues treated by PBS showed negative or weak positive for TNFα.

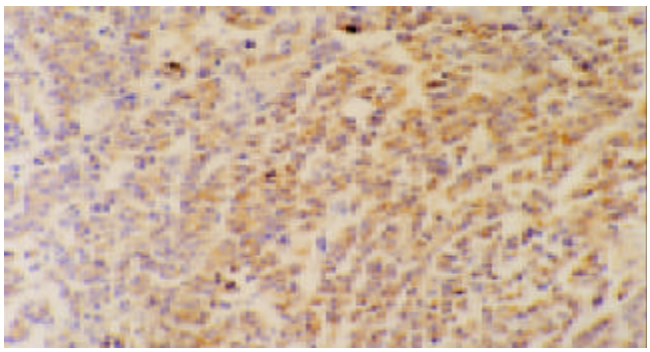

Figure 3 The remnant tumor tissues treated by hscFv$_{25}$-mTNFα were positive for TNFα. The positive granules mainly existed in the cytoplasm of tumor cells. EnVision™ ×200.

DISCUSSION

In the past 20 years, the antibody study has passed through 3 stages: polyclonal antibody, monoclonal antibody and genetic engineering antibody. Among them, the genetic engineering antibody was the most arresting focus of research because of its prominent advantage, such as lower molecular weight, better specificity and affinity[9-12]. It had minimal antigenicity of human against mouse immunoglobulin antibody (HAMA)[13]. Many scFvs against tumors have been used in the phase I-III clinical therapy trials[14-16]. HAb$_{25}$ is a kind of the monoclonal antibody against HCC constructed by our laboratory. The hscFv$_{25}$ against HCC is constructed from HAb$_{25}$. Previous experiment showed that it had better targeting action compared to HAb$_{25}$ [17-19].

The recombinant Fv-immunotoxin was constructed if the scFv C' end was linked to protein toxins, such as pseudomonas exotoxin (PE)[20]. Once bound to the target cells, immunotoxins could kill the tumor cells. Due to PE being nonhuman, to produce effect, it must be internalized into endocytic vesicles where the catalytic protein of the toxin was processed and released into cytosol. Some results of clinical trials using such exotoxin were not satisfactory. Here, we have constructed the single chain recombinant Fv-immunotoxin hscFv$_{25}$-mTNFα. The mTNFα we used was a mutant from natural human TNFα.

The TNFα is one of the strongest active factors in organisms which can kill tumor cells directly. It has severe side effects and is often used in local therapy or targeting therapy by antitumor antibodies[21,22]. Some studies found that the toxicity of TNFα could be reduced by genic fix point mutation or polymeric alteration[23,24]. When natural TNFα' s N-end seven amino acids were cut out and Pro^{8}Ser^{9}Asp^{10} changed to ArgLysArg, and its C-end 157th amino acid of Leu changed to Phe, mTNFα was attained. Compared with natural TNFα, the toxicity of mTNFα was reduced evidently and its cytotoxicity was enhanced greatly[25].

Our study showed the hscFv$_{25}$-mTNFα could kill tumor cells effectively. Compared with dosage of mTNFα and the former experimentation[17], the dosage of hscFv$_{25}$-mTNFα was reduced markedly. Those results revealed that mTNFα could concentrate in tumor tissues and killed tumor cells by the targeting of hscFv$_{25}$. The anti-HCC recombinant Fv-immunotoxin with TNFα replaced by mTNFα could increase its cytotoxicity. Furthermore, we found tumor cells were positive for TNFα in immunohistochemical staining. It also indicated hscFv$_{25}$ had better targeting action.

All these showed the hscFv$_{25}$-mTNFα had better distributive ratio in HCC tissues. It could help local tumor cells to attain a high level of mTNF-α and reduce dose-limiting toxicity. The recombinant Fv-immunotoxin hscFv$_{25}$-mTNFα might have potentiality of clinical application. Due to few nude mice in our study, it maybe lacked rigorous statistical signification. The experimental results need be approved in the future.

REFERENCES

1 **Qian J**, Feng GS, Vogl T. Combined interventional therapies of hepatocellular carcinoma. *World J Gastroenterol* 2003; **9**: 1885-1891

2 **Zeng ZX**, Wang WL, Luo WJ, Wang ZL. Construction of differentially expressed cDNA library in human hepatocellular carcinoma apoptotic cells with suppression subtractive hybridization. *Shijie Huaren Xiaohua Zazhi* 2001; **9**: 1233-1237

3 **Qi YY**, Zhou LG, Wang WX, Chen WJ, Xiang KL, Zhao XY, Yang TH, Yi XZ. Duai-phase enhanced spiral CT in the diagnosis of hepatocellular carcinoma with tumor thrombus in portal vein. *Shijie Huaren Xiaohua Zazhi* 2002; **10**: 384-387

4 **Zhen JY**, Li KZ, Wang WZ. Impact of the expression of P^{27KIPI} on apoptosis and progression of hepatocellular carcinoma. *Shijie Huaren Xiaohua Zazhi* 2002; **10**: 883-886

5 **Rosenblum MG**, Cheung LH, Liu Y, Marks JW 3rd. Design, expression, purification, and characterization, *in vitro* and *in vivo*, of an antimelanoma single-chain Fv antibody fused to the toxin gelonin. *Cancer Res* 2003; **63**: 3995-4002

6 **Reinartz S**, Hombach A, Kohler S, Schlebusch H, Wallwiener D, Abken H, Wagner U. Interleukin-6 fused to an anti-idiotype antibody in a vaccine increases the specific humoral immune response against CA125+ (MUC-16) ovarian cancer. *Cancer Res* 2003; **63**: 3234-3240

7 **Goel A**, Colcher D, Baranowska-Kortylewicz J, Augustine S, Booth BJ, Pavlinkova G, Batra SK. Genetically engineered tetravalent single-chain Fv of the pancarcinoma monoclonal antibody CC49: improved biodistribution and potential for therapeutic application. *Cancer Res* 2000; **60**: 6964-6971

8 **Yuan QA**, Yu WY, Huang CF. Construction and expression of a hepatocellular carcinoma specific rodent and its humanized single-chain Fv fragments in Escherichia coli. *Shengwu Gongcheng Xuebao* 2000; **16**: 86-90

9 **Niv R**, Assaraf YG, Segal D, Pirak E, Reiter Y. Targeting multidrug resistant tumor cells with a recombinant single-chain FV fragment directed to P-glycoprotein. *Int J Cancer* 2001; **94**: 864 -872

10 **McCall AM**, Shahied L, Amoroso AR, Horak EM, Simmons HH, Nielson U, Adams GP, Schier R, Marks JD, Weiner LM. Increasing the affinity for tumor antigen enhances bispecific antibody cytotoxicity. *J Immunol* 2001; **166**: 6112-6117

11 **Cooke SP**, Boxer GM, Lawrence L, Pedley RB, Spencer DI, Begent RH, Chester KA. A strategy for antitumor vascular therapy by targeting the vascular endothelial growth factor: receptor complex. *Cancer Res* 2001; **61**: 3653-3659

12 **van der Poel HG**, Molenaar B, van Beusechem VW, Haisma HJ, Rodriguez R, Curiel DT, Gerritsen WR. Epidermal growth factor receptor targeting of replication competent adenovirus enhances cytotoxicity in bladder cancer. *J Urol* 2002; **168**: 266-272

13 **Whittington HA**, Hancock J, Kemshead JT. Generation of a humanised single chain Fv (scFv) derived from the monoclonal Eric-1 recognising the human neural cell adhesion molecule. *Med Pediatr Oncol* 2001; **36**: 243-246

14 **Turatti F**, Mezzanzanica D, Nardini E, Luison E, Maffioli L, Bambardieri E, de Lalla C, Canevari S, Figini M. Production and validation of the pharmacokinetics of a single-chain Fv fragment of the MGR6 antibody for targeting of tumors expressing HER-2. *Cancer Immunol Immunother* 2001; **49**: 679-686

15 **Mayer A**, Tsiompanou E, O'Malley D, Boxer GM, Bhatia J, Flynn AA, Chester KA, Davidson BR, Lewis AA, Winslet MC, Dhillon AP, Hilson AJ, Begent RH. Radioimmunoguided surgery in colorectal cancer using a genetically engineered anti-CEA single-chain Fv antibody. *Clin Cancer Res* 2000; **6**: 1711-1719

16 **Chester KA**, Bhatia J, Boxer G, Cooke SP, Flynn AA, Huhalov A, Mayer A, Pedley RB, Robson L, Sharma SK, Spencer DI, Begent RH. Clinical applications of phage-derived sFvs and sFv fusion proteins. *Dis Markers* 2000; **16**: 53-62

17 **Sun Z**, Liu Y, Yuan Q, Yu W, Huang C, Ma L, Yu J. Targeting studies of humanized scFv25 fusing to TNFalpha against hepatocellular carcinoma. *Zhonghua Ganzangbing Zazhi* 2000; **8**: 352-354

18 **Cheng H**, Liu YF, Zhang HZ, Shen WN, Zhang J, Zhang J. *In vivo* antitumour activity of PBMCs via genetic modification of single-chain immunotoxin. *Shijie Huaren Xiaohua Zazhi* 2003; **11**: 708-711

19 **Cheng H**, Liu YF, Zhang HZ, Shen WN, Zhang J, Zhang J. *In vitro* cytotoxicity of PBMCs via genetic modification of single-chain immunotoxin. *Shijie Huaren Xiaohua Zazhi* 2003; **11**: 281-284

20 **Fan D**, Yano S, Shinohara H, Solorzano C, Van Arsdall M, Bucana CD, Pathak S, Kruzel E, Herbst RS, Onn A, Roach JS, Onda M, Wang QC, Pastan I, Fidler IJ. Targeted therapy against human lung cancer in nude mice by high-affinity recombinant antimesothelin single-chain Fv immunotoxin. *Mol Cancer Ther* 2002; **1**: 595-600

21 **Thomas PS**, Heywood G. Effects of inhaled tumour necrosis factor alpha in subjects with mild asthma. *Thorax* 2002; **57**: 774-778

22 **Cooke SP**, Pedley RB, Boden R, Begent RH, Chester KA. *In vivo* tumor delivery of a recombinant single chain Fv::tumor necrosis factor-alpha fusion protein. *Bioconjug Chem* 2002; **13**: 7-15

23 **Yamamoto M**, Oshiro S, Tsugu H, Hirakawa K, Ikeda K, Soma G, Fukushima T. Treatment of recurrent malignant supratentorial astrocytomas with carboplatin and etoposide combined with recombinant mutant human tumor necrosis factor-alpha. *Anticancer Res* 2002; **22**: 2447-2453

24 **Terlikowski SJ**. Local immunotherapy with rhTNF-alpha mutein induces strong antitumor activity without overt toxicity-a review. *Toxicology* 2002; **174**: 143-152

25 **Nakamura S,** Kato A, Masegi T, Fukuoka M, Kitai K, Ogawa H, Ichikawa Y, Maeda M, Watanabe N, Kohgo Y. A novel recombinant tumor necrosis factor-alpha mutant with increased anti-tumor activity and lower toxicity. *Int J Cancer* 1991; **48**: 744-748

Edited by Zhu LH **Proofread by** Xu FM

PO Box 2345, Beijing 100023, China
Fax: +86-10-85381893
E-mail: wjg@wjgnet.com www.wjgnet.com

World J Gastroenterol 2004;10(13):1876-1880
World Journal of Gastroenterology
 ISSN 1007-9327

• LIVER CANCER •

Cell apoptosis and regeneration of hepatocellular carcinoma after transarterial chemoembolization

Zhen Li, Dao-Yu Hu, Qian Chu, Jian-Hong Wu, Chun Gao, Yu-Qing Zhang, Yan-Rong Huang

Zhen Li, Dao-Yu Hu, Yu-Qing Zhang, Yan-Rong Huang, Department of Radiology, Tongji Hospital, Tongji Medical College of Huazhong University of Science and Technology, Wuhan 430030, Hubei Province, China
Qian Chu, Department of Neurology, Tongji Hospital, Tongji Medical College of Huazhong University of Science and Technology, Wuhan 430030, Hubei Province, China
Jian-Hong Wu, Chun Gao, Department of Surgery, Tongji Hospital, Tongji Medical College of Huazhong University of Science and Technology, Wuhan 430030, Hubei Province, China
Supported by the Natural Science Foundation of Hubei Province, No. 2002AB130
Correspondence to: Dr. Zhen Li, Department of Radiology, Tongji Hospital, Tongji Medical College of Huazhong University of Science and Technology, Wuhan 430030, Hubei Province, China. doclizhen@hotmail.com
Telephone: +86-27-83663575 **Fax:** +86-27-83643059
Received: 2003-05-11 **Accepted:** 2003-06-02

Abstract

AIM: To evaluate whether cell apoptosis and regeneration were existed in normal liver cells adjacent to carcinoma after transarterial chemoembolization (TACE).

METHODS: Fifty rabbits with hepatic carcinoma were divided into 5 groups at random: group A (control group), groups B and C (TACE treatment groups), groups D and E (partial hepatectomy groups). There were 10 rabbits in each group. Rabbits in groups B-E were treated by transarterial chemoembolization (TACE) and partial hepatectomy (PH) respectively. The changes of S-phase cell fraction (SPF), proliferation index (PI) and cell apoptosis in the normal liver tissue were determined with flow cytometry (FCM) after operations on the first and third days. We determined the mitosis index (MI) with histo-pathological method and the apoptosis index (AI) with TUNEL method at the same time.

RESULTS: Twenty-four hours after operations, compared with control group, the rabbits in TACE group had much higher index of SPF, PI and MI (MI: t=4.89, P<0.001; SPF: t=5.27, P<0.001; PI: t=4.87, P<0.001). Moreover, the proliferation of liver cells in TACE group was much weaker than that of the cells treated by partial hepatectomy, and the differences were significant (MI: t=7.02, P<0.001; SPF: t=4.06, P<0.001; PI: t=2.70, P<0.05). Seventy-two h after operations, FCM showed a small sub-G1 peak in TACE group and PH group, compared with the control group, but there was no difference between them (t=0.41, P>0.05). TACE showed that AI in the treated rabbits was higher than that in control group (t=3.07, P<0.05), and there were no differences between TACE group and PH group, either (t=0.93, P>0.05).

CONCLUSION: Cell apoptosis and regeneration exist in rabbit liver tissues after TACE in some degree, which may be associated with the selective embolization of iodised oil, chemotherapeutic drug and free radical damage.

Li Z, Hu DY, Chu Q, Wu JH, Gao C, Zhang YQ, Huang YR. Cell apoptosis and regeneration of hepatocellular carcinoma after transarterial chemoembolization. *World J Gastroenterol* 2004; 10(13): 1876-1880
http://www.wjgnet.com/1007-9327/10/1876.asp

INTRODUCTION

The efficacy of transarterial chemoembolization (TACE) is greatly determined by the liver function reserve of liver cancer patients. More than 40% patients died of liver failure after TACE, in which most of them were accompanied by poor liver function and damage due to chemotherapy. Therefore, it is important to study the effects of TACE on non-neoplastic liver tissue to decrease the death rate. We have established the animal model of rabbit VX2 hepatic carcinoma. All the rabbits were treated by TACE to detect the effect on cell cycle of non-neoplastic liver tissues after operations[1].

MATERIALS AND METHODS

Establishment of the animal model

Fifty Japanese alpine hares, weighing 2.5-3.3 kg, provided by the Experiment Animal Center of Tongji Medical College were used in this experiment. The rabbits were implanted hepatocellular carcinoma cell VX2, and observed for 3 wk before experiment[2].

Treatment and radiological examination[3,4]

Fifty rabbits with VX2 hepatic carcinoma were randomly divided into 5 groups: Group A (control group), groups B and C (TACE treatment groups), groups D and E (partial hepatectomy groups), 10 rabbits in each group. Three weeks later, at laparotomy of the rabbits, the feeding artery of liver carcinoma was punctured and arteriography was made[5]. A 1 mL of physiological saline was administered to group A. Groups B and C were treated with 0.6-0.8 mL of a mixture of iodine oil (10 mL) and mitomycin (10 mg)[6,7]. Groups D and E were treated by hepatectomy. Groups B and C were performed CT and MRI after TACE[8,9].

Flow cytometry analysis

Rabbits in groups A, B and C were killed on the first day after the procedure, and those in groups D and E were killed on the third day after the procedure. As soon as the rabbits died, a piece of non-neoplastic liver tissue was cut from each rabbit and digested with enzymes. The cells were fixed by 800 mL/L ice ethanol, hatched by 40 μL PC on ice for 30 min, and washed in 1 g/L PBS. At last, they were stained by at 100 μL PI 10 mg/L and 50 μL 1 g/L RNA enzyme for 20 min, then flow cytometry was performed. The cells were detected by FAC Sort FCM machine (Beton Dickson Co, USA). The fluorescence of cells was analyzed with Cellquest software and the cell cycle was studied. The other liver tissues were photographed, fixed with 40 g/L formaldehyde, and stained by HE[10].

Groups B and C were performed CT after TACE, and accumulation of iodized oil was observed. General pathological changes of carcinoma were detected in all the rabbits. Under the microscope, we calculated the number of liver cells in the mitosis

phase per 1 000 liver cells, which was called mitosis index (MI).

FCM analysis

S phase cell fraction (SPF) was calculated according to the equation: SPF=S/(S+G1/G0+G2/M)×100%. Proliferation index (PI) was calculated according to the equation: PI=(S+G2/M)/(S+G1/G0+G2/M)×100%. Apoptosis index (AI) was analyzed by TUNEL method[11], the number of apoptotic cells was calculated under microscope[12].

Statistic analysis

All the data were analyzed by *t* test.

RESULTS

General pathological and radiological findings

Three wk after tumor implantation, the size of VX2 liver carcinoma was 3.5±1.6 cm on average, and appeared as white nodules near the liver surface. There were no definite margins between carcinomas and normal liver tissues. On DSA, there was increased and irregular angiogenesis of the tumor vessels, with tumor stained mainly at the periphery (Figure 1). On MR, the signal of cancer was slightly lower than that of normal liver tissue on T1WI and slightly higher on T2WI (Figure 2). The iodized oil deposited well after TACE on CT[13] (Figure 3).

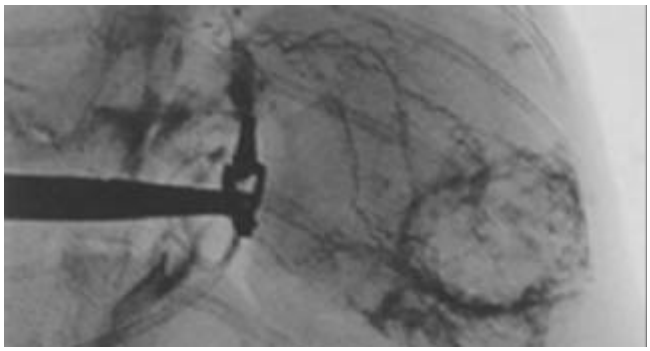

Figure 1 Hepatic arteriography of rabbits. There was increased angiogenesis with thickening and irregularity of the vessels. There was also tumor staining mainly in the periphery of the tumor.

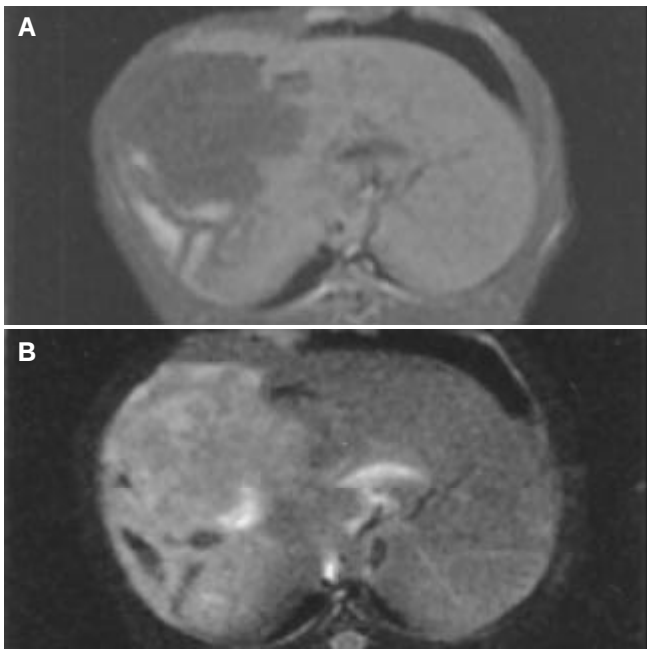

Figure 2 MRI of rabbit liver. The tumor appeared hypointense on T1WI (A) and hyperintense on T2WI (B).

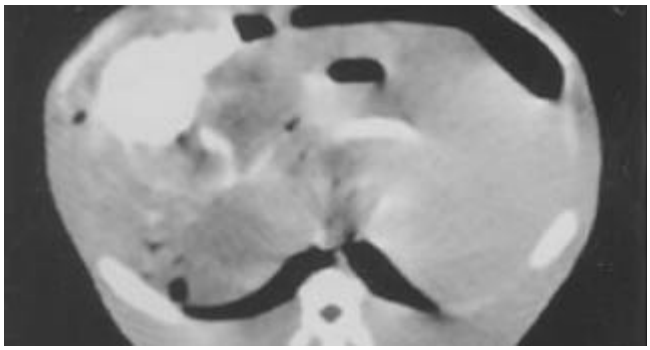

Figure 3 CT scan shows massive retention of iodized oil in tumor after TACE.

Cytological changes

Red fluorescent light could be seen in the cells under laser confocal microscope (Figure 4). Under light microscope (Olympus), we could find cell mitosis clearly, and mitosis index (MI) could be calculated. Flow cytometry showed that S phase and G2/M phase cells in TACE groups and partial hepatectomy groups increased much more on the first day after operations than that in the control group (Figure 5). On the third day after operations, the amount of S-phase and G2/M phase cells in TACE group and partial hepatectomy group was about the same as control group (Figure 6). In the cell apoptosis index (AI) determined by TUNEL method, no significant difference existed between TACE group (Figure 7) and partial hepatectomy group.

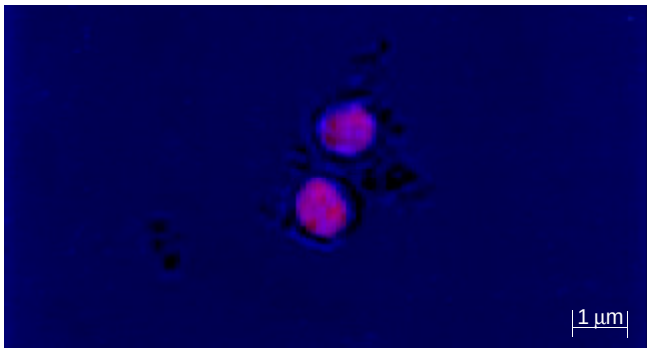

Figure 4 Cells giving out red fluorescent light under laser confocal microscope.

The *t* test values of MI, SPF and PI of TACE groups and control group are listed in Table 1. The *t* test values of MI, SPF and PI of TACE groups and partial hepatectomy groups are listed in Table 2.

Table 1 *t* test value of MI, SPF and PI of TACE groups and control group on the first day after operations

Index	TACE group	Control group	*t* value	*P* value
MI (%)	1.42±0.55	0.51±0.21	4.89	*P*<0.001
SPF (%)	12.46±4.18	4.90±1.76	5.27	*P*<0.001
PI (%)	23.38±8.31	9.93±2.68	4.87	*P*<0.001

Table 2 *t* test value of MI, SPF and PI of TACE groups and partial hepatectomy group on the first day after operations

Index	TACE group	Partial hepatectomy group	*t* value	*P* value
MI (%)	1.42±0.55	3.13±0.54	7.02	*P*<0.001
SPF (%)	12.46±4.18	21.76±5.92	4.06	*P*<0.001
PI (%)	23.38±8.31	32.51±6.75	2.70	*P*<0.05

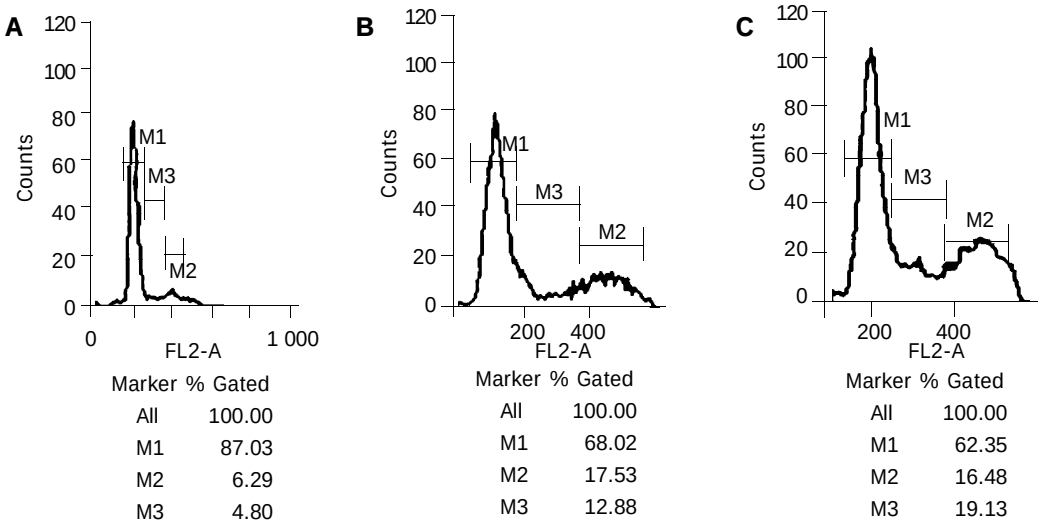

Figure 5 A: Shows the S phase and G2/M phase cells were small in proportion on the first day after operations (4.80%, 6.29%) in control group. B: Shows the S phase and G2/M phase cells grew much more on the first day after operations (17.53%, 12.88%) in TACE group. C: Shows the S phase and G2/M phase cells grew much more on the first day after operations (16.48%, 19.13%) in PH group. *M1 is G0/G1 phase cell ratio/M2 is G2/M phase cell ratio, M3 is S phase cell ratio.

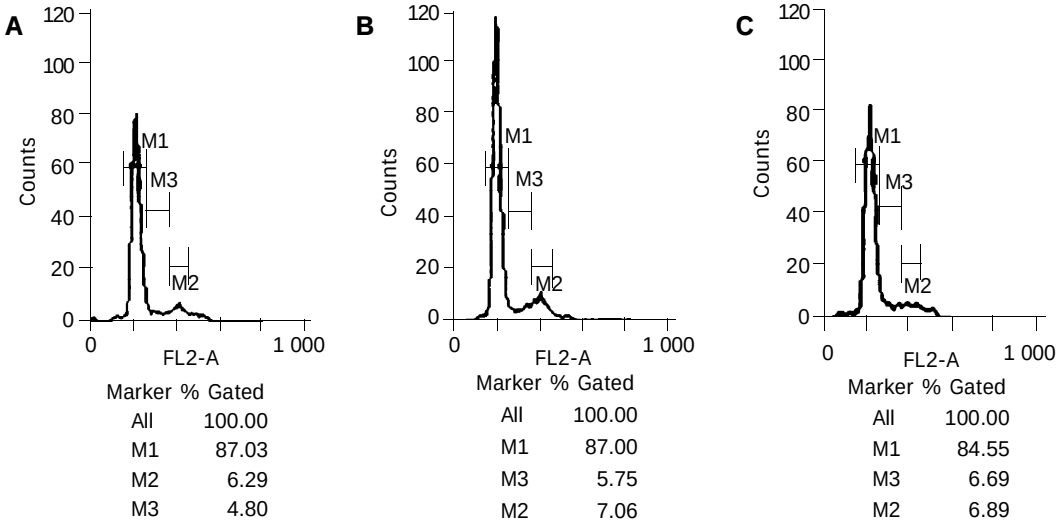

Figure 6 A: Shows the S phase and G2/M phase cells were small in proportion on the third day after operations (4.80%, 6.29%) in control group. B and C: Show the S phase and G2/M phase cells had slight changes on the third day after operations in TACE group and PH group.

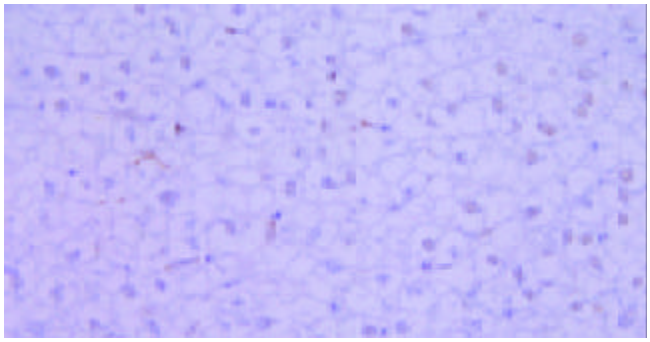

Figure 7 Analysis of apoptosis cells by TUNEL method in TACE group. The nuclei of apoptosis cells appeared brown while those of normal cells appeared blue. It was found that part of the cells were apoptotic cells.

The *t* test values of MI, SPF of TACE groups and control group are listed in Table 3. There was no significant difference between the two groups ($P>0.05$). However, the *P* value of AI and sub-G1 was less than 0.05. The *t* test values of MI, SPF, AI and PI of TACE groups and partial hepatectomy groups are listed in Table 4.

Table 3 *t* test value of MI, SPF, AI, Sub-G1 and PI of TACE groups and control group on the third day after operations

Index	TACE group	Control group	*t* value	*P* value
MI (%)	0.62±0.33	0.51±0.21	0.88	$P>0.05$
SPF (%)	5.70±1.93	4.90±1.76	0.95	$P>0.05$
PI (%)	11.69±1.74	9.93±2.68	1.68	$P>0.05$
Sub-G1 (%)	2.31±1.57	1.18±0.45	2.18	$P<0.05$
AI (%)	20.33±2.36	13.68±1.97	3.07	$P<0.05$

Table 4 *t* test value of MI, SPF, sub-G1 and PI of TACE groups and partial hepatectomy group on the third day after operations

Index	TACE group	Partial hepatectomy group	*t* value	*P* value
MI(%)	0.62±0.33	0.81±0.30	1.28	$P>0.05$
SPF(%)	5.70±1.93	6.62±1.56	1.34	$P>0.05$
PI(%)	11.69±1.74	11.85±2.00	0.17	$P>0.05$
Sub-G1 (%)	2.31±1.57	2.05±1.07	0.41	$P>0.05$
AI(%)	20.33±2.36	22.69±3.79	0.93	$P>0.05$

DISCUSSION

Transarterial chemoembolization (TACE) has been one of the most important and commonly used methods for treatment of hepatocarcinoma[14]. Because most patients died of liver failure after TACE[15,16], it is important to study the condition of postoperative normal liver tissues[17]. The most precise method to evaluate hepatocyte reproduction and apoptosis has been the study of cell cycle[18]. In our research, normal hepatocytes were isolated, fixed and stained, flow cytometry (FCM) was performed and DNA was analyzed. Results showed SPF, PI and MI value of TACE group was much higher than that of control group ($P<0.001$, Table 1). We could conclude that there existed liver regeneration after TACE. From Table 2 at the same time, we could find that hepatocyte regeneration in PH group was stronger than that in TACE group on the first day ($P<0.05$). On the third day after TACE, the difference between TACE group and control group was not significant in all indexes. Furthermore, the difference between TACE group and PH group was not significant either on the third day. From these data, we could conclude that the regeneration process stopped, most of the cells entered the dormancy phase (G_0 phase). However, the value of hypodiploid peak (sub-G1) increased on the third day after TACE ($t=2.18$, $P<0.05$). The difference of sub-G1 between TACE group and PH group was obvious ($P>0.05$, Tables 3, 4). The apoptosis index (AI) became greater on the third day after TACE.

Cell apoptosis (programmed cell death) means the maintenance of stability of internal environment, i.e. the process of autonomic programmed cell death has been controlled by gene[19]. After partial hepatectomy, the hepatocytes would regenerate soon. At the peak of regeneration, cell apoptosis begins. Accompanying cell reproduction, cell apoptosis would eliminate the overgrown cells, and rebuilding of the tissue constitution is achieved. Some authors[20]pointed out that the process was mitogen→cell reproduction→regeneration→cell apoptosis. It was different from the necrosis caused by liver cytotoxic material, which was in the order of cytotoxic material →necrosis→compensatory hyperplasia→cell regeneration. Liver tissue regeneration after PH has been studied comprehensively. When the liver is resected less than 70%, the regeneration is proportional to the volume of the resected portion. Mitosis reaches the peak in 24 h, and completes in 72 h. Liver tissue regeneration exists also after TACE, this is due to the effect of super-selective embolization with iodized oil. The liver regeneration in TACE group was weaker than that in PH group, the reason was that the extent of "medical hepatectomy" was much smaller[21]. However, from Tables 3 and 4, we could find the apoptosis levels between TACE and hepatectomy groups. The apoptosis level following liver regeneration was directly proportional to the regeneration level. It is easy to draw the conclusion that there must exist a new mechanism, which promotes cell apoptosis after TACE. The mechanism might be that mitomycin depressed DNA synthesis and promoted cell apoptosis[22]. Some authors[23] pointed out that mitomycin (5 mg/mL) could cause cell apoptosis after 24 h. Almost all chemotherapeutic drugs could induce cell apoptosis by different ways[24]. For example, vincristine (VCR) and colchicine could induce cell apoptosis by disturbance of microtubule function→loss of hepatocyte function→ identification of the injury by hepatocytes→decrease of protein synthesis→increase of [Ca2+] activation of endonuclease and protein kinase→DNA split→cell apoptosis[25]. On the other hand, there were ischemia and hypoxia of locally embolized tissue, and release of a large amount of free radicals and cell toxins[26,27]. They could induce cell apoptosis[28,29]. For example, free radicals could injure DNA which would lead to activation of polydioadenosine phosphate pibotransferase[30]and accumulation of p53. A cell calcium ion would cause cell apoptosis. It could activate nucleus transcription factors such as NF-κB which would induce cell apoptosis[31]. Normal hepatocyte apoptosis was mainly resulted from the effects of chemotherapeutic drugs and free radical injury rather than from normal tissue repair[32,33].

The regeneration and apoptosis level of normal hepatocytes usually determine the patients' prognosis after transarterial chemoembolization. The obvious apoptosis after TACE was due to chemotherapeutic drugs and free radicals, which made the normal process of apoptosis more rapid. Therefore, excessive dosage of chemotherapeutic drugs may promote apoptosis and injury of normal hepatocytes in non-neoplastic area of the liver, and deteriorate the liver function of patients. We can draw the conclusion that it is important to use chemotherapeutic drugs, because they can protect the liver function of patients and improve their survival rate after treatment.

REFERENCES

1 **El Khaddari S**, Gaudin JL, Abidi H, Picaud G, Rode A, Souquet JC. Chemoembolization in hepatocellular carcinoma: multivariate analysis of survival prognostic factors after the first session. *Gastroenterol Clin Biol* 2002; **26**: 728-734

2 **Lin WY**, Chen J, Lin Y, Han K. Implantation of VX2 carcinoma into the liver of rabbits: a comparison of three direct-injection methods. *J Vet Med Sci* 2002; **64**: 649-652

3 **Li X**, Zheng CS, Feng GS, Zhuo CK, Zhao JG, Liu X. An implantable rat liver tumor model for experimental transarterial chemoembolization therapy and its imaging features. *World J Gastroenterol* 2002; **8**: 1035-1039

4 **Shiozawa S**, Tsuchiya A, Endo S, Kumazawa K, Ogawa K. Transradial approach for transcatheter arterial chemoembolization in patients with hepatocellular carcinoma. *Nippon Shokakibyo Gakkai Zasshi* 2002; **99**: 1450-1454

5 **Yi J**, Liao X, Yang Z, Li X. Study on the changes in microvessel density in hepatocellular carcinoma following transcatheter arterial chemoembolization. *J Tongji Med Univ* 2001; **21**: 321-331

6 **Chen M**, Li J, Zhang Y. Transarterial chemoembolization with high dose iodized oil for the treatment of large hepatocellular carcinoma. *Zhonghua Zhongliu Zazhi* 2001; **23**: 165-167

7 **Pacella CM**, Bizzarri G, Cecconi P, Caspani B, Magnolfi F, Bianchini A, Anelli V, Pacella S, Rossi Z. Hepatocellular carcinoma: long-term results of combined treatment with laser thermal ablation and transcatheter arterial chemoembolization. *Radiology* 2001; **219**: 669-678

8 **Liu H**, Li D, Yang S, Wu Y. Efficacy of TACE in treatment of intraportal tumor thrombi with double helical CT. *Hunan Yike Daxue Xuebao* 1999; **24**: 47-49

9 **Kim HC**, Kim AY, Han JK, Chung JW, Lee JY, Park JH, Choi BI. Hepatic arterial and portal venous phase helical CT in patients treated with transcatheter arterial chemoembolization for hepatocellular carcinoma: added value of unenhanced images. *Radiology* 2002; **225**: 773-780

10 **Jia HS**, Quan XY, Zeng S, Wen ZB. Dynamic evaluation of rabbit VX2 hepatic carcinoma with CT and MRI. *Diyi Junyi Daxue Xuebao* 2002; **22**: 141-144

11 **Xiao E**, Li D, Shen S, Zhou S, Tan L, Wang Y, Luo J, Wu Y, Tan C, Liu H, Zhu H. Effect of preoperative transcatheter arterial chemoembolization on apoptosis of hepatocellular carcinoma cells. *Chin Med J* 2003; **116**: 203-207

12 **Sano B**, Sugiyama Y, Kunieda K, Sano J, Saji S. Antitumor effects induced by the combination of TNP-470 as an angiogenesis inhibitor and lentinan as a biological response modifier in a rabbit spontaneous liver metastasis model. *Surg Today* 2002; **32**: 503-509

13 **Vogl TJ**, Eichler K, Zangos S, Mack M, Hammerstingl R. Hepatocellular carcinoma: Role of imaging diagnostics in detection, intervention and follow-up. *Rofo Fortschr Geb Rontgenstr Neuen Bildgeb Verfahr* 2002; **174**: 1358-1368

14 **Barone M**, Ettorre GC, Ladisa R, Schiavariello M, Santoro C, Francioso G, Vinciguerra V, Francavilla A. Transcatheter arterial chemoembolization (TACE) in treatment of hepatocellular carcinoma. *Hepatogastroenterology* 2003; **50**: 183-187

15 **Ramsey DE**, Kernagis LY, Soulen MC, Geschwind JF.

Chemoembolization of hepatocellular carcinoma. *J Vasc Interv Radiol* 2002; **13**(9 Pt 2): S211-221

16 **Huang YS,** Chiang JH, Wu JC, Chang FY, Lee SD. Risk of hepatic failure after transcatheter arterial chemoembolization for hepatocellular carcinoma: predictive value of the monoethylglycinexylidide test. *Am J Gastroenterol* 2002; **97**: 1223-1227

17 **Grieco A**, Marcoccia S, Miele L, Marmiroli L, Caminiti G, Ragazzoni E, Cotroneo AR, Cefaro GA, Rapaccini GL, Gasbarrini G. Transarterial chemoembolization (TACE) for unresectable hepatocellular carcinoma in cirrhotics: functional hepatic reserve and survival. *Hepatogastroenterology* 2003; **50**: 207-212

18 **Schuchmann M**, Galle PR. Apoptosis in liver disease. *Eur J Gastroenterol Hepatol* 2001; **13**: 785-790

19 **Wright MC**, Issa R, Smart DE, Trim N, Murray GI, Primrose JN, Arthur MJ, Iredale JP, Mann DA. Gliotoxin stimulates the apoptosis of human and rat hepatic stellate cells and enhances the resolution of liver fibrosis in rats. *Gastroenterology* 2001; **121**: 685-698

20 **Neuman MG**. Apoptosis in diseases of the liver. *Crit Rev Clin Lab Sci* 2001; **38**: 109-166

21 **Saccheri S**, Lovaria A, Sangiovanni A, Nicolini A, De Fazio C, Ronchi G, Fasani P, Del Ninno E, Colombo M. Segmental transcatheter arterial chemoembolization treatment in patients with cirrhosis and inoperable hepatocellular carcinomas. *J Vasc Interv Radiol* 2002; **13**: 995-999

22 **Durand RE**, LePard NE. Effects of mitomycin C on the oxygenation and radiosensitivity of murine and human tumours in mice. *Radiother Oncol* 2000; **56**: 245-252

23 **Castaneda F**, Kinne RK. Effects of doxorubicin, mitomycin C, and ethanol on Hep-G2 cells *in vitro*. *J Cancer Res Clin Oncol* 1999; **125**: 1-8

24 **Sato N**, Mizumoto K, Maehara N, Kusumoto M, Nishio S, Urashima T, Ogawa T, Tanaka M. Enhancement of drug-induced apoptosis by antisense oligodeoxynucleotides targeted against Mdm2 and p21WAF1/CIP1. *Anticancer Res* 2000; **20**: 837-842

25 **Crenesse D**, Gugenheim J, Hornoy J, Tornieri K, Laurens M, Cambien B, Lenegrate G, Cursio R, De Souza G, Auberger P, Heurteaux C, Rossi B, Schmid-Alliana A. Protein kinase activation by warm and cold hypoxia- reoxygenation in primary-cultured rat hepatocytes-JNK (1)/SAPK (1) involvement in apoptosis. *Hepatology* 2000; **32**: 1029-1036

26 **Ben-Ari Z**, Hochhauser E, Burstein I, Papo O, Kaganovsky E, Krasnov T, Vamichkim A, Vidne BA. Role of anti-tumor necrosis factor-alpha in ischemia/reperfusion injury in isolated rat liver in a blood-free environment. *Transplantation* 2002; **73**: 1875-1880

27 **Kobayashi T**, Sugawara Y, Ohkubo T, Imamura H, Makuuchi M. Effects of amrinone on hepatic ischemia-reperfusion injury in rats. *J Hepatol* 2002; **37**: 31-38

28 **Barros LF**, Stutzin A, Calixto A, Catalan M, Castro J, Hetz C, Hermosilla T. Nonselective cation channels as effectors of free radical-induced rat liver cell necrosis. *Hepatology* 2001; **33**: 114-122

29 **Karbowski M**, Kurono C, Wozniak M, Ostrowski M, Teranishi M, Nishizawa Y, Usukura J, Soji T, Wakabayashi T. Free radical-induced megamitochondria formation and apoptosis. *Free Radic Biol Med* 1999; **26**: 396-409

30 **Song BC**, Suh DJ, Yang SH, Lee HC, Chung YH, Sung KB, Lee YS. Lens culinaris agglutinin-reactive alpha-fetoprotein as a prognostic marker in patients with hepatocellular carcinoma undergoing transcatheter arterial chemoembolization. *J Clin Gastroenterol* 2002; **35**: 398-402

31 **Factor V**, Oliver AL, Panta GR, Thorgeirsson SS, Sonenshein GE, Arsura M. Roles of Akt/PKB and IKK complex in constitutive induction of NF-kappaB in hepatocellular carcinomas of transforming growth factor alpha/c-myc transgenic mice. *Hepatology* 2001; **34**: 32-41

32 **Won JY**, Lee do Y, Lee JT, Park SI, Kim MJ, Yoo HS, Suh SH, Park SJ. Supplemental transcatheter arterial chemoembolization through a collateral omental artery: treatment for hepatocellular carcinoma. *Cardiovasc Intervent Radiol* 2003; **26**: 136-140

33 **Zaragoza A**, Diez-Fernandez C, Alvarez AM, Andres D, Cascales M. Mitochondrial involvement in cocaine-treated rat hepatocytes: effect of N-acetylcysteine and deferoxamine. *Br J Pharmacol* 2001**; 132**: 1063-1070

Edited by Wang XL and Zhu LH **Proofread by** Xu FM

PO Box 2345, Beijing 100023, China
Fax: +86-10-85381893
E-mail: wjg@wjgnet.com www.wjgnet.com

World J Gastroenterol 2004;10(13):1881-1884
World Journal of Gastroenterology
 ISSN 1007-9327

• LIVER CANCER •

Transjugular intrahepatic portosystemic shunt for palliative treatment of portal hypertension secondary to portal vein tumor thrombosis

Zai-Bo Jiang, Hong Shan, Xin-Ying Shen, Ming-Sheng Huang, Zheng-Ran Li, Kang-Shun Zhu, Shou-Hai Guan

Zai-Bo Jiang, Hong Shan, Xin-Ying Shen, Ming-Sheng Huang, Zheng-Ran Li, Kang-Shun Zhu, Shou-Hai Guan, Department of Radiology, the 3rd Affiliated Hospital of Sun Yat-Sen University, Guangzhou 510630, Guangdong Province, China
Correspondence to: Dr. Hong Shan, the 3rd Affiliated Hospital of Sun Yat-Sen University, Guangzhou 510630, Guangdong Province, China. jzb01@163.net
Telephone: +86-20-85516867 **Fax:** +86-20-87580725
Received: 2003-12-28 **Accepted:** 2004-01-08

Abstract

AIM: To evaluate the palliative therapeutic effects of transjugular intrahepatic portosystemic shunt (TIPS) in portal vein tumor thrombosis (PVTT) complicated by portal hypertension.

METHODS: We performed TIPS for 14 patients with PVTT due to hepatocellular carcinoma (HCC). Of the 14 patients, 8 patients had complete occlusion of the main portal vein, 6 patients had incomplete thrombosis, and 5 patients had portal vein cavernous transformation. Clinical characteristics and average survial time of 14 patients were analysed. Portal vein pressure, ascites, diarrohea, and variceal bleeding and circumference of abdomen were assessed before and after TIPS.

RESULTS: TIPS was successful in 10 cases, and the successful rate was about 71%. The mean portal vein pressure was reduced from 37.2 mmHg to 18.2 mmHg. After TIPS, the ascites decreased, hemorrhage stopped and the clinical symptoms disappeared in the 10 cases. The average survial time was 132.3 d. The procedure failed in 4 cases because of cavernous transformation in portal vein and severe cirrhosis.

CONCLUSION: TIPS is an effective palliative treatment to control hemorrhage and ascites due to HCC complicated by PVTT.

Jiang ZB, Shan H, Shen XY, Huang MS, Li ZR, Zhu KS, Guan SH. Transjugular intrahepatic portosystemic shunt for palliative treatment of portal hypertension secondary to portal vein tumor thrombosis. *World J Gastroenterol* 2004; 10(13): 1881-1884
http://www.wjgnet.com/1007-9327/10/1881.asp

INTRODUCTION

TIPS is effective in treating patients with hemorrhage, intractable ascites and portal hypertensive gastropathy, and many favorable results and experiences have been obtained as well[1-7]. TIPS has been widely used for portal hypertension with portal vein thrombosis (PVT), type-III Budd-Chiari syndrome, even bile duct occlusive diseases, and other portal hypertension[8-17]. But how to treat primary hepatocarcinoma with secondary portal hypertension is a challenge. In 1995, Zhang[18] first reported the clinical experiences that TIPS procedure was applied to HCC patients with variceal hemorrhage, but the portal vein must be opened before TIPS. There were no reports about whether TIPS could be a palliative method for portal vein tumor thrombosis (PVTT). Since 1998 we have tried to study TIPS in the treatment of portal hypertension secondary to PVTT.

MATERIALS AND METHODS

Clinical data

There were 14 patients with end-stage HCC in our hospital from December 1998 to May 2001, 13 men and one woman. The patients aged from 28 to 75 years, and the average age was 56.3 years. Three patients did not receive any treatment before TIPS and the others were treated with transarterial chemoembolization (TACE) and other procedures. One patient survived for 6 years after 8 times of TACE, and 2 patients emerged ascites and hemorrhage after they were treated by radiofrequency ablation. Of the 14 patients, there were three patients with intractable ascites, one patient with simple hemorrhage and 10 patients with hemorrhage and ascites (Tables 1, 2). Their hepatic function was poor and assigned to Child-Pugh class C. The diagnosis of PVTT was based on contrast-enhanced CT and color Doppler sonography while the cavernous transformation in the portal vein was detected by color Doppler sonography, contrast-enhanced CT and angiography.

TIPS procedure

TIPS was performed by using the RTPS 100 (Cook, America) portal venous puncture set. After administration of local anesthetic (20 g/L lidocaine hydrochloride) the Colapinto needle (Cook, America) was advanced into the right hepatic vein, and then the right portal vein was punctured. A wire guide (hydrophilic coating wire guide, Terumo) was introduced through the needle. Because of stenosis, occlusion and cavernous transformation of portal vein trunk and its right and left branches, puncture was difficult. So small branches were also available. With a guiding wire the catheter was advanced into the portal vein trunk. After measurement of the portal venous pressure, the needle track was dilated with a balloon (10 mm-diameter, 40 mm-length). Then an expandable stent (8-10 mm-diameter, 6-8 cm-length) was placed. The number of stents was based on the length of the shunt tract to ensure the stents covering all along stenosis segments arising from tumor emboli. The portal venous pressure was also measured after shunt was established.

RESULTS

The portosystemic shunt was successful in 10 of 14 patients. Shunt tract was achieved with a single stent in four patients, two stents in four patients, and four stents in two patients. The mean portal pressure was 37.2 mmHg and 18.2 mmHg before

and after TIPS. The mean abdomen circumference was 86.3 cm and 77.65 cm before and after the procedure (Table 1). TIPS could be performed for four patients with incomplete occlusion of portal vein trunk as standard TIPS (Figure 1), while it could be performed for six patients with complete occlusion of portal vein trunk by introducing hydrophilic coating wire guide through the potential vascular lumen to superior mesenteric vein (Figure 2). The 4 patients with cavernous transformation in portal vein and severe cirrhosis failed to TIPS procedure, no portal vein trunk and branches but vascular plexus sign was displayed on angiogram. They had no improvement in clinical symptoms and their mean survival time was 34 days, shorter than the successful ones. The needles were punctured out of liver and into the peritoneum cavity in two patients, but they had no severe complications during and after the procedure. The needle tract was passed through the tumor in one patient, but no metastasis was found in 3 mo of follow-up. In all patients the mean content of serum bilirubin and aminotransferase increased transiently after TIPS procedure, and improved after one week of treatment.

Table 1 Clinical characteristics of 14 patients assigned to treatment with transjugular intrahepatic portosystemic stent-shunt procedure

Characteristic	Value
Age (yr)	
Range	28-75
mean±SD	53.6±12.7
Sex (M/F)	13/1
Occlusion of portal vein	
Portal vein trunk (complete/ incomplete)	10/4
Right branch (complete/ incomplete)	10/1
Left branch (complete/ incomplete)	2/2
Tumor type (nodular/massive/diffuse)	2/6/6
With cavernous transformation of PV	5
Times of TACE (mean±SD)	3.7±1.8

Table 2 Portal pressure, ascites and clinical symptoms before and after TIPS procedure in 10 patients receiving stents (mean±SD)

	Before procedure	After procedure	(t/χ^2 value)	*P* Value
Portal vein pressure (mmHg)	37.5±4.8	18.2±1.8	t:13.032	0.000
Circumference of abdomen (cm)	85.3±4.7	79.2±5.2	t:3.823	0.002
Ascites				
Mild	3	8		
Moderate	1	4		
Severe	10	2		
Diarrohea (times/d)	3.8±4.4	0±0	t:3.202	0.007
Hepatic encephalopathy				
0	9	9		
I	3	5		
II	2	0		
Variceal bleeding (times)	1.9±1.5	0±0	T:4.759	0.000

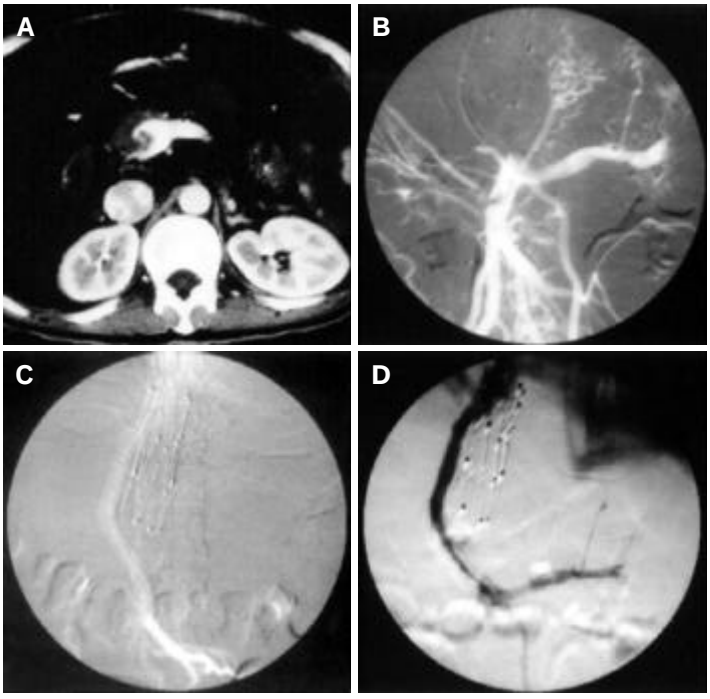

Figure 1 TIPS procedure in patient with incomplete occlusion of portal vein trunk. A: Main portal vein dilation with eccentric tumor thrombi shoven on enhanced Ctgram. B: Superior mesenteric vein dilation with eccentric filling defect and main portal vein occlusion shown on superior mesenteric vein angiogram. C: Open shunt shown on superior mesenteric vein angiogram after stent implantation. D: Recurrence of symptoms of ascites and diarrhoea 30 d after TIPS and shunt stenosis as wall as segmental filling defects shown on follow-up angiogram.

DISCUSSION

The incidence of PVTT in end-staged HCC was very high, about 20-30% in small hepatoma (2-3 cm in diameter) and 50-75% in those above 5 cm in diameter, and 86% of HCC patients with variceal bleeding had PVTT[18]. The tumor emboli resulting in portal hypertension and high resistance made the patients tend to have variceal bleeding and ascites. Tumor thrombosis in main portal vein was more prone to variceal bleeding and more difficult to be treated than that in branches and hepatic vein. Therefore some conservative measures were taken to relieve the patients' ailments, such as endoscopic sclerotherapy and ligation. But these measures were less effective. Because of low efficacy and huge cost, many patients abandoned treatment.

Current status and application of TIPS in PVTT

TIPS procedure is an effective and safe treatment for patients with variceal hemorrhage and intractable ascites, but its use is limited due to its complications of encephalopathy and poor long-term efficacy[19-25]. It was reported that the rate of stenosis of shunt was 33-66% within 1 year and that of encephalopathy was 10-30%[1-2,19,22]. In recent years some scholars applied TIPS to portal hypertension secondary to portal thromblization to ensure the patients to have time for further treatments including liver transplanation[26-29]. But the thrombus must be newly happened because old emboli possibly led to cavernous transformation and made the TIPS and liver transplanation difficult. Some authorities applied TIPS to HCC patients with esophagogastric variceal bleeding, but they thought that patients must be with hepatic function class A or B (Child-Pugh classification), under-controlled or small nodular type hepatoma and without PVTT[18,30-34].

Key skill points in TIPS procedure for PVTT

Of the 14 cases, 10 cases were technically successful and the ratio of success was consistent with that reported[1-2]. It was very difficult to puncture the right main portal branch directly because of portal occlusion, stenosis and cavernous transformation. Even a small branch of portal vein was punctured with good blood regurgitation, and hydrophilic coating wire guide could be introduced into the superior mesenteric vein or splenic vein through the loose thrombus (Figure 2). The stent should cover all the thrombus to prevent tumor from growing into the shunt. The slower the blood flow passing the stent, the more easily the shunt is thrombosed. Esophagogastric vein should be embolized after TIPS procedure because low blood flow tended to form thrombosis in the shunt[8,25]. The embolism of esophagogastric vein could also prevent variceal bleeding, keep high flow and reduce thrombosis in the stent. But esophagogastric vein was not displayed very well because of PVTT in most cases.

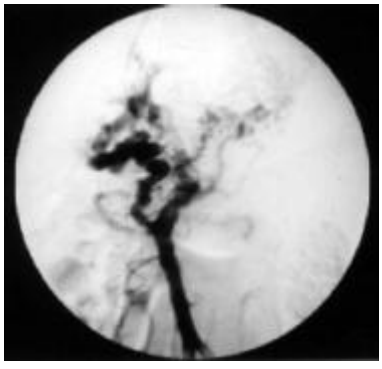

Figure 2 Occlusive portal vein, dialated superior mesenteric vein, portal vein cavernous transformation, and esophagogastric varices shown on portal vein angiogram after introducing a catheter into superior mesenteric vein.

Experiences and clinical effect

TIPS procedure is very effective for diarrhoea secondary to PVTT. A male patient with PVTT had mechanical diarrhoea 12-15 times a day and it lasted for a month with no abnormality in stool examination. Following the decrease of portal pressure after TIPS, ascites and diarrhoea decreased. The causes of diarrhoea were similar to those of ascites. Too high portal vein pressure could make fluid leak out of vessels not only into peritoneal cavity but also into intestinal tract as watery stool.

All patients who failed to TIPS procedure had cavernous transformation. Two patients with tumor thrombus in portal vein had no dilation in superior mesenteric vein and the pressure was not high as well (Figure 3). Considering that the effect was probably not very well in patients with little pressure gradiant, we did not continue further procedure. In these portal hypertension patients there were areas with both a portal and a systemic venous drainage including esophagus, anal canal, retroperitoneum and umbilical region. Partial spleen artery embolization or gastric coronary vein embolization was not effective and variceal rebleeding was inevitable in the following months. In this study only one patient had a successful procedure in five patients with cavernous transformation, so it should be careful to carry out TIPS procedure in such cases.

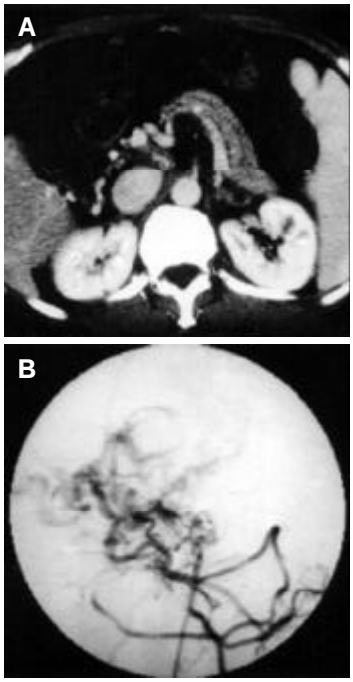

Figure 3 Main portal vein occlusion, hepatic arteric portal shunt and portal cavernous transformation in a 64-year-old patient with refractory ascites and hematemesis. A: Thin splenic and superior mesenteric vein shown on enhanced CT gram. B: Thin superior mesenteric vein and disordered drainage vein shown on angiogram.

A suitable size of stent is important to improve shunt flow, prevent esophagogastric variceal bleeding and decrease ascites[23-34]. Too large a stent could lead to encephalopathy and we used stents of 10 mm in diameter. The shunt stenosed in one patient with a stent of 8 mm in diameter 15 days after TIPS and died of rebleeding after 20 d. Another patient was placed 4 stents because the shunt was too long. Stenosis of the shunt happened 30 d after the stents were placed and the angiogram displayed shunt rugged and segmental filling defects (Figure 1D). Treatment of the shunt stenosis was similar to that of standard TIPS. The rate of shunt stenosis was relatively low in these patients, partly because of short-term follow-up and abnormal coagulatlon. By actively preventing encephalopathy and closely

monitoring condition change, patients in this study did not have encephalopathy of stage II and only 5 patients had transitory encephalopathy of stage I. Although patients died of dyscrasia or liver failure, their quality of life was improved.

REFERENCES

1 **Papatheodoridis GV**, Goulis J, Leandro G, Patch D, Burroughs AK. Transjugular intrahepatic portosystemic shunt compared with endoscopic treatment for prevention of variceal rebleeding: a meta-analysis. *Hepatology* 1999; **30**: 612-622

2 **Schepke M**, Sauerbruch T. Transjugular portosystemic stent shunt in treatment of liver diseases. *World J Gastroenterol* 2001; **7**: 170-174

3 **Xu K**, Zhang HG, He XF, Zhao ZC, Ren K, Jin CY, Han MJ, Wang CL. Preliminary report on portal hypertension in liver cirrhosis treated by transjugular intrahepatic portosystemic stent-shunt: analysis of 8 cases. *Zhonghua Fangshexue Zazhi* 1993; **27**: 294-297

4 **Zhang JS**, Wang MQ, Yang L. Transjugular intrahepatic portosystemic stent shunts. *Zhonghua Yixue Zazhi* 1994; **74**: 150-152

5 **Wang MQ**, Zhang JS, Gao YA. Transjugular intrahepatic portosystemic stent-shunt: an experimental study. *Zhonghua Fangshexue Zazhi* 1993; **28**: 324-327

6 **Trotter JF**, Suhocki PV, Rockey DC. Transjugular intrahepatic portosystemic shunt (TIPS) in patients with refractory ascites: effect on body weight and Child-Pugh score. *Am J Gastroenterol* 1998; **93**: 1891-1894

7 **Han SW**, Joo YE, Kim HS, Choi SK, Rew JS, Kim JK, Kim SJ. Clinical results of the transjugular intrahepatic portosystemic shunt (TIPS) for the treatment of variceal bleeding. *Korean J Intern Med* 2000; **15**: 179-186

8 **Walser EM**, NcNees SW, DeLa Pena O, Crow WN, Morgan RA, Soloway R, Broughan T. Portal venous thrombosis percutaneous therapy and outcome. *J Vasc Interv Radiol* 1998; **9**(1 Pt 1): 119-127

9 **Cwikiel W**, Keussen I, Larsson L, Solvig J, Kullendorff CM. Interventional treatment of children with portal hypertension secondary to portal vein occlusion. *Eur J Pediatr Surg* 2003; **13**: 312-318

10 **Opitz T**, Buchwald AB, Lorf T, Awuah D, Ramadori G, Nolte W. The transjugular intrahepatic portosystemic stent-shunt (TIPS) as rescue therapy for complete Budd-Chiari syndrome and portal vein thrombosis. *Z Gastroenterol* 2003; **41**: 413-418

11 **Ganger DR**, Klapman JB, McDonald V, Matalon TA, Kaur S, Rosenblate H, Kane R, Saker M, Jensen DM. Transjugular intrahepatic portosystemic shunt (TIPS) for Budd-Chiari syndrome or portal vein thrombosis: review of indications and problems. *Am J Gastroenterol* 1999; **94**: 603-608

12 **Sehgal M**, Haskal ZJ. Use of transjugular intrahepatic portosystemic shunts during lytic therapy of extensive portal splenic and mesenteric venous thrombosis: long-term follow-up. *J vasc Interv Radiol* 2000; **11**: 61-65

13 **Yamagami T**, Nakamura T, Tanaka O, Akada W, Takayama T, Maeda T. Transjugular intrahepatic portosystemic shunts after complete obstruction of portal vein. *J Vasc Interv Radiol* 1999; **10**: 575-578

14 **Shibata D**, Brophy DP, Gordon FD, Anastopoulos HT, Sentovich SM, Bleday R. Transjugular intrahepatic portosystemic shunt for treatment of bleeding ectopic varices with portal hypertension. *Dis Colon Rectum* 1999; **42**: 1581-1585

15 **Azoulay D**, Castaing D, Lemoine A, Samuel D, Majno P, Reynes M, Charpentier B, Bismuth H. Successful treatment of severe azathioprine-induced hepatic veno-occlusive disease in a kidney-transplanted patient with transjugular intrahepatic portosystemic shunt. *Clin Nephrol* 1998; **50**: 118-122

16 **Nolte W**, Canelo R, Figulla HR, Kersten J, Sattler B, Munke H, Hartmann H, Ringe B, Ramadori G. Transjugular intrahepatic portosystemic stent-shunt after orthotopic liver transplantation in a patient with early recurrence of portal hypertension of unknown origin. *Z Gastroenterol* 1998; **36**: 159-164

17 **Benador N**, Grimm P, Lavine J, Rosenthal P, Reznik V, Lemire J. Transjugular intrahepatic portosystemic shunt prior to renal transplantation in a child with autosomal-recessive polycystic kidney disease and portal hypertension: A case report. *Pediatr Transplant* 2001; **5**: 210-214

18 **Zhang XT**, Xu K, Zhang HG, Zhang LC, Zhao ZC, Han MJ. Primary hepatocellular arcinoma with portal hypertension treated with TIPSS. *Linchuang Fangshexue Zazhi* 1995; **14**: 236-238

19 **Hausegger KA**, Sternthal HM, Klein GE, Karaic R, Stauber R, Zenker G. Transjugular intrahepatic portosystemic shunt: angiographic follow-up and secondary interventions. *Radiology* 1994; **191**: 177-181

20 **Willkomm P**, Schomburg A, Brensing KA, Reichmann K, Bangard M, Overbeck B, Sauerbruch T, Biersack HJ. Liver perfusion scintigraphy prior to and after transjugular intrahepatic portosystemic shunts (TIPS) in patients with portal hypertension. *Nuklearmedizin* 2000; **39**: 139-141

21 **Zuckerman DA**, Darcy MD, Bocchini TP, Hildebolt CF. Encephalopathy after transjugular intrahepatic portosystemic shunting: analysis of incidence and potential risk factors. *Am J Roentgenol* 1997; **169**: 1727-1731

22 **Sterling RK**, Sanyal AJ. Are TIPS tops in the treatment of portal hypertension? A review on the use and misuse of transjugular intrahepatic portosystemic shunts. *Can J Gastroenterol* 2000; **14**(Suppl D): 122D-128D

23 **Sanyal AJ**. The use and misuse of transjugular intrahepatic portasystemic shunts. *Papatheodoridis G Curr Gastroenterol Rep* 2000; **2**: 61-71

24 **Younossi ZM**, McHutchison JG, Broussard C, Cloutier D, Sedghi-Vaziri A. Portal decompression by transjugular intrahepatic portosystemic shunt and changes in serum-ascites albumin gradient. *J Clin Gastroenterol* 1998; **27**: 149-151

25 **Latimer J**, Bawa SM, Rees CJ, Hudson M, Rose JD. Patency and reintervention rates during routine TIPSS surveillance. *Cardiovasc Intervent Radiol* 1998; **21**: 234-239

26 **Khan TT**, Reddy KS, Johnston TD, Lo FK, Shedlofsky S, Grubb S, Ranjan D. Transjugular intrahepatic portosystemic shunt migration in patients undergoing liver transplantation. *Int Surg* 2002; **87**: 279-281

27 **Hidajat N**, Vogl T, Stobbe H, Schmidt J, Wex C, Lenzen R, Berg T, Neuhaus P, Felix R. Transjugular intrahepatic portosystemic shunt. Experiences at a liver transplantation center. *Acta Radiol* 2000; **41**: 474-478

28 **Liatsos C**, Vlachogiannakos J, Patch D, Tibballs J, Watkinson A, Davidson B, Rolles K, Burroughs AK. Successful recanalization fo portal vein thrombosis before liver transplantation using transjugular intrahepatic portosystemic shunt. *Liver Transpl* 2001; **7**: 453-460

29 **Menegaux F**, Keeffe EB, Baker E, Egawa H, Concepcion W, Russell TR, Esquivel CO. Comparison of transjugular and surgical portosystemic shunts on the outcome of liver transplantation. *Arch Surg* 1994; **129**: 1018-1023

30 **Nicolini A**, Saccheri S, Lovaria A, Maggi A, Cazzaniga M, Panzeri A, Salerno F. Prevention of variceal rebleeding and treatment of liver carcinoma by consecutive transjugular intrahepatic portosystemic shunt and hepatic artery chemoembolization. *Ital J Gastroenterol* 1996; **28**: 269-271

31 **Burger JA**, Ochs A, Wirth K, Berger DP, Mertelsmann R, Engelhardt R, Roessle M, Haag K. The transjugular stent implantation for the treatment of malignant portal and hepatic vein obstruction in cancer patients. *Ann Oncol* 1997; **8**: 200-202

32 **Serafini FM**, Zwiebel B, Black TJ, Carey LC, Rosemurgy AS 2nd. Transjugular intrahepatic portasystemic stent shunt in the treatment of variceal bleeding in hepatocellular cancer. *Dig Dis Sci* 1997; **42**: 59-65

33 **Tazawa J**, Sakai Y, Yamane M, Kakinuma S, Maeda M, Suzuki K, Miyasaka Y, Nagayama K, Kusano F, Sato C. Long-term Observation after transjugular intrahepatic portosystemic stent-shunt in two patients with hepatocellular carcinoma. *J Clin Gastroenterol* 2000; **31**: 262-267

34 **Sakaguchi H**, Uchida H, Maeda M, Matsuo N, Kichikawa K, Ohishi H, Nishida H, Ueno K, Nishimine K, Rosch J. Combined transjugular intrahepatic portosystemic shunt and segmental Lipildol hapatic artery embolization for the treatment of esophagogastric varices and hepatlcellular carcinoma in patients with cirrhosis: Preliminary report. *Cardiovasc Intervent Radiol* 1995; **18**: 9-15

Edited by Wang XL and Zhang JZ **Proofread by** Xu FM

PO Box 2345, Beijing 100023, China
Fax: +86-10-85381893
E-mail: wjg@wjgnet.com www.wjgnet.com

World J Gastroenterol 2004;10(13):1885-1889
World Journal of Gastroenterology
 ISSN 1007-9327

• LIVER CANCER •

Angiogenesis in rabbit hepatic tumor after transcatheter arterial embolization

Xiao-Feng Liao, Ji-Lin Yi, Xing-Rui Li, Wei Deng, Zhi-Fang Yang, Geng Tian

Xiao-Feng Liao, Ji-Lin Yi, Xing-Rui Li, Wei Deng, Zhi-Fang Yang, Geng Tian, Department of General Surgery, Tongji Hospital, Tongji Medical College, Huazhong University of Science and Technology, Wuhan 430030, Hubei Province, China
Correspondence to: Xiao-Feng Liao, Department of General Surgery, Tongji Hospital, Tongji Medical College, Huazhong University of Science and Technology, Wuhan 430030, Hubei Province, China. liaoxiaofeng66@163.com
Telephone: +86-27-83660410
Received: 2003-11-17 **Accepted:** 2003-12-18

Abstract

AIM: To investigate the effect of transcatheter arterial embolization (TAE) on angiogenesis of hepatic tumor.

METHODS: Twenty New Zealand White rabbits were randomly divided into two groups of 10 each and VX2 carcinoma was implanted in the left medial lobes of the livers. Fourteen days later, a silicon catheter was inserted into the left hepatic artery of rabbit with VX2 hepatic tumor and infusion was performed via the hepatic artery using Lipiodol (the TAE group) or saline (the control group). Rabbits were sacrificed 7 d after treatment and tumor tissues were excised. Expression of vascular endothelial growth factor (VEGF) protein and microvessel density (MVD) of tumors were examined using immunohistochemistry. The staining intensity of VEGF was evaluated with a computer-assisted image-analyzer. Reverse transcription-polymerase chain reaction (RT-PCR) was used to detect the VEGF mRNA expression of tumors.

RESULTS: MVD was higher in the TAE group compared with the control group (28.6±10.6 *vs* 16.3±6.9, $P<0.01$). Expression of VEGF protein was enhanced after TAE. The staining intensity of VEGF in the TAE group was 0.162±0.018, significantly higher than in the control group (0.142±0.01, $P<0.01$). At mRNA level, VEGF165 mRNA was significantly higher in the TAE group compared with the control group (2.58±0.42 *vs* 1.99±0.21, $P<0.001$). MVD was well correlated to VEGF expression in both the TAE group ($r=0.69$, $P<0.05$) and the control group ($r=0.72$, $P<0.05$).

CONCLUSION: TAE promotes the development of neovascularization of residual tumors through up-regulation of VEGF expression, possibly due to hypoxic insult.

Liao XF, Yi JL, Li XR, Deng W, Yang ZF, Tian G. Angiogenesis in rabbit hepatic tumor after transcatheter arterial embolization. *World J Gastroenterol* 2004; 10(13): 1885-1889
http://www.wjgnet.com/1007-9327/10/1885.asp

INTRODUCTION

Hepatocellular carcinoma (HCC) is one of the most common malignant tumors in Asia, including China. Surgical resection is still the treatment of first choice for patients with HCC nowadays[1]. However, because of tumor extension, poor hepatic functional reserve due to underlying liver cirrhosis, or both, only a small portion of patients are suitable candidates for surgery[2-4]. Transcatheter arterial chemoembolization (TACE) is considered to be an effective treatment for patients with HCC who are not candidates for surgical resection[5,6]. TACE could reduce tumor size[7-8]. However, intrahepatic or extrahepatic metastasis after TACE is the major factor limiting its overall therapeutic effect[9].

Angiogenesis, the process leading to the formation of new blood vessels from preexisting vessels, plays a central role in the survival of tumor cells, in local tumor growth, and in the development of distant metastasis[10]. Microvessel density (MVD) has been the gold standard for the quantification of tumor angiogenesis, showing a good correlation with the prognosis in a variety of cancers including HCC[11-15]. Among the known angiogenic factors produced by tumor cells, vascular endothelial growth factor (VEGF) is one of the most potent angiogenic factors involved in tumor development. VEGF is a specific mitogenic factor for vascular endothelial cells, which stimulates endothelial cells proliferation, promotes neovascularization and increases vascular permeability. Evidence from preclinical and clinical studies indicates VEGF is associated with formation of metastases and poor prognosis in various cancers[16-18].

VEGF protein is produced by alternative splicing of the primary transcript leading to the production of at least four major isoforms of VEGF: 121, 165, 189, and 206[19]. VEGF189 and VEGF206 contain heparin-binding domains and are highly concentrated in the extracellular matrix. VEGF165 and VEGF121 are diffusible and predominate in most tissues, lacking this particular domain. The presence or absence of these domains affects the properties, actions, and distribution of the isoform produced[19].

Little is known of the changes of angiogenesis and VEGF expression in HCC after TACE. Thus, we established a rabbit model of transcatheter arterial embolization (TAE) with hepatic VX2 carcinoma, and examined MVD and VEGF expression in the hepatic tumors after TAE.

MATERIALS AND METHODS

Implantation procedure

The rabbit VX2 carcinoma was selected for implantation in the liver because of the similarities of its blood supply to that of human hepatomas[20,21]. The VX2 strain (obtained from Dr. Li Xin of Department of Radiology, the Union Hospital, Tongji Medical College of Huazhong University of Science and Technology, Wuhan, China) was maintained by serial passage in rabbit hindlimbs. Twenty male New Zealand White rabbits (3.0 to 3.5 kg) were used for all experiments. Studies with these animals were approved by the Animal Care and Use Committee of Tongji Medical College of Huazhong University of Science and Technology and carried out according to their guidelines. Tumor implantation was performed as described previously[22] with a slight modification. Briefly, rabbits were anesthetized by i.v. injection of sodium pentobarbital (30 mg/kg) via a marginal ear vein. The abdominal area was shaved and

sterilized, and a midline subxyphoid incision was made. The left medial lobe of rabbit liver was gently exposed, and one piece of the VX2 tumor tissue excised from the carrier rabbit and broken into fine pieces (1 mm×1 mm×1 mm in size per piece) in Hanks' solution was implanted into the subcapsule of the left medial hepatic lobe. The implanted site was closed with gelatin sponge to prevent the leakage of tumor cells into the peritoneal cavity. The hepatic lobe was then returned to the abdominal cavity. This method allows the growth of a single solitary, well-demarcated tumor in the liver of each recipient rabbit. The incision was closed in two layers. The tumors were allowed to grow for 2 wk, and studies were performed when the tumors reached 1 to 2 cm in diameter.

TAE procedure

Twenty rabbits were divided into two groups of 10 rabbits each randomly. The animals were relaparotomized through a midline abdominal incision under the general anesthesia as described above, and a silicone catheter (outer diameter 0.8 mm) with a tip in the shape of a hockey-stick was inserted retrogradely into the left hepatic artery via the gastroduodenal artery under the operating microscope (Zeiss OPMI 6-S, Aalen, Germany). The catheter was tightly secured and hepatic arterial infusion was made, with 0.5 mL/kg of lipiodol in TAE group or with the same volume of saline in control group. After the injection, the catheter was removed and the gastroduodenal artery was ligated. The incision was closed in two layers. CT scan was performed 2 d after TAE, and confirmed that the lipiodol had been retained in the tumors of all cases (Figure 1).

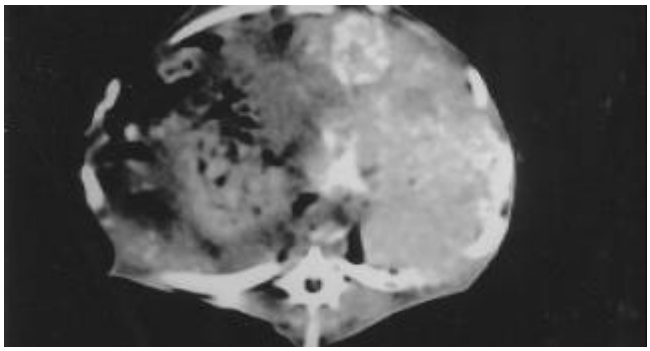

Figure 1 CT scan 2 d following lipiodol infusion.

Tissue preparation

The rabbits were sacrificed 7 d after treatment, and the tumor was removed. Part of the specimen was flash-frozen at –70 ℃ for RT-PCR, and the rest was fixed in 40 g/L formaldehyde and embedded in paraffin for immunohistochemical study.

Immunohistochemistry

Consecutive 4-μm sections were cut and mounted on glass slides. Sections were stained with H&E. VEGF expression was examined immunohistochemically with an anti-VEGF mouse monoclonal antibody (JH121, Neomarkers, Inc., Fremont, CA) at a dilution of 1:80, and by using streptavidin-peroxidase technique with SPtm kit (Zymed Laboratories, Inc., USA). The JC/70 monoclonal antibody (Dako, Glostrup, Denmark) against CD31 was used for microvessel staining using the LSAB method (Dako LSAB kit; Glostrup, Denmark). Negative controls were prepared by PBS substitution for the primary antibodies staining, and known positive controls were included in each staining run.

Morphometric analyses

The positive expression cells of VEGF were ones with brown-yellow granular patterns in the cytoplasm. In intensively positive staining area, three fields of vision were selected at ×400 magnification. Staining intensity of VEGF was assessed morphometrically with a computer-assisted image-analyzer (HPIAS-1 000 high precision color-image measure system, Tongji Qiangping Image Engineer Company). The image analyzer is an integrated system of Windows-based software specially designed for immunohistochemical analysis.

Determination of MVD

MVD was evaluated according to the method described by Gasparini *et al*.[23] The stained sections were screened at low power field (×40), and five areas with the most intense neovascularization (hot spots) were selected. Microvessel counts of these areas were performed at high power field (×200). Any brown-stained endothelial cell or endothelial cell cluster clearly separated from adjacent microvessels, tumor cells, and other connective-tissue elements was counted as one microvessel, irrespective of the presence of a vessel lumen. The mean microvessel count of the five richest vascular areas was taken as the MVD, which was expressed as the absolute number of microvessels per 0.74 mm^2 (×200).

RNA preparation and reverse transcription-polymerase chain reaction (RT-PCR)

Total RNA was extracted using TriZol reagent (Life Technologies, Grand Island, NY) according to the manufacturer's recommendations. Briefly, the tissue was homogenized with a Polytron homogenizer in 1 mL TriZol per 100 mg tissue. The suspension was left at room temperature for 10 min before being centrifuged at 12 000 *g* at 4 ℃ for 10 min. The aqueous supernatant containing the RNA was carefully removed and transferred to a fresh tube. Total RNA was precipitated by addition of isopropanol and centrifuged at 12 000 *g* at 4 ℃ for 10 min. The RNA pellet was washed with 750 mL/L ethanol and re-dissolved in DEPC-treated water. Before being used in RT-PCR these samples were phenol/chloroform extracted and phenol precipitated. The RNA concentration and quality were determined by UV spectrophotometer at absorbances of 260 and 280 nm.

cDNA was synthesized from total RNA with Avian Myeloblastosis Virus and oligo dT-Adaptor Primer (TaKaRa RNA PCR Kit, TaKaRa Bioteth., Dalian, CHN) according to the manufacturer's instructions. Amplification of cDNA was performed using published sense and antisense primers for rabbit β-actin and VEGF[19,24,25]. The primer sequence for β-actin sense was 5' -CCT TCC TGC GCA TGG AGT CCT GG-3' , and the primer sequence for β-actin antisense was 5' -GGA GCA ATG ATC TTG ATC TTC-3' . The sense primer sequence for VEGF was 5' -CAG TGA ATT CGA GAT GAG CTT CCT ACA GCA C-3' , and the antisense primer sequence was 5' -CCT GGA ATT CTC ACC GCC TCG GCT TGT CAC-3' . The PCR cycle profile was at 94 ℃ for 30 s, 59 ℃ for 60 s and 72 ℃ for 60 s, with 30 cycles.

After visualization of the PCR products by 20 g/L agarose gel electrophoresis with ethidium bromide staining gel, images were obtained and the densities of the products were quantified using a digital gel image analysis system (GDS8 000, UVP Co., UK). The PCR fragments were identified according to their molecular mass using a DNA marker (DL2 000 marker, TaKaRa Bioteth., Dalian, China). The relative expression levels were calculated as the density of the product of the respective target genes after normalization with the β-actin internal control.

Statistical analysis

All data are expressed as mean±SD. Differences in staining

intensity of VEGF, quantity of variant VEGF isoforms and MVD between the TAE group and the control group were compared with Student' s *t* test. The correlation of VEGF and MVD was performed with linear regression analysis. $P<0.05$ was considered statistically significant. Statistical analysis was done using SPSS 10.0 for Windows.

RESULTS

MVD and its pathologic features

Figure 2A shows microvessels were stained in brown color. Microvessels were heterogeneously distributed inside the tumor, and, in general, maximal density was observed near the margins of the invasive tumor or in the central regions of tumor where necrosis could be seen. The MVD was 28.6±10.6 in the TAE group, and 16.3±6.9 in the control group. The MVD was significantly higher in the TAE group than that of the control group ($P<0.01$).

Expression of VEGF protein

Immunoreactive products of anti-VEGF antibody were positively detected in the cytoplasm of hepatoma cells and scarcely detected in endothelial cells. In general, hepatoma cells showed stronger VEGF immunoreactivity than endothelial cells. The intensity of immunoreactive products was heterogeneous (Figure 2B). The staining intensity of VEGF in the TAE group was 0.162±0.018, significantly higher compared to the control group (0.142±0.01, $P<0.01$).

There was a significant correlation between MVD and VEGF protein expression in both the TAE group ($r=0.69$, $P<0.05$) and the control group ($r=0.72$, $P<0.05$).

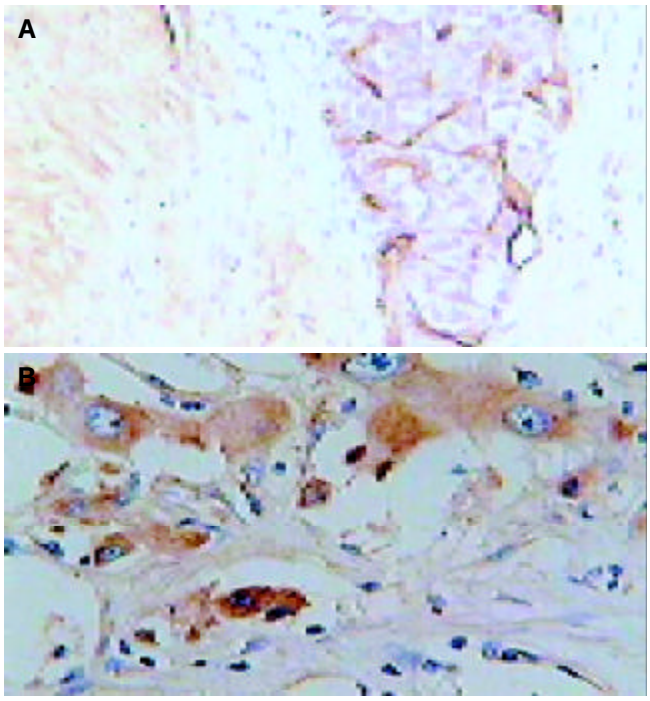

Figure 2 Immunohistochemical staining in hepatic tumor tissues obtained from a rabbit underwent TAE. A: CD31, original magnification ×200; B: VEGF, original magnification ×400.

Expression of VEGF mRNA

PCR amplification of cDNA prepared from frozen sections showed the expression of three bands of 110, 242 and 314 bp corresponding to VEGF121, VEGF165 and VEGF189, respectively (Figure 3A). The band corresponding to VEGF206 was not detected. In both the TAE group and the control group, VEGF165 was strongly detected (Figure 3B). The intensity of VEGF165 mRNA was significantly higher in the TAE group (2.58±0.42), as compared with the control group (1.99±0.21, $P<0.001$). Although the signal of VEGF121 mRNA was slightly higher in the TAE group (1.14±0.19) than that of the control group (0.99±0.11), there was no statistical significance. No significant difference between VEGF189 mRNA in the TAE group (1.03±0.14) and the control group (1.01±0.11) was demonstrated (Figure 3B).

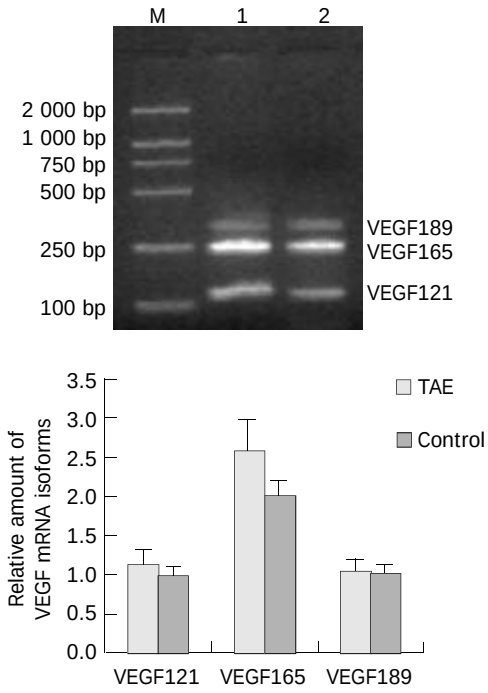

Figure 3 Expression of VEGF mRNA in hepatic tumor tissues. A: Results of RT-PCR of VEGF mRNA in TAE (lane 1), control (lane 2) and M (molecular mass marker); B: quantification of RT-PCR data.

DISCUSSION

TACE has been accepted as one of the most effective palliative treatments for patients with unresectable HCC on the basis of the characterization of its blood supply. Since the blood supply of HCC is derived almost exclusively from hepatic arteries, hepatoma cells undergo ischemic necrosis in TAE. The addition of chemotherapy aimed to enhance the antitumor effect of the ischemia. However, it was only a small proportion of HCC that occurred complete necrosis after TACE[26]. We have occasionally noticed rapid growth and extensive metastasis after multiple TACE treatments. TACE prior to surgical resection may facilitate recurrence of HCC[27]. The recurrence rate after 3 years of treatment is 30-60%[28,29]. It is possible that in addition to the limited ability of chemoembolization to eliminate cancer cells, it may play a role in enhancing the malignant potential of the tumor and the ability of some cells to escape necrosis after treatment[30]. Huang *et al*.[26] and Kim *et al*.[31] reported that the proliferative activity of tumor cells was increased after TACE.

In the present study, we investigated the change of angiogenesis in VX2 hepatic tumor that underwent TAE using immunohistochemical techniques. The results showed that MVD of the tumors markedly increased after TAE. MVD is currently considered the gold standard for histological assessment of the degree of angiogenesis within a tumor. It is an independent predictor for the growth, metastasis and prognosis of tumor. Increasing evidence suggests that there is a clear relationship between the MVD and HCC prognosis[1,14,32,33]. These findings thus provide evidence that the development of neovascularization

in hepatic residual tumors after TAE may be one of the reasons why the majority of tumor nodes do not show complete necrosis and why tumors have an increased tendency to metastasize after TAE.

Until recently, VEGF was the only growth factor proven to be specific and critical for blood vessel formation[34]. Many studies have indicated that VEGF is not only correlated with HCC angiogenesis, but also closely correlated with the invasion and metastasis of HCC. The levels of VEGF in tumor and peripheral blood of patients with HCC might be a useful indicator for both HCC metastasis and poor prognosis[18,35-41]. In our study, the expression of VEGF protein was well correlated to MVD, and the level of VEGF expression in TAE group was increased significantly compared with the control. These findings show that VEGF plays a vital role in the process of angiogenesis in hepatic tumors after TAE.

It has been known that four alternatively spliced products can be generated from the single VEGF gene, yielding different protein products composed of 121, 165, 189 and 206 amino acids, designated as VEGF121, VEGF165, VEGF189 and VEGF206, respectively. Among them, only VEGF121 and VEGF165 are secreted and can induce mitogenesis of endothelial cells; VEGF189 and VEGF206 are membrane anchored and act as vascular permeability factors. To identify the changes of VEGF mRNA isoform expression in hepatic tumors after TAE, we performed RT-PCR. In our study three bands of 110, 242 and 314 bp were shown, corresponding to VEGF121, VEGF165 and VEGF189, respectively. The major VEGF isoform expressed in VX2 hepatic tumor was VEGF165. The significantly enhanced expression of VEGF165 mRNA in the TAE group was observed compared with the control group. Although VEGF121 mRNA was slightly higher in the TAE group than in the control group, there was no statistical significance. We detected no VEGF206 mRNA, consistent with the very restricted expression of this splice variant.

The possible reason for up-regulation of VEGF expression after embolization was anoxia and ischemia of tumor tissues. Hypoxia is known to be a very important stimulus for the new vessel formation seen in tumor angiogenesis by stimulating the expression of VEGF[42,43]. Kim *et al*.[44] reported that hypoxia might induce HCC cells to secrete more VEGF and IGF-II. Moreover, the combination of hypoxia and IGF-II brought an additional induction of VEGF. In the current study, it was found that more microvessel was observed in the tumor margins or areas around the necrotic tissues, which might be resulted from more severe local anoxia in these areas.

Song *et al*.[45] reported that plasma IGF-II level was increased after TACE, which implied that expression of other angiogenic factors besides VEGF might also be changed after TACE.

In conclusion, these results indicate that TAE is involved in the development of neovascularization of hepatic residual tumors after TAE through up-regulation of VEGF expression, possibly due to hypoxic insult. Therefore, the combination of TAE and antiangiogenic therapy may be superior to TAE alone in the treatment of HCC.

REFERENCES

1 **Tang Z**, Zhou X, Lin Z, Yang B, Ma Z, Ye S, Wu Z, Fan J, Liu Y, Liu K, Qin L, Tian J, Sun H, He B, Xia J, Qiu S, Zhou J. Surgical treatment of hepatocellular carcinoma and related basic research with special reference to recurrence and metastasis. *Chin Med J* 1999; **112**: 887-891

2 **Yan FH**, Zhou KR, Cheng JM, Wang JH, Yan ZP, Da RR, Fan J, Ji Y. Role and limitation of FMPSPGR dynamic contrast scanning in the follow-up of patients with hepatocellular carcinoma treated by TACE. *World J Gastroenterol* 2002; **8**: 658-662

3 **Faivre J**, Forman D, Esteve J, Obradovic M, Sant M. Survival of patients with primary liver cancer, pancreatic cancer and biliary tract cancer in Europe. *Eur J Cancer* 1998; **34**: 2184-2190

4 **El-Serag HB**, Mason AC, Key C. Trends in survival of patients with hepatocellular carcinoma between 1977 and 1996 in the United States. *Hepatology* 2001; **33**: 62-65

5 **Acunas B**, Rozanes I. Hepatocellular carcinoma: treatment with transcatheter arterial chemoembolization. *Eur J Radiol* 1999; **32**: 86-89

6 **Tang ZY**. Hepatocellular carcinoma. *J Gastroenterol Hepatol* 2000; **15**(Suppl): G1-7

7 **Poon RT**, Ngan H, Lo CM, Liu CL, Fan ST, Wong J. Transarterial chemoembolization for inoperable hepatocellular carcinoma and postresection intrahepatic recurrence. *J Surg Oncol* 2000; **73**: 109-114

8 **Lo CM**, Ngan H, Tso WK, Liu CL, Lam CM, Poon RT, Fan ST, Wong J. Randomized controlled trial of transarterial lipiodol chemoembolization for unresectable hepatocellular carcinoma. *Hepatology* 2002; **35**: 1164-1171

9 **Liou TC**, Shih SC, Kao CR, Chou SY, Lin SC, Wang HY. Pulmonary metastasis of hepatocellular carcinoma associated with transarterial chemoembolization. *J Hepatol* 1995; **23**: 563-568

10 **Folkman J**. What is the evidence that tumors are angiogenesis dependent? *J Natl Cancer Inst* 1990; **82**: 4-6

11 **Zheng HC**, Sun JM, Li XH, Yang XF, Zhang YC, Xin Y. Role of PTEN and MMP-7 expression in growth, invasion, metastasis and angiogenesis of gastric carcinoma. *Pathol Int* 2003; **53**: 659-666

12 **Abramson LP**, Grundy PE, Rademaker AW, Helenowski I, Cornwell M, Katzenstein HM, Reynolds M, Arensman RM, Crawford SE. Increased microvascular density predicts relapse in Wilms' tumor. *J Pediatr Surg* 2003; **38**: 325-330

13 **Pruneri G**, Ponzoni M, Ferreri AJ, Decarli N, Tresoldi M, Raggi F, Baldessari C, Freschi M, Baldini L, Goldaniga M, Neri A, Carboni N, Bertolini F, Viale G. Microvessel density, a surrogate marker of angiogenesis, is significantly related to survival in multiple myeloma patients. *Br J Haematol* 2002; **118**: 817-820

14 **Poon RT**, Ng IO, Lau C, Yu WC, Yang ZF, Fan ST, Wong J. Tumor microvessel density as a predictor of recurrence after resection of hepatocellular carcinoma: a prospective study. *J Clin Oncol* 2002; **20**: 1775-1785

15 **Ng IO**, Poon RT, Lee JM, Fan ST, Ng M, Tso WK. Microvessel density, vascular endothelial growth factor and its receptors Flt-1 and Flk-1/KDR in hepatocellular carcinoma. *Am J Clin Pathol* 2001; **116**: 838-845

16 **Takahashi R**, Tanaka S, Kitadai Y, Sumii M, Yoshihara M, Haruma K, Chayama K. Expression of vascular endothelial growth factor and angiogenesis in gastrointestinal stromal tumor of the stomach. *Oncology* 2003; **64**: 266-274

17 **White JD**, Hewett PW, Kosuge D, McCulloch T, Enholm BC, Carmichael J, Murray JC. Vascular endothelial growth factor-D expression is an independent prognostic marker for survival in colorectal carcinoma. *Cancer Res* 2002; **62**: 1669-1675

18 **Torimura T**, Sata M, Ueno T, Kin M, Tsuji R, Suzaku K, Hashimoto O, Sugawara H, Tanikawa K. Increased expression of vascular endothelial growth factor is associated with tumor progression in hepatocellular carcinoma. *Hum Pathol* 1998; **29**: 986-991

19 **Watkins RH**, D'Angio CT, Ryan RM, Patel A, Maniscalco WM. Differential expression of VEGF mRNA splice variants in newborn and adult hyperoxic lung injury. *Am J Physiol* 1999; **276**: L858-867

20 **Geschwind JF**, Artemov D, Abraham S, Omdal D, Huncharek MS, McGee C, Arepally A, Lambert D, Venbrux AC, Lund GB. Chemoembolization of liver tumors in a rabbit model: assessment of tumor cell death with diffusion-weighted MR imaging and histologic analysis. *J Vasc Interv Radiol* 2000; **11**: 1245-1255

21 **Ko YH**, Pedersen PL, Geschwind JF. Glucose catabolism in the rabbit VX2 tumor model for liver cancer: characterization and targeting hexokinase. *Cancer Lett* 2001; **173**: 83-91

22 **Geschwind JF**, Ko YH, Torbenson MS, Magee C, Pedersen PL. Novel therapy for liver cancer: direct intraarterial injection of a potent inhibitor of ATP production. *Cancer Res* 2002; **62**: 3909-3913

23 **Gasparini G**, Harris AL. Clinical importance of the determination of tumor angiogenesis in breast carcinoma: much more than a new prognostic tool. *J Clin Oncol* 1995; **13**: 765-782

24 **Ozaki NK**, Beharry KD, Nishihara KC, Akmal Y, Ang JG, Sheikh R, Modanlou HD. Regulation of retinal vascular endothelial

growth factor and receptors in rabbits exposed to hyperoxia. *Invest Ophthalmol Vis Sci* 2002; **43**: 1546-1557

25 **Houck KA**, Leung DW, Rowland AM, Winer J, Ferrara N. Dual regulation of vascular endothelial growth factor bioavailability by genetic and proteolytic mechanisms. *J Biol Chem* 1992; **267**: 26031-26037

26 **Huang J**, He X, Lin X, Zhang C, Li J. Effect of preoperative transcatheter arterial chemoembolization on tumor cell activity in hepatocellular carcinoma. *Chin Med J* 2000; **113**: 446-448

27 **Adachi E**, Matsumata T, Nishizaki T, Hashimoto H, Tsuneyoshi M, Sugimachi K. Effects of preoperative transcatheter hepatic arterial chemoembolization for hepatocellular carcinoma. The relationship between postoperative course and tumor necrosis. *Cancer* 1993; **72**: 3593-3598

28 **Matsui O**, Kadoya M, Yoshikawa J, Gabata T, Arai K, Demachi H, Miyayama S, Takashima T, Unoura M, Kogayashi K. Small hepatocellular carcinoma: treatment with subsegmental transcatheter arterial embolization. *Radiology* 1993; **188**: 79-83

29 **Ohnishi K**, Yoshioka H, Kosaka K, Toshima K, Nishiyama J, Kameda C, Ito S, Fujiwara K. Treatment of hypervascular small hepatocellular carcinoma with ultrasound-guided percutaneous acetic acid injection: comparison with segmental transcatheter arterial embolization. *Am J Gastroenterol* 1996; **91**: 2574-2579

30 **Seki T**, Tamai T, Ikeda K, Imamura M, Nishimura A, Yamashiki N, Nakagawa T, Inoue K. Rapid progression of hepatocellular carcinoma after transcatheter arterial chemoembolization and percutaneous radiofrequency ablation in the primary tumour region. *Eur J Gastroenterol Hepatol* 2001; **13**: 291-294

31 **Kim YB**, Park YN, Park C. Increased proliferation activities of vascular endothelial cells and tumour cells in residual hepatocellular carcinoma following transcatheter arterial embolization. *Histopathology* 2001; **38**: 160-166

32 **Sun HC**, Tang ZY, Li XM, Zhou YN, Sun BR, Ma ZC. Microvessel density of hepatocellular carcinoma: its relationship with prognosis. *J Cancer Res Clin Oncol* 1999; **125**: 419-426

33 **Tanigawa N**, Lu C, Mitsui T, Miura S. Quantitation of sinusoid-like vessels in hepatocellular carcinoma: its clinical and prognostic significance. *Hepatology* 1997; **26**: 1216-1223

34 **Yancopoulos GD**, Davis S, Gale NW, Rudge JS, Wiegand SJ, Holash J. Vascular-specific growth factors and blood vessel formation. *Nature* 2000; **407**: 242-248

35 **Jinno K**, Tanimizu M, Hyodo I, Nishikawa Y, Hosokawa Y, Doi T, Endo H, Yamashita T, Okada Y. Circulating vascular endothelial growth factor (VEGF) is a possible tumor marker for metastasis in human hepatocellular carcinoma. *J Gastroenterol* 1998; **33**: 376-382

36 **Zhou J**, Tang ZY, Fan J, Wu ZQ, Li XM, Liu YK, Liu F, Sun HC, Ye SL. Expression of platelet-derived endothelial cell growth factor and vascular endothelial growth factor in hepatocellular carcinoma and portal vein tumor thrombus. *J Cancer Res Clin Oncol* 2000; **126**: 57-61

37 **Iguchi H**, Yokota M, Fukutomi M, Uchimura K, Yonemasu H, Hachitanda Y, Nakao Y, Tanaka Y, Sumii T, Funakoshi A. A possible role of VEGF in osteolytic bone metastasis of hepatocellular carcinoma. *J Exp Clin Cancer Res* 2002; **21**: 309-313

38 **Yoshiji H**, Kuriyama S, Yoshii J, Ikenaka Y, Noguchi R, Hicklin DJ, Huber J, Nakatani T, Tsujinoue H, Yanase K, Imazu H, Fukui H. Synergistic effect of basic fibroblast growth factor and vascular endothelial growth factor in murine hepatocellular carcinoma. *Hepatology* 2002; **35**: 834-842

39 **Chao Y**, Li CP, Chau GY, Chen CP, King KL, Lui WY, Yen SH, Chang FY, Chan WK, Lee SD. Prognostic significance of vascular endothelial growth factor, basic fibroblast growth factor, and angiogenin in patients with resectable hepatocellular carcinoma after surgery. *Ann Surg Oncol* 2003; **10**: 355-362

40 **Poon RT**, Ng IO, Lau C, Zhu LX, Yu WC, Lo CM, Fan ST, Wong J. Serum vascular endothelial growth factor predicts venous invasion in hepatocellular carcinoma: a prospective study. *Ann Surg* 2001; **233**: 227-235

41 **Gorrin-Rivas MJ**, Arii S, Mori A, Takeda Y, Mizumoto M, Furutani M, Imamura M. Implications of human macrophage metalloelastase and vascular endothelial growth factor gene expression in angiogenesis of hepatocellular carcinoma. *Ann Surg* 2000; **231**: 67-73

42 **von Marschall Z**, Cramer T, Hocker M, Finkenzeller G, Wiedenmann B, Rosewicz S. Dual mechanism of vascular endothelial growth factor upregulation by hypoxia in human hepatocellular carcinoma. *Gut* 2001; **48**: 87-96

43 **Shweiki D**, Itin A, Soffer D, Keshet E. Vascular endothelial growth factor induced by hypoxia may mediate hypoxia-initiated angiogenesis. *Nature* 1992; **359**: 843-845

44 **Kim KW**, Bae SK, Lee OH, Bae MH, Lee MJ, Park BC. Insulin-like growth factor II induced by hypoxia may contribute to angiogenesis of human hepatocellular carcinoma. *Cancer Res* 1998; **58**: 348-351

45 **Song BC**, Chung YH, Kim JA, Lee HC, Yoon HK, Sung KB, Yang SH, Yoo K, Lee YS, Suh DJ. Association between insulin-like growth factor-2 and metastases after transcatheter arterial chemoembolization in patients with hepatocellular carcinoma: a prospective study. *Cancer* 2001; **91**: 2386-2393

Edited by Zhu LH and Chen WW **Proofread by** Xu FM

PO Box 2345, Beijing 100023, China
Fax: +86-10-85381893
E-mail: wjg@wjgnet.com www.wjgnet.com

World J Gastroenterol 2004;10(13):1890-1892
World Journal of Gastroenterology
 ISSN 1007-9327

• COLORECTAL CANCER •

Relationship between serum calcium and CA 19-9 levels in colorectal cancer

Peter Fuszek, Peter Lakatos, Adam Tabak, Janos Papp, Zsolt Nagy, Istvan Takacs, Henrik Csaba Horvath, Peter Laszlo Lakatos, Gabor Speer

Peter Fuszek, Peter Lakatos, Adam Tabak, Janos Papp, Zsolt Nagy, Istvan Takacs, Henrik Csaba Horvath, Peter Laszlo Lakatos, Gabor Speer, 1st Department of Medicine, Faculty of Medicine, Semmelweis University, Budapest, Hungary
Correspondence to: Peter Fuszek MD, 1st Department of Medicine, Faculty of Medicine, Semmelweis University, 1083 Budapest, Korányi S. u. 2/a, Hungary. fuszpet@bel1.sote.hu
Telephone: +36-20-9280-451
Received: 2004-02-20 **Accepted:** 2004-03-13

Abstract

AIM: To examine the calcium metabolism of colorectal cancer (CRC) in patients with colorectal cancer and control patients.

METHODS: Seventy newly diagnosed CRC patients were included. The healthy control group was age and gender matched (n=32). Particular attention was devoted to the relationship between serum calcium of patients, and levels of AFP, CEA, carbohydrate antigen 19-9 (CA 19-9) (that could be considered as prognostic factors). Furthermore, the Ca-sensing receptor (CaSR) gene A986S polymorphism was investigated in these patients, as well as the relationship between different CaSR genotypes and the data stated above.

RESULTS: A lower level of ionized calcium (also corrected for albumin) was found in the serum of CRC patients with normal 25(OH) vitamin D levels. The ionized calcium concentration was inversely correlated with the serum level of CA 19-9. There was no difference in the distribution of CaSR genotypes, between CRC patients and general population. The genotypes did not correlate with other data examined.

CONCLUSION: Based on these results, lower levels of serum calcium might be a pathogenic and prognostic factor in colorectal cancer.

Fuszek P, Lakatos P, Tabak A, Papp J, Nagy Z, Takacs I, Horvath HC, Lakatos PL, Speer G. Relationship between serum calcium and CA 19-9 levels in colorectal cancer. *World J Gastroenterol* 2004; 10(13): 1890-1892
http://www.wjgnet.com/1007-9327/10/1890.asp

INTRODUCTION

Mortality statistics of the developed countries show that colorectal cancer (CRC) is the second leading cause of death. Even though tumorigenesis is a complex process, epidemiological and experimental data indicate that beside the genetic factors, eating habits (and thus the calcium intake) also play a key role in the development of CRC[1]. In the past few years, we have learned more and more about the process, but not every possible factor has been uncovered yet.

Several *in vitro* and *in vivo* studies have confirmed the chemopreventive role of calcium in CRC[1-5]. The experimental data showed that there was a definite connection between low calcium and vitamin D intake and the prevalence of CRC[6,7]. Some researchers described a protective effect against the development of CRC, when the calcium intake was 1 200 mg daily[8]. Alimentary calcium (among others) together with bile acids creating insoluble calcium-soaps inhibite the cytotoxic effect of fatty acids in the bowel, thus protecting the mucus membrane[9-12].

According to twin studies, serum calcium level was mostly determined by genetic factors[13]. One of the key factors of this determination is the calcium-sensing receptor (CaSR), which by sensing the concentration of calcium in target organs could respond to the changes of calcium level, thus regulating calcium homeostasis[13]. Also, a connection has been found between the CaSR gene A986S genotypes (986 Ala/Ser) and serum calcium concentrations within the normal range in healthy adult population[14].

In our work, we examined the calcium metabolism of 70 recently diagnosed CRC patients and analyzed its possible role in the pathogenesis of CRC, and also the relationship between serum levels of AFP, CEA, CA 19-9 (that could be considered as prognostic factors) and parameters of calcium metabolism. Furthermore, we examined the genotype frequencies (CASR A986S) of our patients and the relationship between genotypes and laboratory parameters of calcium homeostasis and tumor markers.

MATERIALS AND METHODS

Patients

Seventy newly diagnosed CRC patients were examined. All the subjects were in good general conditions. Colonoscopy was performed partly for screening purposes (n=10), partly due to symptoms (n=60), such as abdominal pain, discomfort and flatulence, anemia, hematochezia, changes in bowel habits, and partly to search for primary tumor (for example in cases of hepatic metastasis). In each selected case, the histological diagnosis was adenocarcinoma. Clinical stage was Dukes A: 20, B: 32, C: 18. Five patients had liver metastasis at presentation. The clinical data of the patients are presented in Table 1. An age and gender adjusted healthy control group (n=32) was selected for comparison of the laboratory data. The CASR genotype frequency was compared to the genotype frequency of our previously determined control group, consisting of 201 healthy adults. Written informed consent was obtained from all subjects. The study was approved by the Semmelweis University Regional and Institutional Committee of Science and Research Ethics (141/2003).

Laboratory parameters

To analyze the calcium metabolism of the subjects, serum calcium, phosphate and albumin levels were determined by photometric analysis (Roche, Mannheim, Germany). Ionized calcium levels were also measured in a similar way (Easy-Lite, Bedford, USA). The calcium levels were also corrected to the serum albumin levels (corrected calcium). HPLC (Biorad,

Hercules, USA) was used to measure the serum 25(OH) vitamin D levels, while serum levels of parathyroid hormone (PTH) were determined by chemiluminescence assay (Elecsys/Roche, Basel, Switzerland). To measure AFP, CEA and CA 19-9, immunoassays (Axxym/Abbott, North Chicago, USA) were utilized.

Sampling and histology

In each case, the diagnosis was established by colonoscopy (Fujinon, Japan), and tissue samples were taken for histological analysis.

Genotyping

The polymorphic region of *CaSR* gene was amplified by allele specific PCR technique. The following primers were used: primer M: 5' ACG GTC ACC TTC TCA CTG ACG TTT GAT GAG CCT CAG AAG TAC T 3' 43-mer; primer W: 5' GCT TTG ATG AGC CTC AGA AGA TCG ' 24-mer; and primer R: 5' CTC TTC AGG GTC CTC CAC CTC T 3' 22-mer (10 μmol/L final concentration). PCR reaction was carried out in 20 μL final volume containing: 2 μL 10× Mg free reaction buffer, 4 μL dNTP (1 mmol/L), 1.2 μL 25 mmol/L $MgCl_2$, 1 μL DNA (25 ng/mL), 3-2-1 μL (primer R, -W, -M), 0.1 μL (0.5 U/μL) Taq (Promega, Madison, USA) and 5.7 μL 2D PCR water. The PCR conditions were at 94 ℃ for 12 min, 35 cycles at 94 ℃ for 20 min, at 55 ℃ for 20 min, at 72 ℃ for 30 min and at 72 ℃ for 5 min. There were two types of CaSR allels, the allele A and allele S, so the genotypes were AA, AS, SS. Electrophoretic separation was carried out in a 70 g/L Spreadex/acrilamide-bis (29:1) gel (Elchrom, Cham, Switzerland). For the PCR reaction; Hybaid express thermocycler (Teddington, Middlesex, UK) was used.

Statistics

As the first step, the distribution of continuous parameters was analyzed (Kolmogorov-Smirnov test). Logarithmic transformation was performed as needed. However, results were presented using the original units for easier understanding. The average values for CRC and the control population as well as difference between patients with different genotypes were compared using Student *t* test with separate variance estimates. χ^2 test was used to describe the relation between the allele frequency and tumor localization. Finally, we used parametric correlation (Pearson) to describe the relationship between tumor markers and the calcium homeostasis. A P value <0.05 was considered statistically significant. All the statistical analyses were performed using SPSS 9.0 for Windows.

RESULTS

By examining the calcium metabolism of CRC patients, we found that the serum calcium, ionized and corrected calcium levels of our patients were significantly lower, than those of controls. These calcium levels were at the lower limits of the normal range. Serum phosphate and albumin levels were also determined, which were in the lower end of the normal range (Table 1).

There was no difference in serum 25(OH)-vitamin D and PTH values between patients and controls (Table 1). When examining the correlation between calcium metabolism and CEA, AFP, CA 19-9 tumor markers, we found that the ionized calcium levels of our patients were inversely correlated with the serum level of CA 19-9 tumor marker (Table 2).

There was no significant difference in the CaSR A986S genotype frequency between healthy population and CRC patients [(CRC: AA=51/70(73%), AS=19/70(27%), SS=0/70 (0%); control group: AA=145/201(72%), AS=54/201(27%), SS=2/201(1%)].

In case of the different CaSR A986S genotypes of CRC patients, no difference was observed in the examined biochemical parameters and tumor markers (Table 3). Different alleles or genotypes did not show any correlation with the localization of tumor.

Table 1 Laboratory data of CRC patients (mean±SE)

	CRC	Control	*P*	Normal value
Calcium (Ca)	2.26±0.17	2.45±0.09	0.0001	2.25-2.61 mmol/L
Corrected Ca	2.26±0.14	2.37±0.11	0.0001	2.25-2.61 mmol/L
Ionized calcium	1.07±0.07	1.2±0.05	0.0001	1.05-1.25 mmol/L
Phosphate	1.07±0.13	1.2±0.22	0.006	0.85-1.45 mmol/L
Albumin	39.5±4.61	43.87±4.37	0.0001	35-50 g/L
AFP	4.19±2.85	3.34±1.58	NS	0-15 ng/L
CEA	18.84±69	1.79±1.86	0.043	0-10 ng/L
CA 19-9	86.49±406	10.20±9.95	NS	0-37 ng/L
PTH	38.2±16.8	41.5±14.6	NS	10-65 pg/mL
25(OH) vit. D	44.7±73.8	46.84±13.7	NS	20-60 ng/L
Age (yr)	65.6±10.9	63.6±8.2	NS	-

NS=no significant difference.

Table 2 Correlation between tumor marker levels and parameters of calcium metabolism of CRC patients

	Ca	Corrected Ca	*P*	Ca^{2+}	Albumin	PTH	25 (OH) vit. D
AFP	0.67	0.33	0.53	0.40	0.80	0.87	0.30
CEA	0.21	0.79	0.80	0.23	0.15	0.94	0.95
Ca19-9	0.57	0.57	0.63	0.007	0.10	0.74	0.94

Table 3 Laboratory parameters associated with different CaSR A986S genotypes (mean±SE)

	AA	AS	*P*
Calcium	2.23±0.16	2.31±0.18	NS
Corrected Ca	2.24±0.12	2.30±0.14	NS
Phosphate	1.07±0.13	1.08±0.11	NS
Ionized calcium	1.07±0.08	1.09±0.07	NS
Albumin	39.61±4.40	39.20±5.30	NS
AFP	4.18±2.96	4.29±2.68	NS
CEA	9.2±23.8	45±125	NS
CA 19-9	68±379	143±492	NS
PTH	37.3±14.2	41.2±23.0	NS
25(OH) vit. D	51±85	27.3±11.4	NS
Age (yr)	66.18±10.96	64.8±11.2	NS

NS=no significant difference.

DISCUSSION

The results of our study support the role of low serum calcium in the pathogenesis of CRC. Contrasting to previous data of others, we found that beside normal vitamin D values the level of calcium and the concentration of serum phosphate were both lower than that of controls[7], suggesting that in CRC the function of vitamin D receptor (VDR) might be damaged. Our previous study corroborates this hypothesis since we showed that oncogene (HER-2) expression correlated with VDR genotypes in CRC patients[15].

Western style diet (low in calcium and vitamin D and high in fat) has been shown to induce hyperproliferation in colonic epithelial cells. This cell proliferation could be inhibited by calcium and vitamin D supplementation[10,16,17]. By increasing calcium intake, the number of apoptotic cells in colon epithelium increased,

as well[18]. Based on several human studies, high calcium and vitamin D intake might prevent CRC development[1,3,5,6]. A prospective study claimed that the frequency of CRC was three times less in those patients whose serum vitamin D level was above 20 ng/mL[7]. More than 3.75 μg daily vitamin D intake appeared to reduce 50% incidence of CRC, while 1 200 mg daily calcium intake decreased 75% of its incidence[7,8].

Low calcium level may influence CRC pathogenesis in several ways. Calcium ion (Ca^{2+}) is needed for cell proliferation and differentiation. On the other hand, Ca^{2+} could play an important role in intercellular connections and signal-transduction cascades[19-24]. Furthermore, it has an influence on the cell-cycle regulatory genes (p53, K-ras, epidermal growth factor) that had a well-documented role in CRC pathogenesis[25,26]. The functions mentioned above are mediated partly through CaSR. Similarly to other tissues, CaSR could be detected in normal colon epithelial cells as well. Besides, stimulation of the CaSR could increase the expression of E-cadherin and decrease that of beta-catenin. E-cadherin is the inductor of cell differentiation while beta-catenin is responsible for the genesis of malignant phenotype. The fundamental question is whether the low serum calcium level influencing CRC development is present during a life-long period or emerges only in a phase of the patient' s life right before the appearance of cancer. Answering this question is crucial in deciding when to start chemoprevention.

A986S polymorphism of the CaSR gene has been suggested to have a role in the development of parathyroid adenoma. Others have demonstrated that healthy women with CaSR 986 AA homozygote had lower levels of serum calcium compared to women having AS heterozygote and SS homozygote CaSR 986 alleles[14]. Earlier, we demonstrated that CaSR A986S allele frequencies in CRC patients were not different from those in healthy subjects. However, patients with homozygote AA genotype had a significantly higher UICC stage at the time of discovery compared to the heterozygote AS patients. We could not find an association between serum calcium concentrations and CaSR A986S genotypes in our CRC subjects. We also could not detect a correlation between CaSR polymorphism and CRC. The role of CaSR A986S polymorphism in CRC development requires further investigation.

A large array of evidence indicates that CA 19-9 tumor marker had a prognostic role in CRC. Elevated serum levels were associated with the recurrence of CRC or the presence of metastasis. In our patients, serum calcium levels inversely correlated with CA 19-9 concentration, which could support the significance of serum calcium not only as a pathogenic factor but also as a prognostic factor.

In conclusion, our results further strengthen the possibility that serum calcium might be a pathogenic and prognostic factor in the development of colorectal cancer. Our data draw attention to the possibility that by increasing calcium intake, the multi-leveled pathogenic process leading to tumorigenesis might be influenced. In order to prove this, further studies are necessary.

REFERENCES

1 **Pence BC**. Role of calcium in colon cancer prevention: experimental and clinical studies. *Mutat Res* 1993; **290:** 87-95
2 **Buras RR**, Shabahang M, Davoodi F, Schumaker LM, Cullen KJ, Byers S, Nauta RJ, Evans SR. The effect of extracellular calcium on colonocytes: evidence for differential responsive based upon degree of cell differentiation. *Cell Profil* 1995; **28:** 245-262
3 **Greenwald PJ**. Cancer risk factors for selecting cohorts for large-scale chemoprevention trials. *Cell Biochem Suppl* 1996; **25:** 29-36
4 **Lipkin M**. New rodent models for studies of chemopreventive agents. *J Cell Biochem Suppl* 1997; **28-29:** 144-147
5 **Lipkin M,** Newmark H. Calcium and the prevention of colon cancer. *J Cell Biochem Suppl* 1995; **22:** 65-73
6 **Bostick RM**. Human studies of calcium supplementation and colorectal epithelial cell proliferation. *Cancer Epidemiol Biomarkers Prev* 1997; **11**: 971-980
7 **Garland CF,** Comstock GW, Garland FC, Helsing KJ, Shaw EK, Gorham ED. Serum 25-hydroxyvitamin D and colon cancer: eight-year prospective study. *Lancet* 1989; **2:** 1176-1178
8 **Holt PR**, Atillasoy EO, Gilman J, Guss J, Moss SF, Newmark H, Fan K, Yang K, Lipkin M. Modulation of abnormal colonic epithelial cell proliferation and differentiation by low-fat dairy foods: a randomized controlled trial. *JAMA* 1998; **12:** 1074-1079
9 **Pence BC**, Buddingh F. Inhibition of dietary fat-promoted colon carcinogenesis in rats by supplemental calcium or vitamin D3. *Carcinogenesis* 1988; **1:** 187-190
10 **Xue L**, Lipkin M, Newmark H, Wang J. Influence of dietary calcium and vitamin D on diet-induced epithelial cell hyperproliferation in mice. *J Natl Cancer Inst* 1999; **2:** 176-181
11 **Van der Meer R**, Kleibeuker JH, Lapre JA. Calcium phosphate, bile acids and colorectal cancer. *Eur J Cancer Prev* 1991; **1**(Suppl 2): 55-62
12 **Van der Meer R**, Lapre JA, Govers MJ, Kleibeuker JH. Mechanisms of the intestinal effects of dietary fats and milk products on colon carcinogenesis. *Cancer Lett* 1997; **114:** 75-83
13 **Brown EM**, Pollak M. The extracellular calcium-sensing-receptor: Its Role in Health and Disease. *Annu Rev Med* 1998; **49:** 15-29
14 **Cole DE**, Vieth R, Trang HM, Wong BY, Hendy GN, Rubin LA. Association between total serum calcium and the A986S polymorphism of the calcium-sensing receptor gene. *Mol Genet Metab* 2001; **72:** 168-174
15 **Speer G**, Dworak O, Cseh K, Bori Z, Salamon D, Torok I, Winkler G, Vargha P, Nagy Z, Takacs I, Kucsera M, Lakatos P. Vitamin D receptor gene BsmI polymorphism correlates with erbB-2 / HER-2 expression in human rectal cancer. *Oncology* 2000; **58**: 242-247
16 **Llor X**, Jacoby RF, Teng BB, Davidson NO, Sitrin MD, Brasitus TA. K-ras mutations in 1,2-dimethylhydrazine-induced colonic tumors: effects of supplemental dietary calcium and vitamin D deficiency. *Cancer Res* 1991; **51**: 4305-4309
17 **Nobre-Leitao C**, Chaves P, Fidalgo P, Cravo M, Gouveia-Oliveira A, Ferra MA, Mira FC. Calcium regulation of colonic crypt cell kinetics: evidence for a direct effect in mice. *Gastroenterology* 1995; **109**: 498-504
18 **Penman ID**, Liang QL, Bode J, Eastwood MA, Arends MJ. Dietary calcium supplementation increases apoptosis in the distal murine colonic epithelium. *J Clin Pathol* 2000; **53**: 302-307
19 **Buchan AM**, Squires PE, Ring M, Meloche RM. Mechanism of action of the calcium-sensing receptor in human antral gastrin cells. *Gastroenterology* 2001; **120**: 1279-1281
20 **Cerda SR**, Bissonnette M, Scaglione–Sewell B, Lyons MR, Khare S, Mustafi R, Brasitus TA. PKC-δ inhibits anchorage-dependent and -independent growth, enhances differentiation, and increases apoptosis in CaCo-2 cells. *Gastroenterology* 2001; **120:** 1700-1712
21 **Frey MR**, Clark JA, Leontieva O, Uronis JM, Black AR, Black JD. Protein kinase C signaling mediates a program of cell cycle withdrawal in the intestinal epithelium. *J Cell Biol* 2000; **151:** 763-778
22 **Osada S**, Hashimoto Y, Nomura S, Kohno Y, Chida K, Tajima O, Kubo K, Akimoto K, Koizumi H, Kitamura Y. Predominant expression of nPKC eta, a Ca(2+)-independent isoform of protein kinase C in epithelial tissues, in association with epithelial differentiation. *Cell Growth Differ* 1993; **4:** 167-175
23 **Rhee SG**. Regulation of phosphoinositide-specific phospholipase C**.** *Annu Rev Biochem* 2001; **70:** 281-312
24 **Todd C**, Reynolds NJ. Up-regulation of p21WAF1 by phorbol ester and calcium in human keratinocytes through a protein kinase C-dependent pathway. *Am J Pathol* 1998; **153:** 39-45
25 **Kawase T**, Orikasa M, Oguro A, Burns DM. Possible regulation of epidermal growth factor-receptor tyrosine autophosphorylation by calcium and G proteins in chemically permeabilized rat UMR106 cells. *Arch Oral Biol* 1999; **44:** 157-171
26 **Metcalfe S**, Weeds A, Okorokov AL, Milner J, Cockman M, Pope B. Wild-type p53 protein shows calcium-dependent binding to F-actin. *Oncogene* 1999; **18:** 2351-2355

Edited by Wang XL and Chen WW **Proofread by** Xu FM

PO Box 2345, Beijing 100023, China
Fax: +86-10-85381893
E-mail: wjg@wjgnet.com www.wjgnet.com

World J Gastroenterol 2004;10(13):1893-1897
World Journal of Gastroenterology
 ISSN 1007-9327

• VIRAL HEPATITIS •

SEN virus does not affect treatment response in hepatitis C virus coinfected patients but SEN virus response depends on SEN virus DNA concentration

Abdurrahman Sagir, Ortwin Adams, Oliver Kirschberg, Andreas Erhardt, Tobias Heintges, Dieter Häussinger

Abdurrahman Sagir, Oliver Kirschberg, Andreas Erhardt, Tobias Heintges, Dieter Häussinger, Klinik für Gastroenterologie, Hepatologie und Infektiologie, Universitätsklinikum Düsseldorf, Moorenstr 5, 40225 Düsseldorf, Germany
Ortwin Adams, Institut für Virologie der Heinrich-Heine-Universität Düsseldorf, Moorenstr 5, 40225 Düsseldorf, Germany
Correspondence to: Dr. A. Sagir, Klinik für Gastroenterologie, Hepatologie und Infektiologie, Universitätsklinikum Düsseldorf, Moorenstr 5, 40225 Düsseldorf, Germany. sagir@med.uni-duesseldorf.de
Telephone: +49-211-8117820 **Fax:** +49-211-8118752
Received: 2003-10-16 **Accepted:** 2004-02-11

Abstract

AIM: To clarify the effect of SEN virus (SENV) infection on a combination therapy including interferon alfa (IFN-α) or pegylated-IFN with ribavirin in patients with chronic hepatitis and the effect of a combination therapy on SENV.

METHODS: SENV DNA was determined by polymerase chain reaction in serum samples from 95 patients with chronic hepatitis C. Quantitative analysis was done for SENV H DNA.

RESULTS: Twenty-one (22%) of 95 patients were positive for SENV DNA. There was no difference in clinical and biochemical parameters between patients with HCV infection alone and coinfected patients. The sustained response rate for HCV clearance after combination therapy did not differ between patients with SENV (52%) and without SENV (50%, n.s.). SENV DNA was undetectable in 76% of the initially SENV positive patients at the end of follow-up. SENV H response to combination therapy was significantly correlated with SENV DNA level (P=0.05).

CONCLUSION: SENV infection had no influence on the HCV sustained response rate to the combination therapy. Response rate of SENV to the combination therapy depends on SENV DNA level.

Sagir A, Adams O, Kirschberg O, Erhardt A, Heintges T, Häussinger D. SEN virus does not affect treatment response in hepatitis C virus coinfected patients but SEN virus response depends on SEN virus DNA concentration. *World J Gastroenterol* 2004; 10(13): 1893-1897
http://www.wjgnet.com/1007-9327/10/1893.asp

INTRODUCTION

Five hepatitis viruses (A-E) are responsible for more than 80% of cases of viral hepatitis. Recently, a new family of DNA viruses was discovered and designated as "SEN virus" (SENV)[1]. SENV is a single-stranded circular virus of approximately 3 800 nucleotides. By phylogenetic analysis, 8 different strains of SENV have been identified. SENV is a member of the *Circoviridae* family, a group of small, single-stranded, nonenveloped circular DNA virus that includes TT virus, TUS01, SANBAN, and YONBAN[2].

Two strains of SENV (SENV D and SENV H) have been extensively studied and have been shown to be present in approximately 2% of blood donors in the United States, 2% in Italy and 10% in Japan and to be readily transmitted by blood transfusion and other common parenteral routes[3]. Although SENV infection is cleared spontaneously in the majority of patients, approximately 45% develop persistent infection that exceeds 1 year and has been documented as long as 12 years. Hypervariable regions with mutation rates of 7.32×10^{-4} per site per year may be involved in the persistence[4]. Although SENV D and SENV H infections were strongly associated with transfusion-associated non-A to non-E hepatitis in one study, this association does not establish causality and the vast majority of patients infected with SENV did not develop hepatitis at the time of transfusion[3]. However, the clinical role of SENV infection is not yet clear.

HCV is a major cause of post-transfusion hepatitis and chronic liver disease[5]. More than half of patients with HCV infection develop chronic hepatitis that leads to liver cirrhosis, and hepatocellular carcinoma (HCC)[6]. The prevalence of SENV in patients with chronic hepatitis was reported to be between 24% and 40%[3,7]. There is no evidence that SENV infection affects the progression of HCV infection, but the influence of SENV on HCV response to interferon alfa (IFN-α) is not clear[3]. Three studies investigated the influence of SENV on the response to interferon therapy in HCV infected patients[8-10]. Rigas *et al*. and Kao *et al*. investigated the patients with chronic hepatitis treated for 6 mo with 3 million units interferon (IFN) 2 alfa 3 times per week plus 1 000-1 200 mg ribavirin daily. The morning dose was reduced to 400 mg for those weighing less than 72 kg. Rigas *et al.* could demonstrate a negative effect of SENV coinfection on the outcome of therapy[8]. Kao *et al*. showed that SENV infection has no effect on response to combination therapy[10]. The third study investigated 104 patients who were treated with IFN at a dosage of 9 million units (MU) daily for 2 wk, followed by 9 MU 3 times a week for 22 wk (total dose, 720 MU). There was no effect of SENV coinfection on interferon response in this study[9].

None of the studies represent the current therapy scheme. Therapy duration depends on HCV genotype. Patients with HCV genotype 2 or 3 are treated for 24 wk with IFN 3 MU 3 times a week plus ribavirin at a dosage of 1 200 mg or 1 000 mg daily. Patients with genotypes other than 2 or 3 are treated for 48 wk[11,12].

The aim of this study was to determine the prevalence of SENV infection in chronic HCV infected patients, the influence on clinical and virological characteristics and the effect of SENV coinfection on HCV response to combination therapy including IFN and ribavirin.

MATERIALS AND METHODS

Subjekts

Ninety-five patients with chronic hepatitis C virus infection

were seen at the outpatient department of the University of Düsseldorf. Diagnosis of chronic hepatitis C was based on the following criteria: (1) detectable HCV-RNA; (2) absence of detectable hepatitis B surface antigen; (3) exclusion of other liver diseases (autoimmune hepatitis, hemochromatosis, Wilson disease). All patients received combination therapy with IFNα or pegylated-interferon (PEG-IFN)α plus ribavirin, and treated for 24 or 48 wk with IFNα 2a (Intron) or 2b (Roferon)- or PEG-IFNα 2a (PEG-Intron) or 2b (Pegasys), and oral ribavirin (Rebetol, Schering Plough) at a dose of 1 000 mg (weight<75 kg) or 1 200 mg (weight>75 kg) daily. Patients infected with HCV genotype 1 or 4 were treated for 48 wk. Patients with HCV genotype 2 or 3 were treated for 24 wk. Blood samples were taken at baseline, at the end of treatment and six months after the treatment. HCV RNA was detected at baseline, 24, 48 and 24 wk after treatment.

Responders were defined as patients who had undetectable levels of HCV RNA in serum and normal ALT 6 mo after the treatment. Patients, who were positive for HCV-RNA at wk 24 discontinued the treatment and were defined as nonresponders. Patients who relapsed after end of treatment were defined as nonresponders. No patient had a history of or developed decompensated cirrhosis or HCC during the study period and all were negative for the antibody to human immundeficiency virus.

Ninety-five patients entered the study between 1999 and 2002. Forty-nine patients were treated in combination with IFN and 46 patients in combination with PEG-IFN. Fifty-nine of them were men and 36 women with mean age of 42±12 years. Sixty-eight (71%) of them were infected with HCV genotype 1 or 4 and 26(27%) with genotype 2/3 and HCV genotype of 2(2%) patients were undetermined. Mean ALT was 72±73 U/l.

SENV-detection and quantification

The presence of SENV D and SENV H DNA was determined by PCR. Total DNA was extracted from 200 μL serum with the QIAamp blood kit (QIAGEN) and resuspend in 200 μL of elution buffer. The oligonucleotide primers were synthesized according to the published SENV sequences. The selection of the real-time PCR primers for SENV H-virus and SENV D was done with the support of the Primer Express Software (PE Applied Biosystems, Weiterstadt, Germany).

The primer for the SENV H were designated SENV H-F1 (GGTTAACCKSAGCTGACTTCA (K=G/T; S=G/C)) and SENV H-R1 (GGAAGGTGTAGCAAGGGTTGTC), the fluorogenic TaqMan®probe (5' *FAM* TTTCCGTTCTGCTCACCACAAA 3' *TAMRA*). A 69-base pair amplicon in a conserved region of the ORF 1 gene was amplified and detected. The primers for the SENV D were designated SENV D-F1 (CCAGACTTRTGC AAAGTTCCTCTTG (R=A/G)) and SENV D-R1 (GTGGTGAG CAGAACGGATGTT), the fluorogenic TaqMan®probe (5' *FAM* AACTTTGCGGTCAACTGCCGCTG 3' *TAMRA*). A 76-base pair amplicon in a conserved region of the ORF 1 gene was amplified and detected. Each PCR contained 5 μL sample DNA, 300 nmol/L forward and reverse primer, 200 nmol/L fluorogenic Taq-man probe, 200 μmol/L (each) dATP, dCTP, and dGTP, 400 μmol/L dUTP, 10 mmol/L Tris-HCl (pH 8.3), 5 mmol/L $MgCl_2$, 0.5 U uracyl-N-glycosylase (UNG) and 1.25 U *Taq* Gold polymerase in a final volume of 50 μL. Following inactivation of the UNG (2 min, 50 ℃) and activation of the AmpliTaq Gold for 10 min at 95 ℃, 40 cycles (15 s at 95 ℃ and 1 min at 60 ℃) were performed with an thermocycler 5 700 system (PE Applied Biosystems). As a DNA standard for the SENV H-PCR, a SENV H-coding plasmid (pSGSEN-H), encompassing the amplified region of the TaqMan®-PCR, was created by PCR-cloning and serially diluted. The sensitivity of the TaqMan PCR was determined as <5 copies/assay. A standard graph of the C_T values obtained from serial dilutions of the standard was constructed by the software and the C_T values of the unknown samples were plotted on the standard curves and the number of SENV H genomes were calculated. For the SENV D-PCR no standard-plasmid was created and the results were only determined qualitatively.

Serologic testing of hepatitis B and C

The qualitative analysis of HCV-RNA was tested by a commercial PCR assay (Amplicor HCV Amplification 2.0, Roche Diagnostics, Indianapolis, IN). The quantitative analysis of HBV-DNA was made by a commercial assay (Digene Hybrid Capture System HBV DNA Assay). HBs-Ag as a serologic marker of HBV-infection was detected by a commercial immunoassay (Axsym HBs-Ag, Abbott Laboratories, North Chicago, IL).

Genotyping of HCV

The genotype analysis of HCV was performed by a commercial hybridization assay (Inno-Lipa HCV II, Innogenetics, Ghent, Belgium) using HCV-positive amplification products from the PCR assay (Amplicor HCV Amplification 2.0, Roche Diagnostics, Indianapolis, IN).

Statistical analysis

Data were entered in SPSS (version 11.0, Inc., Munich, Germany). A χ^2 or Fisher´s exact test (F-test) was used for the comparison of categorical variables, and a Mann-Whitney test was used for the comparison of continuous variables. The significance level was set at 0.05, and all *P* values were two tailed. All statistical analyses were performed using of SPSS.

ULTS

SENV was detected in 21 (22%) of 95 patients. Of the 21 patients, 16 were infected with SENV H, 4 with SENV D, and one with both strains. The mean SENV H DNA level in serum was 461±381 copies/mL. The mean age and the proportion of men and women were similar in the SENV positive and SENV negative group. There was no significant difference between both groups concerning serum levels of ALT, HCV genotype, number of patients who received PEG-IFN, and the proportion of pretreated patients (Table 1). Therefore, many confounding variables known to influence the outcome of the therapy were excluded. Sustained response rates did not differ significantly between the 21 SENV positive patients and 74 SENV negative patients. Eleven of the 21 SENV positive and 37 of the 74 SENV negative patients were responders (52% *vs* 50%, *P*=1.0).

Table 1 Characteristics of SENV positive and SENV negative patients

	SENV positive (*n*=21)	SENV negative (*n*=74)	*P* value
Median age (yr)	42±12	42±12	0.99[1]
Male, m (%)	13 (62%)	46 (62%)	1.0[2]
Median baseline ALT (IU/L)	81±109	69±60	0.56[1]
Pretreated, *n* (%)	3 (14%)	10 (14%)	1.0[2]
Hepatitis C genotype, *n* (%)			
1,4	16 (76%)	51 (69%)	0.6[2]
2,3	5 (24%)	21 (28%)	0.79[2]
Undetermined	0 (0%)	2 (3%)	
PEG-IFN	11 (52%)	35 (47%)	0.81[2]
Sustained HCV response to therapy	11 (52%)	37 (50%)	1.0[2]

[1]Mann-Whitney test; [2]Fisher´s exact test.

Of the 95 patients receiving combination therapy, 48 were sustained responders, who lost detectable HCV RNA for more than 24 wk after completing the therapy (51%). Of these 48 patients, 30 were infected with HCV genotype 1 or 4 and 16 with HCV genotype 2 or 3 and in 2 patients HCV genotypes were undetermined. Sustained responders were found to be independent in relation to gender, ALT before treatment, HCV genotype, and SENV DNA positivity. Sustained HCV response rate to the combination therapy was correlated inversely with age of the patients ([b]$P<0.01$). A higher mean SENV H DNA level was observed in the nonresponder group, but the difference was not statiscally significant (393±297 *vs* 523±452, $P=0.48$) (Table 2).

Table 2 Clinical, biochemical and viral characteristics in relation to HCV response to combination therapy

	Sustained response (n=48)	No sustained response (n=47)	P value
Male, n (%)	30 (63%)	29 (62%)	0.34[1]
Age (yr)	39±11	45±11	<0.01[2]
ALT	70±78	74±68	0.54[2]
HCV genotype, n (%)			
1 or 4	30 (63%)	37(79%)	
2 or 3	16 (33%)	10 (21%)	0.16[1]
Undetermined	2 (4%)		
SEN positive, n (%)	10 (21%)	11 (23%)	0.81[1]
SENV H-DNA (copies / mL)	393±297	523±452	0.48[2]

[1]Fisher´s exact test; [2]Mann-Whitney test.

We analysed the response of SENV to the combination therapy in 20 of the 21 SENV positive patients. The clinical and virological characteristics are shown in Table 3. Of the 21 patients with SENV DNA, 16 were infected with SENV-H, 3 with SENV-D, and 1 with both. Fifteen (75%) of 20 patients had no detectable SENV DNA after treatment. Two (66%) of the 3 patients infected with SENV D responded to the combination therapy, 12 (75%) of the 16 patients infected with SENV H, and the patient who was infected with both strains responded to combination therapy. SENV response to the combination therapy did not correlate with sex, age, or ALT level (Table 4). SENV H response rates correlated with the SENV-DNA titer before treatment. SENV H-DNA level was significantly lower in patients who responded to the combination therapy (371±276 copies/mL *vs* 820±497 copies/mL, $P=0.05$).

Of the five patients who failed to eradicate SENV, two lost HCV-RNA, one of these two patients did not have ALT normalized.

Table 4 Clinical and virological parameter of SENV response to combination therapy in 20 HCV / SENV-coinfected patients

	SENV response (15)	SENV nonresponse (5)	P
Age (yr,mean)	41±12	48±13	0.23[1]
Male	10 (63%)	3 (60%)	1.0[2]
ALT	85±61	80±123	0.35[1]
SENV H-DNA (copies / mL)	371±276 (n=13)	820±497 (n=4)	0.05[1]

[1]Mann-Withney test; [2]Fisher´s exact test.

DISCUSSION

SENV D or SENV H-DNA was detectable in 22% of the patients, which is comparable to recent reports[13]. The observed frequency of HCV and SENV infection is not surprising because these agents are transmitted by similar routes. SENV has been shown to be associated with blood transfusion and intravenous drug abuse[3,14]. Dual infection with HCV and other

Table 3 Clinical and virological characteristics of patients coinfected with HCV and SENV

No	Age(yr)	SEX	ALT (U / L)	HCV genotype	SENV genotype	SENV H copies / mL	HCV response	SEN V response
1	60	M	62	1	H	218	Yes	Yes
2	47	F	26	1	D / H	74	No	Yes
3	41	F	41	1	D	-	Yes	No
4	31	M	26	1	H	208	Yes	Yes
5	59	F	62	1	H	1304	No	No
6	47	F	169	2	H	1184	No	No
7	31	M	26	1	H	484	Yes	No
8	28	M	32	1	H	308	Yes	Yes
9	63	M	168	1	H	310	No	No
10	59	F	121	4	H	338	No	Yes
11	35	F	42	2	H	38	Yes	Yes
12	36	M	43	1	H	532	No	Yes
13	41	M	24	1	H	848	Yes	Yes
14	41	M	180	1	D	-	Yes	Yes
15	32	F	513	3	H	224	Yes	Yes
16	44	F	36	3	D	-	Yes	Yes
17	28	M	28	2	H	814	Yes	Yes
18	42	M	40	1	H	74	No	Yes
19	37	M	32	4	H	230	No	Yes
20	62	F	41	1	H	662	No	Yes

hepatitis virus (HAV, HBV) has been reported to be associated with a more severe and rapidly progressing liver disease[15-17]. In our study no clinical or biochemical difference was found between patients with HCV infection alone and those coinfected with HCV and SENV. In this and previous studies, there was no evidence to suggest that SENV coinfection leads to increased severity or persistence of chronic hepatitis C[7]. It was demonstrated that infection with SENV in patients with non-A to non-E liver disease has no effect on disease progression[18].

Five independent factors could be identified which are significantly associated with response to antiviral therapy: genotype 2 or 3, viral load less than 2 million copies/mL, age 40 years or less, minimal fibrosis stage, and female sex[11]. Of these five factors, we studied sex, age, ALT, and HCV genotype and found a significant correlation for response of age (P=0.006) but not of sex, ALT, or HCV genotype. This result may reflect the patient selection. We observed on an average, 1.3 times higher SENV DNA level in patients who failed to the therapy compared with patients with sustained response. Nevertheless, this difference was not statistically significant (393±297 *vs* 523±452, P=0.48) and may be due to the small cohort studied.

Response rates to antiviral therapy in hepatitis C has increased after combination therapy consisting of IFN and ribavirin was used. Further increase was observed after introduction of PEG-IFN. Sustained response rates of up to 80% in HCV genotype 2/3 are described[12]. Patients coinfected with other hepatotrophic viruses are still difficult to treat. Coinfection with hepatitis B virus impairs sustained rate[15]. On the other hand, it could be demonstrated that coinfection with TT virus has no influence on response rates to IFN therapy in patients with chronic hepatitis C infection[19,20]. Three studies tried to clarify the influence of SENV on chronic hepatitis C. Rigas *et al*. reported that coinfection with HCV and SENV adversely affected the HCV response to combination therapy with interferon and ribavirin[8]. This cohort was treated for 6 mo with 3 million units IFN 2ab three times per week plus 1 000/1 200 mg ribavirin/day depending on body mass more or less than 72 kg. They did not take into account that antiviral therapy duration in hepatitis C depends on HCV genotype. In contrast, Umemura *et al*. found no influence of SENV coinfection on HCV therapy[9]. They investigated the patients with chronic hepatitis C virus infection, who underwent an IFN-monotherapy. Kao *et al*. studied 100 patients with chronic hepatitis C who were treated with IFN and ribavirin. These patients were treated for 24 wk independent of HCV genotype. They showed that coinfection with SENV has no effect on response to the therapy. However, none of the studies represented the current standard in the therapy of HCV infection.

In our study, patients received combination therapy for a duration depending on HCV genotype. We found no significant difference in sustained response rates between patients with HCV and SENV coinfection and those who had HCV infection alone (52% *vs* 50%, P=1.0). Therefore, our data are in concordance with the results from Umemura *et al*. and Kao *et al*. Overall sustained response rates were higher in our study as compared with the study by Umemura. This results from the higher efficiency of combination therapy compared with IFN-monotherapy.

Sixteen of 20 coinfected patients lost SENV DNA after treatment. There was no influence of the SENV strain on the response rates. SENV D and SENV H response to the combination therapy was not different (2/3 (66%) *vs* 12/16 (75%), P=1.0). This result is in contrast to the results published by Umemura *et al*. The authors reported a response rate of SENV D to a IFN-α therapy of 73% (11/15 patients) and 33% (1/3 patients) for SENV H. This discrepancy may be a result of our cohort. In contrast to their studies we detected more often SENV H than SENV D.

It is well known that virus load is a predictive factor for response to treatment in different virus infections. For example, sustained response rate of HCV therapy correlates with the virus load at initiation of therapy[21]. Patients with high HBV-DNA levels fail more often to antiviral therapy than patients with low HBV-DNA levels[22]. Similarly, a significant difference in SENV DNA levels between patients who lost SENV DNA and whose who did not respond was found. SENV H-DNA levels were significantly lower in the group who lost SENV (P=0.05).

In conclusion, SENV infection is common in patients with HCV infection. SENV coinfection does not influence the clinical course of hepatitis C or the response rates of HCV to the combination therapy. SENV is sensitive to IFN-α, and additional medication with ribavirin does not improve response to IFN-α. The SENV response rate is correlated with the SENV DNA level prior to treatment. Higher levels influence response rate adversely.

REFERENCES

1 **Primi D**, Fiordalisi G, Mantero JL, Mattioli S, Sottini A, Bonelli F. Identifikation of SEN V genotypes. Worlds Intellectual Property Organisation. *May* 2000

2 **Tanaka Y**, Primi D, Wang RY, Umemura T, Yeo AE, Mizokami M, Alter HJ, Shih JW. Genomic and molecular evolutionary analysis of a newly identified infectious agent (SEN virus) and its relationship to the TT virus family. *J Infect Dis* 2001; **183**: 359-367

3 **Umemura T**, Yeo AE, Sottini A, Moratto D, Tanaka Y, Wang RY, Shih JW, Donahue P, Primi D, Alter HJ. SEN virus infection and its relationship to transfusion-associated hepatitis. *Hepatology* 2001; **33**: 303-311

4 **Umemura T**, Tanaka Y, Kiyosawa K, Alter HJ, Shih JW. Observation of positive selection within hypervariable regions of a newly identified DNA virus (SEN virus). *FEBS Lett* 2002; **510**: 171-174

5 **Alter HJ**, Purcell RH, Shih JW, Melpolder JC, Houghton M, Choo QL, Kuo G. Detection of antibody to hepatitis C virus in prospectively followed transfusion recipients with acute and chronic non-A, non-B hepatitis. *N Engl J Med* 1989; **321**: 1494-1500

6 **Alter HJ**, Seeff LB. Recovery, persistence, and sequelae in hepatitis C virus infection: a perspective on long-term outcome. *Semin Liver Dis* 2000; **20**: 17-35

7 **Umemura T**, Alter HJ, Tanaka E, Yeo AE, Shih JW, Orii K, Matsumoto A, Yoshizawa K, Kiyosawa K. Association between SEN virus infection and hepatitis C in Japan. *J Infect Dis* 2001; **184**: 1246-1251

8 **Rigas B**, Hasan I, Rehman R, Donahue P, Wittkowski KM, Lebovics E. Effect on treatment outcome of coinfection with SEN viruses in patients with hepatitis C. *Lancet* 2001; **358**: 1961-1962

9 **Umemura T**, Alter HJ, Tanaka E, Orii K, Yeo AE, Shih JW, Matsumoto A, Yoshizawa K, Kiyosawa K. SEN virus: response to interferon alfa and influence on the severity and treatment response of coexistent hepatitis C. *Hepatology* 2002; **35**: 953-959

10 **Kao JH**, Chen W, Chen PJ, Lai MY, Chen DS. SEN virus infection in patients with chronic hepatitis C: preferential coinfection with hepatitis C genotype 2a and no effect on response to therapy with interferon plus ribavirin. *J Infect Dis* 2003; **187**: 307-310

11 **Poynard T**, Marcellin P, Lee SS, Niederau C, Minuk GS, Ideo G, Bain V, Heathcote J, Zeuzem S, Trepo C, Albrecht J. Randomised trial of interferon alpha2b plus ribavirin for 48 weeks or for 24 weeks versus interferon alpha2b plus placebo for 48 weeks for treatment of chronic infection with hepatitis C virus. International hepatitis interventional therapy group (IHIT). *Lancet* 1998; **352**: 1426-1432

12 **Manns MP**, McHutchison JG, Gordon SC, Rustgi VK, Shiffman M, Reindollar R, Goodman ZD, Koury K, Ling M, Albrecht JK. Peginterferon alfa-2b plus ribavirin compared with interferon alfa-2b plus ribavirin for initial treatment of chronic hepatitis C:

a randomised trial. *Lancet* 2001; **358**: 958-965
13 **Shibata M**, Wang RY, Yoshiba M, Shih JW, Alter HJ, Mitamura K. The presence of a newly identified infectious agent (SEN virus) in patients with liver diseases and in blood donors in Japan. *J Infect Dis* 2001; **184**: 400-404
14 **Wilson LE**, Umemura T, Astemborski J, Ray SC, Alter HJ, Strathdee SA, Vlahov D, Thomas DL. Dynamics of SEN virus infection among injection drug users. *J Infect Dis* 2001; **184**: 1315-1319
15 **Zignego AL**, Fontana R, Puliti S, Barbagli S, Monti M, Careccia G, Giannelli F, Giannini C, Buzzelli G, Brunetto MR, Bonino F, Gentilini P. Impaired response to alpha interferon in patients with an inapparent hepatitis B and hepatitis C virus coinfection. *Arch Virol* 1997; **142**: 535-544
16 **Pontisso P**, Ruvoletto MG, Fattovich G, Chemello L, Gallorini A, Ruol A, Alberti A. Clinical and virological profiles in patients with multiple hepatitis virus infections. *Gastroenterology* 1993; **105**: 1529-1533
17 **Vento S**, Garofano T, Renzini C, Cainelli F, Casali F, Ghironzi G, Ferraro T, Concia E. Fulminant hepatitis associated with hepatitis A virus superinfection in patients with chronic hepatitis C. *N Engl J Med* 1998; **338**: 286-290
18 **Mikuni M**, Moriyama M, Tanaka N, Abe K, Arakawa Y. SEN virus infection does not affect the progression of non-A to -E liver disease. *J Med Virol* 2002; **67**: 624-629
19 **Nishizawa Y**, Tanaka E, Orii K, Rokuhara A, Ichijo T, Yoshizawa K, Kiyosawa K. Clinical impact of genotype 1 TT virus infection in patients with chronic hepatitis C and response of TT virus to alpha-interferon. *J Gastroenterol Hepatol* 2000; **15**: 1292-1297
20 **Kawanaka M**, Niiyama G, Mahmood S, Ifukube S, Yoshida N, Onishi H, Hanano S, Ito T, Yamada G. Effect of TT virus co-infection on interferon response in chronic hepatitis C patients. *Liver* 2002; **22**: 351-355
21 **Lindsay KL**, Trepo C, Heintges T, Shiffman ML, Gordon SC, Hoefs JC, Schiff ER, Goodman ZD, Laughlin M, Yao R, Albrecht JK. A randomized, double-blind trial comparing pegylated interferon alfa-2b to interferon alfa-2b as initial treatment for chronic hepatitis C. *Hepatology* 2001; **34**: 395-403
22 **Niederau C**, Heintges T, Lange S, Goldmann G, Niederau CM, Mohr L, Häussinger D. Long-term follow-up of HBeAg-positive patients treated with interferon alfa for chronic hepatitis B. *N Engl J Med* 1996; **334**: 1422-1427

Edited by Ma JY and Xu FM

PO Box 2345, Beijing 100023, China
Fax: +86-10-85381893
E-mail: wjg@wjgnet.com www.wjgnet.com

World J Gastroenterol 2004;10(13):1898-1901
World Journal of Gastroenterology
 ISSN 1007-9327

• VIRAL HEPATITIS •

Effect of vector-expressed siRNA on HBV replication in hepatoblastoma cells

Jun Liu, Ying Guo, Cai-Fang Xue, Ying-Hui Li, Yu-Xiao Huang, Jin Ding, Wei-Dong Gong, Ya Zhao

Jun Liu, Cai-Fang Xue, Ying-Hui Li, Yu-Xiao Huang, Jin Ding, Wei-Dong Gong, Ya Zhao, Department of Etiology, Fourth Military Medical University, Xi' an 710033, Shaanxi Province, China
Ying Guo, Department of Obstetrics and Gynecology, Second Hospital of Xi' an Jiaotong University, Xi' an 710001, Shaanxi Province, China
Supported by National Natural Science Foundation of China, No. 30100157; Medical Research Fund of Chinese PLA, No. 01MA184; and Innovation Project of FMMU, No. CX99005
Correspondence to: Dr. Jun Liu, Department of Etiology, Fourth Military Medical University, Xi' an 710033, Shaanxi Province, China. etiology@fmmu.edu.cn
Telephone: +86-29-83374536 **Fax:** +86-29-83374594
Received: 2003-12-12 **Accepted:** 2004-01-15

Abstract

AIM: To study the effect of siRNA expressed from DNA vector on HBV replication.

METHODS: Human U6 promoter was amplified from genomic DNA and cloned into plasmid pUC18 to construct a mammalian siRNA expression vector pUC18U6. Then oligonucleotides coding for a short hairpin RNA against HBV were cloned into pUC18U6 to form pUC18U6HBVsir which was introduced into 2.2.15 cells by using liposome-mediated transfection. 2.2.15 cells transfected by pUC18U6 and pUC18U6GFPsir which expressed siRNA against green fluorescent protein and mock-transfected 2.2.15 cells were used as controls. Concentration of HBsAg in the supernatant of the transfected cells was measured by using solid-phase radioimmunoassay.

RESULTS: A mammalian siRNA expression vector pUC18U6 was constructed successfully. Compared with controls, pUC18U6HBVsir which expressed siRNA against HBV decreased concentration of HBsAg significantly by 44%(P<0.05).

CONCLUSION: HBV replication in 2.2.15 cells is inhibited by siRNA expressed from the DNA vector.

Liu J, Guo Y, Xue CF, Li YH, Huang YX, Ding J, Gong WD, Zhao Y. Effect of vector-expressed siRNA on HBV replication in hepatoblastoma cells. *World J Gastroenterol* 2004; 10 (13): 1898-1901

http://www.wjgnet.com/1007-9327/10/1898.asp

INTRODUCTION

RNA interference (RNAi) is a potent gene silencing mechanism conserved in all eukaryotes, in which double-stranded RNAs suppress the expression of cognate genes inducing degradation of mRNAs or blocking mRNA translation[1-3]. The physiological functions of RNAi are not very clear as yet, but it has been used successively as a potent method of gene knockdown in study of gene function and in experimental treatment of some diseases[4-19]. In mammalian cells, double-stranded RNAs inducing RNAi must be short in length (<30 bp) so that they would not activate nonspecific interferon reactions. These short interfering RNAs (siRNAs) can be produced by four different ways: chemical synthesis, *in vitro* transcription, enzymatic digestion of dsRNAs and transfection of DNA vectors encoding siRNAs. Among the four ways, transfection of DNA vectors has some advantages such as low cost, lasting expression of siRNA, easiness of preparation, which make it the preferential method when siRNAs are used in treatment of diseases.

Hepatitis B virus (HBV) is a small enveloped DNA virus which belongs to hepadnaviridae. Human beings are HBV's natural host, though some primates can be infected in laboratory. Liver is the primary target organ of infection and persistent infection of HBV usually leads to severe diseases, such as chronic hepatitis, cirrhosis and hepatocellular carcinoma. Current treatment regimens for chronic HBV infection, namely administration of interferon-γ, lamivudine, adefovir, or different combinations of these drugs have only limited long-term efficacy and many adverse effects or drug resistance[20,21]. Considering the huge population infected by HBV (more than 350 million people are infected by HBV around the world), the exploration of novel treatment strategies is both necessary and urgent. Many ingenious treatment strategies have been tested for inhibition of HBV replication, such as antisense nucleotides, ribozymes, intracellular antibodies, and targeted ribonucleases[22], and all of them have been demonstrated to inhibit HBV replication to various degrees.

To explore RNAi as a novel alternative strategy for treating HBV, we constructed a DNA vector which can express siRNAs in mammalian cells, and then the vector was used to express in 2.2.15 cells a siRNA against HBV to study its effect on HBV replication.

MATERIALS AND METHODS

Cell culture

Human hepatoblastoma Hep G2 cell line 2.2.15 cells stably transfected by HBV genome, were cultured in Dulbecco's modified Eagle's medium (DMEM, from Gibco Life Technologies, Grand Island, NY) supplemented with 100 mL/L fetal calf serum (Sijiqing Biotech Company, Hangzhou, China).

Construction of mammalian siRNA expression vector-pUC18U6

Human genomic DNA was extracted from HepG2 cells with DNeasy™tissue kit (Qiagen, Germany) according to the manufacturer's protocol. Purified human genomic DNA was used as the template in PCR to obtain human U6 promoter. The sequences of the primers are as follows: Forward primer: 5' GCGATCTAGAAAGGTCGGGCAGGAAGAG3', reverse primer: 5' GCGAGGTACCGGTGTTTCGTCCTTTCCACAAG3'.

The underlined bases in forward and reverse primers have recognition sites for *Xba* I and *Kpn* I, respectively. The condition of PCR was at 94 ℃ for 5 min, then 35 cycles at 94 ℃ for 30 s, at 60 ℃ for 30 s, and at 72 ℃ for 1.5 min followed by extension at 72 ℃ for 7 min. The PCR product was analyzed with 100 g/L agarose gel electrophoresis and then purified by PCR fragment recovery kit as recommended by the manufacturer (Takara, Dalian, China). The purified PCR product was digested by *Xba* I and *Kpn* I, ligated with pUC18,

and transformed into competent *E. coli*. The recombinant plasmid was then purified from transformed *E. coli*, and verified by *Xba* I/*Kpn* I digestion analysis and DNA sequencing.

Construction of HBV-siRNA expression vector-pUC18U6HBVsir

Two oligodeoxyribonucleotides encoding shRNA against HBV were synthesized by Bioasia Company (Shanghai) and their sequences are as follows: Oligo 1:5' CAGGCTTTCACTTTCT CGCTCGAGCGAGAAAGTGAAAGCCTGCTTTTTTG3' , Oligo2:5' AATTCAAAAAAGCAGGCTTTCACTTTCTC GCTCGAGCGAGAAAGTGAAAGCCTG3' .

The underlined bases are spacer region and recognition site for *Xho* I. The target of shRNA was 1 086-1 103 nt of HBV genome. To clone the two oligodeoxyribonucleotides, downstream of U6 promoter into pUC18U6, 400 nmol/L for each of the two oligodeoxyribonucleotides was mixed, heated at 100 ℃ for 5 min, and cooled gradually to room temperature to anneal. pUC18U6 was digested with *Kpn* I, blunt-ended with T4 DNA polymerase, then digested with *Eco*R I, purified and ligated with the annealed oligodeoxyribonucleotides. The ligation mixture was transformed into competent *E. coli*. The recombinant plasmid was then purified from transformed *E. coli*, and verified by *Hin*d III/*Xho* I digestion analysis. A control vector, pUC18U6GFPsir, which expressed a siRNA against green fluorescent protein (GFP), was constructed with the same methods and the sequences of the two oligodeoxyribonucleotides encoding the siRNA were synthesized as previously described[23]: Oligo1:5' GGCGAT GCCACCTACGGCAAGCTCGAGCTTGCCGTAGGTG GCATCGCCCCTTTTTTG3' ,Oligo2:5' AATTCAAAAAAG GGCGATGCCACCTACGGCAAGCTCGAGCTTGCCG TAGGTGGCATCGCC3' .

The underlined bases are spacer region and recognition site for *Xho* I.

Transfection

Twenty-four hours before transfection, 2.2.15 cells were seeded into the culture plate at a density of 2×10^8/L. Lipofectamine™ 2000 reagent (Gibco Life Technologies, Grand Island, NY) was used for the transfection of 2.2.15 cells by pUC18U6HBVsir, pUC18U6, pUC18U6GFPsir, or mock solution (DMEM plus Lipofectamine™ 2000 reagent containing no plasmid) according to the manufacturer' s protocol.

Quantification of HBsAg in supernatant of cell culture

Forty-eight hours after the transfection, the supernatant of the cell culture was collected, and HBsAg in the supernatant was quantified using the solid phase radio-immunoassay kit for quantification of HBsAg (Beimian Dongya Biotech Institute, Beijing) according to the manufacturer' s protocol. Briefly, 200 μL of the supernatant was incubated with a plastic tube coated by anti-HBs antibody at 45 ℃ for 1.5 h. After the tube was thoroughly washed with deionized water, 200 μL of ^{125}I-labelled secondary antibody was added and incubated at 45 ℃ for 2 h. The tube was thoroughly washed, and cpm was measured. The concentration of HBsAg of each sample was calculated by comparing the cpm of each sample with a standard curve.

Statistical analysis

One-way ANOVA was used for data analysis. Differences were considered significant when $P<0.05$.

RESULTS

Construction of pUC18U6 and pUC18U6HBVsir

Agarose gel analysis showed that human U6 promoter was amplified from genomic DNA (Figure 1A). Restriction digestion analysis and DNA sequencing indicated a vector suitable for siRNAs expression in mammalian cells, pUC18U6, was successfully constructed (Figure 1B and Figure 2A). We then cloned into pUC18U6, downstream of U6 promoter, the annealed two oligodeoxyribonucleotides encoded a short-hairpin RNA (shRNA) against HBV. shRNAs could be

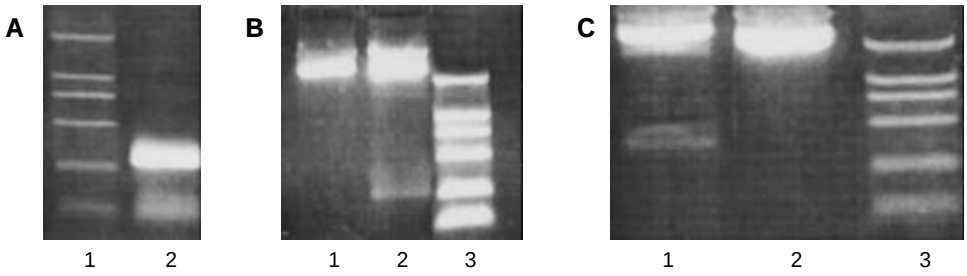

Figure 1 Construction of mammalian siRNA expression vector pUC18U6 and HBV-siRNA expression vector pUC18U6HBVsir. A: Amplification of human U6 promoter by PCR. 1: DNA marker (2 000, 1 000, 750, 500, 250, 100 bp from top to bottom); 2: PCR product. B: Restriction digestion analysis of recombinant vector pUC18U6. 1: pUC18; 2: pUC18U6; 3: DNA marker (2 000, 1 000, 750, 500, 250, 100 bp from top to bottom). C: Restriction digestion analysis of recombinant vector pUC18U6HBVsir. 1: pUC18U6HBVsir; 2: pUC18; 3: DNA marker (2 000, 1 000, 750, 500, 250, 100 bp from top to bottom).

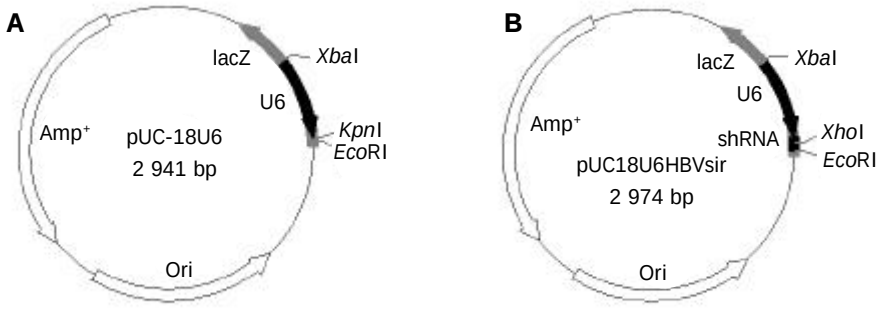

Figure 2 Maps of pUC18U6 and pUC18U6HBVsir. A: pUC18U6. B: pUC18U6HBVsir.

processed into siRNA in cells[24,25]. Since there was no *Xho* I site in pUC18U6, we designed the spacer (CTCGAG) in shRNA recognized by *Xho* I. Therefore, the recombinant vector pUC18U6HBVsir containing the shRNA coding sequence could yield a new 310 bp fragment compared with pUC18U6 after digested with *Xho* I and *Hin*d III (Figure 2B), and this was verified by agarose gel analysis (Figure 1C). This indicated that pUC18U6HBVsir which could express a siRNA against HBV, was successfully constructed (Figure 2B).

Effect of pUC18U6HBVsir expressed siRNA on HBV replication

pUC18U6HBVsir and its control plasmids were transfected into 2.2.15 cells by using liposome. Forty-eight hours after the transfection, the supernatant of the cell culture was collected, and HBsAg in the supernatant was quantified as described in Materials and Methods. As shown in Figure 3, transfection of pUC18U6HBVsir reduced HBsAg significantly as compared with the controls ($P<0.05$), suggesting that siRNA expressed by pUC18U6HBVsir suppressed the replication of HBV, and this suppression was specific because transfection of pUC18U6GFPsir, which expressed siRNA against GFP, had no effect on HBV replication.

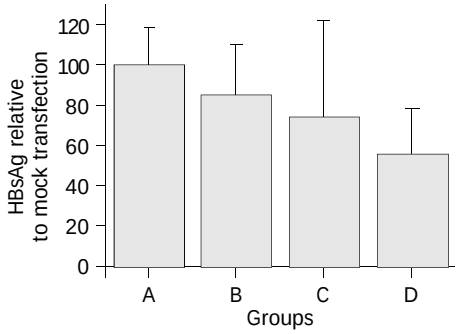

Figure 3 HBsAg concentrations in supernatants of transfected 2.2.15 cells. Groups A-D represent mock-transfected 2.2.15 cells or 2.2.15 cells transfected by pUC18U6, pUC18U6GFPsir and pUC18U6HBVsir, respectively. The concentration of HBsAg in the supernatant of 2.2.15 cells transfected by pUC18U6HBVsir was decreased by 44% as compared with that of mock-transfected 2.2.15 cells.

DISCUSSION

The aim of the present study was to explore siRNAs as a novel strategy in the treatment of HBV infection. Firstly, we first constructed a vector which was suitable to express siRNAs in mammalian cells. siRNAs could be produced *in vitro* and *in vivo*. *In vitro*, siRNAs could be produced by chemical synthesis, *in vitro* transcription, or by enzymatic digestion of dsRNAs[26-29]. siRNAs produced *in vitro* could be transfected directly into mammalian cells to knockdown gene expression. However, *in vitro* produced siRNAs have several shortcomings, such as transient effect, and high cost. To overcome these shortcomings, several groups have developed a couple of DNA-vectors which could express siRNAs i*n vivo*[11,23-25,27,28]. These vectors had different promoters and different backbones, and expressed siRNAs via two approaches: sense and antisense strands of siRNAs transcribed from tandem promoters and then combined to form siRNAs, or short hairpin RNAs transcribed from a single promoter and then processed by Dicer, a key enzyme in RNA interference, to yield siRNAs. The mammalian siRNAs expression vector constructed by us used human U6 promoter, a pol III promoter, to drive the expression of shRNAs. Compared with other reported vectors, our vector has some features which make the cloning of shRNA expression cassettes easy. The *Kpn* I and *Eco*R I sites downstream of the U6 promoter were used for directional cloning of shRNA expression cassettes and the first nucleotide of the *Kpn* I site was guanosine, just the required nucleotide for the +1 position of the U6 promoter. Therefore, there was no need to consider this requirement when we designed shRNA sequences by using our vector. Additionally, our vector has no *Xho* I site. By incorporating *Xho* I site as the spacer in the shRNA sequences, it is easy to identify positive shRNA expression vectors containing shRNA expression cassettes by routine agarose gel analysis of *Xho* I/*Hin*d III digestion products of the vectors. Positive vectors should reveal a new small fragment of about 300 bp which was absent from the negatives (Figures 1C and 2B). Some reported vectors also identify positive shRNA expression by double enzyme digestion. However, the double enzyme digestion sites in these vectors are just the sites used for cloning of shRNA expression cassettes. Therefore, for these vectors it is not easy to identify the positive shRNA expression vectors by routine agarose gel analysis, especially minigel analysis widely used in laboratories, since shRNA expression cassettes are generally 50-60 bp in length, almost the limit of resolving power of routine agarose gel analysis. The same constraint of routine agarose gel analysis also requires shRNA expression cassettes without double enzyme digestion sites, and limit siRNA target site selection. In contrast, there was no such limitation when using our vector to express siRNAs.

Several groups have reported using siRNAs to inhibit HBV replication in cell cultures and animal models[12-19]. Although all of these reports showed that HBV replication was inhibited to various degrees by siRNAs, several factors must be taken into account before siRNAs are used to treat HBV infection. One is target selection. siRNAs target at different sites of the same gene can vary from strong to less inhibition of the gene expression. Up to now, little is known about the mechanism of this selection. Therefore, it is still an empirical matter to design the most effective siRNAs. In our study, we chose 1 086-1 103 nt of HBV genome as the target, different from other groups. Our results suggested that siRNA targeting this site specifically inhibited HBV replication. Considering that HBV genome is 3.2 kb and there are no general rules to predetermine the most effective siRNAs, a systematic comparison by experiments of the efficiency of siRNAs against different targets of HBV genome in inhibiting HBV replication should be done to pick out the most effective siRNAs for treating HBV infection. Another concern of using siRNAs for treatment of HBV infection is viral mutants. RNAi is so specific in gene silencing that even a single-base mismatch between siRNAs and cognate genes can significantly reduce the silencing effect. Since viruses evolve very rapidly, they can gain the resistance to once-effective siRNA molecules in short time. In fact, two recent studies reported HIV and poliovirus escape mutants after extended siRNAs treatment[30,31]. To overcome this obstacle, multiple viral sequences must be targeted simultaneously. In this aspect, our study adds another target when designing multi-target siRNAs to inhibit HBV replication. Further studies are needed to determine the optimal combination of these targets.

REFERENCES

1 **Hannon GJ.** RNA interference. *Nature* 2002; **418:** 244-251
2 **McManus MT,** Sharp PA. Gene silencing in mammals by small interfering RNAs. *Nat Rev Gene* 2002; **3:** 737-747
3 **Dykxhoorn DM,** Novina CD, Sharp PA. Killing the messenger: short RNAs that silence gene expression. *Nat Rev Mol Cell Biol* 2003; **4:** 457-467
4 **Ashrafi K,** Chang FY, Watts JL, Fraser AG, Kamath RS, Ahringer J, Ruvkun G. Genome-wide RNAi analysis of Caenorhabditis elegans fat regulatory genes. *Nature* 2003; **421:** 268-272
5 **Kamath RS,** Fraser AG, Dong Y, Poulin G, Durbin R, Gotta M, Kanapin A, Le Bot N, Moreno S, Sohrmann M, Welchman DP,

Zipperlen P, Ahringer J. Systematic functional analysis of the Caenorhabditis elegans genome using RNAi. *Nature* 2003; **421:** 231-237

6 **Simmer F,** Moorman C, Van Der Linden AM, Kuijk E, Van Den Berghe PV, Kamath R, Fraser AG, Ahringer J, Plasterk RH. Genome-wide RNAi of C. elegans using the hypersensitive rrf-3 strain reveals novel gene functions. *PLoS Biol* 2003; **1:** E12

7 **Hingorani SR,** Jacobetz MA, Robertson GP, Herlyn M, Tuveson DA. Suppression of BRAF (V599E) in human melanoma abrogates transformation. *Cancer Res* 2003; **63:** 5198-5202

8 **Konnikova L,** Kotecki M, Kruger MM, Cochran BH. Knockdown of STAT3 expression by RNAi induces apoptosis in astrocytoma cells. *BMC Cancer* 2003; **3:** 23

9 **Butz K,** Ristriani T, Hengstermann A, Denk C, Scheffner M, Hoppe-Seyler F. siRNA targeting of the viral E6 oncogene efficiently kills human papillomavirus-positive cancer cells. *Oncogene* 2003; **22:** 5938-5945

10 **Jacque JM,** Triques K, Stevenson M. Modulation of HIV-1 replication by RNA interference. *Nature* 2002; **418:** 435-438

11 **Lee NS,** Dohjima T, Bauer G, Li H, Li MJ, Ehsani A, Salvaterra P, Rossi J. Expression of small interfering RNAs targeted against HIV-1 rev transcripts in human cells. *Nat Biotechnol* 2002; **20:** 500-505

12 **Giladi H,** Ketzinel-Gilad M, Rivkin L, Felig Y, Nussbaum O, Galun E. Small interfering RNA inhibits hepatitis B virus replication in mice. *Mol Ther* 2003; **8:** 769-776

13 **McCaffrey AP,** Nakai H, Pandey K, Huang Z, Salazar FH, Xu H, Wieland SF, Marion PL, Kay MA. Inhibition of hepatitis B virus in mice by RNA interference. *Nat Biotechnol* 2003; **21:** 639-644

14 **Shlomai A,** Shaul Y. Inhibition of hepatitis B virus expression and replication by RNA interference. *Hepatology* 2003; **37:** 764-770

15 **Hamasaki K,** Nakao K, Matsumoto K, Ichikawa T, Ishikawa H, Eguchi K. Short interfering RNA-directed inhibition of hepatitis B virus replication. *FEBS Lett* 2003; **543:** 51-54

16 **Ying C,** De Clercq E, Neyts J. Selective inhibition of hepatitis B virus replication by RNA interference. *Biochem Biophys Res Commun* 2003; **309:** 482-484

17 **Chen Y,** Du D, Wu J, Chan CP, Tan Y, Kung HF, He ML. Inhibition of hepatitis B virus replication by stably expressed shRNA. *Biochem Biophys Res Commun* 2003; **311:** 398-404

18 **Konishi M,** Wu CH, Wu GY. Inhibition of HBV replication by siRNA in a stable HBV-producing cell line. *Hepatology* 2003; **38:** 842-850

19 **Klein C,** Bock CT, Wedemeyer H, Wustefeld T, Locarnini S, Dienes HP, Kubicka S, Manns MP, Trautwein C. Inhibition of hepatitis B virus replication in vivo by nucleoside analogues and siRNA. *Gastroenterology* 2003; **125:** 9-18

20 **Conjeevaram HS,** Lok AS. Management of chronic hepatitis B. *J Hepatol* 2003; **38**(Suppl 1): S90-103

21 **Jaboli MF,** Fabbri C, Liva S, Azzaroli F, Nigro G, Giovanelli S, Ferrara F, Miracolo A, Marchetto S, Montagnani M, Colecchia A, Festi D, Reggiani LB, Roda E, Mazzella G. Long-term alpha interferon and lamivudine combination therapy in non-responder patients with anti-HBe-positive chronic hepatitis B: results of an open, controlled trial. *World J Gastroenterol* 2003; **9**: 1491-1495

22 **Beterams G,** Nassal M. Significant interference with hepatitis B virus replication by a core-nuclease fusion protein. *J Biol Chem* 2001; **276:** 8875-8883

23 **Sui G,** Soohoo C, Affar el B, Gay F, Shi Y, Forrester WC, Shi Y. A DNA vector-based RNAi technology to suppress gene expression in mammalian cells. *Proc Natl Acad Sci U S A* 2002; **99:** 5515-5520

24 **Brummelkamp TR,** Bernards R, Agami R. A system for stable expression of short interfering RNAs in mammalian cells. *Science* 2002; **296:** 550-553

25 **Paddison PJ,** Caudy AA, Bernstein E, Hannon GJ, Conklin DS. Short hairpin RNAs (shRNAs) induce sequence-specific silencing in mammalian cells. *Genes Dev* 2002; **16:** 948-958

26 **Elbashir SM,** Harborth J, Lendeckel W, Yalcin A, Weber K, Tuschl T. Duplexes of 21-nucleotide RNAs mediate RNA interference in cultured mammalian cells. *Nature* 2001; **411:** 494-498

27 **Yu JY,** DeRuiter SL, Turner DL. RNA interference by expression of short-interfering RNAs and hairpin RNAs in mammalian cells. *Proc Natl Acad Sci U S A* 2002; **99:** 6047-6052

28 **Calegari F,** Haubensak W, Yang D, Huttner WB, Buchholz F. Tissue-specific RNA interference in postimplantation mouse embryos with endoribonuclease-prepared short interfering RNA. *Proc Natl Acad Sci U S A* 2002; **99:** 14236-14240

29 **Miyagishi M,** Taira K. U6 promoter-driven siRNAs with four uridine 3' overhangs efficiently suppress targeted gene expression in mammalian cells. *Nat Biotechnol* 2002; **20:** 497-500

30 **Gitlin L,** Karelsky S, Andino R. Short interfering RNA confers intracellular antiviral immunity in human cells. *Nature* 2002; **418:** 430-434

31 **Boden D,** Pusch O, Lee F, Tucker L, Ramratnam B. Human immunodeficiency virus type 1 escape from RNA interference. *J Virol* 2003; **77:** 11531-11535

Edited by Zhang JZ and Wang XL **Proofread by** Xu FM

PO Box 2345, Beijing 100023, China
Fax: +86-10-85381893
E-mail: wjg@wjgnet.com www.wjgnet.com

World J Gastroenterol 2004;10(13):1902-1906
World Journal of Gastroenterology
 ISSN 1007-9327

• VIRAL HEPATITIS •

Therapeutic polypeptides based on HBV core 18-27 epitope can induce CD_8^+ CTL-mediated cytotoxicity in HLA-$A2^+$ human PBMCs

Tong-Dong Shi, Yu-Zhang Wu, Zheng-Cai Jia, Li-Yun Zou, Wei Zhou

Tong-Dong Shi, Yu-Zhang Wu, Zheng-Cai Jia, Li-Yun Zou, Wei Zhou, Institute of Immunology, Third Military Medical University, Chongqing 400038, China
Supported by the National Natural Science Foundation of China, No.30271189, and the National 973 Project, No.2001CB510001
Co-correspondents: Dr. Yu-Zhang Wu
Correspondence to: Dr. Tong-Dong Shi, Institute of Immunology, Third Military Medical University, 30 Gaotanyan Street, Chongqing 400038, China. tdshih@yahoo.com.cn
Telephone: +86-23-68752236-801 **Fax:** +86-23-68752789
Received: 2003-12-12 **Accepted:** 2004-01-12

Abstract

AIM: To explore how to improve the immunogenicity of HBcAg CTL epitope based polypeptides and to trigger an HBV-specific HLA I-restricted $CD8^+$ T cell response *in vitro*.

METHODS: A new panel of mimetic therapeutic peptides based on the immunodominant B cell epitope of HBV PreS2 18-24 region, the CTL epitope of HBcAg18-27 and the universal T helper epitope of tetanus toxoid (TT) 830-843 was designed using computerized molecular design method and synthesized by Merrifield's solid-phase peptide synthesis. Their immunological properties of stimulating activation and proliferation of lymphocytes, of inducing T_{H1} polarization, $CD8^+$ T cell magnification and HBV-specific $CD8^+$ CTL mediated cytotoxicity were investigated *in vitro* using HLA-$A2^+$ human peripheral blood mononuclear cells (PBMCs) from healthy donors and chronic hepatitis B patients.

RESULTS: Results demonstrated that the therapeutic polypeptides based on immunodominant HBcAg18-27 CTL, PreS2 B- and universal T_H epitopes could stimulate the activation and proliferation of lymphocytes, induce specifically and effectively $CD8^+$ T cell expansion and vigorous HBV-specific CTL-mediated cytotoxicity in human PBMCs.

CONCLUSION: It indicated that the introduction of immunodominant T helper plus B-epitopes with short and flexible linkers could dramatically improve the immunogenicity of short CTL epitopes *in vitro*.

Shi TD, Wu YZ, Jia ZC, Zou LY, Zhou W. Therapeutic polypeptides based on HBV core 18-27 epitope can induce CD_8^+ CTL-mediated cytotoxicity in HLA-$A2^+$ human PBMCs. *World J Gastroenterol* 2004; 10(13): 1902-1906
http://www.wjgnet.com/1007-9327/10/1902.asp

INTRODUCTION

Despite the existence of effective vaccines against hepatitis B virus (HBV) for many years and massive prophylactic vaccination campaigns, HBV infection remains an important health problem worldwide. HBV can evade the immune defence system and present consistently in hepatocytes. Patients carrying the virus can develop chronic hepatitis, liver cirrhosis, and ultimately hepatocellular carcinoma[1-3]. Currently, the two approved therapies for chronic hepatitis with definite clinical beneficial effects are IFN-α and lamivudine. IFN-α therapy combines antiviral and immunostimulant properties and can result in sustained suppression of HBV replication in one-third of patients. Lamivudine leads to a rapid and almost absolute discontinuation of HBV replication as well as a rapid improvement of the necro-inflammatory activity of the liver disease and to a lesser extent of fibrosis. However, short-term treatment leads to a frequent relapse of HBV replication. On the other hand, long-term treatment has shown to result in virological breakthrough related to the selection of resistant viral variants with a yearly incidence of 15-25%. These outcomes emphasize the need for novel therapeutic approaches[4]. And it is known that cytotoxic T lymphocytes(CTLs) recognize short peptides derived from the intracellular processing of viral antigens in association with HLA class I molecules on the surface of the infected cells, and HLA-I restricted T cell mediated responses, especially virus antigen specific CTL mediated cytotoxicity, play the key role in controlling HBV infection and in the clearance of infected cells[5-7]. Since HBV does not efficiently infect human cells *in vitro*, the use of short synthetic peptides comprised of a set of immunodominant epitopes of virus antigens mimicking the processed antigen fragments can be a rational strategy to stimulate the HBV specific CTL response and break to some extent the immune tolerance to HBV antigens[8-12]. Based on this concept, a new panel of short polypeptides (mimogens) representing the immunodominant CTL, B- and T helper epitopes of the HBcAg, pre-S2 and tetanus toxoid was designed and used for CTL-mediated response analysis. This issue was addressed *in vitro* with HLA-$A2^+$ human peripheral blood lymphocytes (PBMCs) from healthy donors and chronic hepatitis B patients.

MATERIALS AND METHODS

Materials

HLA-$A2^+$ human peripheral blood mononuclear cells (PBMCs) from 9 healthy donors and 9 chronic viral hepatitis B patients were kindly donated by Southwest Hospital, Chongqing municipality, China. Amino acids used for peptide synthesis were purchased from PE & ACT companies. $Na_2{}^{51}GrO_4$ for target cell labeling in standard ^{51}Gr release assay and ^3H-TdR were both from New England Nuclear (NEN™), Boston, USA. Other materials used in this study were as the following: RPMI 1640 medium (Gibco), fetal calf serum (FCS) (HyClone), HLA-A*0201/FLPSDFFPSV tetramer kit (ProImmune, UK) and human IFN-γ ELISpot kit (DiaClone, France).

Methods

Mimetic polypeptides The immunodominant B- and CTL epitopes of HBV pre-S2 and HBcAg were identified on the basis of the HLA-A2.1 binding motifs[13-15]. Peptide1 was chosen from the immunodominant $HBcAg_{18-27}$ CTL epitope (FLPSDFFPSV). The N-termini of peptide 1 linking to the universal T helper sequence of TT 830-843 through a linker of "-Gly-Gly-Gly-" was named as peptide 2 (QYIKANSKFIGITE GGG FLPSDFFPSV). The universal T helper epitope of tetanus

toxoid and the Pre-$S2_{18-24}$ B-epitope were linked to the N- and C-termini of the $HBcAg_{18-27}$ sequence respectively with the linker of"-Ala-Ala-Ala-" and "-Gly-Gly-Gly-" as peptide 3 (QYIKANSKFIGITE AAA FLPSDFFPSV GGG DPRVRGLYFPA). Melanoma associated $MART\text{-}1_{27-35}$ CTL epitope peptide (AAGIGILTV) was used as irrelevant control. All mimogens were calculated and optimized using computerized molecular design theories and methods in O2 workstation(SGI).

The above peptides were synthesized with a Merrifield' s solid-phase peptide synthesis method (PE431A synthesizer), purified by RP-HPLC (WATERS 600) and analyzed by MS/MS (API 2000). All peptides with a purity over 95% were solved in DMSO at the concentration of 10 mg/mL and preserved at -70 ℃.

Lymphocytes proliferation assay

Human PBMCs were separated from peripheral blood by centrifugation on Ficoll-Hypaque gradients and used as fresh samples[16]. PBMCs were plated at a concentration of 2×10^6/mL in 96-well microplates in PRMI 1640 medium supplemented with 100 mL/L fetal bovine serum, 5×10^{-5} mol/L α-mercaptoethanol, and in the presence of 10 μg/mL mimetic peptides respectively. Eighteen to 24 h later, 1 μCi/well of ^{3}H-TdR was added into the medium. Four to 6 h later, lymphocytes were collected and counted using a β-counter. Non-stimulated PBMCs were used as negative control. Results of samples were considered positive if the stimulation index (SI)>2.1.

T_{H1} polarization assay

For the assay of T_{H1} polarization induced by mimetic peptides, IFN-γ ELISPOT kit was used. Briefly[16,17], 96-well PVDF membrane-bottomed plates were coated with capture anti-human IFN-γ mAb at 4 ℃ overnight. Fresh PBMCs were stimulated with 10 μg/mL of mimetic peptide1, 2 and 3 respectively, and then added to triplicated wells at 5×10^3/well and the plates were incubated for 18 h at 37 ℃ in 50 mL/L CO_2. At the end of incubation, cells were washed off and a second biotinylated anti-IFN-γ mAb was added, followed by streptavidin-alkaline phosphatase conjugate and substrates. After the plates were washed with tap water and dried overnight, spots were counted under a stereomicroscope. The number of T_{H1} polarized cells ($HBcAg_{18-27}$-specific $CD8^+$ T cells), expressed as IFN-γ secreting cells(ISCs) /10^6 PBMCs, was calculated after subtracting negative control values (non-stimulated PBMCs). Results of samples were considered as positive if above the mean by three standard deviations and with a cut off of 50 ISCs /10^6 PBMCs above mean background.

Cytotoxicity assay

Peptide-specific CTL lines were primed as follows: at d 0, fresh PBMCs were plated at a concentration of 2×10^5/mL in 24-well microplates (2 mL /well) in RPMI 1640 medium supplemented with 100 mL/L fetal bovine serum and L-glutamine, and in the presence of 10 μg /mL mimetic peptides respectively. Two days later, 30 IU/mL rhIL-2 was added to the medium. Lymphocytes were then re-stimulated weekly for 2 wk as follows: Cells were harvested, washed once, and replated in 24-well plates at the concentration of 2×10^5/mL in the above medium, and restimulated respectively with 10 μg/mL mimetic polypeptides. Twenty hours after last stimulation, cells were harvested, and used as fresh effectors.

CTL-mediated cytotoxicity was detected by standard 4 h ^{51}Cr release assay[17]. T2(HLA-A2) cells were used as targets and pre-incubated with 10 μg/mL of $HBcAg_{18-27}$ peptide 2 h before use. The 1×10^6 target cells were labeled with 3.7×10^6 Bq $Na_2{}^{51}GrO_4$ in 1.0 mL RPMI 1640 medium supplemented with 150 mL/L fetal bovine serum and in the presence of 10 μg/mL of $HBcAg_{18-27}$ peptide for 60 min at 37 ℃, and then washed three times before the addition of effectors. Various concentrations of effector cells were mixed with 1×10^4 targets at effector/target (E/T) ratios of 12.5, 25, 50 and 100 in 200 μL of culture medium in 96-well V-bottomed microplate in triplicate. The microplate was centrifuged for 3 min at 500 r/min, and then incubated for 4 h at 37 ℃ in 50 mL/L CO_2. After the incubation terminated, 100 μL of supernatants was harvested and counted on a γ-counter. Percentage of target cell specific lysis was determined as:(average sample counts-average spontaneous counts/average maximum counts-average spontaneous counts) ×100%. Maximum and spontaneous counts were measured using supernatants from wells receiving 50 g/L SDS or culture medium alone, respectively. In all experiments, spontaneous counts should be less than 30% of maximum counts. CTL responses were considered positive if they exceeded the mean of specific lysis caused by irrelevant mimetic antigen by three standard deviations and by 10%.

$HBcAg_{18-27}$-specific $CD8^+$ CTL quantitative detection

HLA class I^{pep} tetramer-binding assay was used to quantify the $HBcAg_{18-27}$-specific $CD8^+$ T cells from the fresh effectors produced[18]. Briefly, fresh effectors were collected, washed twice with 0.02 mol/L, pH7.2 phosphate buffered saline (PBS), counted and separated equally into different tubes in 1.0 mL of PBS each. The effectors were stained with 2 μL of R-PE-conjugated HLA-A*0201/FLPSDFFPSV and 20 μL of Cy-Chrome-conjugated mouse anti-human CD8 mAb for 30 min at room temperature. R-PE-conjugated avidin and Cy-Chrome-conjugated mouse $IgG_{1,\kappa}$ antibodies were used as isotype control, and non-stimulated PBMCs were used as negative controls. All samples were collected, washed twice, dissolved into 300 μL of PBS and FACS-sorted on a FACstar (Beckton-Dicknson) with Cell Quest software. Results were expressed as percentages of tetramer-binding cells in the $CD8^+$ population. A total of 50 000 events were acquired in each analysis. Results were considered as positive for tetramer-binding cells when above negative controls and by 0.1% $CD8^+$ T cells.

Statistical analysis

All data were expressed as mean±SD. Statistical analysis was performed using a two-tailed Student' s *t* test.

RESULTS

Lymphocytes proliferation assay

Fresh PBMCs were stimulated respectively with three mimetic peptides we designed, and ^{3}H-TdR was used to detect the proliferation of lymphocytes. Data demonstrated that peptide 3 pulsed the most vigorous activation and proliferation of lymphocytes, and with SI>4.1 by average in healthy PBMCs and >3.3 in PBMCs from chronic hepatitis patients. Peptide 2 could also induce weak lymphocytes proliferation, with the mean of SI>2.3 and 2.1 respectively in the PBMCs from healthy donors and chronic hepatitis patients. No activation and proliferation of lymphocytes were detected in peptide 1 stimulated PBMCs (Table 1).

T_{H1} polarization induced by mimetic peptides

$HLA\text{-}A2^+$ human PBMCs were pulsed respectively with three mimetic peptides we initially designed and synthesized, and the T_{H1} polarization induced was detected using IFN-γ ELISPOT method. Spots of IFN-γ secreting cells can be observed in each of the mimetic peptide samples. Peptide1 could induce peptide-specific $CD8^+$ T cells magnification up to approximately 1 667±231 ISCs /10^6 PBMCs in PBMCs from healthy donors and 1 420±253 ISCs /10^6 PBMCs in PBMCs from chronic hepatitis B patients, which were dramatically weaker than those of Peptide 2 and 3, which induced

Table 1 Lymphocytes proliferation assay (mean±SD, n=27)

	^{3}H-TdR counts(*cpm*)			
	Peptide1	Peptide2	Peptide3[b]	Negative controls
PBMCs from healthy donors	4 001.6±328.3	5 882.6±397.2	10 497.6±859.7	2 556.3±211.3
PBMCs from chronic hepatitis patients	3 967.5±285.9	4 912.3±421.1	7 696.2±781.8	2 327.6±169.2

[b]P<0.01 *vs* negative control and peptide1 and 2 groups.

Table 2 Peptide-specific CD8$^+$ T cells induced expressed as ISCs/10^6 PBMCs (mean±SD, n=27)

	ISCs /10^6 PBMCs				
	Peptide1[d]	Peptide2[d]	Peptide3[db]	Irrelevant control	Negative controls
PBMCs from healthy donors	1 667.5±231.3	4 133.7±416.6	9 200.5±1638.1	1 315.5±321.3	233.3±208.6
PBMCs from chronic hepatitis patients	1 420.0±253.5	3 915.7±685.9	8 966.7±1435.3	1 230.0±355.2	245.1±223.3

[b]P<0.01 *vs* peptide1 and 2 groups, [d]P<0.01 *vs* negative control.

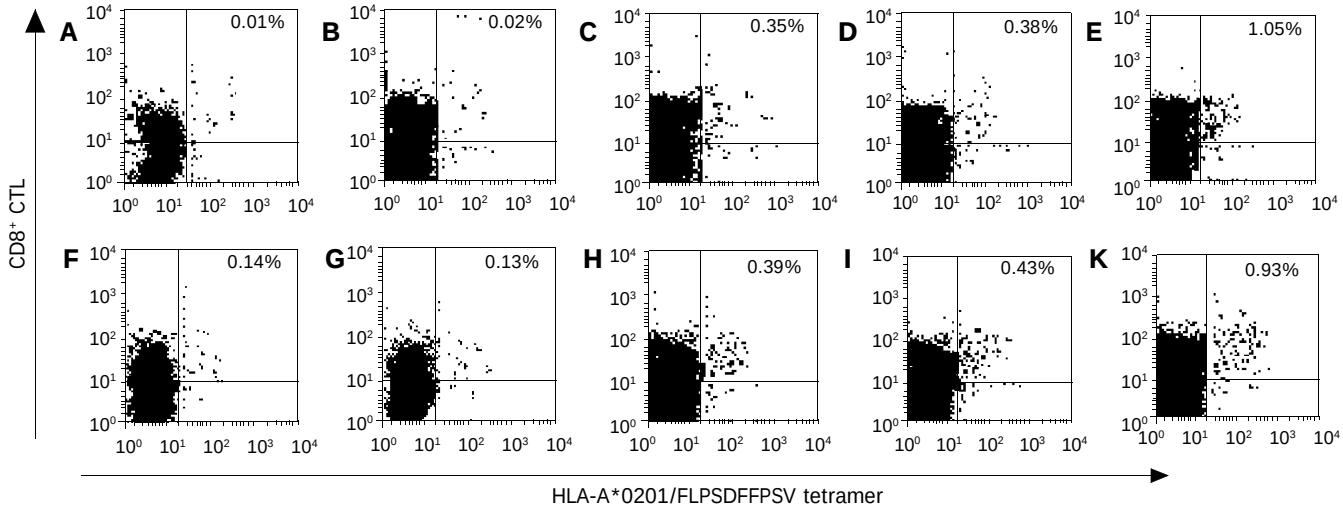

Figure 1 Detection of the HBcAg$_{18\text{-}27}$-specific CD8$^+$ T cells produced with HLA-A*0201/FLPSDFFPSV tetramer-binding assay. A: Non-stimulated HLA-A2$^+$ PBMCs from healthy donors; B: Irrelevant peptide pulsed HLA-A2$^+$ PBMCs from healthy donors; C: Peptide1 pulsed HLA-A2$^+$ PBMCs from healthy donors; D: Peptide2 pulsed HLA-A2$^+$ PBMCs from healthy donors; E: Peptide3 pulsed HLA-A2$^+$ PBMCs from healthy donors; F: Non-stimulated HLA-A2$^+$ PBMCs from chronic hepatitis patients; G: Irrelevant peptide pulsed HLA-A2$^+$ PBMCs from chronic hepatitis patients; H: Peptide1 pulsed HLA-A2$^+$ PBMCs from chronic hepatitis patients; I: Peptide2 pulsed HLA-A2$^+$ PBMCs from chronic hepatitis patients; K: Peptide3 pulsed HLA-A2$^+$ PBMCs from chronic hepatitis patients.

approximately 4 133±416 and 9 200±1 638 ISCs/10^6 PBMCs respectively in PBMCs from healthy donors, and 3 915±685 and 8 966±1 435 ISCs/10^6 PBMCs in PBMCs from chronic hepatitis B patients. These results suggest that all the 3 peptides could pulse T_{H1} polarization of T cells, and peptide 3 was more vigorous than peptide 2 and 1(P<0.01). It showed no difference between the PBMCs from healthy donors and chronic hepatitis patients (Table 2).

Cytotoxicity assay

HLA-A2$^+$ human PBMCs were pulsed with the 3 mimetic peptides and the irrelevant control peptide respectively, and the CTL-mediated cytotoxicity induced was tested by standard 4 h ^{51}Cr release assay against HBcAg$_{18\text{-}27}$ peptide pre-incubated T2 targets. The results demonstrated that all the 3 mimetic peptides could induce positive HBV-specific CTL response, among which peptide 3 induced the most vigorous CTL activity and as high as (68.4±15)% target cell lysis was observed at E/T=100. The percentages of target cells lysed between peptide 1 and 2 pulsing groups were of statistically no difference, and both were dramatically lower than that of peptide 3 (P<0.01). The targets lysis observed in both healthy donors and chronic hepatitis patients showed no statistical difference (Tables 3 and 4).

HBcAg$_{18\text{-}27}$-specific CD8$^+$ CTL detection

HLA-A2$^+$ human PBMCs were pulsed respectively with the above three mimetic peptides and the irrelevant peptide MART-1$_{27\text{-}39}$, the HBcAg$_{18\text{-}27}$-specific CD8$^+$ T cells induced were quantified using HLA-A*0201/FLPSDFFPSV tetramer-binding assay. No HBcAg$_{18\text{-}27}$-specific CD8$^+$ T cells could be detected in the PBMCs pulsed with MART-1$_{27\text{-}35}$ peptide, and the tetramer staining was almost the same as control background (0.02% in PBMCs from healthy donors, and 0.04-0.14% in PBMCs from chronic hepatitis patients). In PBMCs stimulated with peptide 1, 2 and 3, the frequencies of HLA-A*0201/FLPSDFFPSV· CD8 double-positive T cells were on average 0.35%(3 500/10^6 PBMCs), 0.38%(3 800/10^6 PBMCs) and 1.05% (10 500/10^6 PBMCs) respectively in the PBMCs from healthy donors, and 0.39%(3 900/10^6 PBMCs), 0.43%(4 300/10^6 PBMCs) and 0.93%(9 300/10^6 PBMCs) respectively in the PBMCs from chronic patients. Data showed no statistical differences between the PBMCs from healthy donors and chronic hepatitis patients, and between the effects induced by peptide1 and peptide 2 (Figure 1).

Table 3 Percentages of specific targets lysis by HLA-A2$^+$ effector CTLs induced by PBMCs from healthy donors with different peptide antigens (mean±SD, n=27)

E/T ratios	Percentage of specific cell lysis (%)				
	Peptide1[d]	Peptide2[d]	Peptide3[db]	Irrelevant control[a]	Negative controls
12.5	22.7±5.3	21.7±6.1	36.1±7.7	3.7±0.7	3.5±0.7
25	29.3±6.5	28.6±6.3	41.4±9.1	5.7±0.7	3.7±0.7
50	33.5±7.1	33.9±8.2	52.3±12.5	7.3±0.9	6.4±0.9
100	37.2±11.2	36.8±10.9	68.4±14.7	7.4±1.1	8.7±1.3

[a]P>0.05 *vs* negative control, [b]P<0.01 *vs* peptide1 and 2 groups, [d]P<0.01 *vs* negative control.

Table 4 Percentages of specific targets lysis by HLA-A2$^+$ effector CTLs induced by PBMCs from chronic hepatitis B patients with different peptide antigens (mean±SD, n=27)

E/T ratios	Percentage of specific cell lysis (%)				
	Peptide1[d]	Peptide2[d]	Peptide3[db]	Irrelevant control[a]	Negative controls
12.5	18.7±3.6	23.1±4.9	30.2±6.1	5.1±0.8	4.3±0.6
25	22.7±4.1	28.6±5.6	38.4±7.4	4.5±0.7	7.1±1.0
50	31.3±6.0	33.9±6.5	52.7±10.3	7.3±1.1	7.7±1.3
100	35.5±5.7	39.1±7.3	58.5±15.9	9.5±1.7	8.5±1.5

[a]P>0.05 *vs* negative control, [b]P<0.01 *vs* peptide1 and 2 groups, [d]P<0.01 *vs* negative control.

DISCUSSION

HBV-specific CD8$^+$ cytotoxic T cells play a critical role in viral clearance. Low HBV-specific CTL responses in chronic HBV infection may favor the persistence of virus, whereas stimulation and expansion of HBV-specific CTL activity may assist elimination of HBV infection[1-3]. Natural HBV antigens generally contain inappropriate epitopes which could elicit T_{H1}/T_{H2} disequilibrium, immune deviation or immune deficiency, and the conserved amino acid sequences might interfere with intercellular communication and thus elicit immune subversion. Thereby some viruses may evade the immune defence system and present consistently in hepatocytes, and result in chronic hepatitis, liver cirrhosis, and even hepatocellular carcinoma. Thus new generations of therapeutic vaccines should induce CTL responses different from that induced by natural virus infection, and at the same time hold the specificity of HBV antigens[19-22]. According to modern immune theories, effective protection relys on the appropriate match of a set of epitopes[8,23]. Thus, natural antigens should be redesigned or modified using molecular design techniques on the basis of immunodominant epitopes.

Among the different CTL epitopes of HBV core, envelope, and polymerase so far identified, the sequence 18-27 of the HBV core antigen is immunodominant and subdominant in the different supertype of HLA-A2 molecules, and could induce HBV-specific CTL responses in patients of different HLA-A2 subertypes with indistinguishable frequency and magnitude, and represents the main component of a peptide-based therapeutic vaccine aiming at stimulating the antiviral CTL response in patients with chronic hepatitis B. Furthermore, this epitope was also found to stimulate HLA class II restricted T-cell responses. These data illustrate its potential usefulness for the development of therapeutic vaccines[24-26].

As in other infections with noncytopathic viruses, helper T cells control the intensity of CD8$^+$ T-cell responses and helper T-cell responses might be compromised in chronic carriers of HBV, and according to *in vivo* studies, administration of single CTL epitope vaccine could initiate CTL activity, but the magnitude was lower, and the low-level CTL activity was considered not associated with viral clearance[26-30]. In this study, we chose the immunodominant B cell epitope of HBV $PreS_2$ region and the CTL epitope of HBcAg, and introduced the universal T_H epitope of tetanus toxoid to strengthen the T_H response. Three mimetic peptides based on the above epitopes were initially designed and synthesized, and their immunological properties of pulsing lymphocyte activation and proliferation, of inducing T_{H1} polarization and HBV-specific CD8$^+$ CTL-mediated cytotoxicity were preliminarily investigated using human PBMCs from HLA-A2$^+$ healthy donors and chronic hepatitis B patients.

After *in vitro* stimulation, a direct tetramer-binding assay was used to detect the frequencies of HBV-specific CD8$^+$ T cells. The results varied according to the peptides used. The highest frequencies were from peptide3 pulsing group, about 1.05%(10 500/10^6 PBMCs) and 0.93%(9 300/10^6 PBMCs) HLA-A*0201/$HbcAg_{18-27}$· CD8$^+$ CTLs produced in the PBMCs from healthy donors and chronic hepatitis patients respectively, remarkably higher than those of peptide 2 and peptide 1(P<0.01). No $HBcAg_{18-27}$-specific CD8$^+$ T cells could be detected in the PBMCs pulsed with irrelevant peptide, the tetramer staining was almost the same as control background. These data demonstrated the specificity of the therapeutic peptides we designed.

The tetramer-binding assay detects only the number of cells with an appropriate TCR but not their function[31], so chromium release assay, IFN-γ ELISpot assay and lymphocyte proliferation assay were used to detect the function of the effectors pulsed. And a highly significant correlation was found between the frequencies of peptide-specific CD8$^+$ T cells and the functions of responding T cells. All the three mimetic polypeptides designed were potent to induce *in vitro* cultured human PBMCs activation and proliferation, T_{H1} polarization, CD8$^+$ T cell expansion and generation of cytotoxicity. Peptide 3 with the immunodominant B-, CTL and T helper epitope was the most potent. After introduction of T helper epitope into peptide 1, CTL frequency was not remarkably improved, and cytotoxic activity remained low suggesting that this conformation was not sufficient to drive proliferation of CTLs, and its differentiation into mature killer cells. The comparatively higher immunogenicity of peptide 3 was attibutedd to its molecular structure: the introduction of T helper and B-epitopes, and the design of short linkers "-A-A-A-" and "-G-G-G-". The linker was designed and proved to be highly flexible and might act as "hinges". We surmise that this peptide might be recognized by MHC-I/II restricted molecules, and be presented to CD4$^+$ T cells and CD8$^+$ T cells, and ultimately T helper and Tc cells should be activated and function interactively. The results demonstrate that the peptides designed are highly immunogenic and HBV-specific, and the introduction of short and flexible linker and immunodominant T_H plus B- epitopes into short CTL epitopes may dramatically improve the therapeutic peptides' immunogenicity and the possibility of being presented to antigen presenting cells (APCs).

According to reports as yet, the vast majority of polypeptides, especially short epitope peptides can not induce CTL responses vigorous by *in vivo* because of poor immunogenicity[32-35]. Little knowledge is known so far on the molecular mechanisms leading to the difference between the peptides' *in vitro* and *in vivo* functions. In our opinion, *in vivo* induction of cytotoxic activity relys on the efficient presentation by APCs, and the crucial point is how to improve the antigenicity of short peptides and to meet the needs for efficient antigen presentation *in vivo*. In the present study, we redesigned and modified the structure of linear short peptides on the basis of immunodominant

epitopes, changed the molecular properties of the natural peptides, and triggered the direct recognition of the peptides by Tc and T_H cells, and the mimogens sieved were proved to be highly immunogenic *in vitro*. Whether this conformation can meet the needs for efficient antigen presentation *in vivo* needs to be addressed in HLA-A2 transformed HBV transgenic mice.

REFERENCES

1 **Uprichard SL**, Wieland SF, Althage A, Chisari FV. Transcriptional and posttranscriptional control of hepatitis B virus gene expression. *Proc Natl Acad Sci U S A* 2003; **100**: 1310-1315
2 **El-Serag HB.** Hepatocellular carcinoma: an epidemiologic view. *J Clin Gastroenterol* 2002; **35**(5 Suppl 2): S72-S78
3 **Rabe C**, Pilz T, Klostermann C, Berna M, Schild HH, Sauerbruch T, Caselmann WH. Clinical characteristics and outcome of a cohort of 101 patients with hepatocellular carcinoma. *World J Gastroenterol* 2001; **7**: 208-215
4 **Michel ML**. Towards immunotherapy for chronic hepatitis B virus infections. *Vaccine* 2002; **20**(Suppl 4): A83-A88
5 **Huang J**, Cai MY, Wei DP. HLA class I expression in primary hepatocellular carcinoma. *World J Gastroenterol* 2002; **8**: 654-657
6 **Thimme R**, Wieland S, Steiger C, Ghrayeb J, Reimann KA, Purcell RH, Chisari FV. $CD8^+$ T cells mediate viral clearance and disease pathogenesis during acute hepatitis B virus infection. *J Virol* 2003; **77**: 68-76
7 **Thimme R**, Bukh J, Spangenberg HC, Wieland S, Pemberton J, Steiger C, Govindarajan S, Purcell RH, Chisari FV. Viral and immunological determinants of hepatitis C virus clearance, persistence, and disease. *Proc Natl Acad Sci U S A* 2002; **99**: 15661-15668
8 **Chaiken IM**, Williams WV. Identifying structure-function relationships in four-helix bundle cytokines: towards de novo mimetics design. *Trends Biotechnol* 1996; **14**: 369-375
9 **Kessler JH**, Beekman NJ, Bres-Vloemans SA, Verdijk P, van Veelen PA, Kloosterman-Joosten AM, Vissers DC, ten Bosch GJ, Kester MG, Sijts A, Wouter Drijfhout J, Ossendorp F, Offringa R, Melief CJ. Efficient identification of novel HLA-A*0201-presented cytotoxic T lymphocyte epitopes in the widely expressed tumor antigen PRAME by proteasome-mediated digestion analysis. *J Exp Med* 2001; **193**: 73-88
10 **Kakimi K**, Isogawa M, Chung J, Sette A, Chisari FV. Immunogenicity and tolerogenicity of hepatitis B virus structural and nonstructural proteins: implications for immunotherapy of persistent viral infections. *J Virol* 2002; **76**: 8609-8620
11 **Engler OB**, Dai WJ, Sette A, Hunziker IP, Reichen J, Pichler WJ, Cerny A. Peptide vaccines against hepatitis B virus: from animal model to human studies. *Mol Immunol* 2001; **38**: 457-465
12 **Sette AD**, Oseroff C, Sidney J, Alexander J, Chesnut RW, Kakimi K, Guidotti LG, Chisari FV. Overcoming T cell tolerance to the hepatitis B virus surface antigen in hepatitis B virus-transgenic mice. *J Immunol* 2001; **166**: 1389-1397
13 **Preikschat P**, Kazaks A, Dishlers A, Pumpens P, Kruger DH, Meisel H. Interaction of wild-type and naturally occurring deleted variants of hepatitis B virus core polypeptides leads to formation of mosaic particles. *FEBS Lett* 2000; **478**: 127-132
14 **Livingston BD**, Crimi C, Fikes J, Chesnut RW, Sidney J, Sette A. Immunization with the HBV core 18-27 epitope elicits CTL responses in humans expressing different HLA-A2 supertype molecules. *Hum Immunol* 1999; **60**: 1013-1017
15 **Kazaks A**, Dishlers A, Pumpens P, Ulrich R, Kruger DH, Meisel H. Mosaic particles formed by wild-type hepatitis B virus core protein and its deletion variants consist of both homo- and heterodimers. *FEBS Lett* 2003; **549**: 157-162
16 **Guan XJ**, Wu YZ, Jia ZC, Shi TD, Tang Y. Construction and characterization of an experimental ISCOMS-based hepatitis B polypeptide vaccine. *World J Gastroenterol* 2002; **8**: 294-297
17 **Sun Y**, Iglesias E, Samri A, Kamkamidze G, Decoville T, Carcelain G, Autran B. A systematic comparison of methods to measure HIV-1 specific CD8 T cells. *J Immunol Methods* 2003; **272**: 23-34
18 **Kuzushima K**, Hayashi N, Kudoh A, Akatsuka Y, Tsujimura K, Morishima Y, Tsurumi T. Tetramer-assisted identification and characterization of epitopes recognized by HLA A*2402-restricted Epstein-Barr virus-specific $CD8^+$ T cells. *Blood* 2003; **101**: 1460-1468
19 **Bocher WO**, Dekel B, Schwerin W, Geissler M, Hoffmann S, Rohwer A, Arditti F, Cooper A, Bernhard H, Berrebi A, Rose-John S, Shaul Y, Galle PR, Lohr HF, Reisner Y. Induction of strong hepatitis B virus(HBV) specific T helper cell and cytotoxic T lymphocyte responses by therapeutic vaccination in the trimera mouse model of chronic HBV infection. *Eur J Immunol* 2001; **31**: 2071-2079
20 **Blackman MA**, Rouse BT, Chisari FV, Woodland DL. Viral immunology: challenges associated with the progression from bench to clinic.*Trends Immunol* 2002; **23**: 565-567
21 **Kurts C**, Miller JF, Subramaniam RM, Carbone FR, Heath WR. Major histocompatibility complex class I-restricted cross-presentation is biased towards high dose antigens and those released during cellular destruction. *J Exp Med* 1998; **188**: 409-414
22 **Stober D**, Trobonjaca Z, Reimann J, Schirmbeck R. Dendritic cells pulsed with exogenous hepatitis B surface antigen particles efficiently present epitopes to MHC class I-restricted cytotoxic T cells. *Eur J Immunol* 2002; **32**: 1099-1108
23 **Wiesmuller KH**, Bessler WG, Jung G. Solid phase peptide synthesis of lipopeptide vaccines eliciting epitope-spersic, B-, T-helper and T-killer cell response. *Int J Pept Protein Res* 1992; **40**: 255-260
24 **Bertoletti A**, Southwood S, Chesnut R, Sette A, Falco M, Ferrara GB, Penna A, Boni C, Fiaccadori F, Ferrari C. Molecular features of the hepatitis B virus nucleocapsid T-cell epitope 18-27: interaction with HLA and T-cell receptor. *Hepatology* 1997: **26**: 1027-1034
25 **Maini MK**, Boni C, Ogg GS, King AS, Reignat S, Lee CK, Larrubia JR, Webster GJ, McMichael AJ, Ferrari C, Williams R, Vergani D, Bertoletti A. Direct ex vivo analysis of hepatitis B virus-specific CD8(+) T cells associated with the control of infection. *Gastroenterology* 1999; **117**: 1386-1396
26 **Heathcote J**, McHutchison J, Lee S, Tong M, Benner K, Minuk G, Wright T, Fikes J, Livingston B, Sette A, Chestnut R. A pilot study of the CY-1899 T-cell vaccine in subjects chronically infected with hepatitis B virus. *Hepatology* 1999: **30**: 531-536
27 **Ciavarra RP**, Greene AR, Horeth DR, Buhrer K, van-Rooijen N, Tedeschi B. Antigen processing of vesicular stomatitis virus *in situ*. Interdigitating dendritic cells present viral antigens independent of marginal dendritic cells but fail to prime $CD4^+$ and $CD8^+$ T cells. *Immunology* 2000; **101**: 512-520
28 **Carcelain G**, Tubiana R, Samri A, Calvez V, Delaugerre C, Agut H, Katlama C, Autran B. Transient mobilization of human immunodeficiency virus (HIV)-specific CD4 T-helper cells fails to control virus rebounds during intermittent antiretroviral therapy in chronic HIV type 1 infection. *J Virol* 2001; **75**: 234-241
29 **Zhu F**, Eckels DD. Functionally distinct helper T-cell epitopes of HCV and their role in modulation of NS3-specific, $CD8^+$ / tetramer positive CTL. *Hum Immunol* 2002; **63**: 710-718
30 **Livingston BD**, Alexander J, Crimi C, Oseroff C, Celis E, Daly K, Guidotti LG, Chisari FV, Fikes J, Chesnut RW, Sette A. Altered helper T lymphocyte function associated with chronic hepatitis B virus infection and its role in response to therapeutic vaccination in humans. *J Immunol* 1999; **162**: 3088-3095
31 **Cederbrant K**, Marcusson-Stahl M, Condevaux F, Descotes J. NK-cell activity in immunotoxicity drug evaluation. *Toxicology* 2003; **185**: 241-250
32 **Maini MK**, Boni C, Lee CK, Larrubia JR, Reignat S, Ogg GS, King AS, Herberg J, Gilson R, Alias A, Williams R, Vergani D, Naoumov NV, Ferrari C, Bertoletti A. The role of virus-specific CD8(+) cells in liver damage and viral control during persistent hepatitis B virus infection. *J Exp Med* 2000; **191**: 1269-1280
33 **Gripon P**, Rumin S, Urban S, Le Seyec J, Glaise D, Cannie J, Guyomard C, Lucas J, Trepo C, Guguen-Guillouzo C. Infection of a human hepatoma cell line by hepatitis B virus. *Proc Natl Acad Sci U S A* 2002; **99**: 15655-15660
34 **Stebbing J**, Patterson S, Gotch F. New insights into the immunology and evolution of HIV. *Cell Res* 2003; **13**: 1-7
35 **Li D**, Takyar ST, Lott WB, Gowans EJ. Amino acids 1-20 of the hepatitis C virus (HCV) core protein specifically inhibit HCV IRES-dependent translation in HepG2 cells, and inhibit both HCV IRES- and cap-dependent translation in HuH7 and CV-1 cells. *J Gen Virol* 2003; **84**: 815-825

Edited by Zhu LH and Xu FM

PO Box 2345, Beijing 100023, China
Fax: +86-10-85381893
E-mail: wjg@wjgnet.com www.wjgnet.com

World J Gastroenterol 2004;10(13):1907-1910
World Journal of Gastroenterology
 ISSN 1007-9327

Effect of biopsies on sensitivity and specificity of ultra-rapid urease test for detection of *Helicobacter pylori* infection: A prospective evaluation

Li Lin Lim, Khek Yu Ho, Bow Ho, Manuel Salto-Tellez

Li Lin Lim, Khek Yu Ho, Department of Medicine, National University Hospital, Singapore
Bow Ho, Department of Microbiology, National University Hospital, Singapore
Manuel Salto-Tellez, Department of Pathology, National University Hospital, Singapore
Correspondence to: Dr. Khek Yu Ho, Department of Medicine, National University Hospital, 5 Lower Kent Ridge Road, 119074, Singapore. mdchoky@nus.edu.sg
Fax: +65-67794112
Received: 2003-10-27 **Accepted:** 2004-02-09

Abstract

AIM: To prospectively assess the sensitivity, specificity and time to positivity of theUltra-rapid urease test (URUT) for *Helicobacter pylori* (*H pylori*), and compare the results of one with those of two biopsies.

METHODS: Five antral biopsies were taken in consecutive patients undergoing upper endoscopy: one and two biopsies for URUT, and one each for *H pylori* culture and histology. URUT was read at 1, 5, 10, 20 and 30 min, 1, 2, 3 and 24 h after biopsy insertion into the reagent. A positive histology and/or culture was used as positive reference "gold standards".

RESULTS: URUT was more sensitive for detecting *H pylori* with two biopsies rather than one, at all time points up to 120 min. The sensitivity improved from 3.6% to 82.1% for one biopsy and 10.7% to 85.7% for two biopsies from 1 to 120 min. The sensitivity reached 96.4% at 24 h for both, but the specificity reduced from 100% to 96% and 92% for one and two biopsies, respectively.

CONCLUSION: Development of a positive URUT result is hastened by doubling the number of gastric biopsies. We recommend taking two instead of one biopsy to achieve an earlier positive URUT result so that *H pylori* eradication therapy can be initiated before patient is discharged from the endoscopy suite.

Lim LL, Ho KY, Ho B, Salto-Tellez M. Effect of biopsies on sensitivity and specificity of ultra-rapid urease test for detection of *Helicobacter pylori* infection: A prospective evaluation. *World J Gastroenterol* 2004; 10(13): 1907-1910
http://www.wjgnet.com/1007-9327/10/1907.asp

INTRODUCTION

The biopsy urease test was introduced as a simple and convenient method for diagnosing *Helicobacter pylori* (*H pylori*) infection. The biopsy urease test is based on the presence of large amounts of preformed urease enzymes in *H pylori*. The breakdown of urea by urease produces a high local concentration of ammonia, which raises the gastric pH. A phenol indicator that changes the color from yellow at pH 6.8 to magenta at pH 8.4 can detect this pH alteration. The color change with the introduction of the gastric biopsy is an indication for the presence of *H pylori*.

Despite many advances on the study of *H pylori*, the use of the biopsy urease test still remains invaluable in the diagnosis and management of gastroduodenal disease[1,2]. The rapid urease test is able to offer a sensitivity of 80-99% and a specificity of 92-100%[3-5] in untreated patients when compared with histology as the gold standard in the diagnosis of *H pylori* infection.

Since McNulty and Wise first described the biopsy urease test in 1985[6], several modifications of this test have been developed and validated. A test kit (CLOtest, Delta West Limited, W Australia) is commercially available but its costs and the time taken to positive results, which may be up to 24 h, limits its usefulness. The detection rate of *H pylori* at 20 min was 75% and 92% at 3 h and 98% at 24 h[7]. The length of time it takes for CLOtest still poses a hindrance to those clinicians wishing to treat infected patients while they are still in the endoscopy room.

The ultra-rapid urease test (URUT), as described by Arvind[8] is reported to overcome the latter shortcoming by enabling most positive tests to be apparent even before the end of the endoscopy[8].

We had previously reported the sensitivity, specificity, and the time to positivity for the URUT[9]. We found that better sensitivity could be obtained if the test continued to be read over a 24-h period although this was achieved at the expense of an increase in the number of false positive cases. We used only one antral biopsy for the URUT. In the CLOtest, the use of two biopsy specimens has been shown to hasten the time to a positive reaction[10]. Taking two specimens also may theoretically improve the sensitivity and specificity of the test.

The aim of this study was to assess prospectively the sensitivity, specificity and time to positivity for the URUT and compare the results of one biopsy and those of two biopsies in patients undergoing upper endoscopy.

MATERIALS AND METHODS

Patients

From September 1999 to June 2000, 53 consecutive patients who were given routine diagnostic upper gastrointestinal endoscopic examinations by one of the authors (KYH) and who had not been exposed to antibiotics, proton pump inhibitor or bismuth compounds within the past four weeks, and in whom gastric antral biopsies were clinically indicated, were prospectively studied. Patients who had been previously treated for *H pylori* infection and those with an abnormal coagulation profile were excluded from the study.

After an overnight or six-hour fast, each patient underwent esophagogastroduodenoscopy, during which five antral biopsies were taken from within 2 cm of the pylorus using sterilised biopsy forceps (Olympus 16K; Olympus Corp., Tokyo, Japan). Three of the biopsies were used for URUT

wherein the tests were done using one and two of the biopsies, respectively. The remaining two biopsies were sent for culture and histologic examination for *H pylori*. Biopsy specimens for the urease test and culture were taken before those used for histologic examination to avoid contamination with formalin. All patients gave informed consent before endoscopy. The study was conducted in accordance with the provisions of the Declaration of Helsinki and was approved by the Hospital Research & Ethics Committee.

Ultra-rapid urease test

The ultra-rapid urease test kit is composed of a capped polypropylene tube containing 0.5 mL aliquot of 100 g/L unbuffered solution of urea in deionised water (pH 6.8). The solution contains two drops of 10 g/L phenol red, which acts as the indicator[11]. The biopsy specimens for the URUT were removed from the biopsy forceps with a sterile toothpick and placed immediately into the polypropylene tube. Particular care was taken not to shake the tube after placing the biopsy into it so that a rapid positive result could be achieved[12]. The reagent was prepared in large batches, frozen, and was ready for thawing just before use. A positive test result was indicated when there was a color change in the medium surrounding the biopsy from yellow to magenta. The test tube was left at room temperature and examined by experienced observers without knowing the clinical details at pre-determined intervals over 24 h. Convenient times chosen were 1, 5, 10, 20, 30 min and 1, 2, 3 and 24 h after insertion of the biopsy specimen into the urease test reagent.

Histologic assessment

The gastric biopsies for histologic assessment were fixed in 40 g/L neutral buffered formaldehyde paraffin processed and stained with haematoxylin and eosin (H&E) in the normal way. Experienced pathologists without knowledge of the clinical data and URUT results assessed the presence or absence of *H pylori* by examining 3 sets of tissue levels within 12 consecutive sections. Histologic diagnosis *of H pylori* infection with H&E stain was compared with the use of Giemsa[13,14] and thus the Giemsa stain was used only when a few organisms were identified with H&E stain, always confirming the original diagnostic impression.

Culture assessment

For *H pylori* culture, gastric biopsies were smeared on pre-reduced chocolate blood agar plates and incubated in a humidified carbon dioxide incubator at 37 ℃ with 50 mL/L carbon dioxide for 3-4 d. The identity of any colonies grown was confirmed using Gram' s stain and biochemical tests. Experienced microbiologists without knowledge of the clinical data and URUT results assessed the presence or absence of *H pylori*[15,16].

Statistical considerations

Only patients with both culture and histology results were analyzed. Results from the URUT were compared with those from culture and histology of biopsy specimens obtained from the same patient. *H pylori* was considered as positive if either culture or histology demonstrated *H pylori*, and negative if *H pylori* was not detected in both culture and histology. Based on these results, the sensitivity and specificity of the URUT at various time points were determined. For this study, sensitivity was defined as the frequency of a positive URUT in patients with either gastric histology or culture positive for *H pylori*. Specificity was the frequency of a negative test in patients with both negative histology and culture for *H pylori*.

RESULTS

Of the 53 patients included in this study, 39(74%) were Chinese, 7(13%) were Malays, 6(11%) were Indians and 1(2%) was of another race. There were 29(55%) males and 24(45%) females. Their ages ranged from 23 to 85 (median, 52) years. The indications for the endoscopy included abdominal pain in 33 patients (62.2%), anemia or drop in hemoglobin in 6(11.3%), atypical chest pain in 5(9.5%), gastric ulcer follow-up in 1(1.9%), and other symptoms in 8(15.1%). The findings during esophagogastroduodenoscopy were esophagitis in 15(28%), duodenal ulcers in 14(26%), gastric ulcers in 8(15%), gastritis in 8(15%), duodenitis in 3(6%), and others in 5(10%).

H pylori was positive in 28 of the 53 patients (53%), in whom either the histology or culture demonstrated the organism. Twenty-four patients were *H pylori* positive in histology and 28 patients were culture positive.

The results of sensitivity and specificity of URUT at various time points are shown in Table 1. URUT was more sensitive for detecting *H pylori* when two biopsies rather than one were used, at all time points up to 120 min. At 1 min, the sensitivity was 3.6% for one biopsy and 10.7% for two biopsies. At 5 min, the sensitivities improved to 32.1% and 50% respectively. At

Table 1 Ultra-rapid urease test results at various time intervals comparing one *vs* two antral biopsies in 53 patients

		1 m	5 m	10 m	20 m	30 m	60 m	2 h	3 h	24 h
True positive	1 Bx	1	9	13	18	20	23	23	24	24
	2 Bx	3	14	17	21	23	24	24	24	27
True negative	1 Bx	25	25	25	25	25	25	25	25	24p
	2 Bx	25	25	25	25	25	25	25	25	23
False positive	1 Bx	0	0	0	0	0	0	0	0	1
	2 Bx	0	0	0	0	0	0	0	0	2
False negative	1 Bx	27	19	15	10	8	5	5	4	1
	2 Bx	25	14	11	7	5	4	4	4	1
Sensitivity (%)	1 Bx	3.6	32.1	46.4	64.3	71.4	82.1	82.1	85.7	96.4
	2 Bx	10.7	50	60.7	75	82.1	85.7	85.7	85.7	96.4
Specificity (%)	1 Bx	100	100	100	100	100	100	100	100	96
	2 Bx	100	100	100	100	100	100	100	100	92
PPV (%)	1 Bx	100	100	100	100	100	100	100	100	96.4
	2 Bx	100	100	100	100	100	100	100	100	96.4
NPV (%)	1 Bx	48.1	55.6	62.5	71.4	75.8	83.3	83.3	86.2	96
	2 Bx	50	64.1	69.4	78.1	83.3	86.2	86.2	86.2	95.8

Bx=Biopsy, m=minutes, h=hours, PPV=positive predictive value, NPV=negative predictive value.

60 min, the sensitivity was 82.1% for one biopsy and 85.7% for two biopsies. Thereafter there was still some increase in sensitivity with either one or two biopsies, reaching 96.4% at 24 h in each case, but with a reduction in the specificity from 100% to 96% and 92%, for one and two biopsies respectively. Using the receiver operating characteristic curve (Figure 1), the optimal times to read the test appeared to be 1 h when two biopsies were used and 3 h when only a single biopsy was used, and at these time points, the optimal combination of sensitivity and specificity was obtained.

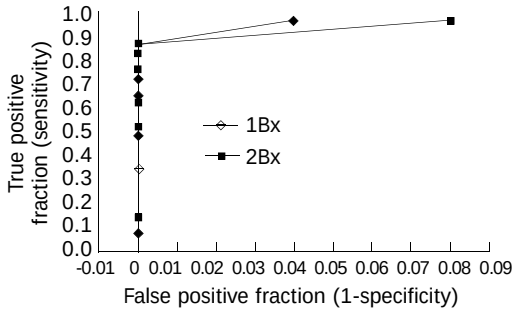

Figure 1 Receiver operating characteristic curve plot of urease test for detection of *H pylori* infection. Bx=Biopsy.

DISCUSSION

The ultra-rapid urease test, as described by Arvind[8] is reported to overcome the shortcoming of the CLOtest which takes a while to become positive. Using this home-made URUT preparation, we had found the test to be highly specific but not very sensitive when interpreted at one minute[9]. However, if the test continued to be read, the sensitivity improved to 87% at 24 h. This was however achieved at the expense of a longer reading time and a reduction in specificity to 90% at 24 h[9]. The development of false positives with delayed reading of the urease tests has previously been noted and attributed to other urease-producing bacteria, or to relatively small numbers of *H pylori*, which are not identified histologically, i.e., false-negative histology[17].

We previously used only one antral biopsy for the ultra-rapid urease test[9]. We hypothesize that if more gastric tissue was sampled, a positive test result might appear earlier, thus improving the test sensitivity without compromising its specificity. The present study confirmed this hypothesis. The URUT was more sensitive in detecting *H pylori* when two biopsies instead of one, were used at all time points up to 60 min. In this study a receiver operating characteristic curve analysis was used to select the optimal time for reading the test. The 1-h reading was found to give the optimal sensitivity/specificity combination when two biopsies were used, this does not automatically ensure that it is the best time to read the test. In many centers in the Asia Pacific region, the URUT is used as an initial screening test, with an additional sample taken for histology, which is sent only if the URUT is negative and when there is a strong clinical suspicion of *H pylori* infection. This approach is of great benefit to avoid the additional cost of the histology. Despite the fact that the *H pylori* infection is a chronic disease, the necessity to treat it soon after endoscopy is desirable to minimize the cost as well as the inconvenience of a second clinic visit. If this is the practice, then the most appropriate time point at which to read the test is 30 min when there is maximal specificity (as false positives will not be checked by histology) and minimal gain in sensitivity by reading the test beyond this time. Most importantly, reading the test at 30 min allows the physician to prescribe *H pylori* eradication treatment to the patient before discharging him or her from the endoscopy suite.

We are unable to explain the initial low sensitivity of the URUT test results found in the this study when compared with the original study[9]. One possible explanation is the reduced size of the biopsy specimens using smaller biopsy forceps as compared with the original study. However, the discrepancy is unlikely to be caused by the difference in the study populations, the incubation temperature of the biopsy specimens, and the volume and concentration of the phenol red used to make the test reagents since these parameters were similar to our previous study[9]. The initially low test sensitivity might not be a major problem as test sensitivity difference between one and two biopsies, and not the initial test sensitivity was the primary concern of this study. The conclusions reached by this study therefore, should remain valid.

There may be additional yield in taking biopsy specimens from different sites of the stomach due to the differences in the geographical distribution of *H pylori*, for example from the gastric body, in addition to the antral biopsies. However, we do not believe the addition of these biopsies would add significantly to the sensitivity of the tests. As part of another protocol (personal communication, KYH), two antral and two body biopsies were taken from 115 consecutive patients, and the specimens stained with H&E to assess the presence or absence of *H pylori*. Of a total of 66 histology positives, only three (4.5%) were correctly identified by the body biopsies while negative in the antral biopsies. Thus body biopsies contributed to an increased yield of only 4.5% in identifying histology positives. Previous other studies to determine the topographic distribution and density of *H pylori* to provide the maximum yield and to reduce the fallacious results due to sampling error have also concluded that biopsies taken from the antrum was sufficient[18-20].

Increasing the number of biopsies to more than two biopsies from the antrum, that is three or even four antral biopsy specimens, may increase the sensitivity given that this probably increases the *H pylori* load and therefore the amount of urease. However, this will prolong the endoscopy time and add inconvenience to the patient.

In our study, *H pylori* positivity was 53% based on either culture or histology result, which is in agreement with the local background *H pylori* colonization rate from our previously published data[9,21]. There were 24 patients who were *H pylori* positive on histology and 28 patients who were culture positive. This difference may reflect the difference in *H pylori* density. In this case, culture appears more sensitive than histology in identifying *H pylori*.

In conclusion, this study showed that the development of a positive URUT result could be hastened by doubling the gastric tissue samples. We recommend to take two biopsies instead of one for the URUT to achieve an earlier positive test result so that appropriate *H pylori* eradication therapy can be prescribed before the patient is discharged from the endoscopy suite.

REFERENCES

1 **Basset C,** Holton J, Ricci C, Gatta L, Tampieri A, Perna F, Miglioli M, Vaira D. Review article: diagnosis and treatment of Helicobacter: a 2002 updated review. *Aliment Pharmacol Ther* 2003; **17**(Suppl 2): 89-97

2 **Versalovic J.** *Helicobacter pylori*. Pathology and diagnostic strategies. *Am J Clin Pathol* 2003; **119**: 403-412

3 **Wong BC,** Wong WM, Wang WH, Tang VS, Young J, Lai KC, Yuen ST, Leung SY, Hu WH, Chan CK, Hui WM, Lam SK. An evaluation of invasive and non-invasive tests for the diagnosis of *Helicobacter pylori* infection in Chinese. *Aliment Pharmacol Ther* 2001; **15**: 505-511

4 **Chen YK,** Godil A, Wat PJ. Comparison of two rapid urease tests for detection of *Helicobacter pylori* infection. *Dig Dis Sci* 1998; **43:**

1636-1640
5 **Viiala CH,** Windsor HM, Forbes GM, Chairman SO, Marshall BJ, Mollison LC. Evaluation of a new formulation CLOtest. *J Gastroenterol Hepatol* 2002; **17**: 127-130
6 **McNulty CA**, Wise R. Rapid diagnosis of Campylobacter associated gastritis (Letter). *Lancet* 1985; **1**: 1443-1444
7 **Marshall BJ**, Warren JR, Francis GJ, Langton SR, Goodwin CS, Blincow ED. Rapid urease test in the management of Campylobacter pyloridis-associated gastritis. *Am J Gastroenterol* 1987; **82**: 200-210
8 **Arvind AS**, Cook RS, Tabaqchali S, Farthing MJG. One minute endoscopy room test for Campylobacter pylori (Letter). *Lancet* 1988; **1**: 704
9 **Ho KY**, Kang JY, Lim TP, Yeoh KG, Wee A. The effect of test duration on the sensitivity and specificity of ultra-rapid urease test for the detection of Helicobacter pylori infection. *Aust NZ J Med* 1998; **28**: 615-619
10 **Laine L**, Chun D, Stein C, El-Beblawi I, Sharma V, Chandrasoma P. The influence of size or number of biopsies on rapid urease test results: a prospective evaluation. *Gastrointest Endosc* 1996; **43**: 49-53
11 **Thillainayagam AV**, Arvind AS, Cook RS, Harrison IG, Tabaqchali S, Farthing MJG. Diagnostic efficiency of an ultra-rapid endoscopy room test for *Helicobacter pylori*. *Gut* 1991; **32**: 467-469
12 **Katelaris PH**, Lowe DG, Norbu P, Farthing MJG. Field evaluation of a rapid, simple and inexpensive urease test for the detection of *Helicobacter pylori*. *J Gastroenterol Hepatol* 1992; **7**: 569-571
13 **Kang JY**, Wee A, Math MV, Guan R, Tay HH. *Helicobacter pylori* and gastritis in patients with peptic ulcer and non-ulcer dyspepsia: ethnic differences in Singapore. *Gut* 1990; **31**: 850-853
14 **Kang JY**, Ho KY, Yeoh KG, Guan R, Wee A, Lee E, Lye WC, Leong SO, Tan CC. Peptic ulcer and gastritis in uraemia, with particular reference to the effect of *Helicobacter pylori* infection. *J Gastroenterol Hepatol* 1999; **14**: 771-778
15 **Hua J**, Ng HC, Yeoh KG, Ho KY, Ho B. Characterization of clinical isolates of *Helicobacter pylori* in Singapore. *Microbios* 1998; **94**: 71-81
16 **Hua JS**, Zheng PY, Fong TK, Mar KM, Bow H. *Helicobacter pylori* acquisition of metronidazole resistance by natural transformation *in vitro*. *World J Gastroenterol* 1998; **4**: 385-387
17 **Laine L**, Estrada R, Lewin DN, Cohen H. The influence of warming on rapid urease test results: a prospective evaluation. *Gastrointest Endosc* 1996; **44**: 429-432
18 **Misra V,** Misra S, Dwivedi M, Singh UP, Bhargava V, Gupta SC. A topographic study of *Helicobacter pylori* density, distribution and associated gastritis. *J Gastroenterol Hepatol* 2000; **15**: 737-743
19 **Vassallo J,** Hale R, Ahluwalia NK. CLO vs histology: Optimal numbers and site of gastric biopsies to diagnose *Helicobacter pylori*. *Eur J Gastroenterol Hepatol* 2001; **13:** 387-390
20 **Kalantar J,** Xia HHX, Ma Wyatt J, Rose D, Talley NJ. Determination of optimal biopsy sites for detection of *H pylori* in patients treated for not treated with antibiotic and anti-secretory drugs. *Gastroenterology* 1997; **112**: A165
21 **Kang JY**, Yeoh KG, Ho KY, Guan R, Lim TP, Quak SH, Wee A, Teo D, Ong YW. Racial differences in *Helicobacter pylori* seroprevalence in Singapore. *J Gastroenterol Hepatol* 1997; **12**: 655-659

Edited by Ma JY **Proofread by** Xu FM

PO Box 2345, Beijing 100023, China
Fax: +86-10-85381893
E-mail: wjg@wjgnet.com www.wjgnet.com

World J Gastroenterol 2004;10(13):1911-1913
World Journal of Gastroenterology
 ISSN 1007-9327

• BASIC RESEARCH •

Effect of rat serum containing Biejiajian oral liquid on proliferation of rat hepatic stellate cells

Li Yao, Zhen-Min Yao, Heng Weng, Ge-Ping Zhao, Yue-Jun Zhou, Tao Yu

Li Yao, Department of Pharmacology, Zhejiang College of Traditional Chinese Medicine, Hangzhou 310053, Zhejiang Province, China
Zhen-Min Yao, Heng Weng, **Yue-Jun Zhou, Tao Yu,** Department of Basic Medicine, Zhejiang College of Traditional Chinese Medicine, Hangzhou 310053, Zhejiang Province, China
Ge-Ping Zhao, Institute of Molecular Medicine, Zhejiang College of Traditional Chinese Medicine, Hangzhou 310053, Zhejiang Province, China
Supported by the Natural Science Foundation of Zhejiang Province, No.398402
Correspondence to: Dr. Li Yao, Department of Pharmacology, Zhejiang College of Traditional Chinese Medicine, Hangzhou 310053, Zhejiang Province, China. ylyj@mail.hz.zj.cn
Received: 2003-08-08 **Accepted:** 2003-09-18

Abstract

AIM: Liver fibrosis is a common pathological process of chronic liver diseases. Activation of hepatic stellate cells (HSCs) is the key issue in the occurrence of liver fibrosis. In this study, we observed the inhibitory action of rat serum containing Biejiajian oral liquid (BOL), a decoction of turtle shell, on proliferation of rat HSCs, and to explore the anti-hepatofibrotic mechanisms of BOL.

METHODS: A rat model of hepatic fibrosis was induced by subcutaneous injection of CCl_4. Serum containing low, medium and high dosages of BOL was prepared respectively. Normal and fibrotic HSCs were isolated and cultured. The effect of sera containing BOL on proliferation of HSCs was determined by ^{3}H-TdR incorporation.

RESULTS: The inhibitory rate of normal rat HSC proliferation caused by 100 mL/mL sera containing medium and high dosages of BOL showed a remarkable difference as compared with that caused by colchicine (medium dosage group: 34.56±4.21% *vs* 29.12±2.85%, $P<0.01$; high dosage group: 37.82±1.32% *vs* 29.12±2.85%, $P<0.01$). The inhibitory rate of fibrotic rat HSC proliferation caused by 100 mL/L serum containing medium and high dosages of BOL showed a remarkable difference as compared with that caused by colchicine (medium dosage group: 51.31±3.14% *vs* 38.32±2.65%, $P<0.01$; high dosage group: 60.15±5.36% *vs* 38.32±2.65%, $P<0.01$). The inhibitory rate of normal rat HSC proliferation caused by 100 mL/L and 200 mL/L sera containing a medium dosage of BOL showed a significant difference as compared with that caused by 50 mL/L (100 mL/L group: 69.02±9.96% *vs* 50.82±9.28%, $P<0.05$; 200 mL/L group: 81.78±8.92% *vs* 50.82±9.28%, $P<0.01$). The inhibitory rate of fibrotic rat HSC proliferation caused by 100 mL/L and 200 mL/L sera containing a medium dosage of BOL showed a significant difference as compared with that caused by 50 mL/L (100 mL/L group: 72.19±10.96% *vs* 61.38±7.16%, $P<0.05$; 200 mL/L group: 87.16±8.54% *vs* 61.38±7.16%, $P<0.01$).

CONCLUSION: Rat serum containing BOL can inhibit proliferation of rat HSCs, and the inhibition depends on the dosage and concentration of BOL. The inhibitory effect on HSC proliferation is one of the main anti-hepatofibrotic mechanisms of BOL.

Yao L, Yao ZM, Weng H, Zhao GP, Zhou YJ, Yu T. Effect of rat serum containing Biejiajian oral liquid on proliferation of rat hepatic stellate cells. *World J Gastroenterol* 2004; 10(13): 1911-1913
http://www.wjgnet.com/1007-9327/10/1911.asp

INTRODUCTION

Liver fibrosis is a common pathological process of chronic liver diseases. Injury factors would cause an unbalance between synthesis and degradation of extracellular matrix (ECM), which results in excessive collagen deposition in the liver[1]. Liver fibrosis could be reversed before developing into liver cirrhosis. Therefore, it is fundamental to prevent and treat cirrhosis to arrest its progression to liver cancer.

There are several steps in treating liver fibrosis in Western medicine, namely to inhibit activation of HSCs and proliferation of fibroblast-like HSCs and/or synthesis of matrix protein, to promote degradation of matrix protein, to impair activation of cytokines which lead to liver fibrosis, and to give gene therapy[2,3]. At the same time, the wide application of Western drugs should be restricted due to their toxicity and side effects.

The anti-hepatofibrotic effect of Biejiajian oral liquid (BOL) has been confirmed in our previous studies[4-6]. At present, we investigated the effect of rat serum containing BOL on the proliferation of rat hepatic stellate cells (HSCs) to further explore its anti-hepatofibrotic mechanisms.

MATERIALS AND METHODS

Materials

One hundred and forty male Wistar rats, weighing (360±20) g, were supplied by Animal Center of Academy of Medical Sciences of Zhejiang Province. Fodder was maize powder (Hangzhou Sijiqing Feed Factory). Lard (commercially available) and cholesterol were produced by Chemical Branch of Guangzhou Medicinal Company (batch number: 980503). Ethanol (A.R) was purchased from Changyuan Chemical Plant of Changshu City (batch number: 980630). BOL was prepared by the Pharmaceutical Laboratory, Zhejiang College of Traditional Chinese Medicine.

Methods

Animal model Except 30 rats for normal control, the rest of 60 Wistar rats received sc 5 mL/kg CCl_4 in the first day of experiment, followed by sc 400 mL/L CCl_4-liquid paraffin mixture 3 mL/kg daily for 3 d. The normal group received an equal amount of 9 g/L NaCl (NS) daily for 6 wk. Except the normal group, each rat was fed with mixed fodder (maize powder with 5 g/L cholesterol and 200 g/L lard) and drank 200 g/L ethanol only. The normal group was fed with general fodder and water. The time required to complete the induction of model was 6 wk[7].

Serum containing BOL preparation Eighty Wistar rats were divided into NS group, colchicine (0.1 mg/kg) group, groups

receiving high (9.2 g/kg), medium (4.6 g/kg) and low dosages (2.3 g/kg) of BOL. Each group received the drug once a day for 7 d. Venous blood was collected from inferior vena cava under asepsis 1 h after the last ig, then serum was separated (3 000 r/min, 20 min, 4 ℃), inactivated at 56 ℃ for 30 min, and stored at -70 ℃ for use.

HSC isolation and culture HSCs were isolated from the livers of normal rats and those with liver fibrosis. Isolation and culture were performed according to the modified Freidman method.

HSC proliferation determination Monolayer HSCs appeared in the 24-well culture plate after they were cultured in 1640 culture medium (Gibco BRC) with sera containing different dosages and concentration of BOL for 48 h. ^{3}H-TdR (Shanghai Institute of Atomic Energy) was added on 92.5 μGBq/well. HSCs were collected after cultured again for 24 h. The HSCs were digested with 2.5 g/L trypsase-1.1 g/L EDTA (Sigma), fixed by 100 mL/L trichloroaceticacid, dehydrated by alcohol, and then oven dried. Dimethylbenzene solution containing 5 mL/L ppo (Amersham) and 0.2 mL/L PoPop was added to measure CPM value of every sample.

Statistical analysis

Statistical analysis was performed with ANOVA. Data were presented as mean±SD. Significant differences were determined by using ANOVA. Results were considered statistically significant when $P<0.05$.

RESULTS

Effect of BOL on rat HSC proliferation

We used 100 mL/L sera containing different dosages of BOL to culture HSCs from normal and hepatofibrotic rats. Results showed that ^{3}H-TdR incorporated into rat HSCs was inhibited obviously by each dosage group, and the higher the dose, the better the effect (Tables 1, 2).

Table 1 Effect of different BOL dosage sera on ^{3}H-TdR incorporation of normal rat HSCs (mean±SD)

Groups	*n*	Cpm / well	Inhibitory rate (%)
Control	6	2 846.31±218.92	
Colchicine	6	2 018.37±39.31[b]	29.12±2.85
Low-dose	6	1 968.42±78.32[b]	30.84±2.71
Intermediate-dose	6	1 870.21±109.45[b]	34.56±4.21[a,d]
High-dose	6	1 779.86±61.12[a,d,f]	37.82±1.32[d,f]

[a]$P<0.05$ *vs* low-dose group, [b]$P<0.01$ *vs* control group, [d]$P<0.01$ *vs* colchicine group, [f]$P<0.01$ *vs* low-dose group.

Table 2 Effect of different BOL dosage sera on ^{3}H-TdR incorporation of hepatofibrotic rat HSCs (mean±SD)

Groups	*n*	Cpm / well	Inhibitory rate (%)
Control	6	1 657.82±67.21	
Colchicine	6	1 022.54±12.18[b]	38.32±2.65
Low-dose	6	994.69±37.86[b]	40.15±5.36
Intermediate -dose	6	828.91±48.19[b,d,f]	51.31±3.14[d,f]
High-dose	6	662.59±17.87[b,d,f]	60.15±5.36[d,f]

[b]$P<0.01$ *vs* control group, [d]$P<0.01$ *vs* colchicine group, [f]$P<0.01$ *vs* low-dose group.

Effect on rat HSC proliferation caused by different concentration sera containing medium dosage of BOL

We used 50 mL/L, 100 mL/L and 200 mL/L sera containing an intermediate dosage of BOL to culture normal and hepatofibrotic rat HSCs, which were controlled with normal rat sera at the same concentration. We observed that ^{3}H-TdR incorporation increased gradually as normal serum concentration increased. ^{3}H-TdR incorporation decreased gradually as drug serum concentration increased. ^{3}H-TdR incorporation in drug serum group at the same concentration was significantly lower than that in control group ($P<0.05$, Tables 3, 4).

Table 3 Effect of different concentration sera containing intermediate dosage of BOL on ^{3}H-TdR incorporation of normal rat HSCs (mean±SD)

Concentration	*n*	Control group (cpm / well)	BOL group (cpm / well)	Inhibitory rate (%)
50 mL / L	6	1 479.79±171.01	701.19±134.25[a]	50.82±9.28
100 mL / L	6	1 990.80±601.42	640.11±209.69[a]	69.02±9.96[c]
200 mL / L	6	2 699.89±789.10	479.59±257.30[a]	81.78±8.92[b]

[a]$P<0.05$ *vs* control group, [b]$P<0.01$ *vs* 50 mL / L concentration, [c]$P<0.05$ *vs* 50 mL / L concentration.

Table 4 Effect of different concentration sera containing intermediate dosage of BOL on ^{3}H-TdR incorporation of hepatofibrotic rat HSCs (mean±SD)

Concentration	*n*	Control group (cpm / well)	BOL group (cpm / well)	Inhibitory rate (%)
50 mL / L	6	987.73±154.02	563.07±124.38[a]	61.38±7.16
100 mL / L	6	1 342.58±701.36	375.92±109.47[a]	72.19±10.96[c]
200 mL / L	6	2 306.39±652.14	299.83±123.51[a]	87.16±8.54[b]

[a]$P<0.05$ *vs* control group, [b]$P<0.01$ *vs* 50 mL / L concentration, [c]$P<0.05$ *vs* 50 mL / L concentration.

DISCUSSION

Mechanism of liver fibrosis

The cells synthesizing extracellular matrix (ECM) in the liver were mainly active HSCs[8]. HSCs are situated in the Disse' s spaces. As liver cells were injured, HSCs would be activated and might increase, and then converted into myofibroblast-like cells (MFBLC), which could express cytokines, receptors, smooth muscle alpha-actin (alpha-SMA) and synthesize a great deal of ECM. Therefore, activation of HSCs is a key step in the pathogenesis of liver fibrosis[9-13]. Activation of local renin-angiotensin system might relate to hepatic fibrosis. Active HSCs could synthesize angiotensin II, which could participate in tissue remodeling in human liver[14]. It is the main source of collagen formation. HSC apoptosis could relieve experimental liver fibrosis in rats. Thus, it is an important pathway for preventing liver cirrhosis that inhibits HSC proliferation and collagen synthesis. Moreover, HSC proliferation is a key phase in liver fibrosis. Inhibiting proliferation of HSCs had an important sense for anti-hepatofibrosis[15,16]. Basement membrane-like matrix could inhibit proliferation of HSCs, estrogen could relieve liver fibrosis, and lipid could induce HSC proliferation[17,18].

Recognition of liver fibrosis in TCM

Researches on preventing and treating liver fibrosis in TCM have been increasing[4-7]. According to the theory of TCM, liver fibrosis is manifested as weakened body resistance while pathogenic factors prevail, damp-heat and blood stasis coexist, and the liver is depressed due to deficiency of Qi and blood in the spleen and kidney. Liver depression and Qi stagnation can result in blood stasis, blood fails to nourish the liver, and the

key pathogenetic mechanism is blood stasis. At beginning, the pathogenetic mechanism is Qi stagnation and blood stasis. If treated improperly, the disease would evolve into blood stasis, so that body resistance is weakened and excessive superficiality is present. The therapy is to promote the circulation and relieve the stasis, and to strengthen the body resistance to eliminate pathogenic factors, to resolve and soften the hard masses.

Anti-hepatofibrotic mechanism of BOL

BOL is an improved preparation from Biejiajian Pill that was recorded in an ancient medical book (*Jinkui Yaolue*). Its ingredients include more than twenty herbs, they are Carapax trionycis, Blackberrylily rhizome, Baical skullcap root, Zingiberis, rhizoma, Radix et rhizoma rhei, Ramulus cinnamomi, Folium pyrrosiae, Magnoliae cortex, Lilac pink herb, Lagerstroemia indica L, Colla corii asini, Radix bupleuri, Catharsius, Paeonia, Ppaeonia suffruticosa, Pruni persicae, semen, Radix ginseng, Pinelliae tuber, Tansymustard seed, Nitrum, Beehive. The combination of ingredients has the effect on promoting circulation and relieving stasis, strengthening body resistance and eliminating pathogenic factors, as well as resolving and softening the hard masses, which is conformable with the principle of treating liver fibrosis. Our previous experiments indicated the mechanisms of anti-hepatofibrosis of BOL as follows. It can prevent hepatocytes from degeneration and necrosis, eliminate liver fibrosis, inhibit the synthesis and secretion of ECM, relieve the capillarization of hepatic sinusoids, and improve the microcirculation of liver. HSCs are sensitive to oxygen and hypoxia could enhance liver fibrosis[19-22]. BOL could also regulate the immune function, and reduce the damage of liver cells[4-6].

In conclusion, serum-containing BOL can inhibit HSC proliferation and the inhibition may be dependent with the dosage and concentration of BOL.

REFERENCES

1 **Bedossa P,** Paradis V. Liver extracellular matrix in health and disease. *J Pathol* 2003; **200**: 504-515

2 **Huang GC**, Zhang JS, Zhang YE. Effects of retinoic acid on proliferation, phenotype and expression of cyclin-dependent kinase inhibitors in TGF-beta1-stimulated rat hepatic stellate cells. *World J Gastroenterol* 2000; **6**: 819-823

3 **Albanis E,** Friedman SL. Hepatic fibrosis. Pathogenesis and principles of therapy. *Clin Liver Dis* 2001; **5**: 315-334

4 **Yao ZM,** Lu GY, Zhao ZY. Experimental study on anti-hepatofibrosis effect of Biejiajian Pill. *Zhejiang Zhongyi Xueyuan Xuebao* 1997; **21**: 45-46

5 **Yao ZM,** Xiong YK, Li JP. Exper imental study on anti-hepatofibrosis effect of Biejia Jian Oral Liquid (BOL). *Zhejiang Zhongyi Xueyuan Xuebao* 2000; **24**: 58-61

6 **Zhao ZY,** Yao ZM, Zhong QP, Zhu FY, Wu CZ, Lu GY, Wang GY. Clinical study on Chinese herb Biejiajian pill for treating hepatic fibrosis. *Zhongxiyi Jiehe Ganbing Zazhi* 2001; **11**: 136-138

7 **Han DW**, Ma XH, Zhao YC. Research on animal model of liver cirrhosis. *Shanxi Yiyao Zazhi* 1979; **4**: 1-5

8 **Schwabe RF,** Bataller R, Brenner DA. Human Hepatic Stellate cells express CCR5 and RANTES to induce proliferation and migration. *Am J Physiol Gastrointest Liver Physiol* 2003; **285**: G949-958

9 **Brenner DA,** Waterboer T, Choi SK, Lindquist JN, Stefanovic B, Burchardt E, Yamauchi M, Gillan A, Rippe RA. New aspects of hepatic fibrosis. *J Hepatol* 2000; **32**(1 Suppl): 32-38

10 **Benyon RC,** Iredale JP. Is liver fibrosis reversible. *Gut* 2000; **46**: 443-446

11 **Rockey DC.** The cell and molecular biology of hepatic fibrogenesis. Clinical and therapeutic implications. *Clin Liver Dis* 2000; **4**: 319-355

12 **Arthur MJ.** Fibrogenesis II. Metalloproteinases and their inhibitors in liver fibrosis. *Am J physiol Gastrointest liver Physiol* 2000; **279**: 245-249

13 **Bataller R,** Brenner DA. Hepatic stellate cells as a target for the treatment of liver fibrosis. *Semin Liver Dis* 2001; **21**: 437-451

14 **Bataller R,** Sancho-Bru P, Gines P, Lora JM, Al-Garawi A, Sole M, Colmenero J, Nicolas JM, Jimenez W, Weich N, Gutierrez-Ramos JC, Arroyo V, Rodes J. Activated human hepatic stellate cells express the renin-angiotensin system and synthesize angiotensin II. *Gastroenterology* 2003; **125**: 117-125

15 **Ikeda H,** Nagashima K, Yanase M, Tomiya T, Arai M, Inoue Y, Tejima K, Nishikawa T, Omata M, Kimura S, Fujiwara K. Involvement of Rho/Rho Kinase Pathway in regulation of apoptosis in rat hepatic stellate cells. *Am J Physiol Gastrointest Liver Physiol* 2003; **285**: G880-886

16 **Bataller R,** Brenner DA. Hepatic stellate cells as a target for the treatment of liver fibrosis. *Semin Liver Dis* 2001; **21**: 437-451

17 **Gaca MD,** Zhou X, Issa R, Kiriella K, Iredale JP, Benyon RC. Basement membrane-like matrix inhibits proliferation and collagen synthesis by activated rat hepatic stellate cells: evidence for matrix-dependent deactivation of stellate cells. *Matrix Biol* 2003; **22**: 229-239

18 **Zhou Y,** Shimizu I, Lu G, Itonaga M, Okamura Y, Shono M, Honda H, Inoue S, Muramatsu M, Ito S. Hepatic stellate cells contain the functional estrogen receptor beta but not the estrogen receptor alpha in male and female rats. *Biochem Biophys Res Commun* 2001; **286**: 1059-1065

19 **Zar HA,** Tanigawa K, Kim YM, Lancaster JR Jr. Rat liver postischemic lipid perixidation and vasconstriction depend on ischemia time. *Free Radic Biol Med* 1998; **25**: 255-264

20 **Ankoma-Sey V,** Wang Y, Dai Z. Hypoxic stimulation of vascular endothelial growth factor expression in activated rat hepatic stellate cells. *Hepatology* 2000; **31**: 141-148

21 **Nagatomi A,** Sakaida I, Matsumura Y, Okita K. Cytoprotection by glycine against hypoxia-induced injury in cultured hepatocytes. *Liver* 1997; **17**: 57-62

22 **Jungermann K,** Kietzmann T. Oxygen: modulator of metablic zonation and disease of the liver. *Hepatology* 2000; **31**: 255-260

Edited by Wang XL and Xu FM

PO Box 2345, Beijing 100023, China
Fax: +86-10-85381893
E-mail: wjg@wjgnet.com www.wjgnet.com

World J Gastroenterol 2004;10(13):1914-1917
World Journal of Gastroenterology
 ISSN 1007-9327

• BASIC RESEARCH •

Effect of traditional Chinese medicinal enemas on ulcerative colitis of rats

Song-Ming Guo, Hong-Bin Tong, Lian-Song Bai, Wei Yang

Song-Ming Guo, Hong-Bin Tong, Department of Traditional Chinese Medicine, Tongji Hospital, Tongji University, Shanghai 200065, China
Lian-Song Bai, Wei Yang, Department of Traditional Chinese Medicine, Shuguang Hospital, Shanghai Traditional Chinese Medicine University, Shanghai 200032, China
Supported by the Science and Technology Development Fund of Shanghai, No. 98DB14586
Correspondence to: Song-Ming Guo, Department of Traditional Chinese Medicine, Tongji Hospital, Tongji University, Shanghai 200065, China. guosm@msn.com
Telephone: +86-21-56741593
Received: 2003-05-11 **Accepted:** 2003-06-02

Abstract

AIM: To investigate the effects of traditional Chinese medicinal enema (TCME) on inflammatory and immune response of colonic mucosa of rats with ulcerative colitis (UC), and to observe the pathogenic mechanism.

METHODS: Thirty UC rats, induced by intestinal enema together with 2.4-dinitrochlorobenzene (DNCB) and acetic acid, were randomly divided into 3 groups, i.e., GI, GII and GIII. Groups GI and GII were administered with TCME and salazosulfapyridine enema (SASPE), respectively. Group GIII was clystered with only normal saline (NSE), served as control. Group GIV was taken from normal rats as reference, once daily, from the 7th day after the establishment of UC for total 28 d. Interleukin-6 (IL-6) in the colonic mucosa was assayed by ^{3}H-TdR incorporation assay. Colonic mucosal lymphocyte subpopulation adhesive molecules, $CD_4^+CD_{11a}^+$, $CD_4^+CD_{18}^+$, $CD_8^+CD_{11a}^+$, $CD_8^+CD_{18}^+$ (LSAM), tumor necrosis factor (TNF)-α, and interferon-γ (IFN-γ), were detected by enzyme linked immunosorbent assay (ELISA). Moreover, the expression of TNF-α mRNA and IFN-γ mRNA in colonic mucosa were detected by polymerase chain reaction (RT-PCR).

RESULTS: Before therapies, in model groups, GI, GII and GIII, levels of IL-6, TNF-α, IFN-γ, $CD_8^+CD_{11a}^+$ and $CD_8^+CD_{18}^+$ were significantly different (38.29±2.61 U/mL, 16.54±1.23 ng/L, 8.61±0.89 ng/L, 13.51±2.31% and 12.22±1.13%, respectively) compared to those in GIV group (31.56±2.47 U/mL, 12.81±1.38 ng/L, 5.28±0.56 ng/L, 16.68±1.41% and 16.79±1.11%, respectively). After therapeutic enemas, in GI group, the contents of IL-6 (32.48±2.53 U/m), TNF-α (13.42±1.57 ng/L) and IFN-γ (5.87±0.84 ng/L) were reduced; then, the contents of $CD_8^+CD_{11a}^+$ (16.01±1.05 %) and $CD_8^+CD_{18}^+$ (16.28±0.19%) were raised. There was no significant difference between groups GI and GIV, but the difference between groups GI and GII was quite obvious (P<0.05). The expressions of TNF-α mRNA and IFN-γ mRNA in group GIII were much higher than those of group GIV, but those in group GI were significantly suppressed by TCME therapy.

CONCLUSION: Ulcerative colitis is related to colonic regional mucosal inflammatory factors and immune imbalance. TCME can effectively inhibit regional mucosal inflammatory factors and improve their disorder of immunity.

Guo SM, Tong HB, Bai LS, Yang W. Effect of traditional Chinese medicinal enemas on ulcerative colitis of rats. *World J Gastroenterol* 2004; 10(13): 1914-1917
http://www.wjgnet.com/1007-9327/10/1914.asp

INTRODUCTION

Ulcerative colitis (UC) is a refractory, chronic and non-specific disease. Its pathogenesis is probably related to the deficiency of autoimmunity and imbalance of immunoregulation[1-5]. The relationship between pathogenesis and immunity of colonic mucosa remains a focus at present[6-11]. In view of poor curative effect and high recurrence rate, traditional Chinese medicinal formulae were used to treat the disease in recent years, and the therapeutic effectiveness is quite satisfactory[12]. In order to explore the mechanism of UC and pharmacological action of the traditional Chinese medicinal formulae, rat models were established to observe the effect of traditional Chinese medicinal enema on immunological and inflammatory factors in colonic mucosa of rats with UC.

MATERIALS AND METHODS

Materials

Six-week-old Wistar rats (n=56), half of male and half of female were purchased from Shanghai Laboratory Animal Center of Chinese Academy of sciences (SLAC. CAS), calf serum, ConA and PHA (Institute of Cell Research of CAS) and mRNA reagent kit and PCR reagent (Promega), IL-6, TNF-α, IFN-γ reagent kit and PE marked CD_{11a}^+, CD_{18}^+ monoclonal antibody (Sigma). ^{3}H-TdR was from Shanghai Atomic Nuclear Institute of CAS. Cell factor primer-detonator was purchased from Shanghai Biological Engineering Center of CAS. The formulae of traditional Chinese medicinal herbs for enema consisted of Huangqi (*astragalus*), Dahuang (*caulis fibraureae*), Huangbai (*cortex phellodendri*), Wubeizi (*galla chinensis*) and Baiji (*rhizoma bletillae*), mixed with 1g crude drug per milliliter by Medicament Section of Shanghai Tongji Hospital. Salazosulfapyridine (SASP, batch No.921101, Shanghai Sine Pharmaceutical Factory) was prepared as suspension (20 mg/mL) at the same section.

UC model establishment

The models were prepared in reference to literature[13]. Fifty six Wistar rats weighing 200±20 g, were fed for 1 week before experiment. Then 38 rats were randomly taken as subjects for experiment. After depilation on back and neck, the rats were administered 0.3 mL of DNCB acetone liquid (DNCB 2.0 g: acetone 100 mL) solution on their bare backs and necks once daily for total 14 d. At the 15th day, 0.25 mL of 0.04 mmol/L DNCB ethanol (500 mL/L) solution was infused through a nylon hose inserted into the colon of rat 8 cm depth. At the 16th day, 2 mL of 80 mL/L-1 acetic acid solution was infused at the same depth. Then, the colon was rinsed with 5 mL normal

saline after 15 s of retention. The remaining 18 rats acted as controls after infusion of normal saline (NS) at 1 week since the preparation of the models, 8 rats were taken respectively from the group of model and group for reference to detect the levels of colonic mucosa lymphocytes: IL-6, TNF-α, IFN-γ and LSAM. The remaining 30 rats were randomly divided into 3 groups of 10 each: GI, GII and GIII were clystered daily with 2 mL of TCM, SASP and NS for 28 d respectively. Another group (GIV) of 10 rats, administered 2 mL of NS daily for 28 d, was taken as reference of normality. At the end of 4 wk experimental period, the lymphocytes were again detected and also the expressions of TNF-α mRNA and IFN-γ mRNA were examined.

Assay of cytokines and immunological factors

Separation and culture of intestinal theca mucosa cells

Mucosa cells were separated and routinely cultured to prepare monolayer culture cells suspension of colonic mucosa, and the suspension was adjusted to 5×10^9/L in RPMI 1640 containing 100 mL/L calf serum. Then, 1.0 mL of suspension, was put in 24-well plate, then 1.0 mL of ConA (final density 5 mg/L) was added, and cultured at 37 ℃ for 24 h in a humidified atmosphere containing 50 mL/L CO_2. The supernatant of the culture was centrifuged at 3 000 r/min and preserved at -20 ℃ for detection of IL-6, TNF-α, IFN-γ and LSAM levels according to the manufacturer' s instructions.

RNA extraction

Total RNA from colonic mucosa tissue of rats was extracted as previously described[14-16]: using single-step method of RNA isolation (acid guanidinium thiocyanate-phenol-chloroform extraction). Formaldehyde denatured electrophoresis stained with ethidium bromide (EB) was used to examine infect RNA. Reverse transcription reaction was performed as previously described[17-19]: a total amount of l μg of RNA as template was mixed with RNasin (40 U/μL) 0.5 μL, 25 μmol/L oligo (dT) 1 μL, 5×RT buffer 5 μL, dNTP (10 mmol/L) 1 μL and AMV (9 U/μL) 1 μL to a total reaction volume of 25 μL, followed by incubation at 37 ℃ for 1 h and at 94 ℃ for 5 min. PCR reaction was carried out as described previously[20-22]: 10 μL cDNA was added with 0.1 μg of primer, 0.05 μg of β-action primer and 2.5 U of *Taq* enzyme (5 U/μL). Total PCR reaction volume was 100 μL. PCR condition was as follows: deraturation at 94 ℃ for 1 min; primer annealing at 54 ℃ for 40 s, and extension at 72 ℃ for 40 s, followed a further extension at 72 ℃for 7 min. Other cycles were as follows: after 30 cycles of amplification, 20 μL of PCR product was electrophoresed on 20 g/L agarose gel, then recorded with camera under ultraviolet for density scanning and calculated the relative expression of the gene.

Statistical analysis

Experimental results were expressed as mean±SD. $P<0.05$ was considered statistically significant. All statistical calculations were performed using the SPSS for Windows version 9.0 software package.

RESULTS

Expression of colonic mucosal cytokines and adhesion molecules in rats of model group (MG) and control group (CG)

At 1 week after setting of models, the expression of cytokines in MG was found to be significantly higher than that in CG ($P<0.01$, Table 1). The expressions of lymphocyte T subpopulation surface adhesive molecules, $CD_8^+CD_{11a}^+$ and $CD_8^+CD_{18}^+$, were remarkably lower in MG than those in CG ($P<0.01$, Table 2).

Colonic mucosal TNF-α mRNA and IFN-γ mRNA

In group GI clystered with TCME, the levels of IL-6, TNF-α and IFN-γ were obviously reduced. Levels of CD_8^+ CD_{11a}^+ and CD_8^+ CD_{18}^+ were remarkably raised, which were no obvious differences compared with those in GIV group (i.e., control group) ($P>0.05$, Tables 3 and 4), but, there were significant differences between groups GI and GII ($P<0.05$, Tables 3 and 4).

Table 1 Expression of colonic mucosal cytokines in MG and RG before therapy (mean±SD)

Group	*n*	IL-6 (U/mL)	TNF-α (ng/L)	IFN-γ (ng/L)
Model	8	38.29±2.61[b]	16.54±1.23[b]	8.61±0.89[b]
Control	8	31.56±2.47	12.81±1.38	5.28±0.56

[b]$P<0.01$ *vs* control group.

Table 2 Comparison between expressions of colonic lymphocyte surface adhesive molecules (mean±SD, %)

Group	*n*	$CD_4^+CD_{11a}^+$	$CD_4^+CD_{18}^+$	$CD_8^+CD_{11a}^+$	$CD_8^+CD_{18}^+$
Model	8	29.81±1.17	26.24±1.12	13.51±2.31[a]	12.22±1.13[a]
Control	8	29.70±1.36	26.89±1.26	16.68±1.41	16.79±1.11

[a]$P<0.05$ *vs* control group.

Table 3 Changes of colonic mucosal cytokines after therapy (n=10, mean±SD)

Group	IL-6 (U/mL)	TNF-α (ng/L)	IFN-γ (ng/L)
GI	32.48±2.53[ae]	13.42±1.57[ae]	5.87±0.84[ae]
GII	34.56±3.21[c]	14.81±1.48[c]	6.36±0.62[c]
GIII	37.32±2.54	16.13±1.36	8.21±0.77
GIV	31.16±2.19	12.71±1.51	5.35±0.63

[a]$P>0.05$, [c]$P<0.05$ *vs* GIV; [e]$P<0.05$ *vs* GII.

Table 4 Expression of colonic mucosal lymphoid T surface adhesive molecules (n=10, mean±SD)

Group	$CD_4^+CD_{11a}^+$ (%)	$CD_4^+CD_{18}^+$ (%)	$CD_8^+CD_{11a}^+$ (%)	$CD_8^+CD_{18}^+$ (%)
GI	27.51±1.13	25.23±1.45	16.01±1.05[ae]	16.28±0.19[ae]
GII	27.35±1.23	25.54±1.50	13.16±1.34[c]	13.27±1.44[c]
GIII	27.42±1.56	25.51±1.28	11.52±1.29	11.34±1.61
GIV	27.61±1.43	25.45±1.26	16.45±1.23	16.56±1.13

[a]$P>0.05$, [c]$P<0.05$ *vs* GIV; [e]$P<0.05$ *vs* GII.

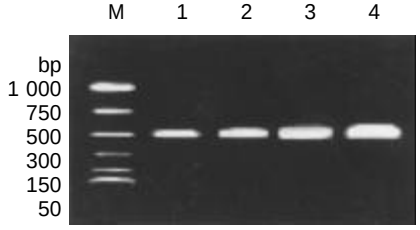

Figure 1 Analysis of TNF-α mRNA expression in UC mice after a 4-week treatment. A 550-bp fragment was amplified by PCR. M: Marker; Lane 1: Group GIV (control); Lane 2: Group GI (TCME); Lane 3: Group GII (SASPE); Lane 4: Group GIII (NSE). The primers used were: upstream, 5'-GGAGCTGCTCA GAGTAAATCAC-3'; and the downstream, 5'-GCACGAGTCA CTCTCGTTTTC-3'[23].

Expression of TNF-α mRNA and IFN-γ mRNA in colonic mucosal tissue

The expression of TNF-α mRNA and IFN-γ mRNA in colonic mucosal tissue, was higher in GIII group than those in GIV group (Figures 1, 2). After treatment, TNF-α mRNA and IFN-γ

mRNA levels were obviously suppressed in groups GI and GII, especially in group GI.

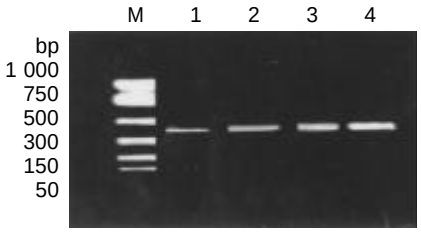

Figure 2 Analysis of IFN-γ mRNA expression in UC mice after a 4-week treatment. A 430-bp fragment was amplified by PCR. M: Marker; Lane 1: Group GIV (control); Lane 2: Group G I (TCME); Lane 3: Group GII (SASPE); Lane 4: Group GIII (NSE). The primers used were: upstream, 5'-TTTTGGGTCTCTTGGCT GTT-3'; and the downstream, 5'-CTCCTTTTTCGCTTCCCTGT-3'[23].

DISCUSSION

The pathogenesis of colonic colitis remains unclear up to now. It is believed that colonic colitis results from the interaction of many factors, such as environment, immunity and heredity, *etc*. Probably, susceptible population in heredity is affected by environmental factors, such as water, food and infection, which trigger excessive reaction of intestinal immunity. The reaction can cause an inflammatory stimulation to intestinal mucosa and damage it[24,25]. More and more attention has been paid to autoimmunity. An opinion suggests that there exists an inevitable correlation between the immunity system of intestinal mucosa and its integrity[26-28]. It has been reported that IL-6, a mononuclear macrophage, is a cytokine secreted by T and B cell. IL-6 can promote proliferation of T cell and enhance T cell reaction to cell toxicity. Our experimental result showed that IL-6 was high active in colonic mucosal tissue of UC models, the higher level of IL-6 can further aggravate the injury on colonic tissue by antigen-antibody reaction and complement activation[29-35]. More endogenous IFN-γ and TNF-α produced by colonic epithelia of UC models cause the changes in epithelia, which may lead directly to scathes of inflammatory epithelia[36,37]. Disorder of autoimmunity is closely related to the imbalance of Th_1 and Th_2 cells. For IFN-γ being on Th_1 cell, abnormal expressions of IFN-γ and IFN-γ mRNA cause inevitably the imbalance of Th_1/Th_2 and result in immune disorder[38-40]. CD_{11a}^+/CD_{18}^+ are cell surface adhesive albumin, also known as lymphocyte function antigen-l (LFA-l), a representative of β_2 integrants. It possesses a series of functions, such as introduction of adhesion, chemotaxis of cell and homing of lymphocytes, *etc*. It expresses on surfaces of white cells, phagocytes and large granular lymphocytes, acting as a key channel in interaction and information between cells. A few of cellular factors, affected by them, such as IL-6, IFN-γ, TNF-α and endotoxin, can affect their expressions[41-43]. $CD_8^+CD_{11a}^+$ and $CD_8^+CD_{18}^+$ (on T_s cell) were found in suffers with moderate and severe ulcerative colitis, and significantly lower than those in normal control rats[44]. This is in conformity to our findings.

Our study showed that expressions of IL-6, TNF-α, TNF-α mRNA, IFN-γ, IFN-γ mRNA were found to be obviously higher and the levels of lymphocyte T surface adhesive molecules, $CD_8^+CD_{11a}^+$ and $CD_8^+CD_{18}^+$ were lower than those in normal rats in colonic mucosal tissue of UC models. The results were in agreement with the findings of others[45]. The results indicated that ulcerative colitis was correlated with disfunction and disorder of autoimmunity. The abnormal expressions of local inflammatory factors and adhesive albumin of cell surface in colonic tissue play a critical role in regulation of immunity. The mutual affects of these factors and abnormality of regulation of immune system are regarded as the core of pathogenesis. The imbalance of regulation between pre-inflammation cytokines and anti-inflammation cytokines is considered an important mechanism of intestine inflammation, including ulcerative colitis.

At present, ulcerative colitis lacks more effective therapy for radical cure. Principally, steroid hormones and salicylic acid preparation are used to control and suppress the inflammation. In recent years, along with the development of immunology and molecular biology, the accumulation of knowledge about the disease and further understanding of the mechanism of drug action, new methods of treatment have come up into being one after another. But the ordinary UC sufferers can not afford remedies due to the exorbitant price of drugs, and the safety of the remedies needs to be further identified. Our study demonstrated that salazosulfapyridine (SASP) is still the principal remedy for ulcerative colitis. It can improve the conditions of patients in mild and moderate states. But the side-effect and high relapse rate after the remedy are unsatisfactory. Traditional Chinese medicine is popular in China. It is characteristic of TCM to treat intestinal diseases with TCM herbs enemas[12]. The study showed that the treatment of TCME was better on UC than SASPE. Our TCME could effectively inhibit the activity of granulocyte, macrophage and monocyte. Also it could reduce immune response and formation of inflammation in colonic mucosal tissue, which might be due to that our TCME could reduce the expressions of IL-6, TNF-α, IFN-γ and raise the levels of surface adhesive molecules ($CD_8^+CD_{11a}^+$ and $CD_8^+CD_{18}^+$), could also suppress the abnormal expressions of IFN-α and IFN-γ mRNA, improve the disorder of immunity in UC and the Baiji could protect colonic mucosa, Bahuang and Huangbai could promote cruor. SASP suspension has more side-effects than the formulae of TCM herbs, although it has a certain effect in treatment of ulcerative colitis clinically. Therefore, the retention enema prepared from TCM herbs may be an ideal choice to manage the disease.

REFERENCES

1 **Furrie E,** Macfarlane S, Cummings JH, Macfarlane GT. Systemic antibodies towards mucosal bacteria in ulcerative colitis and Crohn's disease differentially activate the innate immune response. *Gut* 2004; **53:** 91-98

2 **Ioachim E,** Michael M, Katsanos C, Demou A, Tsianos EV. The immunohistochemical expression of metallothionein in inflammatory bowel disease.Correlation with HLA-DR antigen expression, lymphocyte subpopulations and proliferation-associated indices. *Histol Histopathol* 2003; **18:** 75-82

3 **Ludwiczek O,** Kaser A, Tilg H. Plasma levels of soluble CD40 ligand are elevated in inflammatory bowel diseases. *Int J Colorectal Dis* 2003; **18:** 142-147

4 **Sawada-Hase N,** Kiyohara T, Miyagawa J, Ueyama H, Nishibayashi H, Murayama Y, Kashihara T, Nakahara M, Miyazaki Y, Kanayama S, Nezu R, Shinomura Y, Matsuzawa Y. An increased number of CD40-high monocytes in patients with Crohn's disease. *Am J Gastroenterol* 2000; **95:** 1516-1523

5 **Candelli M,** Nista EC, Nestola M, Armuzzi A, Silveri NG, Gasbarrini G, Gasbarrini A. Saccharomyces cerevisiae-associated diarrhea in an immunocompetent patient with ulcerative colitis. *J Clin Gastroenterol* 2003; **36:** 39-40

6 **Ohman L,** Franzen L, Rudolph U, Harriman GR, Hultgren Hornquist E. Immune activation in the intestinal mucosa before the onset of colitis in Galphai2-deficient mice. *Scand J Immunol* 2000; **52:** 80-90

7 **Fukushima K,** Yonezawa H, Fiocchi C. Inflammatory bowel disease-associated gene expression in intestinal epithelial cells by differential cDNA screening and mRNA display. *Inflamm Bowel Dis* 2003; **9:** 290-301

8 **Fahlgren A,** Hammarstrom S, Danielsson A, Hammarstrom ML. Increased expression of antimicrobial peptides and lysozyme in colonic epithelial cells of patients with ulcerative colitis. *Clin Exp*

Immunol 2003; **131:** 90-101
9 **Carvalho AT,** Elia CC, de Souza HS, Elias PR, Pontes EL, Lukashok HP, de Freitas FC, Lapae Silva JR. Immunohistochemical study of intestinal eosinophils in inflammatory bowel disease. *J Clin Gastroenterol* 2003; **36:** 120-125
10 **Carty E,** De Brabander M, Feakins RM, Rampton DS. Measurement of in vivo rectal mucosal cytokine and eicosanoid production in ulcerative colitis using filter paper. *Gut* 2000; **46:** 487-492
11 **McKaig BC,** McWilliams D, Watson SA, Mahida YR. Expression and regulation of tissue inhibitor of metalloproteinase-1 and matrix metalloproteinases by intestinal myofibroblasts in inflammatory bowel disease. *Am J Pathol* 2003; **162:** 1355-1360
12 **Jiang XL,** Cui HF. An analysis of 10 218 ulcerative colitis cases in China. *World J Gastroenterol* 2002; **8:** 158-161
13 **Padol I,** Huang JQ, Hogaboam CM, Hunt RH. Therapeutic effects of the endothelin receptor antagonist Ro 48-5695 in the TNBS/DNBS rat model of colitis. *Eur J Gastroenterol Hepatol* 2000; **12:** 257-265
14 **Tahara K,** Fujii K, Yamaguchi K, Suematsu T, Shiraishi N, Kitano S. Increased expression of P-cadherin mRNA in the mouse peritoneum after carbon dioxide insufflation. *Surg Endosc* 2001; **15:** 946-949
15 **Xiang X,** Qiu D, Hegele RD, Tan WC. Comparison of different methods of total RNA extraction for viral detection in sputum. *J Virol Methods* 2001; **94:** 129-135
16 **Yamada H,** Koizumi S. Lymphocyte metallothionein-mRNA as a sensitive biomarker of cadmium exposure. *Ind Health* 2001; **39:** 29-32
17 **Fasshauer M,** Kralisch S, Klier M, Lossner U, Bluher M, Chambaut-Guerin AM, Klein J, Paschke R. Interleukin-6 is a positive regulator of tumor necrosis factor alpha-induced adipose-related protein in 3T3-L1 adipocytes. *FEBS Lett* 2004; **27:** 153-157
18 **Barbier M,** Vidal H, Desreumaux P, Dubuquoy L, Bourreille A, Colombel JF, Cherbut C, Galmiche JP. Overexpression of leptin mRNA in mesenteric adipose tissue in inflammatory bowel diseases. *Gastroenterol Clin Biol* 2003; **27:** 987-991
19 **Ridyard AE,** Nuttall TJ, Else RW, Simpson JW, Miller HR. Evaluation of Th1, Th2 and immunosuppressive cytokine mRNA expression within the colonic mucosa of dogs with idiopathic lymphocytic-plasmacytic colitis. *Vet Immunol Immunopathol* 2002; **86:** 205-214
20 **Akazawa A,** Sakaida I, Higaki S, Kubo Y, Uchida K, Okita K. Increased expression of tumor necrosis factor-alpha messenger RNA in the intestinal mucosa of inflammatory bowel disease, particularly in patients with disease in the inactive phase. *J Gastroenterol* 2002; **37:** 345-353
21 **Ogawa A,** Andoh A, Araki Y, Bamba T, Fujiyama Y. Neutralization of interleukin-17 aggravates dextran sulfate sodium-induced colitis in mice. *Clin Immunol* 2004; **110:** 55-62
22 **Sawa Y,** Oshitani N, Adachi K, Higuchi K, Matsumoto T, Arakawa T. Comprehensive analysis of intestinal cytokine messenger RNA profile by real-time quantitative polymerase chain reaction in patients with inflammatory bowel disease. *Int J Mol Med* 2003; **11:** 175-179
23 **Egger B,** Bajaj-Elliott M, MacDonald TT, Inglin R, Eysselein VE, Buchler MW. Characterisation of acute murine dextran sodium sulphate colitis: cytokine profile and dose dependency. *Digestion* 2000; **62:** 240-248
24 **Elson CO,** Sartor RB, Targan SR, Sandborn WJ. Challenges in IBD Research: updating the scientific agendas. *Inflamm Bowel Dis* 2003; **9:** 137-153
25 **Mow WS,** Vasiliauskas EA, Lin YC, Fleshner PR, Papadakis KA, Taylor KD, Landers CJ, Abreu-Martin MT, Rotter JI, Yang H, Targan SR. Association of antibody responses to microbial antigens and complications of small bowel Crohn's disease. *Gastroenterology* 2004; **126:** 414-424
26 **Akazawa A,** Sakaida I, Higaki S, Kubo Y, Uchida K, Okita K. Increased expression of tumor necrosis factor-alpha messenger RNA in the intestinal mucosa of inflammatory bowel disease, particularly in patients with disease in the inactive phase. *J Gastroenterol* 2002; **37:** 345-353
27 **Rioux JD,** Silverberg MS, Daly MJ, Steinhart AH, McLeod RS, Griffiths AM, Green T, Brettin TS, Stone V, Bull SB, Bitton A, Williams CN, Greenberg GR, Cohen Z, Lander ES, Hudson TJ, Siminovitch KA. Genomewide search in Canadian families with inflammatory bowel disease reveals two novel susceptibility loci. *Am J Hum Genet* 2000; **66:** 1863-1870
28 **Obermeier F,** Schwarz H, Dunger N, Strauch UG, Grunwald N, Scholmerich J, Falk W. OX40/OX40L interaction induces the expression of CXCR5 and contributes to chronic colitis induced by dextran sulfate sodium in mice. *Eur J Immunol* 2003; **33:** 3265-3274
29 **Beil WJ,** McEuen AR, Schulz M, Wefelmeyer U, Kraml G, Walls AF, Jensen-Jarolim E, Pabst R, Pammer J. Selective alterations in mast cell subsets and eosinophil infiltration in two complementary types of intestinal inflammation: ascariasis and Crohn's disease. *Pathobiology* 2002-2003; **70:** 303-313
30 **Stucchi AF,** Shebani KO, Leeman SE, Wang CC, Reed KL, Fruin AB, Gower AC, McClung JP, Andry CD, O'Brien MJ, Pothoulakis C, Becker JM. A neurokinin 1 receptor antagonist reduces an ongoing ileal pouch inflammation and the response to a subsequent inflammatory stimulus. *Am J Physiol Gastrointest Liver Physiol* 2003; **285:** G1259-1267
31 **Driessler F,** Venstrom K, Sabat R, Asadullah K, Schottelius AJ. Molecular mechanisms of interleukin-10-mediated inhibition of NF-kappaB activity: a role for p50. *Clin Exp Immunol* 2004; **135:** 64-73
32 **Redwine L,** Hauger RL, Gillin JC, Irwin M. Effects of sleep and sleep deprivation on interleukin-6, growth hormone, cortisol, and melatonin levels in humans. *J Clin Endocrinol Metab* 2000; **85:** 3597-3603
33 **Papadakis KA**, Targan SR. Role of cytokines in the pathogenesis of inflammatory bowel disease. *Annu Rev Med* 2000; **51**: 289-298
34 **Sandborn WJ.** Evidence-based treatment algorithm for mild to moderate Crohn's disease. *Am J Gastroenterol* 2003; **98**(12 Suppl): S1-S5
35 **Gasche C,** Bakos S, Dejaco C, Tillinger W, Zakeri S, Reinisch W. IL-10 secretion and sensitivity in normal human intestine and inflammatory bowel disease. *J Clin Immunol* 2000; **20:** 362-370
36 **Abreu MT,** Taylor KD, Lin YC, Hang T, Gaiennie J, Landers CJ, Vasiliauskas EA, Kam LY, Rojany M, Papadakis KA, Rotter JI, Targan SR, Yang H. Mutations in NOD2 are associated with fibrostenosing disease in patients with Crohn's disease. *Gastroenterology* 2002; **123:** 679-688
37 **Suryaprasad AG,** Prindiville T. The biology of TNF blockade. *Autoimmun Rev* 2003; **2:** 346-357
38 **Loher F,** Bauer C, Landauer N, Schmall K, Siegmund B, Lehr HA, Dauer M, Schoenharting M, Endres S, Eigler A. The interleukin-1 beta-converting enzyme inhibitor pralnacasan reduces dextran sulfate sodium-induced murine colitis and T helper 1 T-cell activation. *J Pharmacol Exp Ther* 2004; **308:** 583-590
39 **Topilski I,** Harmelin A, Flavell RA, Levo Y, Shachar I. Preferential Th1 immune response in invariant chain-deficient mice. *J Immunol* 2002; **168:** 1610-1617
40 **Fuss IJ,** Boirivant M, Lacy B, Strober W. The interrelated roles of TGF-beta and IL-10 in the regulation of experimental colitis. *J Immunol* 2002; **168:** 900-908
41 **Noti JD,** Johnson AK, Dillon JD. Structural and functional characterization of the leukocyte integrin gene CD11d. Essential role of Sp1 and Sp3. *J Biol Chem* 2000; **275:** 8959-8969
42 **Schneeberger EE,** Vu Q, LeBlanc BW, Doerschuk CM. The accumulation of dendritic cells in the lung is impaired in CD18-/- but not in ICAM-1-/- mutant mice. *J Immunol* 2000; **164:** 2472-2478
43 **Tilg H,** Vogelsang H, Ludwiczek O, Lochs H, Kaser A, Colombel JF, Ulmer H, Rutgeerts P, Kruger S, Cortot A, D'Haens G, Harrer M, Gasche C, Wrba F, Kuhn I, Reinisch W. A randomised placebo controlled trial of pegylated interferon alpha in active ulcerative colitis. *Gut* 2003; **52:** 1728-1733
44 **Vainer B,** Brimnes J, Claesson MH, Nielsen OH. Impaired sensitivity to beta 2 integrin-blocking in ICAM-1-mediated neutrophil migration in ulcerative colitis. *Scand J Gastroenterol* 2001; **36:** 621-629
45 **Vainer B,** Sorensen S, Seidelin J, Nielsen OH, Horn T. Expression of ICAM-1 in colon epithelial cells: an ultrastructural study performed on *in vivo* and *in vitro* models. *Virchows Arch* 2003; **443:** 774-781

Edited by Kumar M and Chen WW **Proofread by** Xu FM

PO Box 2345, Beijing 100023, China
Fax: +86-10-85381893
E-mail: wjg@wjgnet.com www.wjgnet.com

World J Gastroenterol 2004;10(13):1918-1922
World Journal of Gastroenterology
 ISSN 1007-9327

• BASIC RESEARCH •

Expression of inducible nitric oxide synthase and cyclooxygenase-2 in pancreatic adenocarcinoma: Correlation with microvessel density

Hans U. Kasper, Hella Wolf, Uta Drebber, Helmut K. Wolf, Michael A. Kern

Hans U. Kasper, Michael A. Kern, Uta Drebber, Department of Pathology, University of Cologne, Germany
Hans U. Kasper, Michael A. Kern, Center of Molecular Medicine of the University of Cologne, Germany
Helmut K. Wolf, Department of Pathology, Johannes-Gutenberg, University of Mainz, Germany
Hella Wolf, Department of Pathology, University of Magdeburg, Germany
Correspondence to: Dr. Hans U. Kasper, Department of Pathology, University of Cologne, Joseph-Stelzmann-Str. 9, D-50931 Koeln, Germany. hans-udo.kasper@uni-koeln.de
Telephone: +49-221-4787223 **Fax:** +49-221-478-6360
Received: 2003-11-18 **Accepted:** 2004-01-17

Abstract

AIM: Cyclooxygenases (COX) are key enzymes for conversion of arachidonic acid to prostaglandins. Nitric oxide synthase (NOS) is the enzyme responsible for formation of nitric oxide. Both have constitutive and inducible isoforms. The inducible isoforms (iNOS and COX-2) are of great interest as regulators of tumor angiogenesis, tumorigenesis and inflammatory processes. This study was to clarify their role in pancreatic adenocarcinomas.

METHODS: We investigated the immunohistochemical iNOS and COX-2 expression in 40 pancreatic ductal adenocarcinomas of different grade and stage. The results were compared with microvessel density and clinicopathological data.

RESULTS: Twenty-one (52.5%) of the cases showed iNOS expression, 15 (37.5%) of the cases were positive for COX-2. The immunoreaction was heterogeneously distributed within the tumors. Staining intensity was different between the tumors. No correlation between iNOS and COX-2 expression was seen. There was no relationship with microvessel density. However, iNOS positive tumors developed more often distant metastases and the more malignant tumors showed a higher COX-2 expression. There was no correlation with other clinicopathological data.

CONCLUSION: Approximately half of the cases expressed iNOS and COX-2. These two enzymes do not seem to be the key step in angiogenesis or carcinogenesis of pancreatic adenocarcinomas. Due to a low prevalence of COX-2 expression, chemoprevention of pancreatic carcinomas by COX-2 inhibitors can only achieve a limited success.

Kasper HU, Wolf H, Drebber U, Wolf HK, Kern MA. Expression of inducible nitric oxide synthase and cyclooxygenase-2 in pancreatic adenocarcinoma: Correlation with microvessel density. *World J Gastroenterol* 2004; 10(13): 1918-1922
http://www.wjgnet.com/1007-9327/10/1918.asp

INTRODUCTION

Cancer of the pancreas is still one of the most dismal malignant diseases with a death to incidence rate of 0.99[1]. In Germany alone, more than 11 000 patients die of this disease per year[2]. The only effective therapy is surgical excision[3]. Adjuvant chemo- and radiotherapy provide only a minimal survival advantage without consistent improvement in outcome[4]. Until now, the molecular biology of pancreatic cancer still is relatively unknown. A number of studies have focused on genetic changes[3,5,6]. But also inflammation has been identified as a significant factor in the development of pancreatic cancer[7]. Both hereditary and sporadic forms of chronic pancreatitis may be associated with increased cancer risk[8]. Cytokines, reactive oxygen species and mediators of the inflammatory pathway have been identified to increase cell cycling, cause loss of tumor suppressor function and stimulate oncogene expression[7]. These cytokines are also part of angiogenesis, being an important step for tumor development and could be a therapeutic target also for pancreatic adenocarcinomas.

Nitric oxide (NO) is a pleiotropic biomolecule with a short half time. It has part in the signal transduction in a great variety of mechanisms including neural transmission, vasodilatation, immunoregulation and defense mechanism as well as influencing cancerogenesis[9]. NO is a product of the conversion of l-arginine to l-citrulline by nitric oxide synthase (NOS)[10]. This enzyme exists in three isoforms, namely the constitutively expressed calcium-dependent endothelial (eNOS) and neuronal (nNOS) nitric oxide synthase and the calcium independent inducible or immunological (iNOS or NOS-2) isoforms[11].

INOS expression in human diseases has long been a matter of investigation. NO production by iNOS in tumor infiltrating macrophages may be part of their antitumoral cytotoxic potential[12]. On the other hand, expression of iNOS in endothelial cells of tumor vessels and in cancer cells itself supports the assumption that the cancer uses this isoform to regulate the tumor vascularisation and blood flow[13,14].

Cyclooxygenases (COX) are enzymes which are involved in the synthesis of prostaglandines (PGs) from arachidonic acid. They catalyze the insertion of molecular oxygen into arachidonic acid to form the unstable intermediate PG-G2 being rapidly converted to PGH2. PGH2 is the source of several biological active PGs, thromboxanes and prostacyclines which contribute to many physiological and pathological processes like hemostasis, kidney and gastric function, pain, inflammation and tumor defense and also tumorigenesis[15].

The two isoforms of COX (COX-1 and COX-2) differ in many respects[16]. COX-1 is constitutively expressed in most tissues and seems to be responsible for the baseline production of PG. COX-2 is not detected in most normal tissues but is highly inducible by inflammatory and mitogenic stimuli. COX-2 is strongly implicated in tumorigenesis and COX-2 inhibitors are discussed as the target for cancer prevention and therapy[17].

Current knowledge regarding the rate of iNOS and COX-2 expressions and their relationship to MVD in pancreatic cancer is rather limited. We investigated therefore iNOS and COX-2 expression in pancreatic adenocarcinomas in comparison to microvessel density to clarify the influence of these mediators in pancreatic carcinomas.

MATERIALS AND METHODS

Tissue specimens

All tissues used in this study were surgical resection specimens obtained from the files of the Department of Pathology, Johannes Gutenberg- University, Mainz, Germany. All pancreatic adenocarcinomas were of ductal origin. Carcinomas from 18 women and 22 men with a mean age of 62.2 years (range 45- 81 years) were investigated. Thirty-three tumors were located in the head of the pancreas, 3 in the corpus and 5 in the tail of the pancreas. TNM- classification according to the TNM classification of malignant tumors was as follows: 5× T1, 27× T2, 7× T3, 1× T4. Twenty-three patients showed lymph node metastases and in 5 patients, distant metastases were known. There were 3 well differentiated, 15 moderately differentiated and 22 poorly differentiated pancreatic carcinomas.

Immunohistochemistry

Resected specimens were fixed overnight in 40 g/L buffered formaldehyde, embedded in paraffin and further processed.

For iNOS detection, 4-μm thick sections were deparaffinized and rehydrated, washed in tap water and distilled water and finally in 0.05 mol/L Tris buffer (pH 7.6). After blocking of nonspecific binding sites (Protein blocking agent, Ultratech, Coulter-Immunotech, Marseille, France), sections were washed and incubated with the primary polyclonal rabbit antibody (Transduction Laboratories, Biomol, Hamburg, Germany) with a dilution of 1:1 200 overnight at 4 ℃. This antibody is directed against the mouse iNOS C-terminal peptide (1 131-1 144) plus additional N-terminated Cys conjugated to KLH (CKKGSALEEPKATRL). According to the manufacturer, the antibody could recognize the human, mouse and rat iNOS 130 kDa protein without cross reaction to eNOS or nNOS. A biotinylated goat anti-rabbit antibody (Vectastain, ABC-AP Elite Kit, Vector Laboratories, Burlingame, USA) served as secondary antibody. After incubation with the avidine-biotin-complex with alkaline phosphatase, as described by the manufacturer, Fast Red chromogen system (Coulter Immunotech) was used for visualization.

For COX-2 immunohistochemistry, antigen retrieval was achieved by microwave treatment 3 times for 5 min with 600 watt in 0.01 mol/L citrate buffer pH 6.0. The monoclonal antibody COX-2 (h-62 sc-7951;Santa Cruz, Santa Cruz, CA USA) was used as primary antibody in a dilution of 1:50. According to the producer, this antibody reacts with COX-2 of mouse, rat and human origin with no cross reaction with Cox-1. For visualization, the envision kit (DAKO, Glostrup, Denmark) was used.

The results of MVD were retrieved from a previous study [18]. In brief, it was determined using a monoclonal mouse anti-CD34 antibody (Biogenex, San Ramon, Clif, USA). After the endogenous peroxidase was blocked with 30 mL/L hydrogen peroxide the staining procedure was automated including detection with DAB (Ventana, Strassbourg, France).

Nuclear counterstaining was done in all sections with hematoxyline. For every staining procedure sections were incubated without the primary antibody as negative controls. Tissues from colorectal cancer were used as positive controls for all three antibodies.

Evaluation

Semiquantitative analysis of the immunostainings for iNOS and COX-2 was performed for the whole tissue sections considering staining intensity and percentage of positive tumor cells. Using a light microscope (Aristoplan, Leitz, Wetzlar, Germany), in ten randomly selected tumor areas the amount of positive tumor cells and the amount of all tumor cells were determined using an ocular grid at 400×. A case without positive tumor cells was considered negative. A case with less than 10% positive tumor cells was scored 1, 10-50% was scored 2, 50-80% was scored 3 and more than 80% was scored 4. The staining intensity was divided in weak (I), moderate (II) and strong (III). An immunoreactive score was calculated by multiplication of staining intensity with the amount of positive cells (lowest end score 0, highest end score 12). This evaluation was performed according to Remmele[19]. Specimens with a grade of more than 1 were regarded as positive.

Intratumoral MVD was measured as previously described [18]. In brief, stained sections were screened at 50× magnification to identify the highest vascular area within the tumor. In these hot spots, individual microvessel count was evaluated at 200× magnification using an ocular grid. Every cluster of cells stained with CD34 was counted as a vessel. Branching structures were counted as single vessels. Vascular counts for each case were calculated.

Statistics

Statistical analysis was performed with the Statistical Program for Social Science (SPSS, Chicago, Ill., USA). The Pearson' s chi-square test and Fischer' s exact test were used to examine the association with the clinicopathological parameters. Nonparametric correlation with Spearman' s rho correlation coefficient was used to compare iNOS and COX-2 expressions as well as MVD. A P-value <0.05 was considered statistically significant.

RESULTS

INOS

Positive iNOS immunostaining was detected in 21 (52.5%) of all 40 cases of pancreatic carcinoma. Immunoreactive tumor cells were both diffusely and focally distributed throughout the tumor. The immunoreaction was seen in the cytoplasm with completely unstained nuclei (Figure 1). Nine cases (22.5%) showed a mild staining intensity (grade I), 8 cases (20%) a moderate staining intensity (grade II) and 4 cases (10%) a strong staining intensity (grade III). One case (2.5%) expressed iNOS only focally in less than 10% of tumor cells. Eight cases (20%) showed immunoreaction in 10- 50% of tumor cells, 11 cases (27.5%) in 50-80% of positive tumor cells. In one case (2.5%) more than 80% of tumor cells were stained (Table 1).

There was no correlation with tumor stage (P=0.971), histological grade (P=0.591), location within the pancreas (P=0.184), lymph node metastases (P=0.652), age (P=0.651) or sex (P=0.546) of the patients. A relationship between iNOS expression and distant metastases was seen, but the low amount of cases with distant metastases did not allow statistical evaluation.

In the surrounding tissue the islets of Langerhans showed positive reaction in several cells. The original acini were negative. In the negative controls, immunoreactivity was completely lacking while the positive controls displayed a clear cut immunopositivity.

COX-2

Positive COX-2 staining was seen in 15 out of the 41 (37.5%) pancreatic carcinomas. The immunoreactivity here was also focally distributed throughout the tumor with cytoplasmic reaction only. Nuclear staining was not observed (Figure 2). The staining intensity in the positive cases differed. Among them, 5 cases (12.5%) were slightly stained (grade I), 4 cases (10%) were moderately stained (grade II) and 6 cases (15%) were intensely stained (grade III). The amount of positive cells was as follows: 3 cases (7.5%) with less than 10% positive tumor cells, 7 cases (17.5%) with 10-50% positive tumor cells, 4 cases (10%) with 50-80% positive tumor cells and 1 case with more than 80% (2.5%) positive tumor cells (Table 1).

Table 1 Comparison between expression of iNOS and COX-2 and clinicopathological features in pancreatic adenocarcinomas (*n*=40)

Variables	No. of patients (%)	INOS positive	INOS negative	*P* value	COX-2 positive	COX-2 negative	*P* value
Tumor stage							
I	5 (12.5)	1	4	0.971	1	4	0.983
II	27 (67.5)	15	12		11	16	
III	7 (17.5)	4	3		3	4	
IV	1 (2.5)	1	0		0	1	
Nodal stage							
n=0	17 (42.5)	10	7	0.652	6	11	0.945
n=1	23 (57.5)	11	12		9	14	
Distant metastases							
M0	35 (87.5)	18	17	0.043	13	22	0.459
M1	5 (12.5)	3	2		2	3	
Grade							
G1	3 (7.5)	2	1	0.591	1	2	0.000
G2	15 (37.5)	10	5		6	9	
G3	22 (55)	9	13		8	14	
MVD		5.7 (+/-2.4)	6.4 (+/-2.9)		6.4 (+/-3)	5.8 (+/-2.4)	

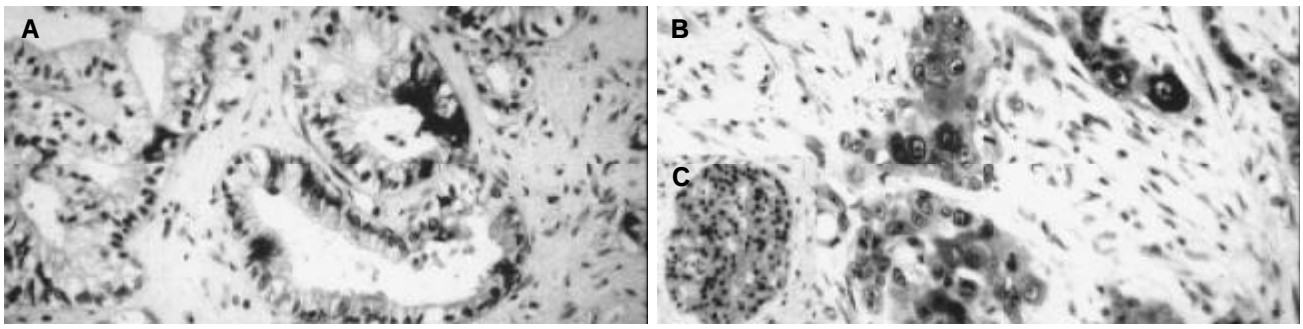

Figure 1 Immunohistochemical demonstration of iNOS expression in cases of pancreatic adenocarcinomas with moderate (A) and strong (B) staining intensity. There was a cytoplasmatic staining pattern with distribution within the tumor. No nuclear staining was observed. Cells of the islets of Langerhans were also positive (C). Original magnification ×200, Hematoxylin counterstaining.

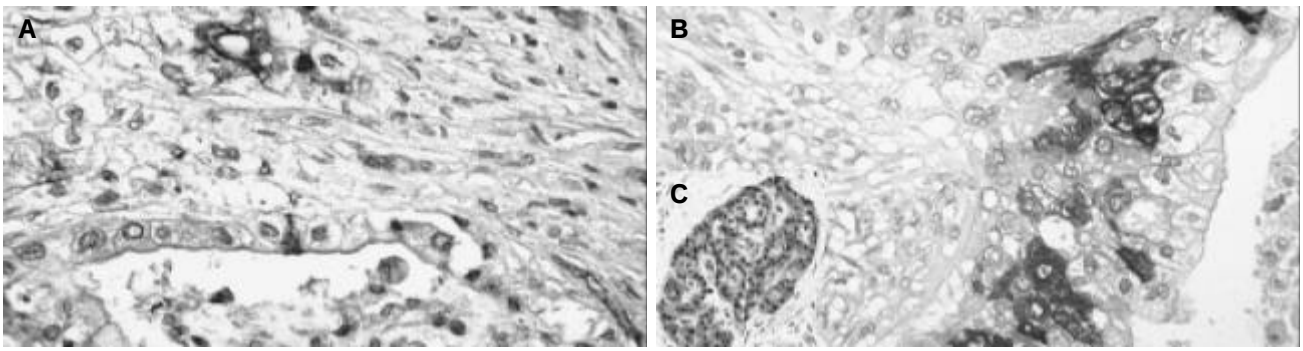

Figure 2 COX-2 immunohistochemistry in pancreatic adenocarcinomas shown in a case with (A) moderate and (B) strong staining intensity. Immunostaining was restricted to the cytoplasm. Even in the case with high staining only a portion of tumor cells expressed COX-2. Cells of the islets of Langerhans were also stained (C). Original magnification ×200, Hematoxylin counterstaining.

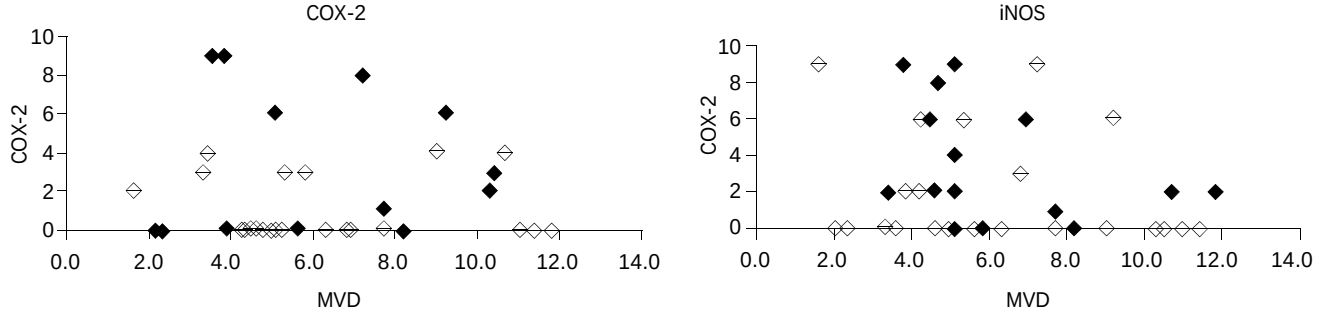

Figure 3 Comparison of iNOS or COX-2 expression with microvessel density. No statistically significant correlation could be noted.

Comparing the immunoreactive score of COX-2 expression with histological grade, a significant relationship could be seen. The more malignant tumors (grade 3) showed a higher COX-2 expression (P=0.000). This association depended stronger on the amount of positive cells (P=0.000). Considering staining intensity alone, no relationship was seen (P=0.118). The carcinomas in the head of the pancreas showed more often COX-2 expression than in other locations (P=0.006).

COX-2 did not correlate with tumor stage (P=0.983), lymph node (P=0.945) or distance metastases (P=0.459), age (P=0.369) or sex (P=0.331) of the patients.

In the surrounding tissue, the islets of Langerhans had positive reaction in several cells. The original acini were negative. In the negative control, immunoreactivity was completely lacking while the positive control displayed a clear cut immunopositivity.

MVD

The mean MVD in pancreatic carcinoma was 6.08 vessels per mm² (range 1.6 to 11.8 vessels per mm² , standard derivation of 2.67 vessels per mm² , median value of 5.25 vessels per mm²).

MVD analysis demonstrated a significant relationship to the age groups (younger or older than 60 years) with higher MVD in the older patients (P=0.024). The was no statistically significant trend regarding the histological grade with more malignant carcinomas (grade 3) having higher MVD (P=0.056).

MVD had no association with tumor stage (P=0.154), location within the pancreas (P=0.678), lymph node (P=0.325) or distance metastases (P=0.137) or sex (P=1.000) of the patients.

Correlation between iNOS, COX-2 and MVD

There was no statistically significant correlation between INOS and COX-2 expression in pancreatic adenocarcinomas (P=0.137, Figure 3). MVD did neither depend on iNOS expression (P=0.160) nor COX-2 expression (P=0.989). Considering only COX-2 positive cases, no correlation of COX-2 with MVD could be found (P=0.459). Also, considering iNOS positive cases alone, there was no relationship between iNOS expression and MVD (P=0.436) noticeable.

DISCUSSION

Folkman *et al*. suggested that the step from prevascular to vascular phase was the prerequisite for the growth and spread of many solid tumors[20]. Thus, angiogenesis contributes significantly to the progression of carcinomas. Intratumoral microvessel density is believed to reflect the overall degree of tumor angiogenesis. It has been accepted as an independent prognostic factor for several types of tumors like breast cancer, colon cancer or lung adenocarcinomas[21-23]. For pancreatic carcinoma, we could not find a correlation with parameters linked to survival[18].

Both COX-2 and iNOS, were play- markers of tumor angiogenesis[24]. Hypoxia induces iNOS together with erythropoietin, the molecule leading to erythropoesis and improvement of oxygen supply. COX-1 could regulate angiogenesis in endothelial cells, whereas COX-2 could regulate the production of nearly all angiogenetic factors in cancer cells[24].

We could show that iNOS was inconstantly expressed in pancreatic adenocarcinomas. This is in concordance with other studies[25,26]. INOS expression has been observed also in other carcinomas such as urothelial carcinomas[27], gynecological cancers[28], breast carcinomas[29], colon cancers[14], and lung tumors[30].

The role of iNOS in cancerogenesis is still not clear. NO, the product of NOS, has several properties in addition to angiogenesis, which might enhance tumor growth. NO has been found to be a mediator of angiogenesis and blood flow[31]. Also, high concentrations of NO could lead to apoptosis, low concentrations might protect many cells from cell death[32-34]. It could be shown that NO induces a G1-arrest followed by apoptosis in pancreatic carcinoma cell lines[35].

Multiple lines of evidence suggest that COX-2 is important in carcinogenesis. For example, COX-2 was upregulated in various forms of cancers[36]. A null mutation for COX-2 caused marked reduction in intestinal polyposis in a murine model of familial adenomatous polyposis[37]. Newly developed selective inhibitors of COX-2 were reported to protect against gastrointestinal tumor formation.

We found COX-2 expression in 15 out of 40 cancer cases. This is slightly lower than that reported in the literature, which was up to 74% by using different methods including Northern and Western blot as well as immunohistochemistry[38-40]. Okami reported a weak staining in most of the investigated carcinoma specimens[41]. COX-2 staining in pancreatic carcinoma was very heterogeneous and there were great variations between specimens.

For pancreatic carcinoma, Koshiba *et al*. suggested that COX-2 might be associated with the degree of malignancy comparing intraductal papillary mucinous adenomas, intraductal papillary carcinomas and intraductal carcinomas[42]. We and others could show that in the group of carcinomas the expression of COX-2 depended on the histological grading, and higher malignant tumors showed more enhanced COX-2 expression. A dependence of histological grade was also described by Niijima[43]. With a higher expression in more malignant tumors COX-2 seems to be a late or bystander effect. In our cohort, we could not prove a positive or negative correlation of COX-2 expression with MVD.

In chronic pancreatitis COX-2 overexpression was also recently observed[44]. The enzyme was found in atrophic acinar cells, hyperplastic ductal cells and islets cells. As chronic pancreatitis is a risk factor for pancreatic cancer, this opens whether COX-2 is involved in the tumorigenesis via chronic inflammation. Apart from positive islets cells, we could not see any COX-2 expression in normal tissues, especially in the surrounding tissue of the tumor. If COX-2 is constantly expressed in chronic inflammation of pancreas one would expect enzyme induction also in the inflamed peritumoral region. Other reports mentioning the nonneoplastic tissue also found no COX-2 expression. It seems therefore unlikely that this enzyme is involved in early tumor development via inflammation.

In summary, approximately half of pancreatic adenocarcinomas express iNOS and COX-2. Both enzymes are heterogeneously distributed in the tumors without any correlation to each other nor to MVD. COX-2 is a phenomenon of higher malignant tumors. Both enzymes do not appear to be a key step in the angiogenesis of pancreatic adenocarcinomas.

ACKNOWLEDGMENTS

The excellent technical assistance by K. Petmecki, the help in editing the manuscript by Y. A. Weidemann and the statistical support by H. Christ are gratefully acknowledged.

REFERENCES

1 **Devesa SS,** Blot WJ, Stone BJ, Miller BA, Tarone RE, Fraumeni JF Jr**.** Recent cancer trends in the united states. *J Natl Cancer Inst* 1995; **87**: 175-182

2 **Bundesamt S**. Statistical year book for the Federal Republic of Germany. *Metzler Poeschel Stuttgart* 1996: 430-433

3 **Yeo TP,** Hruban RH, Leach SD, Wilentz RE, Sohn TA, Kern SE, Iacobuzio-Donahue CA, Maitra A, Goggins M, Canto MI, Abrams RA, Laheru D, Jaffee EM, Hidalgo M, Yeo CJ. Pancreatic cancer.

Curr Probl Cancer 2002; **26**: 176-275
4 **Yeo CJ,** Abrams RA, Grochow LB, Sohn TA, Ord SE, Hruban RH, Zahurak ML, Dooley WC, Coleman J, Sauter PK, Pitt HA, Lillemoe KD, Cameron JL. Pancreaticoduodenectomy for pancreatic adenocarcinoma: Postoperative adjuvant chemoradiation improves survival. A prospective, single-institution experience. *Ann Surg* 1997; **225**: 621-633
5 **Bardeesy N,** DePinho RA. Pancreatic cancer biology and genetics. *Nat Rev Cancer* 2002; **2**: 897-909
6 **Sohn TA**. The molecular genetics of pancreatic ductal carcinoma. *Minerva Chir* 2002; **57**: 561-574
7 **Farrow B,** Evers BM. Inflammation and the development of pancreatic cancer. *Surg Oncol* 2002; **10**: 153-169
8 **Hall Pde L,** Wilentz RE, de Klerk W, Bornman PP. Premalignant conditions of the pancreas. *Pathology* 2002; **34**: 504-517
9 **Knowles RG,** Moncada S. Nitric oxide synthases in mammals. *Biochem J* 1994; **298**(Pt2): 249-258
10 **Moncada S,** Higgs A. The l-arginine-nitric oxide pathway. *N Engl J Med* 1993; **329**: 2002-2012
11 **Forstermann U,** Kleinert H. Nitric oxide synthase: expression and expressional control of the three isoforms. *Naunyn Schmiedebergs Arch Pharmacol* 1995; **352**: 351-364
12 **Kroncke KD,** Fehsel K, Kolb-Bachofen V. Nitric oxide: cytotoxicity versus cytoprotection–how, why, when, and where? *Nitric Oxide* 1997; **1:** 107-120
13 **Ambs S,** Ogunfusika MO, Merriam WG, Bennett WP, Billiar TR, Harris CC. Up-regulation of inducible nitric oxide synthase expression in cancer-prone p53 knockout mice. *Proc Natl Acad Sci U S A* 1998; **95**: 8823-8828
14 **Ambs S,** Merriam WG, Bennett WP, Felley-Bosco E, Ogunfusika MO, Oser SM, Klein S, Shields PG, Billiar TR, Harris CC. Frequent nitric oxide synthase-2 expression in human colon adenomas: implication for tumor angiogenesis and colon cancer progression. *Cancer Res* 1998; **58**: 334-341
15 **Williams CS,** Mann M, DuBois RN. The role of cyclooxygenases in inflammation, cancer, and developme. *Oncogene* 1999; **18**: 7908-7916
16 **Smith WL,** Garavito RM, DeWitt DL. Prostaglandin endoperoxide H synthases (cyclooxygenases)-1 and -2. *J Biol Chem* 1996; **271**: 33157-33160
17 **Lin DT,** Subbaramaiah K, Shah JP, Dannenberg AJ, Boyle JO. Cyclooxygenase-2: a novel molecular target for the prevention and treatment of head and neck cancer. *Head Neck* 2002; **24**: 792-799
18 **Kasper HU,** Ebert M, Malfertheiner P, Roessner A, Kirkpatrick CJ, Wolf HK. Expression of thrombospondin-1 in pancreatic carcinoma: correlation with microvessel density. *Virchows Arch* 2001; **438**: 116-120
19 **Remmele W,** Stegner HE. Recommendation for uniform definition of an immunoreactive score (IRS) for immunohistochemical estrogen receptor detection (ER-ICA) in breast cancer tissue. *Pathologe* 1987; **8**: 138-140
20 **Folkman J**. What is the evidence that tumors are angiogenesis dependent? *J Natl Cancer Inst* 1990; **82**: 4-6
21 **Tarta C,** Teixeira CR, Tanaka S, Haruma K, Chiele-Neto C, da Silva VD. Angiogenesis in advanced colorectal adenocarcinoma with special reference to tumoral invasion. *Arq Gastroenterol* 2002; **39**: 32-38
22 **Sauer G,** Deissler H. Angiogenesis: prognostic and therapeutic implications in gynecologic and breast malignancies. *Curr Opin Obstet Gynecol* 2003; **15**: 45-49
23 **Meert AP,** Paesmans M, Martin B, Delmotte P, Berghmans T, Verdebout JM, Lafitte JJ, Mascaux C, Sculier JP. The role of microvessel density on the survival of patients with lung cancer: a systematic review of the literature with meta-analysis. *Br J Cancer* 2002; **87**: 694-701
24 **Chiarugi V,** Magnelli L, Gallo O. Cox-2, iNOS and p53 as playmakers of tumor angiogenesis (review). *Int J Mol Med* 1998; **2**: 715-719
25 **Kong G,** Kim E, Kim W, Lee Y, Lee J, Paik S, Rhee J, Choi K, Lee K. Inducible nitric oxide synthase (iNOS) immunoreactivity and its relationship to cell proliferation, apoptosis, angiogenesis, clinicopathologic characteristics, and patient survival in pancreatic cancer. *Int J Gastrointest Cancer* 2001; **29**: 133-140
26 **Kong G,** Kim EK, Kim WS, Lee KT, Lee YW, Lee JK, Paik SW, Rhee JC. Role of cyclooxygenase-2 and inducible nitric oxide synthase in pancreatic cancer. *J Gastroenterol Hepatol* 2002; **17**: 914-921
27 **Wolf H,** Haeckel C, Roessner A. Inducible nitric oxide synthase expression in human urinary bladder cancer. *Virchows Arch* 2000; **437**: 662-666
28 **Thomsen LL,** Lawton FG, Knowles RG, Beesley JE, Riveros-Moreno V, Moncada S. Nitric oxide synthase activity in human gynecological cancer. *Cancer Res* 1994; **54**: 1352-1354
29 **De Paepe B,** Verstraeten VM, De Potter CR, Bullock GR. Increased angiotensin II type-2 receptor density in hyperplasia, DCIS and invasive carcinoma of the breast is paralleled with increased iNOS expression. *Histochem Cell Biol* 2002; **117**: 13-19
30 **Ambs S,** Bennett WP, Merriam WG, Ogunfusika MO, Oser SM, Khan MA, Jones RT, Harris CC. Vascular endothelial growth factor and nitric oxide synthase expression in human lung cancer and the relation to p53. *Br J Cancer* 1998; **78**: 233-239
31 **Jenkins DC,** Charles IG, Thomsen LL, Moss DW, Holmes LS, Baylis SA, Rhodes P, Westmore K, Emson PC, Moncada S. Roles of nitric oxide in tumor growth. *Proc Natl Acad Sci U S A* 1995; **92**: 4392-4396
32 **Nicotera P,** Ankarcrona M, Bonfoco E, Orrenius S, Lipton SA. Neuronal necrosis and apoptosis: two distinct events induced by exposure to glutamate or oxidative stress. *Adv Neurol* 1997; **72**: 95-101
33 **Dimmeler S,** Rippmann V, Weiland U, Haendeler J, Zeiher AM. Angiotensin II induces apoptosis of human endothelial cells. Protective effect of nitric oxide. *Circ Res* 1997; **81**: 970-976
34 **Tzeng E,** Kim YM, Pitt BR, Lizonova A, Kovesdi I, Billiar TR. Adenoviral transfer of the inducible nitric oxide synthase gene blocks endothelial cell apoptosis. *Surgery* 1997; **122**: 255-263
35 **Gansauge S,** Nussler AK, Beger HG, Gansauge F. Nitric oxide-induced apoptosis in human pancreatic carcinoma cell lines is associated with a G1-arrest and an increase of the cyclin-dependent kinase inhibitor p21WAF1/CIP1. *Cell Growth Differ* 1998; **9**: 611-617
36 **Ricchi P,** Zarrilli R, Di Palma A, Acquaviva AM. Nonsteroidal anti-inflammatory drugs in colorectal cancer: from prevention to therapy. *Br J Cancer* 2003; **88**: 803-807
37 **Oshima M**, Dinchuk JE, Kargman SL, Oshima H, Hancock B, Kwong E, Trzaskos JM, Evans JF, Taketo MM. Suppression of intestinal polyposis in Apc delta716 knockout mice by inhibition of cyclooxygenase 2 (COX-2). *Cell* 1996; **87**: 803-809
38 **Molina MA,** Sitja-Arnau M, Lemoine MG, Frazier ML, Sinicrope FA. Increased cyclooxygenase-2 expression in human pancreatic carcinomas and cell lines: growth inhibition by nonsteroidal anti-inflammatory drugs. *Cancer Res* 1999; **59**: 4356-4362
39 **Yip-Schneider MT,** Barnard DS, Billings SD, Cheng L, Heilman DK, Lin A, Marshall SJ, Crowell PL, Marshall MS, Sweeney CJ. Cyclooxygenase-2 expression in human pancreatic adenocarcinomas. *Carcinogenesis* 2000; **21**: 139-146
40 **Kokawa A,** Kondo H, Gotoda T, Ono H, Saito D, Nakadaira S, Kosuge T, Yoshida S. Increased expression of cyclooxygenase-2 in human pancreatic neoplasms and potential for chemoprevention by cyclooxygenase inhibitors. *Cancer* 2001; **91**: 333-338
41 **Okami J,** Yamamoto H, Fujiwara Y, Tsujie M, Kondo M, Noura S, Oshima S, Nagano H, Dono K, Umeshita K, Ishikawa O, Sakon M, Matsuura N, Nakamori S, Monden M. Overexpression of cyclooxygenase-2 in carcinoma of the pancreas. *Clin Cancer Res* 1999; **5**: 2018-2024
42 **Koshiba T,** Hosotani R, Miyamoto Y, Wada M, Lee JU, Fujimoto K, Tsuji S, Nakajima S, Doi R, Imamura M. Immunohistochemical analysis of cyclooxygenase-2 expression in pancreatic tumors. *Int J Pancreatol* 1999; **26**: 69-76
43 **Niijima M,** Yamaguchi T, Ishihara T, Hara T, Kato K, Kondo F, Saisho H. Immunohistochemical analysis and in situ hybridization of cyclooxygenase-2 expression in intraductal papillary-mucinous tumors of the pancreas. *Cancer* 2002; **94**: 1565-1573
44 **Schlosser W,** Schlosser S, Ramadani M, Gansauge F, Gansauge S, Beger HG. Cyclooxygenase-2 is overexpressed in chronic pancreatitis. *Pancreas* 2002; **25**: 26-30

Edited by Wang XL **Proofread by** Xu FM

PO Box 2345, Beijing 100023, China
Fax: +86-10-85381893
E-mail: wjg@wjgnet.com www.wjgnet.com

World J Gastroenterol 2004;10(13):1923-1927
World Journal of Gastroenterology
 ISSN 1007-9327

• BASIC RESEARCH •

Increased hepatic expression of nitric oxide synthase type II in cirrhotic rats

Hai Wang, Xiao-Ping Chen, Fa-Zu Qiu

Hai Wang, Xiao-Ping Chen, Fa-Zu Qiu, Liver Center of Tongji Hospital, Tongji Medical College, Huazhong University of Science and Technology, Wuhan 430030, Hubei Province, China
Supported by the Clinical Focal Point Subject Foundation of Ministry of Public Health, No. (2001)321
Correspondence to: Dr. Xiao-Ping Chen, Hepatic Surgery Center of Tongji Hospital, Tongji Medical College, Huazhong University of Science and Technology, Wuhan 430030, Hubei Province, China. chenxp53@sina.com
Telephone: +86-27-83662599 **Fax:** +86-27-83662851
Received: 2002-10-09 **Accepted:** 2002-12-30

Abstract

AIM: To determine the role and effect of nitric oxide synthase type II (NOSII) in cirrhotic rats.

METHODS: Expression of NOSII mRNA was detected by real time RT-PCR. The activity of nitric oxide synthase and serum levels of NO, systemic and portal hemodynamics and degrees of cirrhosis were measured with high sensitive methods. Chinese traditional medicine tetrandrine was used to treat cirrhotic rats and to evaluate the function of NO. Double-blind method was applied during the experiment.

RESULTS: The concentration of NO and the activity of NOS were increased markedly at all stages of cirrhosis, and iNOSmRNA was greatly expressed. Meanwhile the portal-venous-pressure (PVP), and portal-venous-flow (PVF) were significantly increased. NO, NOS and iNOSmRNA were positively correlated to the quantity of hepatic fibrosis. Tetrandrine significantly inhibited NO production and the expression of iNOSmRNA.

CONCLUSION: Increased hepatic expression of NOSII is one of the important causes of hepatic cirrhosis and portal hypertension.

Wang H, Chen XP, Qiu FZ. Increased hepatic expression of nitric oxide synthase type II in cirrhotic rats. *World J Gastroenterol* 2004; 10(13): 1923-1927
http://www.wjgnet.com/1007-9327/10/1923.asp

INTRODUCTION

Nitric oxide (NO) is a vasodilator formerly detected in vascular system, but is currently recognized as a multifunctional molecule widely distributed in many other tissues, such as immune and neuronal systems. NO is synthesized from L-arginine by the NO synthase isozyme family of which three different members have been characterized, namely NOSI, NOSII and NOSIII. NOSI and NOSIII are constitutive and Ca^{2+}/calmodulin-independent. The first was initially discovered in neurons and the second in endothelial cells[1-2]. NOSII is Ca^{2+}-independent, and is located in macrophages and smooth muscle cells, and is induced by appropriate proinflammatory stimuli and bacterial lipolysaccharides[3]. Its activity can be competitively inhibited by several L-arginine analogues such as N^w-nitro-L-arginine.

However, proinflammatory cytokines, endotoxins, and bacterial infections in various pathologic entities are associated with enhanced production of NO, hyporesponsiveness to vasoconstrictors, and development of a hyperdynamic state[4-7]. Vallance and Moncada hypothesized that bacterial endotoxin might account for hemodynamic changes in severe cirrhosis by stimulating the expression of inducible NO synthase (iNOS) to produce NO[8].

Recently, numerous studies have focused on NO as a possible major causative agent of the decreased vascular resistance in cirrhosis. In fact, most investigations are coincident in reporting an increased NO activity in the vasculature of patients and rats with cirrhosis[9-12], a phenomenon in which both NOSII and NOSIII seem to be involved[13]. There is, however, little information on the progress in liver diseases affecting the L-arginine/NO pathway in organs other than the systemic vasculature. This is particularly intriguing in the liver, as it largely affects the consequence of the derangement under pathologic conditions. Whereas most investigations consider NO as an important mediator of hemodynamic alterations in experimental cirrhosis[14].

Chinese traditional medicine tetrandrine has the function of inhibiting calcium influx[15,16], and effect in treatment of liver fibrosis[17]. We postulated that if NO was a key mediator in cirrhosis and portal hypertension, Tetrandrine would affect the level of NO by inhibiting the expression of NOSmRNA and the activity of NOS. Therefore, in this study, mRNAs of NOSII and NOSIII were determined in liver tissue of rats with CCL_4-induced cirrhosis to assess the level of NO. In addition, the NOS activity of liver tissue and the serum levels of NO, hemodynamic changes of portal vein and pathologic changes at all stages of cirrhosis were also investigated.

MATERIALS AND METHODS

Induction of cirrhosis in rats

Hepatic injury and fibrosis were induced in male retired breeder Sprague-Dawley rats (450-550 g) by intragastric administration of carbon tetrachloride as described previously[18]. CCL_4(1.0 mL/kg) in a 1:1 mixture with corn oil was administered by gavage at 7-day intervals. After the second intragastric administration of carbon tetrachloride, Tetrandrine group inhaled the suspension of Tetrandrine (1 mL/0.1 kg). Animal weight was monitored, and the dosage of CCL_4 and Tetrandrine was adjusted accordingly. Portal hypertension (portal venous dilation with portal pressure >10 cm H_2O) was documented in all animals after 10 doses of CCL_4. Controls received corn oil on the same schedule as experimental animals.

In vivo effects of tetrandrine administration

There were 90 conscious rats in this study. Animals were anesthetized with ketamine (100 mg/kg.bm) and prepared with P-50 catheters in portal vein and inferior vena cava. The catheter was connected to a highly sensitive transducer and a multichannel recorder (MX4P and MT4, Lectromed Ltd, Jersey, Chanels Islands, UK) and portal venous pressure and portal venous

flow were recorded. Then, a 2-mL blood sample was taken to measure NO. Blood was immediately centrifuged at 4 ℃ and serum was frozen at -20 ℃ until further analysis. Tissue specimens were obtained from the middle liver lobe in each animal. Liver specimens were fixed in 40 g/L buffered formaldehyde and stained with hematoxylin and eosin, reticulin, and Masson's trichrome for histological examination. Moreover, additional liver tissues were immediately frozen in dry ice and stored in liquid nitrogen until further analysis. Serum NO and liver NOS activity were determined.

Expression of inducible and consititutive NOS mRNA

mRNAs of NOSII and NOSIII were assessed in liver tissues of all groups. Under anesthesia with ketamine (100 mg/kg) animals were exanguinated by cardiac puncture. Liver tissue was dissected, placed in a Petri dish containing a diethyl pyrocarbonate (0.01%)-treated PBS buffer solution, total RNA was extracted by the guanidine isothiocyanate method[19].

NOSII and NOSIII mRNA expression was assessed by real-Time RT-PCR

Reverse transcription (RT) reaction was performed with cDNA synthesis kit (Promega, Madison, WI) and followed the attached protocol with reaction kit. The final volume of the reaction (20 μL) was completed with RNase free water. First strand cDNA synthesis was carried out at 42 ℃ for 30 min in a DNA thermal cycler (PTC-100, MJ Reserch Inc, Watertown, MA). Afterwards, the tubes were incubated at 99 ℃ for 5 min to terminate the reaction. Then each tube was kept at 4 ℃ until PCR was performed.

Real-time RT-PCR

Expression of the target genes (NOSII and NOSIII) was quantified. The primers were designed using the software Primer Express (Applied Biosystems) (Table 1).

RT- PCR was performed according to a TaqMan 2-step method using an ABI PRISM 7 700 sequence detection system (Applied Biosystems). PCR cycling conditions included an initial phase at 50 ℃ for 2 min, followed by at 95 ℃ for 10 min for AmpErase, 40 cycles at 95 ℃ for 15 s, and at 60 ℃ for 1 min. Quantification of the PCR products was based on the TaqMan 5' nuclease assay using the ABI PRISM 7 700 sequence detection system. The starting amount of a specific mRNA in an unknown sample was determined. The standard curve was generated on the basis of the linear relationship between the Ct value and logarithm of the starting quantity. Ct value was the cycle number at which a significant increase in the fluorescence signal was initially detected. The unknown samples were quantified by the software of the ABI PRISM 7 700 sequence detector system, which calculated the Ct value for each sample and then determined the initial amount of the target using the standard curve. The amount of the target was normalized to the reference.

Statistical analysis

One-way ANOVA, Newman-Keuls's, and unpaired Student's *t* tests were used for statistical analysis. Data are expressed as mean±SE, *P* level at 0.05 or less was considered statistically significant.

RESULTS

The cirrhotic liver treated with CCL_4 had a finely granulated surface. Histological examination showed the distinct features of three-grade fibrosis. Tetrandrine group had slight fibrosis in the third grade of cirrhosis.

Pathologic examination

Pathologic examination indicated that tetrandrine had an obvious effect on preventing the necrosis of hepatic cells and delaying the development of hepatic fibrosis (Figure 1).

Serum NO and NOS activity of liver tissue

Serum NO and NOS activity in cirrhotic group were significantly higher than those in normal control, and had no difference between the normal and therapeutic groups (Tables 2, 3).

Table 2 Effects of tetrandrine and on serum NO in cirrhotic rats (μmol/L, mean±SD)

Grade	Tetrandrine (*n*=8)	Cirrhosis (*n*=8)	Negative control (*n*=8)
Earlier period	6.51±0.56[b]	10.27±0.71	5.91±0.67
Metaphase	6.87±0.78[b]	10.88±0.82	6.04±0.98
Late period	6.49±0.83[b]	6.35±1.48[b]	6.17±0.73

[b]*P*<0.01 *vs* cirrhosis.

Table 3 Effects of Tetrandrine on NOS activity in cirrhotic rats (mol/min· g, mean±SD)

Grade	Tetrandrine (*n*=8)	Cirrhosis (*n*=8)	Negative control (*n*=8)
Earlier period	0.5165±1455[a]	1.6916±0.8099	0.4275±0.2037
Metaphase	0.6901±0.2092[a]	1.9756±0.7833	0.5639±0.4275
Late period	0.8483±0.2393[a]	1.9789±0.7690	0.6723±0.5784

[a]*P*<0.05 *vs* cirrhosis.

Hemodynamics

High hemodynamics was observed in cirrhotic rats. Portal-venous-pressure (PVP) and portal-venous-flow (PVF) were significantly increased. But PVP in tetrandrine groups was significantly decreased in all stages of cirrhosis. PVF was only decreased in the metaphase of cirrhosis (Table 4).

Table 1 Oligonucleotides used for PCR

Gene	Quantification method	Primer sequence	cDNA
NOSII	Forward primer	5'-CCCTTCCGAAGTTTCTGGCAGCAG-3'	2 793-2 817
	Reverse primer	5'-GGGCTCCTCCAAGGTGTTGCCC-3'	3 424-3 446
	Probe	5'-(FAM)TCTTCGGTGCGGTCTTTTCCTATGGAGCAA(TAMRA)-3'	3 391-3 421
NOSIII	Forward primer	5'-CAAGACCGATTACACGACAT-3'	31-51
	Reverse primer	5'-GCTGGTTGCCATAGTGACAT-3'	300-321
	Probe	5'-(FAM)GAGTGTTTGGACAAGTCCTCACCGCCTTTT-(TAMRA)-3'	158-188
GAPDH	Forward primer	5'-GAAGGTGAAGGTCGGAGTCA-3'	
	Reverse primer	5'-GAAGATGGTGATGGGA-3'	
	Probe	5'-(JOE)CAAGCTTCCCGTTCTCAGCC(TAMRA)-3'	

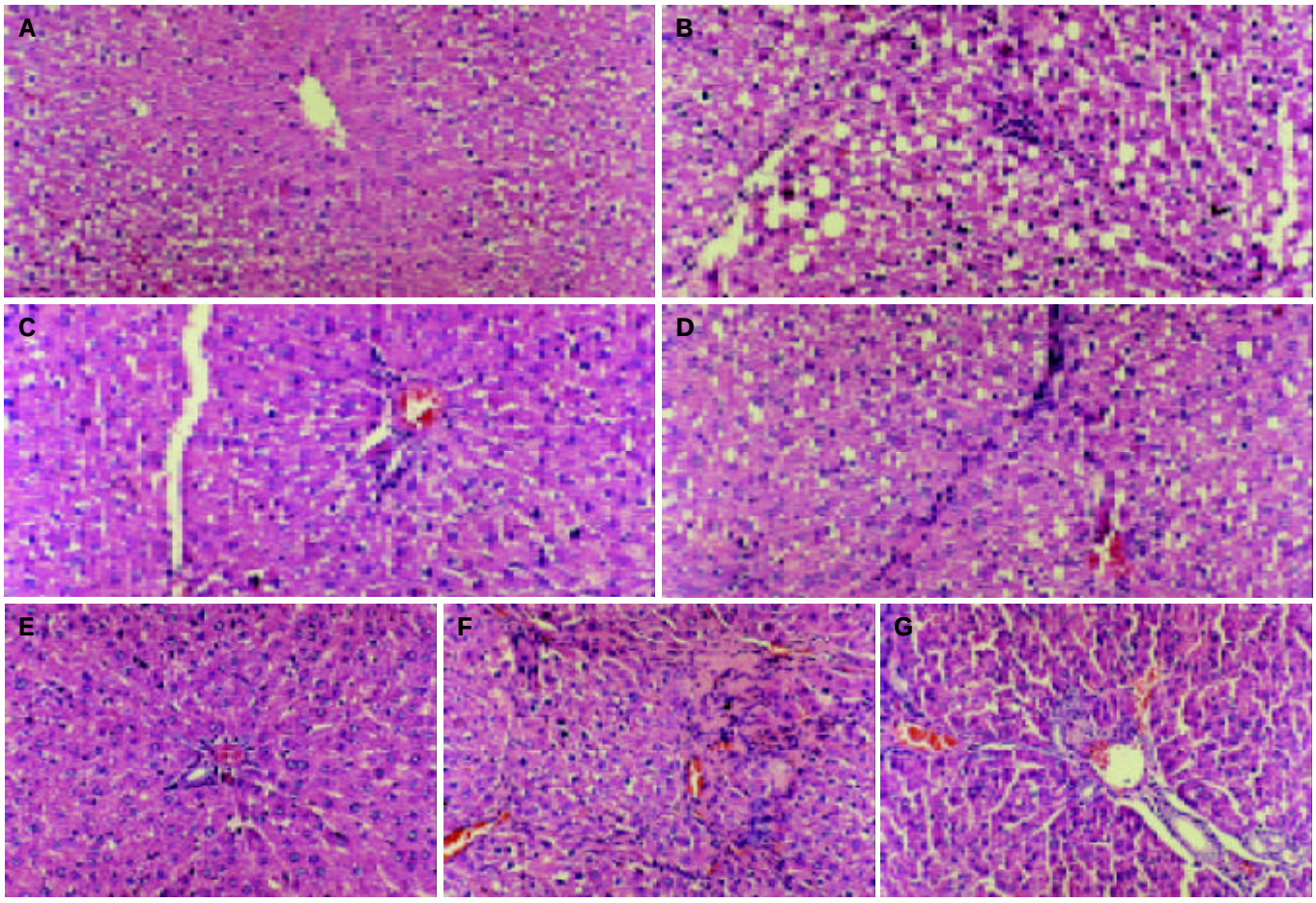

Figure 1 Histological images of three-grade fibrosis and tetrandrine treated group (200×). A: normal group, B: earlier cirrhosis group, C: earlier tetrandrine group, D: metaphase cirrhosis group, E: metaphase tetrandrine group, F: late cirrhosis group, G: late tetrandrine group.

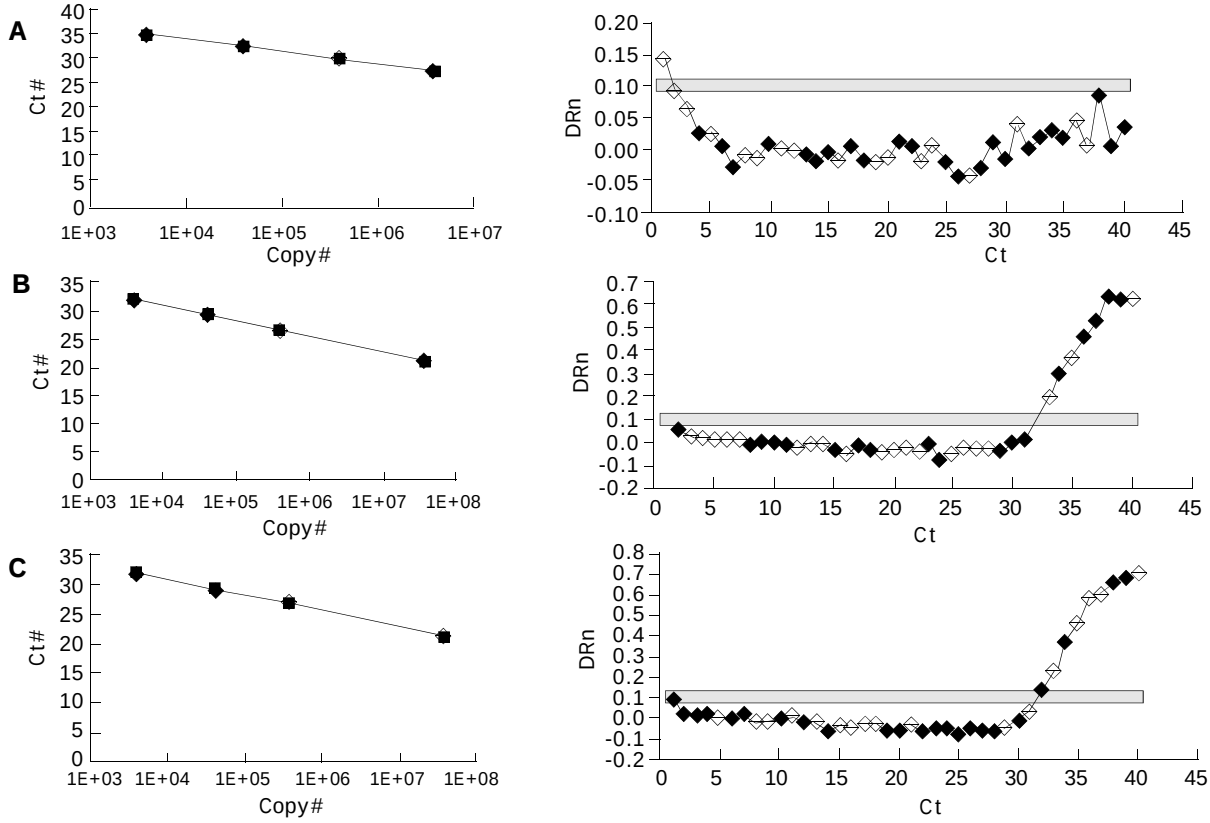

Figure 2 Real-time RT-PCR images: Expression of iNOS in normal hepatic tissue (A), Expression of iNOS in Tetrandrine therapeutic hepatic tissue (B), Expression of iNOS in cirrhotic tissue (C). NOSII was not expressed in normal rat tissue, but highly expressed in cirrhotic rat tissue and NOSII in therapeutic groups was significantly decreased than that in cirrhosis.

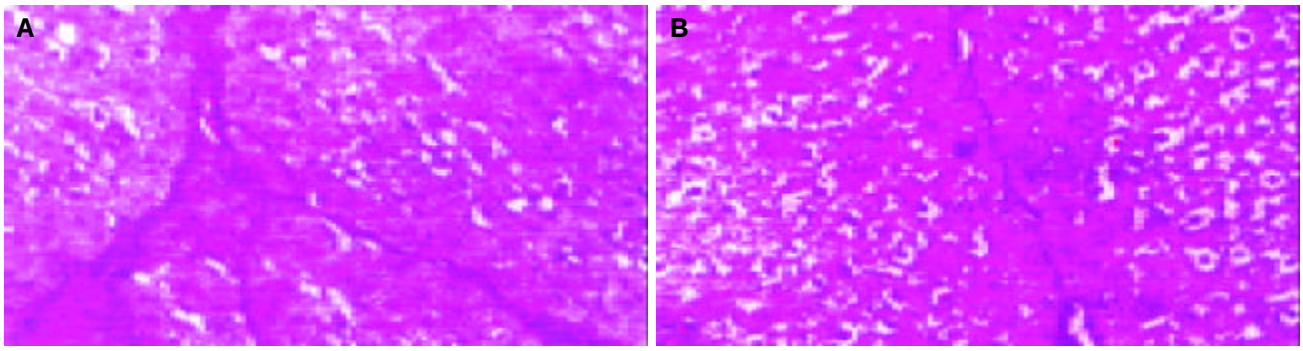

Figure 3 Quantification of cirrhosis: cirrhotic group (A), Tetrandrine group (B).

Table 4 Effects of tetrandrine on hemodynamics in cirrhotic rats (mean±SD)

Stage	Index	Tetrandrine (*n*=8)	Cirrhosis (*n*=8)	Negative control (*n*=8)
Earlier period	PVF	18.37±1.83	21.25±1.76	16.50±1.73
	PVP	1.35±0.25[b]	1.67±0.21	1.18±0.13
	ICVP	0.31±0.04	0.32±0.04	0.31±0.04
	PVR	5.73±0.88	6.38±1.12	5.81±1.04
Metaphase	PVF	14.50±1.61[a]	20.35±1.07	17.75±1.37
	PVP	1.44±0.13[b]	1.72±0.69	1.30±0.21
	ICVP	0.32±0.04	0.31±0.04	0.32±0.04
	PVR	7.98±1.68	9.56±1.29	5.53±0.67
Late period	PVF	15.85±1.23	17.57±1.93	15.42±1.27
	PVP	1.45±0.24[b]	1.67±0.23	1.37±0.10
	ICVP	0.31±0.04	0.32±0.04	0.32±0.04
	PVR	7.44±1.08	8.01±0.79	6.76±0.34

[a]$P<0.05$, [b]$P<0.01$ *vs* cirrhosis.

Relationship between NO and hemodynamics

NO concentration correlated significantly with PVP (r=0.69, $P<0.01$) and PVF (r=0.72, $P<0.01$), but inversely with PVR (r=-0.63, $P<0.01$).

Quantitative RT-PCR

Quantification of the PCR products showed that NOSII was highly expressed in cirrhotic rat tissue (Figure 2C), and NOSII in therapeutic groups was significantly decreased than cirrhosis (Figure 2B) ($P<0.01$). NOSII was not found in normal rat tissue (Figure 2A). NOSIII expression was not different among all groups ($P>0.05$) (Table 5).

Table 5 Quantification of PCR products

Stage	Index	Tetrandrine (*n*=8)	Cirrhosis (*n*=8)	Negative control (*n*=8)
Earlier period	NOSII	0.1723±0.0014	0.5635±0.0104	-
	NOSIII	0.2578±0.0076	0.2694±0.0043	0.2786±0.0107
Metaphase	NOSII	0.1679±0.0093	0.7521±0.0098	-
	NOSIII	0.3210±0.0084	0.3412±0.0113	0.2916±0.0089
Late period	NOSII	0.1876±0.0065	0.6987±0.0078	-
	NOSIII	0.2917±0.0102	0.3002±0.0091	0.2815±0.0098

Quantification of cirrhosis

Quantification of cirrhosis showed that cirrhosis significantly decreased in Tetrandrine group than in cirrhotic group (Figure 3).

DISCUSSION

The function of NO in human beings or experimental animals is invariably associated with marked systemic and portal venous hemodynamic effects, including arterial hypotension, portal hypertension, increased portal venous perfusion. The intensity and full manifestation of this response depend on the expression of NOS and the NOS activity. To ascertain which isoforms of NOS displayed a differential effect on cirrhotic liver of rats, the expressions of NOSII and NOSIII were determined. The study showed that NOSII was markedly increased in cirrhotic rat liver tissues. However, we did not find the expression of NOSII in normal liver tissues. Because macrophages were of central importance in the initiation and regulation of nonspecific and specific immune responses[20], it was considered that NO from these cells was implicated in the nonspecific defense against parasitic diseases and participated in the production of free radicals that are toxic to bacteria and parasites[21]. Rodent macrophages were extremely sensitive to agents promoting NOSII expression[22]. In this study, no difference in NOSIII expression between cirrhotic and normal rats was found. We postulated that NOSIII expression in cirrhotic liver had no effect on portal hypertension. But it might have a great function in cirrhosis due to its expression in big blood vessels[23-25]. Intrahepatic endothelial NO mediated by shear stress-dependence seems impaired by shunt.

Chinese traditional medicine Tetrandrine had a good therapeutic effect for fibrosis[16,17]. It is often used to treat hepatitis of HBV. In a recent study, it was tested to inhibit calcium influx. We therefore postulated that if NO played a role in the mechanism of cirrhosis and portal hypertension, Tetrandrine would have the effect on the inhibition of NO production. This study approved our hypothesis and showed NOSII mRNA was markedly expressed in cirrhotic liver tissues. NOSIII was mainly distributed in endothelial cells and its function was relied on calmodulin(CaM)[26]. Tetrandrine affected NOSIII expression, however, had no effect on NOSIII expression. Thus, we reason the changes of NOSIII could be stimulated by shear stress. NOSII was mainly distributed in microphages and endothelial cells. NOSII did not express in normal physiological conditions. Amino acid sequence analysis showed that NOSII had the conjugated site of calmodulin, and rodent NOSII could be conjugated tightly with CaM without calcium[27]. In this study, an important finding in cirrhotic liver exposed to Tetrandrine was an NO antagonist. Moreover, tetrandrine could also affect NOS enzymatic activity. The results of the present study indicated that portal-venous-pressure and portal-venous-flow decreased by tetrandrine were mediated by lower level NO and cirrhotic blood vessel.

In conclusion, NOSII is markedly expressed in cirrhotic liver, inducing a high hemodynamic change of portal vein and pathologic changes in all stages of cirrhosis. Tetrandrine inhibits NOSII expression, decreases NOS activity and reduces the NO production. The mechanism of fibrosis and portal hypertension is NO mediated, and tetrandrine is effective for improving portal hypertension by reducing NO in cirrhotic patients.

ACKNOWLEDGMENTS

The authors are acknowledged the skillful technical assistance of Dr. Bing-Quan Wu.

REFERENCES

1 **Bredt DS**, Hwang PM, Glatt CE, Lowenstein C, Reed RR, Snyder SH. Cloned and expressed nitric oxide synthase structurally resembles cytochrome P-450 reductase. *Nature* 1991; **351**: 714-718
2 **Lamas S**, Marsden PA, Li GK, Tempst P, Michel T. Endothelial nitric oxide synthase: molecular cloning and characterization of a distinct constitutive enzyme isoform. *Proc Natl Acad Sci U S A* 1992; **89**: 6348-6352
3 **Lowenstein CJ**, Glatt CS, Bredt DS, Snyder SH. Cloned and expressed macrophage nitric oxide synthase contrasts with the brian enzyme. *Proc Natl Acad Sci U S A* 1992; **89**: 6711-6715
4 **Guarner C,** Soriano G, Tomas A, Bulbena O, Novella MT, Balanzo J, Vilardell F, Mourelle M, Moncada S. Increased serum nitrite and nitrate levels in patients with cirrhosis: relationship to endotoxemia. *Hepatology* 1993; **18**: 1139-1143
5 **Lee FY**, Wang SS, Yang MC, Tsai YT, Wu SL, Lu RH, Chan CY, Lee SD. Role of endotoxaemia in hyperdynamic circulation in rats with extrahepatic or intrahepatic portal hypertension. *J Gastroenterol Hepatol* 1996; **11**: 152-158
6 **Lin RS**, Lee FY, Lee SD, Tsai YT, Lin HC, Lu RH, Hsu WC, Huang CC, Wang SS, Lo KJ. Endotoxemia in patients with chronic liver diseases: relationship to severity of liver diseases, presence of esophageal varices, and hyperdynamic circulation. *J Hepatol* 1995; **22**: 165-172
7 **Albillos A,** de la Hera A, Gonzalez M, Moya JL, Calleja JL, Monserrat J, Ruiz-del-Arbol L, Alvarez-Mon M. Increased lipopolysaccharide binding protein in cirrhotic patients with marked immune and hemodynamic derangement. *Hepatology* 2003; **37**: 208-217
8 **Vallance P**, Moncada S. Hyperdynamic circulation in cirrhosis: a role for nitric oxide? *Lancet* 1991; **337**: 776-778
9 **Claria J**, Jimenez W, Ros J, Asbert M, Castro A, Arroyo V, Rivera F, Rodes J. Pathogenesis of arterial hypotension in cirrhotic rats with ascites: role of endogenous nitric oxide. *Hepatology* 1992; **15**: 343-349
10 **Ros J**, Jimenez W, Lamas S, Claria J, Arroyo V, Rivera F, Rodes J. Nitric oxide production in arterial vessels of cirrhotic rats. *Hepatology* 1995; **21:** 554-560
11 **Sieber CC**,Lopez-Talavera JC, Groszmann RJ. Role of nitric oxide in the in vitro splanchnic vascular hyporeactivity in ascitic cirrhotic rats. *Gastroenterology* 1993; **104**: 1750-1754
12 **Morales-Ruiz M**, Jimenez W, Perez-Sala D, Ros J, Leivas A, Lamas S, Rivera F, Arrogo V. Increased nitric oxide synthase expression in arterial vessels of cirrhotic rats with ascites. *Hepatology* 1996; **24**: 1481-1486
13 **Martin PY**, Xu DL, Niederberger M, Weigert A, Tsai P, St John J, Gines P, Schrier RW. Upregulation of endothelial constitutive NOS: a major role in the increased NO production in cirrhotic rats. *Am J Physiol* 1996; **270**: F494-499
14 **Ros J**, Claria J, Jimenez W, Bosch-Marce M, Angeli P, Arroyo V, Rivera F, Rodes J. Role of nitric oxide and prostacyclin in the control of renal perfusion in experimental cirrhosis. *Hepatology* 1995; **22**: 915-920
15 **Liu YL**, Li DG, Lu HM, Xu QF. The control to 3T6 fibroblast from four calcium antagonist. *Beijing Yixue Zazhi* 1996; **18**: 26-29
16 **Wang BE**, Sun M, Bai N, Li XM, Yin WY, Wang TL. The therapeutic observation to experimental liver fibrosis of the active and decongestive Chinese Medicine. *Zhongcaoyao* 1990; **21**: 23
17 **Li DG**, Liu YL, Lu HM, Jiang ZM, Xu QF. The effects of tetrandrine to mitochondrion of cirrhotic rat. *Zhonghua Xiaohua Zazhi* 1994; **14**: 339-342
18 **Andiran F,** Kilinc K, Renda N, Ayhan A, Tanyel FC. Lipid peroxidation and extracellular matrix in normal and cirrhotic rat livers following 70% hepatectomy. *Hepatogastroenterology* 2003; **50**: 805-808
19 **Kimura B,** Kawasaki S, Nakano H, Fujii T. Rapid, quantitative PCR monitoring of growth of Clostridium botulinum type E in modified-atmosphere-packaged fish. *Appl Environ Microbiol* 2001; **67**: 206-216
20 **Kincaid EZ,** Ernst JD. Mycobacterium tuberculosis exerts gene-selective inhibition of transcriptional responses to IFN-gamma without inhibiting STAT1 function. *J Immunol* 2003; **171**: 2042-2049
21 **MacMicking J**, Xie QW, Nathan C. Nitric oxide and macrophage function. *Annu Rev Immunol* 1997; **15**: 323-350
22 **Lyons CR**, Orloff GJ, Cunningham JM. Molecular cloning and functional expression of an inducible nitric oxide synthase from a murine macrophage cell line. *J Biol Chem* 1992; **267**: 6370-6374
23 **Cahill PA**, Redmond EM, Hodges R, Zhang S, Sitzmann JV. Increased endothelial nitric oxide synthase activity in the hyperemic vessels of portal hypertensive rats. *J Hepatol* 1996; **25**: 370-378
24 **Gadano AC**, Sogni P, Yang S, Cailmail S, Moreau R, Nepveux P, Couturier D, Lebrec D**.** Endothelial calcium-calmodulin dependent nitric oxide synthase in the *in vitro* vascular hyporeactivity of portal hypertensive rats. *J Hepatol* 1997; **26**: 678-686
25 **Martin PY**, Xu DL, Niederberger M, Weigert A, Tsai P, St John J, Gines P, Schrier RW. Upregulation of endothelial constitutive NOS: a major role in the increased NO production in cirrhotic rats. *Am J Physiol* 1996; **270**(3 Pt 2): F494-F499
26 **Murthy KS**, Zhang KM, Jin JG, Grider JR, Makhlouf GM. VIP-mediated G protein-coupled Ca2+ influx activates a constitutive NOS in dispersed gastric muscle cells. *Am J Physiol* 1993; **265**(4 Pt 1): G660-G671
27 **Cho HJ**, Xie QW, Calaycay J, Mumford RA, Swiderek KM, Lee TD, Nathan C. Calmodulin is a subunit of nitric oxide synthase from macrophages. *J Exp Med* 1992; **176**: 599-604

Edited by Ren SY and Wang XL **Proofread by** Xu FM

PO Box 2345, Beijing 100023, China
Fax: +86-10-85381893
E-mail: wjg@wjgnet.com www.wjgnet.com

World J Gastroenterol 2004;10(13):1928-1933
World Journal of Gastroenterology
 ISSN 1007-9327

• BASIC RESEARCH •

Isolation of murine hepatic lymphocytes using mechanical dissection for phenotypic and functional analysis of NK1.1$^+$ cells

Zhong-Jun Dong, Hai-Ming Wei, Rui Sun, Bin Gao, Zhi-Gang Tian

Zhong-Jun Dong, Hai-Ming Wei, Rui Sun, Zhi-Gang Tian, Institution of Immunology, University of Science and Technology of China, Hefei 230027, Anhui Province, China
Zhi-Gang Tian, Rui Sun, Shandong Cancer Biotherapy Center, Shandong Academy of Medical Science, Jinan City, Jinan 250062, Shandong Provine, China
Bin Gao, Section on Liver Biology, Laboratory of Physiologic Studies, National Institute on Alcohol Abuse and Alcoholism, National Institutes of Health, Bethesda, Maryland 20892, USA
Supported by the National Science Fund for Distinguished Young Scholars, No. 30125038 and the Key Project of National Natural Science Foundation of China, No. 30230340 and the National High Technology Research and Development Program of China (863 Program), No. 2002AA216151 and Chinese Academy of Sciences, No. KSCX2-2-08
Correspondence to: Dr. Zhi-Gang Tian, School of Life Sciences, University of Science and Technology of China, 443 Huangshan Road, Hefei 230027, Anhui Province, China. ustctzg@yahoo.com.cn
Telephone: +86-551-360-7379 **Fax:** +86-551-360-6783
Received: 2003-08-02 **Accepted:** 2003-10-07

Abstract

AIM: To choose an appropriate methods for the isolation of hepatic lymphocytes between the mechanical dissection and the enzymatic digestion and investigate the effects of two methods on phenotype and function of hepatic lymphocytes.

METHODS: Hepatic lymphocytes were isolated from untreated, poly (I:C)-stimulated or ConA-stimulated mice using the two methods, respectively. The cell yield per liver was evaluated by direct counting under microscope. Effects of digestive enzymes on the surface markers involved in hepatic lymphocytes were represented by relative change rate [(percentage of post-digestion - percentage of pre-digestion)/percentage of pre-digestion]. Phenotypic analyses of the subpopulations of hepatic lymphocytes and intracellular cytokines were detected by flow cytometry. The cytotoxicity of NK cells from wild C57BL/6 or poly (I:C)-stimulated C57BL/6 mice was analyzed with a 4-h ^{51}Cr release assay.

RESULTS: NK1.1$^+$ cell markers, NK1.1 and DX5, were significantly down-expressed after enzymatic digestion and their relative change rates were about 28% and 32%, respectively. Compared with the enzymatic digestion, the cell yield isolated from unstimulated, poly (I:C)-treated or ConA-treated mice by mechanical dissection was not significantly decreased. Hepatic lymphocytes isolated by the mechanical dissection comprised more innate immune cells like NK, NKT and γδ cells in normal C57BL/6 mice. After poly (I:C) stimulation, hepatic NK cells rose to about 35%, while NKT cells simultaneously decreased. Following ConA injection, the number of hepatic NKT cells was remarkably reduced to 3.67%. Higher ratio of intracellular IFN-γ$^+$(68%) or TNF-α$^+$(15%) NK1.1$^+$ cells from poly (I:C)-treated mice was obtained using mechanical dissection method than control mice. There was no difference in viability between the mechanical dissection and the enzymatic digestion, and hepatic lymphocytes obtained with the two methods had similar cytotoxicity against YAC-1 cells.

CONCLUSION: There is no difference in the cell yield and viability of the hepatic lymphocyte isolated with the two methods. The mechanical dissection, but not the enzymatic digestion, may be suitable for the phenotypic analysis of hepatic NK1.1$^+$ cell.

Dong ZJ, Wei HM, Sun R, Gao B, Tian ZG. Isolation of murine hepatic lymphocytes using mechanical dissection for phenotypic and functional analysis of NK1.1$^+$ cells. *World J Gastroenterol* 2004; 10(13): 1928-1933
http://www.wjgnet.com/1007-9327/10/1928.asp

INTRODUCTION

In recent decades, isolated lymphocytes from human or murine liver were universally used to explore the immune mechanisms in the defense of pathogens such as hepatitis virus[1,2] and in the pathogenesis of liver diseases, especially in the autoimmune hepatitis[3] and liver transplantation[4]. Several lymphocyte subpopulations reside in the normal adult human liver. These cells mainly include a large number of T cells, B cells, natural killer (NK) cells and natural killer T (NKT) cells, which are distinct from the peripheral blood lymphocytes (PBL)[5-7]. Up to now, mechanical dissection and enzymatic digestion are two main techniques for isolation of hepatic lymphocytes. The former method started in the early of 1980 and has been used yet. Reportedly, the viability of lymphocyte with this method is poor, and this method also leads to low yield. The latter methods was through incubation with digestive enzymes, 0.5 g/L collagenase IV and 0.01 g/L DNAase I[8] and was considered to have a relative low contamination of PBL. Because the manipulation of the method is difficult to handle for tenderfoots, the prevalent use is limited. Some investigators also discovered that two digestive enzymes used could influence and decrease the percentage of surface markers of human hepatic lymphocytes such as CD56 molecule[9]. However, the effects of two digestive enzymes on the surface markers of murine hepatic lymphocytes especially NK1.1$^+$ cells, remain obscure. Yet there was not any report exclusively focused on the difference between these two methods. To compare these two methods for suitably selecting an appropriate method to analyze the NK1.1$^+$ cells in the liver, we used these methods to isolate the murine hepatic mononuclear cells for the phenotypic and functional analysis.

MATERIALS AND METHODS

Animal

Female C57BL/6 (H-2^b), 6 to 8 week-old, was purchased from Shanghai Experimental Animal Center, Chinese Academy of Sciences (Shanghai, China). All mice were maintained under controlled conditions (22 ℃, 55% humidity, and 12-h day/night

rhythm) in compliance with the regulations of animal care of University of Science and Technology of China.

Reagent

Collagenase IV and DNase I were purchased from Sigma Chemical Co. (St. Louis, MO) and dissolved in the pyrogen-free RPMI 1640 at the concentration of 0.5 g/L and 0.01 g/L, respectively.

Poly (I:C) or ConA treatment

Polyinosinic-polycytidylic acid sodium [Poly (I:C)] and Concanavalin A (Con A) were purchased from Sigma Chemical Co. (St. Louis, MO) and dissolved in the pyrogen-free saline at the concentration of 1 mg/mL. For *in vivo* stimulation of NK cells, mice were intraperitoneally injected with Poly (I:C) (7.5 μg/g· b.m.) for 6 h. For *in vivo* stimulation of NKT cells, mice were intravenously injected with ConA (7.5 μg/g· b.m.) for 6 h.

Protocols for isolation of mononuclear cells (MNC) from liver

Under deep ether anesthesia, mice were euthanized by exsanguinations from the subclavian artery and vein. A needle was inserted into the portal vein. The liver was perfused with 20 mL pH 7.0 PBS, and then the liver was removed. Isolation of hepatic lymphocytes with the mechanical dissection was carried out as follows: step 1, the liver was thoroughly dissected and gently passed through a 200-gauge stainless steel mesh and then suspended in RPMI 1640 medium containing 100 mL/L fetal calf serum (FCS). Step 2, the above cell suspension was centrifuged at 1 500 r/min. The pellet was resuspended in 40% Percoll solution containing 100 U/mL heparin, and then loaded on the layer of 70% Percoll solution followed by centrifugation at 2 000 r/min for 20 min at room temperature. Step 3, the cells were aspirated from the Percoll interface and harvested by centrifugation and washed twice with Hanks' balanced salt solution (HBSS) containing 50 mL/L FCS before use. The procedures for the enzymatic digestions were as follows: step 1, the liver was dissected into 1 mm^3 pieces and 5 mL digestive solution was added. The mixture was incubated at 37 ℃ for 1 h. The supernatant was collected and diluted 1/2 in complete RPMI 1640. Step 2 and 3 were similar to the mechanical dissection.

Assessment of yield and viability of hepatic lymphocytes

Isolated hepatic lymphocytes from different groups (4 mice per group) were diluted 1:20 with 20 mL/L acetic acid, and cell numbers were assessed by direct counting under microscope. Cell viability was assessed by staining with trypan blue, and the stained-positive cells were enumerated to dead cell, while negative cells to viable lymphocyte.

Effects of digestive enzymes on the surface markers

Effects of digestive enzymes, collagenase IV and DNase I, on the surface markers were determined by the percentage in the pre-digestion and post-digestion. It was represented as relative change rate (%). Relative change rate=[(percentage of post-digestion - percentage of pre-digestion)/percentage of pre-digestion].

Immunofluorescence

The phenotype of lymphocytes was analyzed using monoclonal antibody (mAb) in conjunction with two-color or three-color immunofluorescence. The mAb used in this study included fluorescein isothiocyanate (FITC)-, phycoerythrin (PE)-, or Cy5-conjugated gamma/delta T cell receptor (γδ TCR), anti-CD3e, anti-CD25, anti-CD69, anti-IFN-γ, anti-DX5, and anti-NK1.1 mAb (PharMingen, San Diego, CA). For Intracellular cytokine staining, liver mononuclear cells were incubated in the presence of brefeldin A (5 μg/mL; BD PharMingen) and phorbol myristate acetate (PMA) (20 ng/mL; BD PharMingen) for 3 h, and then stained with FITC-conjugated anti-NK1.1 mAb and Cy-5 conjugated anti-CD3e mAb. After fixation with fixation solution and permeabilization with permeabilization solution (Bioscience, Camarillo, USA), intracellular cytokine staining was performed using PE-conjugated anti-IFN-γ or anti-TNF-α mAb. To prevent nonspecific binding, respective isotype antibodies were used as control. Stained cells were acquired by FACSCalibur and analyzed with WinMDI2.8.

Cytotoxicity assay

Target cells used in NK cytotoxicity assay were YAC-1 cells, which were propagated in RPMI 1640 medium supplemented with 100 mL/L heat-inactivated FCS, 2 mmol/L L-glutamine and 25 mmol/L $NaHCO_3$ in a humidified atmosphere containing 50 mL/L CO_2 at 37 ℃. Cytotoxicity assay was carried out as described previously [10]. Labeled target cells (10^4/well) were incubated in a total volume of 200 μL with effector cells in RPMI 1640 containing100 mL/L FCS in 96-well round-bottom microtiter plates at various cell densities in order to achieve effector-to target (E/T) ratios. The plate was incubated for 4 h, and the supernatant was collected after centrifugation and then counted in a gamma counter. The cytotoxicity was calculated as the percentage of releasable counts after subtraction of spontaneous release. The spontaneous release was less than 15% of the maximum release.

Statistical analysis

Data were expressed as mean±SD. Statistical analysis was performed using *t* test. Difference between the groups was considered statistically significant when *P* value was less than 0.05.

RESULTS

Effects of enzymatic digestion on surface molecules of hepatic lymphocytes

To understand the effect of collagenase IV and DNase I on murine hepatic lymphocytes, we detected the percentage of lymphocyte-related markers, CD3, CD4, CD8e, CD25, CD69, NK1.1, DX5 and γδ TCR in the enzyme-treated and untreated hepatic lymphocytes. Surface markers, CD3, CD4, CD8e, CD25, CD69 and γδ-TCR, remained unchanged and two markers associated with NK and NKT cells, NK1.1 and DX5, were significantly decreased in the enzyme-treated group compared to untreated group and their relative change rates were about 28% and 32% in NK1.1 and DX5 groups respectively (Figure 1). The percentages of NK and NKT cells isolated with the mechanical dissection were higher than those in the enzymatic digestion (Table 1, $P<0.05$). This finding suggested that the enzymatic digestion might decrease the proportion of $NK1.1^+$ cells in murine hepatic lymphocytes by decreasing the NK or NKT-related surface molecules, and should be avoided in the study of $NK1.1^+$ in the liver.

Table 1 Subpopulations of hepatic lymphocytes isolated by two the methods (%)

Group	T cell	NK cell	NKT cell	γδ T cell
Mechanical dissection	38.56±5.63	13.35±4.61	20.42±4.65	13.6±3.15
Enzymatic digestion	36.96±4.68	8.35±2.69[a]	13.48±4.25[a]	12.6±2.74

[a]$P<0.05$ *vs* dissection.

Cell yield of the two methods

In normal C57BL/6 mice, the total cell number obtained with the mechanical dissection was about 2.6×10^6 per liver and that

obtained with the enzymatic digestion was 2.9×10^6 per liver, showing no significant difference (Figure 2A). To further investigate the cell yield in the stress condition, two stimuli, Poly (I:C) and ConA, were used to trigger hepatic lymphocytes, respectively. About 7×10^6 hepatic lymphocytes per liver were obtained in Poly (I:C)-stimulated or ConA-stimulated mice using either the mechanical dissection or the enzyme digestion, without any significant difference between the two isolation methods (Figures 2B,C). These results suggested that the mechanical dissection was as effective as the enzymatic digestion in the cell yield.

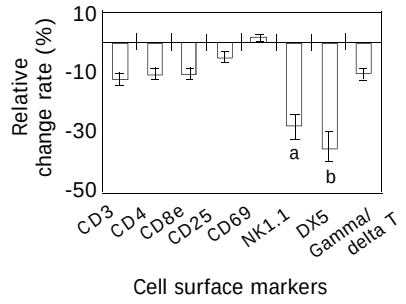

Figure 1 Effects of enzymatic digestion on surface molecules of hepatic lymphocytes. [a]$P<0.05$, NK1.1 *vs* other groups except DX5; [b]$P<0.01$, DX5 *vs* other groups except NK1.1.

Hepatic lymphocytes isolated with mechanical dissection were suitable for phenotypic analysis

Using mechanical dissection, we isolated the hepatic lymphocytes for analyzing the subpopulations of hepatic lymphocytes. Different from other immune organs, hepatic lymphocytes of normal C57BL/6 mice comprised more innate immune cells like NK, NKT and γδ cells, which accounted for 18.60%, 16.62% and 18.60% respectively (Figure 3A). Following Poly (I:C) stimulation, hepatic NK cells increased to about 35% and NKT cells simultaneously decreased, which was consistent with other reports[11] (Figure 3B). Following ConA injection, hepatic NKT cells were remarkably reduced to 3.67%. In addition, after Poly (I:C) stimulation intracellular IFN-γ and TNF-α were significantly augmented to about 68% and 25% within NK ($CD3^-NK1.1^+$) cells, respectively (Figure 3C). Taken together, the results indicated that hepatic lymphocytes obtained with the mechanical dissection could be used for the antibody-based phenotypic analysis of $NK1.1^+$ cells. On the other hand, the liver had the predominance of more innate immune cells.

Hepatic lymphocytes isolated with mechanical dissection were suitable for the functional analysis

In order to understand whether hepatic lymphocytes obtained with mechanical dissection were suitable for functional assays, cell viability was assessed through staining with trypan blue. The cell viability of hepatic lymphocytes from normal C57BL/6 mice accounted for 90% using mechanical dissection method, which was similar to enzyme digestion method (Figure 4A). Next, we examined NK cells cytotoxic function against an NK-sensitive cell line, YAC-1 cells, and found that there was no difference between the two methods (Figure 4B). In the absence of Poly (I:C) stimulation, the cytotoxicity of NK cells to YAC-1 cells was about 15% at the E:T ratio of 1:12.5. After Poly (I:C) stimulation, it increased to 35% at the same E:T ratio. These results indicated that the isolated lymphocytes with the two different methods had the similar viability and were suitable for functional analysis of hepatic lymphocytes prior to or after immune stimulation.

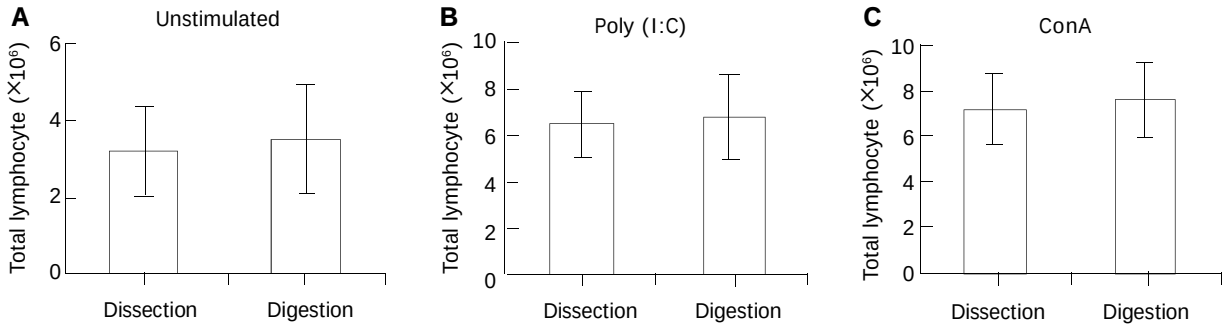

Figure 2 Cell yields between the two isolating methods. Hepatic lymphocytes were isolated using mechanical dissection method and the enzymatic digestion method, respectively, from normal C57BL/6 mice (A), Poly (I:C)-treated C57BL/6 mice (B) or ConA-treated C57BL/6 mice(C).

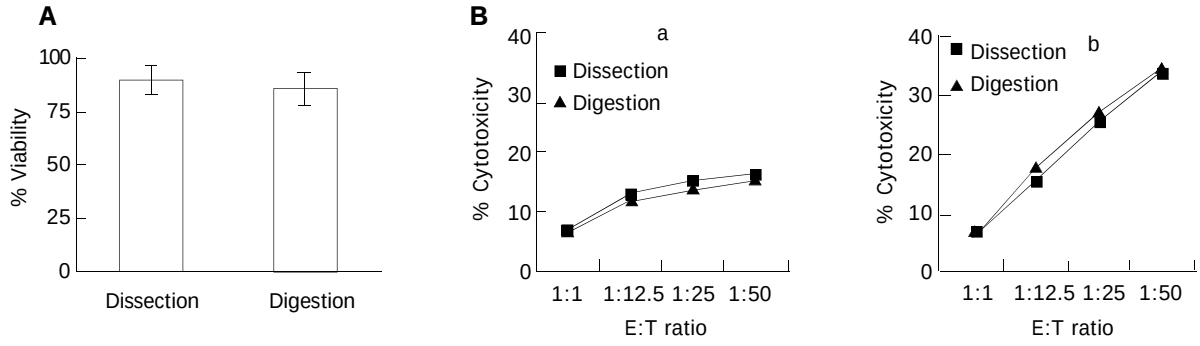

Figure 4 Hepatic lymphocytes isolated with mechanical dissection were suitable for the functional analysis of $NK1.1^+$ cells. A: Viability of hepatic lymphocytes isolated with two methods; B: Cytotoxicity analysis of hepatic lymphocytes. Hepatic lymphocytes were isolated by two different methods, respectively, from control B6 mice (a) or Poly (I:C)-treated B6 mice (b). Their cytotoxicity against YAC-1 cells was tested at the (E/T) ratios.

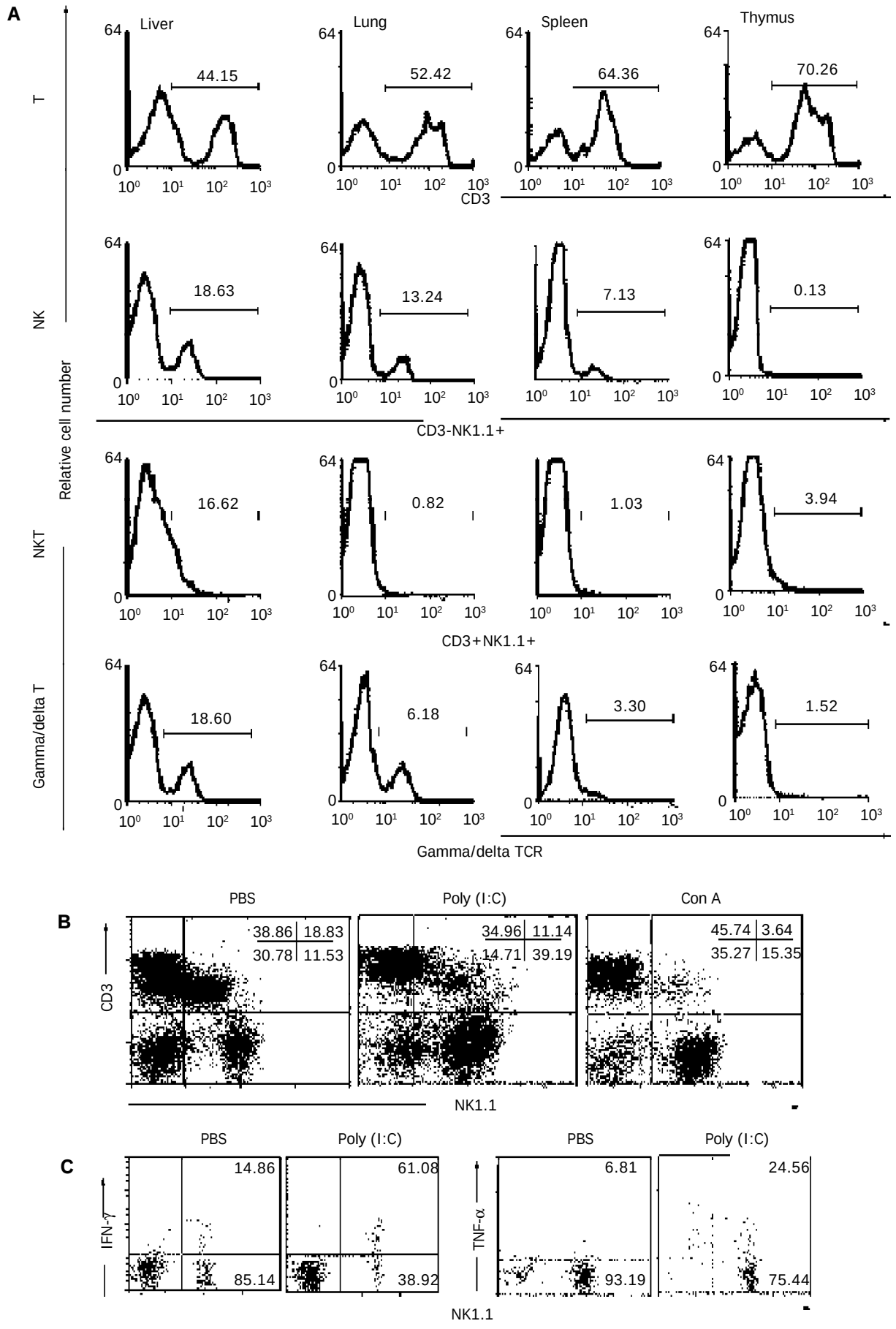

Figure 3 Hepatic lymphocytes isolated with mechanical dissection were suitable for phenotypic analysis of NK1.1$^+$ cells. A: Lymphocytes from liver, lung, spleen and thymus of normal C57BL/6 mice were labeled with two-color immunofluorescence; B, C: C57BL/6 mice were injected with PBS, Poly (I:C) or ConA, respectively. Hepatic lymphocytes were isolated and labeled for phenotype (CD3 and NK1.1) and intracellular cytokine (IFN-γ and TNF-α) detection.

DISCUSSION

Liver has a unique dual blood supply with venous blood from the gut via the portal veins and arterial blood delivered via the hepatic arteries. In view of this distinct anatomy character, liver is thus constantly exposed to gut-derived antigens and infectious organisms in the portal blood. So many unidentified mechanisms have been involved to allow rapid and selective immune responses within this tissue[12,13]. Structurally and functionally, qualification of liver as a lymphoid organ has been reflected by many studies[14,15], and therefore a new term "hepatoimmunology" was emerged in 2002[16]. Liver harbors many innate immune cells, such as NK, NKT and γδ T cells. The predominance of these cells in the liver endows liver with the character of innate immune organ[17], which was supported by the response of NK cells to the innate immune stimulus, Poly (I:C) in our study. However, the exact roles of these cells in the liver remain unclear. NK1.1 molecule is a member of NKR-P1 family, also named as CD161 in human[18], and NK1.1$^+$ cells often have DX5 molecule on their membrane in mice[19]. Their remarkable distinction was that NK1.1 was only expressed by certain strain of mice, such as C57BL/6 and NZB, but not BALB/c[20]. Conventionally, NK1.1$^+$ cells mainly included NK cells and NKT cells. However, upon certain stimulation, activated cytotoxic T cell could also upregulate NK1.1 molecule. NK and NKT cells are two important subpopulations in the liver. They exerted their versatile roles in the defense of pathogens like murine cytomegalovirus (MCMV)[21,22]. Several studies also reported that hepatic NK and NKT cell took part in the antimetastasis of tumor[23-25]. NK1.1$^+$ cells were reported to involve in the pathogenesis of many diseases, like human immunodeficiency virus (HIV) infection and liver disease[26,27]. The demonstration that NK cell or NKT cell could give rise to liver injury had been confirmed by different groups, including our laboratory[28-30]. Accurate assessment of these NK1.1$^+$ cells in the liver required an appropriate technique to purify the hepatic lymphocytes. Various enzymatic or mechanical methods were proposed in the past to isolate lymphocytes from human or murine liver[9]. The Enzymatic digestion was considered to be a satisfied method in the preparation of human organ-specific lymphocytes[31]. In addition, this method has been used to isolate cells like hepatocytes[32]. However, results from different studies appeared to be inconsistent. For example, Trobonjaca *et at.* reported that NKT cells accounted for 35.9% of the total hepatic lymphocytes in normal mice[8], while Osman *et al.* reported that NKT cell accounted for only 16%[33]. This difference may contribute to the different isolating methods taken by them. The roles of collagenase on surface makers of peripheral blood lymphocytes were investigated in 1996. They found collagenase could disrupt the surface markers, such as CD3, CD4, CD8, αβ and γδ TCR by about 20-40%[34]. It was also reported that isolation of intestinal lymphocytes using collagenase released cytotoxic factors, which were found to suppress NK cell activity of isolated cell[35]. Although the mechanical dissection for preparation of hepatic lymphocytes has been used for many years and still used yet, this technique has a defect in cell yield. To make sure the extent, in this study we found that there was no difference in cell yields and viability between the mechanical dissection method and the enzymatic digestion method. We did not observe any decrease in the surface molecules of hepatic lymphocytes in all cases except NK1.1 and DX5, suggesting that enzymatic digestion using collagenase IV and DNase is unsuitable for isolating hepatic lymphocytes for NK1.1$^+$ cell analysis.

ACKNOWLEDGEMENT

We are thankful to Dr. Jing Wang and Dr. Yong-Yan Cheng for their continuous technical helping during this work.

REFERENCES

1 **Vigan I**, Jouvin-Marche E, Leroy V, Pernollet M, Tongiani-Dashan S, Borel E, Delachanal E, Colomb M, Zarski JP, Marche PN. T lymphocytes infiltrating the liver during chronic hepatitis C infection express a broad range of T-cell receptor beta chain diversity. *J Hepatol* 2003; **38**: 651-659
2 **Boisvert J**, Kunkel EJ, Campbell JJ, Keeffe EB, Butcher EC, Greenberg HB. Liver-infiltrating lymphocytes in end-stage hepatitis C virus: subsets, activation status, and chemokine receptor phenotypes. *J Hepatol* 2003; **38:** 67-75
3 **Kaneko Y**, Harada M, Kawano T, Yamashita M, Shibata Y, Gejyo F, Nakayama T,Taniguchi M. Augmentation of Valpha14 NKT cell-mediated cytotoxicity by interleukin 4 in an autocrine mechanism resulting in the development of concanavalin A-induced hepatitis. *J Exp Med* 2000; **191**: 105-114
4 **Otto C**, Kauczok J, Martens N, Steger U, Moller I, Meyer D, Timmermann W, Ulrichs K, Gassel HJ. Mechanisms of tolerance induction after rat liver transplantation: intrahepatic CD4 (+) T cells produce different cytokines during rejection and tolerance in response to stimulation. *J Gastrointest Surg* 2002; **6**: 455-463
5 **Norris S**, Collins C, Doherty DG, Smith F, McEntee G, Traynor O, Nolan N, Hegarty J, O'Farrelly C. Resident human hepatic lymphocytes are phenotypically different from circulating lymphocytes. *J Hepatol* 1998; **28**: 84-90
6 **Luo DZ**, Vermijlen D, Ahishali B, Triantis V, Plakoutsi G, Braet F, Vanderkerken K, Wisse E. On the cell biology of pit cells, the liver-specific NK cells. *World J Gastroenterol* 2000; **6**: 1-11
7 **Doherty DG**, Norris S, Madrigal-Estebas L, McEntee G, Traynor O, Hegarty JE, O'Farrelly C. The human liver contains multiple populations of NK cells, T cells, and CD3$^+$CD56$^+$ natural T cells with distinct cytotoxic activities and Th1, Th2, and Th0 cytokine secretion patterns. *J Immunol* 1999; **163**: 2314-2321
8 **Trobonjaca Z**, Kroger A, Stober D, Leithauser F, Moller P, Hauser H, Schirmbeck R, Reimann J. Activating immunity in the liver. II. IFN-beta attenuates NK cell-dependent liver injury triggered by liver NKT cell activation. *J Immunol* 2002; **168**: 3763-3770
9 **Curry MP**, Norris S, Golden-Mason L, Doherty DG, Deignan T, Collins C, Traynor O, McEntee GP, Hegarty JE, O'Farrelly C. Isolation of lymphocytes from normal adult human liver suitable for phenotypic and functional characterization. *J Immunol Methods* 2000; **242**: 21-31
10 **Luo DZ**, Vermijlen D, Ahishali B, Triantis V, Vanderkerken K, Kuppen PJ, Wisse E. Participation of CD45, NKR-P1A and ANK61 antigen in rat hepatic NK cell (pit cell) mediated target cell cytotoxicity. *World J Gastroenterol* 2000; **6**: 546-552
11 **Hobbs JA,** Cho S, Roberts TJ, Sriram V, Zhang J, Xu M, Brutkiewicz RR. Selective loss of natural killer T cells by apoptosis following infection with lymphocytic choriomeningitis virus. *J Virol* 2001; **75:** 10746-10754
12 **Seki S**, Habu Y, Kawamura T, Takeda K, Dobashi H, Ohkawa T, Hiraide H. The liver as a crucial organ in the first line of host defense: the roles of Kupffer cells, natural killer (NK) cells and NK1.1 Ag+ T cells in T helper 1 immune responses. *Immunol Rev* 2000; **174**: 35-46
13 **Knolle PA**, Gerken G. Local control of the immune response in the liver. *Immunol Rev* 2000; **174**: 21-34
14 **Mehal WZ**, Azzaroli F, Crispe IN. Immunology of the healthy liver: old questions and new insights. *Gastroenterology* 2001; **120**: 250-260
15 **Kita H**, Mackay IR, Van de Water J, Gershwin ME. The lymphoid liver: considerations on pathways to autoimmune injury. *Gastroenterology* 2001; **120**: 1485–1501
16 **Mackay IR**. Hepatoimmunology: a perspective. *Immunol Cell Biol* 2002; **80:** 36-44
17 **Doherty DG**, O'Farrelly C. Innate and adaptive lymphoid cells in the human liver. *Immunol Rev* 2000; **174**: 5–20
18 **Lanier LL**, Chang C, Phillips JH. Human NKR-P1A. A disulfide-linked homodimer of the C-type lectin superfamily expressed by a subset of NK and T lymphocytes. *J Immunol* 1994; **153**: 2417-2428
19 **Rosmaraki EE**, Douagi I, Roth C, Colucci F, Cumano A, Di Santo JP. Identification of committed NK cell progenitors in

adult murine bone marrow. *Eur J Immunol* 2001; **31**: 1900-1909
20 **Arase H**, Saito T, Phillips JH, Lanier LL. Cutting edge: the mouse NK cell-associated antigen recognized by DX5 monoclonal antibody is CD49b (alpha 2 integrin, very late antigen-2). *J Immunol* 2001; **167**: 1141-1144
21 **Lodoen M**, Ogasawara K, Hamerman JA, Arase H, Houchins JP, Mocarski ES, Lanier LL. NKG2D-mediated natural killer cell protection against cytomegalovirus is impaired by viral gp40 modulation of retinoic acid early inducible 1 gene molecules. *J Exp Med* 2003; **197**: 1245-1253
22 **van Dommelen SL**, Tabarias HA, Smyth MJ, Degli-Esposti MA. Activation of natural killer (NK) T cells during murine cytomegalovirus infection enhances the antiviral response mediated by NK cells. *J Virol* 2003; **77**: 1877-1884
23 **Sun R**, Wei H, Zhang J, Li A, Zhang W, Tian Z. Recombinant human prolactin improves antitumor effects of murine natural killer cells *in vitro* and *in vivo*. *Neuroimmunomodulation* 2002; **10**: 169-176
24 **Joo SS**, Kim MS, Oh WS, Lee DI. Enhancement of NK cytotoxicity, antimetastasis and elongation effect of survival time in B16-F10 melanoma cells by oregonin. *Arch Pharm Res* 2002; **25**: 493-499
25 **Park SH**, Kyin T, Bendelac A, Carnaud C. The contribution of NKT cells, NK cells, and other gamma-chain-dependent non-T non-B cells to IL-12-mediated rejection of tumors. *J Immunol* 2003; **170**: 1197-1201
26 **Vergani D**, Choudhuri K, Bogdanos DP, Mieli-Vergani G. Pathogenesis of autoimmune hepatitis. *Clin Liver Dis* 2002; **6**: 439-449
27 **Fleuridor R**, Wilson B, Hou R, Landay A, Kessler H, Al-Harthi L. CD1d-restricted natural killer T cells are potent targets for human immunodeficiency virus infection. *Immunology* 2003; **108**: 3-9
28 **Takeda K**, Hayakawa Y, Van Kaer L, Matsuda H, Yagita H, Okumura K. Critical contribution of liver natural killer T cells to a murine model of hepatitis. *Proc Natl Acad Sci U S A* 2000; **97**: 5498-5503
29 **Abe T**, Kawamura H, Kawabe S, Watanabe H, Gejyo F, Abo T. Liver injury due to sequential activation of natural killer cells and natural killer T cells by carrageenan. *J Hepatol* 2002; **36**: 614-623
30 **Liu ZX**, Govindarajan S, Okamoto S, Dennert G. NK cells cause liver injury and facilitate the induction of T cell-mediated immunity to a viral liver infection. *J Immunol* 2000; **164**: 6480-6486
31 **Flynn L**, Carton J, Byrne B, Kelehan P, O'Herlihy C, O'Farrelly C. Optimisation of a technique for isolating lymphocyte subsets from human endometrium. *Immunol Invest* 1999; **28**: 235-246
32 **Mitry RR**, Hughes RD, Aw MM, Terry C, Mieli-Vergani G, Girlanda R, Muiesan P, Rela M, Heaton ND, Dhawan A. Human hepatocyte isolation and relationship of cell viability to early graft function. *Cell Transplant* 2003; **12**: 69-74
33 **Osman Y**, Kawamura T, Naito T, Takeda K, Van Kaer L, Okumura K, Abo T. Activation of hepatic NKT cells and subsequent liver injury following administration of alpha-galactosylceramide. *Eur J Immunol* 2000; **30**: 1919-1928
34 **Abuzakouk M**, Feighery C, O'Farrelly C. Collagenase and dispase enzymes disrupt lymphocyte surface molecules. *J Immunol Methods* 1996; **194**: 211-216
35 **Gibson PR**, Hermanowicz A, Verhaar HJ, Ferguson DJ, Bernal AL, Jewell DP. Isolation of intestinal mononuclear cells: factors released which lymphocyte viability and function. *Gut* 1985; **26**: 60-68

Edited by Kumar M **Proofread by** Chen WW and Xu FM

PO Box 2345, Beijing 100023, China
Fax: +86-10-85381893
E-mail: wjg@wjgnet.com www.wjgnet.com

World J Gastroenterol 2004;10(13):1934-1938
World Journal of Gastroenterology
 ISSN 1007-9327

• BASIC RESEARCH •

Role of mitochondria in cell apoptosis during hepatic ischemia-reperfusion injury and protective effect of ischemic postconditioning

Kai Sun, Zhi-Su Liu, Quan Sun

Kai Sun, Zhi-Su Liu, Quan Sun, Department of General Surgery, Zhongnan Hospital, Wuhan University, Wuhan 430071, Hubei Province, China
Correspondence to: Professor Zhi-Su Liu, Department of General Surgery, Zhongnan Hospital, Wuhan University, Wuhan 430071, Hubei Province, China. hyfr@mail.wh.cei.gov.cn
Telephone: +86-27-87331752 **Fax:** +86-27-87330795
Received: 2003-06-28 **Accepted:** 2003-10-12

Abstract

AIM: To investigate the role of mitochondria in cell apoptosis during hepatic ischemia-reperfusion injury and protective effect of ischemic postconditioning (IPC).

METHODS: A rat model of acute hepatic ischemia-reperfusion was established, 24 healthy male Wistar rats were randomly divided into sham-operated group, ischemia-reperfusion group (IR) and IPC group. IPC was achieved by several brief pre-reperfusions followed by a persistent reperfusion. Concentration of malondialdehyde (MDA) and activity of several antioxidant enzymes in hepatic tissue were measured respectively. Apoptotic cells were detected by TdT-mediated dUTP-biotin nick end labeling (TUNEL) and expression of Bcl-2 protein was measured by immunohistochemical techniques. Moreover, mitochondrial ultrastructure and parameters of morphology of the above groups were observed by electron microscope.

RESULTS: Compared with IR group, the concentration of MDA and the hepatocellular apoptotic index in IPC group was significantly reduced ($P<0.05$), while the activity of antioxidant enzymes and OD value of Bcl-2 protein were markedly enhanced ($P<0.05$). Moreover, the injury of mitochondrial ultrastructure in IPC group was also obviously relieved.

CONCLUSION: IPC can depress the synthesis of oxygen free radicals to protect the mitochondrial ultrastructure and increase the expression of Bcl-2 protein that lies across the mitochondrial membrane. Consequently, IPC can reduce hepatocellular apoptosis after reperfusion and has a protective effect on hepatic ischemia-reperfusion injury.

Sun K, Liu ZS, Sun Q. Role of mitochondria in cell apoptosis during hepatic ischemia-reperfusion injury and protective effect of ischemic postconditioning. *World J Gastroenterol* 2004; 10(13): 1934-1938
http://www.wjgnet.com/1007-9327/10/1934.asp

INTRODUCTION

Hepatic ischemia-reperfusion injury (IRI) is a common pathological process of traumatic surgical diseases in the liver, such as severe liver trauma, extensive hepatic lobus excision, liver transplantation, shock and infection. When hepatic IRI happens, a series of metabolic and structural and functional disorder of hepatic tissue cells would occur, which directly influence the prognosis of patients[1,2]. At present, the study about the mechanism and intervention method of hepatic IRI has been carried out extensively. It has been confirmed that apoptosis as a way of cell death is significant for maintaining normal cell development and stabilization, and is closely related to the initiation and development of many clinical diseases, and it also participates in IRI of tissues and organs[3-6]. Mitochondria as one of the organelle of cells play an important role in providing energy, adjusting osmotic pressure, calcium balance, and pH value, and cell signaling. Mitochondria perform their function by production of ATP and reactive oxygen species (ROS) which are also known as signals regulating gene expression and triggering cell death[7,8]. At present, mitochondria/ cytochrome C apoptotic pathway has attracted close attention of scholars. Many stimulators such as ROS, Ca^{2+} and cytokines could activate cysteine aspartate-specific proteases (Caspase) by inducing cytochrome C release[9-12]. But the study on the changes of the structure and function of mitochondria in hepatic IRI and the adjusting function of mitochondria in hepatocellular apoptosis was rarely reported at home and abroad. We established a hepatic IRI model in liver of rats, and observed the influence of ischemic postconditioning (IPC) on cell apoptosis in hepatic IRI and the adjustment function of mitochondria. This experiment lays a theoretical foundation for adopting a more reasonable method to restore the blood flow after hepatic ischemia.

MATERIALS AND METHODS

Materials

Twenty-four healthy male Wistar rats, weighing 200-250 g, were supplied by the Experimental Animal Center of Wuhan University. Malondialdehyde (MDA), superoxide dismutase (SOD), catalase (CAT) and glutathione peroxidase (GSH-PX) assay kits were purchased from Nanjing Jiancheng Bioengineering Co.Ltd, China. Mouse anti-rat Bcl-2 monoclonal antibody and SP assay kit were provided by Beijing Zhongshan Biotechnology Co.Ltd, China. Terminal deoxynucleotidyl transferase (TdT) mediated dUTP nick end labeling (TUNEL) *in situ* cell death detection kit was the product of Boehringer Mannhein Co.Ltd, USA.

Animal model

The animals were fed standard laboratory chow. Before the day of experiment, the animals were fasted overnight, but allowed free access to water. They were anesthetized by sodium pentobarbital (30 mg/kg). Hepatoduodenal ligament was separated after entry into the belly, the first porta hepatis was exposed and a rat local hepatic IRI model was established with reference to the previous method[13]. Blood flow of caudate and left lobe of the liver was blocked with non-trauma mini artery clamp, causing 70% liver ischemia. However, the blood flow of right lobe was not blocked to prevent blood clot in portal vein and gastrointestinal tract. Twenty-four rats were randomly divided into three groups (eight in each group) and

subjected to the following treatments. (1) Sham-operated group: only hepatoduodenal ligament was separated after entry into the belly, blood flow of porta hepatis was not blocked. (2) Ischemia-reperfusion group (IR): the livers were undergone ischemia for 60 min followed by reperfusion for 120 min. (3) Ischemic postconditioning group (IPC): the livers were subjected to porta hepatis occlusion for 60 min, then treated for 2 min, 3 min, 5 min, 7 min by brief reperfusion consecutively, each was separated with occlusion for 2 min, followed by a persistent reperfusion for 95 min, which made the total reperfusion time the same as the other two groups.

MDA and antioxidant enzyme measurement

Concentration of MDA and activity of SOD, CAT and GSH-PX in hepatic tissue were measured according to the commercial kit manual.

Immunohistochemical staining

Fresh hepatic tissues, cut from left lobe of the liver, were fixed in formalin for 12-24 h and then embedded in paraffin wax.A 4-μm thick sections were cut and mounted onto slides. They were deparaffinized by passing through xylene and graded series of ethanol, followed by rinsing in tap water and 0.01 mmol/L phosphate buffered saline (PBS) respectively. Endogenous peroxidase activity was quenched by treating the sections with 30 mL/L hydrogen peroxide for 10 min. Nonspecific binding was blocked by incubating sections in PBS containing 10 g/L bovine albumin for 10 min. Then the sections were incubated for an hour in primary antibody (mouse anti-rat Bcl-2 monoclonal antibody). After rinsed in PBS, the sections were treated sequentially with biotin-conjugated second antibody for 10 min and then with streptavidin-peroxidase for another 10 min with PBS rinsing after each step. The sections were stained subsequently with freshly prepared DAB reagent for 3 min, terminated by rinsing in water, then immerged in hematoxylin for 3-5 min and 0.5 mmol/L HCl for 10 s. Finally, after passing through xylene and graded series of ethanol, the sections were covered with coverslips for light analysis. The sections were examined with HAIPS-2 000 image analysis and the Absorbency value was used to evaluate the content of Bcl-2 protein.

Hepatic TUNEL staining

In situ terminal deoxynucleotidyl transferase-mediated dUTP nick-end labeling (TUNEL) of fragmented DNA was performed on paraffin slices using the *in situ* cell death detection kit as described in the commercial kit manual. Positively labeled nuclei (brown color) were identified from negatively unstained nuclei (blue color). The number of positive nuclei was determined by counting (magnification×400) all the positively labeled nuclei present in five random visual fields under a microscope. The percentage of TUNEL positive nuclei to all nuclei counted was used as apoptotic index (AI). The apoptotic cells had the following characteristics: single cells, no inflammation, curling of cell membrane, brown particulate or fragmented nuclei.

Morphopathological observation of ultrastructural organization

One mm^3 fresh hepatic tissue, cut from left lobe of the liver, was pre-fixed with glutaraldehyde at the volume fraction of 2.5 % and post-fixed with 1 g/L osmic acid. Then the specimens were immersed in propylene oxide after dehydration with gradient ethanol, embedded with epoxy resin and made into ultrathin sections. The sections were stained subsequently with lead-uranium and the changes of ultrastructural organization were observed under H-600 transmission electron microscope. Finally, the sections were measured for cross-sectional area (A), cross-sectional perimeter (P) of mitochondria (using Image Pro Plus, USA), and computed specific surface of mitochondria following the formula: $\delta=4P/(\pi A)$.

Statistical analysis

All data were expressed as mean±SD. Comparisons between groups were analyzed with one-way ANOVA and Student-Newman-Keuls *q* test. *P* values less than 0.05 were considered statistically significant.

RESULTS

MDA concentration and antioxidant enzyme activity

The concentration of MDA in hepatic tissue was rapidly elevated after reperfusion in IR and IPC groups against sham group ($P<0.05$), while the activity of SOD, CAT and GSH-PX was significantly reduced ($P<0.05$). Compared with IR group, the concentration of MDA in IPC group was markedly reduced and activity of each antioxidant enzyme was significantly enhanced ($P<0.05$) (Table 1).

Table 1 Measurement of MDA concentration and antioxidant enzyme activity (mean±SD, $n=8$)

Group	MDA (nmol/mg)	SOD (U/mg prot)	CAT (U/mg prot)	GSH-PX (U/mg prot)
Sham	3.42±1.12	241.47±19.52	91.66±8.16	124.17±24.37
IR	17.56±4.80[a]	132.99±22.11[a]	40.24±7.73[a]	51.75±16.43[a]
IPC	10.18±3.56[ab]	176.84±20.50[ad]	64.81±7.19[ad]	89.70±28.15[ad]

[a]$P<0.05$ *vs* sham, [d]$P<0.05$ *vs* IR.

Expression of Bcl-2 protein

The *A* value of Bcl-2 protein in IR group (0.067±0.011) was significantly lower than that in sham group (0.096±0.017) ($P<0.05$). After postconditioning, the expression of Bcl-2 protein was more eminent (*A* value 0.138±0.016) than that in IR group ($P<0.05$) (Figure 1A, B, C).

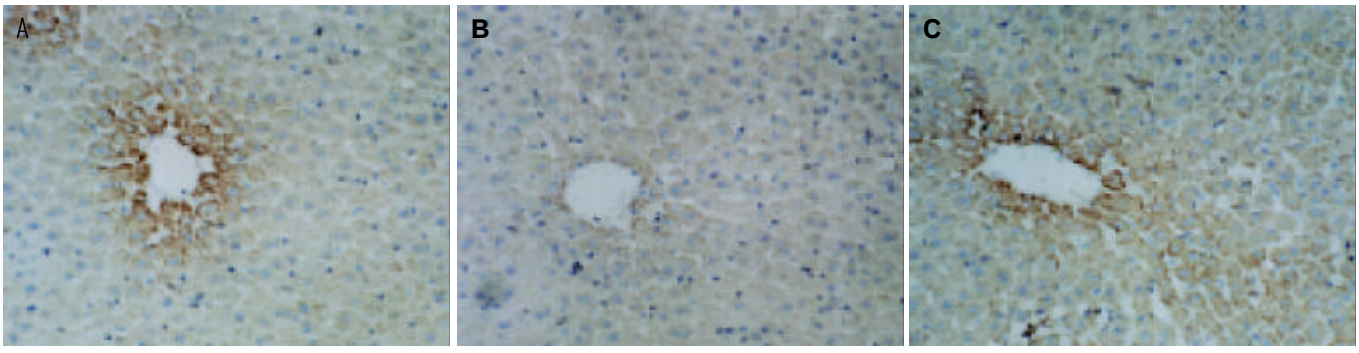

Figure 1 Bcl-2 expression in sham, IR and IPC groups (×200). A: Bcl-2 expression in sham group, B: Bcl-2 expression in IR group, C: Bcl-2 expression in IPC group.

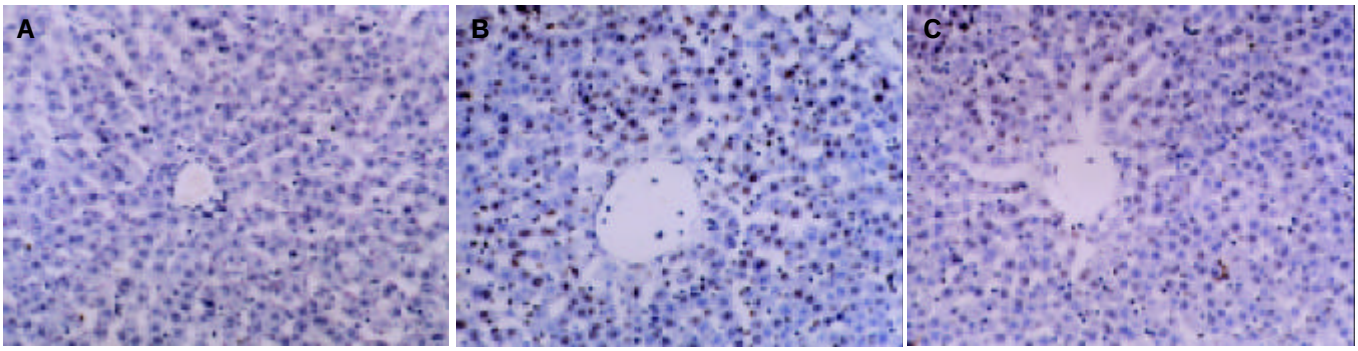

Figure 2 TUNEL staining in sham, IR and IPC groups (×200). A: TUNEL staining in sham group, B: TUNEL staining in IR group, C: TUNEL staining in IPC group.

Effect of IPC on hepatocellular apoptosis

Under light microscope, TUNEL staining indicated that cell injury occurred primarily in the form of apoptosis at the early stage of reperfusion and apoptotic cells were mainly around the central vein (Figure 2A, B, C). Under electron microscope, the early manifestations of apoptosis, such as swelling and rounding of cells, cell exfoliation, and aggregation of chromatin in the edge, as well as the typical manifestations of apoptosis, such as the concentration of cytoplasm and nucleus, and formation of apoptotic body, could be seen (Figure 3). The apoptotic index in IR group (46.53±3.47) was significantly higher than that in sham group (2.05±0.83) (P<0.05). After postconditioning, the apoptotic index (23.16±2.67) was significantly reduced compared with IR group (P<0.05).

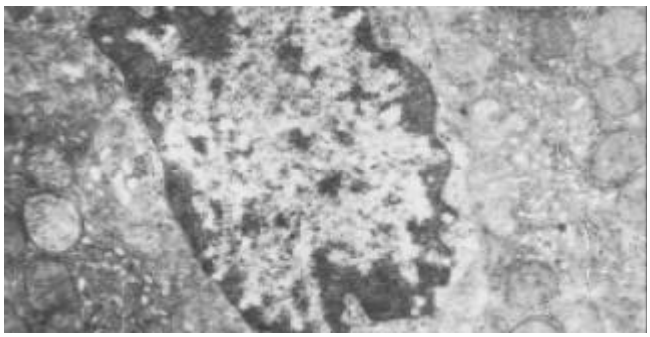

Figure 3 Morphological change of hepatocellular apoptosis in IR group (TEM×15 000).

Ultrastructural changes of mitochondria

In sham group, mitochondrial structure was normal. Mitochondria were orderly arranged in the form of round or ellipsoid without swelling. Mitochondrial membrane was intact and cristae were arranged in the form of concentrical ring or vertical line, congested and clear (Figure 4A). In IR group, mitochondria were swollen obviously. Mitochondrial membrane was vague or partly ruptured and cristae were obviously loose and dissolved, a lot of vacuoluses were formed (Figure 4B). In IPC group, mitochondrial structure was basically normal. Mitochondria were orderly arranged, mitochondrial membrane was basically intact, cristae were congested and there was no vacuolization (Figure 4C).

Quantitive analysis of mitochondrial morphology

The cross-sectional area and perimeter of mitochondria were markedly increased after reperfusion in IR and IPC groups against sham group (P<0.05), while the specific surface of mitochondria was significantly reduced (P<0.05). Compared with IR group, the cross-sectional area and perimeter of mitochondria in IPC group were markedly reduced and the specific surface was significantly increased (P<0.05) (Table 2).

Table 2 Changes of parameters of mitochondrial morphology (mean±SD, n=8)

Group	Area (μm^2)	Perimeter (μm)	Surface (μm^{-1})
Sham	76.2±8.1	22.7±4.6	0.39±0.04
IR	278.3±22.2[a]	60.9±5.9[a]	0.17±0.05[a]
IPC	150.9±16.4[ac]	42.1±4.3[ac]	0.26±0.05[ac]

[a]P<0.05 *vs* sham, [c]P<0.05 *vs* IR.

DISCUSSION

Under the influence of many kinds of stress factors such as ROS, Ca^{2+} overloading, and toxin, mitochondrial ultrastructure and its function were easily damaged, then the active substance originally in mitochondria related to apoptosis including cytochrome C, was released into cytoplasm[14-18]. Recent progress in studies on apoptosis has revealed that cytochrome

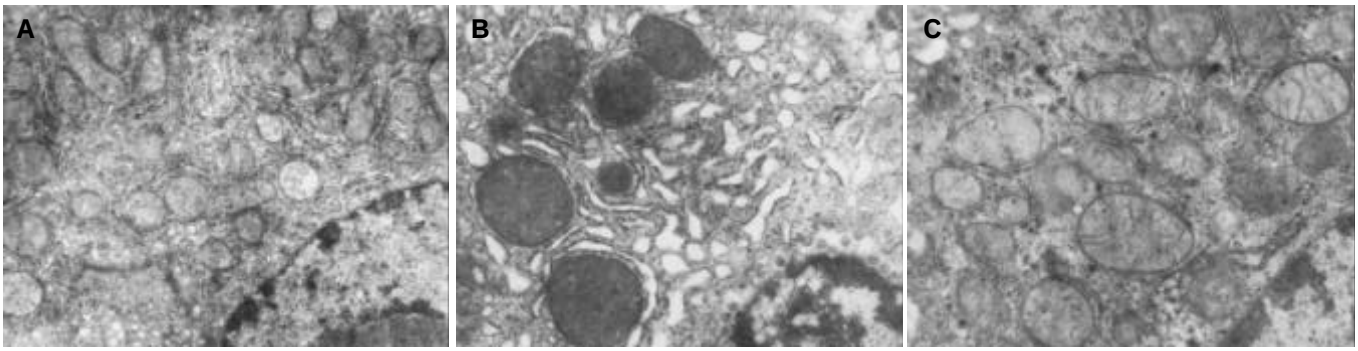

Figure 4 Mitochondrial ultrastructure in sham, IR and IPC groups (TEM×15 000). A: Mitochondrial ultrastructure in sham group, B: Mitochondrial ultrastructure in IR group, C: Mitochondrial ultrastructure in IPC group.

C is a pro-apoptotic factor. It is released at early stage of apoptosis and, by combining with some cytosolic proteins, could activate conversion of the latent apoptosis-promoting protease to its active form[19]. Once cytochrome C was released, cells would die through two ways. One was through quick apoptotic mechanism. Released cytochrome C and apoptotic protease activating factor-1 (Apaf-1) and Caspase-9 were combined, and then Cytc-Apaf-1-Caspase-9 compound was formed, which would lead to the activation of pro-Caspase-9, and subsequently, downstream Caspase-3 was activated, and apoptic cascade reaction was promoted. At the same time, part of the unreleased cytochrome C was steadily combined with cytochrome b-c1 and C oxidase, and adequate ATP was produced to provide energy for apoptosis[20-23]. The other was through necrotic process. Permeability transition pore (PTP) opened, mitochondrial matrix was swollen and ruptured due to hyperosmotic effect, the transmembrane potential ($\Delta \psi m$) of the original mitochondrial membrane quickly collapsed, cytochrome C was released in great amount, electron transferring respiratory chain was blocked, ATP content was radically reduced, effective supply of energy could not be realized and cell necrosed. Consequently, mitochondria could determine the cells to go into apoptosis or necrosis[24]. This experiment proved that early injury of cells after reperfusion occurred mainly in the form of apoptosis. The end product MDA of lipid peroxidation in liver tissue increased after reperfusion, while SOD, CAT and GSH-PX as the major antioxidant enzyme and free radical scavenger were obviously decreased, indicating their capacity of preventing cells from the injury caused by ROS. Excessive oxygen free radicals could directly react with unsaturated fatty acid on the surface of mitochondrial membrane, which led to the destruction of its structure and function. Cytochrome C and other apoptosis-promoting substances were released in great amount, which triggered the apoptosis of cells.

The quantitative analysis of the stereo-form of mitochondria indicated that the major morphological change of mitochondrial injury was swelling. It was considered previously that the apoptotic cells manifested condensed chromatin but intact mitochondria. Now much more evidence revealed that significant changes of mitochondria such as swelling, megamitochondria, mitochondrial pyknosis and disrupted outer-membrane could take place in many apoptotic models[25,26]. Specific surface is the ratio of average area of granular membrane to its volume. It is the objective index to reflect the swelling degree of mitochondria. Our study found that, after reperfusion, the cross-sectional area and perimeter of mitochondria were obviously increased, but specific surface was markedly smaller. The swelling of mitochondria was obvious, and this was in accordance with the changing tendency of mitochondrial ultrastructural organization observed under electron microscope. After postconditioning, the degree of mitochondrial swelling injury was obviously relieved and hepatocellular apoptotic index was also decreased, indicating that the structural and functional changes of mitochondria in apoptotic cells were correlated with the initiation and development of cell apoptosis, suggesting that mitochondrial dysfunction might be the key event in the development of cell apoptosis. Moreover, IPC had a protective effect on the mitochondrial ultrastructure and function.

The exact mechanisms underlying this postconditioning-produced protection remain unclear. It is most likely, though still speculative, that the IPC scheme (reiterative brief pre-reperfusion followed by continuous reperfusion) adopted in this experiment to some extent equaled a controlled slow intermittent reoxygenation, which might reduce the burst production of oxygen free radicals at the early stage of reperfusion and stimulate the release of antioxidant enzymes and free radical scavengers, thus producing protective effects. Compared with IR group, in IPC group MDA in the liver tissue was decreased and every antioxidant enzyme was increased conspicuously, which reduced the injury to mitochondrial membrane lipid peroxidation by toxic oxygen radicals, protected the integrity of the structure and function of mitochondria, and prevented the apoptosis of liver parenchyma cells. Cave *et al.*[27] reported that, in an isolated perfused heart model, compared with sudden reperfusion (remove artery snare occluder abruptly), controllable and slow reperfusion could decrease the occurrence of ventricular fibrillation. The postconditioning treatment in the present study was essentially comparable in some senses to those controlled and slow reoxygenation.

In addition, in order to know the function of mitochondria in apoptotic regulatory pathway, we also measured the change of the content of Bc1-2 protein in liver tissue. Bc1-2 protein as the major representative of apoptotic restraining proteins in Bc1-2 family, functioned through signal-anchor sequence of carboxyl terminal stretching cross mitochondrial membrane[28-31]. Bc1-2 protein could regulate the permeability of PTP on the surface of mitochondrial membrane, or itself could participate in the formation of the specific pathway directly. This could maintain the stability of transmembrane potential and inhibit the release of cytochrome C and other apoptosis-promotion substances, and consequently inhibit the activation of Caspase in cytoplasm and block apoptotic cascade reaction[32-35]. Our experiment confirmed that after postconditioning, the *A* value of Bc1-2 protein was obviously higher than that of IR group, and apoptotic index was obviously decreased. This showed that IPC could decrease apoptosis in liver IRI by up-regulating trans-mitochondrial membrane Bc1-2 protein expression. But the detailed mechanism needs to be further studied.

To sum up, in hepatic IRI, various stress factors can activate the apoptotic pathway mediated by mitochondria, which leads to the increase of apoptosis, and the decrease of the total number of parenchyma cells, and thus the hepatic tissue and liver function are severely damaged. Mitochondrial apoptotic pathway participates in hepatic IRI, and is a ring-point in this complicated mechanism. IPC can protect the mitochondrial ultrastructural organization and function through the inhibition of synthesis of excessive oxygen free radicals after reperfusion and increase trans-mitochondrial membrane Bc1-2 protein expression. Consequently, IPC can inhibit cell apoptosis and reduce hepatic IRI. IPC should carry out after operation and before comprehensive blood perfusion. It is easy to perform and the time is adequate. Undoubtedly, it has direct clinical application value.

REFERENCES

1 **Lei DX**, Peng CH, Peng SY, Jiang XC, Wu YL, Shen HW. Safe upper limit of intermittent hepatic inflow occlusion for liver resection in cirrhotic rats. *World J Gastroenterol* 2001; **7**: 713-717

2 **Kiemer AK**, Heinze SK, Gerwig T, Gerbes AL, Vollmar AM. Stimulation of p38 MAPK by hormonal preconditioning with atrial natriuretic peptide. *World J Gastroenterol* 2002; **8**: 707-711

3 **Oshiro T**, Shiraishi M, Muto Y. Adenovirus mediated gene transfer of antiapoptotic protein in hepatic ischemia-reperfusion injury: the paradoxical effect of Bcl-2 expression in the reperfused liver. *J Surg Res* 2002; **103**: 30-36

4 **Chen MF**, Chen JC, Chiu DF, Ng CJ, Shyr MH, Chen HM. Prostacyclin analogue (OP-2507) induces delayed ex vivo neutrophil apoptosis and attenuates reperfusion-induced hepatic microcirculatory derangement in rats. *Shock* 2001; **16**: 473-478

5 **Sileri P**, Schena S, Morini S, Rastellini C, Pham S, Benedetti E, Cicalese L. Pyruvate inhibits hepatic ischemia-reperfusion injury in rats. *Transplantation* 2001; **72**: 27-30

6 **Ikebe N**, Akaike T, Miyamoto Y, Hayashida K, Yoshitake J, Ogawa M, Maeda H. Protective effect of S-nitrosylated alpha (1)-protease inhibitor on hepatic ischemia-reperfusion injury. *J Pharmacol Exp Ther* 2000; **295**: 904-911

7 **Susin SA**, Zamzami N, Castedo M, Hirsch T, Marchetti P, Ma-

cho A, Daugas E, Geuskens M, Kroemer G. Bcl-2 inhibits the mitochondrial release of an apoptogenic protease. *J Exp Med* 1996; **184**: 1331-1341

8 **Kluck RM**, Bossy-Wetzel E, Green DR, Newmeyer DD. The release of cytochrome c from mitochondria: a primary site for Bcl-2 regulation of apoptosis. *Science* 1997; **275**: 1132-1136

9 **Marchetti P**, Susin SA, Decaudin D, Gamen S, Castedo M, Hirsch T, Zamzami N, Naval J, Senik A, Kroemer G. Apoptosis-associated derangement of mitochondrial function in cells lacking mitochondrial DNA. *Cancer Res* 1996; **56**: 2033-2038

10 **Petit PX**, Susin SA, Zamzami N, Mignotte B, Kroemer G. Mitochondria and programmed cell death: back to the future. *FEBS Lett* 1996; **396**: 7-13

11 **Hengartner MO**. The biochemistry of apoptosis. *Nature* 2000; **407**: 770-776

12 **Desagher S**, Martinou JC. Mitochondria as the central control point of apoptosis. *Trends Cell Biol* 2000; **10**: 369-377

13 **Nauta RJ**, Tsimoyiannis E, Uribe M, Walsh DB, Miller D, Butterfield A. Oxygen-derived free radicals in hepatic ischemia and reperfusion injury in the rat. *Surg Gynecol Obstet* 1990; **171**: 120-125

14 **Liu X**, Kim CN, Yang J, Jemmerson R, Wang X. Induction of apoptotic program in cell-free extracts: requirement for dATP and cytochrome c. *Cell* 1996; **86**: 147-157

15 **Sola S**, Brito MA, Brites D, Moura JJ, Rodrigues CM. Membrane structural changes support the involvement of mitochondria in the bile salt-induced apoptosis of rat hepatocytes. *Clin Sci* 2002; **103**: 475-485

16 **Reichert AS**, Neupert W. Contact sites between the outer and inner membrane of mitochondria-role in protein transport. *Biochim Biophys Acta* 2002; **1592**: 41-49

17 **Xue L**, Borutaite V, Tolkovsky AM. Inhibition of mitochondrial permeability transition and release of cytochrome c by anti-apoptotic nucleoside analogues. *Biochem Pharmacol* 2002; **64**: 441-449

18 **Siskind LJ**, Kolesnick RN, Colombini M. Ceramide channels increase the permeability of the mitochondrial outer membrane to small proteins. *J Bio Chem* 2002; **277**: 26796-26803

19 **Skulachev VP**. Cytochrome c in the apoptotic and antioxidant cascades. *FEBS Lett* 1998; **423**: 275-280

20 **Marcocci L**, Marchi U, Salvi M, Milella ZG, Nocera S, Agostinelli E, Mondovi B, Toninello A. Tyramine and monoamine oxidase inhibitors as modulators of the mitochondrial membrane permeability transition. *J Membr Biol* 2002; **188**: 23-31

21 **Kim TS**, Jeong DW, Yun BY, Kim IY. Dysfunction of rat liver mitochondria by selenite: induction of mitochondrial permeability transition through thiol-oxidation. *Biochem Biophys Res Commun* 2002; **294**: 1130-1137

22 **Rodrigues T**, Santos AC, Pigoso AA, Mingatto FE, Uyemura SA, Curti C. Thioridazine interacts with the membrane of mitochondria acquiring antioxidant activity toward apoptosis–potentially implicated mechanisms. *Br J Pharmacol* 2002; **136**: 136-142

23 **Li P**, Nijhawan D, Budihardjo I, Srinivasula SM, Ahmad M, Alnemri ES, Wang X. Cytochrome c and dATP-dependent formation of Apaf-1/caspase-9 complex initiates an apoptotic protease cascade. *Cell* 1997; **91**: 479-489

24 **Green DR**, Reed JC. Mitochondria and apoptosis. *Science* 1998; **281**: 1309-1312

25 **Frey TG**, Mannella CA. The internal structure of mitochondria. *Trends Biochem Sci* 2000; **25**: 319-324

26 **Wakabayashi T**. Structural changes of mitochondria related to apoptosis: swelling and megamitochondria formation. *Acta Biochim Pol* 1999; **46**: 223-237

27 **Cave AC**, Collis CS, Downey JM, Hearse DJ. Improved functional recovery by ischaemic preconditioning is not mediated by adenosine in the globally ischaemic isolated rat heart. *Cardiovasc Res* 1993; **27**: 663-668

28 **Nguyen M**, Branton PE, Walton PA, Oltvai ZN, Korsmeyer SJ, Shore GC. Role of membrane anchor domain of Bcl-2 in suppression of apoptosis caused by E1B-defective adenovirus. *J Bio Chem* 1994; **269**: 16521-16524

29 **Decaudin D**, Geley S, Hirsch T, Castedo M, Marchetti P, Macho A, Kofler R, Kroemer G. Bcl-2 and Bcl-XL antagonize the mitochondrial dysfunction preceding nuclear apoptosis induced by chemotherapeutic agents. *Cancer Res* 1997; **57**: 62-67

30 **Castedo M**, Hirsch T, Susin SA, Zamzami N, Marchetti P, Macho A, Kroemer G. Sequential acquisition of mitochondrial and plasma membrane alterations during early lymphocyte apoptosis. *J Immunol* 1996; **157**: 512-521

31 **Zamzami N**, Susin SA, Marchetti P, Hirsch T, Gomez-Monterrey I, Castedo M, Kroemer G. Mitochondrial control of nuclear apoptosis. *J Exp Med* 1996; **183**: 1533-1544

32 **Marchetti P**, Castedo M, Susin SA, Zamzami N, Hirsch T, Macho A, Haeffner A, Hirsch F, Geuskens M, Kroemer G. Mitochondrial permeability transition is a central coordinating event of apoptosis. *J Exp Med* 1996; **184**: 1155-1160

33 **Zamzami N**, Marchetti P, Castedo M, Hirsch T, Susin SA, Masse B, Kroemer G. Inhibitors of permeability transition interfere with the disruption of the mitochondrial transmembrane potential during apoptosis. *FEBS Lett* 1996; **384**: 53-57

34 **Akao Y**, Maruyama W, Shimizu S, Yi H, Nakagawa Y, Shamoto-Nagai M, Youdim MB, Tsujimoto Y, Naoi M. Mitochondrial permeability transition mediates apoptosis induced by N-methyl(R) salsolinol, an endogenous neurotoxin, and is inhibited by Bcl-2 and rasagiline, N-propargyl-1(R)-aminoindan. *J Neurochem* 2002; **82**: 913-923

35 **Li S**, Zhao Y, He X, Kim TH, Kuharsky DK, Rabinowich H, Chen J, Du C, Yin XM. Relief of extrinsic pathway inhibition by the Bid-dependent mitochondrial release of Smac in Fas-mediated hepatocyte apoptosis. *J Bio Chem* 2002; **277**: 26912-26920

Edited by Zhu LH and Wang XL **Proofread by** Xu FM

PO Box 2345, Beijing 100023, China
Fax: +86-10-85381893
E-mail: wjg@wjgnet.com www.wjgnet.com

World J Gastroenterol 2004;10(13):1939-1942
World Journal of Gastroenterology
 ISSN 1007-9327

• CLINICAL RESEARCH •

Relationship between encephalopathy and portal vein-vena cava shunt: Value of computed tomography during arterial portography

Qian Chu, Zhen Li, Su-Ming Zhang, Dao-Yu Hu, Ming Xiao

Qian Chu, Su-Ming Zhang, Department of Neurology, Tongji Hospital, Tongji Medical College of Huazhong University of Science and Technology, Wuhan 430030, Hubei Province, China
Zhen Li, Dao-Yu Hu, Ming Xiao, Department of Radiology, Tongji Hospital, Tongji Medical College of Huazhong University of Science and Technology, Wuhan 430030, Hubei Province, China
Supported by the National Natural Science Foundation of China, No. 30070825
Correspondence to: Dr. Qian Chu, Department of Neurology, Tongji Hospital, Tongji Medical College of Huazhong University of Science and Technology, Wuhan 430030, Hubei Province, China. qianchu@163.com
Telephone: +86-27-83691562 **Fax:** +86-27-83612633
Received: 2003-07-17 **Accepted:** 2003-10-07

Abstract

AIM: To assess the value of computed tomography during arterial portography (CTAP) in portal vein-vena cava shunt, and analysis of the episode risk in encephalopathy.

METHODS: Twenty-nine patients with portal-systemic encephalopathy due to portal hypertension were classified by West Haven method into grade I(29 cases), grade II(16 cases), grade III(10 cases), grade IV(4 cases). All the patients were scanned by spiral-CT. Plane scans, artery phase and portal vein phase enhancement scans were performed, and the source images were thinly reconstructed to 1.25 mm. We reconstructed the celiac trunk, portal vein, inferior vena cava and their branches and subjected them to three-dimensional vessel analysis by volume rendering (VR) technique and multiplanar volume reconstruction (MPVR) technique. The blood vessel reconstruction technique was used to evaluate the scope and extent of portal vein-vena cava shunt, portal vein emboli and the fistula of hepatic artery- portal vein. The relationship between the episode risk of portal-systemic encephalopathy and the scope and extent of portal vein-vena cava shunt, portal vein emboli and fistula of hepatic artery- portal vein was studied.

RESULTS: The three-dimensional vessel reconstruction technique of spiral-CT could display celiac trunk, portal vein, inferior vena cava and their branches at any planes and angles and the scope and extent of portal vein-vena cava shunt, portal vein emboli and the fistula of hepatic artery- portal vein. In twenty-nine patients with portal-systemic encephalopathy, grade I accounted for 89.7% esophageal varices, 86.2% paragastric varices; grade II accounted for 68.75% cirsomphalos, 56.25% paraesophageal varices, 62.5% retroperitoneal varices and 81.25% dilated azygos vein; grade III accounted for 80% cirsomphalos, 60% paraesophageal varices, 70% retroperitoneal varices, 90% dilated azygos vein, and part of the patients in grades II and III had portal vein emboli and fistula of hepatic artery-portal vein; grade IV accounted for 75% dilated left renal vein, 50% paragallbladder varices, all the patients had fistula of hepatic artery- portal vein.

CONCLUSION: The three-dimensional vessel reconstruction technique of spiral-CT can clearly display celiac trunk, portal vein, inferior vena cava and their branches at any planes and angles and the scope and extent of portal vein-vena cava shunt. The technique is valuable for evaluating the episode risk in portal-systemic encephalopathy.

Chu Q, Li Z, Zhang SM, Hu DY, Xiao M. Relationship between encephalopathy and portal vein-vena cava shunt: Value of computed tomography during arterial portography. *World J Gastroenterol* 2004; 10(13): 1939-1942
http://www.wjgnet.com/1007-9327/10/1939.asp

INTRODUCTION

Portal-systemic encephalopathy is a kind of syndrome caused by portal hypertension and the construction of lateral branches, leading to a series of metabolic disorders, and is related to many neuron conduction mechanisms[1]. The main clinical manifestation is coma or the alteration of consciousness and behaviors. The syndrome has a close relationship with the construction of portal vein lateral branches. The three-dimensional vessel reconstruction technique of spiral-CT is the best method to display the vascular system[2]. Using this technique, we detected the scope and degree of portal vein-vena cava shunt, analyzed the risk of portal-systemic encephalopathy, and the relationship between them. This is of importance for doctors to make appropriate therapy plan and predict the disease' s prognosis.

MATERIALS AND METHODS

Selection of clinical portal-systemic encephalopathy patients

From April to October 2003, 480 patients were performed spiral-CT because of liver or portal vein diseases. Among them, 59 patients had portal-systemic encephalopathy, including 44 males and 15 females. They aged from 34 to 69 years, averaging 48.9 years. All the patients were diagnosed by clinical symptoms, laboratory examination and radiologic findings. They were classified by West Haven method into grade I (29 cases), grade II (16 cases), grade III (10 cases), grade IV (4 cases).

Based on West Haven method, encephalopathy was divided into 4 grades[3]. Grade I had absence of normal consciousness, euphoria or anxious, shortening of attention time, and other damage manifestations. Grade II had somnolence or indifference, mild disorder of time or space, mild change of personality, unsuitable behaviors, damage of subtraction. Grade III had lethargy, even half coma, reactions to word stimulation, confusion, obvious orientation disorder. Grade IV had coma (The patient had no reaction to word stimulation or harmful stimulation).

Scan technique of spiral-CT

Lightspeed *spiral*-CT (GE Corporation, U.S.A) performed high-speed scan. The parameters[4] were 120 KV, 250 mA, slice thickness 10 mm, pitch 1.375:1, and matrix 512×512. We

performed plane scan at first, and then enhancement scan. The dosage of Ultravist 300 (62.3 mg/mL) was 2 mL/kg, and the injection speed was 3.5 mL/s. The injection was executed by a hyperbaric injection syringe in elbow vein by bolus injection. We performed the artery phase and portal vein phase enhancement scans after the injection[5].

Three-dimensional vessel reconstruction technique of spiral-CT

Double-phase enhancement 10-mm thick images were reconstructed in CT[6], and the reconstructed slices were 1.25-mm thick. Then the images were pushed to the workstation. The three-dimensional blood vessel reconstruction was performed by ADW4.0 software. The reconstructed celiac trunk, portal vein, inferior vena cava and their branches were subjected to three-dimensional vessel analysis by volume rendering (VR) technique[7,8] and multiplanar volume reconstruction (MPVR) technique[9]. The VR technique could utilize any axis as basic axis and carry out 360-degree rotation so that we could observe the vessels in any degree[10]. The MPVR technique could perform any slice cross-sectional analysis[11]. We evaluated the scope and degree of portal vein-vena cava shunt, portal vein emboli and the fistula of hepatic artery- portal vein with the aid of source images and reconstructed images[12], and analyzed the relationship between the above-mentioned changes and the risk of portal-systemic encephalopathy[13,14].

RESULTS

Display effects of three-dimensional vessel reconstruction technique of spiral-CT for portal vein and its branches

Referring to Ishikawa vessel classification method and considering the patients' condition, we classified the portal vein-vena cava shunt into nine types, normally cirsomphalos, paragallbladder varices, lienorenal vein collateral branch opening, retroperitoneal varices, esophageal varices, paraesophageal varices, dilated azygos vein, paragastric varices and dilated left renal vein. At the same time, we observed whether there were portal vein emboli and fistula of hepatic artery- portal vein.

Assessment of hepatic artery- portal vein fistula

The VR technique could display the 3-dimensional vascular structures of celiac trunk, hepatic artery, superior mesenteric artery and their branches at any angle in artery phase. We could analyze the relationship between the arteries and portal vein. The VR technique could display artery- portal vein fistula very well. In the artery phase, the portal vein was visualized early, and the blood in portal vein was seen refluxed (Figure 1A). In portal vein phase, the portal vein was very slightly developed and portal vein-vena cava shunt emerged (Figure 1B).

Detection of portal vein emboli

In the portal vein phase, the VR technique could show the 3-dimensional vascular structures of portal vein and its branches at any angle. The enlarged portal vein and a non-flow region in the trunk could be seen (Figure 2). An image of portal vein was reconstructed by MPVR, and the emboli' s scope and size could be displayed at many angles (Figure 3).

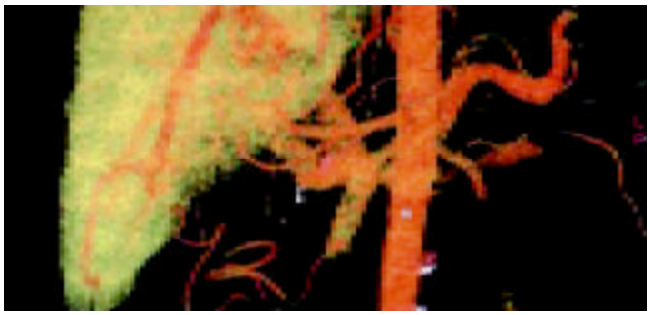

Figure 2 Enlarged portal vein and a non-flow region in the trunk (arrow).

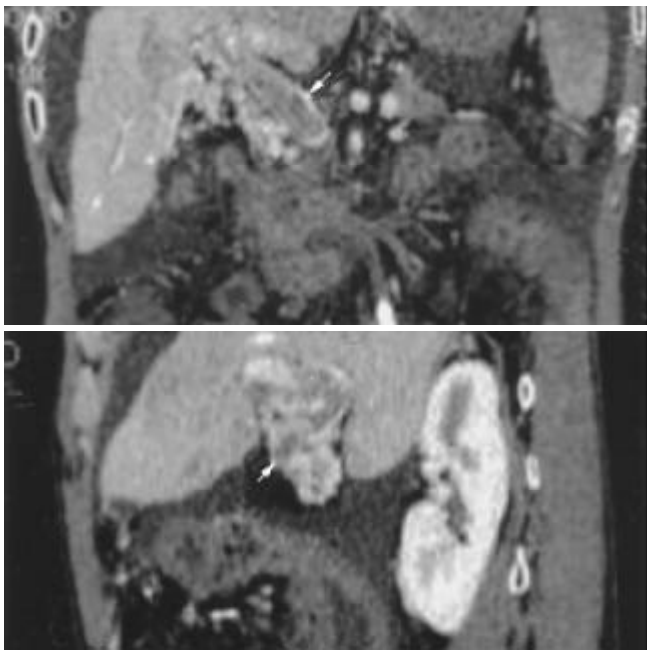

Figure 3 Image of portal vein reconstructed by MPVR. We could see the emboli's scopes and sizes at different planes (arrow).

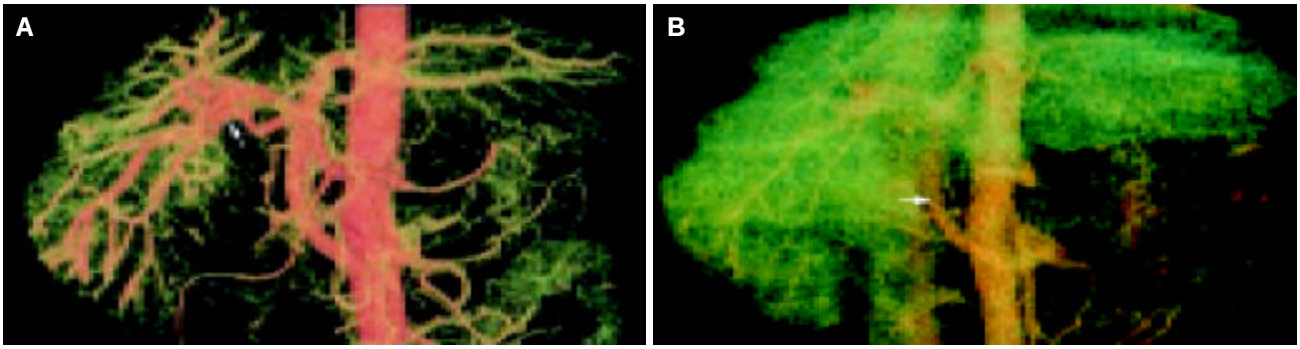

Figure 1 Portal vein in artery phase and in portal vein phase. A: Portal vein in artery phase. VR technique could display artery-portal vein fistula clearly in artery phase, the portal vein was visualized early, even portal vein blood up the stream. The arrow points the fistula aperture between the right hepatic artery and right portal vein. B: Portal vein in portal vein phase. The portal vein was very slightly developed and portal vein-vena cava shunt emerged in the portal vein phase.

Analysis of portal vein-vena cava shunt

The MPVR technique could perform any cross-section analysis. Combining the source images, we evaluated the scope and degree of portal vein-vena cava shunt, portal vein emboli and fistula of hepatic artery- portal vein on MPVR images (Figures 4A, B).

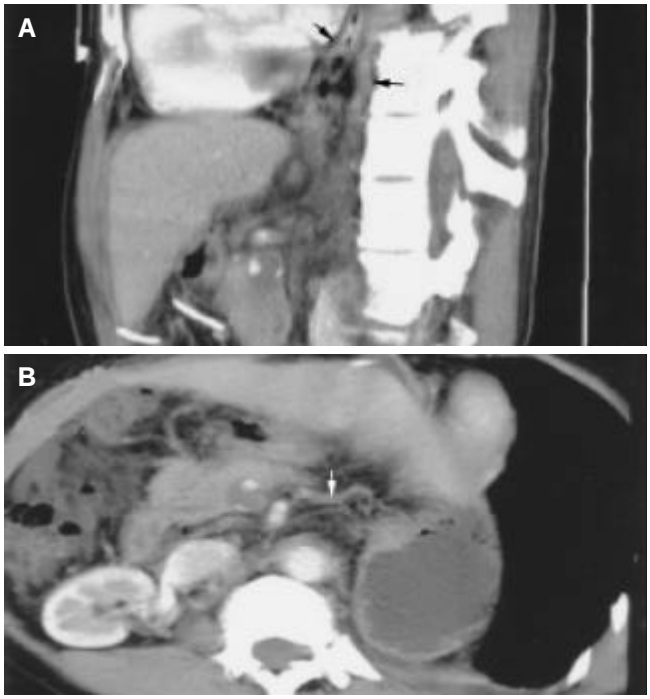

Figure 4 Portal vein-vena cave shunt, portal vein emboli and fistula of hepatic artery-portal vein on MPVR images. A: Paraesophageal varices and dilated azygos vein on MPVR image (arrow). B: Paragastric varices on MPVR image (arrow).

Assessment of portal vein-vena cava shunt in encephalopathy

Referring to Ishikawa vessel classification method, the patients were classified into 4 grades by West Haven method: grade I, 29 cases; grade II, 16 cases; grade III, 10 cases; grade IV, 4 cases. The main portal vein disorders are listed in Table 1.

Table 1 Assessment of portal vein-vena cava shunt in encephalopathy

	Grade I *n*(%)	Grade II *n*(%)	Grade III *n*(%)	Grade IV *n*(%)
Esophageal varices	26(89.7)	9(56.25)	8(80)	4 (100)
Paragastric varices	25(86.2)	11(68.75)	7(70)	3(75)
Cirsomphalos	12(41.3)	11(68.75)	8(80)	4(100)
Retroperitoneal varices	11(37.9)	9(56.25)	6(60)	4(100)
Paraesophageal varices	13(44.8)	10(62.5)	7(70)	3(75)
Dilated azygos vein	6(20.1)	13(81.25)	9(90)	2(50)
Dilated left renal vein	2(6.9)	1(6.25)	1(10)	3(75)
Paragallbladder varices	0(0)	1(6.25)	1(10)	2(50)
Hepatic artery- portal vein fistula	0(0)	3(18.75)	6(60)	4(100)
Portal vein emboli	2(6.9)	8(50)	7(70)	3(75)

As it shows in this table, esophageal varices and paragastric varices were common in grade I. Besides the varices in grade I patients, the patients in grades II and III had cirsomphalos, paraesophageal varices, retroperitoneal varices and dilated azygos vein, and some of them had portal vein emboli and hepatic artery- portal vein fistula. Among the patients in grade IV, dilated left renal vein and paragallbladder varices were usual, and all patients had hepatic artery- portal vein fistula.

DISCUSSION

Encephalopathy is a nervous system syndrome, originating from chronic liver disease and hepatic cirrhosis. It is associated with portal hypertension, hepatic artery- portal vein fistula, portal vein emboli, hyperammonemia and other metabolic disorders. It also has a close relationship with hypertension, portal vein-vena cava shunt and lateral branch formation. The three-dimensional vessel reconstruction technique of spiral-CT can display portal vein, its branches, the scope and degree of portal vein-vena cava shunt. The technique is valuable for evaluating the risk of encephalopathy.

Spiral-CT double-phase (artery phase, portal vein phase) scan and the reconstruction technique could display portal vein-vena cava shunt, hepatic artery- portal vein fistula and portal vein emboli[15]. Computed tomography during arterial portography (CTAP) was one of the best ways to show portal vein disorders[16]. Sixteen-slice spiral-CT had unique superiority for portal vein pictures[17]. To evaluate hepatic artery- portal vein fistula, early visualization of portal vein, enlargement of portal vein and blood of portal vein reflux were the main characteristics[18,19]. The double-phase images of volume rendering technique could not only display the position and size of fistulae, but also the diameter of portal vein and the extent of portal vein reflux. Reflux and fistulae would advance the portal hypertension, accelerate the portal vein-vena cava shunt, decrease the portal vein blood flow into the liver, and increase the opportunity for encephalopathy[20]. There was no hepatic artery- portal vein fistula in grade I patients (n=29), only 18.75% patients had fistulae in grade II (Table 1). However, in grades III and IV patients, 60% and 100% patients had fistulae. We can draw a conclusion that hepatic artery- portal vein fistula increases the risk of encephalopathy, and fistulae would aggravate encephalopathy or indicate the risk of encephalopathy.

On the assessment of portal vein emboli, the VR images in portal vein phase could show the vein because the blood flow was hindered by emboli or the complete obstruction of the trunk. The portal vein embolus was possibly one of the markers that hint the deterioration of encephalopathy[21,22]. Perhaps portal vein embolus could hinder blood flow into the liver[23]. It was believed that encephalopathy would appear if the blood flow of portal vein was less than 692 mL/min[24]. The portal vein embolus would accelerate portal hypertension and induce brain disorder at the same time.

Portal vein-vena cava shunts include[25,26] esophageal varices, paragastric varices[27], paraesophageal varices, cirsomphalos, paraumbilical veins[28,29], retroperitoneal varices (Retzius venous plexus), dilated azygos vein, dilated spleno- renal vein and stomach- renal vein, even internal iliac vein communication[30]. CT and barium meal had the same role in diagnosing esophageal varices and paragastric varices. But CT was more valuable than barium meal and esophagoscope in diagnosing other varices[31,32]. Spiral-CT scan is a kind of volume scan, and its merits include high speed and short reconstruction time. An examination of a patient' s liver can be finished in a breathholding. VR images could display large lateral branch circulation clearly, but the small branches unclearly. The multiplanar volume reconstruction (MPVR) technique could perform any slice cross-sectional analysis of the vessels and disclose their relationship with the surrounding tissues (Figures 2, 3), and esophageal varices, paragastric varices and azygos vein.

In a word, simple esophageal varices, paragastric varices and paraesophageal varices would not induce severe encephalopathy. However, the portal vein emboli, or hepatic artery- portal vein fistula, or wide portal vein-vena cava shunt, particularly the dilated left renal vein and paragallbladder varices, which may hint encephalopathy, would occur or deteriorate.

Not only would portal vein-vena cava shunt induce portal-systemic encephalopathy, but also the liver function of patients,

metabolic status[33] and diseases outside the liver[34]played a role. The relationship between them is still unclear. More work needs to be done. However, the three-dimensional vessel reconstruction technique of spiral-CT can display the celiac trunk, portal vein, inferior vena cava and their branches at any plane and from any angle, and show the scope and degree of portal vein-vena cava shunt. The technique is valuable for evaluating the episode risk in portal-systemic encephalopathy, and helpful for TIPSS.

REFERENCES

1 **Butterworth RF.** Hepatic encephalopathy: a neuropsychiatric disorder involving multiple neurotransmitter systems. *Curr Opin Neurol* 2000; **13**: 721-727

2 **Calculli L**, Casadei R, Amore B, Albini Riccioli L, Minni F, Caputo M, Marrano D, Gavelli G. The usefulness of spiral Computed Tomography and colour-Doppler ultrasonography to predict portal-mesenteric trunk involvement in pancreatic cancer. *Radiol Med* 2002; **104**: 307-315

3 **Ferenci P,** Lockwood A, Mullen K, Tarter R, Weissenborn K, Blei AT. Hepatic encephalopathy-definition, nomenclature, diagnosis, and quantification: final report of the working party at the 11th World Congresses of Gastroenterology, Vienna, 1998. *Hepatology* 2002; **35**: 716-721

4 **Francis IR,** Cohan RH, McNulty NJ, Platt JF, Korobkin M, Gebremariam A, Ragupathi K. Multidetector CT of the liver and hepatic neoplasms: effect of multiphasic imaging on tumor conspicuity and vascular enhancement. *Am J Roentgenol* 2003; **180**: 1217-1224

5 **Matoba M,** Yokota H, Yabuno K, Kuga G, Tinami H, Yamamoto I. Evaluation of two injection protocols by time-density curves for possible application to hepatic dynamic and upper abdominal CT angiography in MDCT: high concentration (350 mgI / ml) with conventional volume (100 ml) *vs* conventional concentration (300 mgI / ml) with larger volume (150 ml) and higher injection rate. *Nippon Igaku Hoshasen Gakkai Zasshi* 2003; **63**: 98-102

6 **Jayakrishnan VK,** White PM, Aitken D, Crane P, McMahon AD, Teasdale EM. Subtraction helical CT angiography of intra- and extracranial vessels: technical considerations and preliminary experience. *Am J Neuroradiol* 2003; **24**: 451-455

7 **Dudeck O,** Hoffmann KT, Wieners G, Pech M, Knollmann F, Felix R. Application of multislice detector spiral computed tomography to intracranial aneurysms: first clinical experience. *Radiologe* 2003; **43**: 310-318

8 **Byun JH,** Kim TK, Lee SS, Lee JK, Ha HK, Kim AY, Kim PN, Lee MG, Lee SG. Evaluation of the hepatic artery in potential donors for living donor liver transplantation by computed tomography angiography using multidetector-row computed tomography: comparison of volume rendering and maximum intensity projection techniques. *J Comput Assist Tomogr* 2003; **27**: 125-131

9 **Frohner S,** Wagner M, Schmitt R, Brunn J, Muller M, Christopoulos G, Coblenz G, Kerber S, Urbanski P. Multi-slice CT of aortocoronary venous bypasses and mammary artery bypasses: evaluation of bypasses and their anastomoses. *Rontgenpraxis* 2002; **54**: 163-173

10 **Fink C,** Hallscheidt PJ, Hosch WP, Ott RC, Wiesel M, Kauffmann GW, Dux M. Preoperative evaluation of living renal donors: value of contrast-enhanced 3D magnetic resonance angiography and comparison of three rendering algorithms. *Eur Radiol* 2003; **13**: 794-801

11 **Kuiper JW,** Geleijns J, Matheijssen NA, Teeuwisse W, Pattynama PM. Radiation exposure of multi-row detector spiral computed tomography of the pulmonary arteries: comparison with digital subtraction pulmonary angiography. *Eur Radiol* 2003; **13**: 1496-1500

12 **Van Straten M**, Venema HW, Streekstra GJ, Reekers JA, den Heeten GJ, Grimbergen CA. Removal of arterial wall calcifications in CT angiography by local subtraction. *Med Phys* 2003; **30**: 761-770

13 **Kobayashi Y,** Nakazawa J, Sakata M. Comparison of the depiction of pancreaticoduodenal arcades and dorsal pancreatic artery, using three-point scale with volume rendering (VR), maximum intensity projection (MIP), and shaded surface display (SSD). *Nippon Hoshasen Gijutsu Gakkai Zasshi* 2002; **58**: 297-300

14 **Piotin M,** Gailloud P, Bidaut L, Mandai S, Muster M, Moret J, Rufenacht DA. CT angiography, MR angiography and rotational digital subtraction angiography for volumetric assessment of intracranial aneurysms. An experimental study. *Neuroradiology* 2003; **45**: 404-409

15 **Nakayama Y,** Imuta M, Funama Y, Kadota M, Utsunomiya D, Shiraishi S, Hayashida Y, Yamashita Y. CT portography by multidetector helical CT: comparison of three rendering models. *Radiat Med* 2002; **20**: 273-279

16 **Kim HC,** Kim TK, Sung KB, Yoon HK, Kim PN, Ha HK, Kim AY, Kim HJ, Lee MG. CT during hepatic arteriography and portography: an illustrative review. *Radiographics* 2002; **22**: 1041-1051

17 **Calculli L,** Casadei R, Amore B, Albini Riccioli L, Minni F, Caputo M, Marrano D, Gavelli G. The usefulness of spiral Computed Tomography and colour-Doppler ultrasonography to predict portal-mesenteric trunk involvement in pancreatic cancer. *Radiol Med* 2002; **104**: 307-315

18 **Choi BI,** Lee KH, Han JK, Lee JM. Hepatic arterioportal shunts: dynamic CT and MR features. *Korean J Radiol* 2002; **3**: 1-15

19 **Lawler LP,** Fishman EK. Extrahepatic arterioportal venous fistula: multidetector CT and volume-rendered angiographic imaging. *Abdom Imaging* 2001; **26**: 616-618

20 **Haussinger D,** Kircheis G. Hepatic encephalopathy. *Schweiz Rundsch Med Prax* 2002; **91**: 957-963

21 **Federico P,** Zochodne DW. Reversible parkinsonism and hyperammonemia associated with portal vein thrombosis. *Acta Neurol Scand* 2001; **103**: 198-200

22 **Olson MM**, Ilada PB, Apelgren KN. Portal vein thrombosis. *Surg Endosc* 2003; **13**: 255-262

23 **Blei AT,** Cordoba J. Hepatic Encephalopathy. *Am J Gastroenterol* 2001; **96**: 1968-1976

24 **Del Piccolo F,** Sacerdoti D, Amodio P, Bombonato G, Bolognesi M, Mapelli D, Gatta A. Central nervous system alterations in liver cirrhosis: the role of portal-systemic shunt and portal hypoperfusion. *Metab Brain Dis* 2003; **18**: 51-62

25 **Watanabe A.** Portal-systemic encephalopathy in non-cirrhotic patients: classification of clinical types, diagnosis and treatment. *J Gastroenterol Hepatol* 2000; **15**: 969-979

26 **Luo JJ**, Yan ZP, Zhou KR, Qian S. Direct intrahepatic portacaval shunt: an experimental study. *World J Gastroenterol* 2003; **9**: 324-328

27 **Tsai HM,** Lin XZ, Chang YC, Lin PW, Hsieh CC. Hepatofugal flow on computed tomography of arterial portography: its correlation with esophageal varices bleeding. *Hepatogastroenterology* 2000; **47**: 1615-1618

28 **Gupta D,** Chawla YK, Dhiman RK, Suri S, Dilawari JB. Clinical significance of patent paraumbilical vein in patients with liver cirrhosis. *Dig Dis Sci* 2000; **45**: 1861-1864

29 **Lin J**, Zhou KR, Chen ZW, Wang JH, Wu ZQ, Fan J. Three-dimensional contrast-enhanced MR angiography in diagnosis of portal vein involvement by hepatic tumors. *World J Gastroenterol* 2003; **9**: 1114-1118

30 **Otake M,** Kobayashi Y, Hashimoto D, Igarashi T, Takahashi M, Kumaoka H, Takagi M, Kawamura K, Koide S, Sasada Y, Kageyama F, Kawasaki T, Nakamura H. An inferior mesenteric-caval shunt via the internal iliac vein with portosystemic encephalopathy. *Intern Med* 2001; **40**: 887-890

31 **Gulati MS,** Paul SB, Arora NK, Berry M. Evaluation of extrahepatic portal hypertension and surgical portal systemic shunts by intravenous CT portography. *Clin Imaging* 1999; **23**: 377-385

32 **Vignaux O,** Gouya H, Augui J, Oudjit A, Coste J, Dousset B, Chaussade S, Legmann P. Hepatofugal portal flow in advanced liver cirrhosis with spontaneous portosystemic shunts: effects on parenchymal hepatic enhancement at dual-phase helical CT. *Abdom Imaging* 2002; **27**: 536-540

33 **Haghighat N,** McCandless DW, Geraminegad P. The effect of ammonium chloride on metabolism of primary neurons and neuroblastoma cells *in vitro*. *Metab Brain Dis* 2000; **15**: 151-162

34 **Akhtar AJ,** Alamy ME, Yoshikawa TT. Extrahepatic conditions and hepatic encephalopathy in elderly patients. *Am J Med Sci* 2002; **324**: 1-4

Edited by Wang XL and Zhu LH **Proofread by** Xu FM

PO Box 2345, Beijing 100023, China
Fax: +86-10-85381893
E-mail: wjg@wjgnet.com www.wjgnet.com

World J Gastroenterol 2004;10(13):1943-1947
World Journal of Gastroenterology
 ISSN 1007-9327

• CLINICAL RESEARCH •

Role of curved planar reformations using multidetector spiral CT in diagnosis of pancreatic and peripancreatic diseases

Jing-Shan Gong, Jian-Min Xu

Jing-Shan Gong, Jian-Min Xu, Department of Radiology, Shenzhen People' s Hospital (Second Affiliated Hospital, School of Medicine, Jinan University), Shenzhen 518020, Guangdong Province, China
Supported by the Medical Research Fund of Guangdong Province, No. A2002634
Correspondence to: Dr. Jing-Shan Gong, Department of Radiology, Shenzhen People' s Hospital (Second Affiliated Hospital, School of Medicine, Jinan University), Shenzhen 518020, Guangdong Province, China. jshgong@sina.com.cn
Telephone: +86-755-25533018 **Fax:** +86-755-25618655
Received: 2003-12-10 **Accepted:** 2004-01-12

Abstract

AIM: To investigate the role of curved planar reformations using multidetector spiral CT (MSCT) in diagnosis of pancreatic and peripancreatic diseases.

METHODS: From October 2001 to September 2003, 47 consecutive patients with pancreatic or peripancreatic diseases, which were confirmed by operation, endoscopic retrograde cholangiopancreatography and clinical follow-up, were enrolled in this study. CT scanning was performed at a MSCT with four rows of detector. A set of images with an effective thickness of 1.0-2.0 mm and a gap of 0.5-1.0 mm (50% overlap) were acquired in all patients for post-processing. Curved planar reformations were carried out by drawing a curved line on transverse source images, coronal or sagittal multiplanar reformations according to certain anatomic structures (such as cholangiopancreatic ducts or peripancreatic vessels) and the position of lesion.

RESULTS: With thin collimation, MSCT could acquire high-quality curved planar reformations to display the profile of the whole pancreas, to trace the cholangiopancreatic ducts and peripancreatic vessels, and to show the relationship of lesions with pancreas and peripancreatic anatomic structures in one curved plane, which facilitates diagnosis and rapid communication of diagnostic information with referring physicians.

CONCLUSION: MSCT with thin collimation could be used to create high-quality curved planar reformations in evaluating pancreatic and peripancreatic diseases with pertinent anatomic information and relative pathologic signs to facilitate the diagnosis and enhance communication with the referring physician. Curved planar reformations can serve as supplements for transverse images in diagnosis and management of pancreatic and peripancreatic diseases.

Gong JS, Xu JM. Role of curved planar reformations using multidetector spiral CT in diagnosis of pancreatic and peripancreatic diseases. *World J Gastroenterol* 2004; 10(13): 1943-1947
http://www.wjgnet.com/1007-9327/10/1943.asp

INTRODUCTION

Pancreas is located in the retroperitoneum with a tortuous course, which is difficult for CT and MR to display the whole pancreas in one slice. There are abundant vessels around the pancreas. It is important to visualize these vessels and the cholangiopancreatic ducts for diagnosing and evaluating the local involvement of pancreatic and peripancreatic lesions. Curved planar reformations can delineate a curved path and display the whole course of pancreas in a single cross-section image according to a curved line drawn on the transverse source images, coronal or sagittal multiplanar reformations (MPR) from a three dimension (3-D) volumetric data set acquired by spiral CT[1,2]. They have been widely used to display vessels and evaluate vascular abnormalities in conjunction with CT angiography[1-7]. Recently the new techniques have been applied to evaluate the pancreas and bile duct system pathologically[8-11]. This article focuses on the role of curved planar reformations using MSCT in the diagnosis of pancreatic and peripancreatic diseases.

MATERIALS AND METHODS

Patients

From October 2001 to September 2003, 47 consecutive patients (21 female and 26 male, age range: 13-72 years, mean age: 53 years) with pancreatic or peripancreatic diseases, which were confirmed by operation (*n*=18), endoscopic retrograde cholangiopancreatography (ERCP) (*n*=6) and clinical follow-up (*n*=23), were enrolled in this study. The diseases included pancreatic carcinoma (*n*=9), cystadenoma (*n*=3), neuroendocrine tumor (*n*=4), chronic pancreatitis with pseudocyst (*n*=16), real cyst of pancreas (*n*=1), choledochal cyst (*n*=2), ampullary carcinoma (*n*=3), choledocholithiasis (*n*=5), duodenal diverticulum (*n*=1), peripancreatic adenopathy (*n*=3) and splenic arterial aneurysm (*n*=1).

CT imaging

CT scans were performed with a MSCT scanner (Toshiba Aquilion, Tokyo, Japan). Seven patients underwent plain scanning, 38 patients underwent both plain and enhanced scanning, and the other two patients a drip infusion CT cholangiography. A scanning with parameters of 120 kVp, 300 mA, 4×1-2 mm collimation, rotation time of 0.5 s, and a pitch of 5.5 was included in all patients during a breathhold of 10-15 s. In patients who underwent both plain and enhanced scanning, this protocol was obtained at the pancreatic parenchyma phase (a delay of 40 s after the beginning of intravenous injection of nonionic contrast media with an iodine content of 300 mg/mL [Omnipaque, Nycomed-Amersham, Shanghai] at 3 mL/s using a power injector). The CT cholangiographic image was acquired 60 min after intravenous drip infusion of iodipamide methyglucamine. A set of images with an effective thickness of 1-2 mm and a gap of 0.5-1.0 mm (50% overlap) was reconstructed and transmitted to workstation for post-processing.

Curved planar reformations

Curved planar reformations were obtained using a cursor to draw a curved line along a special anatomic structure on a stack of axial, sagittal, coronal section at a SGI workstation

(Alatoview 1.21) by an experienced radiologist who was familiar with the pancreatic and peripancreatic anatomic structures and had carefully reviewed all transverse source images. The operator was asked to adjust the trace of the cursor interactively to create several curved planes to display essential anatomic structures, such as cholangiopancreatic ducts and peripancreatic vessels, and the relationship of the lesion with those structures according to diagnostic and clinical need (Figure 1). The section thickness of curved plane will never be larger than the effective section thickness or smaller than the transverse pixel dimensions.

Figure 1 Curve drawn on a transverse image along the pancreatic duct in a patient with pancreatic adenocarcinoma.

RESULTS

With thinner collimation and overlap image data sets, high quality curved planar reformations were obtained in all the 47 patients, displaying the whole pancreas and tracing cholangiopancreatic ducts or peripancreatic vessels in a single cross-section image without any misregistration and steps artifacts (Figures 2-12). For the 20 pancreatic local lesions (9 cases of pancreatic adenocarcinoma, 3 cystic adenomas, 4 neuroendocrine tumors, 3 intrapancreatic pseudocysts and 1 real cyst of pancreas), curved planar reformations demonstrated that the whole or major portions of the lesion was located in the pancreatic parenchyma clearly, which made it easier to determine lesion' s location (Figures 2-5). Curved planar reformations, by tracing a certain vessel, such as the celiac artery, the superior mesenteric artery, the portal vein, could demonstrate changes in the caliber of the vessel and wall invasion, which was helpful for determining whether these vessels were involved and the length of involvement, as in the 9 patients with pancreatic adenocarcinoma and the 3 patients with ampullary carcinoma (Figures 6, 7). Combining with transverse images, curved planar reformations demonstrated 2 positivities and 1 false positivity in predicting respectability, 6 positivities in assessment of unresectability in 9 patients with pancreatic adenocarcinoma. The dilatation of cholangiopancreatic ducts in patients with chronic pancreatitis, pancreatic or ampullary carcinoma and peripancreas lymph nodes enlargement were well depicted on curved planar reformations (Figures 8,9). In 1 patient with pancreatic real cyst, the curved planar reformations after CT cholangiography revealed the beaded dilatation of pancreatic duct and the dilatation and stenosis of the common bile duct. The cyst lay beside the dilated common bile duct (Figure 4). In the 13 patients with pseudocyst beyond the pancreas and the 2 patients with choledochal cyst, curved planar reformations displayed the cystic lesion and the relationship of cysts with pancreas well. Stones' location and cholangiopancreatic ducts morphologic changes distal and proximal to obstruction were depicted on curved planar reformations in all patients with choledocholithiasis (Figure 10). The location and relationship with pancreas of peripancreatic enlarged lymph nodes were easily identified on curved planar reformations, which made differential diagnosis from pancreatic mass more simple (Figure 11). In 1 case of splenic arterial aneurysm, the dilatation of the artery was detected on curved planar reformations but missed on transverse source images due to its small diameter and dilatation along the z axis of CT imaging (Figure 12).

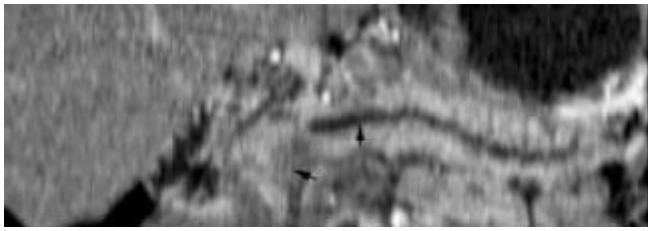

Figure 2 Curve obtained from the curved line on Figure 1 displayed the hypoattenuation tumor at the head of pancreas and the distal dilated pancreatic duct (arrow).

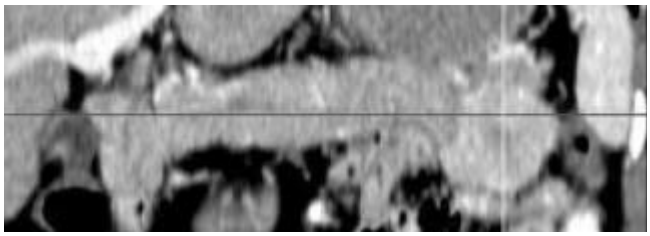

Figure 3 Neuroendocrine tumor of pancreas. Curved planar reformations during pancreatic parenchyma phase demonstrated the enhanced mass located in the tail of pancreas.

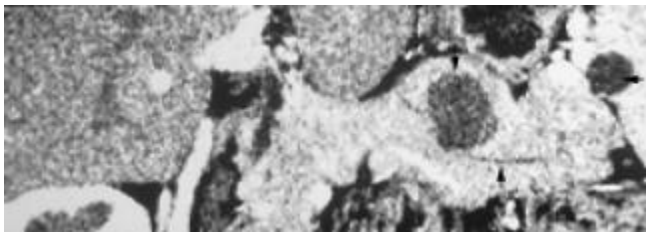

Figure 4 Neuroendocrine tumor of pancreas and peripancreatic pseudocyst. Curved plane showed a non-enhanced hypoattenuation mass located in the pancreatic parenchyma (arrow) and a pseudocyst at the port of spleen during the pancreatic parenchyma phase. The normal pancreatic duct was also well depicted (long arrow).

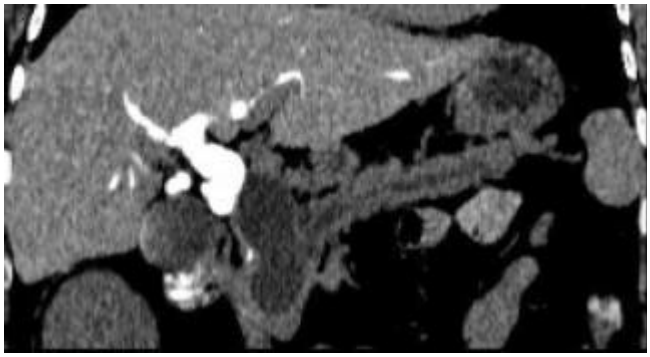

Figure 5 Real cyst of pancreas. Curved planar reformations obtained after CT cholangiography showed the dilatation and obstruction of bile duct system, and the beaded-like dilatation of pancreatic duct. The cyst located beside the common bile duct. There was no contrast media entrancing into cyst.

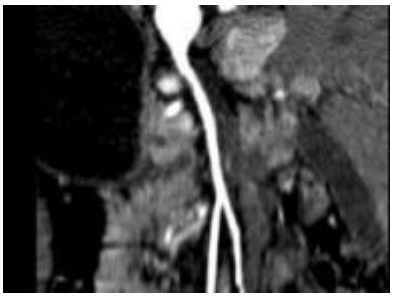

Figure 6 A curved plane tracing superior mesenteric artery of the same patient with Figure 1 and Figure 2 demonstrated the vessel was not involved. The tumor was confirmed to be resectable at operation.

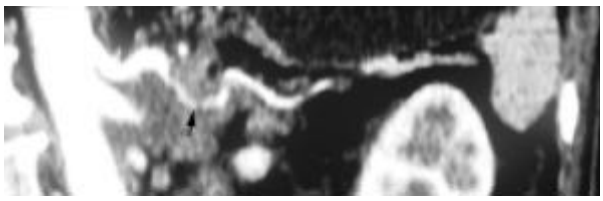

Figure 7 A curved plane tracing the celiac trunk and the splenic artery of a patient with pancreatic adenocarcinoma demonstrated the irregular stricture (arrow).

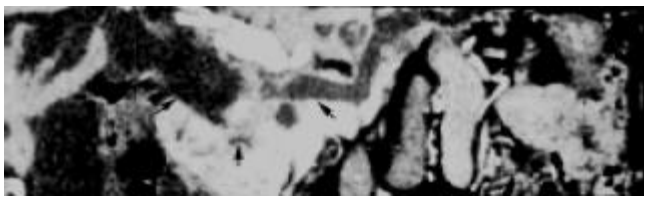

Figure 8 Ampullary carcinoma. Curved planar reformations depicted a low attenuation mass around the pancreatic head and the dilatation of both bile duct (arrow) and pancreatic duct (long arrow).

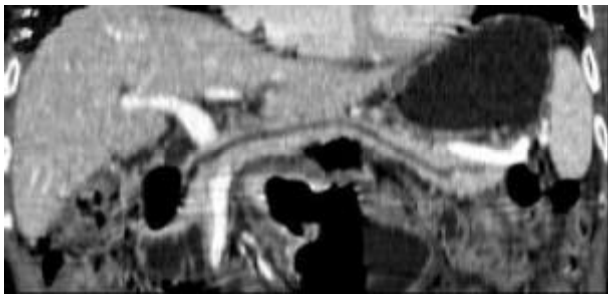

Figure 9 Gastric cancer with peripancreatic adenopathy. Curved planar reformations depicted the dilatation of the pancreatic duct.

Figure 10 Choledocholithiasis of common bile duct. Curved plane displayed the dilatation of the bile duct system and the pancreatic duct. The location of stones was depicted clearly.

Figure 11 Peripancreatic adenopathy. Curved planar reformations showed several enlarged lymph nodes located at the pancreatic head.

Figure 12 Splenic artery aneurysm. Curved planar reformations depicted the local dilatation of splenic artery (arrow).

DISCUSSION

Computed tomography (CT) is the most frequently used imaging modality for the evaluation of patients with suspected pancreatic and peripancreatic diseases, especially for diagnosing and staging pancreatic adenocarcinoma[12-17]. In detection and staging of pancreatic ductal adenocarcinoma, CT had a sensitivity of more than 90% and a positive predictive value in the range of 96% to 100% for determining surgical unresectability[9,12-14]. In determining resectability, the accuracy of CT remained low with positive predictive values ranging from 53% to 79% due to underestimation of vascular invasion and failure to detect small peritoneal and liver metastases[9,12,14]. The introduction of MSCT and the development of three-dimensional (3D) imaging software have significantly improved the ability of CT to image the pancreas and evaluate a wide range of pancreatic and peripancreatic pathology[8-11,17,18].

One major advantage of MSCT over single-detector spiral CT is substantial improvement in the speed of scan acquisition, which permits routine use of very thin collimation covering a large region during breath-hold to acquire volumetric data sets with high resolution along all three axes, especially along z axis, even with isotropic image[9,10,18,19]. The improvement of resolution along the z axis is very helpful for generating high quality multiplanar reformations (MPR) and 3D images. Curved planar reformations are a special form of MPR; which depict the cross-section profile along any curved line the operator draws from the volumetric data sets to trace the course of an anatomic structure. The plane presents results in a 2D image that displays the entire course of the anatomic structure[9]. Thus the techniques are very useful in displaying a complex anatomic structure with a tortuous course. They can delineate the curved vascular structure and display its whole course in one cross-section image. Therefore, curved planar reformations were used to display vessels and evaluate their abnormality[2-7]. This provided a convenient and fast review method for radiologists and an effective format for communicating the pertinent findings to referring physicians. These techniques were especially useful in evaluating those vessels, such as the

carotid siphon, which has a tortuous course and is surrounded by complex bony structures and thus the maximal intensity projection (MIP) and 3D images were difficult to depict them[5]. Recently, the application of curved planar reformations in the pancreatic and bile duct system showed that these techniques could provide helpful unique anatomic information, highlight critical anatomic and pathologic relationships, which were useful for surgical planning[8-11]. The other advantage of curved planar reformations was that the referring physicians could review a few curved planes to acquire critical information instead of reviewing a large number of images in great detail, which enhanced rapid communication[8].

In the present series, curved planar reformations using MSCT were performed in 47 patients with pancreatic and peripancreatic diseases. With thin collimation and overlap reconstruction, high quality curved planar reformations were obtained in all the patients displaying the whole tortuous pancreas in one cross-section image, tracing critical surrounding anatomic structures, such as cholangiopancreatic ducts and peripancreatic vessels, or highlighting relationships of the lesion with essential anatomic structures. All these were helpful for determining the lesion' s location and evaluating its invasion to surrounding anatomic structures. The latter was important to determining the resectability of pancreatic ductal adenocarcinoma. In 9 patients with pancreatic carcinoma, curved planar reformations tracing critical peripancreatic vessels could not only demonstrate the vascular involvement of tumor, but also depict the length of the affected segment. Although one study showed that curved planar reformations were equivalent to transverse images in the detection of pancreatic tumors and determination of surgical resectability[10], we did not assess the resectability according to curved planar reformations only due to their operator dependence, which wound be discussed later. In this series, by combination of curved planar reformations with transverse images, 2 positivities and 1 false positivity in predicting resectability and 6 positivities in determining unresectability in 9 patients with pancreatic adenocarcinoma were obtained. Whether it would improve the accuracy of staging of pancreatic adenocarcinoma by combining curved planar reformation with transverse images was not carried out in this study due to the small sample size of pancreatic carcinoma, which was one limitation of this study. In one case of pancreatic real cyst, curved planar reformations after CT cholangiography demonstrated the beaded dilatation of pancreatic duct and the dilatation and obstruction of the bile duct system. The relationship of the cystic lesion with the pancreatic and bile duct system was depicted clearly. All these could provide guides for operation, although a correct diagnosis was not acquired before operation. For the peripancreatic lesions, such as peripancreatic adenopathy, ampullary carcinoma, duodenal diverticulum and pseudocysts, curved planar reformations depicted the changes of the bile duct system and pancreatic duct, and relationships of lesions with surrounding important anatomic structures, which were helpful for making diagnostic and treatment strategies. Direct display of morphologic changes of bile duct system and stones location in curved planar reformations would be very useful for surgical planning, especially for endoscopic management of choledocholithiasis. With their advantage in demonstrating vascular abnormality, curved planar reformations displayed the small splenic arterial aneurysm easily in this series although it was missed in transverse images. On the one hand, it needs the operator interactively to adjust the path of cursor and work intensively to generate proper curved planar reformations with highlight important diagnostic information. On the other hand, several curved planes may transfer the important information to referring physicians. This reduces the referring physicians' burden to review all the transverse images for useful information.

One limitation of curved planar reformations is that they are exceedingly operator-dependent. Improper path of the cursor may generate spurious stenoses of cholangiopancreatic ducts and vessels, distort the anatomic structures or cause important lesion missed. Therefore, the operator should be familiar with the anatomy of pancreas and carefully review all transverse source images before beginning to draw the line. Although careful view of all transverse source images may be a time-consuming and tedious job, it is helpful to create proper curved planar reformations to highlight critical anatomic structures and pathologic signs. Due to this limitation, in this series a comparison with standard transverse images was not carried out. Curved planar reformations can serve as supplements in evaluating pancreatic and peripancreatic diseases while not a substitute. Recently, Raman *et al*.[20] developed an automated method to generate curved planar reformations with reduced time and effort. With the development of post-processing software, a well-trained radiologic technologists may generate curved planar reformations routinely.

In summary, MSCT with thin collimation can be used to generate high quality curved planar reformations for evaluating pancreatic and peripancreatic diseases. Our preliminary study showed that curved planar reformations could clearly depict essential anatomic structures and highlight critical anatomic information and pathologic signs in several cross-section images, which enhanced the rapid communication with referring physicians. Curved planar reformations can serve as supplements for transverse images in diagnosis and management of pancreatic and peripancreatic diseases.

ACKNOWLEDGEMENTS

We are grateful to Mr. Xiang-Peng Zheng, Ph.D candidate for radiological biology at University of Texas Health Science Center, for language review.

REFERENCES

1 **Rubin GD**, Dake MD, Semba CP. Current status of three-dimensional spiral CT scanning for imaging the vasculature. *Radiol Clin North Am* 1995; **33**: 51-70
2 **Achenbach S**, Moshage W, Ropers D, Bachmann K. Curved multiplanar reconstructions for the evaluation of contrast-enhanced electron beam CT of the coronary arteries. *Am J Roentgenol* 1998; **170**: 895-899
3 **Portugaller HR**, Schoellnast H, Tauss J, Tiesenhausen K, Hausegger KA. Semitransparent volume-rendering CT angiography for lesion display in aortoiliac arteriosclerotic disease. *J Vasc Interv Radiol* 2003; **14**: 1023-1030
4 **Takase K**, Sawamura Y, Igarashi K, Chiba Y, Haga K, Saito H, Takahashi S. Demonstration of the artery of Adamkiewicz at multi- detector row helical CT. *Radiology* 2002; **223**: 39-45
5 **Teasdale E**. Curved planar reformatted CT angiography: utility for the evaluation of aneurysms at the carotid siphon. *Am J Neuroradiol* 2000; **21**: 985
6 **Ochi T**, Shimizu K, Yasuhara Y, Shigesawa T, Mochizuki T, Ikezoe J. Curved planar reformatted CT angiography: usefulness for the evaluation of aneurysms at the carotid siphon. *Am J Neuroradiol* 1999; **20**: 1025-1030
7 **Prokesch RW**, Coulam CH, Chow LC, Bammer R, Rubin GD. CT angiography of the subclavian artery: utility of curved planar reformations. *J Comput Assist Tomogr* 2002; **26**: 199-201
8 **Nino-Murcia M**, Jeffrey RB Jr, Beaulieu CF, Li KC, Rubin GD. Multidetector CT of the pancreas and bile duct system: value of curved planar reformations. *Am J Roentgenol* 2001; **176**: 689-693
9 **Nino-Murcia M**, Jeffrey RB Jr. Multidetector-row CT and volumetric imaging of pancreatic neoplasms. *Gastroenterol Clin North Am* 2002; **31**: 881-896
10 **Prokesch RW**, Chow LC, Beaulieu CF, Nino-Murcia M,

Mindelzun RE, Bammer R, Huang J, Jeffrey RB Jr. Local staging of pancreatic carcinoma with multi-detector row CT: use of curved planar reformations initial experience. *Radiology* 2002; **225**: 759-765

11 **Nino-Murcia M**, Tamm EP, Charnsangavej C, Jeffrey RB Jr. Multidetector-row helical CT and advanced postprocessing techniques for the evaluation of pancreatic neoplasms. *Abdom Imaging* 2003; **28**: 366-377

12 **Tabuchi T**, Itoh K, Ohshio G, Kojima N, Maetani Y, Shibata T, Konishi J. Tumor staging of pancreatic adenocarcinoma using early- and late-phase helical CT. *Am J Roentgenol* 1999; **173**: 375-380

13 **Boland GW**, O'Malley ME, Saez M, Fernandez-del-Castillo C, Warshaw AL, Mueller PR. Pancreatic-phase versus portal vein-phase helical CT of the pancreas: optimal temporal window for evaluation of pancreatic adenocarcinoma. *Am J Roentgenol* 1999; **172**: 605-608

14 **O'Malley ME**, Boland GW, Wood BJ, Fernandez-del Castillo C, Warshaw AL, Mueller PR. Adenocarcinoma of the head of the pancreas: determination of surgical unresectability with thin-section pancreatic-phase helical CT. *Am J Roentgenol* 1999; **173**: 1513-1518

15 **Sheth S**, Hruban RK, Fishman EK. Helical CT of islet cell tumors of the pancreas: typical and atypical manifestations. *Am J Roentgenol* 2002; **179**: 725-730

16 **Demos TC**, Posniak HV, Harmath C, Olson MC, Aranha G. Cystic lesions of the pancreas. *Am J Roentgenol* 2002; **179**: 1375-1388

17 **McNulty NJ**, Francis IR, Platt JF, Cohan RH, Korobkin M, Gebremariam A. Multi–detector row helical CT of the pancreas: effect of contrast-enhanced multiphasic imaging on enhancement of the pancreas, peripancreatic vasculature, and pancreatic adenocarcinoma. *Radiology* 2001; **220**: 97-102

18 **Rydberg J**, Liang Y, Teague SD. Fundamentals of multichannel CT. *Radiol Clin North Am* 2003; **41**: 465-474

19 **Hu H**, He HD, Foley WD, Fox SH. Four multidetector-row helical CT: image quality and volume coverage speed. *Radiology* 2002; **215**: 55-62

20 **Raman R**, Napel S, Beaulieu CF, Bain ES, Jeffrey RB Jr, Rubin GD. Automated generation of curved planar reformations from volume data: method and evaluation. *Radiology* 2002; **223**: 275-280

Edited by Zhu LH and Chen WW **Proofread by** Xu FM

PO Box 2345, Beijing 100023, China
Fax: +86-10-85381893
E-mail: wjg@wjgnet.com www.wjgnet.com

World J Gastroenterol 2004;10(13):1948-1953
World Journal of Gastroenterology
 ISSN 1007-9327

• CLINICAL RESEARCH •

Miniature ultrasonic probes for diagnosis and treatment of digestive tract diseases

Guo-Qiang Xu, Yong-Wei Li, Yong-Mei Han, You-Ming Li, Wei-Xing Chen, Feng Ji, Jing-Hua Li, Qing Gu

Guo-Qiang Xu, You-Ming Li, Wei-Xing Chen, Feng Ji, Jing-Hua Li, Qing Gu, Department of Gastroenterology, First Affiliated Hospital, Medical School of Zhejiang University, Hangzhou 310003, Zhejiang Province, China
Yong-Wei Li, Yong-Mei Han, Department of Rheumatology, First Affiliated Hospital, Medical School of Zhejiang University, Hangzhou 310003, Zhejiang Province, China
Supported by the Initiative Fund for Scientific Research of Zhejiang Personnel Department for Returned Overseas Scholars, No. (2001)275
Correspondence to: Guo-Qiang Xu, Department of Gastroenterology, First Affiliated Hospital, Medical School of Zhejiang University, Hangzhou 310003, Zhejiang Province, China. xuguoqi@mail.hz.zj.cn
Telephone: 13957121569 **Fax:** +86-571-87236611
Received: 2003-12-23 **Accepted:** 2004-01-12

Abstract

AIM: To investigate the clinical value of miniature ultrasonic probes (MUPs) for the diagnosis and treatment of digestive tract diseases.

METHODS: Endoscopic ultrasonography (EUS) was performed for patients with its indications with 7.5-20 MHz MUPs and double-cavity electronic endoscope. According to the diagnosis of MUPs, patients who had indications of treatment received endoscopic resection or surgical excision. Postoperative histological results were compared with the preoperative diagnosis of MUPs. A few patients without endoscopic resection or surgical excision were periodically followed up with MUPs.

RESULTS: A total of 537 patients were examined by MUPs, of them, 256 were diagnosed with gastrointestinal submucosal lesions, 146 with pseudo-submucosal lesions, 50 with digestive tract cancers, 17 with peptic ulcer, 11 with cholecystolithiasis, 8 with chronic pancreatitis, and 2 with achalasia and 47 were diagnosed as normal. After MUPs examinations, 220 patients received endoscopic resection or surgical excision, and the postoperative histological results of 211 patients were completely consistent with the preoperative diagnosis of MUPs. The diagnostic accuracy of MUPs was 95.9%. The result of follow-up with MUPs indicated that gastrointestinal leiomyoma, lipoma, phlebangioma and cyst were unchanged within 1-2 years. The patients who received endoscopic resection or centesis did not have any complications.

CONCLUSION: MUPs are of value in diagnosing gastrointestinal submucosal lesions, staging of digestive tract cancers and biliary-pancreatic diseases. They play a very important role in making therapeutic plans.

Xu GQ, Li YW, Han YM, Li YM, Chen WX, Ji F, Li JH, Gu Q. Miniature ultrasonic probes for diagnosis and treatment of digestive tract diseases. *World J Gastroenterol* 2004; 10(13): 1948-1953
http://www.wjgnet.com/1007-9327/10/1948.asp

INTRODUCTION

With the development of endoscopic ultrasonography (EUS) in clinical application, great progress has been made in diagnostic specificity and sensitivity of digestive tract diseases. EUS has usually been performed with a standard ultrasonic endoscope since the introduction of EUS with miniature ultrasonic probes (MUPs) in clinical diagnosis in the 1990s[1]. In August 2000, MUPs series were adopted in the First Affiliated Hospital of Zhejiang University and since then EUS with MUPs have been performed in 537 patients with digestive tract diseases. In the present article, the clinical values of MUPs in the diagnosis of gastrointestinal submucosal lesions, digestive tract cancers, and biliary-pancreatic diseases were analyzed and reported.

MATERIALS AND METHODS

Patients

A total of 537 patients presenting EUS indications were examined by MUPs. Their mean age was 54 years, ranging from 16 to 89 years. There were 280 men and 257 women.

Instruments

Instruments of EUS with MUPs included Fujino EG-410D double-cavity electronic gastroscope, Olympus-100 electronic colonoscope and Fujino SP-70 high-frequency echoprobe system. The frequency spectrum of the probes is between 7.5-20 MHz.

Methods

The preparation before MUPs examinations was the same as that before gastroscopy and colonoscopy examinations. Intramuscular injection of atropine or scopolamine could also be made. According to the information of the location and size of the lesion in gastrointestine gained by conventional endoscope examinations, microprobes of different frequencies were used. Patients who presented the indications of treatment accepted endoscopic resection or surgical excision according to the diagnosis by MUPs. Postoperative histological examination results of resected lesions were checked with the preoperative diagnosis by MUPs, and for patients with biliary-pancreatic diseases, diagnosis by MUPs was checked with that by ERCP and spiral CT examination. A few patients who did not receive endoscopic resection or surgical excision were periodically followed up with MUPs. The tolerance to EUS with MUPs and complications related to the examination in all these patients were investigated as well.

RESULTS

The results of MUPs examinations of the 537 suspected patients and the histopathologic diagnoses of some cases are summarized in Table 1. After examinations by MUPs, 256 patients were diagnosed with gastrointestinal submucosal lesions, 146 with pseudo-submucosal lesions, 50 with digestive tract cancer, with peptic ulcer, 11 with cholecystolithiasis, 8 with chronic pancreatitis, and 2 with achalasia and 47 were

diagnosed as normal. Among the 256 patients with gastrointestinal submucosal lesions, 162 (64.3%) were diagnosed with leiomyoma. Among the 162 patients with leiomyoma, 96 had esophageal leiomyoma. Of the 96 esophageal leiomyoma cases, 62 had lesions originating from muscularis mucosae and 34 had lesions originating from muscularis propria. Of the 57 gastric leiomyoma cases, 5 had lesions originating from muscularis mucosae and 52 had lesions originating from muscularis propria. Of the 5 duodenal leiomyoma cases, 1 was derived from muscularis mucosae and 4 from muscularis propria. All the 4 cases of colonic leiomyomas were derived from muscularis propria. After MUPs examinations, 122 patients with gastrointestinal true submucosal lesions accepted further treatment of endoscopic resection, surgical excision or puncture. The postoperative pathological diagnosis agreed with the preoperative MUPs diagnosis in 113 cases, thus the accuracy rate of the diagnosis by MUPs was 92.6%. Of the 162 patients with leiomyoma, 86 received either endoscopic resection or surgical excision. In 80 cases, the preoperative MUPs examination results were identical to the postoperative pathological diagnosis. However, the histological results of only 6 patients suffering from leiomyosarcoma (2 cases), gastric neurofibroma, esophageal tuberculosis granuloma, esophageal cyst gland retention, and colonic carcinoid were not consistent with the preoperative diagnoses by MUPs. The accuracy rate of the diagnosis by MUPs was 93%. Among the 146 patients with pseudo-submucosal lesions, 56 were diagnosed with polypus, 37 with inflammatory protruding and thickening of gastrointestinal mucosae, and 53 with extrinsic compression. The polypus and inflammatory protruding were confirmed by pathological biopsy, and the organs of extrinsic compression included spleen (15 cases), gallbladder (9 cases), aorta (8 cases), liver (6 cases), pancreas (4 cases), splenic vein (2 cases), lymph node (3 cases), thoracic vertebrae (2 cases) and mass with unknown nature (4 cases). Of the 11 patients with cholelithiasis, 7 were diagnosed with cholecystolithiasis, and 4 with choledocholith, which was not detected by surface type-B ultrasonogaphy but was confirmed by surgical operation or ERCP. Among the 8 patients with chronic pancreatitis, 4 were diagnosed with pseudocyst of pancreas, 1 with abscess of pancreas, 1 with distension of main pancreatic duct and 2 with pancreatic echo enhancement. Of the 8 patients, 4 were further confirmed by surgical operation or ERCP. The depth and healing of ulcer were verified by examination of EUS in 17 patients with peptic ulcer. According to the MUPs examination, 47 patients had normal stratification and structure of digestive tract. Of them, 5 patients were diagnosed with duodenal accessory papilla. In addition, some patients with gastrointestinal leiomyoma, lipoma, phlebangioma, cyst, inflammatory protruding or thickening were periodically followed up by MUPs, and the results of examinations showed no changes of these lesions in 1-2 years, but some lesions occurred such as inflammatory protruding, thickening and cyst shrank. All the patients could well tolerate this examination without serious complications such as bleeding, perforation and cardiac or pulmonary accident. No complications occurred in patients who received endoscopic resection or puncture.

DISCUSSION

The diameter of MUPs is small, so it can pass through the biopsy tube of a conventional endoscope and be placed anywhere inside the digestive tract to perform EUS. MUPs can reach or pass any small tubule or narrow space where the standard ultrasonic endoscope can not reach. MUPs do not cause compression on organ structures such as esophagus. MUPs can be easily operated. The frequency range of the probes was broad[1]. The significance and experiences in using EUS with MUPs for the diagnosis and treatment of digestive tract diseases are as the following.

Value of MUPs in diagnosing gastrointestinal submucosal lesions

Studies have shown that EUS is the best diagnostic method of gastrointestinal submucosal lesions. EUS could not only confirm if the lesion is a true submucosal lesion, but also ascertain accurately the size, location, origin and nature of the lesion[2-6]. We performed EUS with MUPs, and found 7.5-20 MHz MUPs was very important for the diagnosis of gastrointestinal true submucosal lesions. By this examination, we could

Table 1 MUPs diagnosis of 537 patients and histopathological diagnosis of 211 cases

Diseases	Esophagus	Stomach	Duodenum	Colon	Biliary tract	Pancreas	Total	Confirmation by pathological examination / operation
Leiomyoma	96	57	5	4			162	80 / 86
Leiomyosarcoma	3	4	1				8	8 / 8
Varicosis, Phlebangioma	27	13	2				42	3 / 3
Lipoma	1	4	1	2			8	3 / 3
Cyst	1	3	1	3			8	4 / 5
Brunner adenoma			5				5	4 / 4
Submucosal hematoma of esophagus	2						2	1 / 1
Ectopic pancreas		18					18	7 / 9
Lymphoma		3					3	3 / 3
Polyp	14	32	3	7			56	26 / 26
Inflammatory protruding and thickening	4	31	2				37	37 / 37
Pressure protruding lesions	10	38	3	2			53	8 / 8
Cancer	13	23		8		6	50	42 / 42
Cholecystolithiasis					11		11	11 / 11
Chronic pancreatitis						8	8	4 / 4
Peptic ulcer		16	1				17	
Achalasia	2						2	
Normal							47	
Total	173	242	24	26	11	14	537	211 / 220

determine the size, location, number and origin of the lesion. According to the ultrasonic characteristics of lesions, we could also distinguish the nature of different lesions[7-11]. For example, scanned by MUPs, gastrointestinal leiomyoma presented homogeneous and hypoechoic lesions with a clear margin around the hyperechoic wrapping area, which was derived from muscularis mucosae or muscularis propria (Figure1A). Gastrointestinal lipoma presented homogeneous and hyperechoic lesions with a distinct margin. The lesion often originated from submucosa (Figure 1B). Gastrointestinal cyst presented echoic lesions with a clear margin and enhancement behind. The lesion was often derived from submucosa (Figure 1C). Ectopic pancreas that often appeared in stomach or duodenum revealed non-homogeneous, middle-hyperechoic or patchy echoic lesions with a tubular structure and thickening of muscular layer. The lesions often originated from submucosa or muscularis propria (Figure 1D). Hemangioma and varicosis often appeared in gastric fundus and esophagus as echoic honeycomb-like lesions, and were easy to be deformed by compression. They mostly originated from mucosae or submucosae (Figure 1E). Our clinical research included not only these common submucosal lesions, but also leiomyosarcoma, lymphoma, carcinoid, neurofibroma, abscess, Brunner' s adenoma and hematoma, etc. Leiomyoma was the most common benign tumor in gastrointestinal submucosal lesions, accounting for 64.3% of the total gastrointestinal submucosal lesions. According to our clinical and pathological study on gastrointestinal leiomyoma, leiomyoma mainly occurred in esophagus and stomach, and the incidence in small intestine and colon was much lower than that in esophagus and stomach. The size and layer of the origin of esophageal leiomyoma were obviously different from those of gastric leiomyoma. The majority of esophageal leiomyomas originated from muscularis mucosae, and the size was <1.0 cm. Whereas most of the gastric leiomyomas originated from muscularis propria, and the size was 1-2 cm. Almost all the patients with gastrointestinal leiomyoma only had a single lesion, which often progressed slowly or had no change[12-14]. Among the 256 patients with gastrointestinal true submucosal lesions, 122 patients accepted further treatment of endoscopic resection, surgical excision, or puncture. The results showed that the size, layer, origin and number of the resected lesions were completely consistent with the diagnoses by MUPs. The nature of lesions was in agreement with preoperative diagnosis in 113 patients, and the diagnostic accuracy rate was 92.6%. Current studies with MUPs revealed its significant value in diagnosing gastrointestinal true submucosal lesions[15-19]. In patients who were periodically followed, gastrointestinal leiomyoma, lipoma, ectopic pancrease, cyst and hemangioma remained unchanged within 1-2 years, and no obvious clinical symptoms were observed. This observation indicates that those who are old and can not or do not want to accept further treatment, with lesions located at unusual sites, should be regularly followed up.

Value of MUPs in diagnosing gastrointestinal pseudo-submucosal lesions

Scanning MUPs can display clearly the layer structure and adjacent organs of gastrointestinal tract, so that peudo-submucosal or true submucosal protruding lesions could be accurately identified. According to our clinical experience, pseudo-submucosal lesions mainly included polypus, inflammatory protruding and pressure protruding lesions. Most gastrointestinal tract polypi and inflammatory protruding lesions could usually be diagnosed by conventional endoscopy. In a few patients, the color and structure of polypus or inflammatory prominence were similar to those of the surrounding normal mucosae, so we could not differentiate these lesions from submucosal lesions by conventional endoscopy. By MUPs, according to the origin, layer structure, and changes of the lesion echoes, we could diagnose the lesions easily. As to some superficial and small lesions, we could not only locate them, but also show the layer structure and relationship of the lesions and gastrointestinal wall more clearly by changing probes with different frequencies. Gastrointestinal tract polypus and inflammatory prominences all originated from epithelia and mucosae. Polypus presented homogeneous or non-homogeneous, middle-hyperechoic lesions without envelope (Figure 1F). The latter manifested thickening or loss of epithelia and mucosae, but the layer, structure and echo of the lesions were all normal (Figure 1G). Our diagnostic accuracy rate of extrinsic compression by MUPs was 100%, the same as that reported by Cletti (1993) and Pfau (2002)[20-21]. According to the complete layer and structure of gastrointestinal tract, the curved compression adventitia and the cross section images of surrounding tissues and structures, we could diagnose extrinsic compression easily by MUPs, just as by conventional ultrasonic endoscopy. At the same time, we could precisely distinguish most of the tissues and organs that caused the compression. Of the 537 patients, 53 were diagnosed with extrinsic compression, and the major organs that caused the compression were spleen (Figure 1H), gallbladder, aorta (Figure 1I), liver, pancreas, splenic vein, lymph node and thoracic vertebrae, etc. Furthermore, in most patients the compression was caused by the swelling and lesion of organs and tissues. So our clinical research confirmed the incomparable superiority of MUPs in diagnosing polypus, inflammatory protruding and extrinsic compression of gastrointestinal tract that are often difficult to be found out by conventional endoscopy.

Value of MUPs in diagnosing biliary-pancreatic diseases

When we performed EUS, we placed the ultrasonic probes in the gastrointestinal tract. Compared with surface ultrasonogaphy, the probe closer to biliary tract and pancreas could avoid interference of duodenum and gas, so the images of biliary-pancreatic diseases (especially lesions of the lower middle part of common bile duct and ampulla) taken by EUS were clearer than those taken by surface ultrasonography. According to the literature, the diagnostic sensibility and specificity of EUS for choledocholith were 91% and 100% respectively, which were much higher than those of surface ultrasonography and common CT examination, and similar to those of ERCP, but the complications of EUS were much fewer than those of ERCP[22,23]. In our study, 11 patients were diagnosed with cholelithiasis by a 7.5 MHz microprobe scan (Figure 1J, K). The calculi of the lower part of the common bile duct in 4 of the 11 patients were not detected by surface type B ultrasonography, but confirmed by ERCP or surgical operations. So MUPs are superior to surface ultrasonography and common CT for the diagnosis of calculus of the lower part of the common bile duct, and can greatly improve the diagnostic situations of common bile duct diseases. By MUPs, we could distinguish calculus from tumors in biliary tract by real-time observation and we could also observe the lesions of ampulla directly. Compared with surface ultrasonography, CT, and magnetic resonance cholangiopancreatography (MRCP), MUPs were much superior. Pancreas is deeply located, and its ultrasonic image may be influenced by abdominal gas, so ultrasonography has difficulty to examine it. By examinations with 7.5-12 MHz MUPs, 14 cases were diagnosed with pancreatic diseases. Of them, 8 cases had chronic pancreatitis, including 4 cases of pancreatic pseudocyst(Figure 1L), 1 case of abscess, 1 case of dilation of main pancreatic duct, and 2 cases of pancreatic echo enhancement. The results were consistent with those of spiral CT and ERCP. After examination by MUPs, 9 patients accepted surgical operations and the diagnoses were confirmed by pathologic examinations.

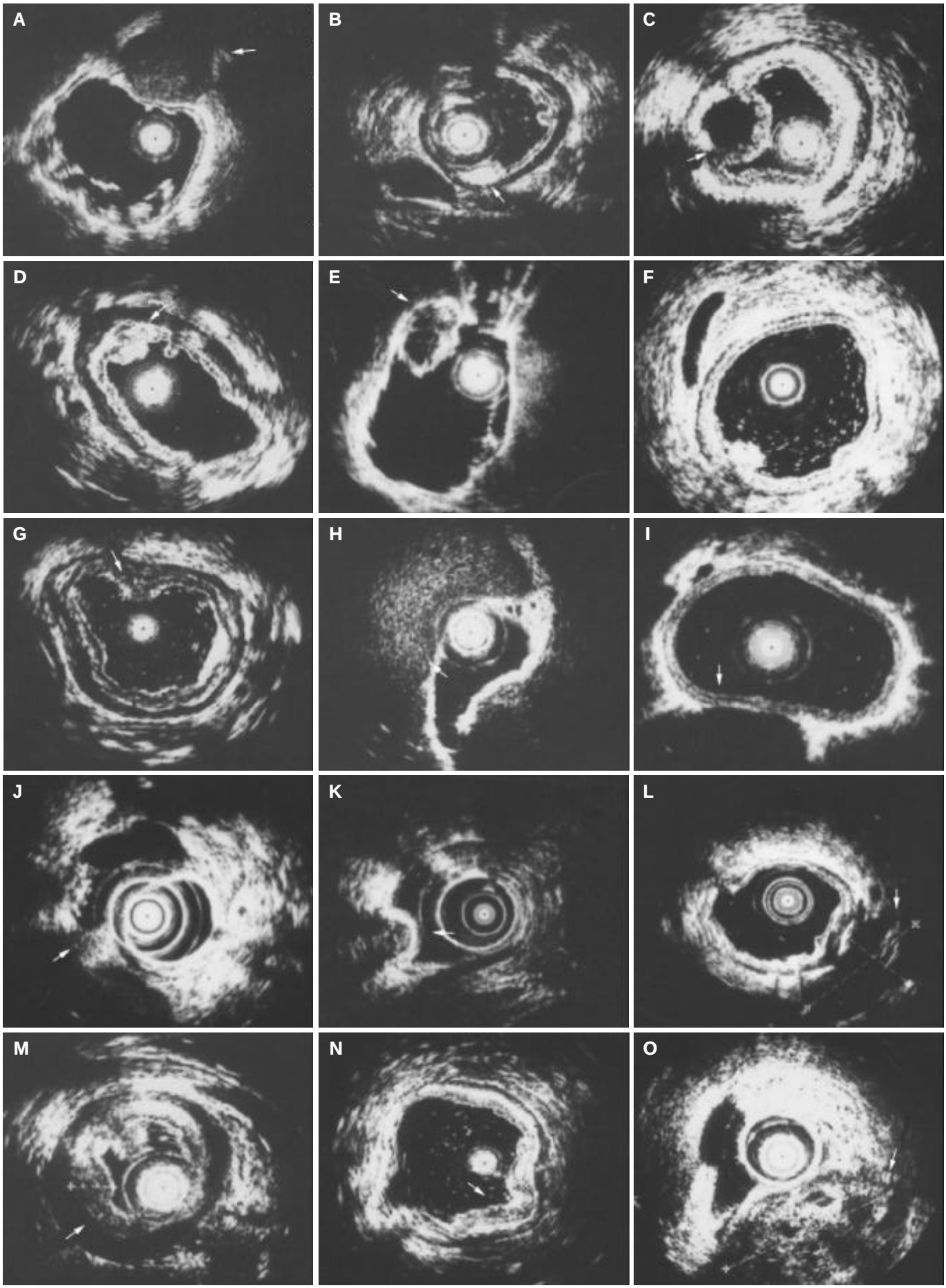

Figure 1 Lesions in digestive tract. A: Gastric leiomyoma, B: Gastric lipoma, C: Gastric cyst, D: Gastric ectopic pancreas, E: Gastric varicosis, F: Gastric polypi, G: Gastric inflammatory protruding, H: Gastric extrinsic compressiom (spleen), I: Esophageal extrinsic compression (aorta), J: Gallstone, K: Choledocholith, L: Pseudocyst of pancreas, M: Linitis plastica, N: Early gastric cancer, O: Pancreatic cancer.

On the basis of these results, we can make the conclusion that EUS with MUPs for pancreatic diseases is of diagnostic value. It can not only detect pancreatic duct, but also observe the changes of pancreatic parenchyma. Compared with ERCP, it was disadvantageous in displaying the full view of pancreatic duct, but it was advantageous in displaying the echo of pancreas, pancreatic calculus, and cyst. Furthermore, there were no ERCP-related complications in examinations by MUPs. So the diagnosis of pancreatic diseases by MUPs was effective, safe and convenient. Recently, there were reports about ultrasonography performed in biliary-pancreatic duct by MUPs[1,24]. It can greatly improves the diagnostic situation of common bile duct and pancreatic parenchymal micro-lesions and has become the best diagnostic method for pancreatic endocrine tumors.

Value of MUPs in diagnosing and TNM staging of digestive tract cancer

TNM staging of digestive tract cancers by EUS is generally accepted. The sensitivity and specificity of EUS for TNM staging of digestive tract cancers were obviously higher than those of surface ultrasonography, conventional endoscopy, CT and MRI, etc, but EUS was inferior to CT and MRI in the diagnosis of stage M cancers[25,26]. With 7.5-20 MHz microprobes, we researched the diagnosis, infiltrating depth and metastasis of surrounding lymph nodes in 50 patients with digestive tract cancers. The results showed the very important value of EUS with MUPs in diagnosing linitis plastica which could not be detected by conventional endoscopy. The growth pattern of this type of gastric cancer was unique. The cancer cells spread and infiltrated into submucosa. So it was hard to be detected by common biopsy. But it had special ultrasonic imaging changes which manifested obviously in diffuse thickening of gastric wall, lose of layer structure and hypoechoic lesion, etc. (Figure 1M). According to these ultrasonographic changes, 8 patients who were diagnosed with linitis plastica were confirmed by surgical operations. Investigations abroad have shown that the diagnostic accuracy rate of EUS for early stage gastrointestinal tract cancers was higher than that by any other examination[24]. Our study also demonstrated that the depth of infiltration and surrounding lymph node metastasis in digestive tract cancers could be diagnosed by MUPs. 12-20 MHz microprobes could display the infiltrating depth of tumors in gastrointestinal wall clearly. A 7.5 MHz probe could show infiltrations in adjacent tissues, organs and lymph nodes, then we could judge whether the cancer lesion was in early stage (Figure 1N) or advanced stage (Figure 1O). The diagnoses by MUPs in 42 patients who received surgical operation or endoscopic resection were consistent with the pathological diagnoses. It is concluded that MUPs can be applied to TNM staging of digestive tract cancers. MUPs are superior to standard ultrasonic endoscopy because it can be inserted into the narrow gastrointestinal tract tumor infiltration or into other small tubules.

Value of MUPs in guiding treatment of digestive tract diseases

Our clinical research demonstrated that MUPs could not only diagnose digestive tract diseases, but also provide treatment plans for these diseases[27-30]. MUPs had a very important diagnostic value in deciding the size, location, layer origin and nature of gastrointestinal submucosal lesions. By this examination, leiomyoma, lipoma and ectopic pancreas originating from above submucosae received endoscopic resection. Cysts derived from submucosa were treated by endoscopic puncture and aspiration. The procedure was effective, safe, economical and simple, and resulted in microtraumas only. Submucosal lesions originating from muscularis propria or adventitia were regarded as contraindications for endoscopic resection. The patients received surgical operation or thoracoscopy or laparoscopy. Patients who did not undergo, or were unfavorable to undergo operations were followed up periodically; therefore, complications such as perforation were avoided. MUPs helped us in ascertaining the indications of endoscopic resection in patients with early stage gastrointestinal tract cancer. They also helped us in formulating scientific, reasonable treatment plans for patients with median or advanced stage of cancer. With the modality, hemangioma and varicosis in gastrointestinal tract were diagnosed, unnecessary biopsy and resection were avoided, and massive hemorrage was prevented. The effective differentiation of inflammatory protruding from pressure protruding lesions helped formulate a correct treatment regimen and give up explorative operation. In addition, difficult biliary-pancreatic diseases could be diagnosed by MUPs; patients could be treated promptly and effectively. In conclusion, MUPs can greatly improve the accuracy rate of diagnosis and treatment of digestive tract diseases.

REFERENCES

1 **Menzel J,** Domschke W. Gastrointestinal miniprobe sonography: the current status. *Am J Gastroenterol* 2000; **58**: 605-616

2 **Varas Lorenzo MJ,** Maluenda MD, Pou JM, Abad R, Turro J, Espinos JC. The value of endoscopic ultrasonography in the study of submucosal tumors of the digestive tract. *Gastroenterol Hepatol* 1998; **18**: 121-124

3 **Rosch T,** Kaper B, Will U, Baronius W, Strobel M, Lorenz R, Ulm K. Accuracy of endoscopic ultrasonography in upper gastrointestinal submucosal lesions: a prospective multicenter study. *Scand J Gastroenterol* 2002; **37**: 856-862

4 **Shen EF,** Arnott ID, Plevris J, Penman ID. Endoscopic ultrasonography in the diagnosis and management of suspected gastrointestinal submucosal tumors. *Br J Surg* 2002; **89**: 231-235

5 **Gress F,** Schmitt C, Savides T, Faigel DO, Catalano M, Wassef W, Roubein L, Nickl N, Ciaccia D, Bhutani M, Hoffman B, Affronti J. Interobserver agreement for EUS in the evaluation and diagnosis of submucosal masses. *Gastrointest Endosc* 2001; **53**: 71-76

6 **Kameyama H,** Niwa Y, Arisawa T, Goto H, Hayakawa T. Endoscopic ultrasonography in the diagnosis of submucosal lesions of the large intestine. *Gstrointest Endosc* 1997; **46**: 406-411

7 **Massari M,** De Simone M, Cioffi U, Gabrielli F, Boccasanta P, Bonavina L. Endoscopic ultrasonography in the evaluation of leiomyoma and extramucosal cysts of the esophagus. *Hepatogastroenterology* 1998; **45**: 938-943

8 **Araki K,** Ohno S, Egashira A, Saeki H, Kawaguchi H, Ikeda K, Kitamura K, Sugimachi K. Esophageal hemangioma: a case report and review of the literature. *Hepatogastroenterology* 1999; **46**: 3148-3154

9 **Lu ZC,** Jing ZD. Submucosal tumors of the esophagus. Modern intralumen ultrasonics. *Beijing: Science Press* 2000: 174-182

10 **Busarini E,** Stasi MD, Rossi S, Silva M, Giangregorio F, Adriano Z, Buscarini L. Endosonographic diagnosis of submucosal upper gastrointestinal tract lesions and large fold gastropathies by catheter ultrasound probe. *Gstrointest Endosc* 1999; **49**: 184-191

11 **Hizawa K,** Matsumoto T, kouzuki T, Suekane H, Esaki M, Fujishima M. Cystic submucosal tumors in the gastrointestinal tract: endosonographic findings and endoscopic removal. *Endoscopy* 2000; **32**: 712-714

12 **Xu GQ,** Zhang BL, Li YM, Chen LH, Ji F, Chen WX, Cai SP. Diagnostic value of endoscopic ultrasonography for gastrointestinal leiomyoma. *World J Gastroenterol* 2003; **9**: 2088-2091

13 **Wang Y,** Sun Y, Liu Y, Wang Z. Transesophageal intraluminal ultrasonography in diagnosis and differential diagnosis of esophageal leiomyoma. *Zhonghua Yixue Zazhi* 2002; **82**: 456-458

14 **Zou XP.** Gastric leiomyoma. Modern Intralumen Ultrasonics. *Beijing: Science Press* 2000: 202-205

15 **Xu GQ,** Li YM, Chen WX, Ji F, Huang HD. Diagnostic value of transendoscopic miniature ultrasonic probes on esophageal and gastric submucosal lesions. *Zhonghua Chaosheng Yingxiangxue Zazhi* 2002; **11**: 188-189

16 **Koch J,** Halvorsen RA Jr, Levenson SD, Cello JP. Prospective com-

parison of catheter-based endoscopic sonography: evaluation of gastrointestinal-wall abnormalities and staging of gastrointestinal malignancies. *Clin Ultrasound* 2001; **29**: 117-124
17 **Catalano MF.** Endoscopic ultrasonography for esophageal and gastric mass lesions. *Gastroenterologist* 1997; **5**: 3-9
18 **Xu GQ**. Benign tumors of the esophagus. Modern Esophagology. *Shanghai: Shanghai Science And Technique Press* 1999: 268-273
19 **Futagami K,** Hata J, Haruma K, Yamashita N, Yoshida S, Tanaka S, Chayama K. Extracorporeal ultrasound is an effective diagnostic alternative to endoscopic ultrasound for gastric submucosal tumours. *Scand J Gastroenterol* 2001; **36**: 1222–1226
20 **Caletti G,** Fusaroli P. Endoscopic ultrasonography. *Endoscopy* 1993; **31**: 95-102
21 **Pfau PR,** Chak A. Endoscopic ultrasonography. *Endoscopy* 2002; **34**: 21-28
22 **Rosch T,** Meining A, Fruhmorgen S, Zillinger C, Schusdziarra V, Hellerhoff K, Classen M, Helmberger H. A prospective comparison of the diagnostic accuracy of ERCP, MRCP, CT and EUS in biliary strictrures. *Gastrointest Endosc* 2002; **55**: 870-876
23 **Kohut M,** Nowakowska E, Marek T, Kaczor R, Nowak A. Accuracy of linear endoscopic ultrasonography in the evaluation of patients with suspected common bile duct stones. *Endoscopy* 2002; **34**: 299-303
24 **Nakazama S.** Recent advances in endoscopic ultrasonography. *J Gastroenterol* 2000; **35**: 257-260
25 **Wakelin SJ,** Deans C, Crofts TJ, Allan PL, Plevris JN, Paterson-Brown S. A comparison of computerized tomography, laparoscopic ultrasound and endoscopic ultrasound in the preoperative staging of oesophagogastric carcinoma. *Eur J Radiol* 2002; **41**: 161-167
26 Hunt GC, Faigel DO. Assessment of EUS for diagnosing, staging and determining respectability of pancreatic cancer: a review. *Gastrointest Endosc* 2002; **55**: 232-237
27 **Izumi Y,** Inoue H, Kawano T, Tani M, Tada M, Okabe S, Takeshita K, Endo M. Endosonography during endoscopic mucosal resection to enhance its safety: a new technique. *Surg Endosc* 1999; **13**: 358-360
28 **kada N,** Higashino M, Osugi H, Tokuhara T, Kinoshita H. Utility of endoscopic ultrasonography in assessing the indications for endoscopic surgery of submucosal esophageal tumors. *Surg Endosc* 1999; **13**: 228-230
29 **Giovannini M,** Bernardini D, Moutardier V, Monges G, Houvenaeghel G, Seitz JF, Derlpero JR. Endoscopic mucosal resection (EMR): results and prognostic factors in 21 patients. *Endoscopy* 1999; **31**: 698-701
30 **Sun S,** Wang M, Sun S. Use of endoscopic ultrasound-guided injection in endoscopic resection of solid submucosal tumors. *Endoscopy* 2002; **34**: 82-85

Edited by Wang XL and Lei LM **Proofread by** Xu FM

PO Box 2345, Beijing 100023, China
Fax: +86-10-85381893
E-mail: wjg@wjgnet.com www.wjgnet.com

World J Gastroenterol 2004;10(13):1954-1957
World Journal of Gastroenterology
 ISSN 1007-9327

• CLINICAL RESEARCH •

Chronic liver disease questionnaire: Translation and validation in Thais

Abhasnee Sobhonslidsuk, Chatchawan Silpakit, Ronnachai Kongsakon, Patchareeya Satitpornkul, Chaleaw Sripetch

Abhasnee Sobhonslidsuk, Patchareeya Satitpornkul, Chaleaw Sripetch, Department of Medicine, Ramathibodi Hospital, Mahidol University, Bangkok, 10400, Thailand
Chatchawan Silpakit, Ronnachai Kongsakon, Department of Psychiatry, Ramathibodi Hospital, Mahidol University, Bangkok, 10400, Thailand
Correspondence to: Abhasnee Sobhonslidsuk, M.D., Department of Medicine, Ramathibodi hospital, 270 Praram 6 road, Bangkok 10400, Thailand. teasb@mahidol.ac.th
Telephone: +66-2-201 1387 **Fax:** +66-2-965 1769
Received: 2003-12-10 **Accepted:** 2004-01-16

Abstract

AIM: Quality of life (QOL) is a concept that incorporates many aspects of life beyond "health". The chronic liver disease questionnaire (CLDQ) was developed to evaluate the impact of chronic liver diseases (CLD) on QOL. The objectives of this study were to translate and validate a liver specific questionnaire, the CLDQ.

METHODS: The CLDQ was formally translated from the original version to Thai language with permission. The translation process included forward translation, back translation, cross-cultural adaptation and a pretest. Reliability and validity of the translated version was examined in CLD patients. Enrolled subjects included CLD and normal subjects with age- and sex-matched. Collected data were demography, physical findings and biochemical tests. All subjects were asked to complete the translated versions of CLDQ and SF-36, which was previously validated. Cronbach's alpha and test-retest were performed for reliability analysis. One-way Anova or non-parametric method was used to determine discriminant validity. Spearman's rank correlation was used to assess convergent validity. *P* -value <0.05 was considered statistically significant.

RESULTS: A total of 200 subjects were recruited into the study, with 150 CLD and 50 normal subjects. Mean ages (SD) were 47.3(11.7) and 49.1(8.5) years, respectively. The number of chronic hepatitis: cirrhosis was 76:74, and the ratio of cirrhotic patients classified as Child A:B:C was 37 (50%): 26(35%): 11(15%). Cronbach's alpha of the overall CLDQ scores was 0.96 and of all domains were higher than 0.93. Item-total correlation was >0.45. Test-retest reliability done at 1 to 4 wk apart was 0.88 for the average CLDQ score and from 0.68 to 0.90 for domain scores. The CLDQ was found to have discriminant validity. The highest scores of CLDQ domains were in the normal group, scores were lower in the compensated group and lowest in the decompensated group. The significant correlation between domains of the CLDQ and SF-36 was found. The average CLDQ score was strongly correlated with the general health domain of SF-36. (*P*=0.69: *P*=0.01).

CONCLUSION: The translated CLDQ is valid and applicable in Thais with CLD. CLDQ reveals that QOL in these patients is lower than that in normal population. QOL is more impaired in advanced stage of CLD.

Sobhonslidsuk A, Silpakit C, Kongsakon R, Satitpornkul P, Sripetch C. Chronic liver disease questionnaire: Translation and validation in Thais. *World J Gastroenterol* 2004; 10(13): 1954-1957
http://www.wjgnet.com/1007-9327/10/1954.asp

INTRODUCTION

The World Health Organization gave the definition of health as being not only the absence of disease and debility but also the presence of physical, mental and social well-being[1]. Quality of life (QOL) is a concept that incorporates many aspects of an individual's experience, general well-being, satisfaction, social and physical function[2]. By definition, QOL is subjective and multi-dimension. It can be influenced by socioeconomic factors, age, gender, presence of disease and treatment[2]. QOL examines how patients experience and perceive. Its results provide a basis for holistic view of the patient and complements the organic outcomes. QOL has been evaluated in a large number of chronic medical and gastrointestinal conditions, such as dyspepsia, inflammatory bowel diseases, liver diseases, *etc*.[3-7]. Well-developed and validated questionnaires have been used as instruments for QOL measurement. Generic and disease-specific instruments measure different aspects of QOL. It is encouraged to use both instruments in clinical research to gain substantial information[5]. Since the development of the first liver-specific questionnaire, the chronic liver disease questionnaire (CLDQ)[7], the QOL research in chronic liver diseases have been steadily reported[6,8-12]. Previous studies in Western patients showed that chronic liver disease (CLD) had negative impact on QOL, and QOL worsened as the severity of disease increased[8,9,12-14]. The study of QOL in gastrointestinal and liver diseases has hardly received attention in Asian population. Our study was aimed to translate and validate a disease specific questionnaire, the CLDQ, to be used in study of QOL in Thai population.

MATERIALS AND METHODS

Ethics

This study received ethics approval from the ethic committee of our hospital. All subjects provided written consent before participation.

Subjects

Between June 1 and September 31, 2003, 150 Thai patients with chronic liver diseases who attended gastroenterological clinic and 50 normal subjects were invited to participate in the study. Chronic liver diseases included chronic hepatitis and cirrhosis. Chronic hepatitis was defined by an elevation of serum transaminases above 1.5 times of upper normal limit for longer than 6 mo and cirrhosis by definition had biochemical and radiological findings consistent with cirrhosis[15]. The staging of cirrhosis was categorized according to Child-Pugh classification: Child (class) A, B and C[16]. Causes of chronic

liver disease were divided into viral hepatitis, alcohol, viral hepatitis combining with alcohol, non-alcoholic fatty liver (NAFLD) and others. Chronic liver disease due to alcohol was defined by the regular intake of alcohol (80 g/d in men, and 40 g/d in women)[17]. History of other medical illness was taken from medical records. Exclusion criteria were concomitant presence of hepatic encephalopathy, other active medical diseases, malignancy, being treated with antiviral agents and those who refused to give consent.

QOL instruments

CLDQ The CLDQ is the first liver specific instrument developed by Younossi *et al*.[7]. The CLDQ includes 29 items in the following domains: abdominal symptoms, fatigue, systemic symptoms, activity, emotional function and worry. The response of CLDQ results in 1 to 7 scales: ranging from "all of the time" to "none of the time"[7]. The original CLDQ was shown to have constructed validity from the studies in chronic liver diseases[7,12].

Translation of CLDQ After the translation permission was granted, the original version of CLDQ was translated into Thai according to the standardized guidelines proposed in 1993[18]. Forward translation from the original English version was performed independently by two Thai native speakers. Reconciliation of both forward versions was done subsequently. A native English speaker living in Thailand who understood Thai language quite well and did not have knowledge about QOL carried out back translation. The semifinal version derived from reconciliation of the original, back translation and forward translation. A pretest in 10 patients with chronic liver diseases was performed. The final version was obtained after the step of cross-cultural adaptation.

Assessment of translated CLDQ The CLDQ and SF-36 questionnaires were administered in 150 patients with chronic liver diseases and in 50 normal subjects. The permission to use the SF-36, a generic questionnaire, in this study was granted from QualityMetric Inc. The study version of SF-36 was previously tested and validated in Thai population[19]. CLDQ was repeated in 25 patients in 1-3 wk apart for test-retest analysis. Reliability was determined from Cronbach' s alpha (reliability coefficient) and test-retest. One-way Anova or non-parametric method was used to determine discriminant validity of scores among different stages of liver diseases. Spearman' s rank correlation was used to assess test-retest and convergent validity. A P value <0.05 was considered to be statistically significant.

RESULTS

Clinical and demographic data

One hundred and fifty patients with CLD and 50 normal subjects were enrolled into the study. Mean ages (SD) of CLD and controlled groups were 47.3(11.7) and 49.1(8.5) years (P=0.40). Of the 150 patients with CLD, 76(51%) had chronic hepatitis and the remainder had cirrhosis. Summarized clinical and demographic data are shown in Table 1. Patients with cirrhosis were older, more unemployed and had lower education levels than those with chronic hepatitis. Viral hepatitis and regular alcohol drinking were the most common causes of CLD. Hepatitis B virus was the major cause of chronic viral hepatitis in this study (68.1%).

Table 1 Clinical and demographic data

Characteristics	Normal (n=50)	Chronic hepatitis (n=76)	Cirrhosis (n=74)	P-value
mean±SD, yr	49.1 (8.5)	43.1 (12.6)	51.6 (8.9)	0.00
Men, n (%)	28 (56)	49 (64.5)	47 (63.5)	0.60
Married, n (%)	40 (81.6)	46 (62.2)	52 (81.3)	0.01
Education, n (%)[1]				
⩾Bachelor degree	20 (40)	29 (39.2)	10 (15.6)	0.004
Career, n (%)[1]				
- White collar	42 (91.3)	44 (69.8)	28 (50)	0.00
- Blue collar	1 (2.2)	4 (6.3)	9 (16)	
- Unemployed	3 (6.5)	15 (23.8)	19 (34)	
Financial burden (+), n (%)[1]	22 (44)	30 (40.5)	29 (45.3)	0.84
Etiologies, n (%)				
- Viral hepatitis		52 (68.4)	41 (55.4)	
- Alcohol		4 (5.3)	20 (27)	0.00
- Viral hepatitis and alcohol		2 (2.6)	7 (9.5)	
- Non-alcoholic fatty liver disease		11 (14.5)	2 (2.7)	
- Others		7 (9.2)	4 (5.4)	
Child-Pugh Classification, n (%)				
- Child A			37 (50)	
- Child B			26 (35)	
- Child C			11 (15)	

[1]Incomplete data.

Reliability

Measurement of internal consistency Cronbach' s alpha of overall scores was 0.96, which was above the acceptable level of 0.70 for comparison between groups[20]. Cronbach' s alpha of domains was higher than 0.93. Item-total correlation (omit that item) was above 0.45 (Table 2).

Test-retest Spearman' s rank correlation of average CLDQ was 0.88 (P=0.00) and domains of CLDQ was higher than 0.67 (P=0.00).

Validity

Discriminant validity The various stages of liver diseases in this study were rearranged as normal, compensated (= chronic hepatitis + Child A cirrhosis) and decompensated (= Child B and Child C cirrhosis) groups. A comparison of domain scores in different groups was performed. All domain scores of CLDQ and SF-36 significantly decreased from normal group to

Table 2 Reliability of CLDQ

CLDQ domains	Mean score (SD)	Cronbach's alpha (if item deleted)	Test-retest reliability	
			Correlation coefficient	P-value
Abdominal symptoms	5.3 (1.3)	0.95	0.85	0.00
Fatigue	4.7 (1.2)	0.94	0.90	0.00
Systemic symptoms	5.3 (1.1)	0.94	0.77	0.00
Activity	5.3 (1.3)	0.94	0.68	0.00
Emotional function	5.2 (1.1)	0.94	0.80	0.00
Worry	5.3 (1.4)	0.94	0.78	0.00
Average CLDQ	5.2 (1.1)	0.93	0.88	0.00

Table 3 Discriminant validity among different groups of patients (mean±SD)

CLDQ domains	Normal (*n*=50)	Compensated group (*n*=113)	Decompensated group (*n*=37)	*P*-value
Abdominal symptoms	5.8 (1.2)	5.3 (1.1)	4.6 (1.6)	0.00
Fatigue	5.4 (1.0)	4.6 (1.1)	4.0 (1.4)	0.00
Systemic symptoms	5.9 (0.9)	5.2 (1.1)	4.7 (1.1)	0.00
Activity	5.9 (1.0)	5.4 (1.1)	4.4 (1.5)	0.00
Emotional function	5.7 (0.9)	5.1 (1.1)	4.8 (1.4)	0.001
Worry	6.3 (0.8)	5.2 (1.4)	4.4 (1.6)	0.00
Average CLDQ	5.8 (0.8)	5.2 (1.0)	4.5 (1.2)	0.00
SF-36 domains				
Physical function	79.4 (14.0)	74.1 (20.2)	59.1 (21.5)	0.00
Role physical	79.5 (34.5)	59.3 (41.1)	34.5 (42.2)	0.00
Bodily pain	76.0 (14.3)	69.4 (22.8)	57.7 (23.8)	0.001
General health	68.6 (19.1)	51.3 (24.2)	42.0 (22.9)	0.00
Vitality	66.1 (14.2)	63.3 (16.3)	57.2 (14.7)	0.03
Social function	85.5 (16.6)	77.5 (20.0)	74.3 (22.0)	0.02
Role emotion	78.0 (36.0)	59.3 (42.9)	39.6 (45.7)	0.00
Mental health	75.2 (15.4)	69.5 (17.7)	65.7 (17.9)	0.03

Table 4 Correlations between CLDQ and SF-36

CLDQ domains	SF-36 domains							
	Physical function	Role physical	Bodily pain	General health	Vitality	Social function	Role emotion	Mental health
Abdominal symptoms	0.28[1]	0.32[1]	0.48[1]	0.49[1]	0.45[1]	0.35[1]	0.38[1]	0.53[1]
Fatigue	0.44[1]	0.52[1]	0.49[1]	0.61[1]	0.58[1]	0.54[1]	0.63[1]	0.59[1]
Systemic symptoms	0.48[1]	0.50[1]	0.63[1]	0.55[1]	0.49[1]	0.48[1]	0.54[1]	0.50[1]
Activity	0.49[1]	0.45[1]	0.47[1]	0.54[1]	0.47[1]	0.44[1]	0.50[1]	0.50[1]
Emotional function	0.38[1]	0.41[1]	0.46[1]	0.59[1]	0.62[1]	0.59[1]	0.54[1]	0.68[1]
Worry	0.38[1]	0.48[1]	0.41[1]	0.68[1]	0.53[1]	0.48[1]	0.49[1]	0.63[1]
Average CLDQ	0.47[1]	0.52[1]	0.56[1]	0.69[1]	0.61[1]	0.55[1]	0.60[1]	0.67[1]

[1]*P*=0.01.

compensated and decompensated groups (Table 3). The CLDQ was found to have good discriminant validity.

Convergen validity Each domain of CLDQ correlated with all domains of SF-36 with correlation coefficient (r) >0.27: *P*=0.01 as shown in Table 4. The average CLDQ score was strongly correlated with the general health domain of SF-36 (*P*=0.69: *P*=0.01).

Influence of disease severity on HRQOL

The CLDQ scores in Thai patients with CLD deteriorated as severity of chronic liver disease increased similarly to previous reports in Western patients[8,9,12-14]. However, we found that average CLDQ, emotional function and activity scores in chronic hepatitis were lower than those in Child A cirrhosis (5.2(1.1) *vs* 5.7(1.2), 5.0(1.1) *vs* 5.5(1.0) and 5.0(0.9) *vs* 5.4 (0.9), respectively; *P*-values were 0.04, 0.02 and 0.03.

DISCUSSION

The original CLDQ is a well-developed and validated disease-specific questionnaire for measuring QOL in CLD[7]. It consists of 29 items which are a suitable number for exploring QOL in patients who have a brief visit to a clinic[7]. It has 7 linkert scale type of answers[7]. To find a standardized disease-specific questionnaire for researches involving QOL in CLD, we translated the CLDQ from the original English to Thai versions by following the proposed guideline[18]. Simple translation of questionnaire from one language to the other without concerning language difference, culture context and lifestyle, jeopardizes the sensibility of the original version. The translated CLDQ used the language which even poorly educated Thais were able to understand the questionnaire meaning, and it was aimed for conceptual and semantic equivalences with the original concept. After the translation and cross-cultural adaptation, the reliability and validity of the translated version were proved to be maintained. Reliability of the CLDQ was confirmed from internal consistency and test-retest. Cronbach' s alpha of overall CLDQ was higher than 0.70, indicating that the translated version had acceptable reliability[20]. Chronic liver diseases greatly impacted QOL, which was confirmed by both generic and disease-specific questionnaires. We arranged chronic hepatitis and cirrhosis Child A into "compensated" group, and Child B and C cirrhosis into "decompensated" group according to the reserved function of the liver. The results from generic and disease-specific questionnaires were in agreement with the fact that a markedly decrease of QOL was seen in advanced stages of chronic liver diseases. On the other hand, it showed that the average CLDQ, activity and emotion function domains in chronic hepatitis were significantly lower than those in Child A cirrhosis. This finding may point out that chronic hepatitis had impairment in some parts of QOL more than Child A cirrhosis which may be a more stable condition. We could not compare the QOL between Child B and C cirrhosis due to the small sample size in both groups. The CLDQ domains correlated significantly with every domain of SF-36. The strongest correlation was seen in the relationship between the average CLDQ score and the general health domain of SF-36. The effect of other demographic and clinical factors on QOL of CLD was inconsistently reported. From a previous study, old age was inversely correlated with physical function of SF-36[8]. However, a subsequent study revealed that younger patients showed more impairment in QOL[9]. Several studies

revealed that chronic viral hepatitis, especially viral hepatitis C-related decreased QOL greater than cholestatic or alcoholic liver disease[8,12]. Other socioeconomic factors, e.g. education, career and financial status may affect QOL as well. The validated CLDQ is found to be a satisfactory tool for future research of QOL in Thai population.

ACKNOWLEDGEMENT

The authors would like to thank Thailand Research Fund (TRF) for the research grant, and Professor Anya Khanthavit for his guidance and comments.

REFERENCES

1 **WHO.** Constitution of the World Health Organization. In: World Health Organization. Handbook of basic documents. 5th ed. *Geneva: Palais des Nations* 1952: 3-20
2 **Glise H,** Wilklund I. Health-related quality of life and gastrointestinal disease. *J Gastroenterol Hepatol* 2002; **17**(Suppl): S72-S84
3 **Talley NJ,** Weaver AL, Zinsmeister AR. Impact of functional dyspepsia on quality of life. *Dig Dis Sci* 1995; **40:** 584-589
4 **Irvine EJ,** Feagan B, Rochon J, Archambault A, Fedorak RN, Groll A, Kinnear D, Saibil F, McDonald JW. Quality of life: a valid and reliable measure of therapeutic efficacy in the treatment of inflammatory bowel disease. *Gastroenterology* 1994; **106:** 287-296
5 **Younossi ZM,** Guyatt G. Quality -of- life assessments and chronic liver disease. *Am J Gastroenterol* 1998; **93:** 1037-1041
6 **Borgaonkar MR,** Irvine EJ. Quality of life measurement in gastrointestinal and liver disorders. *Gut* 2000; **47:** 444-454
7 **Younossi ZM,** Guyatt G, Kiwi M, Boparai N, King D. Development of a disease specific questionnaire to measure health related quality of life in patients with chronic liver disease. *Gut* 1999; **45:** 295-300
8 **Younossi ZM,** Boparai N, McCormick M, Price LL, Guyatt G. Assessment of utilities and health-related quality of life in patients with chronic liver disease. *Am J Gastroenterol* 2001; **96:** 579-583
9 **Marchesini G,** Bianchi G, Amodio P, Salerno F, Merli M, Panella C, Loguercio C, Apolone G, Niero M, Abbiati R. Factors associated with poor health-related quality of life of patients with cirrhosis. *Gastroenterology* 2001; **120:** 170-178
10 **Chong CA,** Gulamhussein A, Heathcote EJ, Lilly L, Sherman M, Naglie G, Krahn M. Health-state utilities and quality of life in hepatitis C patients. *Am J Gastroenterol* 2003; **98:** 630-638
11 **Bianchi G,** Loguercio C, Sgarbi D, Abbiati R, Brunetti N, De Simone T, Zoli M, Marchesini G. Reduced quality of life of patients with hepatocellular carcinoma. *Dig Liver Dis* 2003; **35:** 46-54
12 **Younossi ZM,** Boparai N, Price LL, Kiwi ML, McCormick M, Guyatt G. Health-related quality of life in chronic liver disease: the impact of type and severity of disease. *Am J Gastroenterol* 2001; **96:** 2199-2205
13 **Arguedas MR,** DeLawrence TG, McGuire BM. Influence of hepatic encephalopathy on health-related quality of life in patients with cirrhosis. *Dig Dis Sci* 2003; **48:** 1622-1626
14 **Cordoba J,** Flavia M, Jacas C, Sauleda S, Esteban JI, Vargas V, Estaban R, Guardia J. Quality of life and cognitive function in hepatitis C at different stages of liver disease. *J Hepatol* 2003; **39:** 231-238
15 **Leevy CM,** Sherlock S, Tygstrup N, Zetterman R. Disease of the liver and biliary tract. Standardization of nomenclature, diagnostic criteria and prognosis. *New York, Raven Press* 1994: 61-68
16 **Sherlock S,** Dooley J. Disease of the liver and biliary system. 10th ed. *Oxford: Blackwell Science* 1997: 135-180
17 **Sherlock S,** Dooley J. Disease of the liver and biliary system. 10th ed. *Oxford: Blackwell Science* 1997: 385-403
18 **Guillemin F,** Bombardier C, Beaton D. Cross-cultural adaptation of health-related quality of life measures: literature review and proposed guidelines. *J Clin Epidermiol* 1993; **46:** 1417-1432
19 **Kongsakon R**, Silpakit C. Thai version of the medical outcome study in 36 items short form health survey: an instrument for measuring clinical results in mental disorder patients. *Rama Med J* 2000; **23:** 8-19
20 **McDowell I,** Nevell C. Measuring health: a guide to rating scales and questionnaire. *New York: Oxford University Press* 1987

Edited by Wang XL **Proofread by** Xu FM

PO Box 2345, Beijing 100023, China
Fax: +86-10-85381893
E-mail: wjg@wjgnet.com www.wjgnet.com

World J Gastroenterol 2004;10(13):1958-1960
World Journal of Gastroenterology
 ISSN 1007-9327

• BRIEF REPORTS •

Comparison of three PCR methods for detection of *Helicobacter pylori* DNA and detection of *cag*A gene in gastric biopsy specimens

SI Smith, KS Oyedeji, AO Arigbabu, F Cantet, F Megraud, OO Ojo, AO Uwaifo, JA Otegbayo, SO Ola, AO Coker

SI Smith, Molecular Biology and Biotechnology Division, Nigerian Institute of Medical Research, P.M.B. 2013, Yaba, Lagos, Nigeria
KS Oyedeji, Microbiology Division, Nigerian Institute of Medical Research, P.M.B. 2013, Yaba, Lagos, Nigeria
AO Arigbabu, Department of Surgery, Obafemi Awolowo University Teaching Hospital Complex, Ile-Ife
F Cantet, F Megraud, Laboratoire de Bacteriologie, Bordeaux, Cedex, France
OO Ojo, AO Uwaifo, Department of Biochemistry, University of Ibadan, Ibadan, Nigeria
JA Otegbayo, SO Ola, Department of Medicine, University of Ibadan, Ibadan, Nigeria
AO Coker, College of Medicine, University of Lagos, Idi-Araba, Lagos, Nigeria
Supported by Inserm Fellowship, France, awarded to Dr. SI Smith
Correspondence to: Dr. SI Smith, Molecular Biology and Biotechnology Division, Nigerian Institute of Medical Research, P.M.B. 2013, Yaba, Lagos, Nigeria. stellaismith@yahoo.com
Fax: +2341-342-5171
Received: 2004-01-15 **Accepted:** 2004-04-14

Abstract

AIM: To comparatively evaluate PCR and other diagnostic methods (the rapid urease test and / or culture) in order to determine which of the three PCR methods (*ureA*, *glmM* and 26-kDa, SSA gene) was most appropriate in the diagnosis of *Helicobacter pylori* (*H pylori*) infection and also to evaluate the detection of a putative virulence marker of *H pylori*, the *cag*A gene, by PCR in biopsy specimens.

METHODS: One hundred and eighty-nine biopsy specimens were collected from 63 patients (three biopsies each) undergoing upper gastroduodenal endoscopy for various dyspeptic symptoms. The PCR methods used to detect *H pylori* DNA directly from biopsies were the *glmM*, 26-kDa, *ureA* and then *cag*A was used to compare the culture technique and CLO for urease with the culture technique being used as the gold standard.

RESULTS: Thirty-five percent of the biopsies were positive for *H pylori* DNA using the 3 PCR methods, while 68% of these were positive for the *cagA* gene. Twenty-four percent of the biopsies were negative for *H pylori* DNA in all PCR methods screened. The remaining 41% were either positive for *ureA* gene only, *glmM* only, 26-kDa only, or *ureA* + *glmM*, *ureA* + 26-kDa, *glmM* + 26-kDa. Out of the 35% positive biopsies, 41% and 82% were positive by culture and CLO respectively, while all negative biopsies were also negative by culture and *cagA*. Cag A+ infection was also predominantly found in *H pylori* DNA of the biopsies irrespective of the clinical diagnosis.

CONCLUSION: This method is useful for correctly identifying infections caused by *H pylori* and can be easily applied in our laboratory for diagnostic purposes.

Smith SI, Oyedeji KS, Arigbabu AO, Cantet F, Megraud F, Ojo OO, Uwaifo AO, Otegbayo JA, Ola SO, Coker AO. Comparison of three PCR methods for detection of *Helicobacter pylori* DNA and detection of *cag*A gene in gastric biopsy specimens. *World J Gastroenterol* 2004; 10(13): 1958-1960
http://www.wjgnet.com/1007-9327/10/1958.asp

INTRODUCTION

Culture has been for long the method of choice to detect infectious agents. However, for some organisms that are growing slowly like *Helicobacter pylori* (*H pylori*), it may take several days to obtain a result. Furthermore, culture is very much dependent on infrastructure conditions and in developing countries may be jeopardized by shortage in electrical power supply.

Recently, assays based on PCR technology have been developed to detect the presence of microbial DNA, including *H pylori* DNA, by using several gene targets directly from the biopsies[1-3]. The targets of these PCR methods include the urease A (*ureA*) gene[4], the 26-kDa species-specific antigen (SSA) gene[5] and the phosphosamine mutase (*glmM*) gene[3] to mention a few. It can be standardized to diagnose different agents. With such methods, all the experiments are not lost in case of shortage of power supply as they can be easily repeated. A similar approach has been applied in difficult environments such as in Russia.

The present study was therefore aimed (i) to comparatively evaluate PCR and other diagnostic methods (the rapid urease test and / or culture) in order to determine which of the three PCR methods was most appropriate in the diagnosis of *H pylori* infection, and to evaluate the detection of a putative virulence marker of *H pylori*, the *cag*A gene, by PCR in biopsy specimens.

MATERIALS AND METHODS

Patients

A total of 189 specimens from 63 patients (three biopsies each) undergoing upper gastroduodenal endoscopy for various dyspeptic symptoms were included in this study and 3 biopsies each were taken from the antrum of the patients for CLO test, culture and DNA, respectively.

The specimens were obtained from four centres in Nigeria: Lagos University Teaching Hospital (LUTH), Lagos; Mount Pleasant Medical and Endoscopy clinic, Ojuelegba, Lagos; University College Hospital, Ibadan; and Obafemi Awolowo Teaching Hospital Complex (OAUTHC), Ile-Ife.

Bacterial strains

Twelve *H pylori* isolates were used in this study: one *cag*A-positive reference strain (26695), and 11 clinical isolates.

Other strains tested included local isolates of *Campylobacter jejuni* (4), *C. coli* (4) and *C. fetus* (3). The strains were tested by PCR to assess the specificity of the primers.

DNA extraction from biopsies was by the method of Marais *et al*.[6]. Briefly, the biopsy samples were ground and centrifuged for 5 min at 10 000×g. The pellet was resuspended in 300 μL extraction buffer (20 mmol/L Tris-HCl, pH 8.0; 0.5% Tween 20) and proteinase K (0.5 mg/mL final concentration). The mixture was incubated at 56 ℃ for one hour after which

Table 1 Conditions for four different PCR methods

Target (reference), nucleotide (nt) positions amplified, and size of PCR products	Primer names and sequences	PCR conditions
26-kDa SSA gene (5),	Primer 3, 5'-TGGCGTGTCTATTGACAGCGAGC-3'	98 ℃, 10 min (1cycle);
nt 474–776, 303 bp	Primer 4, 5'-CCTGCTGGGCATACTTCACCAG-3'	92 ℃, 30 s; 68 ℃, 1 min (37cycles); 92 ℃, 30 s 68 ℃, 1 min; 72 ℃, 2 min (6 cycles)
Urease A gene (4),	HPU1, 5'-GCCAATGGTAAATTAGTT-3'	94 ℃, 1 min; 45 ℃, 1 min
nt 304 – 714, 411 bp	HPU2, 5'-CTCCTTAATTGTTTTTAC-3'	72 ℃, 1 min (35 cycles)
*glm*M gene (3)	Forward primer, 5'-AAGCTTTTAGGGGTGTTAGGGGTTT-3'	93 ℃, 1 min; 55 ℃, 1 min;
nt 784–1 077, 294 bp	Reverse primer, 5'-AAGCTTACTTTCTAACACTAACGC-3'	72 ℃, 1 min (35 cycles)
CagA gene	Primer 1, 5'-CCATGAATTTTTGATCCGTTCGG-3'	94 ℃, 1 min, 58 ℃, 1 min; 72 ℃, 1 min (40 cycles)
nt 394 bp	Primer 2, 5'-GATAACAGGCAAGCTTTTGAGGGA-3'	

the enzyme was inactivated by boiling for 10 min.

Five μL of DNA was used as the template for each PCR. Each sample was examined by four different PCRs. Primers used in this study were from, 26-kDa SSA gene (303 bp), urease A gene (411 bp), *glm*M gene (294 bp) and the *cag*A1 gene sequence (394 bp).

PCR reaction was carried out in a 50 μL volume in GeneAmp 9700 (Perkin Elmer). The primer sequences, conditions and sizes of these PCR methods are listed in Table 1.

Detection of amplified DNA products

A volume of seven μL of each PCR mixture was subjected to gel electrophoresis (1%) and ethidium -bromide staining for the detection of amplified DNA products.

RESULTS

Specificity of PCR assays with bacterial isolates

The specificity of PCR primers targeting *ure*A, *glm*M, 26-kDa and *cag*A gene was determined by testing 12 bacterial strains from related genus.

The 26-kDa PCR amplified the expected 303-bp fragment from the reference *H pylori* strain, while none from the other *Campylobacter* strains was amplified. Likewise, the *glm*M gene amplified the expected 294-bp fragment, *ure*A, 411-bp fragment and *cag*A, 394-bp fragment in *H pylori* reference and not in *Campylobacter* spp.

Detection of the three genes by PCR

Out of the 63 biopsies screened, 22(35%) were positive in all three PCR methods (26-kDa, *glm*M, *ure*A), 11 were positive for *ureA*, five for *glmM*, two for 26-kDa, two each for *ureA* and *glmM* and one each for *glmM*/ 26-kDa and *ureA* /26-kDa. Fifteen (24%) of the biopsies screened were negative for all three genes screened. Of these, 22 were positive for *H pylori* DNA, only nine (41%) were culture positive (Table 2). All negative biopsies from the 3 genes were negative by culture and CLO test. Two culture negative biopsies were positive in all three genes screened.

Detection of the cagA gene

Of the 22 biopsies that showed positive amplification in all three genes, 15(68%) were positive for the *cag*A gene. These comprised three biopsies from patients with cancer positive for the cagA gene. The patients with normal findings also had two out of three biopsies positive for the *cag*A gene. Out of the ten biopsies screened from patients with duodenitis or duodenal ulcer, only three (30%) were negative for the *cag*A gene (Table 3). All the biopsies that were positive for *cagA* were also positive for their corresponding isolates. All negative biopsies were also negative for *cag*A gene.

Table 2 Results of three PCR methods and cagA gene for the detection of *H pylori* from gastric biopsy

Biopsy (*n*=63)	*ureA*	*glmM*	26-kDa	Cag A +	Culture	CLO
22	+	+	+	15	9+, 13-	18+, 4-
11	+	-	-	-	11-	3+, 8-
5	-	+	-	-	5 -	3+, 2-
2	-	-	+	-	2 -	2-
4	+	+	-	-	4 -	2-, 2+
2	+	-	+	-	1+, 1-	2 +
2	-	+	+	-	1+, 1-	2 +
15	-	-	-	-	15 -	15 -

–: negative, +: positive.

Table 3 Positive and negative predictive values of three different PCR methods

Value	Results [(%, No. of samples with value / total No.)] for PCR method		
	ureA gene	*glmM* gene	26-kDa gene
Positive predictive[1]	91 (10 / 11)	91 (10 / 11)	100 (11 / 11)
Negative predictive[2]	44 (23 / 52)	56 (29 / 52)	67 (35 / 52)

[1]Compared with 11 culture- positive samples, [2]Compared with 52 culture- negative samples.

DISCUSSION

The *ureA* gene PCR had a very poor specificity in our study, as it amplified 29 of the 52 (npv=44%) culture negative biopsy specimens. This was contrary to the report by Lu *et al*.[1], but they concluded that the sensitivity was unsatisfactory and could be due to sequence polymorphism in the loci.

However, the positive predictive value was 91%. The 26-kDa gene primer amplified all 100%(11/11) (ppv=100%) of *H pylori* culture positive biopsy samples and produced 17 false positive results on 52 culture negative specimens (npv=67%) (Table 2).

The *glmM* gene PCR amplified 10 out of the 11 culture positive biopsy specimens (ppv, 91%), with a low sensitivity, as 23 of 52 culture negative biopsy specimens (npv, 56%) were amplified.

Lage *et al*.[2] however, reported in their study that there

were no false positive or negative biopsies amplified by the *glmM*. The reason for this is quite obvious as there are no problems of power outages in their environment and so it is easy to culture *H pylori* as a result of the steady power supply as opposed to our environment where constant power outages threaten the isolation of *H pylori*.

A comparison of the urease test using the CLO test kit (Delta West, pty, Australia) showed that a total of 25 biopsies positive for urease test were negative by culture. This was possible as a result of the fact that the CLO test kit could detect the presence of *H pylori* even when they were very small, while when there was power outage the possibility of detecting the organism was small. In addition, occassionally the biopsy forcep could be contaminated during the passage of the endoscope in the stomach, resulting in growth of some other urease positive organisms from the biopsies[7]. Another general explanation for the poor specificity of all tests compared to culture was as a result of incessant power outages in our country, thus decreasing the possibility of isolating *H pylori* (a fastidious organism) by culture.

Sixty-eight percent of the biopsies that were positve for all three PCR methods were positive for *cagA*. The presence of *cagA*, a virulence factor, was found to be common irrespective of the clinical diagnosis, similar to a previous study by Smith *et al*.[8].

In conclusion, the 26-kDa gene, was found to be the most appropriate of the three different PCR methods for the detection of *H pylori* from biopsies. The study also showed that PCR had a potential value for studying *cagA* and possibly other virulent factors directly from biopsies, although it might not be important in rapidly detecting a patient that is at high risk of peptic ulcer since the frequency is similar to those of non-ulcer dyspepsia and more importantly the method could be adapted for our environment, where there is constant power outage.

REFERENCES

1 **Lu JJ**, Perng CL, Shyu RY, Chen CH, Lou Q, Chong SKF, Lee CH. Comparison of five PCR methods for detection of *Helicobacter pylori* DNA in gastric tissues. *J Clin Microbiol* 1999; **37**: 772-774

2 **Lage A**, Godfroid E, Fauconnier A, Burette A, Butzler JP, Bollen A, Glupczynski Y. Diagnosis of *Helicobacter pylori* infection by PCR: comparison with other invasive methods. *J Clin Microbiol* 1995; **33**: 2752-2756

3 **Bickley J**, Owen RJ, Fraser AG, Pounder RE. Evaluation of the polymerase chain reaction for detecting the urease C gene of *Helicobacter pylori* in gastric biopsy samples and dental plaque. *J Med Microbiol* 1993; **39**: 338–344

4 **Clayton CL**, Kleanthous H, Coates PJ, Morgan DD, Tabaqchali S. Sensitive detection of *Helicobacter pylori* by using polymerase chain reaction. *J Clin Microbiol* 1992; **30**: 192- 200

5 **Hammar M**, Tyszkiewicz T, Wadstrom T, O'Toole PW. Rapid detection of Helicobacter pylori in gastric biopsy material by polymerase chain reaction. *J Clin Microbiol* 1992; **30**: 54–58

6 **Marais A**, Monteiro L, Occhialini M, Pina M, Lamoliatte H, Megraud F. Direct detection of *Helicobacter pylori* resistance to macrolides by a polymerase chain reaction/DNA enzyme immunoassay in gastric biopsy specimens. *Gut* 1999; **44**: 463–467

7 **Smith SI**, Oyedeji KS, Arigbabu A, Anomneze EE, Chibututu CC, Atimomo CA, Atoyebi A, Adesanya A, Coker AO. Prevalence of H pylori in patients with gastritis and peptic ulcer in Western, Nigeria. *Biomedical Lett* 1999; **60**: 115–120

8 **Smith SI**, Kirsch C, Oyedeji KS, Arigbabu AO, Coker AO, Ekkehard B, Miehlke S. Prevalence of Helicobacter pylori vacA, cagA and iceA genotypes in Nigerian patients with duodenal ulcer disease. *J Med Microbiol* 2002; **51**: 851–854

Edited by Wang XL and Xu FM

PO Box 2345, Beijing 100023, China
Fax: +86-10-85381893
E-mail: wjg@wjgnet.com www.wjgnet.com

World J Gastroenterol 2004;10(13):1961-1963
World Journal of Gastroenterology
 ISSN 1007-9327

• BRIEF REPORTS •

Frequencies of poor metabolizers of cytochrome P450 2C19 in esophagus cancer, stomach cancer, lung cancer and bladder cancer in Chinese population

Wei-Xing Shi, Shu-Qing Chen

Wei-Xing Shi, Department of Public Health, School of Medicine, Zhejiang University, Hangzhou 310031, Zhejiang Province, China
Shu-Qing Chen, Department of Biochemistry and Molecular Biology, College of Pharmaceutical Sciences, Zhejiang University, Hangzhou 310031, Zhejiang Province, China
Supported by Research funding from Health Bureau of Zhejiang Province (G20030697) and Research Fund from Hangzhou Tobacco Factory
Correspondence to: Dr Shu-Qing Chen, Department of Biochemistry and Molecular Biology, College of Pharmaceutical Sciences, Zhejiang University, Hangzhou 310031, Zhejiang Province, China. chenshuqing@zju.edu.cn
Telephone: +86-571-87217406 **Fax:** +86-571-87217406
Received: 2004-01-15 **Accepted:** 2004-02-12

Abstract

AIM: To investigate the association between cytochrome P450 2C19 (CYP2C19) gene polymorphism and cancer susceptibility by genotyping of CYP2C19 poor metabolizers (PMs) in cancer patients.

METHODS: One hundred and thirty-five cases of esophagus cancer, 148 cases of stomach cancer, 212 cases of lung cancer, 112 cases of bladder cancer and 372 controls were genotyped by allele specific amplification-polymerase chain reaction (ASA-PCR) for CYP2C19 PMs. The frequencies of PMs in cancer groups and control group were compared.

RESULTS: The frequencies of PMs of CYP2C19 were 34.1% (46/135) in the group of esophagus cancer patients, 31.8% (47/148) in the stomach cancer patients, 34.4%(73/212) in the group of lung cancer patients, only 4.5%(5/112) in the bladder cancer patients and 14.0%(52/372) in control group. There were statistical differences between the cancer groups and control group (esophagus cancer, χ^2=25.65, P<0.005, OR=3.18, 95%CI=2.005-5.042; stomach cancer, χ^2=21.70, P<0.005, OR=2.86, 95%CI=1.820-4.501; lung cancer, χ^2=33.58, P<0.005, OR=3.23, 95%CI=1.503-6.906; bladder cancer, χ^2=7.50, P<0.01, OR=0.288, 95%CI=0.112-0.740).

CONCLUSION: CYP2C19 PMs have a high incidence of esophagus cancer, stomach cancer and lung cancer, conversely they have a low incidence of bladder cancer. It suggests that CYP2C19 may participate in the activation of procarcinogen of esophagus cancer, stomach cancer and lung cancer, but may involve in the detoxification of carcinogens of bladder cancer.

Shi WX, Chen SQ. Frequencies of poor metabolizers of cytochrome P450 2C19 in esophagus cancer, stomach cancer, lung cancer and bladder cancer in Chinese population. *World J Gastroenterol* 2004; 10(13): 1961-1963
http://www.wjgnet.com/1007-9327/10/1961.asp

INTRODUCTION

Individuals vary widely in their susceptibility to carcinogens. One attractive genetic mechanism to account for this variability is the activity of polymorphically expressed cytochrome P450 enzymes that activate procarcinogens or conversely detoxify carcinogens. Cytochrome P450 2C19 (CYP2C19) is a clinically important metabolic enzyme responsible for the metabolism of a number of therapeutic drugs, such as S-mephenytoin, omeprazole, diazepam, proguanil, propranolol and certain antidepressants[1]. Recently, there were several papers concerning the CYP2C19 polymorphism and cancer susceptibility. Wadelius *et al*.[2] found no association between CYP2C19 polymorphism and prostate cancer. Roddam *et al*.[3] reported an increased risk of CYP2C19 poor metabolizers (PMs) to develop adult acute leukaemia and Sachse *et al*.[4] found CYP2C19*2 had an decreased risk of colorectal cancer. Normally, Oriental people had a higher incidence of CYP2C19 poor metabolizers, which was usually about 13-16%, but in Caucasian people it was only 1-3% as well. So, for the purpose of investigating association between CYP2C19 polymorphism and cancer susceptibility, it is more easy to draw a conclusion in Oriental population. The aim of this study was to evaluate the relationship between CYP2C19 polymorphism and susceptibility to different kind of cancer by means of CYP2C19 genotyping among Chinese subjects.

MATERIALS AND METHODS

Reagents

Taq DNA polymerase, dNTPs, PCR buffer and 25 mmol/L $MgCl_2$ were purchased from Promega USA, Primers (Sangon, Shanghai), Igepal CA-630 (Sigma, USA), DNA Ladder (Huamei, Shanghai), Agarose (Pharmacia, Sweden), *Sma*I and *Ham*HI were obtained from MBI, USA. Other chemicals were of analytical grade.

Equipments

PCR machine (Hybaid, USA), electrophoresis apparatus (Pharmacia, Sweden), gel imaging system (Stratagene, USA), high speed centrifuge (Hitachi, Japan) and electro-balance (Mettle, France) were used.

Subjects

Cancer patients were from No 1 and No 2 hospitals affiliated to Zhejiang University. Healthy controls were recruited randomly around the same area. This study was approved by the Medical Institutional Review Board of the University and all subjects were provided informed consent prior to their participation. All the subjects were Chinese Han Nationality.

Methods

DNA extraction and detection of CYP2C19*2 and CYP2C19*3 A 5 mL blood sample was collected from each subject and DNA was extracted from blood for CYP2C19 genotyping according to Lahiri *et al*.[5]. For the detection of CYP2C19*2, paired PCR reactions were set, one containing CYP2C19*2 primers and the other containing wild-type

primers (Table 1). Each PCR reaction (50 μL) containing 10 mmol/L Tris-HCl, pH 8.3, 50 mmol/L KCl, 2.0 mmol/L $MgCl_2$, 0.2 mmol/L of each dNTPs, 0.2 μmol/L of each primers and 50-1 000 ng of DNA template, 1 unit of Taq DNA polymerase was amplified through 35 cycles, each cycle consisting of denaturation at 94 ℃ for 1 min, primer annealing at 61 ℃ for 1 min, and extension at 72 ℃ for 1.5 min. Finally, a further extension was carried out at 72 ℃ for 10 min. The amplicon was analyzed on 20 g/L agarose gel electrophoresis. For detection of CYP2C19*3, paired PCR reactions were set, one containing CYP2C19*3 primers and the other containing wild-type primers (Table 2). Each PCR reaction (50 μL) containing 10 mmol/L Tris-HCl pH 8.3, 50 mmol/L KCl, 2.0 mmol/L $MgCl_2$, 0.2 mmol/L of each dNTPs, 0.2 μmol/L of each primers and 50-1 000 ng of DNA template, 1 unit of Taq DNA polymerase was amplified through 35 cycles, each cycle consisting of denaturation at 94 ℃ for 1 min, primer annealing at 58 ℃ for 1 min and extension at 72 ℃ for 30 s. Finally, a further extension was performed at 72 ℃ for 10 min. The amplicon was analyzed on 20 g/L agarose gel electrophoresis.

Table 1 Primers designed for detection of CYP2C19*2

Genotype		Sequences
Wild-type	Forward	5'-AAT TAC AAC CAG AGA GCT TGG C-3'
	Reverse	5'-GTA ATT TGT TAT GGG TTC C<u>C</u>-3'
Mutant	Forward	5'-AAT TAC AAC CAG AGA GCT TGG C-3'
	Reverse	5'-GTA ATT TGT TAT GGG TTC C<u>T</u>-3'

Table 2 Primers designed for detection of CYP2C19*3

Genotype		Sequences
Wild-type	Forward	5'-TAT TAT TAT CTG TTA ACT AAT ATG A-3'
	Reverse	5'-AAC TTG GCC TTA CCT GGA T<u>C</u>-3'
Mutant	Forward	5'-TAT TAT TAT CTG TTA ACT AAT ATG A-3'
	Reverse	5'-AAC TTG GCC TTA CCT GGA T<u>T</u>-3'

The genotypes were judged by shown up of goal fragments in the paired PCR amplifications. For CYP2C19*2 allele, the goal fragment (139 bp band) could be seen only in the lane of CYP2C19*2 PCR reaction means homozygous CYP2C19*2 allele (*2/*2), only in the lane of wild-type reaction means homozygous wild-type (*1/*1), and in both reaction means heterozygous CYP2C19*2 (*1/*2). For CYP2C19*3 allele, the goal fragment (253 bp band) could be seen only in the lane of CYP2C19*3 PCR reaction means homozygous CYP2C19*3 allele (*3/*3), only in the lane of wild-type reaction means homozygous wild-type (*1/*1), and in both reaction means heterozygous CYP2C19*3 (*1/*3). In the consideration of both alleles, the other genotype could be *2/*3.

Quality control checks of PCR procedures indicated DNA samples genotyped in a double-blinded fashion yielded the same alleles as found during previous genotyping of DNA. The genotypes were checked for reliability by comparing with PCR-RFLP procedure[6,7].

RESULTS

Genotyping of CYP2C19

Four pairs of primers were designed according to CYP2C19 wild-type sequence and the mutations in CYP2C19*2 and CYP2C19*3 by the principle of allele-specific amplification. PCR amplification conditions were tested to find the optimum annealing temperature and $MgCl_2$ concentration. The method was proved to be quick, accurate and less contamination (Figures 1, 2).

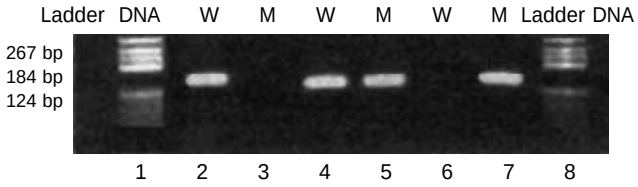

Figure 1 Typical electrophoresis pattern in detection of CYP2C19*2. Goal fragment was 139 bp. Lanes 1 and 8: DNA ladder; Lanes 2, 4 and 6: wild-type primers; Lanes 3, 5 and 7: mutant primers; Sample 1: homozygous wild-type (lanes 2 and 3); Sample 2: heterozygote (lanes 4 and 5); Sample 3: homozygous mutant (lanes 6 and 7).

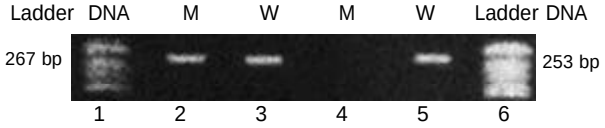

Figure 2 Typical electrophoresis pattern in detection of CYP2C19*3. Goal fragment was 253 bp. Lanes 1 and 6: DNA ladder; Lanes 2 and 4: mutant primers; Lanes 3 and 5: wild-type primers. Sample 1: heterozygote (lanes 2 and 3); Sample 2: homozygous wild-type (lanes 4 and 5); No homozygous mutant found in this study.

Frequency study of poor metabolizers in the cancer groups and the control group

The frequencies of poor metabolizers of CYP2C19 (genotypes of *2/*2 and *2/*3, no *3/*3 was found in this study) were of 34.1%(46/135) in the group of esophagus cancer patients, 31.8%(47/148) in the stomach cancer patients, 34.4%(73/212) in the group of lung cancer patients, only 4.5%(5/112) in the bladder cancer patients and 14.0%(52/372) in control group. There were statistical differences between cancer groups and control group (esophagus cancer, χ^2=25.65, P<0.005, OR=3.18, 95%CI=2.005-5.042; stomach cancer, χ^2=21.70, P<0.005, OR=2.86, 95%CI=1.820-4.501; lung cancer, χ^2=33.58, P<0.005, OR=3.23, 95%CI=1.503-6.906; bladder cancer, χ^2=7.50, P<0.01, OR=0.288, 95%CI=0.112-0.740). It was obviously that CYP2C19 PMs had a high incidence of esophagus cancer, stomach cancer and lung cancer, conversely CYP2C19 PMs had a low incidence of bladder cancer (Table 3).

Table 3 Frequencies of EMs and PMs in different cancer groups and control group

Group	Total cases	EMs (*1/*1, *1/*2, *1/*3)		PMs (*2/*2,*2/*3)	
		Cases	%	Cases	%
Esophagus cancer	135	89	65.9	46	34.1
Stomach cancer	148	101	68.2	47	31.8
Lung cancer	212	139	65.6	73	34.4
Bladder cancer	112	107	95.5	5	4.5
Control	372	320	86.0	52	14.0

Esophagus cancer, χ^2=25.65, P<0.005, OR=3.18, 95%CI=2.005-5.042; Stomach cancer, χ^2=21.70, P<0.005, OR=2.86, 95%CI=1.820-4.501; Lung cancer, χ^2=33.58, P<0.005, OR=3.23, 95%CI=1.503-6.906; Bladder cancer, χ^2=7.50, P<0.01, OR=0.288, 95%CI=0.112-0.740.

DISCUSSION

With the completion of the Human Genome Project, great opportunities exist to investigate the effects of genetic variation of the cancer susceptibility to environment exposure. It is known to all cigarette smoke can cause lung cancer, but the fact is not every smoker suffering from lung cancer. What is

the mechanism of which smoker is more susceptible to lung cancer, which smoker may not catch the disease. One of the answers may lie on the gene polymorphisms of drug metabolising enzymes. This rule may also apply to esophagus cancer, stomach cancer and bladder cancer.

Cytochrome P450s are the main drug metabolizing enzymes in human body, and are always found to participate in the metabolism of carcinogens or procarcinogens. Some are involved in the activation of procarcinogens, some may take part in the inactivation of carcinogens. That depends on what kind of carcinogens and what kind of cancers, and what kind of mechanism of carcinogenesis.

CYP2C19-one of the most important cytochrome P450s, is known as a key enzyme in the *in vivo* metabolism of a number of related hydantoins and barbiturates, as well as in the metabolism of structurally unrelated drugs such as omeprazole, lansoprazole, progunil, mephenytoin and citalopram[1]. Individuals can be divided into two groups, poor metabolizers (PMs) and extensive metabolizers (EMs), depending on the hydroxylation ability of S-mephenytoin. There are two main enzyme deficient alleles called CYP2C19*2 (CYP2C19m1) and CYP2C19*3 (CYP2C19m2). CYP2C19*2 is a single base pair G_{681}→A mutation in exon 5 of CYP2C19 and accounts for 75% and 85% of Oriental and Caucasian mutant alleles, respectively[6]. CYP2C19*3 is a single base pair G_{636}→A mutation in exon 4 of CYP2C19 which results in a premature stop codon[7]. It accounts for 10-25% of Oriental mutant alleles and is rare in Caucasians. An individual who inherits two mutant CYP2C19 alleles, whatever same kind (*2/*2, *3/*3) or different kind (*2/*3), has a reduced capacity to metabolize CYP2C19 substrates and is a PM. Individuals who are homozygous (*1/*1) or heterozygous (*1/*2, *1/*3) for wild-type CYP2C19*1 have efficient enzyme to metabolize CYP2C19 substrates and are EMs. Although there are several other reports about rare enzyme defect alleles, it is recognized that the purpose of prediction of CYP2C19 phenotype can be achieved by genotyping CYP2C19 only with CYP2C19*2 and CYP2C19*3 in Chinese population[8].

In this study, 135 esophagus cancer patients, 148 stomach cancer patients, 212 lung cancer patients, 112 bladder cancer patients and 372 controls were genotyped for CYP2C19. Among them, 34.1% of esophagus cancer patients, 31.8% of stomach cancer patients and 34.4% of lung cancer patients, but only 4.5% of bladder cancer patients and 14.0% of healthy controls were genotyped as CYP2C19 PMs. Statistical analysis of the frequencies of PMs in cancer groups and control group showed significant differences (Table 3). It means CYP2C19 PMs are more susceptible to esophagus cancer, stomach cancer and lung cancer, but it is unsusceptible to Bladder cancer.

Several studies on CYP2C19 polymorphism and its association with carcinogenesis have shown self-contradiction results[2-4]. However, our data indicated that CYP2C19 polymorphism was associated with esophagus cancer, stomach cancer, lung cancer and bladder cancer. Furthermore, we found that CYP2C19 PMs had increased risk of esophagus cancer, stomach cancer and lung cancer, and a decreased risk of bladder cancer. However, Klose *et al*.[9] reported that CYP2C19 was only expressed in liver and duodenum. How it functioned so differently in different organs remained a mystery. But from the organs listed above, it is deducible that CYP2C19 PMs are more susceptible to the cancers of upper or systemic organs, such as esophagus, stomach, lung and blood. And they are unsusceptible to the cancers of lower organs, like bladder and colorectal cancers. Prostate cancer was another example which showed no relationship between CYP2C19 polymorphism and carcinogenesis. It implies that different type of cancers may have different oncological mechanisms.

The genetic background and living environment of an individual are most important factors for carcinogensis[10]. The relationship between genetic polymorphism of *CYP* genes[11,12], ABO blood groups[13] and well water pollution are widely recognized. But more efforts needed to elucidate the correlation of different types of cancer to so many different factors, the development of biochip technology may speed it up[14].

REFERENCES

1 **Xie HG**, Kim RB, Wood AJ, Stein CM. Molecular basis of ethnic differences in drug disposition and response. *Annu Rev Pharmacol Toxicol* 2001; **41**: 815-850

2 **Wadelius M**, Autrup JL, Stubbins MJ, Andersson SO, Johansson JE, Wadelius C, Wolf CR, Autrup H, Rane A. Polymorphisms in NAT2, CYP2D6, CYP2C19 and GSTP1 and their association with prostate cancer. *Pharmacogenetics* 1999; **9**: 333-340

3 **Roddam PL**, Rollinson S, Kane E, Roman E, Moorman A, Cartwright R, Morgan GJ. Poor metabolizers at the cytochrome P450 2D6 and 2C19 loci are at increased risk of developing adult acute leukaemia. *Pharmacogenetics* 2000; **10**: 605-615

4 **Sachse C**, Smith G, Wilkie MJ, Barrett JH, Waxman R, Sullivan F, Forman D, Bishop DT, Wolf CR. A pharmacogenetic study to investigate the role of dietary carcinogens in the etiology of colorectal cancer. *Carcinogenesis* 2002; **23**: 1839-1849

5 **Lahiri DK**, Nurnberger JI Jr. A rapid non-enzymatic method for the preparation of HMW DNA from blood for RFLP studies. *Nucleic Acids Res* 1991; **19**: 5444

6 **de Morais SM**, Wilkinson GR, Blaisdell J, Meyer UA, Nakamura K, Goldstein JA. Identification of a new genetic defect responsible for the polymorphism of (S)-mephenytoin metabolism in Japanese. *Mol Pharmacol* 1994; **46**: 594-598

7 **de Morais SM**, Wilkinson GR, Blaisdell J, Nakamura K, Meyer UA, Goldstein JA. The major genetic defect responsible for the polymorphism of S-mephenytoin metabolism in humans. *J Biol Chem* 1994; **269**: 15419-15422

8 **Shu Y**, Zhou HH. Individual and ethnic differences in CYP2C19 activity in Chinese populations. *Acta Pharmacol Sin* 2000; **21**: 193-199

9 **Klose TS**, Blaisdell JA, Goldstein JA. Gene structure of CYP2C8 and extrahepatic distribution of the human CYP2Cs. *J Biochem Mol Toxicol* 1999; **13**: 289-295

10 **Yoshimura K**, Hanaoka T, Ohnami S, Kohno T, Liu Y, Yoshida T, Sakamoto H, Tsugane S. Allele frequencies of single nucleotide polymorphisms (SNPs) in 40 candidate genes for gene-environment studies on cancer: data from population-based Japanese random samples. *J Hum Genet* 2003; **48**: 654-658

11 **Bartsch H**, Nair U, Risch A, Rojas M, Wikman H, Alexandrov K. Genetic polymorphism of CYP genes, alone or in combination, as a risk modifier of tobacco-related cancers. *Cancer Epidemiol Biomarkers Prev* 2000; **9**: 3-28

12 **Ribeiro Pinto LF**, Teixeira Rossini AM, Albano RM, Felzenszwalb I, de Moura Gallo CV, Nunes RA, Andreollo NA. Mechanisms of esophageal cancer development in Brazilians. *Mutat Res* 2003; **544**: 365-373

13 **Su M**, Lu SM, Tian DP, Zhao H, Li XY, Li DR, Zheng ZC. Relationship between ABO blood groups and carcinoma of esophagus and cardia in Chaoshan inhabitants of China. *World J Gastroenterol* 2001; **7**: 657-661

14 **Landi S**, Gemignani F, Gioia-Patricola L, Chabrier A, Canzian F. Evaluation of a microarray for genotyping polymorphisms related to xenobiotic metabolism and DNA repair. *Biotechniques* 2003; **35**: 816-820

Edited by Kumar M **Proofread by** Xu FM

PO Box 2345, Beijing 100023, China
Fax: +86-10-85381893
E-mail: wjg@wjgnet.com www.wjgnet.com

World J Gastroenterol 2004;10(13):1964-1966
World Journal of Gastroenterology
 ISSN 1007-9327

• BRIEF REPORTS •

Allelotyping for loss of heterozygosity on chromosome 18 in gastric cancer

Jing-Cui Yu, Kai-Lai Sun, Buo Liu, Song-Bin Fu

Jing-Cui Yu, Department of Medical Genetics, China Medical University, Shenyang 110001, China; Department of Clinical Pharmacology, the Second Affiliated Hosptial, Harbin Medical University, Harbin 150086, Heilongjiang Province, China
Song-Bin Fu, Laboratory of Medical Genetics, Harbin Medical University; Bio-pharmaceutical Key Laboratory of Heilongjiang Province, Harbin 150086, Heilongjiang Province, China
Kai-Lai Sun, Department of Medical Genetics, China Medical University, Shenyang 110001, Liaoning Province, China
Buo Liu, Chinese National Human Genome Center, Beijing 100176, China
Supported by the Teaching and Research Award Program for Outstanding Young Teachers in Higher Education Institutions by Ministry of Education of China and the National Natural Science Foundation, No. 30370783 and the Key Project of Science and Technology of Heilongjiang Province, No. GB03C601-1
Correspondence to: Dr. Song-Bin Fu, Laboratory of Medical Genetics, Harbin Medical University, Harbin 150086, Heilongjiang Province, China. fusb@ems.hrbmu.edu.cn
Telephone: +86-451-86674798 **Fax:** +86-451-86669576
Received: 2003-12-23 **Accepted:** 2004-02-01

Abstract

AIM: To investigate the association between loss of heterozygosity (LOH) on chromosome 18 and sporadic gastric cancer.

METHODS: Multiplex PCR was used to screen 14 highly polymorphic microsatellite markers on chromosome 18 in 45 cases of primary gastric cancer. PCR products were separated on polyacrylamide gels and the electrophoresis maps were analyzed with Genescan and Genotyper.

RESULTS: The LOH frequencies in gastric cancer at all 14 markers ranged from 10% to 58%. Eleven markers were found with over 20% LOH frequencies, in which 9 markers located in 18q, and 2 markers in 18p. Two overlapping deleted regions were identified: R1 between D18S61-D18S1161 at 18q22 (9cM) with 24% LOH frequency; R2 between D18S462-D18S70 at 18q22-23(6cM) with 32% LOH frequency.

CONCLUSION: LOH of chromosome 18 (18q and 18p) may be involved in gastric tumorigenesis. Two overlapping deleted fragments suggested that there might be unidentified tumor suppressor genes in those two regions.

Yu JC, Sun KL, Liu B, Fu SB. Allelotyping for loss of heterozygosity on chromosome 18 in gastric cancer. *World J Gastroenterol* 2004; 10(13): 1964-1966

http://www.wjgnet.com/1007-9327/10/1964.asp

INTRODUCTION

Inactivation of tumor suppressor genes (TSGs) has been considered to be one of the most important mechanisms during the human tumorigenesis[1]. Earlier studies have shown that loss of heterozygosity (LOH) on specific chromosomal loci is related to the inactivation of TSGs. The Knudson "two-hit" hypothesis has provided the rationale for identifying TSGs by mapping regions of LOH. Analysis of LOH has been developed and fully exploited for the detection of TSGs in a variety of tumors through comparison of copy number changes in tumor DNA with matched control DNA[2]. Different chromosomal regions that are harboring putative TSGs can be found in tumors by searching for LOH markers. Furthermore, by identifying genetic distance between these markers and TSGs, the allelic loss regions can be narrowed step by step and the TSGs can be finally cloned.

Gastric cancer (GC) is one of the most frequent malignancies and remains a main cause of mortality in China[3-5]. Many regions of LOH on different chromosomes have been found in GC[6]. Allelic loss on the long arm of chromosome 18 (18q LOH) is highly related to GC[7]. Little is known about allelic loss on the short arm of chromosome 18 (18pLOH) in GC, although a significant incidence of 18pLOH (specially 18q11) has been found in tumors of the lung, brain and breast[8]. So in this paper, we chose fourteen highly polymorphic microsatellite markers spanning chromosome 18p and 18q and performed genome-wide allelotyping in 45 primary gastric cancers. We identified the chromosomal loci and overlapping regions that are frequently lost in GC for clarifying the roles of 18pLOH and 18qLOH in GC and providing evidences for finding new important TSGs.

MATERIALS AND METHODS

Sample collection and DNA extraction

Forty-five primary gastric tumors and corresponding non-tumorous tissue specimens were obtained at surgery from the First Hospital and the Second Hospital of Harbin Medical University. All the patients were confirmed by routine histologic examination and received no treatment before surgery. Each specimen was frozen immediately and stored at -80 ℃ until use. Genomic DNA was extracted using DNAzo1^R reagent-genomic DNA isolation reagent (Gibcol).

Fluorescent microsatellite analysis

Along chromosome 18, we chose 14 polymorphic microsatellite markers (5 markers at 18p, 9 markers at 18q) at a density of approximately one marker every 9 cM (http://www.gdb.org). The oligonucleotides were labeled with FAM, HEX and NED three different fluorescent dyes for allelotyping (primers were obtained from the ABI PRISM Linkage Mapping Set v. 2, Perkin-Elmer). Multiplex PCR was carried on in a Gene Amp^R PCR system 9600 (Perkin-Elmer) for amplifying matched pairs of normal and tumor DNAs. PCR reaction conditions were as follows: 5 μL final volume included 0.5 μL of 10×PCR buffer, 0.6 μL of 25 mmol/L $MgCl_2$, 0.1 μL of 10 mmol/L dNTP, 0.25 U of Hot-start tag polymerase, 0.04 μL of each primer and 50 ng of DNA. The following PCR run conditions were used: (a) an initial denaturation at 94 ℃ for 12 min; (b) 15 cycles each at 94 ℃ for 30 s, 63 ℃ for 1 min (0.5 ℃ decreased per cycle), 72 ℃ for 1 min 50 s; (c) 24 cycles each at 94 ℃ for 30 s, 56 ℃ for 1 min, 72 ℃ for 1 min 50 s; and (d) a final extension at 72 ℃ for 15 min. A portion of each PCR product (0.7 μL) was combined with 1 μL of the loading mix (ABI internal size standard and formamide loading buffer). After denaturation

at 95 ℃ for 5 min, products were electrophoresed on 4.5% polyacrylamide gels with 7 mol/L urea on ABI prism 377 DNA sequencer (Perkin-Elmer) for 2.5 h. The data were collected automatically and analyzed using ABI prism Genescan 3.1 and Genotyper 2.1 software. Two fragments amplified from normal DNA indicated heterozygote and alleles were defined as the two highest peaks within the expected size range of heterozygote. A ratio of T_1:T_2/N_1:N_2 (less than 0.67 or greater than 1.3) was scored as a LOH (Figure 1). A single fragment amplified from normal DNA (homozygote) and these PCR reactions in which fragments were not clearly amplified were scored as non-informative. The LOH frequency of a site was equal to the percentage of the number between allelic losses and informative cases.

RESULTS

LOH at various frequencies were found in GC patients, ranging from 10% to 58%, with the highest rate at D18S70 (21/36, 58%). Of the 45 cases of GC studied, 36(80%) exhibited allelic losses at least at one site, 25 at over two sites. Figure 1 shows allelic losses in partial patients on several markers. Figure 2 shows LOH frequencies of 14 markers and cytogenetic locations. Eleven markers were found with over 20% LOH frequencies, including 2 markers at 18p and 9 markers at 18q. They were as follows: D18S59 (18p11.3, 28%), D18S452 (18p11.3, 24%), D18S478 (18q11.1-11.2, 37%), D18S1102 (18q12, 29%), D18S474 (18q21, 22%), D18S64 (18q21, 30%), D18S68 (18q21, 25%), D18S61 (18q22, 26%), D18S1161 (18q22, 21%), D18S462 (18q22-23, 29%) and D18S70 (18q23, 58%). Two overlapping deleted regions (Figure 2) were identified at 18q22 (between D18S61 and D18S1161, 9 cM or approximately 5 Mb DNA sequence, overlapping fragment LOH 24%) and 18q22-23 (between D18S462 and D18S70, 6 cM or approximately 3 Mb DNA sequence, overlapping fragment LOH 32%), respectively.

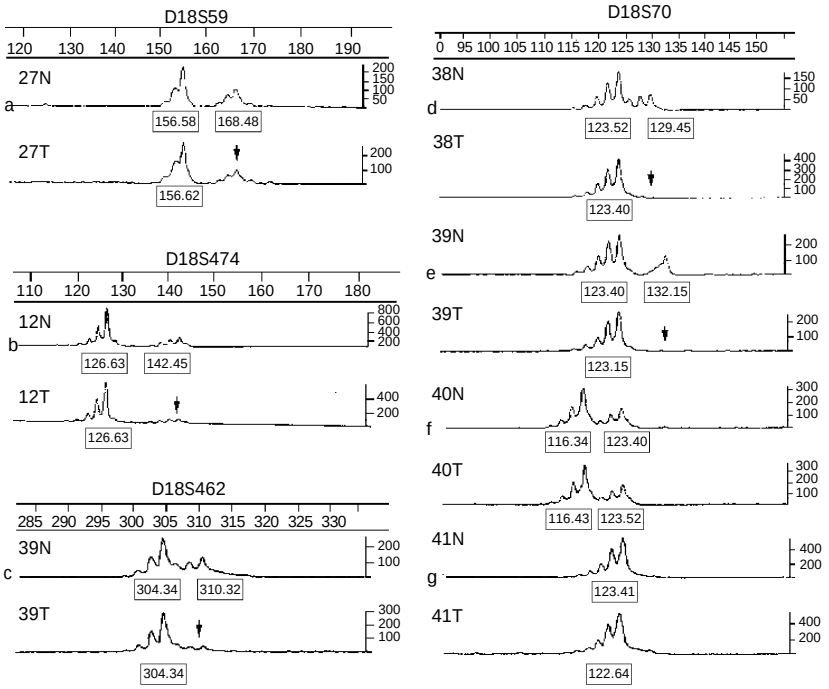

Figure 1 Representative LOH analysis of chrosomose 18. The scales on the top and right side of each figure represent the size (bp) and the intensity, respectively; N: Nontumorous control; T: Tumor; Arrow: Informative case with allelic loss (a, b, c, d, e); f: An informative case without allelic loss (heterozygote); g: An non-informative case (homozygote).

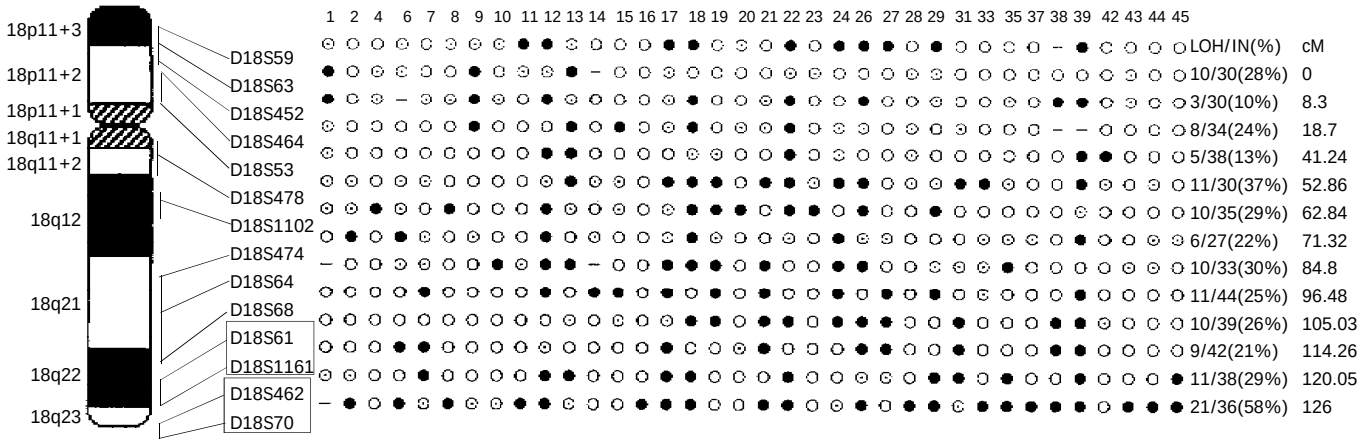

Figure 2 Results of analysis for LOH on chromosome 18. Top: the number of GC patient with LOH; Left: An ideogram of chromosome 18 with the physical order of 14 microsatellite markers according to Genome Database; Right: Allelotyping results from 36 GC patients; ●: Loss of heterozygosity (informative, IN);O: Retention of heterozygosity (informative, IN); ⊙: Homorozygote (non-informative);-: Not available; Black frame: Overlapping deleted region.

DISCUSSION

Genetic instability is often observed in tumor cells[9]. Losses of fragments in some chromosomes may lead to allelic losses of TSGs. In the present study, more extensive genome screening was conducted on chromosome 18 in 45 cases of primary GC using 14 microsatellite markers (5 markers at 18p, 9 markers at 18q). Thirty-six out of 45 GC patients (80%) exhibited allelic losses at least one marker, allelic losses of over two markers were seen in 25 cases of GC patients. We found that two markers (D18S59 and D18S452) with over 20% LOH frequencies on chromosome band 18p11.3. DAL-1 gene (18p11.32) localizes between the two markers, which undergoes allelic losses in lung tumors and a significant proportion of ductal carcinomas *in situ* of the breast. It has been revealed that the DAL-1 protein suppresses the growth of MCF-7 breast cancer cell lines in part through the induction of apoptosis and that expression of DAL-1 increases attachment of these cells to a variety of extracellular matrices[10]. DAL-1 plays a critical role in the suppression of lung tumor formation and metastasis[11]. Our results support the role of DAL-1 gene in gastric carcinogenesis. Future investigations need to be carried on to understand the biological importance of the two putative loci and their clinical relevance in the pathogenesis of GC.

18qLOH is a frequent event in tumors, especially head and neck, colon, lung and gastric cancers[12-14]. All of our 9 markers on this chromosomal arm have shown allelic loss frequencies exceeding 20%. D18S70 was the highest rate of LOH (21/36, 58%) marker on which frequent allelic loss has been reported in head and neck cancers[15] and serous ovarian carcinoma[16]. On the chromosome 18q22-23, Takebayashi *et al*. have identified three loci (D18S39, D18S61 and D18S70) which are lost in 70-75% of head and neck primary tumor cell lines. Lassus *et al*. observed that 59% of serous carcinomas have shown allelic loss at one or more sites and have been associated with tumor grade and poor survival. Moreover, they have identified two minimal common regions of loss at D18S465-D18S61 (18q22, 3.9 cM) and D18S462-D18S70 (18q23, 5.8 cM). Our data, together with these findings of others, suggest that D18S70 is a new putative tumor suppressor site in GC and support the existence of at least one candidate TSG near the site. Significant LOH of the two overlapping lost fragments identified by us appears novel for GC and no candidate TSGs have been reported in the two overlapping deleted regions so far. LOH frequencies of the two overlapping fragments suggest the presence of as yet unidentified TSGs. Although TSGs harboured in the two overlapping lost fragments have not been defined yet, the two regions are useful candidates for further allelotyping with higher-density microsatellite markers and may help us narrow the sites of frequent allelic loss in order to search for new critical TSGs involved in the development of GC.

The molecular genetic mechanisms of GC remain unclear. Investigators have postulated that, like other tumors, the multistep processes with a variety of factors are involved in GC. Step-wise accumulation of DNA damage from "normal" to tumor tissue serves as the basis of the tumor progression models [17]. Our findings have shown that allelic losses are widespread on chromosome 18 and gastric tumorigenesis may be involved in synthetic effect of multiple TSGs.

ACKNOWLEDGEMENTS

We are grateful to Dr. Shen Yan (Chinese National Human Genome Center, Beijing) for his helpful advice.

REFERENCES

1 **Wang GS,** Wang MW, Wu BY, You WD, Yang XY. A novel gene, GCRG224, is differentially expressed in human gastric mucosa. *World J Gastroenterol* 2003; **9:** 30-34
2 **Tomlinson IPM,** Lambros MBK, Roylance RR. Loss of heterozygosity analysis: practically and conceptually flawed? *Genes Chromosomes Cancer* 2002; **34:** 349-353
3 **Wang GT**. Progress in studies of mechanism of gastric precancerous lesions, carcinogenesis and their reversion. *Shijie Huaren Xiaohua Zazhi* 2000; **8:** 1-4
4 **Deng DJ**, E Z. Overview on recent studies of gastric carcinogenesis: human exposure of N-nitrosamides. *Shijie Huaren Xiaohua Zazhi* 2000; **8:** 250-252
5 **Pan CJ,** Liu KY. Proliferation / apoptosis and expression of P53 and Bcl-2 in gastric carcinoma. *Shijie Huaren Xiaohua Zazhi* 2003; **11:** 526-530
6 **Du JJ,** Dou KF, Cao YX, Wang ZH, Wang WZ, Gao ZQ. CA11, a down-regulated gene in gastric cancer: a functional study. *Shijie Huaren Xiaohua Zazhi* 2002; **10:** 525-529
7 **Ren Q,** Wang ZN, Luo Y, Ao Y, Lu C, Jiang L, Xu HM, Zhang X. Loss of heterozygosity on chromosome 18 in microdissected gastric cancer cells. *Shijie Huaren Xiaohua Zazhi* 2003; **11:** 310-313
8 **Tran Y,** Benbatoul K, Gorse K, Rempel S, Futreal A, Green M, Newsham I. Novel regions of allelic deletion on chromosome 18p in tumors of the lung, brain and breast. *Oncogene* 1998; **17**: 3499-3505
9 **Lengauer C,** Kinzler KW, Vogelstein B. Genetic instability in colorectal cancers. *Nature* 1997; **386:** 623-627
10 **Charboneau AL,** Singh V, Yu T, Newsham IF. Suppression of growth and increased cellular attachment after expression of DAL-1 in MCF-7 breast Cancer Cells. *Int J Cancer* 2002; **100:** 181-188
11 **Yageta M,** Kuramochi M, Masuda M, Fukami T, Fukuhara H, Maruyama T, Shibuya M, Murakami Y. Direct association of TSLC1 and DAL-1, two distinct tumor suppressor proteins in lung cancer. *Cancer Res* 2002; **62:** 5129-5133
12 **Wu CL**, Kirley SD, Xiao H, Chuang Y, Chung DC, Zukerberg LR. Cables enhances cdk2 tyrosine 15 phosphorylation by weel, inhibits cell growth, and is lost in many human colon and squamous cancers. *Cancer Res* 2001; **61:** 7325-7332
13 **Tan D**, Kirley S, Li Q, Ramnath N, Slocum HK, Brooks JS, Wu CL, Zukerberg LR. Loss of cables protein expression in human non-small cell lung cancer: a tissue microarray study. *Hum Pathol* 2003; **34:** 143-149
14 **Candusso ME**, Luinetti O, Villani L, Alberizzi P, Klersy C, Fiocca R, Ranzani GN, Solcia E. Loss of heterozygosity at 18q21 region in gastric cancer involves a number of cancer-related genes and correlates with stage and histology, but lacks independent prognostic value. *J Pathol* 2002; **197:** 44-50
15 **Takebayashi S**, Ogawa T, Jung KY, Muallem A, Mineta H, Fisher SG, Grenman R, Carey TE. Identification of new minimally lost regions on 18q in head and neck squamous cell carcinoma. *Cancer Res* 2000; **60:** 3397-3403
16 **Lassus H**, Salovaara R, Aaltonen LA, Butzow R. Allelic analysis of serous ovarian carcinoma reveals two putative tumor suppressor loci at 18q22-q23 distal to *SMAD*4, *SMAD*2, and DCC. *Am J Pathol* 2001; **159:** 35-42
17 **Powell CA,** Klares S, O'Connor G, Brody JS. Loss of heterozygosity in epithelial cells obtained by bronchial brushing: clinical utility in lung cancer. *Clinical Cancer Research* 1999; **5:** 2025-2034

Edited by Chen WW and Kumar M **Proofread by** Xu FM

PO Box 2345, Beijing 100023, China
Fax: +86-10-85381893
E-mail: wjg@wjgnet.com www.wjgnet.com

World J Gastroenterol 2004;10(13):1967-1970
World Journal of Gastroenterology
 ISSN 1007-9327

• BRIEF REPORTS •

Effects of *Radix Puerariae* flavones on liver lipid metabolism in ovariectomized rats

Ji-Feng Wang, Yan-Xia Guo, Jan-Zhao Niu, Juan Liu, Ling-Qiao Wang, Pei-Heng Li

Ji-Feng Wang, Yan-Xia Guo, Jan-Zhao Niu, Juan Liu, Ling-Qiao Wang, Pei-Heng Li, Department of Biochemistry, Beijing University of Chinese Medicine, Beijing 100029, China
Supported by the National Natural Science Foundation of China, No. 30330220 and the Natural Science Foundation of Beijing, No. 7032024
Correspondence to: Professor Ji-Feng Wang, Department of Biochemistry, Beijing University of Chinese Medicine, Beijing 100029, China
Telephone: +86-10-64286995 **Fax:** +86-10-64286995
Received: 2003-09-15 **Accepted:** 2003-12-10

Abstract

AIM: To study the effects of *Radix Puerariae* flavones (RPF) on liver lipid metabolism in ovariectomized (OVX) rats.

METHODS: Forty adult female Wistar rats were randomly divided into four groups: OVX group; sham-OVX group; OVX+estrogen group and OVX+RPF group. One week after operation rats of the first two groups were treated with physiological saline, rats of OVX+estrogen group with estrogen (1 mg/kg·b.w.) and rats of OVX+RPF group with RPF (100 mg/kg·b.w.), respectively for 5 weeks. After the rats were killed, their body weight, the weight of the abdominal fat and uterus were measured, and the levels of total cholesterol (TC) and triglyceride (TG) in liver homogenate were determined.

RESULTS: Compared with the sham-OVX group, the body mass of the rats in OVX group was found increased significantly; more abdominal fat in store; TC and TG in liver increased and uterine became further atrophy. As a result, the RPF was found to have an inhibitive action on those changes of various degrees.

CONCLUSION: RPF has estrogen-like effect on lipid metabolism in liver and adipose tissue.

Wang JF, Guo YX, Niu JZ, Liu J, Wang LQ, Li PH. Effects of *Radix Puerariae* flavones on liver lipid metabolism in ovariectomized rats. *World J Gastroenterol* 2004; 10(13): 1967-1970
http://www.wjgnet.com/1007-9327/10/1967.asp

INTRODUCTION

Estrogen plays an important role not only in maintaining the reproductive function and the secondary sex characters of the female animals, but also in so-classical target tissues, such as the brain, bone, liver, kidney and the cardiovascular system[1,2]. With the decreases of estrogen in postmenopausal women, the incidences of fracture in osteoporosis, cardiovascular and neurodegenerative diseases often increase[3-5]. Estrogens replacement therapy is able to attenuate symptoms of menopausal syndrome and to reduce the incidence of above-mentioned diseases[6-9].

Phytoestrogens are naturally occurring plant chemicals that can produce an estrogen-like effect in the body, used as a natural alternative to hormone replacement therapy and to reduce menopausal symptoms. They are not chemically the same as the estrogens made in the body, but when digested and absorbed they can act somewhat as estrogen in the body[10]. *Radix Puerariae* is the dried root of *Pueraria lobata Ohwior Pueraria thomsonii Benth*. Sweet in taste and neutral in nature, it can strengthen the spleen and stomach, invigorate the spleen and replenish *Qi*. Its main component is flavone. Recent research has found leguminous plants rich in flavone have a certain kind of estrogen-like effect[11-13]. In this study extraction of *Radix Puerariae* was given to ovariectomized (OVX) rats and its estrogen-like effects were observed.

Previous studies in our laboratory have illustrated that when the female rats were OVX, the estrogen level in their body decreased, which might lead to the body weight gains, abdominal fat stores, increase of liver fat and atrophy of uterine[12]. Therefore, the OVX rats can be used as models to reflect the pathologic changes in perimenopausal or postmenopausal women.

MATERIALS AND METHODS

Animals

All of the 40 female Wistar rats, 220±10 g in body mass, were purchased from the Experimental Animal Center of Chinese Academy of Medical Sciences. They were raised in an air-conditioned animal house at 25±1 ℃ with a light-dark cycle of 12 h, and fed with free forge and running water. The rats were randomly divided into four groups: OVX group; sham-OVX group; OVX+estrogen group and OVX+RPF group. After anesthetized with 15 g/L sodium pentobarbital intraperitoneally, the rats of OVX, OVX + estrogen and OVX+RPF groups were OVX. Rats from sham-OVX received only a squeeze in the connecting point between the ovary and the fallopian tube without having their ovary removed. Starting from the second week of the operation, the rats of OVX group and sham-OVX group were treated with saline, the rats of OVX+estrogen group were treated with estrogen (1 mg/ kg· b.w.) and rats from OVX+RPF group were treated with RPF (100 mg/kg· b.w.) respectively for 5 wk. The average feed consumption and mass of the rats from various groups were measured once a week.

Drugs and reagents

The RPF, provided by Biochemistry Department of Beijing University of Chinese Medicine, was made into suspension of required concentration (10 g/L). The positive control drug was nilestriol (batch number: 20000403) provided by Beijing Four Rings Pharmaceutical Factory. TG and TC kit were provided by Beijing Zhong-Sheng High-Technology Bioengineering Company.

Instruments

The Semi-automatic Biochemistry Analyzer MD 100 was made in USA. The electronic analytical balance was produced by Shimadzu Co. in Japan and the high speed centrifuge TLLC

was manufactured by Beijing Sihuan Scientific Instrumental Company.

Collection and measurement methods of specimens

Five weeks after the operation, the animals were anesthetized with 15 g/L sodium pentobarbital and the liver, abdominal fat and uterus were taken weighed and frozen. Some liver specimens were collected after operation, fixed in 40 g/L formaldehyde, embedded in paraffin, sectioned and stained with hematoxylin and eosin for light microscopy. Some liver specimens were frozen stored at -20 ℃. Liver triglyceride and total cholesterol concentration were measured with the TC kit and the TG kit on a MD100 Semi-automatic biochemistry analyzer respectively after lipid extraction.

Statistical analysis

Data were presented as mean±SD, and Student' s *t* test was used to determine changes between different groups. $P<0.05$ was considered significant.

RESULTS

Effect of RPF on body weight of OVX rats

The mean body mass of the OVX group increased significantly after the operation, compared to the OVX group, RPF was found to have a long term effect on body weight gains ($P<0.05$). The mean body weight of the OVX group started to exceed that of the sham-OVX group significantly ever from the first week ($P<0.05$). The mean body mass of OVX+RPF group had a statistical difference from the mean body weight of OVX group after 3 wk ($P<0.05$). From the fifth week, the body mass of all rats began to drop, but the final data showed that RPF could control the weight gain caused by ovariectomy. During feeding, rats from the OVX+estrogen group were found with colporrhagia, magersucht, and anorexia, but no such symptoms found in the OVX+RPF group (Table 1).

Effect of RPF on abdominal fat and fat factor of OVX rats

The mean weight of abdominal fat of the OVX group was obviously higher than that of the sham-OVX group ($P<0.05$). Both estrogen and RPF could inhibit the storing of abdominal fat caused by ovariectomy, the mean data was only 52.1% and 64.35% compared with OVX group, respectively (Table 2).

Effect of RPF on liver lipid metabolism of OVX rats

TC and TG in liver of the OVX group were 16.4±5.0 mg/dL and 119±26 mg/dL, respectively, which were significantly higher than other groups ($P<0.05$). In the sham-OVX group they were only 11.4±4.4 mg/dL and 65±18 mg/dL. The RPF was found to have a marked effect on controlling liver TC level, with TC 10.2±2.0 mg/dL and TG 46±24 mg/dL which were even lower than sham-OVX group and OVX+estrogen group (Table 3).

Effect of RPF on wet uterus weight of OVX rats

Six weeks after the operation, the uteri of the rats from the OVX group were found with severe atrophy with a quarter of the uterus weight of the sham OVX group. The uterus weight of the estrogen group was higher than the sham-OVX group ($P<0.05$). RPF has again been proved to have some effects on maintaining the uterus weight ($P<0.05$) in OVX group (Table 4).

Table 4 Effect of RPF on wet uterus weight of OVX rats

Group	*n*	Uterus (g)	Uterus factor (‰)
OVX	8	0.11±0.02[c]	0.40±0.10[c]
Sham-OVX	9	0.39±0.14	1.70±0.60
OVX+estrogen	10	0.46±0.34[a]	2.10±1.50[a]
OVX+RPF	10	0.15±0.03[a]	0.70±0.10[a]

Results expressed as mean±SD. [a]$P<0.05$ *vs* OVX group, [c]$P<0.05$ *vs* sham-OVX.

Table 1 Effect of RPF on body mass of OVX rats

Group	*n*	Body mass after operation (g)	Body weight during recovery period (g)	Wk 1 (g)	Wk 2 (g)	Wk 3 (g)	Wk 4 (g)	Wk 5 (g)	Change rate
OVX	8	215±15	233±17	250±16	266±16[c]	276±15[c]	284±16[c]	268±20[c]	22.1%
Sham OVX	9	235±4.7	230±4	232±7	235±6	241±9	246±11	237±14	7.1%
OVX+estrogen	10	236±17	242.4±21	249±18	248±16[a]	239±14[a]	248±18[a]	239±19[a]	1.1%
OVX+RPF	10	216±15	233.3±16	243±17	251±20	249±16[a]	246±19[a]	245±17[a]	5.6%

Results expressed as mean±SD. [a]$P<0.05$ *vs* OVX group, [c]$P<0.05$ *vs* sham-OVX.

Table 2 Effect of RPF on abdominal fat and fat factor of OVX rats

Group	*n*	Abdominal fat (g)	Compared with OVX (%)	Fat factor (%)	Compared with OVX (%)
OVX	8	13.2±2.1[c]	–	5.1±0.4[c]	–
Sham OVX	9	10.6±3.2	80.4	4.6±1.2	91.2
OVX+estrogen	10	6.8±3.6[a]	52.1	3.1±1.6[a]	60.1
OVX+RPF	10	8.5±2.5[a]	64.4	3.7±1.2[a]	72.1

Results expressed as mean±SD. [a]$P<0.05$ *vs* OVX group, [c]$P<0.05$ *vs* sham-OVX.

Table 3 Effect of RPF on liver lipid metabolism of OVX rats

Group	*n*	TC (mg/dL)	Compared with OVX (%)	TG (mg/dL)	Compared with OVX (%)
OVX	8	16.4±5.0[c]	–	119±26[c]	–
Sham-OVX	9	11.4±4.4	81±27	65±18	54±15
OVX+estrogen	10	10.2±1.7[a]	62±10	54±31[a]	45±26
OVX+RPF	10	10.2±2.0[a]	76±15	46±24[a]	39±20

Results expressed as mean±SD. [a]$P<0.05$ *vs* OVX group, [c]$P<0.05$ *vs* sham-OVX, OVX+estrogen and OVX+RPF group.

DISCUSSION

Unlike the animal models that are often prepared by giving high fat diets for hyperlipemia study, the OVX rats were used in the present study. Results of the experiments showed that the animals with ovariectomy tended to have body weight gain, accumulated abdominal fat, increased TC and TG levels in liver and atrophied uterus, which are very similar to menopausal symptoms. Experience from our past studies has proved that animal models thus prepared are stable, which can be used in the study of lipid metabolic disturbance.

Current studies on phytoestrogen both at home and abroad are mainly focused on soy bean and its extracts, and there are very rare reports of *Radix Puerariae*, a plant from the leguminous family. In fact, the phytoestrogen content in *Radix Puerariae* is much higher than that in soy bean. The aim of the present research was to study the effects of extracts from *Radix Puerariae* on lipid metabolism in OVX rats, which mimicked the postmenopausal situation of the disorders of lipid metabolism. And we obtained a series of satisfactory results.

We found in the study that there was an obvious lipid metabolic disturbance in OVX rats. Five weeks after the operation, the TC concentration in liver in OVX group was found obviously higher than those in other groups. RPF could lower the TC concentration to the normal value. However, the mechanism for this change is not quite clear yet. The increased insulin concentration in OVX rats may accelerate the dephosphorylation effect of the hydroxymethylglutaryl CoA reductase (HMGCoA reductase), which is a rate-limiting enzyme of the composition of cholesterol. As a result, it accelerates the activity of the enzyme[14-16]. Insulin could also induce the composition of the HMGCoA reductase directly to increase the composition of cholesterol[17-19]. For the cholesterol metabolism *in vivo*, there are two transport pathways-the endogenous cholesterol transport and the reverse cholesterol transport. In the former, the cholesterol by exogenous absorption and synthesis in the liver is utilized when it, in the form of LDL-C, is combined with the receptors of the extra hepatic tissue, and the ligand combined with LDL receptors are mainly the apolipoprotein of apo B100 and apo E[20-23]. In the latter, the extrahepatic cholesterol, in the form of HDL-C, is conveyed back to the liver and expelled out of the body after further metabolism[24]. Some experiments have shown that estrogen can enhance the activity of the LDL receptors and promote the endogenous transport so as to lower the TC levels[25]. In conclusion, the high insulin level in OVX rats may lead to a high level of cholesterol concentration, while, the low level of estrogen concentration may result in the low level of LDL-R concentration and activity, both of which can cause an accumulation of LDL. The increased production and decreased consumption together make a high level of cholesterol concentration in the body, followed by the hypercholeste and adiposis hepatica.

A high level of TG concentration was also found in the OVX rats. Extrinsic estrogen can be supplemented to reduce the TG accumulation in liver. It was found in our study that RPF had a similar effect. The histological sections revealed a great number of grease spots in the OVX group, while not so many in the estrogen treated group and RPF treated group. The mechanism may be as follows: First, glucose was promoted to change into TG by a high level of insulin concentration in OVX rats[26]. Second, the high level of TC directly damaged the structure of hepatic sinusoid and chylomicrons that contained a high level of TG coming into the Disse' s spaces without been treated. Therefore, the liver cell ingested a large amount of TG from the blood. Profound studies are still needed to further confirm its mechanisms.

We also noticed the side effects and risks of estrogen in this study. In clinic, the commonly encountered side effects of HRT are edema (fluid retention), nausea, breast tenderness, and headache. Other side effects include rash, increased growth of facial hair, dizziness, and hypophrodisia. More serious potential health risks to consider of HRT are breast cancer, uterine cancer, blood clotting, and liver and gallbladder diseases[27-29]. Today, selective estrogen receptor modulators (SERMs) have been used as an alternative approach to activate estrogen signaling pathways in a tissue-specific manner[30,31]. Phytoestrogens have a similar chemical structure to estrogen, and could bind to the estrogen receptor (ER)-beta. Once they bind each other, the ER is occupied, and the real estrogen can not get in. Phytoestrogens then dispatch estrogen-like messages to the cells. Although it is a weak message, it is strong enough to produce some of the positive effects of estrogen but it is still too weak to stimulate the growth of cancer cells[32, 33]. When the estrogen levels are too high, this competition appears to reduce the effects of estrogen by replacing estrogen with the weaker phytoestrogen. When the estrogen levels are too low, it appears that phytoestrogen simulates the effects of estrogen and partially makes up for the deficiency[34].

In conclusion, our data suggest that as a natural estrogen replacement, the RPF could regulate the lipid metabolic disturbance in liver in the OVX rats. Furthermore, there may be a possible protective action against cardiovascular diseases and osteoporosis caused by deficiency of estrogen in menopausal women. However, our data was limited. More work is still needed to confirm its profound pharmacological effects.

REFERENCES

1 **Diel P.** Tissue-specific estrogenic response and molecular mechanisms. *Toxicol Lett* 2002; **127**: 217-224

2 **Dubey RK,** Oparil S, Imthurn B, Jackson EK. Sex hormones and hypertension. *Cardiovasc Res* 2002; **53**: 688-708

3 **Diaz Lopez JB,** Rodriguez Rodriguez A, Ramos B, Caramelo C, Rodriguez Garcia M, Cannata Andia JB. Osteoporosis, estrogens, and bone metabolism. Implications for chronic renal insufficiency. *Nefrologia* 2003; **23**(Suppl 2): 78-83

4 **DeSoto MC.** Drops in estrogen levels affect brain, body and behavior: reported relationship between attitudes and menopausal symptoms. *Maturitas* 2003; **45**: 299-301

5 **Ahlborg HG,** Johnell O, Turner CH, Rannevik G, Karlsson MK. Bone loss and bone size after menopause. *N Engl J Med* 2003; **349**: 327-334

6 **Levine JP.** Long-term estrogen and hormone replacement therapy for the prevention and treatment of osteoporosis. *Curr Womens Health Rep* 2003; **3**: 181-186

7 **Miura S,** Tanaka E, Mori A, Toya M, Takahashi K, Nakahara K, Ohmichi M, Kurachi H. Hormone replacement therapy improves arterial stiffness in normotensive postmenopausal women. *Maturitas* 2003; **45**: 293-298

8 **Cohen LS,** Soares CN, Poitras JR, Prouty J, Alexander AB, Shifren JL. Short-term use of estradiol for depression in perimenopausal and postmenopausal women: a preliminary report. *Am J Psychiatry* 2003; **160**: 1519-1522

9 **Hodgin JB,** Maeda N. Minireview: estrogen and mouse models of atherosclerosis. *Endocrinology* 2002; **143**: 4495-4501

10 **Stark A,** Madar Z. Phytoestrogens: a review of recent findings. *J Pediatr Endocrinol Metab* 2002; **15**: 561-572

11 **Uesugi T,** Toda T, Tsuji K, Ishida H. Comparative study on reduction of bone loss and lipid metabolism abnormality in ovariectomized rats by soy isoflavones, daidzin, genistin, and glycitin. *Biol Pharm Bull* 2001; **24**: 368-372

12 **Wang JF,** Niu JZ, Li H, Zhang C, Liu LQ, Gao BH. Effects of soy extract on lipid metabolism in ovariectomized rats. *Zhongguo Zhongyao Zazhi* 2002; **27**: 285-288

13 **Boue SM,** Wiese TE, Nehls S, Burow ME, Elliott S, Carter-Wientjes CH, Shih BY, McLachlan JA, Cleveland TE. Evaluation of the estrogenic effects of legume extracts containing phytoestrogens. *J Agric Food Chem* 2003; **51**: 2193-2199

14 **Feoli AM,** Roehrig C, Rotta LN, Kruger AH, Souza KB, Kessler AM, Renz SV, Brusque AM, Souza DO, Perry ML. Serum and liver lipids in rats and chicks fed with diets containing different

oils. *Nutrition* 2003; **19**: 789-793
15 **Jang I,** Hwang D, Lee J, Chae K, Kim Y, Kang T, Kim C, Shin D, Hwang J, Huh Y, Cho J. Physiological difference between dietary obesity-susceptible and obesity-resistant Sprague Dawley rats in response to moderate high fat diet. *Exp Anim* 2003; **52**: 99-107
16 **Colandre ME,** Diez RS, Bernal CA. Metabolic effects of trans fatty acids on an experimental dietary model. *Br J Nutr* 2003; **89**: 631-639
17 **Guerin M,** Egger P, Soudant C, Le Goff W, van Tol A, Dupuis R, Chapman MJ. Dose-dependent action of atorvastatin in type IIB hyperlipidemia: preferential and progressive reduction of atherogenic apoB-containing lipoprotein subclasses (VLDL-2, IDL, small dense LDL) and stimulation of cellular cholesterol efflux. *Atherosclerosis* 2002; **163**: 287-296
18 **Marino M,** Pallottini V, D'Eramo C, Cavallini G, Bergamini E, Trentalance A. Age-related changes of cholesterol and dolichol biosynthesis in rat liver. *Mech Ageing Dev* 2002; **123**: 1183-1189
19 **Dubrac S,** Parquet M, Blouquit Y, Gripois D, Blouquit MF, Souidi M, Lutton C. Insulin injections enhance cholesterol gallstone incidence by changing the biliary cholesterol saturation index and apo A-I concentration in hamsters fed a lithogenic diet. *J Hepatol* 2001; **35**: 550-557
20 **Demonty I,** Deshaies Y, Lamarche B, Jacques H. Interaction between dietary protein and fat in triglyceride metabolism in the rat: effects of soy protein and menhaden oil. *Lipids* 2002; **37**: 693-699
21 **Perrella J,** Berco M, Cecutti A, Gerulath A, Bhavnani BR. Potential role of the interaction between equine estrogens, low-density lipoprotein (LDL) and high-density lipoprotein (HDL) in the prevention of coronary heart and neurodegenerative diseases in postmenopausal women. *Lipids Health Dis* 2003; **2**: 4
22 **Stangl H,** Graf GA, Yu L, Cao G, Wyne K. Effect of estrogen on scavenger receptor BI expression in the rat. *J Endocrinol* 2002; **175**: 663-672
23 **Karjalainen A,** Heikkinen J, Savolainen MJ, Backstrom AC, Kesaniemi YA. Mechanisms regulating LDL metabolism in subjects on peroral and transdermal estrogen replacement therapy. *Arterioscler Thromb Vasc Biol* 2000; **20**: 1101-1106
24 **Bobkova D,** Poledne R. Lipid metabolism in atherogenesis. *Cesk Fysiol* 2003; **52**: 34-41
25 **Yoon M,** Jeong S, Lee H, Han M, Kang JH, Kim EY, Kim M, Oh GT. Fenofibrate improves lipid metabolism and obesity in ovariectomized LDL receptor-null mice. *Biochem Biophys Res Commun* 2003; **302**: 29-34
26 **Sugimoto T,** Kimura T, Fukuda H, Iritani N. Comparisons of glucose and lipid metabolism in rats fed diacylglycerol and triacylglycerol oils. *J Nutr Sci Vitaminol* 2003; **49**: 47-55
27 **Chlebowski RT,** Hendrix SL, Langer RD, Stefanick ML, Gass M, Lane D, Rodabough RJ, Gilligan MA, Cyr MG, Thomson CA, Khandekar J, Petrovitch H, McTiernan A. Influence of estrogen plus progestin on breast cancer and mammography in healthy postmenopausal women: the Women's Health Initiative Randomized Trial. *JAMA* 2003; **289**: 3243-3253
28 **Sidelmann JJ,** Jespersen J, Andersen LF, Skouby SO. Hormone replacement therapy and hypercoagulability. Results from the Prospective Collaborative Danish Climacteric Study. *BJOG* 2003; **110**: 541-547
29 **Gallus S,** Negri E, Chatenoud L, Bosetti C, Franceschi S, La Vecchia C. Post-menopausal hormonal therapy and gallbladder cancer risk. *Int J Cancer* 2002; **99**: 762-763
30 **Khosla S.** Estrogen, selective estrogen receptor modulators and now mechanism-specific ligands of the estrogen or androgen receptor? *Trends Pharmacol Sci* 2003; **24**: 261-263
31 **Fontana A,** Delmas PD. Selective estrogen receptors modulators in the prevention and treatment of postmenopausal osteoporosis. *Endocrinol Metab Clin North Am* 2003; **32**: 219-232
32 **Hu JY,** Aizawa T. Quantitative structure-activity relationships for estrogen receptor binding affinity of phenolic chemicals. *Water Res* 2003; **37**: 1213-1222
33 **Latonnelle K,** Fostier A, Le Menn F, Bennetau-Pelissero C. Binding affinities of hepatic nuclear estrogen receptors for phytoestrogens in rainbow trout (*Oncorhynchus mykiss*) and Siberian sturgeon (*Acipenser baeri*). *Gen Comp Endocrinol* 2002; **129**: 69-79
34 **Bolego C,** Poli A, Cignarella A, Paoletti R. Phytoestrogens: pharmacological and therapeutic perspectives. *Curr Drug Targets* 2003; **4**: 77-87

Edited by Zhu LH and Chen WW **Proofread by** Xu FM

PO Box 2345, Beijing 100023, China
Fax: +86-10-85381893
E-mail: wjg@wjgnet.com www.wjgnet.com

World J Gastroenterol 2004;10(13):1971-1974
World Journal of Gastroenterology
 ISSN 1007-9327

• BRIEF REPORTS •

Anti-cancer effects of COX-2 inhibitors and their correlation with angiogenesis and invasion in gastric cancer

Suo-Lin Fu, Yun-Lin Wu, Yong-Ping Zhang, Min-Min Qiao, Ying Chen

Suo-Lin Fu, Yun-Lin Wu, Yong-Ping Zhang, Min-Min Qiao, Ying Chen, Department of Gastroenterology, Ruijin Hospital, Shanghai Second Medical University, Shanghai 200025, China
Supported by the Science and Technology Development Foundation of Shanghai, No. 02ZB14042
Correspondence to: Professor Yun-Lin Wu, Department of Gastroenterology, Ruijin Hospital, Shanghai Second Medical University, Shanghai 200025, China. fusuolin@163.com
Telephone: +86-21-64370045-665246
Received: 2004-02-14 **Accepted:** 2004-03-04

Abstract

AIM: To observe the anti-cancer effects of COX-2 inhibitors and investigate the relationship between COX-2 inhibitors and angiogenesis, infiltration or metastasis in SGC7901 cancer xenografts.

METHODS: Thirty athymic mice xenograft models with human stomach cancer cell SGC7901 were established and divided randomly into 3 groups of 10 each. Sulindac, one non-specific COX inhibitor belonging to non-steroidal anti-inflammatory drugs (a series of COX inhibitors known as NSAIDs) and celecoxib, one selective COX-2 inhibitor (known as SCIs) were orally administered to mice of treatment groups. Immunohistochemistry was used to examine the expression of PCNA, CD44v6 and microvessel density (MVD). Apoptosis was detected by using TUNEL assay.

RESULTS: Tumors in sulindac and celecoxib groups were significantly smaller than those in control group from the second week after drug administration ($P<0.01$). In treatment group, the cell proliferation index was lower ($P<0.05$) and apoptosis index was higher ($P<0.05$) than those in control groups. Compared with the controls, microvessel density was reduced ($P<0.01$) and expression of CD44v6 on tumor cells was weakened ($P<0.05$) in treatment groups.

CONCLUSION: COX-2 inhibitors have anticancer effects on gastric cancer. They play important roles in angiogenesis and infiltration or metastasis of stomach carcinoma. The anticancer effects of COX-2 inhibitors may include inducing apoptosis, suppressing proliferation, reducing angiogenesis and weakening invasiveness.

Fu SL, Wu YL, Zhang YP, Qiao MM, Chen Y. Anti-cancer effects of COX-2 inhibitors and their correlation with angiogenesis and invasion in gastric cancer. *World J Gastroenterol* 2004; 10(13): 1971-1974

http://www.wjgnet.com/1007-9327/10/1971.asp

INTRODUCTION

Gastric cancer is one of the commonest malignancies of human beings. The incidence of gastric cancer is typically high in China and as a result, more than 170 000 people die of it each year. It has important significance if certain drugs are found to lower its incidence or prevent it.

Chemoprevention of NSAIDs against colorectal cancer has been observed for long[1]. Since cyclooxygenase-2 (COX-2), one of the isoenzymes catalyzing the production of prostaglandins, was discovered in early 1990s[2], its gene construction, biochemical property and biological role have been understood step by step. The discovery of COX-2 has enlightened people to pay more attention to its relation with neoplasm. More and more selective COX-2 inhibitors (SCIs) have been found out, further facilitating the cognition to COX-2[3]. Although the roles COX-2 inhibitors play in various cancers and their mechanisms are being widely studied recently, few people have gone deep into *in vivo* experiments[4]. Based on *in vitro* cytologic experiments[5-7], this study went further into *in vivo* experiments so as to clarify the anti-cancer mechanisms of COX-2 inhibitors.

MATERIALS AND METHODS

Cell line

Human moderately differentiated gastric cancer cell line SGC7901 was cultured in RPMI 1640 medium at 37 ℃ in a humidified box (Hareus) with 50 mL/L CO_2 in our laboratory. When cells were amplified to a certain amount, they were dissociated, collected and suspended in PBS at a density of 5×10^7/mL.

Animals

Thirty male athymic mice (BALB/c nu/nu, 6 wk old, 17-20 g) were purchased from Shanghai Experimental Animal Center of Chinese Academy of Sciences. Mice were maintained under specific pathogen-free conditions (Micro-FLO positive air supply rodent cage system) and fed with sterilized food and autoclaved water. Experiments were started after 3 d of acclimatization.

Agents

Gum arabic (50 mg/kg) was dissolved in sterilized water at a concentration of 10 mg/mL. Sulindac (8 mg/kg; Sigma inc.) and celecoxib (10 mg/kg) were agitated and suspended with gum arabic (50 mg/kg) in water at a same concentration, respectively, by using a homogenizer.

Animal experiment procedure

Each mouse was inoculated with a subcutaneous injection of SGC7901 cells (5×10^6 in 0.1 mL PBS) into the right forelimb after weighed individually. Then these 30 mice were randomized into control, sulindac, and celecoxib groups. From the same day, the mice were orally administered different agents once daily (0.1mL; according to mouse weight of 20 g): the controls with gum arabic, the sulindac group with sulindac, and the celecoxib group with celecoxib. Mice' s diet, activity, stool, urine, and tumor growth were observed daily and shortest and longest diameters of xenografts were measured weekly. The tumor volume was deduced according to the formula[8]: volume (mm^3)=(the shortest diameter)^2×(the longest diameter) /2. Both

body weight and tumor size of each mouse were measured again before they were killed by cervical dislocation on the 32 nd day. All tumors were dissected from the body and weighed, then divided along the longest diameter. Halves of the specimens were frozen in liquid nitrogen while the other halves were fixed in 40 g/L phosphate-buffered formaldehyde.

Immunohistochemical assays

The formalin-fixed tissues were embedded in paraffin, and sectioned at a thickness of 4 μm. The sections were deparaffinized and hydrated gradually, and examined by histology of HE staining, immunohistochemistry, and TUNEL technique respectively. EnVision kits, the reagents of immunohistochemical assay, were purchased from GeneTech Co. Tests were performed according to the two step procedure. After incubated with 3% H_2O_2 for 10 min at room temperature and unmasked antigens by heat treatment, sections were covered with animal serum for 20 min. Specimens were then incubated with primary antibodies PCNA (PC10; 1/100; Santa Cruz), CD44v6 (ZM-0052; Beijing Zhongshan), or CD34 (BD) at 4 ℃ over night and further treated with EnVision kits for 30 min at room temperature. They were visualized by diaminobenzidin (DAB) and counter-stained by hematoxylin. TBS took the place of primary antibodies as a negative control. Sections were observed under microscope after mounted. The results of staining were analyzed and evaluated with American Image-Pro Plus software. The percentage of positive cells with PCNA staining in five 400× sights was counted as proliferation index (PI). The average of vessels with CD34 staining in three hot regions was calculated as MVD.

Apoptosis detection by TUNEL method

The reagent kit for apoptosis detection, TdT-FragEL DNA fragmentation detection kit was bought from ONCOGENE. Test procedures consisting of the following sections were provided in the brochure of the kit. The specimens were deparaffinized and hydrated gradually, and rinsed with 1× TBS, then incubated with proteinase K (20 μg/mL in 10 mmol/L Tris-HCl) for 20 min. After immersed in 30 mL/L H_2O_2 at room temperature for 5 min and in TdT labeling reaction mixture at 37 ℃ for 1.5 h, specimens were covered with 1× conjugate for 30 min, visualized by DAB and counter-stained by hematoxylin afterwards. TBS took the place of primary antibodies as a negative control. After mounted, sections were observed under microscope. The results of staining were analyzed and evaluated with American Image-Pro Plus software. The percentage of positive cells with TUNEL staining in five 400× sights served as apoptosis index (AI).

Statistical analysis

Data were analyzed by software of SAS 6.12 and shown in a default form of mean±SD.

RESULTS

Animal experiments

During the experiment, the growth, diet, activity, *etc*. of mice were carefully observed, no hematuresis and hematochezia were shown during experiment. Two mice died accidentally in the process however, which might be caused by the operation of enema clyster. The body weight among groups was not significantly different, nor did the weight change during the experiment. The growth of xenografts in treatment groups was significantly suppressed compared with the controls, but there was no difference between two treatment groups (Figure 1).

Difference of tumor growth in different groups was shown from the second week (Table 1).

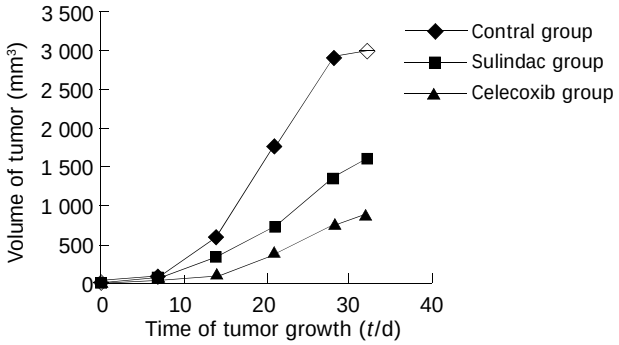

Figure 1 Effects of sulindac and celecoxib on the growth of human gastric cancer xenografts in athymic mice.

Table 1 Tumor volume of three groups (mean±SD)

Group	Date (d)				
	7	14	21	28	32
Contro l	45.2±35.5	609±289	1 779±366	2 920±776	2 984±589
Sulindac	78±137	351.5±227.0	723±514	1 370±832	1 590±1 009
Celecoxib	19.5±14.8	108±105	408±390	788±701	891±764
P	0.30	0.0002	0.0001	0.0001	0.0001

F=27.95, P<0.01 *vs* control group. No significant difference in volume was shown between sulindac group and celecoxib group.

In each group, five mice out of ten were picked out randomly and dissected with no obvious erosion, bleeding, or ulcer of stomach and no neoplasm metastasis.

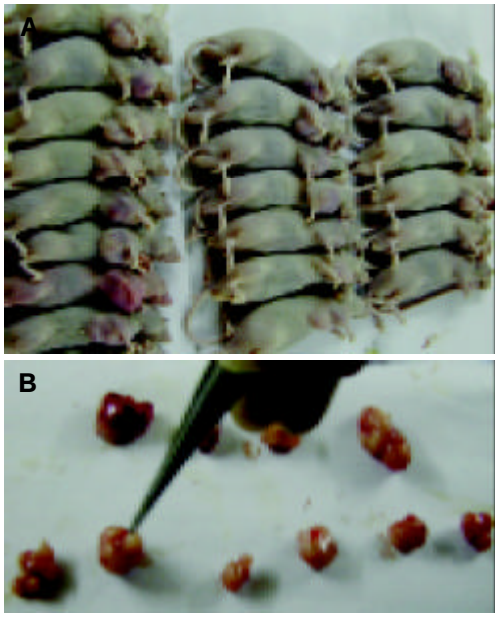

Figure 2 Histology of tumors. A: *In vivo* appearance of xenografts; B: *In vitro* appearance of xenografts.

Tumor histology

Xenograft took on an appearance of big globular neoplasia or cluster of several small neoplastic nods (Figure 2). Necrosis could be seen comparatively common in cut of tumors, and the size of necrotic area seemed to be related to the volume of tumor. With regard to HE-stained sections, deeply stained tumor cells with big nuclei were arranged tightly with no cavum structure found under microscope, which coincided with the characteristics of tumor histology. Tumor cells among all groups showed no difference in morphology, while necrosis could be commonly seen under microscope.

Cell proliferation and apoptosis

PI of control group was significantly higher than that of sulindac group and celecoxib group ($P<0.05$), but the difference was not notable between two treatment groups. AI in two treatment groups was higher than that in the control group ($P<0.05$), while there was also no difference between the two groups. The AI/PI value was calculated and compared among all groups. Consequently, it was apparently larger in two treatment groups ($P<0.01$), however no difference was shown between them.

Tumor angiogenesis

Immunohistochemical staining of CD34 revealed that celecoxib and sulindac could suppress angiogenesis of SGC7901 xenografts. MVD in sulindac and celecoxib groups was apparently lower than that in the control ($P<0.01$). Although it was lower in celecoxib group, the difference is not notable.

Invasiveness of tumor cells

Membranes of tumor cells were stained brown by CD44v6 staining. By analysis of staining intensity and quantity of positive cells with Image-Pro Plus software, the expression of CD44v6 was markedly weakened by the treatment with sulindac and celecoxib ($P<0.05$), but there was no apparent difference between sulindac and celecoxib groups.

DISCUSSION

COX-2 was successfully cloned and its structure has been clearly recognized more than ten years before[9]. It is an inducible isoenzyme that catalyzes production of a series of prostaglandins. Participating in inflammatory reaction, COX-2 is expressed by a variety of tumor cells and correlated to tumorigenesis. Several researches have revealed the prophylactic effect of NSAIDs on colorectal carcinoma and their therapeutic effect on colon polyps[10]. Here the mechanism of NSAIDs is considered as inhibiting COX-2. Non-specific COX inhibitors inhibit COX-1 at the same time, which may cause fatal side effects. As a result, they are not so ideal in long-term application for preventing tumorigenesis. Lately developed selective COX-2 inhibitors shed light on chemoprevention of neoplasms. Nevertheless a series of researches have to be carried out to confirm its effectiveness, reliability and virtues before extensive clinical application.

The expression of COX-2 also existed in gastric cancer while the positive rate might reach 61.4%[11]. We have shown that human moderately differentiated gastric cancer cell SGC7901 can express COX-2. Its growth was suppressed *in vitro* after the treatment of sulindac, both proliferation and apoptosis were affected[5]. This time we inoculated athymic mice with SGC7901 to observe the effects of sulindac and celecoxib, a clinically applied selective COX-2 inhibitor, on *in vivo* tumor by establishing animal models of gastric cancer. The results showed that both drugs had a notable inhibition on gastric cancer growth. Although the effect of celecoxib was better than of sulindac, no statistical difference was shown.

To explore the anticancer mechanisms of COX-2 inhibitors, we evaluated the influence of two drugs on tumor cell proliferation and apoptosis in xenografts by immunohistochemistry, which verified the results of *in vitro* researches. Administration of both sulindac and celecoxib increased apoptosis of cancer cells *in vivo*. The AI/PI, a value reflecting cytokinetics, showed a more significant difference.

The growth of tumor cells depends on nutrition supply, which largely relies on angiogenesis. Ischemia can induce tumor cell apoptosis, speeding up necrosis and cell extinction. Many researches verified the relation between COX-2 and angiogenesis[12] and the inhibition effects of NSAIDs on blood vessel endothelial cells[13]. We observed that sulindac and celecoxib obviously decreased the blood vessel quantity of xenografts and reduced the MVD compared to that of the control group. COX-2 inhibitors realized their anti-cancer effects by repressing the expression of anti-apoptosis gene *Bcl-2*[14] and reducing angiogenesis in stomach carcinoma, thereby impairing the nutrition supply of the tumor, further inhibiting proliferation and inducing apoptosis of gastric cancer cells. Our results were similar to those of Sawaoka *et al*.[15].

Some studies suggested the expression of COX-2 was correlated to the clinicopathologic characteristics of gastric cancer, such as infiltration, lymphatic or hematogenous metastasis, prognosis, *etc*[16]. As a cell surface adhesive molecule, CD44 was the receptor of hyaluronic acid and involved in cell-to-cell and cell-to-matrix interactions. Especially, the expression of its spliced variant 6 was closely correlated to cell movement, carcinogenesis, progress, incursion and metastasis of gastric carcinoma[17]. In this study we evaluated COX-2 inhibitors' influence on the CD44v6 expression by using animal models, finding the positive cells of expressing CD44v6 (pigmented in membrane) often existed in the periphery of tumors with a tendency to surround blood vessels. The positivity of CD44v6 staining was strong in the control group and significantly weakened in two medication groups, which demonstrating that COX-2 inhibitors play a role in depressing invasiveness and reducing metastasis of gastric cancer, which could be one of their anti-cancer effects. No obvious metastasis was found by rough anatomy of mice in our study however. It requires improved experiment design.

In brief, the mechanisms of COX-2 inhibitors resisting the growth of gastric cancer might include suppressing cell proliferation, inducing apoptosis, reducing angiogenesis and weakening invasiveness. But selective COX-2 inhibitors were not observed obviously more effective than non-specific COX inhibitors. The former did not show any advantage in side effects either, such as gastrorrhagia, ulceration, and so on, which may be relevant to experiment animal model and short experiment duration. Further studies are required. This study also showed comparatively more necrosis of tumors, but its correlation to drug administration was unclear. In comparison, Japanese researchers discovered no relation between drug treatment of indomethacin or NS398 in MKN45 cell xenografts[15].

This is the first part of a serial study, and we will verify the results afterwards using Western blotting, RT-PCR, *etc*.

REFERENCES

1 **Kune GA**, Kune S, Watson LF. Colorectal cancer risk, chronic illnesses, operations, and medcations: case control results from the Melbourne Colorectal Cancer Study. *Cancer Res* 1988; **48**: 4399-4404

2 **Xie WL**, Chipman JG, Robertson DL, Erikson RL, Simmons DL. Expression of a mitogen-reponsive gene encoding prostaglandin synthase is regulated by mRNA splicing. *Proc Natl Acad Sci U S A* 1991; **88**: 2692-2696

3 **Kawamori T**, Rao CV, Seibert K, Reddy BS. Chemopreventive activity of celecoxib, a specific cyclooxygenase-2 inhibitor, against colon carcinogenesis. *Cancer Res* 1998; **58**: 409-412

4 **Hahm KB**, Lim HY, Sohn S, Kwon HJ, Lee KM, Lee JS, Surh YJ, Kim YB, Joo HJ, Kim WS, Cho SW. *In vitro* evidence of the role of COX-2 in attenuating gastric inflammation and promoting gastric carcinogenesis. *J Environ Pathol Toxicol Oncol* 2002; **21**: 165-176

5 **Sun B**, Wu YL, Zhang XJ, Wang SN, He HY, Qiao MM, Zhang YP, Zhong J. Effects of Sulindac on growth inhibition and apoptosis induction in human gastric cancer cells. *Shijie Huaren Xiaohua Zazhi* 2001; **9**: 997-1002

6 **Wu YL**, Sun B, Zhang XJ, Wang SN, He HY, Qiao MM, Zhong J, Xu JY. Growth inhibition and apoptosis induction of Sulindac on Human gastric cancer cells. *World J Gastroenterol* 2001; **7**: 796-800

7 **Li JY**, Wang XZ, Chen FL, Yu JP, Luo HS. Nimesulide inhibits proliferation via induction of apoptosis and cell cycle arrest in human gastric adenocarcinoma cell line. *World J Gastroenterol* 2003; **9**: 915-920

8 **Ovejera AA**, Houchens DP, Barker AD. Chemotherapy of human tumor xenografts in genetically athymic mice. *Ann Clin Lab Sci* 1978; **8**: 50-56

9 **Hla T**, Neilson K. Human cyclooxygenase-2 cDNA. *Proc Natl Acad Sci U S A* 1992; **89**: 7384-7388

10 **Labayle D**, Fischer D, Vielh P, Drouhin F, Pariente A, Bories C, Duhamel O, Trousset M, Attali P. Sulindac causes regression of rectal polyps in familial adenomatous polyposis. *Gastroenterology* 1991; **101**: 635-639

11 **Joo YE**, Oh WT, Rew JS, Park CS, Choi SK, Kim SJ. Cyclooxygenase-2 expression is associated with well-differentiated and intestinal-type pathways in gastric carcinogenesis. *Digestion* 2002; **66**: 222-229

12 **Tsujii M**, Kawano S, Tsuji S, Sawaoka H, Hori M, DuBois RN. Cyclooxygenase regulates angiogenesis induced by colon cancer cells. *Cell* 1998; **93**: 705-716

13 **Sun B**, Wu YL, Zhang XJ, He HY, Wang SN, Qiao MM. Growth inhibition of Sulindac and Indomethacin on human umbilical vein endothelial cells ECV304. *Zhongliu* 2003; **23**: 370-372

14 **Sun B**, Wu YL, Wang SN, Zhang XJ, He HY, Qiao MM, Zhang J. The effects of sulindac on induction of apoptosis and expression of cyclooxygenase-2 and Bcl-2 in human hepatocellular carcinoma cells. *Zhonghua Xiaohua Zazhi* 2002; **22**: 338-340

15 **Sawaoka H**, Tsuji S, Tsujii M, Gunawan ES, Sasaki Y, Kawano S, Hori M. Cyclooxygenase inhibitors suppress angiogenesis and reduce tumor growth *in vivo*. *Lab Invest* 1999; **79**: 1469-1477

16 **Ohno R**, Yoshinaga K, Fujita T, Hasegawa K, Iseki H, Tsunozaki H, Ichikawa W, Nihei Z, Sugihara K. Depth of invasion parallels increased cyclooxygenase-2 levels in patients with gastric carcinoma. *Cancer* 2001; **91**: 1876-1881

17 **Joo M**, Lee HK, Kang YK. Expression of E-cadherin, beta-catenin, CD44s and CD44v6 in gastric adenocarcinoma: relationship with lymph node metastasis. *Anticancer Res* 2003; **23**: 1581-1588

Edited by Wang XL and Chen WW **Proofread by** Xu FM

PO Box 2345, Beijing 100023, China
Fax: +86-10-85381893
E-mail: wjg@wjgnet.com www.wjgnet.com

World J Gastroenterol 2004;10(13):1975-1978
World Journal of Gastroenterology
 ISSN 1007-9327

• BRIEF REPORTS •

Loss of heterozygosity on chromosome 10q22-10q23 and 22q11.2-22q12.1 and *p53* gene in primary hepatocellular carcinoma

Guang-Neng Zhu, Li Zuo, Qing Zhou, Su-Mei Zhang, Hua-Qing Zhu, Shu-Yu Gui, Yuan Wang

Guang-Neng Zhu, Li Zuo, Qing Zhou, Su-Mei Zhang, Hua-Qing Zhu, Shu-Yu Gui, Yuan Wang, Laboratory of molecular Biology and Department of Biochemistry, Anhui Medical University, Hefei 230032, Anhui Province, China
Li Zuo, Qing Zhou, Su-Mei Zhang, Hua-Qing Zhu, Shu-Yu Gui, Yuan Wang, Anhui Province Key Laboratory of Genomic Research, Hefei 230032, Anhui Province, China
Guang-Neng Zhu, Department of Biochemistry, Bengbu Medical College, Bengbu 233003, Anhui Province, China
Shu-Yu Gui, Department of Respiratory Disease, the First Affiliated Hospital of Anhui Medical University, Hefei 230032, Anhui Province, China
Supported by the Natural Science Foundation of Anhui Province, No.99044312 (YW), No.01043716(SYG) and Natural Science Foundation of Anhui Educational Commission, No.JL-97-077 (YW)
Correspondence to: Professor Yuan Wang, Laboratory of Molecular Biology and Department of Biochemistry, Anhui Medical University, Hefei 230032, Anhui Province, China. wangyuan@mail.hf.ah.cn
Telephone: +86-551-5161140
Received: 2003-09-09 **Accepted:** 2003-10-12

Abstract

AIM: To analyze loss of heterozygosity (LOH) and homozygous deletion on *p53* gene (exon2-3, 4 and 11), chromosome 10q22-10q23 and 22q11.2 -22q12.1 in human hepatocellular carcinoma (HCC).

METHODS: PCR and PCR-based microsatellite polymorphism analysis techniques were used.

RESULTS: LOH was observed at D10S579 (10q22-10q23) in 4 of 20 tumors (20%), at D22S421 (22q11.2-22q12.1) in 3 of 20(15%), at TP53.A (*p53* gene exon 2-3) in 4 of 20 (20%), at TP53.B (*p53* gene exon 4) in 6 of 20(30%), and at TP53.G *(p53* gene exon 11) in 0 of 20(0%). Homozygous deletion was detected at 10q22-10q23(8/20; 40%), 22q11.2-22q12.1(8/20; 40%), p53 gene exon 2-3(0/20;0%), *p53* gene exon 4(6/20; 30%), and *p53* gene exon 11(2/20; 10%).

CONCLUSION: There might be unidentified tumor suppressor genes on chromosome 10q22-10q23 and 22q11. 2-22q12.1 that contribute to the pathogenesis and development of HCC.

Zhu GN, Zuo L, Zhou Q, Zhang SM, Zhu HQ, Gui SY, Wang Y. Loss of heterozygosity on chromosome 10q22-10q23 and 22q11.2-22q12.1 and *p53* gene in primary hepatocellular carcinoma. *World J Gastroenterol* 2004; 10(13): 1975-1978
http://www.wjgnet.com/1007-9327/10/1975.asp

INTRODUCTION

Hepatocellular carcinoma (HCC) is a primary liver malignancy with high mortality. It is among the most common malignancies worldwide, especially in Asia, Africa and Southern Europe[1]. It has been generally accepted that HCC is highly associated with chronic hepatitis B virus (HBV) or hepatitis C virus (HCV) infection or alcohol intake which induces cirrhosis[2]. High intake of aflatoxin B found in many kinds of food is also reported to be a risk factor for HCC[3,4]. Like other solid tumors, It has been proposed that hepatocarcinogenesis and metastasis of HCC is a multi-step process requiring the accumulation of genetic alterations, but the precise molecular pathogenesis is far from clear.

Loss of heterozygosity (LOH) analysis has become an effective way to identify informative loci and candidate tumor suppressor genes (TSGs). Molecular chromosomal studies of tumors by using polymerase chain reaction (PCR) -based polymorphic markers can detect small loci of anomalies that may harbor TSGs. Search for novel TSGs is based largely on the identification of common regions of deletion on chromosomes. LOH has been found in many types of tumors, including HCC. LOH in HCC has been detected on chromosomal arms 1p, 2q, 4p, 4q, 5q, 6q, 8p, 8q, 9p, 9q, 11p, 13q, 16p, 16q and 17p[5-11]. However, deletion of 10q22-10q23, and 22q11.2-22q12.1 and p53 gene exon 2-3 and 11 in HCC has not been investigated.

In the present study, we detected LOH and homozygous deletion on chromosome 10q, and chromosome 22q near the NF2 gene locus, and *p53* gene locus in 20 cases of HCC.

MATERIALS AND METHODS

Specimens

Surgical specimens of HCC were collected from the First Affiliated Hospital of Anhui Medical University and the Affiliated Hospital of Bengbu Medical College. The patients were born and grew in different places of Anhui Province, China. Both tumor and corresponding non-tumor liver tissues were immediately put into liquid nitrogen after separation and then stored at -80 ℃ until DNA extraction. Diagnosis of HCC was confirmed by pathological examination.

DNA extraction

Genomic DNA was extracted from tissues with the standard proteinase K-phenol/choloroform method. To each of the samples, 500 μL of DNA extraction buffer containing 200 mmol/L NaCl, 10 g/L sodium dodecyl sulfate, 2 mmol/L EDTA, 0.1 mol/L Tris-HCl was added during the process of homogenization. After 0.2 mg/mL proteinase K was added, the sample was shaken for 12 h at 37 ℃. After phenol-chloroform extraction, DNA was precipitated with cold ethanol overnight at -20 ℃. After centrifugation, the pellet was dried and resuspended in 50 μL TE buffer (Tris-EDTA buffer). DNA was stored at -20 ℃ until polymerase chain reaction (PCR) amplification was performed.

Pcr amplification

PCR amplification primer pairs for p53 gene, 10q22-10q23 and 22q11.2-22q12.1 are as follows (Table 1).

Polyacrylamide gel electrophoresis

PCR product (12 μL) was mixed with 3 μL 950 g/L deionized formamide and 3 μL DNA loading buffer containing 2.5 g/L

Table 1 PCR amplification primer pairs for p53 gene, 10q22-10q23 and 22q11.2-22q12.1

Markers name	Forward	Reverse	Annealing (T℃)	Size (bp)
TP53.A1/TP53.A2 (p53 gene exon 2-3)	TGGATCCTCTTGCAGCAGCC	AACCCTTGTCCTTACCAGAA	54	270
TP53.B1/TP53.B2 (p53 gene exon 4)	ATCTACAGTCCCCCTTGCCGGC	AACTGACCGTGCAAGTCA	57	296
TP53.G1/TP53.G2 (p53 gene exon 11)	TCTCCTACAGCCACCTGAAG	CTGACGCACACCTATTGCAA	58	122
D10S579	CCGATCAATGAGGAGTGCC	ATACACCCAGCCAATGCTGC	60	260
D22S421	CTGCTGCCCCTAACATATCAC	GGCCAGGAGTGTCTGAATTTTA	65	163
CDK4[1]	GGAGGTCGGTACCAGAGTG	CATGTAGACCAGGACAGG	60	364

[1]The aim of PCR amplification of CDK4 gene was to confirm that genomic DNA had been truly extracted from all samples. These primer sequences were retrieved from the Genome Database (http://gdbwww.gdb.org). PCR amplification was performed in a 50 μL reaction volume containing 400 ng template DNA, 0.2 mmol/L of each deoxynucleotide triphosphate, 20 mmol/L of each primer, 1.5 mmol/L $MgCl_2$, 1× reaction buffer and 2 U Taq DNA polymerase. The reaction mixture was denatured for 5 min at 94℃. DNA was subsequently amplified for 35 cycles with 94℃ for 30 s, 54-65℃ for 30 s, 72℃ for 40 s, and a final extension at 72℃ for 8 min. PCR product (8 μL) was electrophoresed in a 20 g/L agarose gel, visualized by staining with ethidium bromide and ultraviolet illumination, and documented by a computer-linked camera. The target DNA fragments were confirmed by comparing to a 100 bp DNA ladder.

Table 2 Clinical and genetic features of 20 patients with HCC (*, LOH; △, homozygous deletion; O, no deletion; +, HBsAg positive; -, HBsAg negative)

Case No.	Age (yr)	Sex	HBsAg	TP53.A	TP53.B	TP53.G	D10S579	D22S421
1	49	M	+	*	*	O	*	O
2	55	M	+	O	△	O	O	△
3	39	M	+	O	△	O	△	△
4	55	F	+	*	O	O	O	*
5	72	F	+	O	*	△	△	O
6	40	M	+	O	O	O	O	O
7	34	F	+	O	*	O	△	△
8	56	M	+	O	O	O	O	O
9	27	F	_	O	*	O	△	O
10	50	M	+	O	O	O	O	△
11	48	M	+	O	△	O	△	△
12	52	M	+	O	O	O	△	O
13	63	F	+	O	△	△	△	△
14	60	M	+	O	△	O	*	△
15	65	M	+	O	O	O	*	O
16	34	M	+	O	*	O	O	O
17	64	M	+	*	*	O	*	*
18	52	F	+	O	O	O	△	O
19	32	F	+	O	△	O	O	△
20	38	M	+	*	O	O	O	*
LOH rate (%)				20	30	0	20	15
Homozygous deletion rate (%)				0	30	10	40	40

xylene cyanol FF, 2.5 g/L bromophenol blue, and 300 g/L glycerin. The mixture was denatured at 95 ℃ for 5 min, put onto ice for 10 min, loaded onto 80 g/L denaturing polyacrylamide gel containing 3.3 mol/L urea and then electrophoresed at 100 V for 2 h. The gel was silver-stained[13]. LOH was determined by visual evaluation, which compared the allele bands from tumors and the corresponding non-tumor tissues. The complete loss of one polymorphic allele from those seen in the paired control DNA was scored as allelic loss by three independent observers. PCR reactions were performed twice to confirm LOH.

RESULTS

HCC tumor and corresponding non-tumor liver tissues of 20 patients were studied for LOH on 10q22-10q23 (D10S579), 22q11.2-22q12.1 (D22S421), and 17p13.1 by five microsatellite markers, and the rate of LOH was 20%(4/20), 15%(3/20), 50%(10/20), respectively (Table 2). Homozygous deletion was observed in 8 of 20 cases (40%) for the marker D10S579, 8 of 20 cases (40%) for D22S421, 6 of 20 cases (30%) for TP53.B, 2 of 20 cases (10%) for TP53.G, and in 0 of 20 cases (0%) for the marker TP53.A.

Results of 20 g/L agarose gel electrophoresis are shown in Figure 1. LOH in tumor and corresponding non-tumor liver tissues are shown in Figure 2.

DISCUSSION

HCC is one of most malignant tumors. The mechanism of hepato-carcinogenesis is a multi-factor and multi-step process requiring the accumulation of genetic alterations, including chromosomal aberration, oncogene activation, inactivation of TSGs and abnormality of growth factors and growth factor

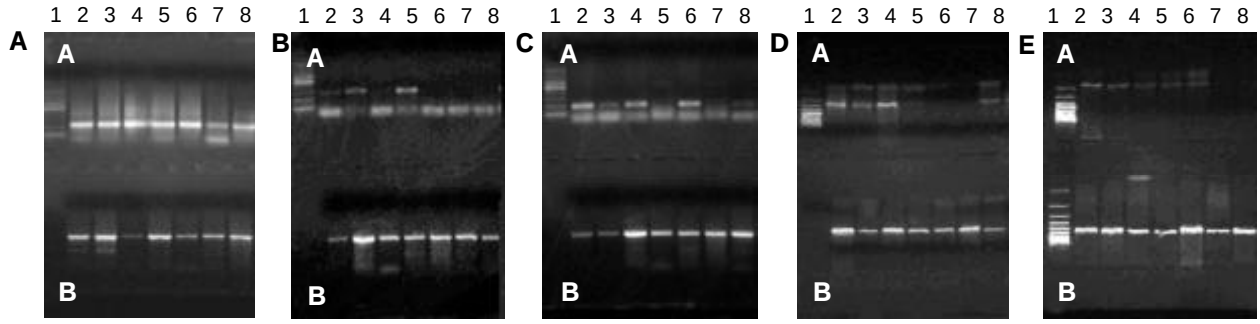

Figure 1 Agarose gel electrophoresis of PCR products of p53 gene exons 2-3, 4, 11, and chromosome 10q22-10q23 and 22q11.2-22q12.1. A: PCR products of p53 exon 2-3. Lane 1, 100 bp DNA marker; Lanes 2-8, PCR products of p53 exon2-3 (A) and CDK4 gene (B, as a control) amplified from HCC genomic DNA. No homozygous deletion of p53 exon 2-3 was found in all HCC specimens. B: PCR products of p53 exon 4. Lane 1, 100 bp DNA marker; Lanes 2-8, PCR products of p53 exon4 (A) and CDK4 gene (B, as a control) amplified from HCC genomic DNA. Lines 4, 6-8, homozygous deletion. C: PCR products of p53 exon11. Line 1, 100 bp DNA ladder; Lanes 2-8, PCR products of p53 exon11 (A) and CDK4 gene (B, as a control) amplified from HCC genomic DNA. Lanes 5 and 7, homozygous deletion. D: PCR products of 10q22-10q23. Lane1, 100 bp DNA marker; Lanes 2-8, PCR products of 10q22-10q23 (A) and CDK4 gene (B, as a control) amplified from HCC genomic DNA. Lines 6 and 7, homozygous deletion. E: PCR products of 22q11.2-22q12.1. Lane 1, 100 bp DNA ladder; Lanes 2-8, PCR products of 22q11.2-22q12.1 (A) and CDK4 gene (B, as a control) amplified from HCC genomic DNA. Lanes 7 and 8, homozygous deletion.

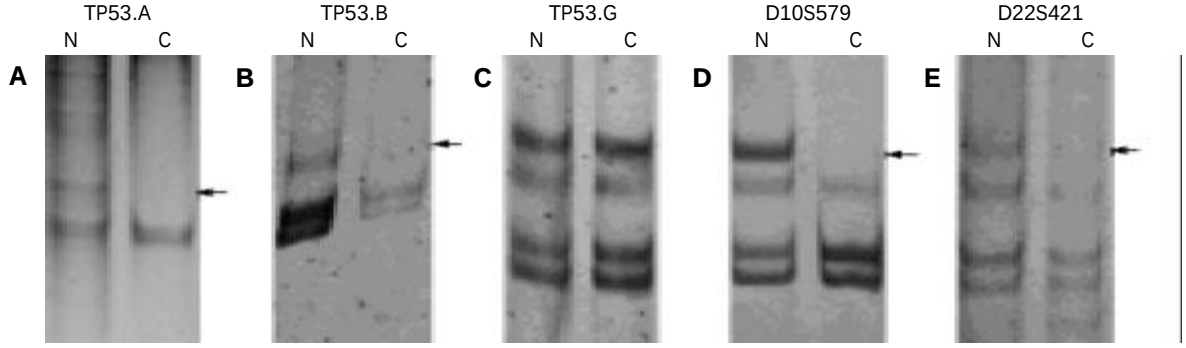

Figure 2 Representative illustrations of LOH detected with the microsatellite markers TP53.A, TP53.B, TP53.G, D10S579, D22S421 in human hepatocellular carcinomas (C) as compared to non-tumor liver tissues (N). The arrows show the location of the missing alleles. A: TP53.A (case 4); B: TP53.B (case 17); C: TP53.G (case 19,no LOH); D: D10S579 (case 17); E: D22S421 (case 20).

receptors. Of these factors, inactivation of TSGs is a very important factor.

Allelic loss on chromosome 17p is among the most common genetic abnormalities in many human cancers. *p53* gene is thought to be the gene associated with the genesis of these cancer types, including HCC[12]. *p53* is activated in response to DNA damage, inducing either cell cycle arrest to permit DNA repair or apoptosis. Loss of p53 function occurs mainly through allelic deletions at chromosome 17p13, where *p53* gene is located. In human HCC, LOH at chromosome 17p13 has been reported in 25-60% of tumors, and the worldwide prevalence of p53 mutation is around 28% with, however, important geographic variations. In this study, LOH was observed at exon 2 and 3 (TP53.A) and exon 4 (TP53.B), of the gene in 20% and 30% of HCC cases, respectively, but not detected at exon 11 (TP53.G). In addition, all but one (19/20) patients were positive with HBsAg. These data also support the idea that LOH at *p53* gene and HBV infection are highly associated with the pathogenesis and development of HCC.

LOH on D10S579 has been reported in renal cell carcinoma (RCC)[13]. We investigated 20 HCCs in the present study, and found four cases had LOH and eight cases had homozygous deletion on 10q22-10q23(D10S579). Our finding suggests that on 10q22-10q23, there might be unidentified TSG(s) that plays an important role in the pathogenesis of hepatocellular carcinoma.

22q11.2-22q12.1(D22S421) is near the locus of *NF2* gene. *NF2* (neurofibromatosis 2) gene, which is located on chromosome 22q12.2-22q12.2, is postulated to be a tumor suppressor gene. It encodes for a protein with 595 amino acids, designated as merlin or schwannomin which belongs to a family of cytoskeletal proteins. The majority of *NF2* gene mutations are deletions, insertions, and point mutations, all of which lead to a nonfunctional, truncated protein[14].

LOH at the *NF2* locus has been observed in many tumors, including schwannoma[15], meningioma[16], malignant mesothelioma[17], gastrointestinal stromal tumor[18], colorectal carcinoma[19]. However, Handel-Fernandez *et al*.[20] found that there was no LOH at *NF2* gene in pancreatic adenocarcinoma, but 37% of the cases had deletions which were clustered into two separate areas of chromosome 22 - one proximal and one distal to *NF2* gene. In the present study, we detected LOH on 22q11.2-22q12.1 in three of 20 HCCs and homozygous deletion on 22q11.2-22q12.1 in eight of 20 HCCs. Our finding suggests that 22q11.2-22q12.1 likely contains an unidentified tumor suppressor gene that contributes to the pathogenesis and the development of HCC, that the region plays an important role of cis-acting element similar to *NF2* gene, or that it acts the part of trans-acting factor similar to other TSGs, such as *p53* gene.

In conclusion, we have obtained important new information on LOH and homozygous deletion in chromosome 10q, 22q and 17p, in a subset of HCC. Inactivation of p53 gene and unidentified tumor suppressor gene(s), present in regions of 10q22-10q23 and 22q11.2-22q12.1, may play an important role in the pathogenesis of HCC.

REFERENCES

1 **Simonetti RG**, Camma C, Fiorello F, Politi F, D'Amico G, Pagliaro L. Hepatocellular carcinoma. A worldwide problem and the major risk factors. *Dig Dis Sci* 1991; **36**: 962-972

2 **Harris CC**. Hepatocellular carcinogenesis: recent advances and speculations. *Cancer Cells* 1990; **2**: 146-148

3 **Yakicier MC**, Legoix P, Vaury C, Gressin L, Tubacher E, Capron F, Bayer J, Degott C, Balabaud C, Zucman-Rossi J. Identification of homozygous deletions at chromosome 16q23 in aflatoxin B1 exposed hepatocellular carcinoma. *Oncogene* 2001; **20**: 5232-5238

4 **Martins C**, Kedda MA, Kew MC. Characterization of six tumor suppressor genes and microsatellite instability in hepatocellular carcinoma in southern African blacks. *World J Gastroenterol* 1999; **5**: 470-476

5 **Fujimori M**, Tokino T, Hino O, Kitagawa T, Imamura T, Okamoto E, Mitsunobu M, Ishikawa T, Nakagama H, Harada H. Allelotype study of primary hepatocellular carcinoma. *Cancer Res* 1991; **51**: 89-93

6 **Fujimoto Y**, Hampton LL, Wirth PJ, Wang NJ, Xie JP, Thorgeirsson SS. Alterations of tumor suppressor genes and allelic losses in human hepatocellular carcinomas in China. *Cancer Res* 1994; **54**: 281-285

7 **Hsu HC**, Peng SY, Lai PL, Sheu JC, Chen DS, Lin LI, Slagle BL, Butel JS. Allelotype and loss of heterozygosity of p53 in primary and recurrent hepatocellular carcinomas. A study of 150 patients. *Cancer* 1994; **73**: 42-47

8 **Boige V**, Laurent-Puig P, Fouchet P, Flejou JF, Monges G, Bedossa P, Bioulac-Sage P, Capron F, Schmitz A, Olschwang S, Thomas G. Concerted nonsyntenic allelic losses in heperploid hepatocellular carcinoma as determined by a high-resolution alleltype. *Cancer Res* 1997; **57**: 1986-1990

9 **Nagai H**, Pineau P, Tiollais P, Buendia MA, Dejean A. Comprehensive allelotyping of human hepatocellular carcinoma. *Oncogene* 1997; **14**: 2927-2933

10 **Shao J**, Li Y, Li H, Wu Q, Hou J, Liew C. Deletion of chromosomes 9p and 17 associated with abnormal expression of p53, p16/MTS1 and p15/MTS2 gene protein in hepatocellular carcinomas. *Chin Med J* 2000; **113**: 817-822

11 **Herath NI**, Kew MC, Walsh MD, Young J, Powell LW, Leggett BA, MacDonald GA. Reciprocal relationship between methylation status and loss of heterozygosity at the $p14^{ARF}$locus in Australian and South African hepatocellular carcinomas. *J Gastroenterol Hepatol* 2002; **17**: 301-307

12 **Levine AJ**. p53, the cellular gatekeeper for growth and division. *Cell* 1997; **88**: 323-331

13 **Alimov A**, Li C, Gizatullin R, Fredriksson V, Sundelin B, Klein G, Zabarovsky E, Bergerheim U. Somatic mutation and homozygous deletion of PTEN/MMAC1 gene of 10q23 in renal cell carcinoma. *Anticancer Res* 1999; **19**(5B): 3841-3846

14 **Lasota J**, Fetsch JF, Wozniak A, Wasag B, Sciot R, Miettinen M. The neurofibromatosis type 2 gene is mutated in perineurial cell tumors: a molecular genetic study of eight cases. *Am J Pathol* 2001; **158**: 1223-1229

15 **Mohyuddin A,** Neary WJ, Wallace A, Wu CL, Purcell S, Reid H, Ramsden RT, Read A, Black G, Evans DG. Molecular genetic analysis of the NF2 gene in young patients with unilateral vestibular schwannomas. *J Med Genet* 2002**; 39:** 315-322

16 **Leuraud P**, Marie Y, Robin E, Huguet S, He J, Mokhtari K, Cornu P, Hoang-Xuan K, Sanson M. Frequent loss of 1p32 regin but no mutation of the p18 tumor suppressor gene in meningiomas. *J Neurooncol* 2000; **50**: 207-213

17 **Pylkkanen L**, Sainio M, Ollikainen T, Mattson K, Nordling S, Carpen O, Linnainmaa K, Husgafvel-Pursiainen K. Concurrent LOH at multiple loci in human malignant mesothelioma with preferential loss of NF2 gene region. *Oncol Rep* 2002; **9**: 955-959

18 **Fukasawa T**, Chong JM, Sakurai S, Koshiishi N, Ikeno R, Tanaka A, Matsumoto Y, Hayashi Y, Koike M, Fukayama M. Allelic loss of 14q and 22q,NF2 mutation, and genetic instability occur independently of c-kit mutation in gastrointestinal stromal tumor. *Jpn J Cancer Res* 2000; **91**: 1241-1249

19 **Sugai T**, Habano W, Nakamura S, Yoshida T, Uesugi N, Sasou S, Itoh C, Katoh R. Use of crypt isolation to determine loss of heterozygosity of multiple tumor suppressor genes in colorectal carcinoma. *Pathol Res Pract* 2000; **196**: 145-150

20 **Handel-Fernandez ME**, Nassiri M, Arana M, Perez MM, Fresno M, Nadji M, Vincek V. Mapping of genetic deletions on the long arm of chromosome 22 in human pancreatic adenocarcinomas. *Anticancer Res* 2000; **20**: 4451-4456

Edited by Xia HHX and Xu FM

PO Box 2345, Beijing 100023, China
Fax: +86-10-85381893
E-mail: wjg@wjgnet.com www.wjgnet.com

World J Gastroenterol 2004;10(13):1979-1983
World Journal of Gastroenterology
 ISSN 1007-9327

• BRIEF REPORTS •

Reversal of 5-flouroucial resistance by adenovirus-mediated transfer of wild-type p53 gene in multidrug-resiatant human colon carcinoma LoVo/5-FU cells

Zhi-Wei Yu, Peng Zhao, Ming Liu, Xin-Shu Dong, Ji Tao, Xue-Qin Yao, Xin-Hua Yin, Yu Li, Song-Bin Fu

Zhi-Wei Yu, Peng Zhao, Ming Liu, Xin-Shu Dong, Department of Abdominal Surgery, the Third Affiliated Hospital of Harbin Medical University, Harbin 150040, Heilongjiang Province, China
Ji Tao, Department of General Surgery, The fifth Hospital of Harbin Medical University, Harbin 150040, Heilongjiang Province, China
Xue-Qin Yao, Department of General Surgery, Nanfang Hospital, Guangzhou 510515, Guangdong Province, China
Xin-Hua Yin, Department of Geriatrics,the Second Affiliated Hospital of Harbin Medical University, Harbin 150096, Heilongjiang Provinece, China
Yu Li, Song-Bin Fu, Department of Molecular Biology, Harbin Medical University, Harbin 150057, Heilongjiang Province, China
Correspondence to: Zhi-Wei Yu, Department of Abdominal Surgery, the Third Affiliated Hospital of Harbin Medical University, Harbin 150040, Heilongjiang Province, China. yuzhiwei1974@163.com
Telephone: +86-451-6677580-2146
Received: 2003-07-04 **Accepted:** 2003-08-28

Abstract

AIM: To observe the reversal effects of wide-type p53 gene on multi-drug resistance to 5-FU (LOVO/5-FU).

METHODS: After treatment with Ad-p53, LOVO/5-FU sensitivity to 5-Fu was investigated using tetrazolium dye assay. Multidrug resistance gene-1 (MDR1) gene expression was assayed by semi-quantitative reverse transcription-polymerase chain reaction and the expression of p53 protein was examined by Western blotting.

RESULTS: The reversal activity after treatment with wide-type p53 gene was increased up to 4.982 fold at 48 h. The expression of MDR1 gene decreased significantly after treatment with wide-type p53 gene, and the expression of p53 protein lasted for about 5 d, with a peak at 48 h, and began to decrease at 72 h.

CONCLUSION: Wide-type p53 gene has a remarkable reversal activity for the high expression of MDR1 gene in colorectal cancers. The reversal effects seem to be in a time dependent manner. It might have good prospects in clinical application.

Yu ZW, Zhao P, Liu M, Dong XS, Tao J, Yao XQ, Yin XH, Li Y, Fu SB. Reversal of 5-flouroucial resistance by adenovirus-mediated transfer of wild-type p53 gene in multidrug-resiatant human colon carcinoma LoVo/5-FU cells. *World J Gastroenterol* 2004; 10(13): 1979-1983

http://www.wjgnet.com/1007-9327/10/1979.asp

INTRODUCTION

Resistance to cytotoxic agents is the major cause of failure of medical treatment of human cancer and it is known that tumor cells can become resistant to anticancer drugs by a variety of different mechanisms[1]. MDR (multidrug-resistance) is a form of drug resistance characterized by decreased cellular sensitivity to a broad range of chemotherapeutic agents and due significantly to the over expression of MDR1 mRNA and its product P-gp[2,3]. As an integral membrane protein, the M_r 170 000 P-gp is thought to be an energy-dependent membrane pump involved in the excretion of toxins in normal cells[4]. Elevated expression of P-gp in malignant cells results in increased efflux and therefore reduced intracellular accumulation of cytotoxic agents, such as 5-FU, anthracyclines, Vinca alkaloids, and epipodophyllotoxins, but is not cross-resistant to alkylating agents, antimetabolites, and cisplatin. This decrease is considered as the basic mechanism of the MDR phenomenon[4-7]. While a number of pharmacological agents have been shown to partially reverse MDR *in vitro*[8], there remains a need to identify more potent, more specific, and less toxic chemosensitizers for clinical use.

Inactivity of p53 gene by missense mutation or deletion is the most common genetic alteration in human cancers[9]. The loss of p53 function has been reported to enhance cellular resistance to a variety of chemotherapeutic agents [10-13]. Our preliminary experiments[14] also showed that there was a strong relationship between the MDR1 gene expression and mutated p53 gene in colorectal cancers.

Thus, in light of the fact that MDR1 is over-expressed in colorectal cancer that often lacks a functional p53[14], we ask whether p53 plays a role in the control of MDR1 gene. Therefore, we sought to determine whether the introduction of the wild - type p53 gene in LOVO/5-FU cells by an adenoviral vector could increase the sensitivity of cells to a DNA cross-linking agent 5-FU *in vitro* and *in vivo*.

MATERIALS AND METHODS

Cell culture

LoVo cells were derived from a human colon adenocarcinoma. 5-FU-resistant LoVo sub-line (LoVo/5-FU) was obtained from the LoVo cell line by selection with 5-FU[15], and maintained in medium containing 5 ng/mL 5-FU as described previously. LoVo/5-FU cells were kindly provided by Dr. Xue-Qing Yao. Monolayer cultures of LoVo and LoVo/5-FU were maintained in RPMI 1640 medium supplemented with 150 g/L heat-inactivated fetal calf serum (Sigma Chemical Co), 10 mL/L of a 200 mmol/L glutamine solution, 100 U/mL penicillin, 100 μg/mL streptomycin, and 10 g/L vitamin solution for minimum essential Eagle' s medium purchased from GIBICO-BRL (Gaithersburg, MD). Cell lines grown in the presence of agents were passed in drug-free medium 2 to 3 times prior to use. All cells were grown at 37 ℃ in a humidified atmosphere of 50 mL/L CO_2 and 950 mL/L air.

Adenovirus vectors

Construction and identification of Ad-p53 and Ad-LacZ were finished and kindly provide by Dr. Xin-Hua Yin. Briefly, recombinant p53 adenovirus, Ad5CMV-p53 containing cytomegalovirus promoter, wild-type p53 cDNA, and SV40

early lopyadenylation signal in a minigene cassette was inserted into the E1-deletion region of modified Ad5. p53 shuttle vector and recombinant plasmid pJM 17 were cotransfected into 293 cells (Ad-transformed human embryonic kidney cells) by a liposome-mediated technique. The culture supernatant of 293 cells showing the complete cytopathic effect was collected and used for subsequent infections. Control Ad-LacZ virus was generated in a similar manner. Viral titers were determined by plaque forming activity in 293 cells. Concentrated virus was dialyzed, aliquoted, and stored at -80 ℃. Cells were harvested 36-40 h after infection, pelleted, resuspended in PBS, and lysed. Cell debris was removed by double cesium chloride gradient ultracentrifugation.

Transient transfections

Adherent cells were plated in the wells of a 12-well plate. After 24 h, Ad-LacZ was transfected into the cells in different diluting densities. Forty-eight transfection, the cells were washed twice with PBS and fixed for 2 h with 40 g/L formaldehyde solution at 4 ℃, then washed twice again with PBS and stained with 1 g/L X-gal solution for about 8 h at 37 ℃. Observed under the electron microscope, the cells with blue staining were positive cells with LacZ expression, and calculated to determine the transfection efficiency.

Drug sensitivity testing

Chemosensitizers in the various cell lines were determined by using the tetrazolium-based colorimetric assay (MTT [*i.e.*, 3-(4,5-dimethy1-2-thiazoly1)- 2m 5-dipheny1-2H-tetrazolium bromide] assay). Cells (LoVo/5-FU/Ad-p53 cells, LoVo/5-FU cells, LoVo cells;) were seeded in a 96-well microtiter plate at a density of 1×10^5 cells/well and each well contained 200 μL medium. Cells were exposed 24 h after plating to various concentrations of 5-FU for 4 h. After treatment, medium was removed and replaced with 200 μL of drug-free medium. Plates were incubated for further 72 h. At this time, 15 μL of MTT (4 mg/mL) solution was added to each well. After a 4-h incubation at 37 ℃, the cellular supernant was gently aspirated, and insoluble formazan crystals were dissolved by adding 180 μL 1 000 g/L DMSO (dimethyl sulfoxide) to each well, then the plates were shaken for about 10 min. The absorbance of each well was determined by a spectrophotometry at the wavelength of 570 nm with a microculture plate reader. Inhibition of cell growth was determined as a percentage of absorbance of vehicle-treated control cultures. IC_{50} was the concentration of drugs that reduced staining (A_{570}) to 50% of vehicle-treated controls.

The effect of chemosensitizers on drug resistance was studied by exposing cells to a range of concentrations of cytotoxic drugs in the absence or presence of concentrations of chemosensitizers. Dose-response curves were corrected for the inhibition of cell growth caused by chemosensitizers alone, and the "fold reversal" of MDR for 5-FU plus chemosensitizer combination was calculated as follows:

$$\text{Fold reversal}=\frac{IC_{50}\ \text{drug alone}}{IC_{50}\ \text{drug +chemosensitizer}}$$

Western blot analysis of wild-type p53 expression

Cells infected with the indicated adenovirus and MOI were grown to about 80% confluence in 10-cm plates. After washed with PBS, cells were scraped from the plate, washed once with ice-cold PBS containing 1 mmol/L phenylmethylsulfonyl fluoride, and centrifuged at 1 000 r/min for 4 min. The cell pellet was resuspended in ice-cold radioimmunoprecipitation assay buffer (1% NP40, 0.5% sodium deoxycholate, and 1 g/L SDS, 10 μg/mL aprotinin, 10 μg/mL leupeptin and 1 μg/mL pepstatin A) and sonicated. After centrifugation at 12 000 *g* at 4 ℃ for 20 min, the resulting supernatant was harvested as the total cell lysate. The protein was aliquoted and stored at -70 ℃ until use. Protein samples were electrophoresed through a 125 g/L polyacrylamide gel containing 1 g/L SDS and the gel was run at 30 mA for 3 h. Separated proteins were transferred onto nitrocellulose paper by electroblotting. After blocked with 50 mL/L blocking reagent, the nitrocellulose membrane was probed with a monoclonal antibody against human wild-type p53 from Oncogene Science. Detection was accomplished using ECL western blotting detection reagents from Amersham Pharmacia Corp.

Determination of MDR1 mRNA expression by RT-PCR

Expression of the MDR1 gene was determined by measuring the mRNA level from total RNA by SUPERSCRIPT™ first-strand synthesis system (GIBCO BRL,Gaithersburg, MD), using MDR1-specific primer pairs. Briefly, total RNA was extracted from established lines with TRIzol reagent (Life Technologies, Inc.). Equal amounts of RNA, as determined by absorbance at 260 nm, were denatured and size was fractionated by electrophoresis through a 12 g/L agarose gel containing formaldehyde and 2 μg/dL ethidium bromide (Figure 1). Equal amounts (1 μg) of total RNA from each tissue were treated with RNase-free DNAse I to remove any contaminated DNA. DNAse-treated RNA was then used to synthesize single-strand cDNAs by AMV reverse transcriptase in the presence of random primers, followed by PCR amplification. The primers used for PCR reaction were: MDR1-1, GTA CCC ATC ATT GCA ATA GC and MDR1-2, CAA ACT TCT GCT CCT GAG TC. These two MDR1 primers bracketed the COOH-terminal region of the MDR1 cDNA and gave a PCR product of 147 bp. PCR amplification was performed by pre-denaturing at 95 ℃ for 3 min, and then running 30 cycles in the following conditions: denaturation at 94 ℃ for 40 s, annealing for 40 s at 55 ℃, and extension at 72 ℃ for 50 s. As internal control, RT-PCR for β-actin was carried out using 5' CGT GGG CCG CCC TAG GCA CCA 3' (forward primer) and 5' TTG GCC TTA GGG TTC AGG GGG 3' (reverse primer) in the same conditions as described for MDR1, and showed a PCR product of 243 bp. The PCR products were electrophoresed in a 20 g/L agarose gel with 0.5 μg/mL ethidium bromide and visualized under UV light. Quantitation of relative band volume counts was performed using Molecular analyst for windows software. To estimate MDR1 expression levels, a MDR1 index was designated as a band volume count ratio of MDR1 to constitutively expressed β-actin, because β-actin mRNA was expressed constitutively in cells. The higher the MDR1 index, the higher the expression level of MDR1 mRNA in cells.

RESULTS

Sensitivity of LoVo and LoVo/5-FU to 5-flurouracil

The sensitivity of LoVo and LoVo/5-FU cells to 5-furouracil was evaluated using the MTT assay as shown in Table 1. Previous studies utilizing MTT assays have shown that the LoVo/5-FU cell line is 8.988-fold more resistant to 5-flurouracil than parental LoVo cells. We found the two cell lines showed differences in sensitivity to 5-flurouracil, too. The concentration inducing 50% inhibition of cell proliferation for 5-Flurouracil was 0.82 μg/mL for the parental line and 7.37 μg/mL for the LoVo/5-FU cells.

Effect of wtp53 gene on cell growth in LoVo/5-FU cells

Figure 1 showed the effect of wild-type p53 on the LoVo/5-FU cells. It suggested that the dose of Ad-p53 for experiment didn' t affect the growth rate of LoVo/5-FU cells during the six days after transfection.

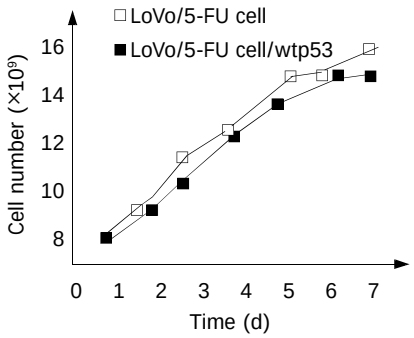

Figure 1 Effect of wild-type p53 on the growth rate of LoVo/5-FU cells.

Effect of wild-type p53 on LoVo/5-FU cells sensitivity to 5-flurouracil

The effect of wild-type p53 on 5-flurouracil sensitivity was examined using the MTT assay. A dose of 8.17×10^{10} pfu/mL Ad-p53 was chosen as the dose to modulate 5-flurouracil sensitivity. For this study, cells were treated with wild-type p53 for 48 h, 5-flurouracil was then added to the final concentration of 0.25 to 15 μg/mL for 3 h, and then the medium was removed and replaced with a fresh medium without drugs and the incubation was continued. Cell growth was determined after an addition for 72 h. Treatment with wild-type p53 appeared to decrease the resistance of LoVo/5-FU cells to 5-flurouracil (Table 1).

Table 1 Effect of wild-type p53 on LoVo/5-FU sensitivity to 5-flurouracil

Cell lines	IC_{50} (μg/mL)	Resistant time	Reverse time
LoVo cells	0.82		
LoVo/5-FU cells	7.37	8.988	
LoVo/5-FU cells+wild-type p53	1.48[b]	1.804	4.982

[b]$P<0.01$ compared with LoVo/5-FU cell control group.

Expression of wild-type p53 protein in cell lines

The X-gal staining suggested that the dilution of 1:20 for Ad-p53 could make about more than 80% cells infected successfully. LoVo/5-FU was transduced *in vitro* with the human wild-type -p53 cDNA by exposing to Ad-p53 (1:20). To make sure that the constructed p53 expression vector, Ad-p53, efficiently expressed functional wild-type p53, we determined its protein expression and transactivating function. Western blot analysis showed a higher level of wild-type p53 protein expression as early as 48 h after infection with Ad-p53, and which lasted for 5 d, then decreased significantly on the sixth day. But no wild-type p53 was detected in parental (uninfected) cells or control cells infected with Ad-LacZ (data not shown), suggesting that the transfer and expression of p53 by Ad-p53 were highly efficient (Figure 2).

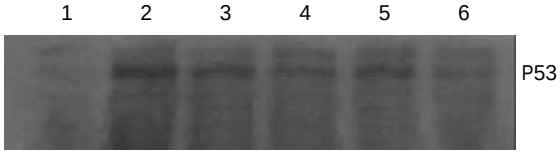

Figure 2 Western blot analysis of wild-type p53 in LoVo/5-FU cell line and LoVo/5-FU cells transiently transfected with p53 expression vector (Ad-p53). Lane 1: LoVo/5-FU cell line. Lanes 2, 3, 4, 5, 6: LoVo/5-FU cells transiently transfected with Ad-p53 for 2, 3, 4, 5, 6 d accordingly. Levels of wild-type p53 protein (lanes 2-6) were determined by Western-blot analysis with an antibody which could detect wild-type forms of p53 protein.

Expression of wild-type p53 suppressed endogenous MDR1 gene expression

We asked whether wild-type p53 expression could indeed inhibit endogenous MDR1 gene expression in LoVo/5-FU cells. Successful generation of cell lines constantly expressing wild-type p53 was tested in human LoVo/5-FU cells transfected with Ad-p53 as above, and these cells constantly maintained wild-type p53 for about 6 d and provided a valuable reagent for studying drug sensitivity. As seen in Figure 2, vector-transfected LoVo/5-FU cells expressing wild-type p53, had a lower MDR1 mRNA expression than LoVo/5-FU cells without wild-type p53 expression, as determined by RT-PCR. There was a decrease in MDR1 transcripts compared with the empty vector-transfected cell line, suggesting that constitutive expression of p53 could inhibit endogenous MDR1 transcription in LoVo/5-FU cells, and this suppression showed a time-dependent mode Figure 3, 4 and Tables 2, 3.

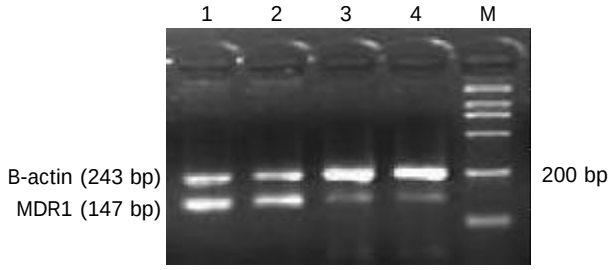

Figure 3 Results of RT-PCR for expression of MDR1 mRNAs in p53-null and wild-type p53 expressing LoVo/5-FU cells. M: marker; Lanes 1 and 2: results of untransfected LoVo/5-FU cells; Lanes 3 and 4: results of transfected LoVo/5-FU cells.

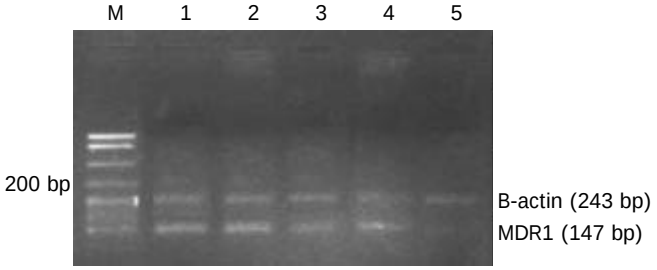

Figure 4 Results of RT-PCR for expression of MDR1 mRNAs of transfected LoVo/5-FU cells at different time. M: marker; Lanes 1, 2, 3, 4, 5: the cells transfected with Ad-p53 for 2, 3, 4, 5, 6 d accordingly.

Table 2 MDR1 expression in different cell lines

	Lane 1	Lane 2	Lane 3	Lane 4
MDR1/β-actin	1.26	1.19	0.42	0.33

Table 3 MDR1 expression of LoVo/5-FU cells on different day after dealing with Ad-p53

Time/d	2	3	4	5	6
MDR1/β-actin	1.22	1.24	1.06	0.86	0.42

DISCUSSION

Tumor cell resistance to chemotherapeutic drugs represents a major problem in clinical oncology; patients with colorectal

cancer are generally unresponsive to chemotherapy. The goal of our current cancer research was to find ways to improve the efficacy of gene replacement therapy for cancer by investigating interactions between the gene products and chemotherapeutic drugs.

Resistance to cytotoxic agents is the major cause of failure of medical treatment of human cancer and it is known that tumor cells could become resistant to anticancer drugs by a variety of mechanisms[1]. In numerous *in vitro* models, this resistance has been shown to be mediated by MDR1 gene, whose product P-gp is thought to be an energy-dependent membrane pump involved in the excretion of toxins in normal cells. Elevated expression of P-gp in malignant cells could result in increased efflux and therefore reduced intracellular accumulation of cytotoxic agents. This decrease has been considered as the basic mechanism of the MDR phenomenon[2-7].

LoVo/5-FU cells were selected from the LoVo parental cell line through culture in the presence of 5-flurorucial and were resistant to 5-FU which was toxic to LoVo parental cells. LoVo/5-FU cells had cross-resistance to the drugs comprising the classical MDR phenotype[15]. In this study, we found the resistance subline overexpressed MDR1 mRNA and no wild-type p53 protein was expressed.

An adenovirus system has potential advantages for gene delivery *in vivo*, such as easy production of high titer virus, high infection efficiency, and infectivity for many types of cells[16-18]. The stability and duration of the expression of introduced gene are still controversial. For chemo-gene therapy, the expression levels and high infectivity may be more significant than the duration of expression because drugs can kill infected cells within several days. In our model, the expression of wild-type p53 gene was driven independently by the cytomegalovirus promoter contained in an Ad-p53 vector. The expression of wild-type p53 protein by Ad-p53 peaked after 48 h and decreased to a low level by the sixth day. This suggests that a transiently high level of wild-type p53 expression is sufficient to initiate the cytotoxic program in cancer cells.

We found that pretreatment of LoVo/5-FU cells with Ad-p53 was capable of restoring cell sensitivity to 5-flurorucial. In the parental cell line, however, Ad-p53 did not potentiate 5-flurorucial toxicity. The functional reversal of MDR by Ad-p53 in LoVo/5-FU cells appeared to be mediated by changes of the MDR1 gene expression.

Several agents have been described to affect MDR1 gene expression or the MDR phenotype in human or rodent cells, such as the Ca^{2+} channel blocker, verapamil, calmodulin inhibitor, trifluoperazine, which have been shown to reverse the MDR phenotype *in vitro* through direct competition with drugs for P-gp binding in the absence of changes in P-gp expression. Treatment with these agents could result in increased intracellular concentrations of cytotoxic drugs, which are thus a final common pathway in the reversal of the multidrug-resistant phenotype. They are presently used in clinical trials to patients with drug refractory tumors. However, they could induce significant cardiotoxicity, thus which limiting their clinical usefulness[19,20]. The Ad-p53 concentrations reported here are active *in vivo* in the absence of significant toxicity.

Wild-type p53, a M_r 53 000 nuclear phosphoprotein involved in the control of cell growth and apoptosis is the most commonly altered gene in human tumors[21]. Its role as a tumor suppressor has been well documented as its inactivation was strongly correlated with human cancer[21-23]. p53 protein had different domains for DNA binding, transactivation, and tetramerization functions[24,25]. After binding to consensus for DNA sequences, p53 could positively regulate the expression of downstream effctor genes, including Gadd45, p21(WAF1/CIP1)[26], and mouse muscle creation kinase[27]. In addition, wild-type p53 could also negatively regulate a variety of genes that lack a p53 consensus binding site, including DNA topoisomerase II[28], MDR1[29-32], c-fos[33], and other viral and cellular promoters. It has been suggested that transcriptional repression by p53 could result from its direct interactions with transcription factors, such as TATA-binding protein[34,35], Sp1[36,37] and CCAAT-binding factor[28]. Taken together, these observations strongly imply that p53 acts directly with the transcription machinery to modulate MDR1 transcription.

Many tumors have no functional p53, and others express high levels of MDR1. Whether there is a direct connection has remained to be determined[38]. However, our results suggested that restoration of wild-type p53 in tumor cells could overcome the uncontrolled up-regulation of MDR1 gene expression, and could add to the beneficial effect of wild-type p53 gene therapy that would restore cell growth inhibition and apoptosis pathway to facilitate drug-induced cell killing.

A variety of treatment protocols, including surgery, chemotherapy, and radiotherapy, have been tried for human colorectal cancer, but the long-term survival rate remains unsatisfactory. The combination therapy we present here might be effective as an adjuvant treatment to prevent local recurrence following primary tumor resection or as a treatment that could be given by intralesional injections in drug-resistant primary, metastatic, or locally recurrent colorectal cancer. Protocols are being developed to explore these clinical applications.

REFERENCES

1 **Zhu XH**, Li JY, Xia XM, Zhu MQ, Geng MJ, Chen L, Zhang JQ. Multidrug resistance mechanisms in cell line HL-60/VCR. *Aizheng* 2002; **21**: 1310-1313

2 **Tsuruo T,** Naito M, Tomida A, Fujita N, Mashima T, Sakamoto H, Haga N. Molecular targeting therapy of cancer: drug resistance, apoptosis and survival signal. *Cancer Sci* 2003; **94**: 15-21

3 **Tsuruo T**. Molecular cancer therapeutics: recent progress and targets in drug resistance. *Intern Med* 2003; **42**: 237-243

4 **Fromm MF.** The influence of MDR1 polymorphisms on P-glycoprotein expression and function in humans. *Adv Drug Deliv Rev* 2002; **54**: 1295-1310

5 **Johnstone RW,** Ruefli AA, Smyth MJ. Multiple physiological functions for multidrug transporter P-glycoprotein? *Trends Biochem Sci* 2000; **25**: 1-6

6 **Shapiro AB,** Ling V. Effect of quercetin on Hoechst 33342 transport by purified and reconstituted P-glycoprotein. *Biochem Pharmacol* 1997; **53**: 587-596

7 **Abu-Qare AW**, Elmasry E, Abou-Donia MB. A role for P-glycoprotein in environmental toxicology. *J Toxicol Environ Health B Crit Rev* 2003; **6**: 279-288

8 **Thomas H,** Coley HM. Overcoming multidrug resistance in cancer: an update on the clinical strategy of inhibiting p-glycoprotein. *Cancer Control* 2003; **10**: 159-165

9 **Tullo A,** D'Erchia AM, Sbisa E. Methods for screening tumors for p53 status and therapeutic exploitation. *Expert Rev Mol Diagn* 2003; **3**: 289-301

10 **Chang BD,** Swift ME, Shen M, Fang J, Broude EV, Roninson IB. Molecular determinants of terminal growth arrest induced in tumor cells by a chemotherapeutic agent. *Proc Natl Acad Sci U S A* 2002; **99**: 389-394

11 **Yazlovitskaya EM,** DeHaan RD, Persons DL. Prolonged wild-type p53 protein accumulation and cisplatin resistance. *Biochem Biophys Res Commun* 2001; **283**: 732-737

12 **Yuan R,** Meng Q, Hu H, Goldberg ID, Rosen EM, Fan S. P53-independent downregulation of p73 in human cancer cells treated with Adriamycin. *Cancer Chemother Pharmacol* 2001; **47**: 161-169

13 **Hawkins DS,** Demers GW, Galloway DA. Inactivation of p53 enhances sensitivity to multiple chemotherapeutic agents. *Cancer Res* 1996; **56**: 892-898

14 **Yu ZW,** Dong XS, Wang XH. The relationship between the mdr1 gene expression and mutations of p53 gene and ras gene in colorectal cancer. *Chin J Oncol* 2002; **24**: 480

15 **Yao XQ,** Qing SH, Yang Y. Establishment of multidrug-resistant human colorectal cancer cell line LoVo / 5-FU: a preliminary study of biological characterization. *J First Mil Med Univ* 2001; **21**: 19-21
16 **Xu ZL,** Mizuguchi H, Mayumi T, Hayakawa T. Regulated gene expression from adenovirus vectors: a systematic comparison of various inducible systems. *Gene* 2003; **309**: 145-151
17 **Mohr L,** Geissler M. Gene therapy: new developments. *Schweiz Rundsch Med Prax* 2002; **91**: 2227-2235
18 **Park J,** Ries J, Gelse K, Kloss F, von der Mark K, Wiltfang J, Neukam FW, Schneider H. Bone regeneration in critical size defects by cell-mediated BMP-2 gene transfer: a comparison of adenoviral vectors and liposomes. *Gene Ther* 2003; **10**: 1089-1098
19 **Durie BG,** Dalton WS. Reversal of drug-resistance in multiple myeloma with verapamil. *Br J Haematol* 1988; **68**: 203-206
20 **Epstein J,** Xiao HQ, Oba BK. P-glycoprotein expression in plasma cell myeloma is associated with resistance to VAD. *Blood* 1989; **74**: 913-917
21 **Vogelstein B,** Kinzler KW. p53 function and dysfunction. *Cell* 1992; **70**: 523-526
22 **Baker SJ,** Markowitz S, Fearon ER, Willson JK, Vogelstein B. Suppression of human colorectal carcinoma cell growth by wide-type p53. *Science* 1990; **249**: 912-915
23 **Zambetti GP,** Levine AJ. A comparison of the biological activities of wild-type p53 and mutant p53. *FASEB J* 1993; **7**: 855-865
24 **Cho Y,** Gorina S, Jeffrey PD, Pavletich NP. Crystal structure of a p53 tumor suppressor-DNA complex: understanding tumorigenic mutations. *Science* 1994; **265**: 346-355
25 **Wolcke J,** Reimann M, Klumpp M, Gohler T, Kim E, Deppert W. Analysis of p53 "latency" and "activation" by fluorescence correlation spectroscopy: Evidence for different modes of high affinity DNA binding. *J Biol Chem* 2003; **278**: 32587-32595
26 **Sowa Y,** Sakai T. Gene-regulating chemoprevention against cancer–as a model for "molecular-targeting prevention" of cancer. *Nippon Eiseigaku Zasshi* 2003; **58**: 267-274
27 **Zambetti GP,** Bargonetti J, Walker K, Prives C, Levine AJ. Wild-type p53 mediates positive regulation of gene expression through a specific DNA sequence element. *Genes Dev* 1992; **6**: 1143-1152
28 **Wang Q,** Zambetti GP, Suttle DP. Inhibition of DNA topoisomerase II alpha gene expression by the p53 tumor suppressor. *Mol Cell Biol* 1997; **17**: 389-397
29 **Chin KV,** Ueda K, Pastan I, Gottesman MM. Modulation of activity of the promoter of the human MDR1 gene by Ras and p53. *Science* 1992; **255**: 459-462
30 **Zastawny RL,** Salvino R, Chen J, Benchimol S, Ling V. The core promoter region of the P-glycoprotein gene is sufficient to conger differential responsiveness to wild-type p53 and mutant p53. *Oncogene* 1993; **8**: 1529-1535
31 **Thottassery JV,** Zambetti GP, Arimori K, Schuetz EG, Schuetz JD. P53-dependent regulation of MDR1 gene expression causes selective resistance to chemotherapeutic agents. *Proc Natl Acad Sci U S A* 1997; **94**: 11037-11042
32 **Bush JA,** Li G. Regulation of the Mdr1 isoforms in a p53-deficient mouse model. *Carcinogenesis* 2002; **23**: 1603-1607
33 **Elkeles A,** Juven-Gershon T, Israeli D, Wilder S, Zalcenstein A, Oren M. The c-fos proto-oncogene is a target for transactivation by the p53 tumor suppressor. *Mol Cell Biol* 1999; **19**: 2594-2600
34 **Seto E,** Usheva A, Zambetti GP, Momand J, Horikoshi N, Weinmann R, Levine AJ, Shenk T. Wild-type p53 binds to the TATA-binding protein and represses transcription. *Proc Natl Acad Sci U S A* 1992; **89**: 12028-12032
35 **Huang H,** Kaku S, Knights C, Park B, Clifford J, Kulesz-Martin M. Repression of transcription and interference with DNA binding of TATA-binding protein by C-terminal alternatively spliced p53. *Exp Cell Res* 2002; **279**: 248-259
36 **Borellini F**, Glazer RI. Induction of Sp1-p53 DNA-binding heterocomplexes during granulocyte / macrophage colony-stimulating factor-dependent proliferation in human erythroleukemia cell line TF-1. *J Biol Chem* 1993; **268**: 7923-7928
37 **Liedtke C**, Groger N, Manns MP, Trautwein C. The human caspase-8 promoter sustains basal activity through SP1 and ETS-like transcription factors and can be up-regulated by a p53-dependent mechanism. *J Biol Chem* 2003; **278**: 27593-27604
38 **Galmarini CM,** Kamath K, Vanier-Viornery A, Hervieu V, Peiller E, Falette N, Puisieux A, Ann Jordan M, Dumontet C. Drug resistance associated with loss of p53 involves extensive alterations in microtubule composition and dynamics. *Br J Cancer* 2003; **88**: 1793-1799

Edited by Wang XL and Xu FM

PO Box 2345, Beijing 100023, China
Fax: +86-10-85381893
E-mail: wjg@wjgnet.com www.wjgnet.com

World J Gastroenterol 2004;10(13):1984-1988
World Journal of Gastroenterology
 ISSN 1007-9327

• BRIEF REPORTS •

Influence of survivin and caspase-3 on cell apoptosis and prognosis in gastric carcinoma

Yun-Hong Li, Chen Wang, Kui Meng, Long-Bang Chen, Xiao-Jun Zhou

Yun-Hong Li, Department of Gastroenterology, Gulou Hospital, Medical College of Nanjing University, Nanjing 210008, Jiangsu Province, China
Chen Wang, Medical College of Nanjing University, Nanjing 210093, Jiangsu Province, China
Long-Bang Chen, Department of Oncology, Clinical School of Medical College of Nanjing University/Nanjing General Hospital of Nanjing Command, Nanjing 210002, Jiangsu Province, China
Kui Meng, Xiao-Jun Zhou, Department of Pathology, Clinical School of Medical College of Nanjing University/Nanjing General Hospital of Nanjing Command, Nanjing 210002, Jiangsu Province, China
Correspondence to: Dr. Yun-Hong Li, Department of Gastroenterology, Gulou Hospital, Medical College of Nanjing University, 321 Zhongshan Road, Nanjing 210008, Jiangsu Province, China. liyunhong37@vip.sina.com.cn
Telephone: +86-25-86522328 **Fax:** +86-25-83307016
Received: 2003-12-23 **Accepted:** 2004-01-15

Abstract

AIM: To evaluate the role of survivin and caspase-3 in apoptosis of gastric carcinoma, as well as in prognosis of patients with gastric carcinoma.

METHODS: Expressions of survivin and caspase-3 were investigated immunohistochemically in 80 gastric carcinoma patients without a history of chemo-radiation therapy. Tumor cell apoptosis was examined by TUNEL method.

RESULTS: Immunohistochemical analysis showed that survivin expression was positive in 61 of 80 patients (76%) with gastric carcinoma. In contrast, no expression of survivin in adjacent normal tissues was detected. Expression level of caspase-3 was higher in normal tissues than in carcinoma. Patients with higher expression of survivin had worse histological grades and pathological stages. Expression of caspase-3 was significantly associated with histological stages, but not with the pathological stages. Although survivin expression in carcinoma was not inversely related to caspase-3, patients with survivin (-) and caspase-3(+) had the maximum apoptosis index.

CONCLUSION: Expression level of survivin was associated with histological grades and pathological stages of the tumor, indicating that survivin may be a poor prognosis factor for gastric carcinoma. Unlike caspase-3, survivin (an apoptosis inhibitor) can markedly inhibit the apoptosis of tumor cells.

Li YH, Wang C, Meng K, Chen LB, Zhou XJ. Influence of survivin and caspase-3 on cell apoptosis and prognosis in gastric carcinoma. *World J Gastroenterol* 2004; 10(13): 1984-1988
http://www.wjgnet.com/1007-9327/10/1984.asp

INTRODUCTION

Abnormalities in cell death control are implicated as a cause or contributing factor in a range of diseases, including cancer, autoimmunity, and degenerative disorders[1]. This control involves several proteins that promote or inhibit apoptosis and an evolutionarily conserved multistep cascade[2]. A number of proteins, such as Bcl-2, Fas and Bax affect upstream of the cascade[3,4]. Survivin, a recently discovered inhibitor of apoptosis, may prolong cell survival by targeting the terminal effector caspase-3[5,6]. Located at the end of cascade, caspase-3 acts as both initiators and executors in the apoptotic process. So survivin and caspase-3 have been the focus of debate regarding apoptosis.

In the last decade, molecular abnormalities of tumor cells have emerged as important prognostic indicators of gastric carcinoma. As a candidate molecule to influence the apoptosis balance, survivin has unique properties such as undetectable in normal adults tissues and overexpression in a variety of human cancers *in vivo*[7]. Although studies indicated that survivin was a prognostic tumor marker[8-13], little is known about its potential role in gastric carcinoma. In this study we sought to investigate the expression of survivin and caspase-3 in gastric carcinoma and to dissect their potential prognostic value, and discuss the relationship between survivin, caspase-3 and tumor cell apoptosis.

MATERIALS AND METHODS

Patients and samples

A total of 80 patients with gastric adenocarcinoma did not receive any treatment prior to surgery. Of them 56 were males and 24 were females, with a mean age of 60 years. Surgically resected specimens were fixed in 10% neutral formalin, embedded in paraffin, and stained by haematoxylin-eosin. Histological grades and pathological stages were conformed to the criteria of UICC (Figure 1). The subjects consisted of 17 cases in stage I, 34 cases in stage II, and 29 cases in stage III. Tumor tissues and normal tissues from every patient were detected.

Immunohistochemical staining for survivin and caspase-3

A pilot study using the anti-survivin antibody and anti-caspase-3 antibody was conducted on various neoplasms, including gastric carcinoma, lung cancer, breast cancer and non-Hodgkin's lymphoma to determine an appropriate dilution. The immunostaining was performed, and negative control slides processed without primary antibody were incubated for each staining. Paraffin-embedded slides were deparaffinized and put in 400 mL EDTA solution (0.001 mol/L, pH 6.0). Then the solution was heated in a pressure cooker and boiled for 2 min while maintaining the pressure. After cooling the slides were incubated with the primary antibody (mouse anti-human survivin or caspase-3 monoclonal antibody purchased from NEO MAEKERS) overnight at 4 ℃ and rinsed by PBS (0.01 mol/L, pH 7.4) three times. Then the slides were incubated with an anti-mouse conjugate containing horseradish peroxidase at 37 ℃ for 30 min and rinsed by PBS three times. Finally 3,3-diaminobenzidine was used for color development and hematoxylin was used for counterstaining. The mean percentage of positive tumor cells was determined in at least five areas at 400-fold magnification and assigned to one of the following five categories[14]: -, <5%; +, 5-25%; ++, 26-50%; +++, 51-75%; ++++, >75%.

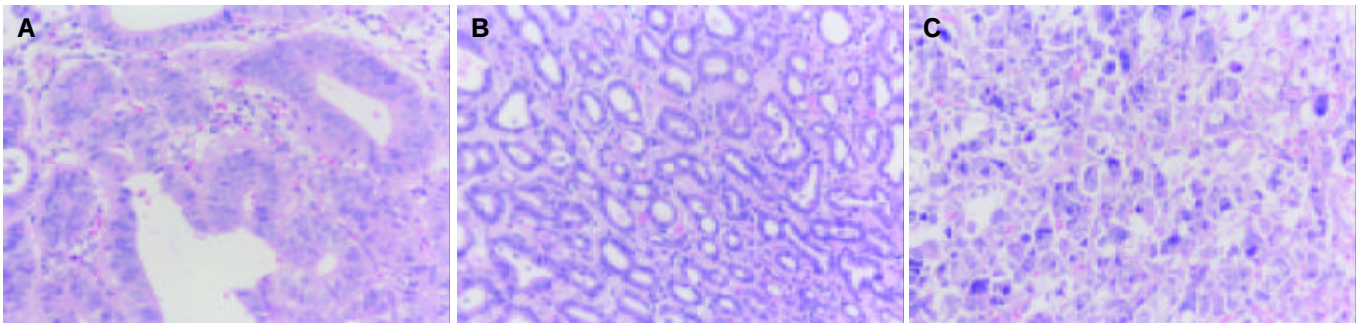

Figure 1 HE staining of gastric carcinoma. A: well differentiated gastric carcinoma; B: Moderately differentiated gastric carcinoma; C: Poorly differentiated gastric carcinoma (Original magnification: ×200).

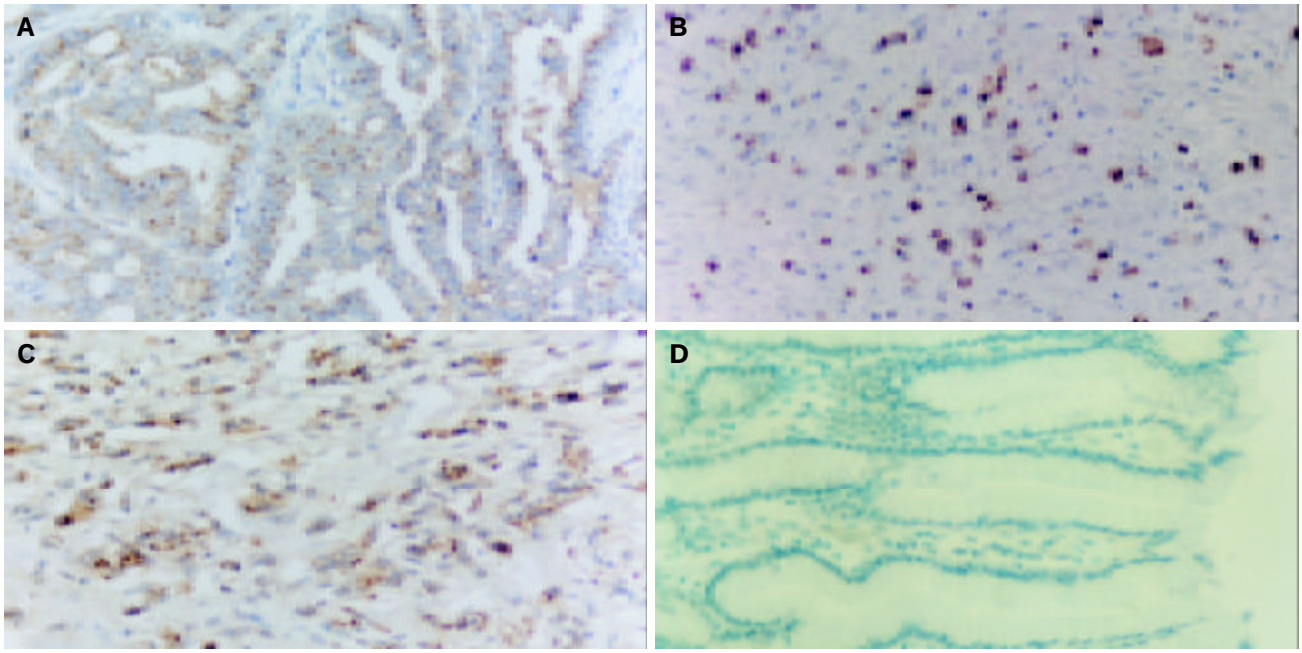

Figure 2 Survivin expression in gastric carcinoma. A: well differentiated gastric carcinoma; B: Moderately differentiated gastric carcinoma; C: Poorly differentiated gastric carcinoma; D: Substitution for antibody with PBS as negative control (Original magnification: ×200).

Histochemical detection of apoptosis

All cases received detection of apoptosis except those with both survivin and caspase-3 negativities. Apoptotic cells and apoptotic bodies were detected by *in situ* labeling using a TUNEL kit purchased from Borrinman Company. In brief, deparaffinized and rehydrated sections were digested with proteinase K for 20 min at room temperature and washed. After quenching in 30 mL/L hydrogen peroxide for 10 min and washing with PBS, terminal deoxynucleotidyl transferase enzyme was pipetted onto the sections, which were then incubated at 37 ℃ for 1 h. After stopping the reaction by putting sections in PBS and washing, anti-digoxin-peroxidase was added to the slides. Finally slides were washed with PBS, stained with 3,3-diaminobenzidine, and counterstained with hematoxylin. Substitution for terminal deoxynucleotidyl transferase with distilled water was used as negative control. Positive cells were determined according to the method described previously[15]. In brief, positive cells had dark or dark brown nuclei and some morphological characteristics, including chromatin condensation, nuclear disintegration, and formation of crescent caps of condensed chromatin at the nuclear periphery. Counting method was the same as described previously.

Statistical analysis

Differences of positivity rates between different groups were assessed by *t*-test. Kruskal-Wallis' rank sum test was used to assess the differences between ranked data. Linear correlation hypothesis test was used to evaluate the extent of correlation between two groups. All of the statistical analyses were performed with SAS statistical package.

RESULTS

Immunohistochemical staining revealed that anti-survivin mAb 8E2 specifically reacted with gastric carcinoma cells, with positive staining in cytoplasm and near the Golgi apparatus, whereas no expression of survivin was observed in adjacent normal tissues. A total of 61 cases of gastric carcinoma in this series were defined as positive staining (76%, Figure 2), with the mean percentage of 29.83%.

Of the 80 cases of gastric carcinomas, 75 cases (94%) of the adjacent normal tissues were positive for caspase-3, while 68 cases (85%) of the tumors were caspase-3 positive (Figure 3). Student' s *t*-test showed that caspase-3 expressed higher in normal tissue than in carcinoma. Survivin and caspase-3 were not positive at the same position in cancer cells. Expression of survivin in carcinomas showed a negative but not linear correlation with that of caspase-3 (r=-0.18, P>0.05).

Through Kruskal-Wallis' rank sum test, we found that the expression of both survivin and caspase-3 had significant differences between tissues with different histological grades (Tables 1, 3). The expression of survivin was significantly associated with pathological stages, but caspase-3 was not (Tables 2, 4).

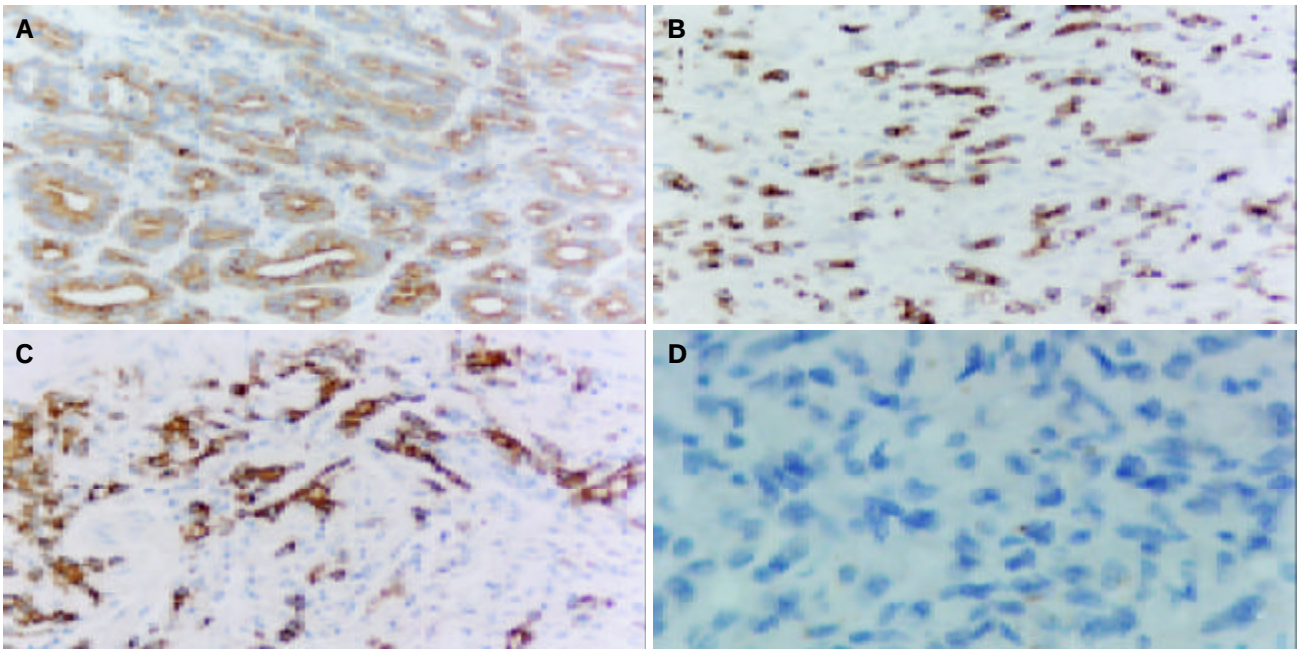

Figure 3 Expression of caspase-3 in gastric carcinoma. A: well differentiated gastric carcinoma; B: Moderately differentiated gastric carcinoma; C: Poorly differentiated gastric carcinoma; D: Substitution for antibody with PBS as negative control (Original magnification: ×200).

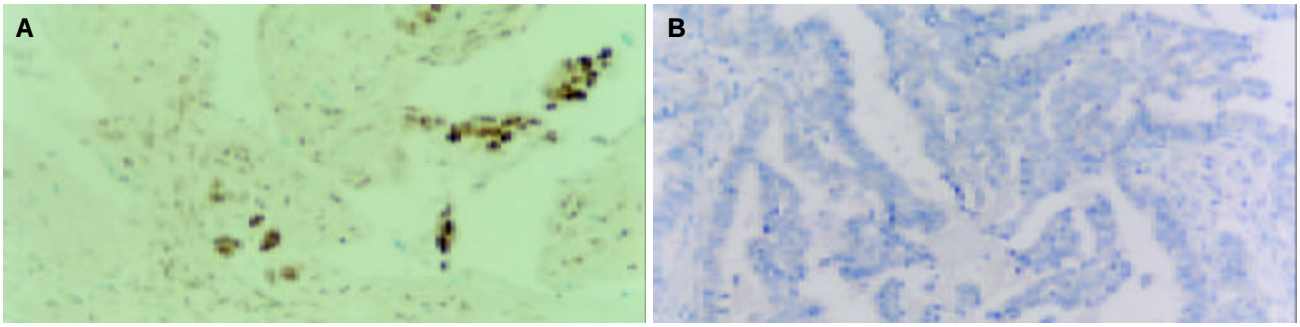

Figure 4 Apoptosis in gastric carcinoma. A: Positive; B: Substitution for terminal deoxynucleotidyl transferase with distilled water as negative control (Original magnification: ×200).

Table 1 Correlation between histological grades and survivin expression

Positive degree	Poorly differentiated	Moderately differentiated	Well differentiated	Sum	Mean ranks
+	1	13	4	18	9.5
++	8	11	1	20	28.5
+++	10	5	1	16	46.5
++++	4	3	0	7	58
n	23	32	6	61	

Hc=12.8, *P*<0.005 between poorly, moderately and well differentiated gastric carcinomas.

Table 2 Correlation between pathological stages and expression of survivin

Positive degree	Stage I	Stage II	Stage III	Sum	Mean ranks
+	8	6	4	18	9.5
++	3	15	2	20	28.5
+++	1	3	12	16	46.5
++++	1	2	4	7	58
n	13	26	22	61	

Hc=15.1, *P*<0.005 between stages I, II and III.

Table 3 Correlation between histological grades and expression of caspase-3

Positive degree	Poorly differentiated	Moderately differentiated	Well differentiated	Sum	Mean ranks
+	6	2	0	8	3.5
++	10	14	1	25	17.5
+++	8	19	2	29	42.5
++++	1	1	4	6	63
n	25	36	7	68	

Hc=11.7, *P*<0.005 between poorly, moderately and well differentiated gastric carcinomas.

Table 4 Correlation between pathological stages and expression of caspase-3

Positive degree	Stage I	Stage II	Stage III	Sum	Mean ranks
+	1	5	2	8	4.5
++	7	7	11	25	21
+++	5	14	10	29	48
++++	3	2	1	6	65.5
n	16	28	24	68	

Hc=0.54, *P*>0.75 between stages I, II and III.

Apoptotic cells and apoptotic bodies were observed in gastric carcinoma by using *in situ* labeling (Figure 4). The mean apoptotic index (AI) of the 80 cases was 0.84%. The mean AI in survivin-positive tumors was 0.59%, which was significantly lower than the mean AI of 1.26% observed in survivin-negative tumors ($P<0.005$). The mean AI in caspase-3-positive tumors (0.97%) was significantly higher than that in caspase-3-negative tumors (0.56%, $P<0.05$). Tumors with survivin(-) and caspase-3 (+) had the highest AI of 1.58%.

DISCUSSION

Recently, several inhibitors of apoptosis (IAP) related to the baculovirus IAP gene have been identified in humans, mice, and *Drosophila*[4]. Recombinant expressions of IAP proteins counteract various forms of apoptosis *in vivo*[16] and *in vitro*[17]. These molecules are thought to block an evolutionarily conserved step in apoptosis. At least in the case of X-linked IAP, this may involve direct inhibition of the terminal effectors caspase-3 and caspase-7 through a BIR-dependent recognition[18]. Among the recently described IAP family, survivin is characterized by a unique structure with a single BIR and no-zinc-binding domain known as the RING finger[19,20], and by the selective distribution in common human cancers[4,7]. In this study, specific staining for survivin was detected in 61 cases (76%), with a variable proportion of positive tumor cells (10-85%). In contrast, the adjacent normal tissues or the infiltrating lymphocytes did not express survivin, consistent with similar studies[13]. As the histological differentiation decreased and pathological stage increased, positivity rate and expression level of survivin were elevated. So survivin expression has prognostic value in human gastric carcinoma.

Alessandra[21] reported that survivin was expressed in G_2-M phase of the cell cycle in a cell cycle-regulated manner and associated with mitotic spindle microtubules. In this study, survivin-positive patients had lower AI as compared with survivin-negative patients, suggesting that the overexpression of survivin in cancer might obliterate the checkpoint of the cell cycle and allow aberrant progression through the G2-M phase checkpoint in gastric carcinoma.

In normal gastric tissues, caspase-3 was mainly expressed in gastric surface mucous cells, being in accord with the gastric cell turnover. Caspase-3 expression was increased in well differentiated tumors and apoptotic cells were increased in tumors with caspase-3 positivity, indicating that the expression of caspase-3 promoted apoptosis of tumor cells. It is well known that a number of genetic alterations are required for malignant transformation. Therefore we can speculate that abnormal differentiation leads to decreased expression of caspase-3 in tumor cells.

As a key effector molecule of apoptosis, caspase-3 can inactivate number proteins, which are associated with the structure and cycle of normal cells. Survivin showed an inversed function compared with caspase-3, which can be illustrated by the results that cases with survivin (-) and caspase-3 (+) had higher AI than cases with survivin (+) and caspase-3 (-). Then what we wanted to know was, if survivin inhibited directly the expression or function of caspase-3. Although our results indicated that expression of survivin was inversely associated with that of caspase-3, statistic analysis showed no linear correlation. So we think survivin did not inhibit the function of caspase-3 by directly inhibiting its expression. One of the relevant points to this issue was that survivin induced caspase-9 deactivation first[22,23], and then caspase-3 could not be activated at the end of the cascade. Some other reports suggested that survivin inhibited caspase pathway of apoptosis, and controled apoptosis and mitotic spindle checkpoint[19,24]. We speculate that survivin mainly oppresses caspase-3 activation or possesses effect on the upstream promoter activity, but not its expression. Further studies are needed to confirm the process of how survivin inhibits caspase-3.

As long as survivin affects terminal effector of apoptosis and exists in tumor cells, it would be an ideal target of apoptosis-based therapy. One of the roles of chemotherapy is inducing apoptosis, and caspase-3 has been proved to participate in this process[25], so acting on this target might also enhance sensitivity to chemotherapy or reduce the effect of drug-resistance. A recent *in vitro* study demonstrated that anti-survivin RNA down-regulated the expression of endogenous survivin in transformed cells and induced apoptotic cell death[26]. Targeted antagonists of survivin may offer a new therapeutic method for gastric carcinoma. A homeland study[27] revealed that antisense oligonucleotide targeting survivin induced decrease of survivin expression, increase of cell apoptosis, inhibition of cell proliferation in hepG2 cells. It also has been reported[28] that survivin-based plasmids could induce apoptosis in gastric cancer cells and sensitize gastric cancer cells to chemotherapeutic agents. Gene therapy targeting survivin gene expression may offer a new approach to cancer therapy.

REFERENCES

1 **Cross M**, Dexter TM. Growth factors in development, transformation, and tumorigenesis. *Cell* 1991; **64**: 271-280
2 **Thompson CB**. Apoptosis in the pathogenesis and treatment of disease. *Science* 1995; **267**: 1456-1462
3 **Barinaga M**. Death by dozens of cuts. *Science* 1998; **280**: 32-34
4 **Tamm I,** Wang Y, Sausville E, Scudiero DA, Vigna N, Oltersdorf T, Reed JC. IAP-family protein survivin inhibits caspase activity and apoptosis induced by Fas (CD95), Bax, caspases, and anti-cancer drugs. *Cancer Res* 1998; **58**: 5315-5320
5 **Ambrosini G**, Adida C, Altieri DC. A novel anti-apoptosis gene, survivin, expressed in cancer and lymphoma. *Nat Med* 1997; **3**: 917-921
6 **Adida C**, Haioun C, Gaulard P, Lepage E, Morel P, Briere J, Dombret H, Reyes F, Diebold J, Gisselbrecht C, Salles G, Altieri DC, Molina TJ. Prognostic significance of survivin expression in diffuse large B-cell lymphomas. *Blood* 2000; **96**: 1921-1925
7 **Kawasaki H**, Altieri DC, Lu CD, Toyoda M, Tenjo T, Tanigawa N. Inhibition of apoptosis by survivin predicts shorter survival rates in colorectal cancer. *Cancer Res* 1998; **58**: 5071-5074
8 **Islam A**, Kageyama H, Hashizume K, Kaneko Y, Nakagawara A. Role of survivin, whose gene is mapped to 17q25, in human neuroblastoma and identification of a novel dominant-negative isoform, survivin-beta / 2B. *Med Pediatr Oncol* 2000; **35**: 550-553
9 **Tanaka K**, Iwamoto S, Gon G, Nohara T, Iwamoto M, Tanigawa N. Expression of survivin and its relationship to loss of apoptosis in breast carcinomas. *Clin Cancer Res* 2000; **6**: 127-134
10 **Asanuma K**, Moriai R, Yajima T, Yagihashi A, Yamada M, Kobayashi D, Watanabe N. Survivin as a radioresistance factor in pancreatic cancer. *Jpn J Cancer Res* 2000; **91**: 1204-1209
11 **Lu CD**, Altieri DC, Tanigawa N. Expression of a novel antiapoptosis gene, survivin, correlated with tumor cell apoptosis and p53 accumulation in gastric carcinoma. *Cancer Res* 1998; **58**: 1808-1812
12 **Lu C**, Tanigawa N. Spontaneous apoptosis is inversely related to intratumoral microvessel density in gastric carcinoma. *Cancer Res* 1997; **57**: 221-224
13 **Duckett CS**, Nava VE, Gedrich RW, Clem RJ, Van Dongen JL, Gilfillan MC, Shiels H, Hardwick JM, Thompson CB. A conserved family of cellular genes related to the baculovirus iap gene and encoding apoptosis inhibitors. *EMBO J* 1996; **15**: 2685-2694
14 **Hay BA**, Wassarman DA, Rubin GM. *Drosophila* homologs of baculovirus inhibitor of apoptosis proteins function to block cell death. *Cell* 1995; **83**: 1253-1262
15 **Takahashi R**, Deveraux Q, Tamm I, Welsh K, Assa-Munt N, Salvesen GS, Reed JC. A single BIR domain of XIAP sufficient for inhibiting caspases. *J Biol Chem* 1998; **273**: 7787-7790
16 **Giodini A**, Kallio MJ, Wall NR, Gorbsky GJ, Tognin S, Marchisio PC, Symons M, Altieri DC. Regulation of microtubule stability

and mitotic progression by survivin. *Cancer Res* 2002; **62**: 2462-2467
17 **Reed JC**. The Survivin saga goes *in vivo*. *J Clin Invest* 2001; **108**: 965-969
18 **Shi Y**. Survivin structure: crystal unclear. *Nat Struct Biol* 2000; **7**: 620-623
19 **Shankar SL**, Mani S, O'Guin KN, Kandimalla ER, Agrawal S, Shafit-Zagardo B. Survivin inhibition induces human neural tumor cell death through caspase-independent and -dependent pathways. *J Neurochem* 2001; **79**: 426-436
20 **Li F**, Ambrosini G, Chu EY, Plescia J, Tognin S, Marchisio PC, Altieri DC. Control of apoptosis and mitotic spindle checkpoint by survivin. *Nature* 1998; **396**: 580-584
21 **Sun XM**, MacFarlane M, Zhuang J, Wolf BB, Green DR, Cohen GM. Distinct caspase cascades are initiated in receptor-mediated and chemical-induced apoptosis. *J Biol Chem* 1999; **274**: 5053-5060
22 **Sasaki H**, Sheng Y, Kotsuji F, Tsang BK. Down-regulation of X-linked inhibitor of apoptosis protein induces apoptosis in chemoresistant human ovarian cancer cells. *Cancer Res* 2000; **60**: 5659-5666
23 **Hauser HP**, Bardroff M, Pyrowolakis G, Jentsch S. A giant ubiquitin-conjugating enzyme related to IAP apoptosis inhibitors. *J Cell Biol* 1998; **141**: 1415-1422
24 **Miller LK**. An exegesis of IAPs: salvation and surprises from BIR motifs. *Trends Cell Biol* 1999; **9**: 323-328
25 **Sun C**, Cai M, Gunasekera AH, Meadows RP, Wang H, Chen J, Zhang H, Wu W, Xu N, Ng SC, Fesik SW. NMR structure and mutagenesis of the inhibitor-of-apoptosis protein XIAP. *Nature* 1999; **401**: 818-822
26 **Kappler M**, Kotzsch M, Bartel F, Fussel S, Lautenschlager C, Schmidt U, Wurl P, Bache M, Schmidt H, Taubert H, Meye A. Elevated expression level of survivin protein in soft-tissue sarcomas is a strong independent predictor of survival. *Clin Cancer Res* 2003; **9**: 1098-1104
27 **Wang Y**, Wang JL. Antisense oligonucleotide targeting survivin inducing apoptosis of hepatic cancer cells. *Zhonghua Xiaohua Zazhi* 2003; **23**: 11-14
28 **Tan JH,** Tu SP, Zou B, Ma TL, Zhong J, Zhang CL, Qiao MM, Jiang SH. Experimental study on apoptosis induced by pcDNA3-survivin mutant in gastric cancer cell lines. *Zhonghua Xiaohua Zazhi* 2003; **23**: 199-202

Edited by Chen WW and Zhu LH **Proofread by** Xu FM

PO Box 2345, Beijing 100023, China
Fax: +86-10-85381893
E-mail: wjg@wjgnet.com www.wjgnet.com

World J Gastroenterol 2004;10(13):1989-1991
World Journal of Gastroenterology
 ISSN 1007-9327

• BRIEF REPORTS •

Enhanced antitumor efficacy on hepatoma-bearing rats with adriamycin-loaded nanoparticles administered into hepatic artery

Jiang-Hao Chen, Rui Ling, Qing Yao, Ling Wang, Zhong Ma, Yu Li, Zhe Wang, Hu Xu

Jiang-Hao Chen, Rui Ling, Qing Yao, Ling Wang, Zhong Ma, Department of Vascular and Endocrine Surgery, Xijing Hospital, Fourth Military Medical University, Xi' an 710033, Shaanxi Province, China
Yu Li, Department of Cell Biology, Fourth Military Medical University, Xi' an 710033, Shaanxi Province, China
Zhe Wang, Department of Pathology, Fourth Military Medical University, Xi' an 710033, Shaanxi Province, China
Hu Xu, Department of Orthopaedics, Xijing Hospital, Fourth Military Medical University, Xi' an 710033, Shaanxi Province, China
Correspondence to: Dr. Jiang-Hao Chen, Department of Vascular and Endocrine Surgery, Xijing Hospital, Fourth Military Medical University, Xi' an 710033, Shaanxi Province, China. chenjh@fmmu.edu.cn
Telephone: +86-29-83375271
Received: 2003-12-19 **Accepted:** 2004-01-15

Abstract

AIM: To investigate the antitumor activity of adriamycin (ADR) encapsulated in nanoparticles (NADR) and injected into the hepatic artery of hepatoma-bearing rats.

METHODS: NADR was prepared by the interfacial polymerization method. Walker-256 carcinosarcomas were surgically implanted into the left liver lobes of 60 male Wistar rats, which were divided into 4 groups at random (15 rats per group). On the 7th day after implantation, normal saline (NS), free ADR (FADR), NADR, or ADR mixed with unloaded nanoparticles (ADR+NP) was respectively injected via the hepatic artery (i.a.) of rats in different groups. The dose of ADR in each formulation was 2.0 mg/kg body weight and the concentration was 1.0 mg/mL. Survival time, tumor enlargement ratio, and tumor necrosis degree were compared between each group.

RESULTS: Compared with the rats that received NS i.a., the rats that received FADR or ADR+NP acquired apparent inhibition on tumor growth, as well as prolonged their life span. Further significant anticancer efficacy was observed in rats that received i.a. administration of NADR. Statistics indicated that NADR brought on a more significant tumor inhibition and more extensive tumor necrosis, as compared to FADR or ADR+NP. The mean tumor enlargement ratio on the 7th day after NADR i.a. was 1.106. The mean tumor-bearing survival time was 39.50 days. Prolonged life span ratio was 109.22% as compared with rats that accepted NS.

CONCLUSION: Therapeutic effect of ADR on liver malignancy can be significantly enhanced by its nanopaticle formulation and administration via hepatic artery.

Chen JH, Ling R, Yao Q, Wang L, Ma Z, Li Y, Wang Z, Xu H. Enhanced antitumor efficacy on hepatoma-bearing rats with adriamycin-loaded nanoparticles administered into hepatic artery. *World J Gastroenterol* 2004; 10(13): 1989-1991
http://www.wjgnet.com/1007-9327/10/1989.asp

INTRODUCTION

Transhepatic arterial chemotherapy (TAC) is recognized as an efficient therapy for liver primary and metastatic tumors by increasing the drug concentration in tumor and improving the therapeutic effect subsequently. It was reported that administration of ADR via the hepatic artery (i.a.) was able to increase the drug concentration in tumor by 3-fold as compared to intravenous administration[1]. In patients with cancers, the i.a. administration of ADR reduced the plasma AUC by about 30%[2].

During recent years, nanoparticles have been extensively applied as carriers of antitumor drugs. *In vivo* studies have demonstrated that nanoparticles are specifically concentrated to the reticuloendothelial system (RES), especially to liver and spleen, after administered into body[3]. On the basis of these experiences, we hypothesized that a further significant therapeutic effect could be expected by TAC in combination with nanoparticle techniques. We carried out a randomized control study to test it.

MATERIALS AND METHODS

NADR preparation and characterization

NADR was prepared by the interfacial polymerization method[4]. α-polybutylcyanoacrylate (PBCA) was used as polymeric materials. The final product had an appearance of reddish, colloidal, semi-transparent solution. Under transmission electron microscopy (TEM), NADR showed a global, regular contour with a homogenous size and distribution. The diameter of particles ranged from 22 to 130 nm (mean, 93.1 nm). The drug-embedding ratio was 82.6%, the drug-loading ratio was 40.9%, and the effusion rate was less than 3% three months later.

Animals and anesthetic

Sixty male Wistar rats weighing 230-270 g (mean, 250 g) were provided by Laboratory Animal Center of our university and randomly divided into 4 groups, with 15 in each. Sumianxin (Changchun Agricultural Pastoral University) was used as anesthetic.

Establishment of hepatoma model

One mL of suspension containing 10^7 Walker-256 (W256) carcinosarcoma cells (Shanghai Medical Industrial Institution) was injected into the thigh muscle of a carrier rat (not included in experimental rats). One week after inoculation, a palpable tumor generated at the injected site. Viable tumor tissue was excised under sterile conditions and soaked in 20 mL of Hanks balanced salt solution. Tissue was diced into approximately 1 mm×1 mm×1 mm fragments. Experimental rats were anesthetized with intramuscular injection of Sumianxin at 0.2 mL/kg. Median incision beneath the metasternum was made and the liver was exposed. The tumor fragment was implanted into the left liver lobe.

Administration i.a.

On the 7th day after tumor implantation, all animals received laparotomy again. The longest (a) and shortest (b) diameters of

the tumor were measured. The tumor volume was calculated as

$$\frac{a \times b^2}{2}$$

By cannulation method described previously[5], normal saline (NS), free ADR (FADR), NADR, or ADR mixed with unloaded nanoparticles (ADR+NP) was injected into the hepatic artery of rats in groups 1-4 respectively. The dose of ADR in each formulation was 2.0 mg/kg body weight. The concentration of ADR was 1.0 mg/mL.

Assessment of therapeutic effect

Tumor growth inhibition Seven days later, all animals received the third laparotomy. The longest (a) and shortest (b) diameters of the tumor were measured again and the tumor volume after administration was calculated. The tumor volume ratio (TVR) was calculated as

$$TVR = \frac{\text{Tumor volume after administration}}{\text{Tumor volume before administration}}$$

Tumor necrosis degree Seven random rats in each group were killed and anatomized. Hepatoma was removed completely and fixed in 40 g/L formaldehyde. Three 5-μm thick sections in each tumor were cut on the maximal transverse plane and mounted on glass slides overnight at room temperature. After HE staining, the sections were examined under microscope. According to the percentage of necrosis area, tumors were graded on the following criteria: I, 0-30%; II, 30-70%; III, 70-100%.

Increased life span Survival time of the remaining 8 rats in each group was recorded. The mean survival time of NS group was reckoned as control. Increased life span (%ILS) was calculated as

$$\%ILS = \left(\frac{\text{Mean survival of treated group}}{\text{Mean survival of control group}} - 1\right) \times 100\%$$

Statistical analysis

SPSS 10.0 for windows was used for statistical analysis. Statistical significance was tested by ANOVA and Dunnett test for tumor growth inhibition, log rank test for survival time. $P<0.05$ was considered statistically significant.

RESULTS

Tumor growth inhibition

No difference in tumor volume was found among groups before treatment ($P>0.05$, Table 1). After treatment, the tumor grew rapidly in rats that received NS. The mean tumor volume was 31.55 times greater than that before treatment. Metastases were observed in about half of these rats. In contrast, the speed of tumor growth lowered apparently in rats that received FADR or ADR+NP ($P<0.01$). No difference between FADR and ADR+NP was observed ($P>0.05$). The slowest tumor growth was found in rats that received i.a. administration of NADR. Statistics indicated that NADR brought on a further significant tumor inhibition, as compared with FADR or ADR+NP ($P<0.01$). In addition, no metastasis was found in rats that received NADR.

Tumor necrosis degree

Under microscope, W256 tumor cells in rats that received NS appeared active proliferation and extensive mitoses. Small areas of necroses were observed in the center of tumor tissue and accompanied with a few inflammatory cells (Table 2). Moderate to severe necroses were found in tumors of rats that received FADR or ADR+NP. Grade III of tumor necroses was found in 5 of 7 tumors after administration of NADR, including 2 cases of complete tumor necrosis.

Increased life span

Compared with the survival time (18.88 d) in saline controls, the tumor-bearing survival time was greatly prolonged in animals that received NADR (mean, 39.50 d), or FADR (mean, 27.75 d), or ADR+NP (mean, 26.13 d) (Table 3). NADR prolonged the life span by 109.22%, which was longer than FADR (46.98%) and ADR+NP (38.40%) ($P<0.05$).

Table 1 Tumor volume (V) and tumor volume ratio (TVR) after treatment (mean±SD)

Group	V (cm^3)		TVR
	Before treatment	After treatment	
NS	0.086±0.049	2.521±0.840	31.550±7.975
FADR	0.083±0.035	0.149±0.072	1.883±0.708[b]
ADR+NP	0.079±0.036	0.161±0.105	1.896±0.565[b]
NADR	0.079±0.033	0.087±0.038	1.106±0.275[d]

[b]$P<0.01$, *vs* NS; [d]$P<0.01$, *vs* FADR, ADR+NP.

Table 2 Tumor necrosis degree after treatment

Grade	NS	FADR	ADR+NP	NADR
I	6	2	1	0
II	1	3	5	2
II	0	2	1	5[1]

[1]Complete necrosis in 2 cases.

Table 3 Mean survival time and increased life span (%ILS) after treatment (mean±SD)

Group	Mean survival time (d)	%ILS
NS	18.88±2.80	-
FADR	27.75± 6.34	46.98[b]
ADR+NP	26.13±5.75	38.40[b]
NADR	39.50±8.97	109.22[a]

[a]$P<0.05$, *vs* FADR, ADR+NP; [b]$P<0.01$, *vs* NS.

DISCUSSION

We did not include intravenous administration (i.v.) in the present experiment because the i.a. route was much more efficient than i.v. in the treatment of liver malignancies. Different from the liver parenchyma, which receives more than 70% of its blood supply from the portal vein and the rest from the hepatic artery, hepatoma receives approximately 90% of its blood supply from the hepatic artery. The speciality of liver blood supply determines the great difference between the two routes of administration. The difference did not warrant repeat comparison in our study.

The results of our experiments demonstrated that the antitumor activity of ADR could be markedly enhanced when the drug was encapsulated in nanoparticles and administered into the hepatic artery. Equivalent or similar effects could not be acquired using FADR or ADR+NP. Compared with FADR or ADR+NP, NADR produced a more significant tumor inhibition and more extensive tumor necrosis. The average tumor volume on the 7th day after treated with NADR was 0.087 cm^3, nearly the half of 0.161 cm^3 of the volume after treated with ADR+NP. The survival time of rats that received NADR was evidently increased. Compared with saline

controls, NADR prolonged the life span by 109.22%.

The likely explanations for the improved therapeutic activity in four aspects are as follows. First, it has been testified that the cytocidal effect of ADR depends on the concentration and duration of exposure[6]. Increasing ADR concentration in tumor cells or slowing its elimination could certainly enhance its antitumor efficacy. Secondly, encapsulating the drug into nanoparticles might modify its distribution pattern in tissues. After administered into body, nanoparticles were taken up selectively by RES, such as the liver, spleen, and bone marrow. Accumulation of biodegradable nanoparticles with associated drugs in Kupffer cells would create a gradient of drug concentration for a massive and prolonged diffusion of the free drug towards neoplastic tissues[3]. Thirdly, *in vitro* studies reported that compared to FADR, NADR exhibited a 3-fold enhancement of cytotoxicity, as determined by cell growth inhibition and DNA synthesis, after continuous exposure to 0.02 and 0.04 μg/mL[7]. Further studies showed that nanoparticular pharmaceutics were able to enter specifically certain types of tumor tissues or tumor cells[8]. Fourthly, the tiny size of nanoparticle could increase its contact areas significantly, which would result in an apparent improvement in its bioavailability. A recent study compared carbendazim, a novel anticancer drug, with its nanoparticles. The result confirmed that nanoparticle formulation improved the drug bioavailability by 166%[9].

Our experiments support the hypothesis that the therapeutic effect could be dramatically enhanced by TAC in combination with nanotechnology. We conclude that nanoparticles can be used as a promising drug carrier in TAC for the treatment of liver primary and metastatic tumors.

REFERENCES

1 **Ridge JA,** Collin C, Bading JR, Hancock C, Conti PS, Daly JM, Raaf JH. Increased adriamycin levels in hepatic implants of rabbits Vx-2 carcinoma from regional infusion. *Cancer Res* 1988; **48:** 4584-4587

2 **Eksborg S,** Cedermark BJ, Strandler HS. Intrahepatic and intravenous administration of adriamycin - a comparative pharmacokinetics study in patients with malignant liver tumours. *Med Oncol Tumor Pharmacother* 1985; **2:** 47-54

3 **Chiannilkulchai N,** Ammoury N, Caillou B, Devissaguet JP, Couvreur P. Hepatic tissue distribution of doxorubicin-loaded nanoparticles after i.v. administration in reticulosarcoma M 5076 metastasis-bearing mice. *Cancer Chemother Pharmacol* 1990; **26:** 122-126

4 **Andrieu V,** Fessi H, Dubrasquet M, Devissaguet JP, Puisieux F, Benita S. Pharmacokinetic evaluation of indomethacin nanocapsules. *Drug Des Deliv* 1989; **4:** 295-302

5 **Zou YY,** Ueno M, Yamagishi M, Horikoshi I, Yamashita I, Tazawa K, Gu XQ. Targeting behavior of hepatic artery injected temperature sensitive liposomal adriamycin on tumor-bearing rats. *Sel Cancer Ther* 1990; **6:** 119-127

6 **Rupniak HT,** Whelan RD, Hill BT. Concentration and time-dependent inter-relationships for antitumour drug cytotoxicities against tumour cells *in vitro*. *Int J Cancer* 1983; **32:** 7-12

7 **Astier A,** Doat B, Ferrer MJ, Benoit G, Fleury J, Rolland A, Leverge R. Enhancement of adriamycin antitumor activity by its binding with an intracellular sustained-release form polymethacrylate nanospheres, in U-937 cells. *Cancer Res* 1988; **48:** 1835-1841

8 **Jordan A.** Nanotechnology and consequences for surgical oncology. *Kongressbd Dtsch Ges Chir Kongr* 2002; **119:** 821-828

9 **Jia L,** Wong H, Wang Y, Garza M, Weitman SD. Carbendazim: disposition, cellular permeability, metabolite identification, and pharmacokinetic comparison with its nanoparticle. *J Pharm Sci* 2003; **92:** 161-172

Edited by Zhang JZ and Wang XL **Proofread by** Xu FM

PO Box 2345, Beijing 100023, China
Fax: +86-10-85381893
E-mail: wjg@wjgnet.com www.wjgnet.com

World J Gastroenterol 2004;10(13):1992-1994
World Journal of Gastroenterology
 ISSN 1007-9327

• BRIEF REPORTS •

Effect of glutamine on change in early postoperative intestinal permeability and its relation to systemic inflammatory response

Zhu-Fu Quan, Chong Yang, Ning Li, Jie-Shou Li

Zhu-Fu Quan, Chong Yang, Ning Li, Jie-Shou Li, Research Institute of General Surgery, Jinling Hospital, Medical College of Nanjing University, Nanjing 210002, Jiangsu Province, China
Correspondence to: Dr. Zhu-Fu Quan, Research Institute of General Surgery, Jinling Hospital, Medical College of Nanjing University, Nanjing 210002, Jiangsu Province, China. quanzhufu@hotmail.com
Telephone: +86-25-85137085 **Fax:** +86-25-84803956
Received: 2003-06-16 **Accepted:** 2003-09-18

Abstract

AIM: To study the effects of glutamine (Gln) on the change of intestinal permeability and its relationship to systemic inflammatory response in early abdominal postoperative patients.

METHODS: A prospective, randomized, double-blind and controlled trial was taken. Twenty patients undergoing abdominal surgery were randomized into Gln group (oral administration of glutamine, 30 g/d, for 7 d, *n*=10) and placebo group (oral administration of placebo, 30 g/d, for 7 d, *n*=10). Temperatures and heart rates of all patients were daily recorded. White blood cell counts(WBC) and biochemical variables were measured before operation and 4 and 7 d after drug administration. Serum concentrations of glutamine, endotoxin, diamine oxidase and malondialdehyde and urine lactulose/mannito (L/M) ratio were measured before and 7 d after drug administration.

RESULTS: The patients in the 2 groups were comparable prior to drug administration. Serum Gln concentration was significantly decreased in the placebo group and increased in the Gln group 7 d after drug administration. Urine L/M ratio was significantly increased in the placebo group and decreased in the Gln group. The serum concentration of endotoxin, diamine oxidase and malondialdehyde was significantly decreased in the Gln group compared with those in the placebo group. Temperatures, heart rates and WBC counts were significantly lower in the Gln group than those in the placebo group.

CONCLUSION: Gut is one of the sources of systemic inflammatory response in abdominal postoperative patients and glutamine can decrease intestinal permeability, maintain intestinal barrier and attenuate systemic inflammatory response in early postoperative patients.

Quan ZF, Yang C, Li N, Li JS. Effect of glutamine on change in early postoperative intestinal permeability and its relation to systemic inflammatory response. *World J Gastroenterol* 2004; 10(13): 1992-1994
http://www.wjgnet.com/1007-9327/10/1992.asp

INTRODUCTION

Gut has been considered as one of the central organs responding to stresses in surgical patients[1]. In the last few years, animal experiments and clinical researches have proved that the intestinal permeability increases during stresses, such as severe trauma, operation. Glutamine as a semi-essential amino acid is a special nutrient to intestinal mucosal cells. It can reduce the permeability of gut, but becomes increasingly exhausted after severe trauma or operation. In this research we studied the effects of glutamine on the change of intestinal permeability and its relationship to systemic inflammatory response in abdominal postoperative patients.

MATERIALS AND METHODS

Patient grouping

A prospective, randomized, double-blind and controlled trial was taken. Twenty abdominal surgical patients aged 18-65 years and without any severe disease in liver, kidney, cardiovascular system and hematopoietic system, were randomized into Gln group (oral administration of glutamine, 30 g/d, for 7 d, *n*=10) and placebo group (oral administration of placebo, 30 g/d, for 7 d, *n*=10). Their sex, age, body mass and operation type were similar (Tables 1, 2).

Table 1 General data of two groups

	Placebo group	Glutamine group
Age (yr)	48.3±12.2	48.3±10.8
Male/Female	7/3	6/4
Weight (kg)	54.2±11.1	56.7±12.1

Drug dose and administration

Glutamine was dissolved in warm water (1 g in 10 mL) and orally taken or by gastric tube (10 g one time, and 3 times per day) after operation for 7 d. Placebo was administered as glutamine.

Measurement

Temperature and heart rate of all patients were daily recorded from the day before operation to the end of drug administration.

Peripheral blood was sampled on the morning of the day before operation, the day before drug administration, 4 and 7 after drug administration. Liver and kidney functions were measured.

Peripheral blood was sampled on the morning of the day before and 7 d after drug administration for the measurement of the concentration of the serum glutamine (Gln)[2], diamine oxidase (DAO)[3] and malondialdehyde (MDA)[4] .

Peripheral blood was sampled before and 7 d after drug administration for the measurement of the concentration of serum endotoxin with an endotoxin detection kit (Shanghai Yihua Clinical Technology Company).

On the morning before and the 7th dafter administration, 6 h' s urine was collected after 50 mL lactulose/mannito (L/M) solution (lactulose 10 g and mannito 5 g) was taken for the measurement of the levels of lactulose and mannito with method of enzyme[5,6] and calculation of the ratio of L/M.

Statistic method

Results were expressed as mean±SD and analyzed with Student *t*-test. $P<0.05$ was considered statistically significant.

Table 2 Detailed clinical data of patients in two groups

Group	Case(*n*)	Sex	Age(yr)	Diagnosis	Operation type
Gln group	1	Male	55	Cardiac orifice cancer	Total gastrectomy
	2	Male	30	Acute suppurative cholangitis	Cholecystectomy choledochostomy
	3	Female	40	Rectal cancer	Anterior resection of rectum
	4	Male	47	Sigmoid cancer	Sigmoidectomy
	5	Male	62	Cardiac orifice cancer	Proximal subtotal gastrectomy
	6	Female	28	Rectal cancer	Anterior resection of rectum
	7	Female	52	Cholecystolithiasis	Cholecystectomy
	8	Male	49	Gastric cancer	Subtotal gastrectomy
	9	Male	60	Gastric cancer	Subtotal gastrectomy
	10	Male	60	Cardiac orifice cancer	Proximal subtotal gastrectomy
Placebo group	1	Male	50	Pancreas pseudocyst	Cyst-jejunal Roux-en-y anastomosis
	2	Female	56	Ascending colon cancer	Right semi-colectomy
	3	Female	60	Rectal cancer	Anterior resection of rectum
	4	Female	54	Sigmoid cancer	Sigmoidectomy
	5	Male	48	Cardiac orifice cancer	Proximal subtotal gastrectomy
	6	Male	43	Ascending colon cancer	Right semi-colectomy
	7	Male	64	Gastric cancer	Proximal subtotal gastrectomy
	8	Female	29	Gastric cancer	Proximal subtotal gastrectomy
	9	Male	43	Sigmoid cancer	Sigmoidectomy
	10	Male	36	Acute biliary pancreatitis	Selective cholecystectomy

RESULTS

General condition

During the research, there were no complication and death in both Gln group and placebo group.

Temperature

The highest, average and lowest temperatures increased after operation. The highest and average temperatures from d 3 to 6 and the lowest temperatures from d 2 to 6 in the Gln group were significantly lower than those in the placebo group.

Heart rate

The highest, average and lowest heart rates increased after operation in patients of both groups. The highest and average heart rates on d 2, 3 and 5 and the lowest heart rates from d 2 to 5 were significantly lower in the Gln group than in the placebo group.

WBC count

WBC counts increased from the first day after operation in both groups with the maximum being above 12.0×10^9/L. WBC counts decreased to normal level 4 d later in the Gln group, but 7 d later in the placebo group.

Serum concentration of Gln

In the placebo group, the serum concentration of Gln decreased from 432.17±142.68 μmol/L to 250.78±77.10 μmol/L (P<0.05), whereas in the Gln group the serum concentration of Gln increased from 361.17±161.25 μmol/L to 583.22±171.52 μmol/L (P <0.05). The serum concentration of Gln in the Gln group was significantly higher than that in the placebo group (P<0.01) (Table 3).

Table 3 Serum levels of Gln in two groups (μmol/L)

Group	Before drug administration	7 d after drug administration
Placebo group	432.17±142.68	250.78±77.10[b]
Gln group	361.17±161.25	583.22±171.52[ad]

[a]P<0.05, [b]P<0.01, *vs* before drug administration; [d]P<0.01, *vs* placebo group.

Serum DAO concentration

Serum DAO concentrations were not significantly different in the 2 groups before drug administration. Seven days after drug administration, serum DAO concentrations increased in the placebo group and decreased in the Gln group (P<0.01). The difference in serum DAO concentrations was very significant (P<0.01) between the two groups (Table 4).

Table 4 Serum DAO levels in two groups (U/mL)

Group	Before drug administration	7 d after drug administration
Placebo group	2.06±0.48	3.18±1.13
Gln group	2.26±0.63	1.25±0.65[bd]

[b]P<0.01 *vs* before administration; [d]P<0.01 *vs* placebo group.

Serum MDA concentration

Serum MDA concentrations were not significantly different in the 2 groups before drug administration. Seven days after drug administration, they increased in the placebo group and decreased in the Gln group (P<0.01). The serum MDA concentrations were significantly different between the two groups (P<0.01) after drug administration (Table 5).

Table 5 Serum MDA levels in two groups (nmol/mL)

Groups	Before drug administration	7 d after drug administration
Placebo group	3.94±0.56	4.85±0.63[b]
Gln group	4.46±0.67	3.53±0.59[bd]

[b]P<0.01 *vs* before drug administration; [d]P<0.01 *vs* placebo group.

Table 6 Levels of serum endotoxin in two groups (EU/mL)

Group	Before drug administration	7 d after drug administration
Placebo group	0.21±0.07	0.25±0.08
Gln group	0.23±0.05	0.18±0.06[ab]

[a]P<0.05 *vs* before drug administration; [b]P<0.01 *vs* placebo group.

Serum endotoxin concentration

Levels of serum endotoxin in the 2 groups were not significantly different before drug administration. After 7 d, the serum endotoxin concentrations increased in the placebo group significantly and decreased in the Gln group (P<0.05) with a very significant difference between the two groups (P<0.01, Table 6).

Ratio of urine L/M

The ratio of L/M was not significantly different in the 2 groups initially, which was 134.00±18.48 in the placebo group and 146.102±20.21 in the Gln group. After 7 d, the ratio of L/M significantly increased in the placebo group ($P<0.01$), and significantly decreased in the Gln group ($P<0.05$). Then, the ratio of L/M was significantly lower in the Gln group than in the placebo group ($P<0.01$, Table 7).

Table 7 Changes of urine L/M ratio in two groups

Group	Before drug administration	7 d after drug administration
Placebo group	134.00±18.48	194.83±45.31[b]
Gln group	146.10±20.21	117.47±25.68[ad]

[a]$P<0.05$, [b]$P<0.01$, *vs* before drug administration; [d]$P<0.01$ *vs* placebo group.

DISCUSSION

Normally, besides digestion and absorption, the gut functions as a mucosal barrier to bacteria, endotoxin and some other toxins. Whether the mucosal barrier works well or not is closely related to intestinal permeability. To measure it, some material with large molecular weight was used as a probe. Lactulose/mannito was most often used[7]. During the period of severe trauma or operation, the intestinal mucosal barrier was damaged, and therefore the intestinal permeability increased from which bacteria and endotoxin can easily transfer through the intestinal mucosa and invade tissue and blood, which is called bacterial translocation. Then the bacteria and endotoxin in blood would inversely affect the intestinal mucosal barrier and get it further damaged, thus forming a vicious circle. The more critical condition was that systemic inflammatory response syndrome (SIRS) and multiple organ dysfunction sysdrome (MODS) could even occur[8]. Therefore, how to maintain the function of intestinal mucosal barrier in severe trauma or postoperative patients and how to decrease the permeability and bacterial translocation to avoid the occurrence of SIRS and MODS have become a very important problem.

Brooks *et al*.[9] took L/M as a molecular probe to measure the intestinal permeability in 25 cases of gastrointestinal tumor. The ratio of L/M was greatly increased in the placebo group. Li *et al*.[10] measured 24 hours' urine ^{99m}T-DTPA taken orally in 8 cases of postoperative patients 7 d after operation. The excretory rate of ^{99m}T-DTPA was 13.71±4.85%, which almost doubly increased to that before operation (6.64±3.95%). In this research, serum Gln concentration decreased by 41.97%, and increased by 61.48% in the Gln group after administration of Gln for 7 d, when compared with the level before administration. It was significantly higher in the Gln group than in the placebo group. The ratio of L/M was not significantly different in the two groups initially. After 7 d, the ratio of L/M significantly increased in the control group and significantly decreased in the Gln group. The ratio of L/M was significantly lower in the Gln group than in the placebo group. This result showed that supplement of ectogenetic Gln could significantly decrease the intestinal permeability. Jiang *et al*.[11,12] also proved this in surgical patients. Supplement of alanyl-glutamine could increase serum Gln level and decrease urine L/M ratio.

Li *et al*.[13-16] studied that measurement of serum DAO was helpful to determine the degree of intestinal mucous damage. In their research after administration of Gln, serum DAO level significantly increased in the placebo group and significantly decreased in the Gln group compared with the level before drug administration. The change in serum endotoxin level was similar in the 2 groups. This change of serum endotoxin level was related to the fact that high serum Gln level could enhance the function of intestinal mucosal barrier. Low serum endotoxin level was helpful to reduce SIRS in patients. Some reseaches showed that endotoxin in early trauma could lead to the increase of production and release of cytokines such as TNF-α,IL-6, IL-8, which could take part in the generation of SIRS[17].

Haga *et al*.[18] studied the postoperative conditions of 292 gastrointestinal patients. The result was that 245 patients had SIRS early after operation, which was 83.9%. The possibility of postoperative complication and MODS in these patients was much higher than that in those without SIRS. The results in our study indicate that SIRS can be reduced in early postoperative patients.

REFERENCES

1 **Wilmore DW,** Smith RJ, O'Dwyer ST, Jacobs DO, Ziegler TR, Wang XD. The gut: a central organ after surgical stress. *Surgery* 1988; **104**: 917-923

2 **You ZY,** Yu B, Lei ZH, Zhao Y. The determination of Glu and Gln in plasma and tissue by RP-HPLC. *Disan Junyi Daxue Xuebao* 1995; **17:** 152-153

3 **Hosoda N**, Nishi M, Nakagawa M, Hiramatsu Y, Hioki K, Yamamoto M. Structural and functional alterations in the gut of parenterally or enterally fed rats. *J Surg Res* 1989; **47:** 129-133

4 **Zhang JX**, Gao SG. Malondialdehyde Kit for determining serum lipoperoxide. *Nanjing Tiedao Yixueyuan Xuebao* 1997; **16:** 63-64

5 **Behrens RH**, Docherty H, Elia M, Neale G. A simple enzymatic method for the assay of urinary lactulose. *Clin Chim Acta* 1984; **137**: 361-367

6 **Lunn PG**, Northrop CA, Northop AJ. Automated enzymatic assays for the determination of intestinal permeability probes in urine. 2. Mannitol. *Clin Chim Acta* 1989; **183:** 163-170

7 **Bjarnason I**, MacPherson A, Hollander D. Intestinal permeability: an overview. *Gastroenterology* 1995; **108:** 1566-1581

8 **Saadia R**, Schein M, MacFarlane C, Boffard KD. Gut barrier function and the surgeon. *Br J Surg* 1990; **77:** 487-492

9 **Brooks AD**, Hochwald SN, Heslin MJ, Harrison LE, Burt M, Brennan MF. Intestinal permeability after early postoperative enteral nutrition in patients with upper gastrointestinal malignancy. *JPEN* 1999; **23:** 75-79

10 **Li N**, Liu FN, Li YS, Kang J, Li FJ, Li JS. The changes of plasma glutamine and its influence on intestinal permeability after abdominal surgery. *Changwai Yu Changnei Yingyang* 1998; **5:** 3-6

11 **Jiang ZM**, Wang LJ, Qi Y, Liu TH, Qiu MR, Yang NF, Wilmore DW. Comparison of parenteral nutrition supplemented with L-glutamine or glutamine dipeptides. *JPEN* 1993; **17:** 134-141

12 **Bai MX,** Jiang ZM, Liu YM, Wang WT, Li DM, Wilmore DW. Effects of alanyl-glutamine on gut barrier function. *Nutrition* 1996; **12**: 793-796

13 **Li JY,** Lu Y, Xue LB. The effect of oral administration of glutamine on free amino acids concentration in the plasma of scalded rat. *Anjisuan He Shengwuziyuan* 2000; **22**: 51-56

14 **Lu Y,** Li JY, Sun SR, Jin H, Jiang XG, Sun XQ, Sheng ZY. Relationship between change of plasma diamine oxidase activity and gut injury in rats during gut ischemia-reperfusion. *Anjisuan He Shengwuziyuan* 2000; **22**: 50-54

15 **Li JY,** Lu Y, Fu XB, Jin H, Hu S, Sun XQ, Sheng ZY. The significance of changes in diamine oxidase activity in intestinal injury after tranma. *Zhongguo Weizhongbing Jijiu Yixue* 2000; **12**: 482-484

16 **Li JY,** Lu Y , Hao J, Jin H, Xu HJ. Determination of diamine oxdase activity in intestinal tissue and blood using spectrophotometry. *Anjisuan He Shengwuziyuan* 1996; **18**: 28-30

17 **Jiang JX**, Tian KL, Chen HS. Zhu PF, Wang ZG. Changes of plasma cytokines in patients with severe trauma and their relation ship with organ damage. *Zhonghua Waike Zazhi* 1997; **35:** 406-407

18 **Haga Y**, Beppu T, Doi K, Nozawa F, Mugita N, Ikei S, Ogawa M. Systemic inflammatory response syndrome and organ dysfunction following gastrointestinal surgery. *Crit Care Med* 1997; **25:** 1994-2000

Edited by Wang XL and Xu FM

PO Box 2345, Beijing 100023, China
Fax: +86-10-85381893
E-mail: wjg@wjgnet.com www.wjgnet.com

World J Gastroenterol 2004;10(13):1995-1997
World Journal of Gastroenterology
 ISSN 1007-9327

• BRIEF REPORTS •

Safe major abdominal operations: Hepatectomy, gastrectomy and pancreatoduodenectomy in elder patients

Yu-Lian Wu, Jun-Xiu Yu, Bin Xu

Yu-Lian Wu, Jun-Xiu Yu, Bin Xu, Department of Surgery, 2nd Affiliated Hospital, School of Medicine, Zhejiang University, Hangzhou 310009, Zhejiang Province, China
Correspondence to: Dr. Yulian Wu, Department of Surgery, 2nd Affiliated Hospital, School of Medicine, Zhejiang University, Hangzhou 310009, Zhejiang Province, China. wuyulian@medmail.com.cn
Telephone: +86-571-87784604 **Fax:** +86-571-87784604
Received: 2003-12-10 **Accepted:** 2004-01-08

Abstract

AIM: To evaluate the impact of advanced age on outcome after hepatectomy, gastrectomy and pancreatoduodenectomy.

METHODS: Two hundreds and eleven patients undergone hepatectomy, gastrectomy and pancreatoduodenectomy from January 1998 to September 2002 were analyzed retrospectively. Clinicopathologic features and operative outcome of 83 patients aged 65 years or more were compared with that in 128 younger patients aged less than 65 years.

RESULTS: The nutritional state, such as pre-operation level of serum albumin and hemoglobin in the older patients was poorer than that in the younger patients. The older patients had higher comorbidities than the younger patients (48.2% *vs* 15.6%). No significant difference was observed in perioperative mortality, and complication rate between the older and younger patients (2.4% *vs* 1.6% and 22.9% *vs* 20.3%, respectively). Multivariate analysis demonstrated that pancreatoduodenectomy, hepatectomy with resection of more than 2 segments and comorbidities were independent predictors of postoperative complication, whereas age was not (P=0.3172).

CONCLUSION: It is safe for patients aged 65 years or more to undergo hepatic, pancreatic and gastric resection if great care is taken during perioperative period.

Wu YL, Yu JX, Xu B. Safe major abdominal operations: Hepatectomy, gastrectomy and pancreatoduodenectomy in elder patients. *World J Gastroenterol* 2004; 10(13): 1995-1997
http://www.wjgnet.com/1007-9327/10/1995.asp

INTRODUCTION

The number and proportion of the elderly in our population have increased progressively as a result of increased life expectancy. The population over the age of 65 years is growing at the fastest rate than any other age groups[1]. But surgery for potentially curable disease frequently leaves elderly patients numerically de-represented[2]. Worrying about surgical risks and morbidity may be one reason accounting for this phenomenon. There are different opinions about whether elderly surgical patients have poor outcome. Some studies suggested that elderly surgical patients had high morbidity and mortality[3,4]. Other reports showed that there was no significant difference in the rate of complications and death between the older and the younger surgical patients[5,6]. Two hundreds and eleven patients undergone major abdominal operations, including hepatectomy, gastrectomy and pancreatoduodenectomy in recent 5 years were analyzed retrospectively to see whether the older patients face more risks than younger patients.

MATERIALS AND METHODS

Two hundreds and eleven patients who underwent hepatectomy, gastrectomy or pancreatoduodenectomy in our hospital from January 1998 to September 2002 were studied retrospectively. The patients were divided into two groups: older group (age ≥65 years) and younger group (age<65 years). The patients' age and sex, diagnosis, comorbidities, preoperative laboratory values, type of operation, clinical and pathologic characteristics of local lesion, postoperative complications and death, operative blood loss and transfusion, relaparotomy, length of hospital stay were obtained from the operative records and medical notes. The primary carcinoma was divided into different stages according to TNM staging system defined by Union Internationale Contre le Cancer (UICC, 1997). The patients were considered to have comorbidity when treatment was required in additional organ systems. Complications were defined by the classification proposed by Clavien *et al.*[7]. Because grade I complications (minor and were likely to resolve spontaneously) were difficult to collect due to retrospective audits, only grade IIa complications (requiring drug for treatment), grade IIb complications (requiring reoperation or invasive procedure), grade III complications (events with residual or lasting disability including organ resection), grade IV complications (death as a result of any complication) were included in this study. Mortality was defined as death from any cause within 30 days of the operation.

Data were analyzed with the SAS 8.0 statistical software. Differences were analyzed with the Chi-square test or Fisher' s exact test for group contingency analysis and the Student' *t* test and Mann-Whitney non-parametric test for continuous variables. Using logistic regression, the influence of different variables on the complication was studied. Length of hospital stay of the two groups was compared with a nonparametric product-limit method analogous to a Kaplan-Meier survival analysis. P<0.05 was considered statistically significant.

RESULTS

0f the 211 patients, 150 cases were men and 61 cases were women. The median age was 60 years (range, 18 to 88).

The older group consisted of 83 patients, including 51 cases (≥65 years), 21 cases (>70 years), 6 cases (>75 years), and 5 cases (>80 years). Diagnosis included primary hepatic carcinoma (31 cases), hepatic adenoma (1 case), hepatic chronic granuloma (1 case), metastatic cancer in liver (5 cases), gastric carcinoma (30 cases), gastric carcinoid (1 case), pancreatic carcinoma (4 cases), periampullary cancer (8 cases), and chronic pancreatitis (2 cases).

The younger group consisted of 128 patients. Diagnosis included primary hepatic carcinoma (45 cases), hepatic malignant stroma (1 case), focal nodular hyperplasia of liver

(1 case), metastatic cancer in liver (1 case), gastric carcinoma (37 cases), gastric ulcer (1 case), gastric malignant stoma (1 case), pancreatic carcinoma (15 cases), periampullary cancer (23 cases), chronic pancreatitis (2 cases), and benign biliary stricture (1 case).

No difference in stage of primary cancer was seen between the older group and younger group, but the levels of serum albumin and hemoglobin in older group were lower than those in younger group (Table 1). A 48.2% of total patients in older group had one or more comorbidities, which was significantly higher than that in younger group (15.6%). There was no difference in the constitution of operative procedure in the older and younger group. Median operative blood loss and transfusion were similar in both groups (500 mL *vs* 500 mL and 2 units *vs* 2 units, Table 1).

Table 1 Comparison of clinicopathologic features between the two age groups

Clinicopathologic Features	Younger group (<65 yr)	Older group (≥65 yr)	*P* value
Age (median)	52	69	
Gender (*n*)			0.2142[1]
Male	87	63	
Female	41	20	
Diagnosis (*n*)			0.1105[2]
Liver			
Hepatic carcinoma	45	31	
Others	3	7	
Stomach			
Gastric carcinoma	37	30	
Others	2	1	
Pancrea			
Pancreatic carcinoma	15	4	
Periampullary carcinoma	23	8	
Others	3	2	
Serum albumin (mean±SD, g/dL)	3.84±0.46	3.65±0.50	0.0045[3]
Hemoglobin (mean±SD, g/dL)	12.05±2.39	11.16±2.33	0.0082[3]
Stage of primary cancer (*n*)			0.5658[1]
I	18	12	
II	32	13	
III	53	34	
IV	17	13	
Comorbidity	15.6% (20/128)	48.2% (40/83)	<0.0001[1]

[1]Chi-squere test; [2]Fisher's exact test; [3]Student's *t* test.

There was no apparent difference in complication rates between the older and younger group (22.9% *vs* 20.3%, Table 2). The most common complications were wound infection. Other complications included pneumonia, bile leak, pancreatic fistula, delayed gastric emptying, gastrointestinal fistula, cerebrovascular accident, abdominal bleeding, gastric bleeding, DIC, hepatic encephalopathy, pleural effusion, and renal failure. Two patients (2.4%) were re-operated because of gastric bleeding and bile leak in older group. Three patients (2.3%) were re-operated because of intestinal fistula, abdominal bleeding and bile leak in younger group. There was no significant difference in the rate of the re-operation between the two groups (Table 2). In older group, one patient died of DIC and severe metabolic acidosis 4 d after operation, another patient died of pneumonia 24 d after operation. In younger group, two patients died of abdominal hemorrhage and hepatic encephalopathy 13 and 27 d, respectively, after operation. The older patients had almost same perioperative mortality rate as the younger patients (2.4% and 1.6%, respectively). The median hospital stay was 24 d (range, 8 to 147 d) in the older group, which was significantly longer than that in the younger group (median, 21 d, and range, 4 to 128 d) (Figure 1).

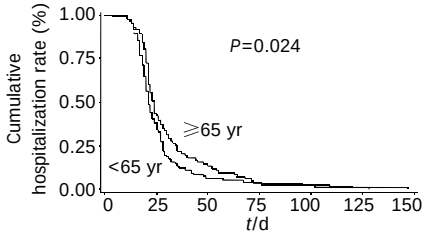

Figure 1 Length of hospital stay of the two age groups. Kaplan-Meier curves showed that the hospital stay in older group was significantly longer than that in younger group (*P*=0.024).

Table 3 Multivariate analysis of factors influencing major post-operative complications

Variables	Odds ratio	95% confidence interval	*P* value
Pancreatoduodenectomy	3.7736	1.7699-8.0145	0.0006
Hepatectomy>2 segments	1.0858	1.0060-1.1834	0.0334
Comorbidity	3.2787	1.5361-6.9930	0.0021
Age (as continuous variable)	1.0173	0.9833-1.0537	0.3172

Logistic regression analysis showed pancreatoduodenectomy and hepatectomy with resection of more than 2 segments and comorbidities were independent factors for complications, whereas age was not.

Table 2 Comparison of therapeutic characteristics between the two age groups

Therapeutic characteristics	Younger group (<65 yr)	Older group (≥65 yr)	*P* value
Operative procedures			0.1708[1]
Hepatectomy≤2 segments	26	23	
Hepatectomy>2 segments	22	15	
Gastrectomy-total/proximal	13	11	
Gastrectomy-distal	26	20	
Pancreatoduodenectomy	41	14	
Operative blood loss (median, mL)	500 (100-20 000)	500 (50-3 500)	0.6480[3]
Operative blood transfusion (median, units)	2 (0-36)	2 (0-13)	0.3395[3]
Rate of complications	20.3% (26/128)	22.9% (19/83)	0.6550[1]
Reoperative rate	2.3% (3/128)	2.4 % (2/83)	1.0000[2]
Perioperative mortality (within 30 d)	1.6% (2/128)	2.4 (2/83)	0.6470[2]
Hospital length of stay (median, d)	21 (4-128)	24 (8-147)	0.0241[4]

[1]Chi-squere test; [2]Fisher's exact test; [3]Mann-Whitney non-parametric test; [4]Kaplan-Meier method.

The multivariate analysis by a stepwise logistic regression model identified three independent significant variables for postoperative complications in the both groups: pancreatoduodenectomy, hepatectomy with resection of more than 2 segments and comorbidities. Sex, reasons of operations, serum albumin, hemoglobin did not influence the morbidity as an independent factor. Calendaric age (in years) was not an independent predictor of complication (P=0.3172) (Table 3).

DISCUSSION

Our study suggests that there is no difference between the older patients and the younger patients in postoperative morbidities and mortalities. Similar results have been reported by others. Hodul *et al*.[6] studied in 122 patients with pancreatoduodenectomy, including 48 patients aged over 70 years, and reported no significant difference between older group and younger group comparing the rate of complications, such as wound infection, abdominal abscess, pancreatic leak, and so on. A retrospective study carried out on 97 patients with a gastric tumor measuring 10 cm or more in diameter showed age was not the influencing factor of frequency of complications[5]. Furthermore, analysis of extended hepatectomy (more than four liver segments) demonstrated age was not a contributor to in-hospital mortality[8].

The improvement in perioperative management was a vital reason for reducing the morbidity and mortality[9]. Developed guidelines for perioperative care may contribute the safety of operation for the elderly, for example, less use of nasogastric tubes can decrease the pulmonary complications, routine drainage being avoided in most cases or limited to a short period can facilitate early mobilization[10]. Preoperative assessment of elderly and formulation of an effective anesthetic plan according the "individual principle" can decrease the risks of anesthesia[11]. The surgeon's skill was enhanced due to specialization and made the major abdominal operation become safety. Special team including surgeons, physicians, anesthetists and nurses for unstable elderly patients can decrease the morbidity and mortality[12]. The environment of operation room[13] was improved, the operative instruments were updated, which could attenuate the stress of an operation. Positive and effective treatment in surgical intensive care unit (SICU) helps elderly patients live through the crisis after operation.

Older patients need more perioperative care. First, older patients have more comordities require to manage than younger patients. Blair *et al*.[14] reported older cases had more comorbidities than the younger (49% *vs* 25%) in a series of 179 patients undergone gastrectomy and pancreatectomy. In our study, nearly half of older patients had one or more comorbidities, which were significantly higher than that in younger patients. Second, the nutrition of older patients is poorer than younger patients. Our study showed the level of serum albumin and hemoglobin in older group was lower than younger group. More comorbidities and poorer nutrition mean the older patients need more waiting time for operation and more time for postoperative management, which lead more length of hospital stay in the older cases. Thus, the median hospital stay was longer significantly in older group longer than that in younger group in our study.

In this study, the level of serum albumin and hemoglobin were not the independent predictors for complications, suggesting that short-term nutritional support before operation could improve the nutritional status and reduce the risks of the surgery and anesthesia[15]. Comorbidity was an independent factor for complication in our study because the comorbidity could not be controlled in short-term. Comorbidity must be treated during perioperative period, which is a positive measure to reduce perioperative morbidity and mortality.

The patients with complex major operation should receive more perioperative care. Pancreatoduodenectomy and hepatectomy with resection of more than 2 segments were independent predictors of complication in our study. The result was supported by more recent reports. Jarnagin *et al*.[16] studied in 1803 consecutive cases with hepatic resection over the past decade, and reported that the number of hepatic segments resected and operative blood loss were the independent predictors of both perioperative morbidity and mortality. So, the authors figured out that the major operation has more complications than minor operation[16].

In conclusion, the present data suggest that advanced age does not predict high morbidity and mortality after major abdominal operations. Surgeons should not advise against an operation just because the patient is old.

REFERENCES

1 **Etzioni DA,** Liu JH, Maggard MA, Ko CY. The aging population and its impact on the surgery workforce. *Ann Surg* 2003; **238**: 170-177

2 **Kmietowicz Z.** Call for greater care of elderly people in surgery. *BMJ* 1999; **319**: 1324B

3 **Pavlidis TE,** Galatianos IN, Papaziogas BT, Lazaridis CN, Atmatzidis KS, Makris JG, Papaziogas TB. Complete dehiscence of the abdominal wound and incriminating factors. *Eur J Surg* 2001; **167**: 351-354

4 **Saghir JH,** McKenzie FD, Leckie DM, McCourtney JS, Finlay IG, McKee RF, Anderson JH. Factors that predict complications after construction of a stoma: a retrospective study. *Eur J Surg* 2001; **167**: 531-534

5 **Yasuda K,** Shiraishi N, Adachi Y, Inomata M, Sato K, Kitano S. Risk factors for complications following resection of large gastric cancer. *Br J Surg* 2001; **88**: 873-877

6 **Hodul P,** Tansey J, Golts E, Oh D, Pickleman J, Aranha GV. Age is not a contraindication to pancreaticoduodenectomy. *Am Surg* 2001; **67**: 270-275

7 **Clavien PA,** Sanabria JR, Strasberg SM. Proposed classification of complications of surgery with examples of utility in cholecystectomy. *Surgery* 1992; **111**: 518-526

8 **Melendez J,** Ferri E, Zwillman M, Fischer M, DeMatteo R, Leung D, Jarnagin W, Fong Y, Blumgart LH. Extended hepatic resection: a 6-year retrospective study of risk factors for perioperative mortality. *J Am Coll Surg* 2001; **192**: 47-53

9 **Beliveau MM,** Multach M. Perioperative care for the elderly patient. *Med Clin North Am* 2003; **87**: 273-289

10 **Kehlet H,** Wilmore DW. Multimodal strategies to improve surgical outcome. *Am J Surg* 2002; **183**: 630-641

11 **Muravchick S**. Preoperative assessment of the elderly patient. *Anesthesiol Clin North America* 2000; **18**: 71-89

12 **Demetriades D,** Sava J, Alo K, Newton E, Velmahos GC, Murray JA, Belzberg H, Asensio JA, Berne TV. Old age as a criterion for trauma team activation. *J Trauma* 2001; **51**: 754-756

13 **Jin F,** Chung F. Minimizing perioperative adverse events in the elderly. *Br J Anaesth* 2001; **87**: 608-624

14 **Blair SL,** Schwarz RE. Advanced age does not contribute to increased risks or poor outcome after major abdominal operations. *Am Surg* 2001; **67**: 1123-1127

15 **Cohendy R,** Gros T, Arnaud-Battandier F, Tran G, Plaze JM, Eledjam J. Preoperative nutritional evaluation of elderly patients: the Mini Nutritional Assessment as a practical tool. *Clin Nutr* 1999; **18**: 345-348

16 **Jarnagin WR,** Gonen M, Fong Y, DeMatteo RP, Ben-Porat L, Little S, Corvera C, Weber S, Blumgart LH. Improvement in perioperative outcome after hepatic resection: analysis of 1 803 consecutive cases over the past decade. *Ann Surg* 2002; **236**: 397-406

Edited by Kumar M **Proofread by** Xu FM

PO Box 2345, Beijing 100023, China
Fax: +86-10-85381893
E-mail: wjg@wjgnet.com www.wjgnet.com

World J Gastroenterol 2004;10(13):1998-2001
World Journal of Gastroenterology
 ISSN 1007-9327

• BRIEF REPORTS •

Gastrointestinal decompression after excision and anastomosis of lower digestive tract

Wen-Zhang Lei, Gao-Ping Zhao, Zhong Cheng, Ka Li, Zong-Guang Zhou

Wen-Zhang Lei, Gao-Ping Zhao, Zhong Cheng, Ka Li, Zong-Guang Zhou, Department of Gastrointestinal Surgery, West China Hospital, Sichuan University, Chengdu 610041, Sichuan Province, China
Correspondence to: Dr. Gao-Ping Zhao, Department of Gastrointestinal Surgery, West China Hospital, Sichuan University, Chengdu 610041, Sichuan Province, China. zhgaoping@yahoo.com.cn
Telephone: +86-28-68126226 **Fax:** +86-28-68123364
Received: 2004-02-02 **Accepted:** 2004-02-24

Abstract

AIM: To discuss the clinical significance of postoperative gastrointestinal decompression in operation on lower digestive tract.

METHODS: Three hundred and sixty-eight patients with excision and anastomosis of lower digestive tract were divided into two groups, i.e. the group with postoperative gastrointestinal decompression and the group without postoperative gastrointestinal decompression. Clinical therapeutic outcome and incidence of complication were compared between two groups. Furthermore, an investigation on application of gastrointestinal decompression was carried out among 200 general surgeons.

RESULTS: The volume of gastric juice in decompression group was about 200 mL every day after operation. Both groups had a lower girth before operation than every day after operation. No difference in length of the first passage of gas by anus and defecation after operation was found between two groups. The overall incidence of complications was obviously higher in decompression group than in non-decompression group (28% *vs* 8.2%, $P<0.001$). The incidence of pharyngolaryngitis was up to 23.1%. There was also no difference between two groups regarding the length of hospitalization after operation. The majority (97.5%) of general surgeons held that gastrointestinal decompression should be placed till passage of gas by anus, and only 2.5% of surgeons thought that gastrointestinal decompression should be placed for 2-3 d before passage of gas by anus. Nobody (0%) deemed it unnecessary for placing gastrointestinal compression after operation.

CONCLUSION: Application of gastrointestinal decompression after excision and anastomosis of lower digestive tract cannot effectively reduce gastrointestinal tract pressure and has no obvious effect on preventing postoperative complications. On the contrary, it may increase the incidence of pharyngolaryngitis and other complications. Therefore, it is more beneficial to the recovery of patients without undergoing gastrointestinal decompression.

Lei WZ, Zhao GP, Cheng Z, Li K, Zhou ZG. Gastrointestinal decompression after excision and anastomosis of lower digestive tract. *World J Gastroenterol* 2004; 10(13): 1998-2001
http://www.wjgnet.com/1007-9327/10/1998.asp

INTRODUCTION

At present, gastrointestinal decompression after excision and anastomosis of lower digestive tract is still widely used in clinic. Although some researches regarding the application of gastrointestinal decompression after digestive tract operation were made, few researches related to the value of decompression after lower digestive tract have been carried out. Therefore, we performed a prospective randomized controlled study on 368 patients undergoing excision and anastomosis of lower digestive tract in West China Hospital, Sichuan University between July 2002 and October 2003. We also made an investigation in the application of gastrointestinal decompression among 200 general surgeons in China.

MATERIALS AND METHODS

Cases selection

Three hundred and sixty-eight cases underwent excision and anastomosis of lower digestive tract were divided into two groups. One group underwent gastrointestinal decompression after operation and the other group did not.

Clinical data

Of one hundred and eighty-six cases underwent postoperative gastrointestinal decompression, 109 were males and 77 were females, aged between 21-82 years with an average age of 56.8 years. Of the 182 cases in the group who did not undergo postoperative gastrointestinal decompression, 112 were males and 70 were females, aged between 23-84 years with a mean age of 57.2 years. In decompression group, there were 4 cases of small intestinal tumor, 6 cases of benign colon disease, 31 cases of carcinoma of colon and 145 cases of rectal cancer. In non-decompression group, there were 5 cases of small intestinal tumor, 8 cases of benign colon disease, 28 cases of carcinoma of colon and 141 cases of rectal cancer. Partial excision of small intestine was performed for small intestinal tumors. Patients with benign colon disease and colon carcinoma underwent partial or subtotal excision of colon, and those with rectal cancer received anterior resection.

Methods

A nasogastric tube was placed in all patients during operation. The tube was removed in the group with gastrointestinal decompression after passage of gas by intestines with continuous vacuum aspiration. The nasogastric tubes in the group without gastrointestinal decompression were immediately removed after operation. Then, the following procedures were carried out. The gastric juice of patients was collected and measured after operation, the postoperative girth was measured by circling umbilical region in the morning as a comparison value with preoperative one, the time for passage of gas by intestines and defecation, the length of hospitalization after operation and the incidence of complications and prognosis were observed and recorded. Those suffering from anastomotic leaks were subjected to treatments such as anti-infective treatment, nutrition support or colostomy. Correspondingly, acute dilatation of stomach was subjected

to gastrointestinal decompression and vacuum aspiration, pulmonary infection to anti-infective therapy, wound infection to local drainage, and cough and throat pain to oral nursing and fog inhalation therapy.

Clinical investigation

An investigation was carried out among 200 general surgeons from 18 hospitals by way of communication. The contents of investigation included the length of placing gastrointestinal decompression after excision and anastomosis of lower digestive tract by these surgeons and their cognition of the significance of placing gastrointestinal decompression.

Statistical analysis

SPSS 10.0 software was used to conduct statistical analysis.

RESULTS

General data

There were no significant differences between two groups in terms of sex ($P>0.05$), age ($P>0.05$). No statistical difference was found between two groups in case distributions ($P=0.892$).

Table 1 Girth of 368 cases before and after operation on lower digestive tract (mean±SD)

Girth	Decompression group (n=186)	Non-decompression group (n=182)	P value
Before operation (cm)	76.3±17.6[b]	75.1±16.2[d]	0.051
After operation (cm)			
Day 1	82.4±21.5	81.5±20.7	0.562
Day 2	82.8±19.8	83.6±21.8	0.367
Day 3	82.2±21.5	84.7±21.2	0.551

[b]$P<0.001$, [d]$P<0.001$ *vs* the three initial days after operation.

Clinical observation

None of the 368 cases died due to operation. The volume of gastric juice in the group with gastrointestinal decompression was 10-520 mL every day after operation (146.5±87.4 mL on the 1st day, 204.9±92.5 mL on the 2nd day, and 205.3±107.1 mL on the 3rd day, respectively). The volume of gastric juice on the 1st day was lower than that on the 2nd and 3rd days ($P<0.001$). However, there was no statistical difference between the volumes on the 2nd and 3rd days ($P>0.05$). There was no significant difference between two groups in terms of girth before and after operation ($P>0.05$). However, the preoperative girth of two groups was less in comparison with the postoperative one ($P<0.001$) (Table 1). The time for passage of gas by anus was 3.2±1.1 d in the group with gastrointestinal decompression and 3.2±1.3 d in the group without gastrointestinal decompression ($P<0.05$). The time for the first defecation of the group with gastrointestinal decompression and the group without gastrointestinal decompression was 4.5±1.4 and 4.6±1.6 d, respectively ($P>0.05$). The time of hospitalization after operation was 9.0±4.5 d for the group with gastrointestinal decompression and 8.6±4.0 d for the group without gastrointestinal decompression ($P>0.05$). All patients were completely recovered from such illnesses and discharged from hospital.

Incidence of complications

Table 2 shows the incidence of complications after operation. Symptoms as fever and leakage of intestinal contents were diagnosed as anastomotic leakage. There were 5 cases suffering from the lesion in the two groups. All the leakages occurred during excision and anastomosis of lower or ultra-lower rectal tumor and healed after clinical therapy. Those who suffered from abdominal distension, emesis and succussion splash of stomach were diagnosed with acute dilatation of stomach and then subjected to gastrointestinal decompression. Four cases of pulmonary infection were found in two groups by chest X-ray and cured through anti-inflammatory therapy. Any symptom with throat upset or pain was diagnosed as pharyngolaryngitis, 23.1% of patients suffered from pharyngolaryngitis in decompression group and only 4.4% in non-decompression group. Through statistical analysis, the incidence rate of pharyngolaryngitis in decompression group was obviously higher than that in non-decompression group ($P<0.001$). No statistical difference was found in terms of other complications ($P>0.05$). Compared with non-decompression group, the total incidence of complications in decompression group was evidently higher ($P<0.001$).

Investigation results

We conducted an investigation among 200 general surgeons in China, 97.5%(195/200) of surgeons routinely placed nasogastric tube for the passage of gas by anus after excision and anastomosis of lower digestive tract, while 2.5%(5/200) of surgeons discarded gastrointestinal decompression 2-3 d after operation before the passage of gas by anus. All patients of these surgeons underwent gastrointestinal decompression after operation and this kind of management was assumed as a matter of course by the surgeons investigated. Ninety-five percent of the surgeons (190/200) held that gastrointestinal decompression should be maintained till the passage of gas by anus, 4.5%(9/200) of surgeons thought it unnecessary for placing gastrointestinal decompression till passage of gas by anus.

DISCUSSION

Present status of application of gastrointestinal decompression after excision and anastomosis of lower digestive tract

At present, it is still generally believed that gastrointestinal decompression should be performed after operation on abdominal region. The monographs on operation pointed out that gastrointestinal decompression should be conducted for the passage of gas by anus[1]. A randomized study on general surgeons showed that 72% of them performed routine gastrointestinal decompression after excision of small intestine and 49% of them performed routine gastrointestinal decompression after excision and anastomosis of large intestine[2]. The present study revealed that 97.5% of surgeons thought gastrointestinal decompression should be performed for the passage of gas by anus after excision and anastomosis of lower digestive tract, suggesting that it has become a routine

Table 2 Complications of 368 cases after operation on lower digestive tract

Patient froup	Anastomotic leakage (n, %)	Acute dilation of stomach (n, %)	Pulmonary infection (n, %)	Pharyngolaryngitis (n, %)	Wound infection (n, %)
Decompression group (n=186)	3(1.6)	1(0.5)	3(1.6)	43(23.1)[b]	2(1.1)
Non-decompression group (n=182)	2(1.1)	2(1.1)	1(0.5)	8(4.4)	1(0.5)

[b]$P<0.001$ *vs* non-decompression group.

procedure after excision and anastomosis of lower digestive tract.

Effects of gastrointestinal decompression

Paralysis of intestine is a natural and transient physiological process after operation on abdominal region. Some researches[3,4] regarding the relationship between such a phenomenon and gastrointestinal decompression have been made. However, there were few reports focusing on the theoretical basis of this field. It is well-known that the volume of secreted digestive juices was about 5 300-9 500 mL, and the gas secreted by deglutition and intestines was about 30-300 mL[5]. Nevertheless, the volume extracted by gastrointestinal decompression every day was less than 10% of digestive juices. This study showed the volume extracted by gastrointestinal decompression every day was 200 mL. It is thus evident that gastrointestinal decompression could not effectively extract digestive juices. After operations on abdominal region, gastrointestinal motor function was reduced and the function of intestinal absorption was not greatly influenced. This research showed that the postoperative girth was increased as compared with preoperative girth, demonstrating that there exists paralysis of intestines after operation and paralysis of intestines is a normal and brief process. Clevers *et al*.[3] reported that paralysis of intestine could not be alleviated by gastrointestinal decompression. The present study demonstrated that there were no significant differences between two groups in terms of passage of gas by anus and the length of defecation. The findings made it clear that gastrointestinal decompression could not get rid of paralysis of intestine or shorten the length of paralysis of intestine. There was no statistical difference between two groups in the increase of girth after operation, demonstrating that with the aid of gastrointestinal decompression, the liquid and gas were difficult to be extracted from intestines and there was no obvious effect upon postoperative abdominal distension. The above research results showed that gastrointestinal tract pressure could not be effectively reduced by means of gastrointestinal decompression.

Influence of gastrointestinal decompression upon postoperative complication

It is undoubtedly that the risk of incidence of anastomotic leakage would increase with the increased tract pressure after anastomosis. One of the purposes of gastrointestinal decompression was to reduce the inner pressure of gastrointestinal tract and the incidence rate of anastomotic leakage. This study revealed that there was no significant difference between two groups in the development of anastomotic leakage, which might be correlated with the fact that gastrointestinal decompression could not effectively reduce stoma pressure of gastrointestinal tract, and especially that gastrointestinal decompression played a small role in reducing the pressure of stoma of lower digestive tract. In the two groups, 3 cases suffered from acute dilation of stomach and no statistical difference was found between two groups. Of the 3 cases of acute dilation of stomach, 1 was from the non-decompression group and cured by the gastrointestinal decompression for 28 d. Although there was an increased probability of acute dilation of stomach without gastrointestinal decompression, its incident rate was lower and easily treated when it happened. In the two groups, there were 4 cases of pulmonary infection. Although gastrointestinal decompression was not the immediate cause for pulmonary infection, it could lead to cough and expectoration, and indirectly induce pulmonary infection. Owing to a low incidence rate of pulmonary infection, further researches for more cases need to be conducted. According to the report by Huerta *et al*.[6], the incidence rate of pulmonary infection in those with gastrointestinal decompression after operation on abdominal region was 10 times higher than that in those without gastrointestinal decompression. In addition, this report deemed that it was improper to perform gastrointestinal decompression as a routine procedure and that gastrointestinal decompression could be only used for the treatment of paralysis and dilation of stomach. Pharyngolaryngitis could be immediately induced by long-term irritation and compression of throat by gastrointestinal decompression tubes. Nathan *et al*.[2] reported that the incidence rate of throat pain was greatly increased in gastrointestinal decompression group. This study revealed that the incidence rate of pharyngolaryngitis in decompression group was up to 23.1%, 5 times as high as in non-decompression group, showing that pharyngolaryngitis was related to nasogastric tubes. This kind of pharyngolaryngitis could be easily dealt with through treatments as fog inhalation therapy and oral nursing after removal of the tube. Michowitz *et al*.[7] revealed that the incidence rate of complications was obviously increased in the group with gastrointestinal decompression after operations on abdominal region, and that postoperative hyperpyrexia and atelectasis were markedly enhanced. Another randomized research report showed that 70% of severe upsets were caused by gastrointestinal decompression[8]. This study demonstrated that gastrointestinal decompression could not effectively prevent severe postoperative complications such as anastomotic leakage and instead, resulted in an increased incidence rate of pharyngolaryngitis.

Influence of gastrointestinal decompression upon prognosis

According to some research reports[9,10], there were no increase in incidence rate of complications and no obvious influence upon prognosis by fluid feeding from the 1st day after operation on gastrointestinal tract without gastrointestinal decompression. Researches showed that it was unnecessary for gastrointestinal decompression after operation on abdominal region, which could reduce the incidence rate of pneumonia and recover the tract functions as early as possible[11-16]. The present study showed that there was no obvious difference between two groups in terms of passage of gas by anus and length of defecation time, implying that there was no adverse influence upon recovery of intestinal functions without gastrointestinal decompression. Despite of no significant difference in the time of postoperative hospitalization, the total incidence rate of complications in decompression group was obviously higher than that in non-decompression group, demonstrating that it was more beneficial to the recovery of patients without gastrointestinal decompression.

In conclusion, gastrointestinal decompression following excision and anastomosis of lower digestive tract cannot reduce the pressure of gastrointestinal tract and has no obvious effects upon preventing of postoperative complications. Contrary to expectations, it may increase the incidence rate of pharyngolaryngitis and other complications. Therefore, it is more beneficial to the patients' recovery without gastrointestinal decompression.

REFERENCES

1 **Li JS**, Wu MC, Huang ZQ. The Complete works of surgery-general surgery volume. 1sted. Beijing: *People's Military Surgeon Press* 1996: 344-548

2 **Nathan BN**, Pain JA. Nasogastric suction after elective abdominal surgery: a randomised study. *Ann R Coll Surg Engl* 1991; **73**: 291-294

3 **Clevers GJ**, Smout AJ. The natural course of postoperative ileus following abdominal surgery. *Neth J Surg* 1989; **41**: 97-99

4 **Ying FM**. Reports on 112 cases with decompression operation on biliary tract without nasogastric tube. *Linchuang Waike Zazhi* 1999; **7**: 104

5 **Tang YS**, Zhang XZ, Han DC. Human medical parameters and concepts. 1sted. *Jinnan: Jinan Press* 1995: 80-115
6 **Huerta S**, Arteaga JR, Sawicki MP, Liu CD, Livingston EH. Assessment of routine elimination of postoperative nasogastric decompression after Roux-en-Y gastric bypass. *Surgery* 2002; **132**: 844-848
7 **Michowitz M**, Chen J, Waizbard E, Bawnik JB. Abdominal operations without nasogastric tube decompression of the gastrointestinal tract. *Am Surg* 1988; **54**: 672-675
8 **Koukouras D**, Mastronikolis NS, Tzoracoleftherakis E, Angelopoulou E, Kalfarentzos F, Androulakis J. The role of nasogastric tube after elective abdominal surgery. *Clin Ter* 2001; **152**: 241-244
9 **Hoffmann S**, Koller M, Plaul U, Stinner B, Gerdes B, Lorenz W, Rothmund M. Nasogastric tube versus gastrostomy tube for gastric decompression in abdominal surgery: a prospective, randomized trial comparing patients' tube-related inconvenience. *Langenbecks Arch Surg* 2001; **386**: 402-409
10 **Gouzi JL**, Moran B. Nasogastric tubes after elective abdominal surgery is not justified. *J Chir* 1998; **135**: 273-274
11 **Colvin DB**, Lee W, Eisenstat TE, Rubin RJ, Salvati EP. The role of nasointestinal intubation in elective colonic surgery. *Dis Colon Rectum* 1986; **29**: 295-299
12 **Wolff BG**, Pembeton JH, van Heerden JA, Beart RW Jr, Nivatvongs S, Devine RM, Dozois RR, Ilstrup DM. Elective colon and rectal surgery without nasogastric decompression. A prospective, randomized trial. *Ann Surg* 1989; **209**: 670-673
13 **Racette DL**, Chang FC, Trekell ME, Farha GJ. Is nasogastric intubation necessary in colon operations? *Am J Surg* 1987; **154**: 640-642
14 **Dinsmore JE**, Maxson RT, Johnson DD, Jackson RJ, Wagner CW, Smith SD. Is nasogastric tube decompression necessary after major abdominal surgery in children? *J Pediatr Surg* 1997; **32**: 982-984
15 **Savassi-Rocha PR,** Conceicao SA, Ferreira JT, Diniz MT, Campos IC, Fernandes VA, Garavini D, Castro LP. Evaluation of the routine use of the nasogastric tube in digestive operation by a prospective controlled study. *Surg Gynecol Obstet* 1992; **174**: 317-320
16 **MacRae HM**, Fischer JD, Yakimets WW. Routine omission of nasogastric intubation after gastrointestinal surgery. *Can J Surg* 1992; **35**: 625-628

Edited by Wang XL and Chen WW **Proofread by** Xu FM